IODP - ICDP
Kolloquium 2010
„Geozentrum“ Frankfurt

9. - 11. März 2010
Goethe-Universität Frankfurt

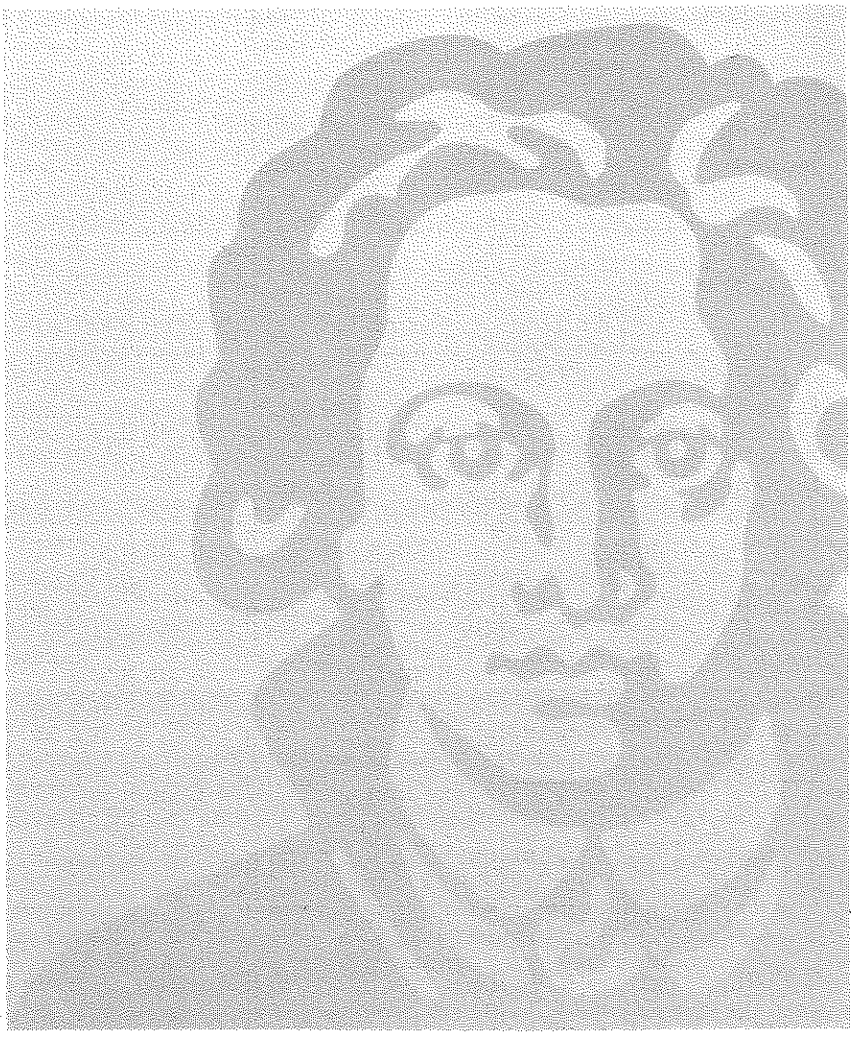

Deutsche
Forschungsgemeinschaft

DFG

Eocene-Oligocene transition Expedition 320/321

Dienstag, 09. März 2010		
10:00	13:00	**Registrierung im Foyer Geowissenschaften**
13:00	13:30	**Eröffnung im Hörsaal Chemie N/B1** Universitätsleitung G. Lüniger, DFG Koordinatoren - Gastgeber
Berichte / Entwicklungen		
13:30	13:50	J. Erbacher / R. Stein IODP Rückblick auf 2009 - Wie geht es weiter?
13:50	14:10	R. Oberhänsli / R. Emmermann ICDP Deutschland – Wie geht es weiter?
14:10	14:25	J. O. Herrle, N. Gussone, E. Hathorne, A. Holbourn, T. Westerhold, and Exp. 320/321 Scientists **Expedition 320/321 "Pacific Equatorial Age Transect (PEAT)"**
14:25	14:40	J. Gottschalk, A.J. Kopf, M. Melles, and El'gygytgyn Scientific Party **School Project about paleoclimate research: ICDP Expedition at Lake El'gygytgyn enters the class room**
14:40	14:55	A.J. Kopf, T. Wiersberg, Shipboard Science Party Exp. 319 **IODP Expedition 319: NanTroSEIZE Stage 2: Preliminary results**
14:55	15:10	A. Hüpers, V.B. Heuer, Y. Kitamura, S. Kutterolf, and IODP Exp. 322 Scientists **Preliminary results of sedimentology and physical properties from IODP Expedition 322 (NanTroSEIZE Stage 2: subduction inputs)**
15:10	15:20	W. Eder **Stand und Perspektiven des „International Year of Planet Earth" (IYPE)**
15:20	17:00	**Posterpräsentation** der Themen: Berichte und Entwicklungen, Seismogene Zone, Hangstabilitäten, Impaktstrukturen, Gashydrate, Gase, Fluide **Kaffeepause**
Seismogene Zone / Hangstabilitäten		
17:00	17:20	M. Stipp, Y. Kitamura, J.H. Behrmann, B. Leiss **Geotechnical experiments indicate deformation partitioning in the soft sediments of the Nankai accretionary prism (NEXT- NanTroSEIZE)**
17:20	17:40	J.H. Behrmann, S. Meissl **Superfast sedimentation and submarine slides, Gulf of Mexico continental slope: insights into transport processes from fabrics and geotechnical data**
Stoffkreisläufe / Tiefe Biosphäre		
17:40	18:00	M. Reuschel, H. Strauss, V.M. Melezhik, A. Lepland, P. Caritgny, L.R. Kump, Y. Deines, A. Romashkin, D. Rychanchik **The global sulfur cycle across the Archean-Paleoproterozoic transition: Evidence from FAR-DEEP**
18:00	18:20	C. Illing, H. Strauss, R. Summons, A. Lepland, V.M. Melezhik, & the FAR-DEEP Scientists **Molecular and organic carbon isotopic evidence for the evolution of key metabolic pathways during the Archean-Proterozoic transition**
18:20	18:40	J. Griess, K. Mangelsdorf, D. Wagner **Microbial driven methane dynamic in the Siberian Arctic during glacial-interglacial climate changes**
ab 19:00		**Icebreaker** im Foyer Geowissenschaften

Mittwoch, 10. März 2010		
Stoffkreisläufe / Tiefe Biosphäre		
09:00	09:20	P. Meister, B. Brunner, T.G. Ferdelman, M.E. Böttcher, B.B. Jorgensen **Sulphur- and carbon-isotopes document dynamic sulphate methane interface (Peru Margin, Leg 201 Site 1229)**
09:20	09:40	L.M. Wehrmann, T.G. Ferdelman, B. Brunner, C. März, Y. Huh, M. Ikehara, N. Risgaard-Petersen, H. Schrum, E.A. Walsh, S. D`Hondt, A.C. Ravelo, K. Takahashi, C. Alvarez-Zarikian, and IODP Exp. 323 Scientists **Microbial respiration and diagenetic redox cycling in sediments of the high productivity Bering Sea (IODP Expedition 323)**
9:40	11:00	**Posterpräsentation** der Themen: Stoffkreisläufe, Tiefe Biosphäre, Magmatische Petrologie, Metamorphismus **Kaffeepause**
Magmatische Petrologie / Metamorphismus		
11:00	11:20	H. Behrens, A.V. Simonyan, S. Dultz, J. Fiebig **From magma degassing to carbonation of rocks - studies related to the Unzen Drilling Project**
11:20	11:40	N. Jöns, W. Bach, F. Klein, T. Schroeder **Influence of melt veins on the mineralogical and structural evolution of abyssal peridotites**
11:40	12:00	C. Kirchner, J. Koepke, H. Behrens **Time scales for vertically moving axial magma chambers at fast-spreading ocean ridges and involved magmatic reactions: insights from IODP Site 1256**
12:00	12:20	Y. Lavallée, C.P. De Campos, D. Morgavi, R. Heistek, L. Morgan, K.U. Hess, D.B. Dingwell **Towards timescales of assimilation and magma mixing in the large igneous province of Snake River Plain – Yellowstone, Northwest United States: Why deep-drilling? Preliminary results**
12:20	12:40	C. Virgil, A. Hördt, S. Ehmann, M. Leven, E. Steveling, J. Kück, F. Dietze **3-komponentige Magnetfeldmessungen in der Outukumpu-Bohrung (Finnland)**
12:40	14:00	**Mittagspause + Poster**
Paläozeanographie / Paläoklima		
14:00	14:20	P. Hofmann, L. Handly, H.M. Talbot, T. Wagner **A warming pulse in the subtropical North Atlantic during Oceanic Anoxic Event 1a, ODP Site 641C Galicia Margin**
14:20	14:40	L. Diester-Haass, K. Billups, K.-C. Emeis **Marine biological productivity, carbon cycling and climate cooling during the Oligocene to Miocene transition**
14:40	16:30	**Posterpräsentation** der Themen: Paläozeanographie, Paläoklima **Kaffeepause**
16:30	16:50	N. Riedel, T. Litt **Einflüsse prähistorischen Vulkanismus auf die Vegetationsgeschichte Ostanatoliens. Vorläufige Untersuchungsergebnisse holozäner Sedimente des Vansees (Türkei)**
16:50	17:10	M. Sumita, H.-U. Schmincke **Onland tephra record around Lake Van as a stratigraphic, compositional, temporal and alteration framework for the Palevan drilling project**
17:10		**Transfer**
19:00	21:00	**Campus Westend (Hörsaal HZ1)** **Grußwort von Frau Nicola Beer,** Hessische Staatssekretärin für Europaangelegenheiten **Öffentliche Abendvorträge:** Ralf Tiedemann Jochem Marotzke **Das „2° C Ziel“ - Szenarien und Vorhersagen**

Donnerstag, 11. März 2010

Paläozeanographie / Paläoklima

8:30	8:50	B. Zolitschka, C. Ohlendorf, C. Gebhardt, A. Hahn, P. Kliem, and the PASADO Science Team **Characterisation of the 106 m long lacustrine sediment record from Laguna Potrok Aike, Argentina (ICDP-project PASADO)**
08:50	09:10	B. Wagner, H. Vogel, and the SCOPSCO Science Team **The sediment record of Lake Ohrid, Albania and Macedonia – modern and past sedimentation and inferences of climatic and environmental change over the last glacial-interglacial cycle**
09:10	09:30	C. Karas, D. Nürnberg, R. Tiedemann, D. Garbe-Schönberg **Mid-Pliocene restriction of the Indonesian Gateway and its implication on ocean circulation and climate**
09:30	09:50	S. de Schepper, M.J. Head, J. Groeneveld, D. Naafs **Mid-Pliocene North Atlantic palaeoceanography based on palynology, Mg/Ca of planktonic foraminifers and alkenones**
09:50	10:10	M. Kucera, L. Numberger, H. Schulz, U. Röhl, A. Mackensen **Marine isotopic stage 11 in the eastern Mediterranean Sea**
10:10	11:30	**Posterpräsentation** der Themen: Neue Projekte, Projektvorschläge, Paläozeanographie, Paläoklima **Kaffeepause**
11:30	11:50	L. Perez, J. Lorenschat, M. Brenner, B. Scharf, A. Schwalb **Environmental history of Lago Petén Itzá, Guatemala, during the Deglacial and Last Glacial Maximum**
11:50	12:10	O. Juschus, V. Wennrich, M. Melles, C. Gebhardt **Quaternary mass movement events in Lake El'gygytgyn, northeastern Siberia – their effects on the 'pelagic' sediment record and first results from the deep drilling project**

Neue Projekte / Projektvorschläge

12:10	12:30	S. Stegmann, P. Henry, A. J. Kopf, N. Sultan, V. Spiess, G. de Lange, K. Moran, J.K. Morgan, S. Migeon, A. Camerlenghi, Y. Yamada, A. Solheim, S. Tinti, P. Charvis **Drilling and monitoring of natural and man-made landslide trigger mechanisms at the Ligurian slope (W'Mediterranean Sea): the Nice Airport Landslide NAIL.**
12:30	13:00	**Posterprämierung und Schlussworte**
13:00		**Tagungsende**

Donnerstag, 11. März 2010

Im **Anschluß** an das IODP/ICDP Kolloquium

14:00	**GESEP School 2010: Wissenschaftliches Kernbohren in Lockersedimenten**

Der modulare Kurs, organisiert von GESEP, Potsdam, wird von Ingenieuren und Wissenschaftlern aus Braunschweig, Bremen, Essen, Frankfurt und Potsdam mit langer Erfahrung in IODP und ICDP gehalten und soll jungen Wissenschaftlern Grundkenntnisse in Bohrtechnik, Bohrlochgeophysik und Monitoring, Antragstellung und Management vermitteln.

ENDE: **Freitag, 12. März 2010, ca. 17.00 Uhr**

Teilnehmerliste

Name	Vorname	Institution und Ort
Almeev	Renat	Institut für Mineralogie, Leibniz Universität Hannover
Bach	Wolfgang	Universität Bremen
Bachmann	Gerhard	Universität Halle
Bagdassarov	Nikolai	Universität Frankfurt
Beer	Nicola	Hessisches Ministerium der Justiz, für Integration und Europa, Wiesbaden
Behrens	Harald	Institut für Mineralogie, Leibniz Universität Hannover
Behrmann	Jan	IFM-GEOMAR, Kiel
Berthold	Susann	Dresdner Grundwasserforschungszentrum e.V.
Bickert	Torsten	MARUM, Universität Bremen
Böhm	Evelyn	Universität Heidelberg
Böhm	Florian	IFM-GEOMAR, Kiel
Börner	Frank	Dresdner Grundwasserforschungszentrum e.V.
Bohrmann	Gerhard	MARUM, Universität Bremen
Bollmann	Jörg	Universität Toronto
Bolte	Torsten	Institut für Mineralogie, Leibniz Universität Hannover
Bosch	Frank	RWTH Aachen
Botcharnikov	Roman	Institut für Mineralogie, Leibniz Universität Hannover
Bräuer	Karin	Helmholtz-Zentrum für Umweltforschung - UFZ, Halle
Breuker	Anja	Bundesanstalt für Geowissenschaften und Rohstoffe, Hannover
Brückmann	Warner	IFM-GEOMAR, Kiel
Buske	Stefan	Freie Universität Berlin
Chapligin	Bernhard	Alfred-Wegener-Institut für Polar- und Meeresforschung, Bremerhaven
Cichy	Sarah B.	Institut für Mineralogie, Leibniz Universität Hannover
Cukur	Deniz	IFM-GEOMAR, Kiel
Cypionka	Heribert	ICBM Oldenburg
De Campos	Cristina	Universität München
De Schepper	Stijn	Universität Bremen, Fachbereich Geowissenschaften
Dersch-Hansmann	Michaela	Hessisches Ministerium der Justiz, für Integration und Europa, Wiesbaden
Deutsch	Alex	Universität Münster
Diester-Haass	Liselotte	Universität des Saarlandes, Saarbrücken
Dietze	Frank	KIT Karlsruhe
Drath	Gabriela	Bundesanstalt für Geowissenschaften und Rohstoffe, Hannover
Dultz	Stefan	Institut für Bodenkunde, Leibniz Universität Hannover
Dziony	Wanja	Institut für Mineralogie, Leibniz Universität Hannover
Eckert	Sebastian	ICBM Oldenburg
Eder	Wolfgang	Universität München
Emmermann	Rolf	GeoForschungsZentrum Potsdam
Engelen	Bert	ICBM Oldenburg
Engelhardt	Tim	ICBM Oldenburg
Erbacher	Jochen	Bundesanstalt für Geowissenschaften und Rohstoffe, Hannover
Erdmann	Martin	Institut für Mineralogie, Leibniz Universität Hannover
Erzinger	Jörg	GeoForschungsZentrum, Potsdam
Etourneau	Johan	Universität Kiel
Fenner	Juliane	Bundesanstalt für Geowissenschaften und Rohstoffe, Hannover
Ferdelman	Timothy	MPI Bremen
Fiebig	Jens	Universität Frankfurt
Flaws	Asher	Universität München
Frank	Ute	GeoForschungsZentrum Potsdam
Friedrich	Oliver	Universität Frankfurt
Gaedicke	Christoph	Bundesanstalt für Geowissenschaften und Rohstoffe, Hannover
Gärtner	Claudia	Universität Münster
Gebhardt	Catalina	Alfred-Wegener-Institut für Polar- und Meeresforschung, Bremerhaven
Gischler	Eberhard	Universität Frankfurt
Gottschalk	Julia	Universität Bremen
Grein	Michaela	Staatliches Museum für Naturkunde, Stuttgart
Grieß	Juliane	Alfred-Wegener-Institut für Polar- und Meeresforschung, Bremerhaven
Grützner	Jens	Alfred-Wegener-Institut für Polar- und Meeresforschung, Bremerhaven
Gussone	Nikolaus	Institut für Mineralogie, Universität Münster
Gutjahr	Stine	Freie Universität Berlin
Haberzettl	Torsten	Universität Jena
Hahn	Annette	Universität Bremen
Handiani	Dian	Universität Bremen
Harms	Ulrich	GeoForschungsZentrum Potsdam
Hathorne	Ed	IFM-GEOMAR, Kiel
Heide	Klaus	Universität Jena
Heldt	Matthias	Bundesanstalt für Geowissenschaften und Rohstoffe, Hannover
Hensen	Christian	IFM-GEOMAR, Kiel
Hepp	Daniel A.	Universität Bremen
Herrle	Jens	Universität Frankfurt
Hess	Kai-Uwe	Earth and Environmental Sciences, LMU München
Hesse	Reinhard	McGill University, Montreal
Heuer	Verena	MARUM, Universität Bremen
Heydolph	Ken	IFM-GEOMAR, Kiel
Hoerdt	Andreas	TU Braunschweig
Höfig	Tobias	IFM-GEOMAR, Kiel
Hoffmann	Nadine	RWTH Aachen
Hofmann	Peter	Universität Köln
Holbourn	Ann	Universität Kiel
Holtz	François	Institut für Mineralogie, Leibniz Universität Hannover
Hüpers	Andre	MARUM, Universität Bremen
Illing	Christian	Universität Münster
Jöns	Niels	Fachbereich Geowissenschaften, Universität Bremen
Juschus	Olaf	TU Berlin

Kämpf	Horst	GeoForschungsZentrum Potsdam
Karas	Cyrus	IFM-GEOMAR, Kiel
Kastner	Stephanie	GEOPOLAR, Institut für Geographie, Universität Bremen
Khélifi	Nabil	Universität Kiel
Kirchner	Clemens	Institut für Mineralogie, Leibniz Universität Hannover
Kitamura	Yujin	IFM-GEOMAR, Kiel
Kliem	Pierre	Universität Bremen
Klügel	Andreas	Universität Bremen
Koepke	Jürgen	Institut für Mineralogie, Leibniz Universität Hannover
Kopf	Achim	MARUM, Universität Bremen
Kotthoff	Ulrich	Universität Hamburg
Krastel	Sebastian	IFM-GEOMAR, Kiel
Kucera	Michal	Universität Tübingen
Kudraß	Hermann-Rudolf	Bundesanstalt für Geowissenschaften und Rohstoffe, Hannover
Kuhn	Thomas	Bundesanstalt für Geowissenschaften und Rohstoffe, Hannover
Kuhnt	Wolfgang	Universität Kiel
Kunze	Sabine	Bundesanstalt für Geowissenschaften und Rohstoffe, Hannover
Lazarus	David	Museum für Naturkunde, Berlin
Leythaeuser	Detlev	RWTH Aachen
Lezius	Jeannette	Alfred-Wegener-Institut für Polar- und Meeresforschung, Bremerhaven
Lindhorst	Katja	IFM-GEOMAR, Kiel
Lipp	Julius	MARUM, Universität Bremen
Lippold	Jörg	Universität Heidelberg
Lischka	Martin	Universität Greifswald
Lorenschat	Julia	TU Braunschweig
Lücke	Andreas	FZ Jülich
Lückge	Andreas	Bundesanstalt für Geowissenschaften und Rohstoffe, Hannover
Lüniger	Guido	DFG, Bonn
März	Christian	ICBM, Universität Oldenburg
Mang	Christoph	KIT Karlsruhe
Marotzke	Jochem	Max-Planck-Institut für Meteorologie, Hamburg
Mayr	Christoph	Universität Erlangen
Meissl	Sandra	IFM-GEOMAR, Kiel
Meister	Patrick	MPI Bremen
Montoya Pino	Carolina	Universität Frankfurt, Institut für Geowissenschaften
Naafs	David	Alfred-Wegener-Institut für Polar- und Meeresforschung, Bremerhaven
Nürnberg	Dirk	IFM-GEOMAR, Kiel
Oberhänsli	Roland	Institut für Geowissenschaften, Potsdam
Ockert	Charlotte	Universität Münster
O'Connor	John	Alfred-Wegener-Institut für Polar- und Meeresforschung, Bremerhaven
Ohlendorf	Christian	GEOPOLAR, Institut für Geographie, Universität Bremen
Oschmann	Wolfgang	Universität Frankfurt
Ostertag-Henning	Christian	Bundesanstalt für Geowissenschaften und Rohstoffe, Hannover
Palamenghi	Luisa	Universität Bremen
Pèrez Alvarado	Liseth	TU Braunschweig
Planert	Lars	IFM-GEOMAR, Kiel
Pletsch	Thomas	Bundesanstalt für Geowissenschaften und Rohstoffe, Hannover
Raddatz	Jacek	IFM-GEOMAR, Kiel
Raschke	Ulli	Museum für Naturkunde, Berlin
Rausch	Svenja	Universität Bremen
Reusch	Anna	Universität Bremen
Reuschel	Marlene	Universität Münster
Riedel	Nils	Steinmann-Institut, Universität Bonn
Riethdorf	Jan	IFM-GEOMAR, Kiel
Rommerskirchen	Florian	MARUM, Universität Bremen
Roth-Nebelsick	Anita	Universität Tübingen
Sahlberg	Monika	Universität Oldenburg
Sarnthein	Michael	Institut für Geowissenschaften, Universität Kiel
Schäbitz	Frank	Universität Köln
Schippers	Axel	Bundesanstalt für Geowissenschaften und Rohstoffe, Hannover
Schmidt-Schierhorn	Friederike	Universität Bremen
Schmincke	Hans-Ulrich	IFM-GEOMAR, Kiel
Schneider	Ralph	Universität Kiel
Schreck	Michael	Alfred-Wegener-Institut für Polar- und Meeresforschung, Bremerhaven
Schulte	Peter	Institut für Geologie-Mineralogie, Universität Erlangen
Schulz	Hartmut	Institut für Geowissenschaften, Tübingen
Schumann	Jens	GeoForschungsZentrum Potsdam
Schwalb	Antje	Institut für Umweltgeologie, Braunschweig
Schwamborn	Georg	Alfred-Wegener-Institut für Polar- und Meeresforschung, Potsdam
Shishkina	Tatiana	Universität Hannover
Simonyan	Anna	Universität Hannover, Institut für Bodenkunde
Smolka	Peter P.	Universität Münster
Stadler	Susanne	Bundesanstalt für Geowissenschaften und Rohstoffe, Hannover
Stein	Rüdiger	Alfred-Wegener-Institut für Polar- und Meeresforschung, Bremerhaven
Steinke	Stephan	MARUM, Universität Bremen
Stipp	Michael	IFM-GEOMAR, Kiel
Strack	Dieter	International Oil & Gas Consultant, Ratingen
Strauch	Gerhard	Helmholtz-Zentrum für Umweltforschung - UFZ, Halle
Sumita	Mari	IFM-GEOMAR, Kiel
Szurlies	Michael	Universität Potsdam
Teichert	Barbara	Universität Münster
Tiedemann	Ralf	Alfred-Wegener-Institut für Polar- und Meeresforschung, Bremerhaven
Timmerman	Martin	Universität Potsdam
Trampe	Anna F.	Universität Bremen
Uenzelmann-Neben	Gabriele	MARUM, Universität Bremen
van Bramann	Ullrich	TU Braunschweig

Virgil	Christopher	Institut für Geophysik und Extraterrestrische Physik, TU-Braunschweig
Voigt	Silke	Universität Frankfurt
von der Handt	Anette	Universität Freiburg
Wagner	Bernd	Universität Köln
Wallrabe-Adams	Hans-Joachim	MARUM, Universität Bremen
Weber	Michael E.	Universität Köln
Wefer	Gerold	MARUM, Universität Bremen
Wehrmann	Laura	MPI Bremen
Wennrich	Volker	Universität Köln
Westerhold	Thomas	MARUM, Universität Bremen
Weyer	Stefan	Universität Köln
Wiersberg	Thomas	GeoForschungsZentrum Potsdam
Wille	Michael	Universität Köln
Winkelmann	Daniel	IFM-GEOMAR, Kiel
Wonik	Thomas	LIAG Hannover
Wortmann	Ulrich	Universität Toronto
Zolitschka	Bernd	GEOPOLAR, Institut für Geographie, Universität Bremen

Fahrtberichte

Preliminary results from IODP Expedition 313 (New Jersey Shallow Shelf)

KOTTHOFF, ULRICH[1], STADLER, SUSANNE[2], AND THE IODP EXPEDITION 313 SCIENCE PARTY[3]

[1]Department of Geosciences, Hamburg University, Bundesstrasse 55, D-20146 Hamburg, Germany, e-mail: ulrich.kotthoff@uni-hamburg.de
[2]Federal Institute for Geosciences and Natural Resources (BGR), Stilleweg 2, D-30655 Hannover, Germany, e-mail: susanne.stadler@bgr.de
[3]ECORD Science Operator, Edinburgh, United Kingdom

IODP Expedition 313 aims at estimating amplitudes, rates and mechanisms of sea-level change and at the evaluation of sequence stratigraphic facies models that predict depositional environments, sediment compositions, and stratal geometries in response to sea-level change. Several hundred cores from three sites (313-M0027, M0028, and M0029) from the New Jersey shallow shelf (~35 m water depth) were retrieved during May to July 2009. The drilling was executed using an ECORD "mission-specific" jack-up platform 45 to 67 km off the coast of New Jersey. The recovery rate for the three sites surpassed 80%, with 1311 m total core length. The deepest hole (M0029A) reached 757 mbsf; the oldest sediment recovered is from the late Eocene (Hole M0027A) according to biostratigraphy, magnetostratigraphy and Sr-isotopy-based age estimates.

With the coring of the three holes from the shallow shelf, the coastal plain (ODP Legs 150X, 174AX), outer shelf and slope (Legs 150 and 174A) core datasets are complemented, building up a large “New Jersey transect” across the US Atlantic passive margin. In addition to the coring, wireline logs– gamma ray, resistivity, magnetic susceptibility, sonic, acoustic televiewer and vertical seismic profiles – have been collected for all three sites, which together with multisensor core logs on unsplit cores provide very precise ties between core-logs and seismic profiles.

The lithostratigraphic reconstruction of the cored sediments shows that they were deposited in two general contexts: (1) mixed-wave to river-dominated shelf with well-sorted silt and sand deposited in off- shore to shoreface environments and (2) clinoform slope/rollover degradation periods dominated by interbedding of poorly sorted silts, debris flow and turbidite sands, and toe-of-slope silt and silty clays. The depositional systems are usually silt-rich supply systems that show a notable paucity of clays. The open shelf experiences frequent periods of dysoxia with cyclical repetitions. No evidence was found of exposure at the clinoform inflection point (depositional shelf break), but the periodic occurrences of shallow-water facies along the slope of clinoforms and of deepwater facies on the topset of the clinoforms suggest large-amplitude changes in relative sea level in the range of 60m.

Zonation of multiple fossil groups (foraminifers, organic-walled dinoflagellate cysts and nannoplankton), Sr-isotopic ages measured on molluscs and forams, magnetic reversal chronology, and pollen-based reconstructions of hinterland vegetation imply a nearly continuous record of ~1 myr sea-level cycles and climate variations which may explain facies changes along the slopes of the clinoforms. Planned post-cruise works include stratigraphic backstripping (with calculation of sediment compaction and crustal loading) to derive a more precise estimate of the magnitude of eustatic sea-level change.

Preliminary results from IODP Expedition 317 (Canterbury Basin, New Zealand)

D.A.. HEPP[1], J. S. LIPP[1], IODP EXPEDITION 317 SHIPBOARD SCIENTISTS

[1]MARUM – Center for Marine Environmental Sciences and Department of Geosciences, University of Bremen, Leobener Strasse, 28359 Bremen, Germany

IODP Expedition 317 (November 4, 2009 to January 4, 2010) aimed to understand the relative importance of global sea level changes (eustasy) versus local tectonic and sedimentary processes in controlling continental margin sedimentary cycles (Expedition 317 Scientists, 2010).

The main focus was on the sequence stratigraphy of the late Miocene to recent, when the global sea level change was dominated by glacioeustasy. Drilling in the Canterbury Basin, on the eastern margin of the South Island of New Zealand, takes advantage of high rates of Neogene sediment supply, which preserves a high-frequency (0.1-0.5 m.y.) record of depositional cyclicity.

The Canterbury Basin provides an opportunity to study the complex interactions between processes responsible for the preserved stratigraphic record of sequences because of the proximity of an uplifting mountain chain (Southern Alps), and strong ocean currents. The overarching objectives of this expedition were:

Date clinoform seismic sequence boundaries and sample associated facies to estimate eustatic amplitudes.

Drill the Marshall Paraconformity in the offshore basin.

Constrain the erosion history of the Southern Alps.

Determine sediment drift depositional histories and paleoceanographic record.

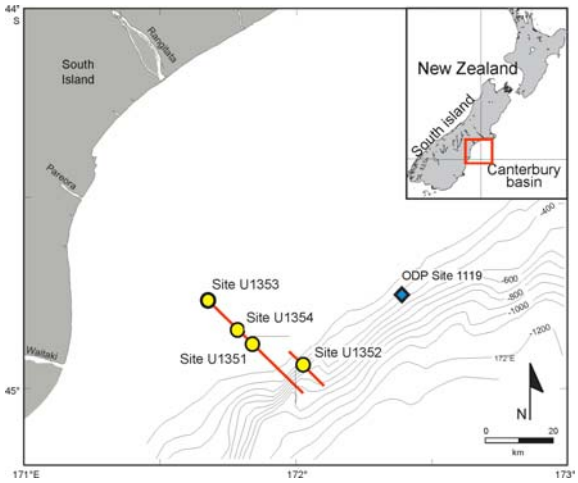

Figure 1: Map of the study area on the eastern margin of South Island, New Zealand shows site locations drilled during Expedition 317 (red) and Site 1119 (ODP Leg 181). Red lines = locations of dip profiles shown in Figure 2 (modified from Expedition 317 Scientists, 2010).

To meet these objectives, sedimentary sequences were cored in a transect of three Sites on the continental shelf (landward to basinward, Sites U1351, U1353, U1354, Fig. 1) and one Site on the continental slope (U1352; Fig. 1). The transect provides a stratigraphic record of depositional cycles across the shallow water environment most directly affected by relative sea level change. Seismic sequence boundaries were tentatively correlated with lithological boundaries observed in cores. This record will be refined postcruise and used to estimate the timing and amplitude of global sea level change and to document the sedimentary processes that operate during sequence formation.

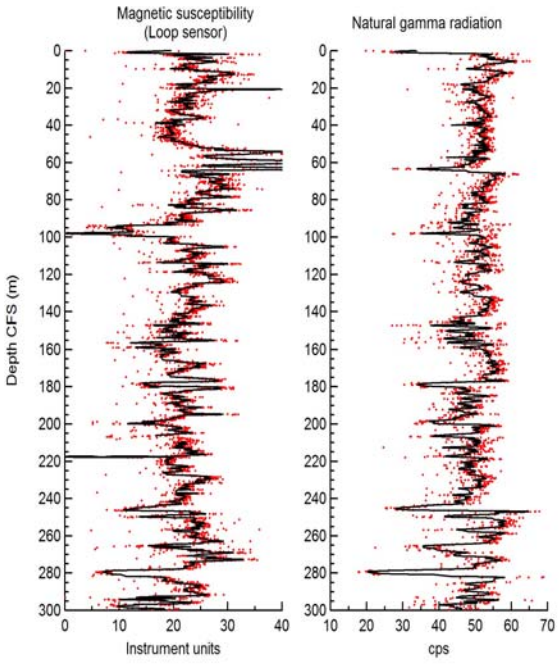

Figure 2: Raw (red) and Gaussian low pass filtered data (black) for magnetic susceptibility (loop sensor) for the upper 300 m of Hole U1352B.

Sites U1351, U1353 and U1354 provide a high resolution record of Holocene and late Quaternary glacial cycles in a continental shelf setting. Site U1352 (Fig. 2), located on the continental slope, represents a record from modern slope terrigenous sediment to hard Eocene limestone, with all associated lithologic, biostratigraphic, physical, geochemical, and microbiological transitions. The site also provides a record of ocean circulation and fronts during the last ~35 m.y.

The early Oligocene (~30 Ma) Marshall Paraconformity was the deepest target of Expedition 317 and is hypothesized to represent intensified current erosion or nondeposition associated with the initiation of thermohaline circulation and the proto Antarctic Circumpolar Current.

Nineteen regional middle Miocene to Pleistocene sequence-bounding unconformities were identified from high-frequency sequence stratigraphy on the shelf-slope sediment prism of the offshore Canterbury Basin (U1-19; Fig. 3). The unconformities can be divided into three larger seismic units, the youngest of which indicates increasing exposure during sea level lowstands. Each unconformity is typically accompanied by a significant hiatus.

The smaller scale cycles documented by Expedition 317 drilling are in part similar to the Milankovitch-scale rhythms documented from nearby ODP Site 1119 (Fig. 1) and the New Jersey shelf, and correspond to cycles with inferred lengths of 100,000 and 40,000 years. Cycles drilled during Expedition 317 have differing sedimentary architectures dependent upon whether they were deposited seaward (Site U1352) or landward (Sites U1353 and U1354) relative to the inferred position of the lowstand shore line (~125 m). Site U1351 at 122 m water depth is located almost exactly at the lowstand shore line.

The observed middle Miocene to recent sedimentary sequences are generally correlative with previous ODP drilling of sedimentary sequences for sequence stratigraphic and sea level objectives, particularly drilling on the New Jersey Margin (ODP Legs 150, 150X, 174A, and 174AX; IODP Expedition 313) and in the Bahamas (ODP Leg 166), but includes an expanded Pliocene section. Completion of at least one transect across a geographically and tectonically distinct siliclastic margin was the necessary next step in deciphering continental margin stratigraphy. Expedition 317 also complements ODP Leg 181 drilling, which focused on drift development, with the landward part of the Eastern New Zealand oceanic sedimentary system.

Expedition 317 marked a new direction for IODP by incorporating drilling in shallow water on the continental shelf with unusually deep penetrations using the JOIDES Resolution, and set a number of scientific ocean drilling for microbiological studies (1925 m at Site U1352; Fig. 3C-D).

Reference:

Expedition 317 Scientists, 2010. Canterbury Basin Sea Level: Global and local controls on continental margin stratigraphy. IODP Prel. Rept., 317. doi:10.2204/iodp.pr.317.2010

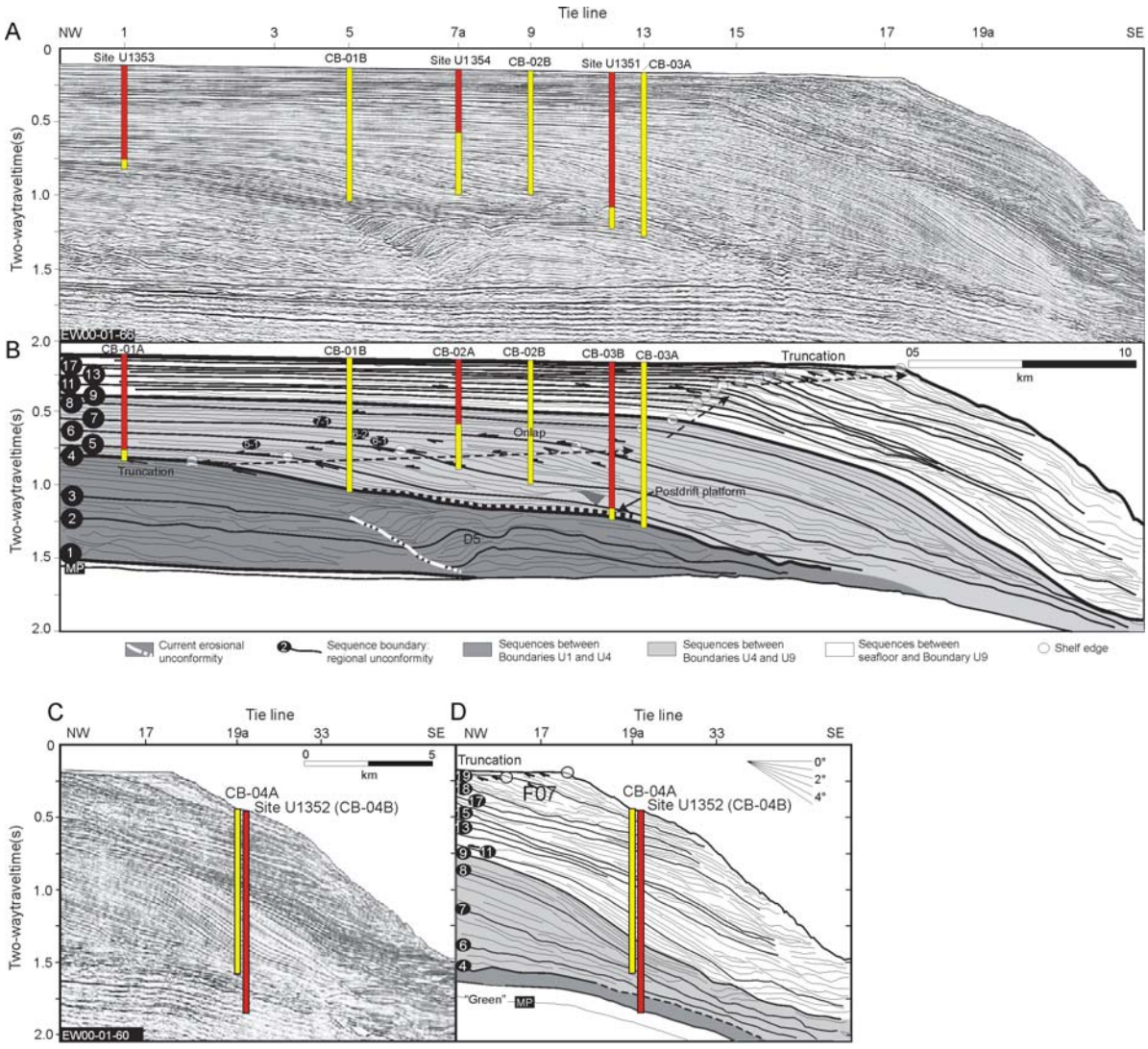

Figure 3: (A, C) Uninterpreted and (B, D) interpreted multichannel seismic profile showing locations of drilled (red) and alternative (yellow) sites, sequence boundaries and selected locations of reflection truncation (arrows), clinoform breakpoints representing paleoshelf edges (circles) and unconformities (U1-17; Expedition 317 Scientists, 2010).

IODP Expedition 319 NanTroSEIZE Stage 2 – Preliminary results

A. KOPF[1], T. WIERSBERG[2], SHIPBOARD SCIENCE PARTY EXP 319

[1]MARUM, Univ. Bremen
[2]GeoForschungsZentrum Potsdam

The Nankai Trough Seismogenic Zone Experiment (NanTroSEIZE) is a coordinated, multiexpedition drilling project designed to investigate fault mechanics and seismogenesis along subduction megathrusts through direct sampling, in situ measurements, and long-term monitoring in conjunction with allied laboratory and numerical modeling studies. The fundamental scientific objectives of the NanTroSEIZE project include characterizing the nature of fault slip and strain accumulation, fault and wall rock composition, fault architecture, and state variables throughout the active plate boundary system. As part of the NanTroSEIZE program, operations during Integrated Ocean Drilling Program (IODP) Expedition 319 included riser drilling, analyses of cuttings and core samples, downhole measurements and logging, and casing at Site C0009 in the Kumano forearc basin as well as riserless drilling, logging while drilling (LWD), casing, and observatory operations at Site C0010 across a major splay fault (termed the "megasplay") that bounds the seaward edge of the forearc basin near its updip terminus. In addition, we drilled at contingency Site C0011 to collect logging-while-drilling data in advance of planned coring operations scheduled as part of IODP Expedition 322.

Site C0009 marked the first riser drilling in IODP history. This allowed several scientific operations unprecedented in IODP, including carefully controlled measurements of in situ pore pressure, permeability and minimum principal stress magnitude, real-time mud gas analysis, and laboratory analyses of cuttings throughout the entire riser-drilled depth range (~700–1600 meters below seafloor [mbsf]). We conducted a leak-off test at one depth interval and successfully deployed the wireline Modular Formation Dynamics Tester 12 times to directly measure in situ stress magnitude, formation pore pressure, and permeability. During all phases of riser drilling, we collected mud gas for geochemical analyses and cuttings samples were collected throughout the entire riser-drilled depth range. Integration of data from cuttings, wireline

logging, and cores (from a limited depth interval) allowed definition of a single integrated set of lithologic units and comparison with previously drilled IODP Site C0002 to determine the evolutionary history of the forearc basin. After casing the borehole, we conducted a long-offset (up to 30 km) two-ship active seismic experiment, recording shots within the borehole to image the megasplay and master décollement beneath the borehole, and to evaluate seismic velocity and anisotropy of the forearc basin and accretionary prism sediments around the borehole.

At riserless Site C0010, operations included drilling with measurement while drilling (MWD)/LWD across the megasplay fault to 555 mbsf, casing the borehole with screens at the depth of the fault, conducting an observatory dummy run to test future strainmeter and seismometer deployment procedures, and installation of a temporary pore pressure and temperature monitoring system in advance of planned future permanent observatory emplacement. The observatory system (termed a "smart plug") marks the first observatory installation of the NanTroSEIZE program. MWD/LWD data at this site were used to define unit boundaries and the fault zone target interval for placement of the casing screens. Through comparison with previously drilled Site C0004 these data also provide insights into along-strike differences in the architecture of the megasplay fault and hanging wall.

Expedition 320/321 „Pacific Equatorial Age Transect (PEAT)“

J.O. HERRLE[1], N. GUSSONE[2], E. HATHORNE[3], A. HOLBOURN[4], T. WESTERHOLD[5], AND THE EXPEDITION 320/321 SCIENTISTS

[1]Institute of Geosciences, Goethe University Frankfurt, Altenhoeferalle 1, D-60438 Frankfurt am Main, Germany
2Institut für Mineralogie, Westfälische Wilhelms-Universität Münster, Corrensstrasse 24, 48149 Münster, Germany
[3]IFM-GEOMAR, Leibniz Institute of Marine Sciences, University of Kiel, Wischhofstrasse 1-3, D-24148 Kiel, Germany
[4]Institut für Geowissenschaften, Christian-Albrechts-Universität zu Kiel, Olhausenstrasse 40, 24098 Kiel, Germany
[5]Center for Marine Environmental Sciences (MARUM), University of Bremen, PO Box 330440, 28334 Bremen, Germany

Integrated Ocean Drilling Program (IODP) Expeditions 320 and 321, “Pacific Equatorial Age Transect” (PEAT) recovered a continuous sedimentary archive, which captures the evolution of the equatorial climate system throughout the Cenozoic. Expeditions 320 and 321 cored eight sites with a total of 23 holes along the position of the paleo-equator in the Pacific that allow us to decipher paleoceanographic and paleoclimatic changes during critical periods of Earth’s history. Intervals of major interest, characterised by an excellent recovery, moderate to well preserved siliceous and calcareous microfossils, and high sedimentation rates, include the (i) early Eocene Climatic Optimum (EECO, Zachos et al., 2001a), (ii) the Middle Eocene Climatic Optimum (MECO, Bohaty and Zachos, 2003), (iii) the middle through late Eocene high carbonate accumulation events (CAE events, Lyle et al., 2005), (iv) the Eocene-Oligocene transition (Oi-1; Coxall et al., 2005), (v) the early to late Oligocene glaciation events (Oi-1a to Oi-2c, Pekar et al., 2002, Pälike et al., 2006), (vi) the late Oligocene warming event (Pälike et al., 2006), (vii) the Oligocene–Miocene transition (Zachos et al., 2001), and (viii) the middle Miocene glaciation intensification event (Mi-3, Holbourn et al., 2005).

One of the primary objectives of the PEAT program was to detail the nature and changes of the carbonate compensation depth (CCD) throughout the Cenozoic in the equatorial Pacific. Shipboard results reveal that the early Eocene equatorial CCD is much shallower than previously thought, as shown by results from Site U1332, where we did not recover any carbonate in the basal sediment section above basement, in contrast to Site U1331, which is only ~2 m.y. older. Our estimated CCD at ~49 Ma is only ~3000 m paleodepth. Surprisingly, our results also show a shallower CCD than previously known during the late Oligocene, perhaps 300 m shallower in the time interval between 23 and 27 Ma. This shallower CCD, at a paleodepth of ~4.5 km, and associated reduced carbonate fluxes to the seafloor could be linked to the gradual late Oligocene cooling (Pälike et al., 2006). The design of our drilling locations in combination with existing data will allow us to generate a 3-D view of CCD evolution during the Cenozoic during postcruise research. Preliminary results from high resolution XRF core scanning suggest that the new records from Site U1333 and U1334 consist of higher carbonate contents than Site 1218 (Leg 199) providing an expanded, more complete record for the late Eocene.

Another highlight of the Expedition 320 and 321 was the recovery of well preserved and diverse assemblages in both the siliceous (radiolarians and diatoms) and calcareous plankton and benthic groups (planktic and benthic foraminifers and calcareous nannofossils) for most parts of the late Paleogene and Neogene. All groups exhibit prominent downcore variations in abundance and preservation that appear related to major changes in primary production, export flux, and water-column and seafloor dissolution, thus reflecting fundamental changes in global climate. The “carbonate crash”, an extended period of low carbonate deposition, widely recorded throughout the eastern Pacific Ocean at ~ 9-11 Ma (Lyle et al., 1995; Farrell et al., 1995), is marked by sharp decreases or disappearance of planktic foraminifers, high benthic to planktic foraminifer ratios and generally impoverished benthic foraminifer assemblages. During episodic expansion of the Antarctic ice-sheets in particular for the Eocene/Oligocene transition (Oi-1), the early to late Oligocene (Oi-1a, Oi-2b, Oi-2c) as well as during the mid Miocene (at ~14-15 Ma), calcareous microfossils (planktic and benthic) exhibit overall good preservation and relatively high diversity, suggesting a vigorous Pacific Ocean circulation and deep CCD. Postcruise studies will provide an opportunity to further investigate temporal and spatial variations in microfossil distribution across the equatorial Pacific Ocean and to unravel links with global climatic and oceanographic events during the Cenozoic.

The shipboard geochemical analyses of the interstitial water and bulk sediment samples reflect the large variations in the sediment composition resulting from shifts in biogenic carbonate versus opal production and the large scale redox state and diagenetic processes of the sediment column, which are related to the overall changes in sediment composition. The interstitial water chemistry indicates seawater circulation in the basement. The most interesting profiles of dissolved constituents were those of Sr^{2+} and Li^{+} that mirrored each other at the various sites.

This implies the presence of an active source for Sr^{2+}, most likely carbonate recrystallisation, and an enigmatic sink for Li^{+}, in the sediment column at PEAT sites.

References:
Bohaty, S.M., Zachos, J.C., 2003. Significant Southern Ocean warming event in the late middle Eocene. Geology, 31, 1017-1020.
Coxall, H.K., Wilson, P.A., Pälike, H., Lear, C.H., Backman, J., 2005. Rapid stepwise onset of Antarctic glaciation and deeper calcite compensation in the Pacific Ocean. Nature 433, 53-57.
Farrell, J.W., Raffi, I., Janecek, T.R., Murray. D.W., Levitan, M., Dadey, K.A., Emeis, K.-C., Lyle, M., Flores, J.-A., and Hovan, S., 1995. Late Neogene sedimentation patterns in the eastern equatorial Pacific. In: Pisias, N.G., et al. (eds.), Proc. ODP, Init. Repts., Sc. Res., 138: College Station, TX (Ocean Drilling Program), 717-756.
Holbourn, A., Kuhnt, W., Schulz, M. & Erlenkeuser, H., 2005. Impacts of orbital forcing and atmospheric carbon dioxide on Miocene ice-sheet expansion. Nature 438, 483–487.
Lyle, M., Dadey, K. & Farrell, J., 1995. The Late Miocene (11-8 Ma) eastern Pacific carbonate crash: Evidence for reorganization of deep water circulation by the closure of the Panama Gateway. In: Pisias, et al. (eds.), Proc. ODP, Init. Repts., Sc. Res., 138: College Station, TX (Ocean Drilling Program), 821-837.
Lyle, M., Olivarez Lyle, A., Backman, J., Tripati, A., 2005. Biogenic sedimentation in the Eocene equatorial Pacific the stuttering greenhouse and Eocene carbonate compensation depth. In Lyle, M., Wilson, P.A., Janecek, T.R., et al., Proc. ODP, Init. Repts., 199: College Station, TX (Ocean Drilling Program), 1-35. doi:10.2973/odp.proc.sr.199.219.2005
Pälike, H., Norris, R.D., Herrle, J.O., Wilson, P.A., Coxall, H.K., Lear, C.H., Shackleton, N.J., Tripati, A.K. & Wade, B.S., 2006. The heartbeat of the Oligocene climate system. Science 314, 1894-1898.

Preliminary results of sedimentology and physical properties from IODP Expedition 322 (NanTroSEIZE Stage 2: subduction inputs)

A. HÜPERS[1], V.B. HEUER[1], Y. KITAMURA[2], S. KUTTEROLF[2], AND THE IODP EXPEDITION 322 SCIENTISTS

[1] MARUM - Center for Marine Environmental Sciences, University of Bremen, P.O. Box 330440, 28334 Bremen, Germany.
[2] IFM-GEOMAR, Leibniz Institute of Marine Sciences at the University of Kiel, Wischhofstraße 1-3, 24149 Kiel, Germany.

The Nankai Trough Seismogenic Zone Experiment (NanTroSEIZE) is a multistage, multiplatform drilling project of the Integrated Ocean Drilling Program (IODP) to investigate fault mechanics and seismogenesis along a subduction megathrust. The interdisciplinary project comprises direct sampling, in situ measurements, and long-term monitoring of the Nankai subduction system off Kii peninsula (SE Japan; Fig. 1) supplemented by shore-based experimental and numerical modelling studies. IODP Expedition 322 with DV Chikyu (1 September - 10 October 2009) is one of two expeditions of the project's second stage conducted in 2009. Its overarching aim was to provide a reference for the sediments and basement of the subduction zone by characterizing the incoming sedimentary strata and igneous basement of the Shikoku Basin prior to their arrival in the Nankai Trough.

Expedition 322 established two drill sites (Fig. 1) to document the incoming material with regard to the seafloor relief which strongly influences the presubduction geometry of sedimentary facies. Site C0011 is located on the northeastern flank of a bathymetric high (Kashinosaki Knoll). Logging while drilling had already been conducted at this site during the final days of Expedition 319 and provides a comprehensive data set for Shikoku Basin sediments. Coring started at 340 m core depth below seafloor (CSF) and aimed to penetrate the sediment/basalt interface at ca. 1050 m CSF but was prematurely abandoned at 876 m CSF without reaching ignous basement because of destruction of the drill bit. Site C0012 is located on the crest of the knoll. Coring started at 60 m CSF and continued to a total depth of 576 m CSF. The sediment/basalt interface was penetrated at 537.81 m CSF and 38.2 m of basement were cored with 18% recovery.

Although some sediment intervals could not be cored, the initial results capture all important lithologies of the Shikoku Basin and the underlying basement with a good correlation of unit boundary ages between the two sites (Fig. 2). When viewed together, the cored material documents the evolution of the Shikoku Basin. Five distinct lithological units of dominantly hemipelagic silty clay with Quarternary to middle Miocene age are overlying early Miocene pelagic clay and the igneous basement. A set of interbeds of late Miocene volcaniclastic and tuffaceous sandstones was sampled for the first time in the Shikoku Basin for which reason the interval is designated as a discrete formation named middle Shikoku Basin facies. An older system of abundant silt- and sandstone interbeds developed during the middle Miocene. It is in analogy to the turbiditic hemipelagic facies of the lower

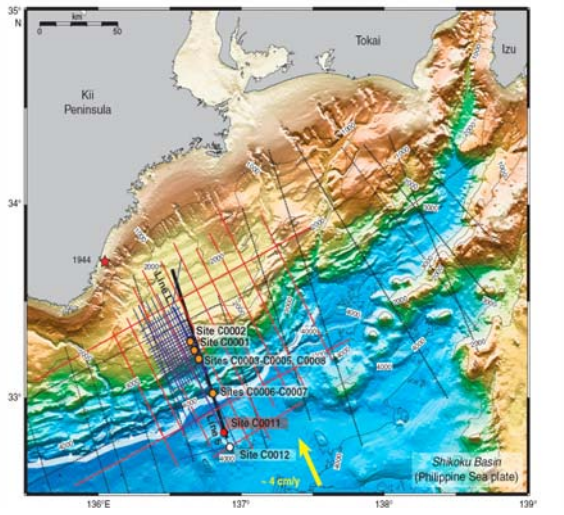

Fig. 1: Bathymetric map of the Nankai Trough showing Expedition 322 drilled Sites C0011 (red) and C0012 (white). The white barbed line shows the position of deformation front of Nankai accretionary prism. The arrow indicates the convergence vector between Philippine Sea plate and Japanese Islands (Eurasian plate). Other lines indicate 2-D multichannel seismic profile locations and orange dotes Stage 1 drill sites (from Underwood, M.B., Saito, S., Kubo, Y., and the Expedition 322 Scientists. 2009).

Shikoku Basin at ODP Site 1177. The oldest sedimentary formation is the pelagic clay. The unit was penetrated only at Site C0012 where it is documented as a thin layer (9.3m) of red and green calcareous claystones overlying directly the igneous basement. On the basis of nannofossils from pelagic clay, the age of the basement is >18.9 Ma at Site C0012. The recovered basement consists of pillow lava basalts, basalts, and basaltic-hyaloclastite breccia. The lithological results clearly reveal that basement highs modulate sedimentation rates in the Shikoku Basin as suggested by the condensed stratigraphic column of Site C0012. Deposition of sandy detritus on the crest of the knoll may be the result of thick turbidity currents and/or

upslope flow of gravity flows. Furthermore, chaotic deposits in middle Shikoku Basin facies (Fig.1) also suggest mass wasting processes at the northeastern flank of the knoll, probably by gravitational sliding.

Physical properties for both sites are consistent with normal consolidation trends. Profiles show downhole increases in bulk density, electrical resistivity, thermal

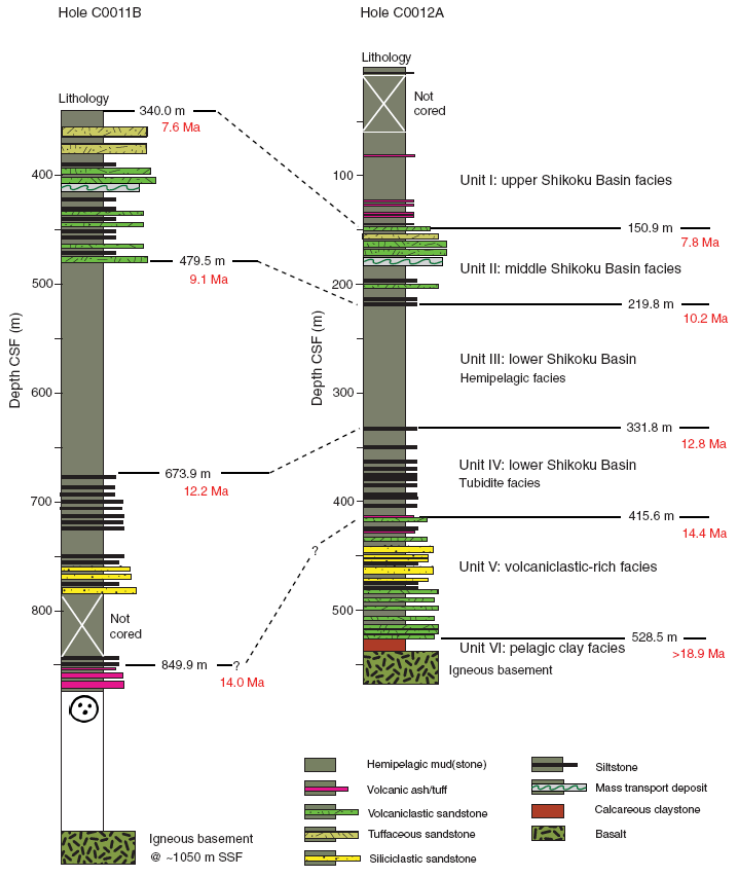

Fig. 2: Stratigraphic correlation between Sites C0011 and C0012. For Site C0011, coring started at 340 m CSF. Unit boundary ages are taken from integrated age-depth models (from Underwood, M.B., Saito, S., Kubo, Y., and the Expedition 322 Scientists, 2009).

conductivity and P-wave velocity, associated with a downhole decrease of porosity. Unfortunately, widespread occurrence of water-filled microcracks due to drilling disturbance led to large scatter in all physical property data. Geochemical analysis of pore-water constituents and dissolved gases suggest the intriguing possibility of two fluids from different sources migrating through the sedimentary strata seaward of the trench. One regime is driven by the explusion of fluids from the subducting systems (by compaction, and opal plus clay mineral dehydration) and migration through high permeability horizons in the subduction inputs. The geochemical fingerpints are fluid freshening and the presence of higher hydrocarbons. The other flow regime is driven by migration of a seawater-like fluid through the upper oceanic crust into the overlying sediment pile.

In conclusion, Expedition 322 achieved its proposed objectives. All important geologic properties have been documented providing a reference to study changes down the subduction system. Numerous whole-round samples were taken for further on-shore laboratory investigations of composition, geotechnical properties, frictional properties, and porosity/permeability.

References:

Underwood, M.B., Saito, S., Kubo, Y., and the Expedition 322 Scientists, 2009. NanTroSEIZE Stage 2: subduction inputs. IODP Prel. Rept., 322. doi:10.2204/iodp.pr.322.2009.

Preliminary Results IODP Expedition 323 (Bering Sea)

C. MÄRZ[1], L.M. WEHRMANN[2], A.C. RAVELO[3], K. TAKAHASHI[4], C. ALVAREZ-ZARIKIAN[5], AND IODP EXPEDITION 323 SCIENTISTS

[1]AG Mikrobiogeochemie, Institut für Chemie und Biologie des Meeres, Carl-von-Ossietzky-Strasse 9-11, 26129 Oldenburg, Germany
[2]AG Biogeochemie, Max-Planck-Institut für Marine Mikrobiologie, Celsiusstrasse 1, 28359 Bremen, Germany
[3]Ocean Sciences Department, University of California, 1156 High Street, Santa Cruz CA 95064, USA
[4]Department of Earth and Planetary Sciences, Kyushu University, Hakozaki 6-10-1, Higashi-ku, Fukuoka 812-8581, Japan
[5]Integrated Ocean Drilling Program, Texas A&M University, 1000 Discovery Drive, College Station TX, 77845-9547, USA

The main scientific objective of IODP Expedition 323 to the Bering Sea (July 4th – September 5th, 2009; Victoria/Canada – Yokohama/Japan) was to study the paleoceanographic development of this region over the last 5 Million years. Additionally, the expedition aimed to access microbial respiration, subseafloor biomass and community composition in the Deep Biosphere of this high-productivity area.

The position of the Bering Sea at the intersection of the North Pacific and the Arctic Ocean (Fig. 1) makes it an ideal target to study environmental processes related to Pliocene-Pleistocene climate fluctuations and the development of the Northern Hemisperic Ice Sheet. In addition, the Bering Sea is one of the most productive ocean regions worldwide, resulting in high deposition of biogenic remains, which in turn are supposed to fuel microbial processes in the sediment and related early diagenesis. Together with the high input of detrital matter from surrounding land masses, ice-rafted debris, and volcanic material from the Aleutian Arc, the sediments of the Bering Sea represent a unique and diverse paleoenvironmental archive. This was already recognized during DSDP Leg 19 (Fig. 1), but no continuous high-quality sediment records were cored.

During Expedition 323, seven sites were drilled along the northeastern Bering Sea slope (U1339, U1343-U1345) and on Bowers Ridge (U1340-U1342) in water depths of 850 to 3,200 m (Fig. 1). A total of more than 5.7 km of core were recovered, mostly with APC technique which provided high quality records. At least three holes were drilled at each site, drilling at most sites was complemented by an additional shallow (50-60 m) microbiology-dedicated hole. Recovered sediments consisted of a variable mixture of siliciclastic clay, silt and sand, isolated pebbles, biogenic remains (mostly diatoms), volcanic ash layers, and authigenic minerals (e.g. carbonates, pyrite). At Site U1342, around 100 m of volcaniclastic hardrock were drilled. The age of the sediment at all sites was determined by combined bio- and magnetostratigraphy and reached around 5 Million years at Sites U1340 and U1341. Estimated sedimentation rates varied from 10 to 50 cm/1000 years, with lowest rates determined for the Bowers Ridge sites and highest rates discovered for the sites along the continental slope. The degree of bioturbation ranged from strong with abundant burrows and mottles, over intermediate with indistinct bedding, to absent in finely laminated intervals. Sediments were of mostly greenish to greyish colour, depending on the relative proportion of terrigenous to biogenic material.

High-resolution pore-water and solid-phase profiles gave evidence for high present-day microbial activity in sediments from the continental slope sites while sites on Bowers Ridge were characterized by low rates of microbial respiration. At the slope sites, very high gas contents of the deposits frequently caused sediment extrusion on the rigfloor and catwalk. Production of methane in these sediments was presumably driven by intense biogeochemical degradation of organic matter. The occurrence of authigenic phases in most of the cores and paleomagnetic studies imply that the primary sediment composition was significantly overprinted by early diagenetic processes related to transformations of the sulphur and iron cycle.

The recovered Bering Sea sediments offer great potential to provide new insights of the paleoenvironmental development of this climate-sensitive region, its implications for global climate history, and the activity of the Deep Biosphere in a high-latitude, high productivity region.

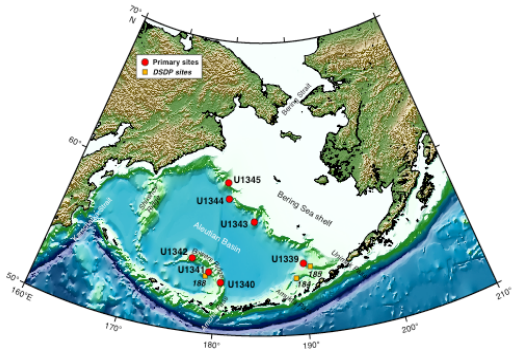

Fig. 1: Map of the Bering Sea region with drill sites of DSDP Leg 19 (orange) and IODP Expedition 323 (red) on the Umnak Plateau, the Bowers Ridge, and along the Bering Sea slope.
.

IODP

Preliminary geochemical and petrological results from Shatsky Rise volcanic rocks, IODP Expedition 324: Shatsky Rise Formation

K. HEYDOLPH[1], R. ALMEEV[2], A.R. GREENE[3], A. ISHIKAWA[4], A.A.P. KOPPERS[5], J.J. MAHONEY[3], M. MIYOSHI[6], J.H. NATLAND[7], K. SHIMIZU[4], M. WIDDOWSON[8] AND IODP EXPEDITION 324 SCIENTIFIC PARTY

[1]Leibniz-Institute of Marine Sciences, IFM-GEOMAR, Wischhofstr.1-3, D-24148, Germany, kheydolph@ifm-geomar.de
[2]Institute of Mineralogy, University of Hannover, Callinstrasse 3, D-30167 Hannover, Germany
[3]Department of Geology and Geophysics, University of Hawaii, 1680 East-West Road, Honolulu HI 96822, USA
[4]Insitute for Research on Earth Evolution (IFREE), Japan Agency of Marine-Earth Sciences and Technology (JAMSTEC), 2-15 Natsushima-Cho, Yokosuka, Kanagawa 237-0061, Japan
[5]College of Oceanic and Atmospheric Sciences, Oregon State University, 104 COAS Admin. Building, Corvallis OR 97331-5503, USA
[6]Beppu Geothermal Research Laboratory, Institute for Geothermal Sciences, Kyoto University, Noguchibaru, Beppu, Oita 874-0903, Japan
[7]Rosenstiel School of Marine and Atmospheric Science, University of Miami, 4600 Rieckenbacker Causeway, Miami FL 33149, USA
[8]Department of Earth and Environmental Sciences, The Open University, Walton Hall, Milton Keynes MK7 6AA, UK

Results from onboard investigations: The submarine Shatsky Rise Plateau is a unique large igneous province (LIP) in the northwest Pacific Ocean ca. 1500 km east of Japan. It is the only large intraoceanic plateau worldwide, which formed during the Late Jurassic to Early Cretaceous. During this time period numerous reversals of the Earth's magnetic field caused alternating magnetic lineation in the ocean floor, which allowed a detailed reconstruction of the original tectonic setting. Accordingly the three main volcanic edifices Tamu, Ori and Shirshov massif formed along a southwest - northeast trending, rapidly spreading triple junction. However, the Shatsky Rise shows characteristics for both a ridge-controlled and a plume head origin. Therefore one main objective of this expedition is to test both hypotheses (plume head versus ridge-controlled) for the plateau genesis.

During expedition 324 five sites have been cored, with one site (U1346) on the summit of Shirshov Massif and two sites on Ori (U1349 and U1350) and on Tamu (U1347 and U1348) respectively. With the exception of site U1348 all sites revealed basaltic lava flows, which occur as packages of pillow basalt and massive inflation units, frequently interbedded with volcaniclastic sediments. The largest massive inflation flows have a maximum thickness ~ 23m and the thickest occur on Tamu Massif, comparable to massive flows cored on Ontong Java Plateau during ODL Leg 192. Massive flows are also found at Sites U1349 and U1350, on Ori Massif summit and flank, respectively, though an entire ~50 m succession of igneous rocks from Site U1346 (Shirshov Massif summit) consists of pillow lavas. Ori Massif flow units are generally thinner than on Tamu Massif, presumably indicating that the average eruptions become smaller and less effusive from Tamu to Ori to Shirshov massifs. Cores from site U1348 contained a thick sequence (~120 m) of highly altered volcaniclastic sediments with shallow-water carbonaceous sandstones on top. The cored basaltic lava flows ranging from relatively fresh (Sites U1347 and U1350) to moderately to highly altered (Sites U1346 and U1349). Additional recovered basement rocks from two summit sites (U1346 and U1349) showed the most severe alteration, whereas rocks from Sites U1347 and U1359 are apparently less affected by fluid flow and temperatures. Preliminary shipboard geochemical data show that the recovered lava flows consist of variably evolved tholeiitic basalts, with Sites U1347 and U1350 samples having similar compositions to basalts from previous ODP Site 1213 on Tamu Massif. In general, their compositions overlap with Ontong Java Plateau samples as well as with mid-ocean-ridge basalts (MORB). Some samples from Site U1350 have Zr/Ti ratios similar to MORB values. This led to the first broad assumption that the source of Shatsky Rise basalts is slightly enriched in incompatible elements compared to MORB, consistent with slightly lower degrees of partial melting and possibly the presence of residual garnet. Alteration-resistant element ratios (e.g. Zr/ Ti) seem to indicate, that the more altered basalts from Sites U1346, U1348 and U1349 are also of tholeiitic composition. Basaltic lava flow samples from Site U1349 appear to represent significantly less differentiated magmas than those from other sites and have similarities to picritic Ontong Java Plateau basalts.

Post-cruise research objectives: Samples collected by two German participants of the Expedition 324 (K. Heydolph, IFM-GEOMAR and R.Almeev, Uni Hannover) will be further investigated in the course of their post-cruise studies. Two new DFG-proposals running in the frame of SPP "IODP" have been recently submitted.

At IFM-GEOMAR we want to generate an integrated high-quality geochemical data set (i.e. Sr-Nd-Pb-Hf isotopes) to further determine the source composition for the Shatsky Rise Plateau. In addition we are going to establish a comprehensive interlaboratory high-quality Ar-Ar geochronology data base to further constrain the southwest-northeast trending age progression as indicated by multiple magnetic lineations on the seafloor. Our combined new absolute age and Sr-Nd-Pb-Hf isotopic composition data will help to determine the origin, temporal and spatial evolution of source compositions and melting conditions. Ultimately the new geochemical data should help to differentiate between classical hotspot plume head and plate fracturing models for the origin of the Shatsky Rise Plateau and oceanic plateaus in general.

At Hannover we would like to focus on the determination of magma storage conditions and to the simulation of magma differentiation processes in Shatsky Rise oceanic plateau. This information will be gained from (1) the study of mineral, glass and melt inclusion compositions, from (2) crystallization experiments and (3) thermodynamic modeling. The Shatsky Rise is also an ideal region to study pristine pre-eruptive volatile abundances in LIP basalts, due to the lack of contamination with continental lithosphere. The quantitative information on volatile budget, composition, oxygen fugacity, and volatile release in Shatsky Rise basaltic magmas will be obtained from a complementary approach combining analysis of natural samples, investigation of phase relationships at controlled oxygen fugacity and volatile activities. This is a prerequisite information to quantify the

degassing of mantle plume derived melts and the possible climatic impact in Earth's history.

Bericht

Stand und Perspektiven des ‚International Year of Planet Earth' (IYPE)

WOLFGANG EDER[1]

[1]Dept. Earth Sciences, Uni München, Luisenstr. 37, 80333 München; w.eder-geo@iaag.geo.uni-muenchen.de

Das "Internationale Jahr des Planeten Erde" (IYPE) war eine gemeinsame Initiative der Internationalen Union der Geowissenschaften, IUGS, und der UNESCO, der UN-Organisation für Bildung, Wissenschaft, Kultur und Kommunikation. Das eigentliche „Jahr" konzentrierte sich auf 2008, wie es im Dezember 2005 die Generalversammlung der Vereinten Nationen beschlossen hatte. Projekte und Veranstaltungen rund um das „IYPE" umfassten jedoch den Zeitraum 2007 bis 2009; einige Vorhaben (national und international) werden als Erbe des IYPE (‚legacy projects of IYPE') über das IYPE „Planet Erde Triennium" hinaus wirken.

Die Trägerorganisation des IYPE, die in den USA eingetragene IYPE-Corporation, und ihr in Trondheim beim norwegischen geologischen Dienst angesiedeltes Sekretariat werden Ende Juni 2010 ihre koordinierende und organisatorische Arbeit einstellen.

Das IYPE hat sich 2009, in der Auslaufphase des „IYPE Trienniums 2007 – 2009", global stabilisiert - zum Jahresende 2009 waren 80 Nationalkomitees aktiv. Die Aktivitäten in Deutschland waren überdurchschnittlich, vor allem dank der Unterstützung durch DFG und BMBF. Diese Aktivitäten und die Zusammenarbeit unter dem Dach der „GeoUnion" wurden international gewürdigt: Anlässlich des „Planet Earth Lisbon Event" (PELE, November 2009) wurde die Beteiligung Deutschlands am IYPE mit einem Sonderpreis bedacht. Insgesamt wurden 17 Länder auf diese Weise ausgezeichnet.

Trotzdem bleibt festzuhalten, dass es nicht einfach war, deutsche Geowissenschaftler in der Breite für das IYPE zu begeistern und zu mobilisieren. Dies ist wohl vor allem eine Folge des außerordentlich erfolgreichen deutschen „Jahres der Geowissenschaften" (2002). Neue, eigens für das IYPE geschaffene Vorhaben gab es nur vereinzelt - selbstkritisch betrachtet blieb das deutsche Engagement am IYPE somit insgesamt unter Deutschlands Möglichkeiten.

Derzeit wird beraten, wie die im IYPE geschaffene globale und multidisziplinäre Zusammenarbeit sinnvoll fortzusetzen ist; vor allem sollen die in vielen Ländern neugeschaffenen Strukturen (Nationalkomitees) genutzt und erhalten werden. Diskutiert werden die Gründung eines „Planet Earth Institute", das sich als Stiftung vornehmlich der Öffentlichkeitsarbeit widmen soll, und die Einrichtung einer „Global Geoscience Initiative", die die globale Erdsystem-Forschung in den nächsten Dekaden besser international ausrichten soll.

Abstracts

IODP

Petrogenesis of oceanic plagiogranites: constraints from partial melting experiments on gabbro in the presence of NaCl-rich H_2O-CO_2 fluids

R. ALMEEV[1], J. KOEPKE[1], S.SILANTIEV[2], N.STRUBE[1]

[1]Institute of Mineralogy, Leibniz University of Hannover
[2]Vernadsky Insitute for Geochemistry and Analytical Chemistry, Moscow

Oceanic plagiogranites (e.g. diorites, tonalites, trondjhemites) are intermediate to felsic plutonic rocks, widely reported in ophiolite complexes and from recently formed oceanic crust. The mechanisms proposed for their genesis include late-stage differentiation of a parental MORB melt and partial melting of gabbroic rocks triggered by water-rich fluids. Recently the last mechanism has received realistic experimental confirmation (Koepke et al., 2004). It was demonstrated that at temperatures in excess of 900 °C and at low pressures (200 MPa) the hydrous partial melting of different typical oceanic gabbros and gabbro-norites can lead to melt compositions close to natural plagiogranites. The key result of these experiments is the requirement of H_2O-bearing fluid phase to produce melts silicic in composition, however the nature of these water-rich fluids (magmatic or seawater-derived) is still under debate (Koepke et al., 2007). There is a number of geological and geochemical observations suggesting the involvement of deep, seawater-derived fluids in anatexis of the lower crust that results in formation of oceanic plagiogranites. These are: (1) close spatial relationships of oceanic plagiogranites and active high-temperature hydrothermal systems (e.g. Mid-Atlantic Ridge (MAR), 12-17°N, (Silantyev et al., 2008)); (2) data on halite-rich fluid inclusions in the MAR gabbro with entrapment temperature exceeding 700°C (Kelley & Delaney, 1987); (3) the presence of high-temperature amphibole with high Cl contents (up to 2 wt%) which are probably seawater-derived (Koepke et al., 2008); (4) geochemical evidence for enrichment in LREE as well as high (compared to the host rocks) $^{87}Sr/^{86}Sr$ characteristics of oceanic plagiogranites (Silantyev et al., 2005); (5) First in-situ analyses of Sr isotopes in those interstitial minerals assumed to be residual phases after a hydrous anatexis event (Koepke et al., 2008).

It is well known that Cl strongly affects the solid/fluid partitioning behaviour of many elements (e.g. LILE, REE, Zn, Cu, Mo, Au, Ag, PGE, U, Th). The addition of Cl to a fluid can noticeably change the phase equilibria and especially the melt composition coexisting with solid phases (Botcharnikov et al., 2007). In addition, it was demonstrated recently that the Na_2O content of melts coexisting with a fluid phase is strongly dependent on the Cl content of the system (granitic composition in equilibrium with HCl-NaCl-KCl-enriched H_2O-bearing fluid; Frank et al., 2002; Simon and Pettke, 2009). However, there is a lack of appropriate experimental information on (1) the role and behaviour of a NaCl-rich fluid during partial melting of gabbro and on (2) the partitioning of major and trace elements between melt, fluid and saline liquid.

The understanding of the role of hydrothermal driven anatexis in the genesis of the felsic rocks in modern oceanic settings may have an important implication to the problem of formation of the early crust on the Earth. It has been shown recently (Rollinson, 2008) that compositions of modern oceanic plagiogranites are reminiscent of the archaen TTG rocks (Condie, 1981). It was suggested for example, that the high Na_2O content and LREE-enrichment of oceanic plagiogranites and some of the archaen tonalites and trondjhemites can be explained by the involvement of the sodium-rich sea-water derived fluids in the processes of partial melting (Rollinson, 2008). Thus, the experimental investigation of deep anatexis within the ocean crust driven by water- and Cl-rich fluids has also the potential to shed light on the formation of the first continental crust in the early Earth history within a period of exclusively basaltic magmatism.

Our project started in 2010 is aimed to perform partial melting experiments in the presence of NaCl-rich H_2O-CO_2 fluids (modelled seawater-derived fluid) at pressure 200 MPa to (1) investigate the specifics of generating SiO_2-rich melts by partial melting of oceanic gabbros and (2) to study the effect of NaCl in the fluid on major and trace element partitioning. In the course of our experimental work it is planned to use core samples of the plagiogranites (trondhjemitic and felsic veins) together with their gabbroic hosts as starting material for the experiments from the site U1309, Expedition 304/305 of the Integrated Ocean Drilling Program (IODP), MAR 30°10.12′N, 42°07.11′W, the central dome of Atlantis Massif. For better comparison we plan to run simultaneously (the same PT-conditions) samples with pure H_2O, pure H_2O-CO_2 fluid and with fluid composed of H_2O, CO_2, and 3.2 wt% NaCl. Depending on the experimental results we may test fluids with higher salinity. The experimental setup and conditions will be chosen so that the products contain large melt pools allowing us to analyze our experimental glasses with respect to trace elements and to constrain the effect of NaCl in the fluid on trace element partitioning. For this purpose additional prerequisite methodological experiments may be required. At last, it is also planned to check qualitatively the role of NaCl-rich hydrous fluid on element partitioning during partial melting by changing the ratio fluid/melt in the experiments.

References:

Botcharnikov, R. E., Holtz, F. & Behrens, H. (2007): Eur J Mineral 19, 671-680.
Condie, K. C. (1981): Archean Greenstone Belts. Amsterdam: Elsevier
Frank, M.R., Candela, P.A., Piccoli, P.M., and Glascock, M.D. (2002): GCA, 66(21), 3719-3732.
Kelley, D. S. & Delaney, J. R. (1987): EPSL, 83, 53-66
Koepke, J., Feig, S. T., Snow, J. & Freise, M. (2004): CMP, 146, 414-432.
Koepke, J., Berndt, J., Feig, S. T. & Holtz, F. (2007): CMP, 153, 67-84.
Koepke, J. et al. (2008): G3, 9, 1-29
Simon, A.C.& Pettke, T. (2009): GCA, 73(2), 438-454.
Silantyev, S. A. et al., (2005): InterRidge News, 14, 1-4.
Silantyev, S. A. et al., (2008): Petrology, 16, 73-100
Simon, A.C.& Pettke, T. (2009): GCA, 73(2), 438-454.
Rollinson, H. (2008): Terra Nova, 20(5), 364-369.

ICDP

Magma Storage Conditions of Indian Batt and Cougar Point Tuff Rhyolites, Yellowstone Hotspot Track – Experimental Simulations at 200 MPa

R. ALMEEV[1], B. NASH[2], F. HOLTZ[1]

[1]Institute of Mineralogy, Leibniz University of Hannover
[2]Department of Geology and Geophysics, University of Utah

Mantle plumes play a crucial role in the Earth's thermal and tectonic evolution. Plumes have long been implicated in the breakup and rifting of continents and plume-derived melts play a significant role in the creation and modification of sub-continental mantle lithosphere. Hotspot volcanism in oceanic lithosphere has been the subject of intense investigations, whereas hotspot volcanism within continental lithosphere has not been studied in the detail because of limited exposures and mainly because of the complex interactions between mantle-derived melts and crustal-derived melts. One example allowing us to gain insights in the complex interrelationship of coupled mantle and crustal igneous processes is the Yellowstone hotspot (YHS) because its activity has not been overprinted by later geologic processes. The hotspot produced first the Columbia River Basalts (17 Ma) and a thermal anomaly migrated eastwards to its current position below Yellowstone volcanic system. Fundamental questions on the existence of a hotspot or alternatively of a thermal anomaly below Yellowstone as well as on the formation of the basalts are still under debate (e.g., Christiansen et al., 2002; Shervais et al., 2005, 2006; Leeman, 2005) but the formation and the source of the considerable volumes of rhyolitic magmas that have been erupted in the last 15 Ma are even more enigmatic (e.g., Nash et al., 2006).

The rhyolitic volcanism related to the YHS has been investigated in a number of studies (see for example two recent special volumes in McCurry et al., 2008 and Morgan et al., 2009 and references therein). The bulk compositions of the YHS rhyolites mimic that of average crust. Pb isotopic data are consistent with an ancient source, whereas Sr and Nd isotopic data preclude direct melting of the Precambrian basement underlying much of the YHS volcanic province (Leeman & Bonnichsen, 2005). YHS rhyolites contain a significant juvenile component – either younger crustal source material (such as Idaho batholith) or inputs of hydrothermally altered SRP basalt or inputs of both. Similarly to the basalts, the isotopic compositions of the rhyolites indicate a change of the lithospheric composition between East and West, which is marked by the transition from accreted oceanic terrains (in the West) to Precambrian basement (in the East).

The rhyolites range from low to high silica, medium to high K_2O and display classical characteristics of A-type granites. The evolutionary trends can be explained by fractionation of plagioclase (Pl), quartz (Qtz), pyroxenes (Cpx and Pig), Fe-Ti-oxides (Mt and Ilm). The particular feature is the anhydrous mineral assemblage, consistent with high temperatures. Using classical geothermometers (compositions of mineral pairs, zircon saturation) a general decrease of temperature with time has been observed. The earliest erupted silicic magmas in the western part of the YHS province (16-17 Ma) were probably extremely hot (up to 1080 °C; Nash & Perkins, 2005) whereas the younger rhyolites in the eastern part (particularly Yellowstone) have lower pre-eruptive temperatures (down to 850 °C) and contain biotite or hornblende (Christiansen & McCurry, 2008), indicating a change of magma storage conditions with time and space. In addition to changing temperatures, other pre-eruptive conditions such as the volatile contents of magmas and the depth of magma chambers may have changed concomitantly. For example, considering that several rhyolitic suites contain Pl, feldspar (Fsp, sanidine) and Qtz, the water contents of the early high temperature rhyolitic magmas are expected to be very low (e.g. Holtz et al., 2001) and should be significantly higher in the low temperature younger hornblende-bearing magmas. However, the exact water content of the melts is still under debate and there is nearly no data on the depth of the main magma chambers. The experimental determination of phase equilibria at high pressure and temperature is one of the methods commonly applied to constrain pre-eruptive conditions and this study reports our attempt to constrain experimentally the magma storage conditions of high temperature rhyolitic magmas belonging to the Bruneau Jarbidge eruptive center (12.5-10.0 Ma old).

An experimental study was carried out to constrain phase relations in Cougar Point Tuff (CPT) and Indian Batt (IB) rhyolites, representatives of explosive and effusive stages of silicic volcanism at Bruneau-Jarbidge eruptive center (Cathey & Nash, 2004), the locus of Yellowstone hotspot between 12.7 and 10.5 Ma. CPT consists of 10 large-volume (> 102-103 km3 each) rhyolitic ash-flow tuffs which are generally crystal poor (5-25%) metaluminous ferroan rhyolites, characterized by anhydrous phenocryst assemblage including Pl, Fsp, Cpx, Pig, Qtz, Mt, Ilm, fayalite (Fa), and accessory zircon (Zir) and apatite (Ap). Previous investigations (e.g. Honjo et al., 1992; Perkins & Nash, 2002) favored relatively high pre-eruptive temperatures (900-1000°C) and low fO_2 (~QFM) and aH_2O for CPT magmas. Recent studies on rhyolitic airfall glasses (Cathey and Nash, 2004) confirm high temperature storage conditions over long periods implying the existence of a dynamically evolving magma reservoir that was chemically and thermally zoned and periodically recharged, leading to successive eruptive units. IB rhyolite is post-CPT lava flow (10-9.5 Ma) which is composed of less silicic, Fe and Ti rich rhyolites, which denote the compositional trend of CPT-magmas as well as all Yellowstone rhyolites.

Crystallization experiments were performed at 200 MPa in CSPV at 800-850°C, and in IHPV at 850-1000°C with run duration varied from 7 to 40 days. The water activity (aH_2O) of the experimental charges was varied by adding a fluid composed of a mixture of H_2O and CO_2. In CSPV the oxygen fugacity was monitored by adding a solid Ni-NiO oxygen buffer, whereas in IHPV all experiments were conducted at intrinsic oxygen conditions, corresponding to NNO+2.6 under H_2O-saturated and to ~QFM at nominally dry conditions. Water concentrations in most of the experimental glasses were determined using infrared spectroscopy (FTIR).

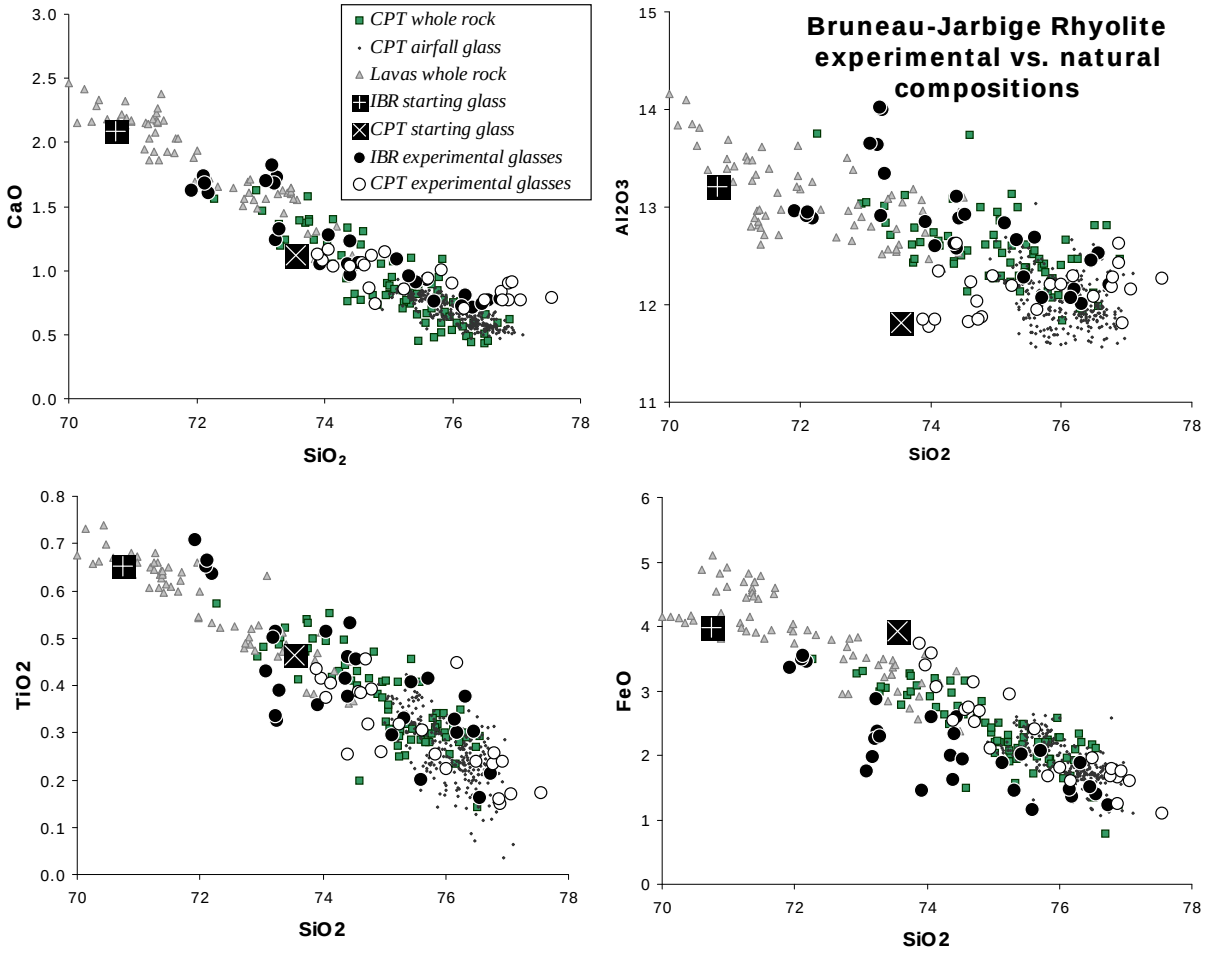

Figure 1. Comparison of natural Cougar Point Tuff (CPT) rhyolitic ignimbrites and lavas with compositions of residual glasses produced in experiments with Indian Batt rhyolite (IBR) and CPT starting compositions. Note that most of the experimental glassses follow the trend defined by natural compositions.

With the CPT starting composition, rhyolitic melt was coexisting with Mt at 1000°C in the whole range of melt H2Om concentrations. With decreasing temperature, Mt was followed by the crystallization of Fsp up to ~ 1 wt % H2Om. In nominally dry run (< 0.5 wt % H2Om) at 950°C and in the runs with H2Om < 1.4 wt % at 900°C Qtz and Pig and Cpx were observed. Fayalite and Pl were stable at temperatures below 900°C and H2Om < 1.5-2.0 wt % in experiments at the lowest fO2 conditions (<QFM in nominally dry runs in CSPV) and were not stable in experiments at fO2 ~ QFM (in IHPV) at similar temperatures. In low temperature runs at reducing conditions (T=850°C, H2Om = 0.3 wt %, H2Om = 1.5 wt %) the three phases Qtz, Pl and Fsp were observed (in addition to mafic phases), indicating that the melt had a eutectic composition.

Using the IB starting composition, the most anhydrous (H2Om < 0.8 wt%) and high temperature (950-1000°C) runs resulted in the crystallization of a Cpx+Pig+Plag+Mt association. From 950°C to 875°C in the H2Om interval of 0.5-1.5 wt%, Fsp and Qtz started to crystallize, whereas Pl and Pig are not observed. We still did not observe coexisting Pl and Fsp, although additional experiments are in progress.

The phase relationships determined experimentally can be used to bracket the conditions of crystallization of natural rhyolitic magmas. The natural mineral assemblage Pl+Fsp+Cpx+Pig+Mt+Qtz±Fa was experimentally reproduced only in the runs with low water concentration in the melt (< 1.5 wt%) and low fO2 (<QFM) at a temperature of 850°C. The coexistence of Cpx and Pig observed in IB rhyolite only at the highest temperatures and lowest H2Om also strengthen the validity of temperature estimates based on Cpx-Pig geothermometer (up to 1050°C). Our experiments indicate that Pl and Fsp only coexist at lower temperatures when compared to the temperature at which Cpx and Pig do coexist. This is also in agreement with the results from two-feldspar and two-pyroxene geothermometry, indicating that the crystallization temperature of feldspars may be lower than that of pyroxenes by ~50°C.

The low water contents and oxygen fugacities required in our experiments to reproduce natural mineral association of the CPT rhyolites are in general agreement with previous ideas on the nearly anhydrous character of the YHS silicic magmatism (Honjo et al., 1992; Perkins & Nash, 2002; Cathey and Nash, 2004). However, from the results at 200 MPa obtained in this study, the temperature at which the full natural mineral assemblage is reproduced (conditions of multiple saturation in CPT rhyolite) can not be higher than 900 °C, contradicting with the relatively

high (950-1000°C) pre-eruptive temperatures obtained as a result of mineral thermometry (e.g. Honjo et al., 1992; Cathey and Nash, 2004). The main problem to reproduce the high temperatures predicted from geothermometry is the absence of plagioclase (in experiments with CPT composition) and Fsp (in experiments with IB composition) in the phase assemblage at the studied experimental conditions, even in nearly dry runs.

There are different possible explanations for the discrepancy between data from geothermometry and from the experimental dataset. It is possible that part of the natural mineral assemblage is not in equilibrium with the magma. In this case plagioclase could be inherited from another source (e.g., low temperature magma tapped during ascent) or the mineral assemblage could result from a mixture of different portions of magmas in a chemically and thermally zoned magmatic reservoir. On the other hand ilmenite which is present in some of the natural rocks has not been reproduced in our experiments, indicating that the experimental conditions may be too oxidizing. A change of the redox conditions may affect the stability of magnetite, which would in turn affect the stability field of clinopyroxene and plagioclase. Preliminary calculations and data obtained for other compositions show that the stability of pigeonite is strongly dependent on oxygen fugacity at low water concentrations.

Our new crystallization experiments support that crystal fractionation is the dominating mechanism responsible for chemical variations in rhyolite from the Bruneau-Jarbidge eruptive center. This is illustrated by the good overlap of natural CPT petrochemical trend (lava flows, ignimbrites, air fall glasses) with experimentally determined liquid lines of descent (see figure 1).

Further objectives: Rhyolites: the conditions at which the Cougar Point Tuff rhyolites have been generated and stored (magma chamber conditions) is a priority in the research program. It appears extremely important to check if the temperature of the rhyolites is as high as postulated in previous studies. The experimental conditions will be varied to check (1) if pressure may play a role (experiments are in progress at 500 MPa, and it is already clear that pressure influences strongly the pyroxene and quartz stability fields), (2) to which extent the oxygen fugacity influences the stability of ferromagnesian phases and of plagioclase and (3) to which extent small compositional changes of the bulk composition may affect the plagioclase stability field. We also plan to use the recently proposed Ti-in-quartz thermometer and try to calibrate it for the investigated compositions.

References:

Cathey & Nash. (2004): The Cougar Point Tuff: Implications for Thermochemical Zonation and Longevity of High-Temperature, Large-Volume Silicic Magmas of the Miocene Yellowstone Hotspot, Journal of Petrology, 45, 27-58.

Christiansen, R. L., Foulger, G. R. & Evans, J. R. (2002). Upper-mantle origin of the Yellowstone hotspot. Geological Society of America Bulletin 114, 1245-1256.

Christiansen, E. and McCurry, M., 2008. Contrasting origins of Cenozoic silicic volcanic rocks from the western Cordillera of the United States. Bulletin of Volcanology, 70(3): 251-267.

Holtz F., Johannes W., Tamic N. & Behrens H. (2001) Maximum and minimum water contents of granitic melts: a reexamination and implications. Lithos 56: 1-14.

Honjo, N., Bonnichsen, B., Leeman, W.P., and Stormer, J.C. (1992) Mineralogy and Geothermometry of High-Temperature Rhyolites from the Central and Western Snake River Plain. Bulletin of Volcanology, 54(3), 220-237.

Leeman, W. P. (2005). Lithospheric vs. asthenospheric contributions to basaltic magmatism in the Snake River Plain - Yellowstone (SRPY) hot-spot track. Geochimica et Cosmochimica Acta 69, A140-A140.

Leeman, W. P. & Bonnichsen, B. (2005). Overview of silicic volcanism of the Snake River Plain - Yellowstone (SRPY) province. Geochimica et Cosmochimica Acta 69, A237-A237.

McCurry M., Christiansen E. H. & Leeman W.P. (ed.) (2008): Petrogenesis and volcanology of anorogenic rhyolites: a special issue dedicated to Bill Bonnichsen. Bul.Volc. 70(3). 247-434

Morgan, L.A., Cathey, H. & Pierce, K.L. (ed.) (2009): The Track of the Yellowstone Hotspot - What do Neotectonics, Climate Indicators, Volcanism, and Petrogenesis Reveal about Subsurface Processes? JVGR. 188 (1-3). 1-304

Nash, B. P. & Perkins, M. E. (2005). The Yellowstone hotspot in space and time: Evidence from silicic volcanism. Geochimica et Cosmochimica Acta 69, A142.

Nash, B.P., Perkins, M.E., Christensen, J.N., Der-Chuen Lee, Halliday, A.N. (2006) The Yellowstone hotspot in space and time: Nd and Hf isotopes in silicic magmas. Earth and Planetary Science Letters 247, 143-156.

Perkins, M.E., and Nash, B.P. (2002) Explosive silicic volcanism of the Yellowstone hotspot: The ash fall tuff record. Geological Society of America Bulletin, 114(3), 367-381.

Shervais, J. W., Kauffman, J. D., Gillerman, V. S., Othberg, K. L., Vetter, S. K., Hobson, V. R., Zarnetske, M., Cooke, M. F., Matthews, S. H. & Hanan, B. B. (2005). Basaltic volcanism of the central and western Snake River Plain: A guide to fi eld relations between Twin Falls and Mountain Home, Idaho. In: Pederson, J. & Dehler, C. M. (eds.) Interior Western United States, 1-26, doi: 10.1130/2005.fl d1006(1102).

Shervais, J. W., Vetter, S. K. & Hanan, B. B. (2006). Layered mafic sill complex beneath the eastern Snake River Plain: Evidence from cyclic geochemical variations in basalt. Geology 34, 365-368.

IODP

Phase relations in oceanic serpentinites as a guide to hydrogen production during seawater-peridotite interactions

W. BACH[1], F. KLEIN[1,2], N. JÖNS[1], M. HENTSCHER[1], T.M. MCCOLLOM[3],

[1]Geoscience Department, University of Bremen, Klagenfurter Str., 28359 Bremen

[2]Now at: Woods Hole Oceanographic Institution, Woods Hole, MA02543, USA

[3]CU Center for Astrobiology & Laboratory for Atmospheric and Space Physics, Campus Box 392, University of Colorado, Boulder CO 80309, USA

In a newly funded grant, the composition and assemblages of secondary minerals will be used as a guide to serpentinization processes. Phase petrology and geochemical reaction path modeling will be used in estimating of gas fugacities, solute activities, temperatures and overall water fluxes of the serpentinization system. The role of the rock composition will be explicitly addressed. In combination, the results are going to provide new insights into the process of serpentinization and its consequences for hydrogen (i.e., food for microbes) production, and petrophysical property evolution during serpentinization. Our work is planned to be an expansion of studies conducted in serpentinites from ODP Leg 209, which provided many new insights into serpentinization processes (funded through DFG-SPP 1144). It is a logical and timely step to take this approach and apply it to many other sites, since petrographic descriptions and petrophysical data indicate that the reaction pathways during serpentinization are incredibly variable.

Despite a renewed interest in serpentinization of the seafloor, the underlying peridotite-water reactions are still poorly constrained. Type and sequence of serpentinization reactions depend on the conditions of water-rock reactions, chiefly temperature and water flux. The relative reaction rates of olivine and pyroxene determine the compositions of interacting fluids, in particular pH and silica activity

(Allen and Seyfried, 2003). Bach et al. (2004) demonstrated that the mineral reactions deduced from the rock record are consistent with theoretical predictions and experimental results. They found evidence in ODP Leg 209 drill cores from the Mid-Atlantic Ridge 15ºN area for peridotite-seawater interactions that took place under a wide rage of temperature, pH, and redox conditions and involved fluids with variable silica activities. It is apparent that apart from the physicochemical conditions of peridotite-seawater reactions, protolith composition, presence of gabbro intrusions, and structural features (e.g., detachment faults, normal fault gauges) contribute to the large diversity in alteration types observed. This diversity of peridotite-seawater reaction products may be common in structurally complex settings, such as oceanic core complexes.

More recently, the role of silica activities and Fe-Mg exchange equilibria in controlling hydrogen production during serpentinization has been highlighted (Sleep et al., 2004; Bach et al., 2006; Frost and Beard, 2007; Evans, 2008; McCollom and Bach, 2009). Understanding the phase relations and their dependence on rock composition, water-to-rock ratios, and temperature is of paramount importance in unraveling the enigma of strongly reduced conditions in serpentinization. Serpentinization causes hydrogen and methane fluxes into the oceans that are an order of magnitude greater than the fluxes associated with magmatic accretion of the oceanic crust. Because hydrogen drives methanogenesis, organosynthesis, and microbial metabolism in serpentinite-hosted hydrothermal systems (Kelley et al., 2005; Proskurowski et al., 2008) and in ultramafic basement rocks (e.g., Alt and Shanks, 1998), a detailed understanding of its production is of interest. These improved insights are also required to understand how the physical properties of serpentinizing lithospheric mantle develops during exhumation and uplift of mantle peridotite.

To date, comprehensive phase petrological studies of seafloor serpentinites and associated rocks are restricted to two areas on the Mid-Atlantic Ridge, specifically Sites 1268-1274 (Bach and Klein, 2009; Jöns et al., 2009; Klein and Bach, 2009; Klein et al., 2009) and 1309 (Frost and Beard, 2007; Frost et al., 2008; Beard et al., 2009). Our studies from Leg 209 indicate that unprecedented details about the reaction sequences during serpentinization may be obtained from merging careful petrographic, magnetic, and spectroscopic analyses with comprehensive thermodynamic modeling. These studies have revealed much new insight, but the phase relations are going to be different in other sites. We need to study many of them in order to develop general ideas and sharpen the predictive power of our petrological models. We therefore plan to investigate serpentinized ultramafic rocks from mid-ocean ridge, rifted continental margin, and convergent margin (fore-arc) settings to provide a detailed account of phase relations, iron distribution and redox state during serpentinization at a range of temperatures. We propose to focus our investigation on mid-ocean ridge settings, rifted continental margins, and fore arc serpentine mud volcanoes. Sites to be investigated include: 779/780 (Conical Seamount), 1200 (South Chamorro Seamount), 897/899/1068/1070 (Iberian Margin), 895 (Hess Deep), and 920 (MARK area). These settings span a wide range in physicochemical conditions of serpentinization, allowing us to make empirical observations and compare them with results of comprehensive water-rock reaction simulations along specific reaction paths.

The specific aims of this project are to use observational data: (i) microchemical variations in relation to serpentinite texture and precursor phase compositions, (ii) opaque mineral phase relations within serpentinized peridotites, (iii) textural data, apparent reaction sequences and zonations, and (iv) magnetic intensity measurements and Mößbauer spectroscopy in order to allow the computations of gas fugacities in the system and the aqueous solute activities in the intergranular fluid. Obvious chemical potential gradients between different lithologies and rock domains can then be identified as driving force for reaction and mass transfer. These observations and phase petrological constraints are merged with results from geochemical reaction path modeling designed to examine the dependencies of fluid-rock reactions on temperature, water-to-rock ratio, and rock composition. Specifically, we plan to

(I) examine the controls of precursor rock composition (dunite, harzburgite, lherzolite, websterite, etc.) on equilibrium phase assemblages

(II) estimate the hydrogen and hydrogen sulfide fugacities of the reactions revealed by petrographic observations using Fe-Ni-Co-O-S phase relations

(III) estimate temperature and water flux during serpentinization and related processes (rodingitization)

(IV) compute chemical co-evolution paths of rock and fluid to further develop and test the most likely reaction sequences

(V) compare the computed fluid chemistries with those of fluids venting from serpentinite-hosted hydrothermal systems on the seafloor to identify the specific mineral-fluid reactions that govern fluid composition

(VI) compute evolution paths of density and magnetic susceptibility of peridotites undergoing serpentinization

These insights will then be used to develop a conceptual model of peridotite-seawater interactions in the oceans. By studying serpentinites from a range of settings and with widely variable compositions and alteration conditions we are going to reveal systematic differences in phase assemblages and mineral compositions, in particular the distribution of iron and its oxidation state in serpentinite. In an iterative approach we will use both empirical observations and thermodynamic modeling to derive the fundamental processes governing serpentinization. Although not the focus of the proposed work, we will use hydrothermal experimental data for groundtruthing thermodynamic calculations and to guide our interpretation of natural rocks. As high hydrogen fugacity is the major driver of methanogenesis and other organic synthesis reactions, our results are going to provide a theoretical foundation of how much of what organic compound may form in peridotite-seawater interactions.

References:

Allen, D.E. and Seyfried, W.E.J., 2003. Compositional controls on vent fluids from ultramafic-hosted hydrothermal systems at mid-ocean ridges: An experimental study at 400ºC, 500 bars. Geochim. Cosmochimi.Acta, 67: 1531-1542.

Alt, J.C. and Shanks, W.C., 1998. Sulfur in serpentinized oceanic peridotites: Serpentinization processes and microbial sulfate reduction. J. Geophys. Res., 103: 9917-9929.

Bach, W., Garrido, C.J., Harvey, J., Paulick, H. and Rosner, M., 2004. Variable seawater-peridotite interactions – First insights from ODP Leg

209, MAR 15ºN. Geochem., Geophys., Geosyst., 5(9): Q09F26, doi: 10.1029/2004GC000744.
Bach, W. and Klein, F., 2009. Petrology of rodingites: Insights from geochemical reaction path modeling. Lithos,112: 103-117.
Bach, W. et al., 2006b. Unraveling the sequence of serpentinization reactions; petrography, mineral chemistry, and petrophysics of serpentinites from MAR 15° N (ODP Leg 209) Geophysical Research Letters, 33(13): L13306, doi:10.1029/2006GL025681.
Beard, J.S., et al., 2009. Onset and Progression of Serpentinization and Magnetite Formation in Olivine-richTroctolite from IODP Hole U1309D. J. Petrol., 50: 387-403.
Evans, B.W., 2008. Control of the Products of Serpentinization by the Fe2+Mg–1 Exchange Potential of Olivine and Orthopyroxene. J. Petrol., 49: 1873-1887.
Frost, B.R. and Beard, J.S., 2007. On silica activity and serpentinization. J. Petrol., 48: 1351-1368.
Frost, B.R., Beard, J.S., McCaig, A. and Condliffe, E., 2008. The Formation of Micro-Rodingites from IODP Hole U1309D: Key to Understanding the Process of Serpentinization. J. Petrol., 49(9): 1579-1588.
Kelley, D.S. et al., 2005. A serpentinite-hosted ecosystem: The Lost City Hydrothermal Field. Science, 307: 1428-1434
Klein, F. and Bach, W., 2009. Fe-Ni-Co-O-S phase relations in peridotite-seawater interactions. J. Petrol., 50: 37-59.
Klein, F., Bach, W., Jöns, N., Berquo, T. and Moskowitz, B (2009). Iron Partitioning and Hydrogen Generation During Serpentinization of Abyssal Peridotites. Geochim. Cosmochim. Acta. 73(22) 6868-6893
McCollom, T.M. and Bach, W., 2009. Thermodynamic constraints on hydrogen generation during serpentinization of ultramafic rocks. Geochim. Cosmochim. Acta, 73: 856-879.
Jöns, N., Bach, W. and Schroeder T., 2009. Formation and alteration of plagiogranites in an ultramafic-hosted detachment fault at the Mid-Atlantic Ridge (ODP Leg 209), Contrib. Mineral. Petrol. 157: 625-639
Proskurowski, G. et al., 2008. Abiogenic Hydrocarbon Production at Lost City Hydrothermal Field. Science, 319: 604-607.
Seyfried, W.E., Jr., Foustoukos, D.I. and Fu, Q., 2007. Redox evolution and mass transfer during serpentinization: An experimental and theoretical study at 200°C, 500 bar with implications for ultramafic-hosted hydrothermal systems at Mid-Ocean Ridges. Geochim. Cosmochim. Acta, 71: 3872- 3886
Sleep, N.H., Meibom, A., Fridiksson, T., Coleman, R.G. and Bird, D.K., 2004. H_2-rich fluids from serpentinization: geochemical and biotic implications. Proc. Natl. Acad. Sci., 104: 12818-12823.

ICDP

Colorado Plateau Coring Project (CPCP): 100 Million Years of Climatic, Tectonic, and Biotic Evolution in Continental Cores

G.H. BACHMANN[1], M. SZURLIES[2], P.E. OLSEN[3], D.V. KENT[4], J.W. GEISSMAN[5], R. MUNDIL[6], G.E. GEHRELS[7], R.B. IRMIS[8], R. BLAKEY[9], W.M. KÜRSCHNER[10], J. SHA[11], R. MOLINA-GARZA[12]

[1]Institut für Geowissenschaften, Martin-Luther-Universität Halle-Wittenberg, 06120 Halle (Saale), gerhard.bachmann@geo.uni-halle.de
[2]Institut für Erd- und Umweltwissenschaften, Universität Potsdam, 14476 Potsdam, michael.szurlies@geo.uni-potsdam.de
[3]Lamont-Doherty Earth Observatory, Columbia University, Palisades, NY, USA
[4]Department of Earth and Planetary Sciences, Rutgers University, Piscataway, NJ, USA
[5]Department of Earth and Planetary Sciences, University of New Mexico, Albuquerque, NM, USA
[6]Berkeley Geochronology Center, Berkeley, CA, USA
[7]Department of Geosciences, University of Arizona, Tucson, AZ, USA
[8]Museum of Paleontology, University of California, CA, USA
[9]Department of Geology, Northern Arizona University, Flagstaff, AZ, USA
[10]Department o Biology, Universiteit Utrecht, NL
[11]Chinese Academy of Sciences, Nanjing, CHN
[12]Universidad Nacional Autónoma de México, Querétaro, MEX

Goals: To recover continuous Triassic and Jurassic reference sections of one of the most data-rich epicontinental basins worldwide with the goal of understanding the links between major events in the history of life, climate change, and Earth System crises in the Early Mesozoic. Major foci will include the two major and two minor mass extinction events, the ascent of the dinosaurs, and the origin of modern biota, because the Colorado Plateau and environs have produced some of the richest fossil assemblages in the world spanning these events.

Place 100 million years of biotic, climatic, tectonic evolution of western equatorial to temperate Pangea into a precise and globally relevant chronostratigraphic and paleogeographic context.

Outcrops: Visually superb, but large parts inaccessible, covered, very weathered! Major lithostratigraphic, biostratigraphic, chronostratigraphic problems!

Drilling areas and concept: Three long (~1 km) and two shorter cores in clear stratigraphic superposition

Expected outcomes: High resolution magnetostratigraphic & chemostratigraphic reference sections - age-calibrated by high-precision U-Pb zircon dates from several discrete levels in Triassic strata - for regional and global chronostratigraphic correlations

Rates and magnitudes of transition from the Paleozoic to essentially modern terrestrial ecosystems

Biotic, climatic, and tectonic connections between Colorado Plateau and rifting of Pangea, emplacement of the CAMP, opening of the Atlantic Ocean, and other large igneous provinces (Karoo-Ferrar, Siberian traps) and other major Earth System events

Interplay between basin stratigraphy, accommodation space, uplift, and eustasy?

Climate trends vs. plate position changes in “hot house” Pangaea

Comparison of paleoclimate record against other parts of the World for tests of climate models

Response of depositional environments to cyclical climate changes; e.g., fluvial vs. eolian

Lithostratigraphic, biostratigraphic and sequence stratigraphic correlations, ages and extents of regional unconformities and possible relationship to eustatic fluctuations

1st Workshop: November, 14-16, 2007, St. George, UT, USA, 45 international researchers – outline CPCP concept

2nd Workshop: May, 8-11, 2009, Albuquerque, NM, USA, 40 international researchers – to form international science team and plan

Full Proposals to NSF and ICDP: April, 2009, July 2009 (Phase 1), January 2010, February 2010. – five years total duration, estimated ~5 M USD.

Results as of February 2010: Phase 1, ~500 m Petrified Forest Core was favorably reviewed and NSF (Sedimentary Geology & Paleobiology) intends to fund (~1.2 M USD for science only); preliminary proposal for full project was positively reviewed and recommended for full proposal development. Start date and specific budget to be determined.

IODP

Superfast sedimentation and submarine slides, Gulf of Mexico continental slope: insights into transport processes from fabrics and geotechnical data

J.H. BEHRMANN[1], S. MEISSL[2]

[1] MARINE GEODYNAMICS, LEIBNIZ-INSTITUT FÜR MEERESWISSENSCHAFTEN, IFM-GEOMAR, 24148 KIEL, GERMANY (JBEHRMANN@IFM-GEOMAR.DE)

The Gulf of Mexico continental slope seaward of the Missisippi Delta is the site of extremely fast (up to 2.5 cm/year) sedimentation in the last 60000 vears, building thick sequences of underconsolidated muds and clays. These are severely overpressured (e.g. Flemings et al., 2008), and, where located on the gently inclined continental slope, are subject to frequent submarine sliding, creating mass transport deposits (MTD). In the Ursa Basin, a region of extensive offshore hydrocarbon production, IODP drilling (Flemings, Behrmann, John et al., 2006, Behrmann, Flemings, John et al., 2006) has shown that major sliding events occur about every 5000 years, moving up to about 30 cubic kilometers of sediment.

When unconsolidated or poorly consolidated sedimentary rock masses are moved in the form of slumps, debris flows or mud flows there are variable degrees of clay realignment by remolding and shearing. Especially the clay fabric seems to influence the geotechnical properties. It is thought that during mobilization the sediments become fluidized through temporary fabric collapse (in the case of sensitive clays), or by grains becoming buoyant during the ingress of externally derived fluids. In fossil sediments there is some documentation that weak grain preferred orientations, and thus a higher degree of consolidation does form during slumping near the ocean floor, and is retained in the later diagenetic history. Although overprinting of these fabrics by further compaction of sediments is likely, the effects of submarine mass transport are expected to leave a lasting imprint on the sediment fabrics and textures, and will, in principle, result in different geotechnical properties.

Here we document that submarine mass transport in the Ursa Basin is made possible by extremely low coefficients of friction and shear strengths of the sediments, in combination with the prevailing high pore pressures. MTD formation strongly modified the sediment fabric and pore space, strengthened the material overall, and left a distinctive imprint on the AMS (Anisotropy of Magnetic Susceptibility) fabric.

Specimens from Sites U1322 and U1324 were tested in consolidated undrained (CU) triaxial experiments and ring shear experiments. Peak shear strenghts are broadly similar to those obtained from the simple shipboard penetrometer tests (Fig. 1). Friction coefficients are in the range of 0.13 to 0.31, with internal angles of friction of approximately 7.4° to 17.2° in ring shear experiments. At intermediate (7.624 MPa) to high (15.237 MPa) overburden pressures the majority of the samples tested shows velocity weakening, whereas lower overburden pressures do not give a clear trend regarding velocity weakening or strengthening of the samples. In CU triaxial tests, peak shear stresses observed are between 27 and 140 kPa. One sample coming from close to the base of a MTD at Site U1322 is the weakest one tested, with a cohesion of only about 30-40 kPa, at a borehole depth of over 220 m. This leaves the possibility for reactivation of slide surfaces at this depth, and thus mobilization of very voluminous slides at extremely low shear stresses.

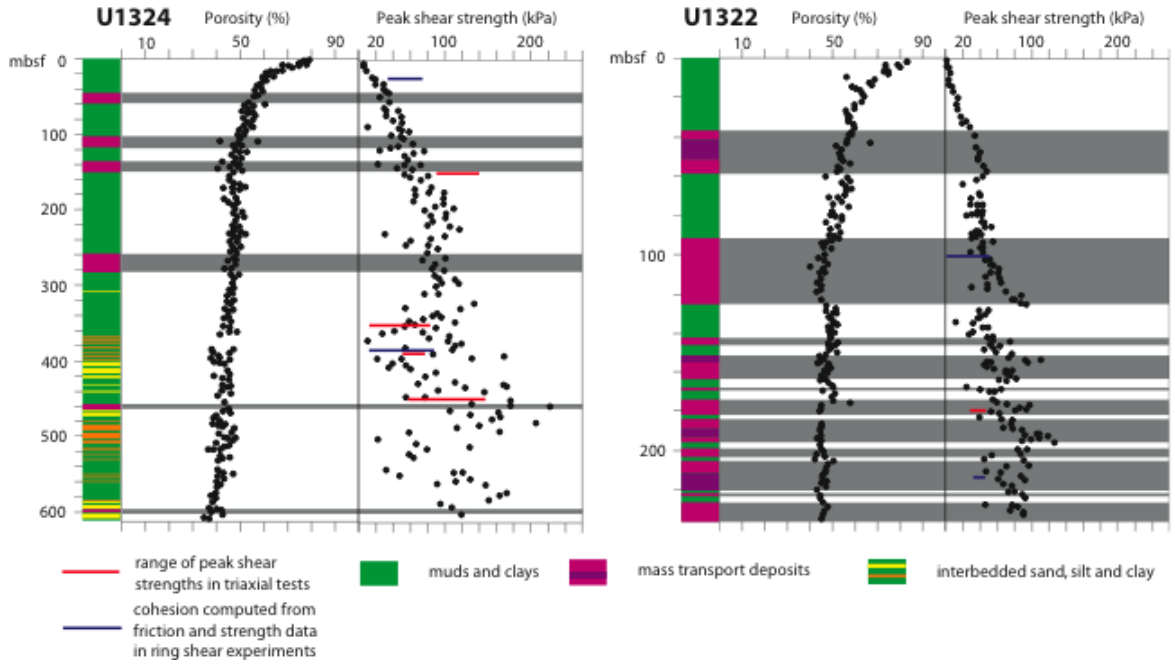

Fig. 1: Logs from IODP Sites U1322 and U1324, Ursa Basin, showing sediment type, porosity, and shear strength data (penetrometer, ring shear and triaxial tests). See text for discussion.

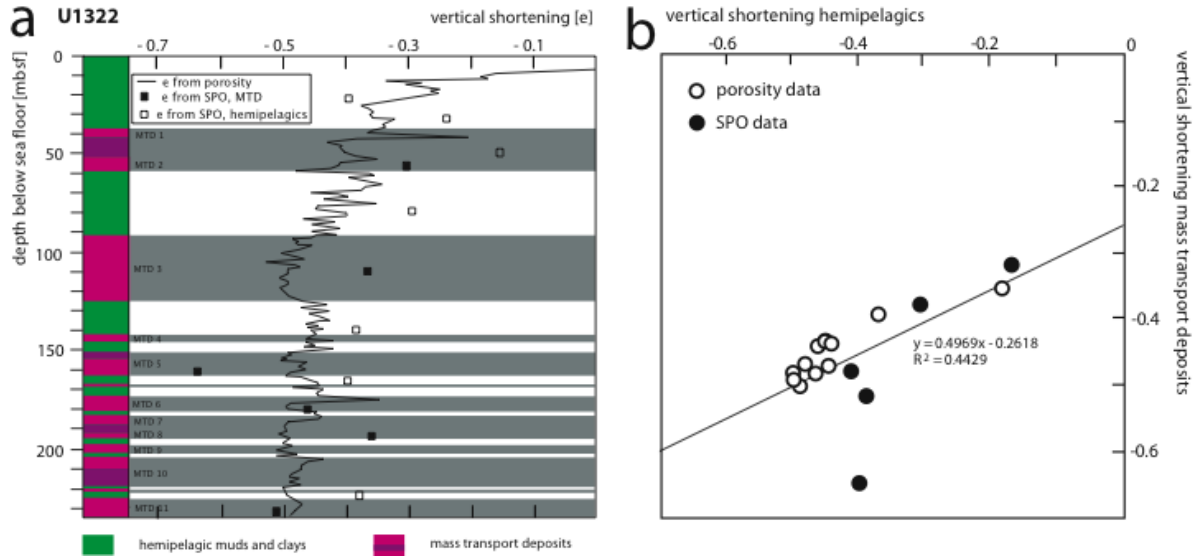

Fig. 2: Deformation data, Site U1322. a) Shortening from porosity and SPO data. B) shortening in MTD plotted against shortening in overlying layer of hemipelagic sediments. See text.

Vertical shortening in the sediments can be calculated from porosity data, and from the intensity of shape preferred orientation (SPO) of clay-sized particles. In the example of IODP Site U1322 (Fig. 2) it can be seen that vertical shortening (elongation = e) from porosity loss (initial porosity was taken to be the average porosity recorded in the uppermost ten meters of sediment) is in broad agreement with vertical shortening values obtained from SPO, using the March model for strain induced fabrics (Fig 2a). At maximum borehole depth, almost 50% of the initial sediment volume is lost by compaction, with the average compaction of MTD being distinctly larger than that of the overlying layers of hemipelagics. This is best seen when observing the graph showing e from porosity at the upper boundaries of MTD 5, 6, 7 and 10 (Fig. 2a).

When average shortening values from MTD and the immediately overlying layer of hemipelagic sediments are plotted against each other (Fig. 2b) it is evident that the two values are related by a slope with a slope less than one. The deviation of the slope from from the 45° angle then depicts the amount of shortening added by the mass transport process. In the case of the uppermost pair of hemipelagics this discrepancy is between 14 and 16 percent, indicating that the submarine sliding is capable of inducing at least this amount of volume loss by additional compaction in the MTD during transport. Deeper in the drillhole, the discrepancy becomes smaller, an effect to be expected, as the couples of hemipelagics and MTD are subjected to a common diagenetic history after deposition and – in the case of MTD – sliding.

Measurements of anisotropies of magnetic susceptibility (AMS) were performed on a very extensive set of samples from Site U1322. Work was carried out at RCOM, Bremen with a Geofyzika Brno KLY_2 Kappa Bridge and the ANISOFT 20 software package. We used standard p-mag samples. Because of very high magnetisation (Franke, pers. comm., 2007) standard volumes had to be reduced by about 25% to carry out the tests. Every sample was measured in 15 orientations to determine the magnetic vectors $K_{max,}$ K_{int} and K_{min}. We represent the results in standard Flinn Diagrams and P/T plots of the magnetic shape factor (Jelinek's shape factor; see examples in Figs 3b and 3c).

The results show that the intensity of the AMS fabric varies methodically between the sediment sections produced by suspension fallout (the hemipelagic sections; white in the Log seen in Fig. 3a), and those sections affected by sliding (geay MTD sections in Fig. 3a) In the hemipelagics values for Kmax and Kint do not differ very much, pointing to a generally oblate fabric shape. This is to be expected in normally sedimented clay-rich sediment. In contrast, the sediments affected by mass transport processes, show triaxial ellipsoid shapes, and a generally higher difference between Kmax and Kmin. Transitions are very sharp, and coincide with the boundaries of the two types of deposit. Our interpretation of the data seen in Fig. 3a is that weak, oblate magnetic fabrics in the sediments were severely overprinted and modified during the sliding process in MTD bodies, so that the fabric building process can be seen as a superpostion of the effects vertical uniaxial shortening, and shearing during the MTD event. The difference in the AMS fabric shape is clearly shown in the P/T and Flinn plots in Fig. 3b for the example of MTD 3 and the subjacent package of hemipelagic sediments. MTD-related fabric building must have occurred during the transport process and not afterwards, as the subjacent sediments were not affected.

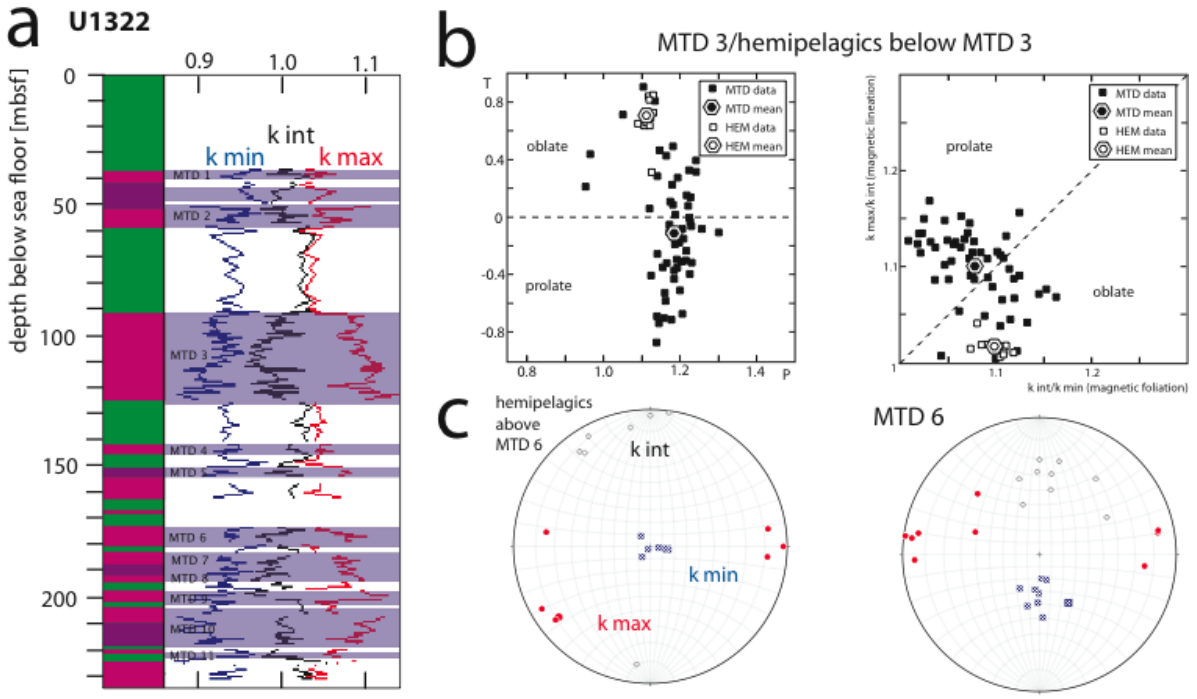

Fig. 3: Anisotropies of magnetic susceptibility (AMS) in muds and mudstones from Site U1322. a) Downhole variations of the kong (kmax) intermediate (kint) and short (kmin) axes of the AMS ellipsoid. b) P/T-diagram (left) and Flinn plot (right) showing the differences in the shapes of AMS ellipsoids for MTD 3 and in the layer of hemipelagic sediments overlying MTD 3. c) Orientations of the three principal axes of the AMS ellipsoid in samples from MTD 6 (right) and the layer of hemipelagic sediments overlying MTD 6 (left). Equal angle, lower hemisphere projections. See text.

A very important aspect of fabric building is discovered when the principal magnetic fabric axes are reoriented with repect to geographic coordinates. This is seen for the example of MTD 6 and the overlying hemipelagic sediments (Fig. 3c). In both packets K_{max} is oriented east-west, depicting the downslope suspension transport off Mars ridge to the west (see Flemings, Behrmann, John et al., 2006, for the regional geological context of Ursa Basin). Clear differences exist, however, in the orientations of the K_{int} and K_{min} axes (Fig. 3c). In the hemipelagics K_{min} is vertical, reflecting the orientation of the uniaxial shortening axis. In the the MTD the K_{min} axial orientation is tilted 10°-40° against the north-south direction of MTD transport. This reflects the position of incremental shortening axis of simple shear strain that the MTD undergoes during transport.

In summary, the most important conclusions to be drawn from our work are:

Submarine sliding leaves a strong and irreversible imprint on the sediment: it changes magnetic and shape fabric intensities and geometries, and partly destructs the pore space. This is clearly a transport phenomenon, which leads to expulsion of large amounts of pore fluids during the sliding event. This may be as much as 150-200 liters of pore water per cubic meter of sediment. All this means that MTD transport is “en masse”, probably as a cohesive body akin to an avalanche of wet snow on land. Resulting from this it can be stated that the geohazard potential of such slides is considerable.

The young sediments in the Ursa Basin are extremely weak, and show very low friction angles. While bases of some MTDs seem to experience strengthening by the sliding, the sediments below the bases remain weak, and slides are thus susceptible to reactivation, including the possibility to form multi-stage, stacked slide deposits. Very minor changes in pore pressures may lead to renewed or reactivated sliding anytime.

References

Behrmann, J.H., Flemings, P.B., John, C.M., and the Expedition 308 Scientists, 2006. Rapid sedimentation, overpressure and focused fluid flow, Gulf of Mexico continental margin. – Scientific Drilling, 3, 12-17. doi:10.2204/iodp.sd.3.03.2006

Flemings, P.B., Behrmann, J.H., John, C.M., and the Expedition 308 Scientists, 2006. Proc. IODP, 308: College Station TX (Integrated Ocean Drilling Program Management International, Inc.).doi:10.2204/iodp.proc.308.101.2006.http://iodp.tamu.edu/publications/exp308/308title.htm

Flemings, P.B., Long, H., Dugan, B., Germaine, J., John, C., Behrmann, J.H., Sawyer, D. and IODP Expedition 308 Scientists, 2008. Pore pressure penetrometers document high overpressure near the seafloor where multiple landslides have occurred on the continental slope offshore Louisiana, Gulf of Mexico (Vol 269, pg 309, 2008). Earth and Planetary Science Letters, 274, 269-283.

ICDP

SYNCO-Log: A synthetic log to identify density-driven convection in deep boreholes

S. BERTHOLD, F. BÖRNER

DGFZ Dresdner Grundwasserforschungszentrum e.V., Meraner Str. 10, 01217 Dresden, Germany

Boreholes locally distort the natural flow field and open up an additional possibility of vertical heat and mass transfer between rock formations (e.g. aquifers), surrounding, and atmosphere. A variety of processes can cause heat and mass input or exchange through the fluid column (Fig. 1). Density-driven convection (also called free convection or natural convection) plays an important role among them (Börner and Berthold, 2009).

Density-driven convective flows have adulterating effects on fluid samples and in-situ measurements in boreholes. Gases and other substances are possibly transported into new depths where varying chemical processes may arise. Consequently, knowing about the existence of vertical density-driven flows in fluid columns is crucial for hydrological investigations and for borehole geophysics. Moreover, temperatures in fluid columns and in the proximate formation may depart significantly from the ones in the surrounding rock when affected by vertical convection (Berthold and Börner, 2008). Thus, understanding convective flow within the borehole is also important for subsurface water movement investigations and geothermics.

So far, no particular logging device or interpretation algorithm was available that could detect free convection in deep boreholes. The SYNCO-Log approaches the problem. The general objective of the research presented here, is the development of an interpretation method for the detection and differentiation of various types of vertical mass and heat transport processes in the fluid column of the deep boreholes of the International Continental Drilling Program (ICDP). Outcome of the interpretation method is a so-called Synthetic Convection Log (SYNCO-Log).

The foundations were laid in a project which dealt with the investigation of free vertical convection in groundwater monitoring wells and its quantification according to its data adulterating effect (Berthold and Börner, 2008). These investigations of convective processes included numerical simulations, medium scale experiments, and field tests (borehole measurements). Additionally, two computational algorithms were developed for detecting and quantifying vertical flows in the water column. Fundamental elements have been already tested in numerous shallow boreholes (< 400 m). The occurrence of density-driven convective transport processes could be proven in many monitoring wells and shallow boreholes under normal conditions, as the critical threshold for the onset of a density-driven flow is considerably low.

Within the scope of the new research project, the borehole log interpretation method is adapted to deep boreholes. The difficulty is to obtain a similar good result of interpretation using available data from deep ICDP boreholes. The characteristic properties of these borehole logs include e.g. higher speed while lowering the probe, larger sampling interval, and higher viscosity of the fluid (mud). Additionally to the differences related to the measurement technique, some of the deep boreholes are characterized by very distinct temperature gradients.

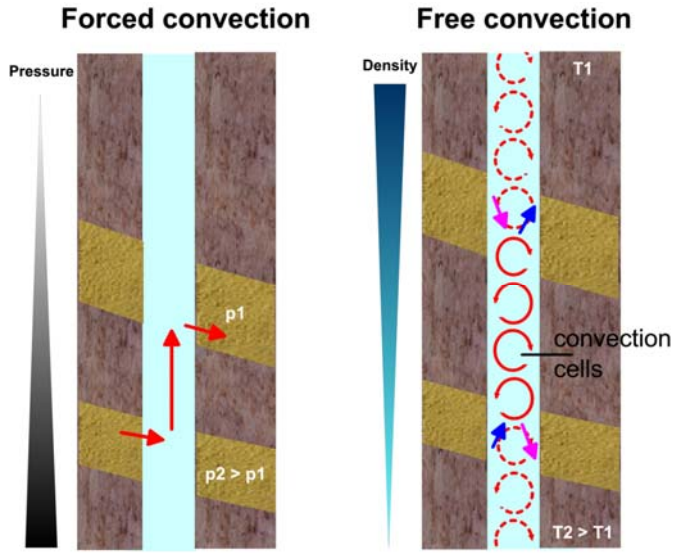

Fig. 1: Vertical convection in boreholes: forced convection due to a pressure gradient (left) and free, density-driven convection due to a temperature gradient (right).

With the kind permission of several principal investigators (PIs), numerous data from different borehole locations could be acquired. In addition to the available data, simultaneous temperature and fluid conductivity measurements were conducted in the KTB main hole. The KTB-borehole and the infrastructure of the KTB-field laboratory were provided by the Helmholtz Centre Potsdam GFZ German Research Centre for Geosciences. The measurements themselves were realized with equipment of the DGFZ Dresdner Grundwasserforschungszentrum e.V in October 2008. Measurements were realized using a low downhole logging velocity (2 m/min) and a high sampling interval (1cm). Such high-resolved temperature and mud resistivity measurements were conducted for the first time, as regards the KTB main hole.

Meanwhile, the interpretation algorithm was successively adapted on the special drill and measurement technique related parameters and the geothermal conditions of the deep ICDP boreholes. The adaptation includes: input unit selection, identification of measurement parameters from the input data, filtering according to measurement precision, implementation of an additional density formula for saline fluids, and automatic choice of the relevant density formula (Fig. 2).

The SYNCO-Log combines two approaches realized in two independently working algorithms. With one algorithm the causes (driving forces) and with the other one the effects (forced, free convection or double diffusion) of vertical transport processes can be detected. The combination of both algorithms considerably improves the reliability of the interpretation. The Synthetic Convection Log, that way, enables in-situ detection and even identification of free convective, including double-diffusive, flows using state-of-the-art geophysical borehole measurements like temperature and water conductivity/mud resistivity logs. In the sense of a quick look interpretation, the SYNCO-Log visually divides the fluid column into sections that are characterized by density-driven flow and sections that are characterized by no density-driven convective flow. Additionally, it classifies the sections with density-driven flow according to its flow type.

Before applying the SYNCO-Log to the obtained borehole logs, the available data were ascertained in detail. Their categorization was the first step towards an adaptation of the interpretation algorithm. The logs were evaluated according to the prevailing conditions during the measurements. Not always are simultaneous temperature and mud resistivity logs available. In these cases, interpretation is limited and assumptions on the missing parameters have to be made. Sparse sampling or especially high logging velocities in many cases required the implementation of an elaborated filtering.

The applicability of the SYNCO-Log and relevance of the results is presented in Figure 3 based on results from the KTB main hole (KTB-MH). Maximum depth for the October 2008 measurement was 525 m below surface due to equipment-related limitations (cable length). Analysis of the results concerning density-driven vertical flows revealed that at measurement time the entire investigated fluid column of the KTB-MH was subject to free convective flow. The existence of revolving flows was confirmed by both interpretation algorithms: cause- and effect-oriented interpretation.

According to the Synthetic Convection Log, the main part of the fluid column is influenced by thermosolutal convection. That means temperature as well as salinity gradients have a destabilizing effect resulting in a distinct, intensive flow. Based on the analysis it can be assumed that a constant upward directed heat flow and a constant downward directed salt flow exist in the investigated part of the fluid column. To what extent the heat flow induced in the borehole affects, for example, the determination of reliable heat flow densities of the surrounding rock formation remains to be clarified. However, this is beyond the scope of the project.

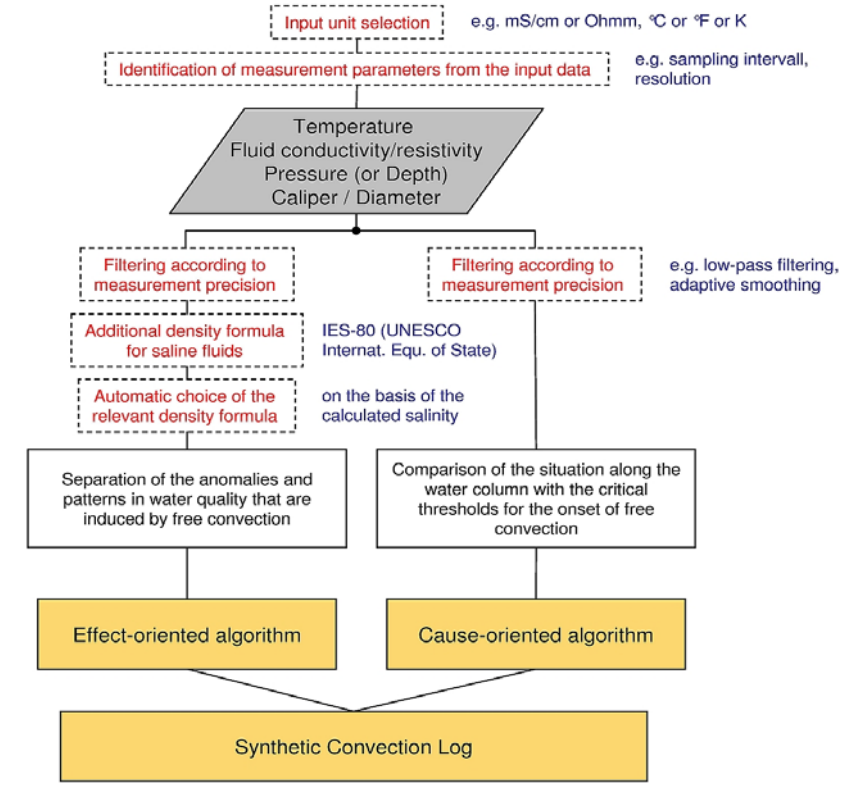

Fig. 2: The Synthetic Convection Log (SYNCO-Log) adaptated to deep boreholes of the ICDP

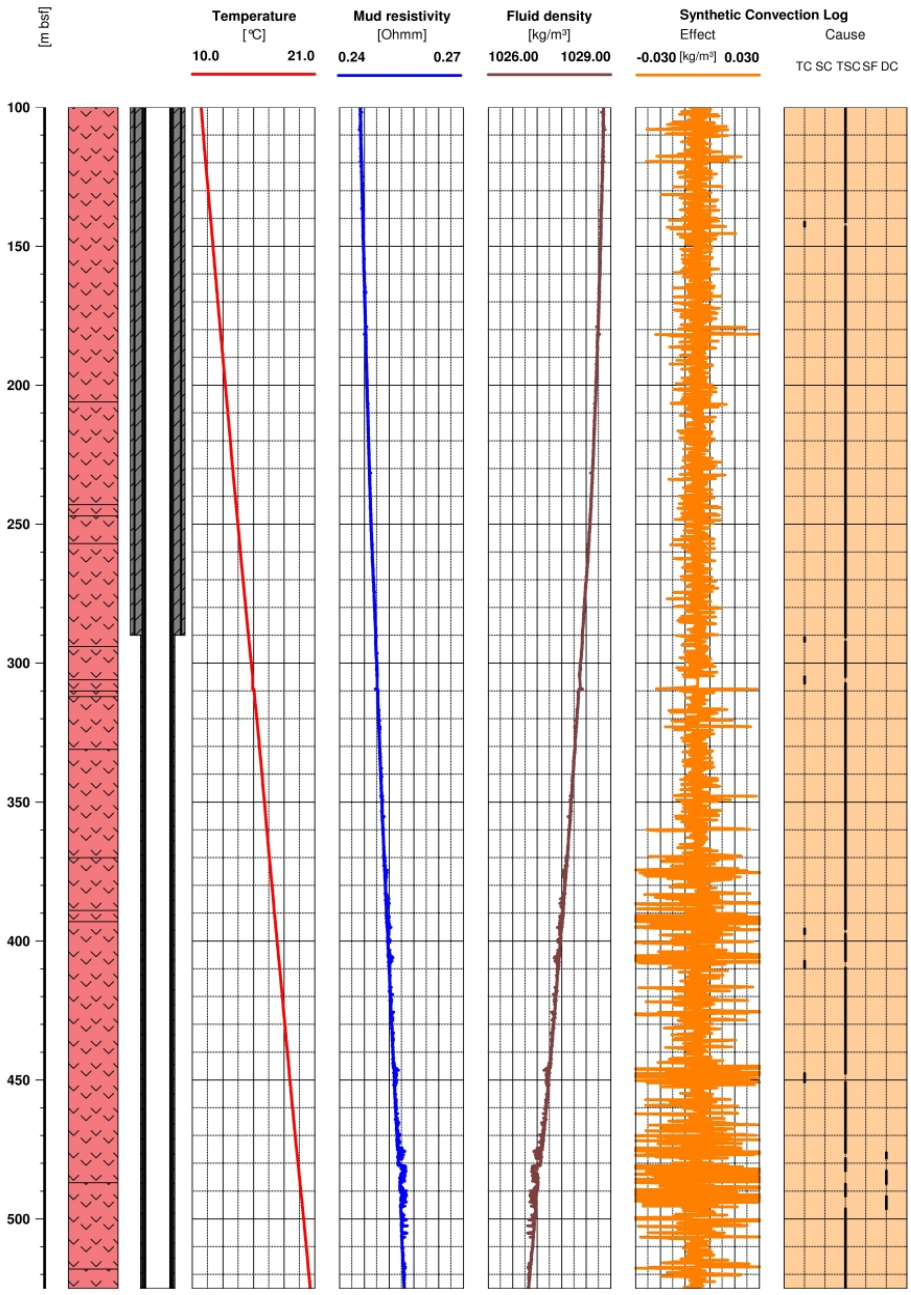

Fig. 3: KTB main hole measurement results along with the new SYNCO-Log

The research is funded by the German Research Foundation (DFG) under the label BO 1082/10-1 within the priority program 1006 “International Continental Drilling Program (ICDP)”.

References:

Berthold S., Börner F. (2008): Detection of free vertical convection and double-diffusion in groundwater monitoring wells with geophysical borehole measurements, Environmental Geology 54(7), S. 1547-1566.

Börner F., Berthold S. (2009): Vertical flows in groundwater monitoring wells, In: Kirsch, R. (ed.), Groundwater Geophysics – A Tool for Hydrogeology, 2nd ed., Springer-Verlag, Berlin, Heidelberg, S. 367-389.

IODP

Calcium and strontium isotopes in low temperature alteration carbonates of the ocean crust

F. BÖHM[1], A. EISENHAUER[1], S. RAUSCH[2], W. BACH[2], A. KLÜGEL[2]

[1] IFM-GEOMAR, Kiel, Germany
[2] Geoscience Department, University of Bremen, Germany

During low temperature alteration (LTA) $CaCO_3$ precipitates in veins and vesicles of the ocean crust [1]. We analyzed Sr/Ca, Mg/Ca, $\delta^{18}O$, $\delta^{13}C$, $^{87}Sr/^{86}Sr$, and $\delta^{44/40}Ca$ of $CaCO_3$ from basement samples of DSDP and ODP drill cores from the Atlantic and Pacific Oceans. The 87Sr/86Sr ratios point to seawater as the major source for Sr in most Cenozoic samples. This interpretation is corroborated by

low d18O temperatures (0-5°C), close to bottom water values, and by normal marine $\delta^{13}C$ values. In contrast, samples of Cretaceous and Jurassic age show up to 65% of basement derived calcium and $\delta^{18}O$ temperatures between 15 and 50°C.

Calcium isotope values (d44/40Ca) range from -0.7 ‰ to 1.8 ‰ (SRM 915a). In accord with previous studies [2,3] d44/40Ca differs between aragonite (-0.2 to +0.3 ‰) and calcite (0.9 to 1.8 ‰). A negative correlation of $\delta^{44/40}Ca$ and Sr/Ca ratios is explained by precipitation rates varying between <10-2 to 102 µmol/m2/h [4]. The calcites with the highest $\delta^{44/40}Ca$ and lowest Sr/Ca values probably formed close to isotopic equilibrium [5]. The $\delta^{44/40}Ca$ of LTA calcites (1.6 ‰ for Cenozoic sites) is very high compared to biogenic carbonates (0.6 ‰ for modern biogenic carbonates [5]). Thus LTA carbonates represent a sink for heavy Ca isotopes, both with respect to the land-ocean calcium cycle and to the crust-mantle Ca exchange.

References:
[1] Alt J.C., Teagle D.A.H. (1999) Geochim. Cosmochim. Acta., 63, 1527-1535.
[2] Amini M., et al. (2008) Geochim. Cosmochim. Acta, 72, 4107-4122.
[3] Gussone N., et al. (2005) Geochim. Cosmochim. Acta, 69, 4485-4494.
[4] Tang J., et al. (2008) Geochim. Cosmochim. Acta, 72, 3733-3745.
[5] Fantle, M.S., DePaolo, D.J. (2007) Geochim. Cosmochim. Acta, 71, 2524-2546.

IODP

Fabric and Micro-fabric of ODP Leg 204 gas hydrates, Cascadia margin

G. BOHRMANN[1], S. A. KLAPP[1], W.F. KUHS[2]

[1]Fachbereich Geowissenschaften der Univeristät Bremen, Klagenfurterstr., D-28359 Bremen
[2]Geowissenschaftliches Zentrum der Universität Göttingen, Goldschmidtstr.1, D-37077 Göttingen

Ocean Drilling Program (ODP) Leg 204 to Hydrate Ridge, located on the continental slope offshore Oregon (USA), was the first drilling expedition dedicated to understanding gas hydrate processes in accretionary complexes and provided a test-bed for a number of different techniques for estimating the gas hydrate content of sediments. Gas hydrate estimates based on a variety of geophysical and geochemical techniques indicate a heterogeneous distribution of gas hydrate, which results in part because of different regimes for delivery of gas to the gas hydrate stability zone. In the "normal regime," which is pervasive throughout the study region, the average gas hydrate content of the sediments is relatively low (2%–8% of the pore space), no gas hydrate is present in the upper ~30 mbsf because the methane content of the pore water is below saturation, and the fine-scale distribution of gas hydrate depends strongly on lithology.

Superimposed on the normal regime is a "transport-dominated regime" in which gas is focused into a stratigraphically controlled conduit and is transported as free gas to the structural summit. At the summit, high gas pressure drives free gas into and through the gas hydrate stability zone, resulting in a shallow deposit in which gas hydrate comprises ~25% of the total sediment volume to a depth of ~25 mbsf. Geochemical data indicate that most of the gas that forms the summit deposit has migrated from greater depth and has either a thermogenic or altered biogenic character, and modeling suggests that abundant free gas is needed to form gas hydrate in these conditions.

From six ODP 204 drill sites we investigated a total of 65 frozen whole-round samples using X-ray computerized tomographic (CT) imaging. Although most of the whole-round samples stored in liquid nitrogen showed widespread decomposition of gas hydrate, the original presence of gas hydrate in the sediment cores was indicated by low-density anomalies. In many cases the gas hydrate itself was no longer present and had been replaced by a distinctive fabric that reflects the frozen state of a soupy sediment full of bubbles. Detailed fabric analyses of the samples showed that the hydrates had been present in layers with a variety of dips. Shallow hydrate layers parallel or subparallel to bedding are interpreted to result from gas bubble injections parallel to the layering of sedimentary deposits. Deeper than 40 mbsf, hydrate layers are characterized by steeper dip angles of 30°–90° and are interpreted as precipitates in open fractures or joints, consistent with a model in which free gas migrates through the sediments by opening cracks, which close as gas hydrate is precipitated. At Hydrate Ridge the approximate sediment depth at which the force of gas hydrate crystallization cannot overcome the overburden stress is approximately 25 mbsf. Accordingly, in the deeper sediments gas hydrates form only along surfaces of cracks and fractures and have distinctly different fabrics than the shallower hydrates.

Preliminary investigations of ODP Leg 204 hydrates revealed the crystallite sizes of natural gas hydrates for the first time. The crystallite sizes revealed that the crystallites were in the range of 300 µm to 600 µm. So far, five different samples of the ODP 204 drillings were investigated; however, a tendency seems to exist that larger crystallites exist at greater depths. Smaller crystallites instead were found at shallower depths not only at Hydrate Ridge but also at other places, e.g. in shallow hydrate deposits in the Black Sea.

IODP

Studying the change of petrophysical properties with depth of sedimentary rock layers at New Jersey Shallow Shelf (USA) and Wilkes Land margin (Antarctica)

F.P. BOSCH[1], A. FEHR[1], R. PECHNIG[2], C. CLAUSER[1]

[1]Applied Geophysics and Geothermal Energy, E.ON Energy Research Center, RWTH Aachen University, Mathieustr. 6, D-52074 Aachen
[2]Geophysica Beratungsgesellschaft mbH, Lütticher Str. 32, D-52064 Aachen

The main objective of this study is to analyse the change of petrophysical properties as thermal conductivity and its controlling factors porosity and permeability of sedimentation areas with depth. Data and rock samples from IODP expeditions no. 313 "New Jersey Shallow Shelf" and no. 318 "Wilkes Land Glacial History" of certain prominent sediment layers at different depths will be used. The changes of these parameters control fluid and heat transport properties and consequently environment properties of the investigated sedimentation zones.

Lab measurements of thermal conductivity, electrical resistivity and nuclear magnetic resonance (NMR) on rock samples from both expeditions will be performed. Lab data will be intergrated with down hole logging and multi scanner core logging measurements. In order to re-create in-situ conditions of the rock samples according to the depth taken from, the samples will be compacted by a centrifuge prior to measurements. Further compaction will simulate the conditions at even greater depths.

Results from this experiments will be used to simulate the temperature history of these two sedimentation areas at different depths and to develop concepts for the sedimentological classification of rocks from downhole logging data.

IODP

Improvement of methods for the quantification of microorganismns in oligotrophic carbonate rich marine sediments of North Pond

A. BREUKER, A. SCHIPPERS

Bundesanstalt für Geowissenschaften und Rohstoffe (BGR), Stilleweg 2, 30655 Hannover

The microbiology of the oligotrophic, carbonate rich sediments of North Pond located on the cold western flank of the middle Atlantic ridge is subject of this study. The abundance and distribution of microorganismns are of interest to study life in oligotrophic sediments which cover the major part of the ocean floor but have been little addressed in deep biopshere studies so far. Here we present our first results for North Pond sediments which were sampled during the IODP site survey cruise R/V Maria S. Merian 11/1 in February/March 2009. The application of published protocols for total cell counts and real-time PCR quantification (qPCR) of Bacteria and Archaea resulted in a high variability and a low reliability of the data. Thus the established protocols had to be modified for these carbonate rich sediments by an additional treatment with inorganic acids. For validation of the improved protocols sterilized sediment samples were spiked with different cell numbers of pure cultures and the percentage of recovered cells was calculated for each protocol and sample. Results are shown in Figure 1. Concerning qPCR, a high cell recovery was achieved using the protocol by Webster et al. (2003) with a preceeding washing step with 0.1 mM HCl or HI for extraction of prokaryotic DNA. Concerning total cell counts, a good cell recovery could be achieved with an additional washing step with 0.1 mM HCl for the protocols described by Weinbauer et al. (1998) and Kallmeyer et al. (2008). For the latter protocol a further improvement was achievd by omission of the carbonate step which allowed a reproducible and reliable total cell counting especially for samples with very low cell numbers. Overall, our first North Pond data for four sediment sites indicate low cell numbers with a dominance of Archaea over Bacteria with an average difference of two orders of magnitude. Depths profiles of cell numbers for several sites will be shown.

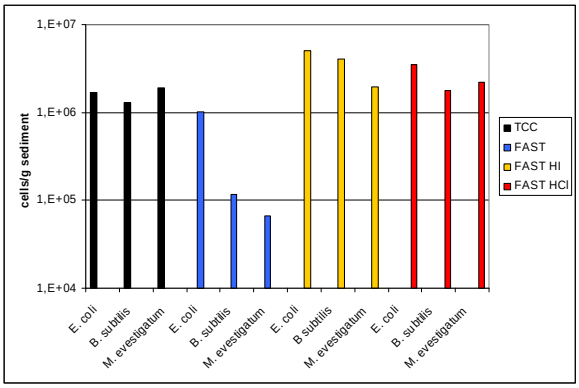

Figure 1a. Validation of the improved protocols for cell number determination in North Pond sediments by qPCR analysis. Sterilzed sediments were spiked with known cell numbers of pure cultures and afterwards analyzed by qPCR after extraction of DNA with FAST PREP KIT after Webster et al. (2003) with additional modifications. TCC: Total cell number of the spiked sediments, determined by SYBR Green direct counting; FAST: Cell numbers with extraction of DNA after Webster et al. (2003) without additional modifications. FAST HI or FAST HCl: Cell numbers after extraction of DNA with FAST PREP KIT after Webster et al. (2003) with an additional washing step with 0.1 mM HI or HCl respectively. The 16S rRNA gene copy numbers per cell used for calculation of cell numbers were: Escherichia coli: 5, Bacillus subtilis: 10, Methanohalobium evestigatum: 1.5.

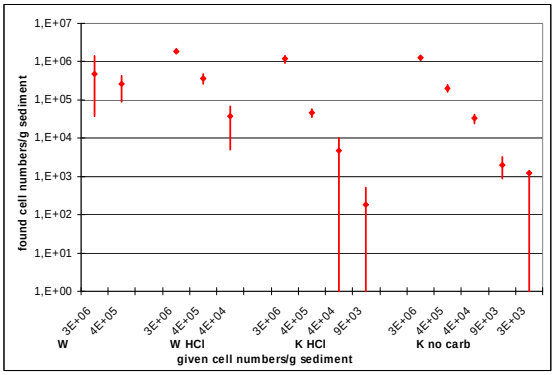

Figure 1b. Validation of the improved protocols for cell number determination in North Pond sediments by SYBR Green direct counting. Sterilized sediments were spiked with known cell numbers of pure cultures and afterwards analyzed by different methods. W: Method by Weinbauer et al. (1998); W HCl: Method by Weinbauer et al. (1998) with an additional washing step with HCl; K HCl: Method by Kallmeyer et al. (2008) with an additional washing step with HCl; K no carb: Method by Kallmeyer et al. (2008) without carbonate dissolution step. Dots indicate mean cell numbers of triplicate determinations, bars indicate standard deviation.

References:

Kallmeyer, J., D.C. Smith, A.J. Spivack, and S. D'Hondt. 2008. New cell extraction procedure applied to deep subsurface sediments. Limnol. Oceanogr. Methods 6: 236–245.

Webster, G., C.J. Newberry, J. Fry, and A.J. Weightman. 2003. Assessment of bacterial community structure in the deep sub-seafloor biosphere by 16S rDNA-based techniques: a cautionary tale. J. Microbiol. Meth. 55: 155-164.

Weinbauer, M.G., C. Beckmann, and M.G. Höfle. 1998. Utility of green fluorescent nucleic acid dyes and aluminum oxide membrane filters for rapid epifluorescence enumeration of soil and sediment bacteria. Appl. Environ. Microbiol. 64: 5000-5003.

ICDP

From method development to climate reconstruction - $\delta^{18}O$ analysis of biogenic silica from Lake El'gygytgyn, NE Siberia

B. CHAPLIGIN[1], H. MEYER[1], H. FRIEDRICHSEN[2], A. MARENT[3], H.-W. HUBBERTEN[1]

[1]Alfred Wegener Institute for Polar and Marine Research, Research Unit Potsdam, Telegrafenberg A43, D-14473 Potsdam, Germany
[2]MS-Analysentechnik, Aßmannshauser Str.12, D-14197 Berlin, Germany
[3]Technische Universität Berlin, Hardenbergstr. 36, D-10623 Berlin, Germany

Abstract: Especially in climate-sensitive areas such as the Arctic, longer drilling records for paleo-climate reconstructions are rare (BRIGHAM-GRETTE et al., 2007). Therefore, in 2003, a 16.50 m sediment core was drilled at Lake El'gygytgyn (Lake E), NE Russia (dating back to app. 340 ka) in an area of the Northern Hemisphere which has not been glaciated at least during the last five glacial/interglacial cycles. In regions of high latitude, where carbonates are absent, the oxygen isotope composition from lacustrine biogenic silica, i. e. diatoms, is the best proxy for reconstructing past climate changes such as air temperatures as well as the isotope composition of precipitation (LENG and MARSHALL, 2004). In this study, the preparation of the samples as well as the contamination assessment had to be revised due to the pecularity (only small diatoms < 10 µm available) of the material. In addition, a new approach for the dehydration/dehydroxylation process and for a high performance (fast, precise) oxygen isotope analysis was developed. The reliability of the method has been verified by analysing quartz and biogenic standards with a standard deviation < 0.2 ‰. Preliminary results of 50 samples from Lake E show variations in $\delta^{18}O$ that reflect glacial-interglacial cycles throughout the whole core , ranging between $\delta^{18}O$ = 18.6 ‰ and $\delta^{18}O$ = 23.0 ‰. This is the first proxy record from an Arctic lake sediment core dating back more than 300 ka directly responding to paleo-precipitation changes.

Method development: For the analysis of $\delta^{18}O$ Si very pure (>97 %) diatom samples are needed. Former studies included different purification techniques (MORLEY et al., 2004; RINGS et al., 2004; SHEMESH et al., 1995). However every sediment core has to be treated individually according the specific material involved (LENG et al., 2009). Various preparation steps treatment have been performed in order to gain a most clean diatom sample from the original sediment: (1) drying, (2) H_2O_2/HCl treatment, (3) wet sieving, (4-7) heavy liquid separation and (8) $HClO_4/HNO_3$ treatment. For the Lake E record the <10 µm fraction had to be selected as only this fraction contained enough purified sample material (>3 mg) throughout the whole core.

The degree of purity was verified under light microscope and by Energy Dispersive X-ray Spectroscopy (EDS) under the Scanning Electron Microscope (SEM) as any contamination can significantly change the $\delta^{18}O$ values (BREWER et al., 2008). The percentage of contamination was surveyed for all preparation steps 1-8 in Lake samples. Figure 1 shows the change in SiO_2 [%] after each step analysed by EDS. The dried, uncleaned sample contains app. 70 % SiO2. The SiO_2 content increases throughout the purification process to a percentage of > 96 % (which was our target value). Out of 115 samples, app. 90% show a final content of SiO_2 > 96 % and Al_2O_3 < 3 % (Al_2O_3 being an indicator for clay minerals).

Amorphous silica contains OH groups within the SiO2 skeleton as well as chemically-combined water. The OH

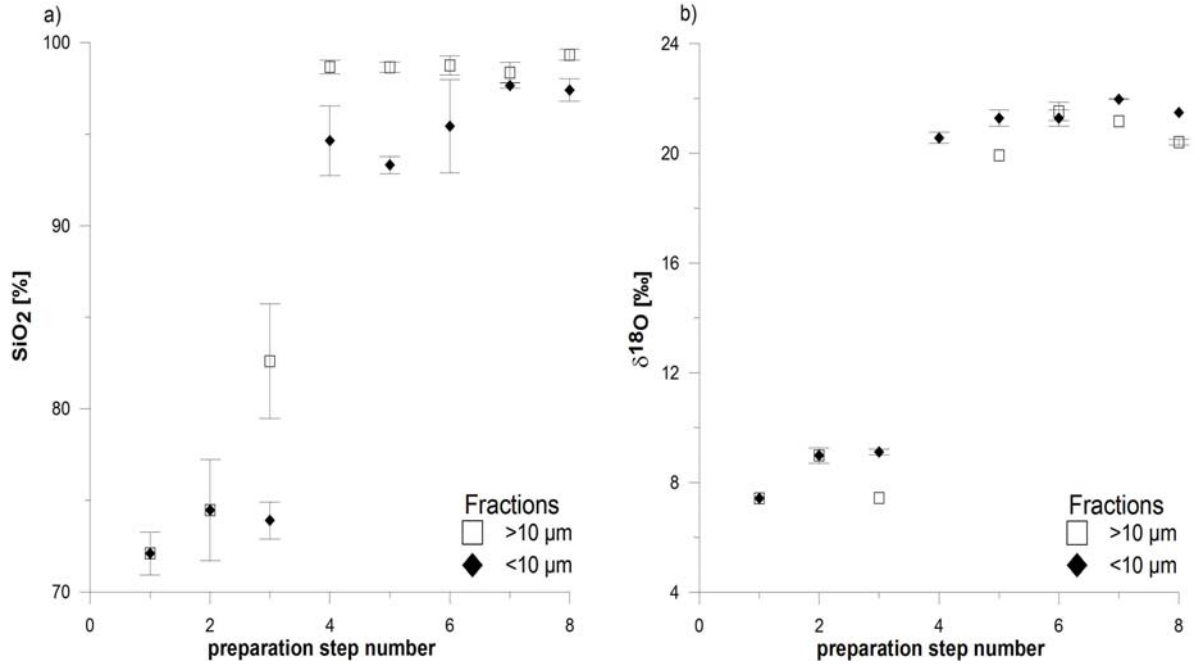

Fig. 1: The development of the SiO_2 content (a) and the isotopic composition (b) throughout the different purification stages was assessed. Both fractions (>10 µm, <10 µm) show a final purity degree of >97 %, the last four purification steps are only essential for the <10 µm fraction. The δ18O values reach a plateau after the 5th purification step. The final acid cleaning with $HClO_4/HNO_3$ slightly lowers the values.

groups and chemically-combined water have to be removed prior to isotope analysis as their oxygen is easily exchanged and,thus, may not reflect the original isotopic composition of the water. Various methods have been established in the past 20 years for the dehydration and dehydroxylation of amorphous silica (Alexandre et al., 2006; Labeyrie and Juillet, 1982; Lücke et al., 2005; Schmidt et al., 1997; Sharp, 1990), including Controlled Isotopic Exchange (CIE) followed by fluorination, Stepwise Fluorination (SWF) and inductive High-Temperature carbon reduction (iHTR).

Here, we present a new method we called Helium Flow Dehydration (HFD) which removes the "hydrous layer" by exposing the sample to an increased temperature (maximum 1100°C) within app. 7h in an oven with a continuous Helium stream leading away all exchangeable oxygen (Fig. 2).

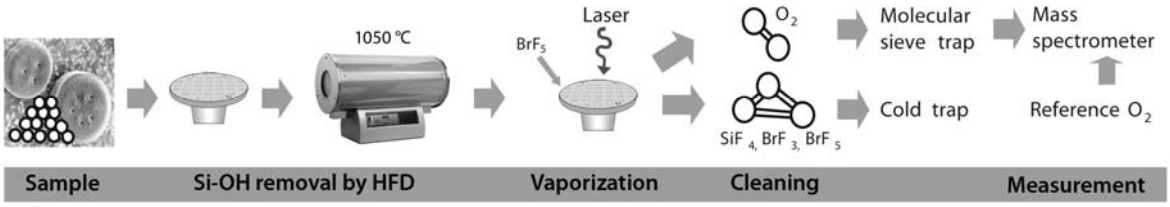

Fig. 2: The sample was heated at 1100°C under a He flow to remove the Si-OH layer by Helium Flow Dehydration (HFD). Through the use of a CO2 laser, the sample is vaporized and under BrF5, the O2 is released and the non-oxygen gas is trapped in a cryogenic trap. The oxygen is transported to the molecular sieve and then transferred to the mass spectrometer for isotope measurement.

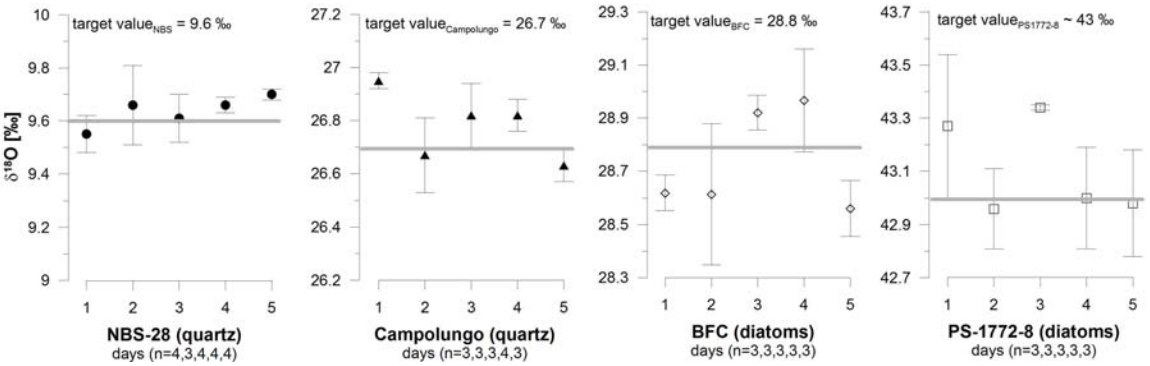

Fig. 3: Verification of the method with quartz (filled symbols) and pure diatom standards (open symbols). The target values originate from IAEA (NBS-28), University of Bonn (Campolungo) and the National Environment Research Council (UK, BFC and PS1772-8). The daily standard deviation is <0.2‰ apart from BFC (2) and PS1772-8 (1). The reproducibility between the days is similar: NBS-28 (Avg: 9.64 ‰; SD:0.09 ‰; n=19), Campolungo (26.78 ‰; 0.14‰; 16), BFC (28.73‰; 0.22‰; 15) and PS1772-8 (43.11‰, 0.11‰; 15).

The isotope analysis was performed with a PDZ-Europa 2020 mass spectrometer. The oxygen was liberated from the sample by laser-fluorination under BrF5 atmosphere. The whole procedure is shown in Figure 2. Specially designed software and a video camera were used to survey and record the process in the reaction chamber and allowed a quick, half-automated, remote operation. This guaranteed maximum safety as the mass spec was installed in a different room than the reagent (BrF5), the reaction chamber, and the laser unit arranged under a hood. The fluorination periphery is directly coupled to the mass spectrometer, making an online analysis possible. In addition, a direct comparison of oxygen was enabled omitting the intermediate step of reacting oxygen to CO or CO2. Tests on standard material (Quartz: NBS 28, Campolungo, biogenic silica: BFC, PS1772-8) showed a standard deviation <0.2 ‰ (Fig. 3).

Core analysis: In 2003, a 16.50 m sediment core (Lz-1024) was drilled at Lake El'gygytgyn, NE Siberia which dates back to app. 340 ka. Preliminary studies have shown that mainly two diatom species are present in the lake: Cyclotella ocellata which occurs throughout the whole core and Pliocaenicus costatus mainly existing in the Holocene (CHERAPANOVA et al., 2007). In total, 115 samples were purified and the contamination was assessed according to the developed procedures described above. As Pliocaenicus costatus is of a size >10 µm, the purified samples <10 µm almost exclusively consist of a single species (Cyclotella ocellata). This is important as there are still a few discrepancies regarding the existence of species-dependent isotope fractionation in diatoms (BRANDRISS et al., 1998; MOSCHEN et al., 2005; SCHMIDT et al., 2001; SCHMIDT et al., 1997).

By now, around 50 different samples were measured (N=2-4) with a special emphasis on the time periods between 0-30 ka BP (resolution ~ 1k) and 100-170 ka BP (resolution ~ 3 k). The mean standard deviation between the repetitions was $1\sigma < 0.3$ ‰. The downcore variations of $\delta^{18}O$ show that glacial-interglacial cycles are present throughout the whole core (Figure 4) including the Holocene Thermal Maximum (HTM; $\delta^{18}O = 21.5$ ‰), the Last Glacial Maximum (LGM; $\delta^{18}O = 18.6$ ‰) and the Eemian interglacial period (δ18O = 23.0 ‰) By the time of the conference, more samples will be analysed and presented for the first time.

Conclusions: A fast and precise approach was developed to analyse the oxygen isotope composition of biogenic silica: up to 15 samples per day can be analysed with a SD < 0.2 ‰. Novelties include a remote and half-automated analysis by new software development, a safe approach by installing the instrument in two different rooms and a new method to remove the "hydrous layer" by heating the sample at 1100°C in a Helium flow (Helium Flow Dehydration). All different applied methods are part of an on-going inter-laboratory comparison of eight laboratories coordinated by AWI.

The first 50 samples from the 16.50 m sediment core (dating back to app. 340 ka) drilled at Lake El'gygytgyn (NE Russia) were analysed and show variations of the $\delta^{18}O$ values that reflect glacial-interglacial cycles. The Holocene Thermal Maximum, the Last Glacial Maximum as well as

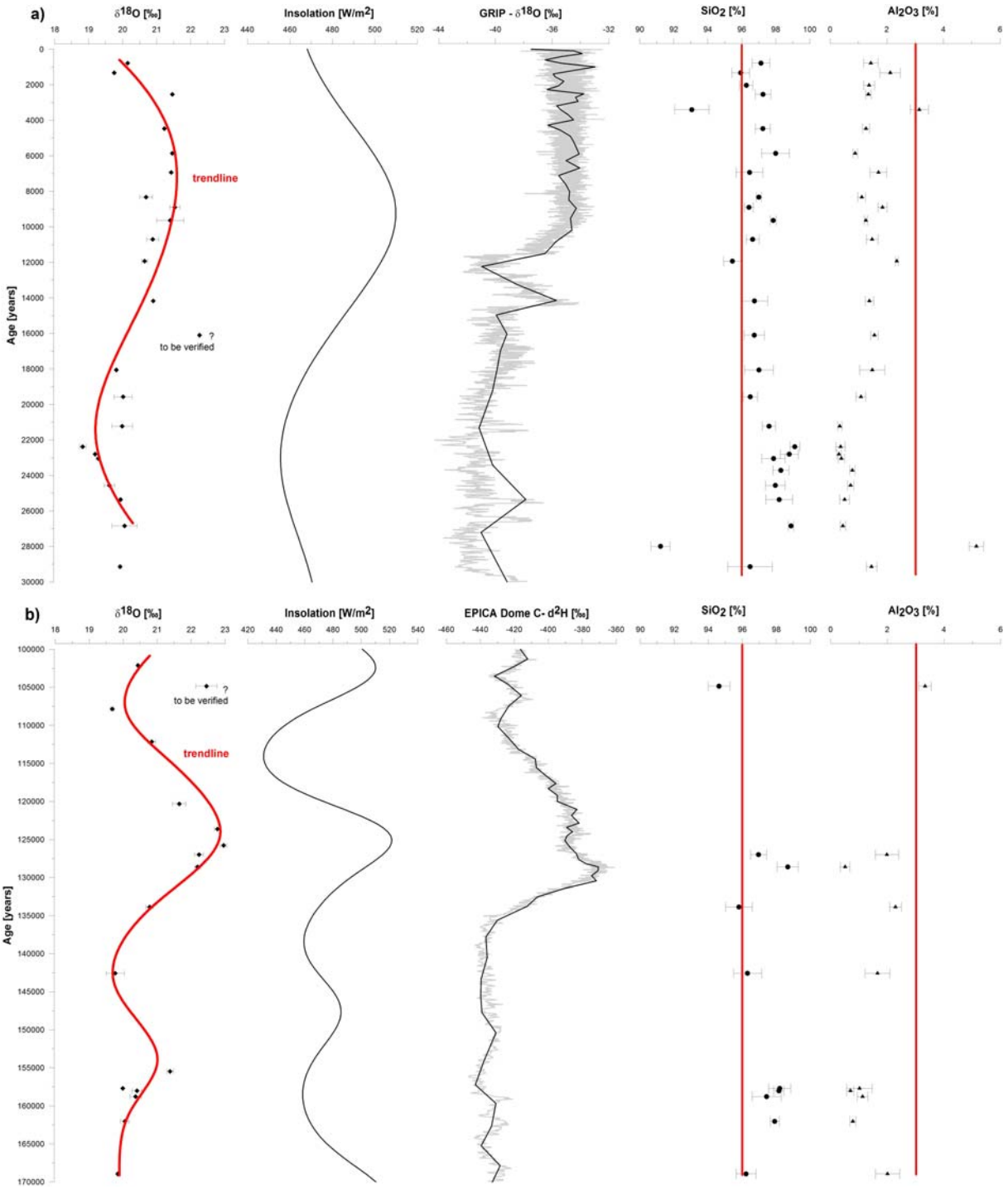

Fig. 4: Preliminary $\delta^{18}O$ results from time intervals 0-30ka (a) and 100-170 ka (b). The trendline clearly shows climate- related isotope variations e.g. HTM and LGM (both in a) and further downcore an isotope maximum during the Eemian interglacial (b). The local insolation and ice core data from GRIP ($\delta^{18}O$ for 0-30ka) as well as EPICA Dome-C (dD for 100-170ka) were plotted for comparison (grey: all data, black: spline smoothing to 50 points). The EDS results from the contamination assessment of the purified samples show SiO_2 percentages of mostly >96 % and Al_2O_3 <3 %. No corrections are applied to the isotope data so far, as not all samples have yet been analysed for both, EDS and $\delta^{18}O$.

the Eemian interglacial and the interglacial period corresponding to MIS 7 are clearly visible. Further analyses will increase the resolution, close the gaps between the time intervals analysed up to now and allow a better interpretation of the paleo-climate variations. This work can be expanded to the long lake sediment core (dating back to about 3.6 Ma), which was drilled within the ICDP program at Lake El'gygytgyn in early 2009.

References:

Alexandre, A., Basile-Doelsch, I., Sonzogni, C., Sylvestre, F., Parron, C., Meunier, J.-D., and Colin, F., 2006. Oxygen isotope analyses of fine silica grains using laser-extraction technique: Comparison with oxygen isotope data obtained from ion microprobe analyses and application to quartzite and silcrete cement investigation. Geochimica et Cosmochimica Acta 70, 2827-2835.

Brandriss, M. E., O'Neil, J. R., Edlund, M. B., and Stoermer, E. F., 1998. Oxygen isotope fractionation between diatomaceous silica and water. Geochimica et Cosmochimica Acta 62, 1119-1125.

Brewer, T. S., Leng, M. J., Mackay, A. W., Lamb, A. L., Tyler, J. J., and Marsh, N. G., 2008. Unravelling contamination signals in biogenic silica oxygen isotope composition; the role of major and trace element geochemistry. JQS. Journal of Quaternary Science 23, 321-330.

Brigham-Grette, J., Melles, M., Minyuk, P. S., and Party, S., 2007. Overview and significance of a 250 ka paleoclimate record from El'gygytgyn Crater Lake, NE Russia. Journal of Paleolimnology 37, 1-16.

Cherapanova, M. V., Snyder, J. A., and Brigham-Grette, J., 2007. Diatom stratigraphy of the last 250 ka at Lake El'gygytgyn, northeast Siberia. Journal of Paleolimnology 37, 155-162.

Labeyrie, L. D. and Juillet, A., 1982. Oxygen isotopic exchangeability of diatom valve silica; interpretation and consequences for paleoclimatic studies. Geochimica et Cosmochimica Acta 46, 967-975.

Leng, M., Swann, G. E. A., M.J., H., Tyler, J. J., Patwardhan, S. W., and Sloane, H. J., 2009. The Potential use of Silicon Isotope Composition of Biogenic Silica as a Proxy for Environmental Change. Silicon 1, 65–77.

Leng, M. J. and Marshall, J. D., 2004. Palaeoclimate interpretation of stable isotope data from lake sediment archives. Quaternary Science Reviews 23, 811-831.

Lücke, A., Moschen, R., and Schleser, G. H., 2005. High-temperature carbon reduction of silica: A novel approach for oxygen isotope analysis of biogenic opal. Geochimica et Cosmochimica Acta 69, 1423-1433.

Morley, D. W., Leng, M. J., Mackay, A. W., Sloane, H. J., Rioual, P., and Battarbee, R. W., 2004. Cleaning of lake sediment samples for diatom oxygen isotope analysis. Journal of Paleolimnology 31, 391-401.

Moschen, R., Lücke, A., and Schleser, G. H., 2005. Sensitivity of biogenic silica oxygen isotopes to changes in surface water temperature and palaeoclimatology. Geophysical Research Letters 32, 4pp.

Rings, A., Lücke, A., and Schleser, G. H., 2004. A new method for the quantitative separation of diatom frustules from lake sediments. Limnol. Oceanogr.: Methods 2, 25-34.

Schmidt, M., Botz, R., Rickert, D., Bohrmann, G., Hall, S. R., and Mann, S., 2001. Oxygen isotopes of marine diatoms and relations to opal-A maturation. Geochimica et Cosmochimica Acta 65, 201-211.

Schmidt, M., Botz, R., Stoffers, P., Anders, T., and Bohrmann, G., 1997. Oxygen isotopes in marine diatoms: A comparative study of analytical techniques and new results on the isotope composition of recent marine diatoms. Geochimica et Cosmochimica Acta 61, 2275-2280.

Sharp, Z. D., 1990. A laser-based microanalytical method for the in situ determination of oxygen isotope ratios of silicates and oxides. Geochimica et Cosmochimica Acta 54, 1353-1357.

Shemesh, A., Burckle, L. H., and hays, J. D., 1995. Late Pleistocene oxygen isotope records of biogenic silica from the Atlantic sector of the Southern Ocean. Paleoceanography 10, 179-196.

ICDP

Experimental investigations on pre-eruptive conditions and dynamic processes during eruption of Mt.Unzen in 1991-1995

S.B. CICHY[1], R.E. BOTCHARNIKOV[1], F. HOLTZ[1], H. BEHRENS[1], H. SATO[2]

[1]Institut fuer Mineralogie, Leibniz Universitaet Hannover, Callinstr. 3, 30167 Hannover, Germany, (s.cichy@mineralogie.uni-hannover.de)
[2]Dept. of Earth and Planetary Science, Kobe University, Japan

The compositional and morphological characteristics of rocks produced during volcanic eruptions provide constraints on the magma storage conditions prior to eruption and on the dynamic processes occuring in magma chamber and during magma ascent. However, the quantitative interpretation of chemical and morphological variations in terms of eruptive dynamics requires an accurate calibration via experimental approaches. In the particular example of the Unzen eruption in 1991-95, a variety of experimental studies (phase relations, solubility of volatiles in melts, viscosity and decompression experiments) have been combined with petrological, geochemical and geophysical approaches for the erupted rocks as well as for rocks in magmatic conduit drilled by the ICDP (Unzen Scientific Drilling Project), leading to a general overview of the magmatic processes prior to and during the eruption. Our goal is to simulate experimentally the magma ascent from ca. 10 to 1.5 km depth (below ICDP target) as well as to the surface. Therefore, two main experimental approaches have been used: (i) crystallization experiments in a broad range of temperatures and pressures to reproduce the equilibrium phase relations in rhyodacitic magmas at different conditions; (ii) isothermal decompression experiments conducted at different temperatures and decompression rates to investigate kinetic processes of magma degassing and crystallization, occuring on magma ascent.

We have conducted phase stability experiments on the rhyodacitic groundmass composition of the 1991-1995 Unzen eruption at pressures in the range from 50 to 300 MPa, at temperatures in the range from 800 to 1000 °C, as well as at different activity of water, varying from ~0.1 to 1.0. Preliminary results are shown in the phase diagrams (Fig. 1 and 2). Additional phase stability experiments are in progress. The particular attention has to be focused on the appearance of the amphibole and plagioclase.

The determined P-T range for the magma chamber of the 1991-1995 Unzen eruption are considered to be in the range of 870 to 930°C at pressure of ~300 MPa (e.g. Nishi et al., 1995; Venezky and Rutherford, 1999; Holtz et al., 2005). The occurrence of the mineral phases, especially amphibole (Amph) and plagioclase (Plag), are very sensitive to the activity of water in the system ($aH_2O \sim X_{H2O}^{fluid}$) at these conditions. Based on the experiments with dacite, Holtz et al. (2005) suggested that Plag, Amph and Opx were the major mineral phases stable at 300 MPa prior to the eruption. Our data illustrate that this mineral assemblage in rhyodacitic magma is only stable at temperatures ≤ 850°C and in the systems with water activity close to 0.9-1.0 (Fig.1 and 2). As pressure decreases, the stability field of Amph shifts to lower temperatures and to a wider range of X_{H2O} (> 0.5). At

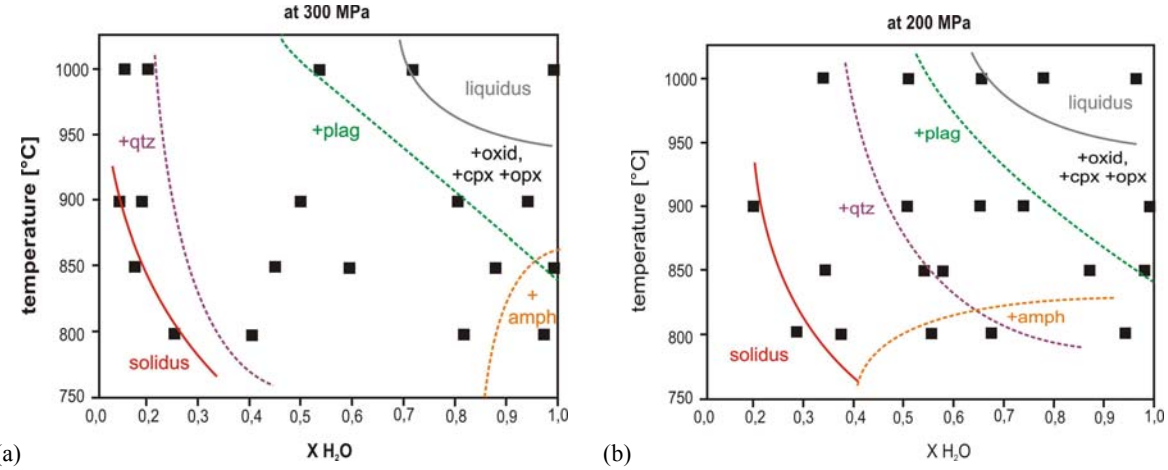

Fig. 1: Phase diagrams for Unzen's rhyodacitic groundmass at 300 MPa (a) and at 200 MPa (b) with a temperature range from 800 to 1000°C. Abbreviations: plag= plagioclase; cpx= clinopyroxene; opx= orthopyroxene; amph= amphibole; qtz= quartz; X_{H2O}= mole fraction of water in the fluid phase after the experiment (~water activity in the system, aH_2O).

water-saturated conditions (X_{H2O} = 1.0), Plag starts to crystallize close to or below 200 MPa. As water activity decreases in the fluid-saturated system, Plag becomes even stable at higher pressures and temperatures. These observations are very useful to interpret the results of our decompression experiments and furthermore, the textures of natural samples.

decompression rate. In the H_2O-bearing system, the nucleation and growth of Plag is accompanied by an increase of BND.

The onset of crystallization, observed from changes in the chemical composition of the residual melt, occurs at decompression rates < 0.1 MPa/s. At the lowest decompression rate (0.0002 MPa/s), the chemical

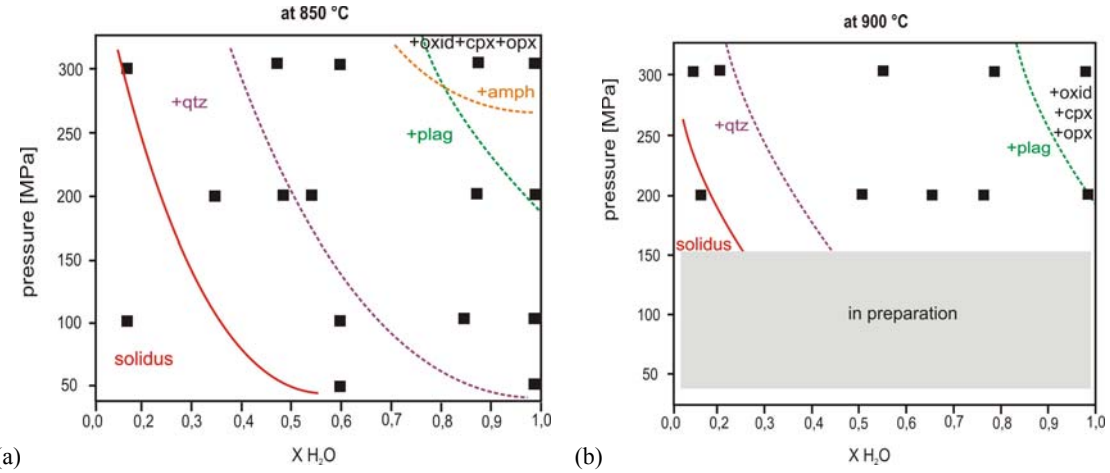

Fig. 2: The stability of minerals phases in rhyodacitic groundmass of Unzen at 850°C (a) and at 900°C (b) and in the pressure range of 50 to 300 MPa. Abbreviations: plag= plagioclase; cpx= clinopyroxene; opx= orthopyroxene; amph= amphibole; qtz= quartz; X_{H2O}= mole fraction of water in the fluid phase.

In decompression experiments, simulating magma ascent from depths with pressure of 300 MPa to those with pressure of 50 MPa at 850°C (set-I; Cichy et al., submitted), equilibrium concentrations of water in the residual glasses are reached at decompression rates ≤ 1 MPa/s for the H_2O+CO_2-bearing system and ≤ 0.1 MPa/s for the H_2O-bearing system. The bubble number density (BND) values range from $10^{11.5}$ m^{-3} to 10^{14} m^{-3} in both the H_2O-bearing and the H_2O+CO_2-bearing systems. In the H_2O+CO_2 system, the BND decreases with decreasing decompression rate, which is attributed to the increasing influence of bubble growth and coalescence on the processes of volatile exsolution from melts with decreasing

composition of the residual melt in the H_2O+CO_2-bearing system becomes similar to the natural matrix glass composition. There is no significant variation of the microlite number density (MND) value as a function of the decompression rate. The MND values range from $10^{2.4}$ mm^{-3} to $10^{3.0}$ mm^{-3} and are at least two order of magnitude lower than those from natural samples (10^5-10^6 mm^{-3})

In this set of decompression experiments we can clearly see that plagioclase microlites only nucleated and grew in experiments of the H_2O-bearing system with the two lowest conducted decompression rates (0.0005 and 0.0002 MPa/s). The length of those plagioclases reaches up to 200-250 µm which is consistent with the size of

plagioclase microlites in natural samples. Plagioclase microlites in the H_2O+CO_2-bearing system were already present in the starting assemblage at 300 MPa and grew to a maximum size of ~80 μm during decompression. In this study, we were able to show that the size and shape of microlites nucleating and crystallizing during decompression (plagioclase in our experimental dataset set-I) are useful to constrain ascent rates at the onset of the crystallization of the corresponding phase. In the case of Unzen magmas, the size of plagioclases is compatible with magma ascent rates of ~ 30-50 m/h (average velocity estimated for the pressure range 200 to 50 MPa).

As a next step, we have conducted additional sets of decompression experiments and at least two more sets are in progress (see Table 1). Two types of experiments have been conducted: high-pressure decompression (HPD) experiments and low-pressure decompression (LPD) experiments. In HPD experiments, we start at 300 MPa, corresponding to Unzen's magma chamber depth, and decrease pressure to final pressures of 50 MPa, which is similar to the pressure of the ICDP target at a depth of 1.5 km, or higher. In LPD experiments, we simulate the magma ascent until surface pressures (0.1 MPa). This will provide a better insight into the bubble and microlite nucleation and growth processes at different stages (=depths) during magma ascent.

ensure the similarity of the starting material for each experimental run by synthesizing large batches of fluid-saturated glass in big capsules, which were then quenched and cut into smaller cylinders before the different decompression experiments were run. On the other hand, the continuous pressure release in cold-sealed pressure vessels (CSPV) were realizable only in experiments which did not take longer than one hour total decompression time, as most of the work necessary had to be done manually. Therefore, we have constructed and installed, in cooperation with the petrology work group of Prof. Marcus Nowak (University Tübingen), a new decompression valve allowing continuous decompression even at lower decompression rates, providing more realistic simulation of decompression processes. After a series of test runs using the new decompression valve only under pressure, we have conducted a set of HDP experiments (set VI) investigating in detail the effects of the three different decompression methods continuous, multi-step and single-step on bubble nucleation and growth. The high temperature above the liquidus (at 1200 °C) of set VI experiments has been used to exclude the effect of microlite nucleation and growth on the bubble forming processes. Additionally, we have used here two series of fluid-saturated systems: one containing only H2O in the fluid and the second having a mixture of H2O, Cl and CO2. We have added chlorine (and water) as

#	fluid saturated system	P start [MPa]	P final [MPa]	T [°C]	type of vessel	decompression method	decompression rate [MPa/s]
set I	H_2O, H_2O+CO_2	300	50	850	CSPV	continuous + multi-step	20 – 0.0002
set II	H_2O, H_2O+CO_2	300	100	850	CSPV	continuous	20 – 0.1
set III	H_2O, H_2O+CO_2	300	200	850	CSPV	continuous + multi-step	20 – 0.0002
set IV	H_2O	200	0.1	850	CSPV	multi-step	0.1 – 0.0001
set V	H_2O	50	0.1	850	CSPV	multi-step	0.1 – 0.0001
set VI	H_2O, HCl+CO_2	300	50	1200	IHPV	continuous + multi-step + single-step	0.1 – 0.0013
set VII	H_2O, H_2O+CO_2	300	50	930	IHPV	continuous (new valve)	(1 – 0.0002)
set VIII	H_2O	50	0.1	930	IHPV	continuous (new valve)	(1 – 0.0001)

Table 1: Conditions of already conducted (set I to VI) and planned (set VII to VIII) decompression experiments within the project.

As the temperature of the mixed magma prior to the 91-95 Unzen eruption has been estimated to be 900 ± 30°C (e.g. Venezky & Rutherford, 1999), we have been conducting HPD and LPD experiments at a temperatue of 930°C. The results of phase stability experiments shown in Fig. 1 provide estimates for the equilibrium phase assemblages that are expected in HT-decompression experiments. For instance, at the starting pressure of 300 MPa neither plagioclase nor amphibole should be stable at 930°C. While at this temperature amphibole is only stable at pressures above 300 MPa, plagioclase will nucleate and grow during decompression as the decompression path crosses its stability field at lower pressures.

Additionally, there have been made some efforts to enhance the quality of the conducted decompression experiments. Since the nucleation of bubbles and microlites can be influenced by the properties of starting material, special attention should be paid to minimize the textural and compositional inhomogeneity in the initial system. To do this, we have changed the preparation of the samples to HCl to the glass powder. It has been proven by melt inclusion analyses that chlorine is an important volatile in the mixed magma, containing ~500 ppm Cl in the melt prior to the eruption (Botcharnikov et al., 2008).

The experimental products from HT, LPD and HPD experiments have been analyzed by synchrotron-based X-ray tomographic microscopy (TOMCAT) at the Paul Scherrer Institute, Villigen (Switzerland). This non-destructive technique allows 3D visualization of textural characteristics with high resolution (about 0.3 □m voxel size). The significant difference in density between silicate glass and fluid bubbles provides excellent opportunity to reconstruct 3D textures of vesiculated samples. On the other hand, lower density contrast between glass and microlites and quite small size of microlite crystals (typically about 5-15 μm) makes the quantification of crystal size distribution challenging. About 30 samples have been analyzed in February 2010, and the obtained analytical data are now in processing.

The results of our decompression and phase relation experiments will be used to interprete textural features of natural samples from surface and depth which were analysed for the distribution of microlites and bubbles. The quantitative interpretation will provide constraints on magma ascent processes during Unzen eruption.

References:
Cichy SB., Botcharnikov RE., Holtz F. & Behrens H. (submitted) Vesiculation and Microlite Crystallization in the Ascending Rhyodacitic Magma During the 1991-95 Eruption of Unzen Volcano, Japan, Journal of Petrology .
Botcharnikov RE., Holtz F., Almeev RR., Sato H. & Behrens H. (2008) Storage conditions and evolution of andesitic magma prior to the 1991–95 eruption of Unzen volcano: Constraints from natural samples and phase equilibria experiments, Journal of Volcanology and Geothermal Research 175, 168-180
Holtz F., Sato H., Lewis J., Behrens H. & Nakada S. (2005) Experimental petrology of the 1991-1995 Unzen Dacite, Japan. Part I: phase relations, phase composition and preeruptive conditions. J. Petrol, 46, 319-337
Nishi K., Ishihara K., Kamo K., Ono H. & Mori H. (1995). Positioning of magma reservoir at Unzen volcano by GPS survey. Bulletin of Volcanology Society of. Japan 40, 43-51, in Japanese with English abstract.
Venezky D.Y. & Rutherford M.J. (1999). Petrology and Fe-Ti oxide reequilibration of the 1991 Mount Unzen mixed magma. Journal of Volcanology and Geothermal Research 89, 212-230.

IODP

Marine biological productivity, carbon cycling, and climate cooling during the Oligocene to Miocene transition

L.DIESTER-HAASS[1], K.BILLUPS[2], K.-C. EMEIS[3]

[1]Universität des Saarlandes, Zentrum für Umweltforschung, 66041 Saarbrücken.[l.haass@mx.uni-saarland.de]
[2]School of Marine Science and Policy ,University of Delaware ,700 Pilottown Road ,Lewes, DE 19958 , [kbillups@udel.edu]
[3]Institut fuer Biogeochemie und Meereschemie, Universitaet Hamburg , Bundesstr. 55, [kay.emeis@zmaw.de]

The Oligocene to Miocene boundary (the so-called Mi1 event) marks one of the major Cenozoic cooling steps. A corresponding but slightly out of phase $\delta^{13}C$ maximum has been attributed to increased organic matter burial associated with global climate cooling (e.g., Zachos et al., 2001). To test this idea we have constructed records of marine biological productivity (based on benthic foraminiferal accumulation rates, BFAR) to parallel the stable isotope records from 20-25 Ma at three sites from the Atlantic Ocean (ODP Sites 926, 1265 and 1090) sampling different hydrographic regimes. Our data show that the $\delta^{18}O$ and $\delta^{13}C$ maximum that characterize the Oligocene/Miocene boundary is accompanied by a pronounced maximum in BFAR derived paleoproductivity at all sites. In the subtropical Atlantic (Site 1265) and the Southern Ocean (Site 1090), productivity increases about 500 kyr prior to Mi1 in tune with the beginning of enhanced amplitude variations in the benthic foraminiferal $\delta^{13}C$ record. In the tropical Atlantic (Site 926), where we have appropriate sampling resolution (~10 kyr), eccentricity-scale variations in paleoproductivity are coherent with the stable isotope records and in-phase with the $\delta^{18}O$ values. Paleoproductivity leads $\delta^{13}C$ at the 400 kyr period by about 18 kyrs in agreement with the lead of $\delta^{18}O$ values with respect to $\delta^{13}C$ values. These results illustrate that the link between Oligocene to Miocene climate transition and the carbon cycle is one of marine primary productivity both during the glacial event of Mi1 as well as on eccentricity time scales. The late Oligocene (24 Ma) increase of productivity suggests that a reduction of atmospheric CO_2 levels mediated by increased biological productivity may have lead to climate cooling at the Oligocene to Miocene boundary.

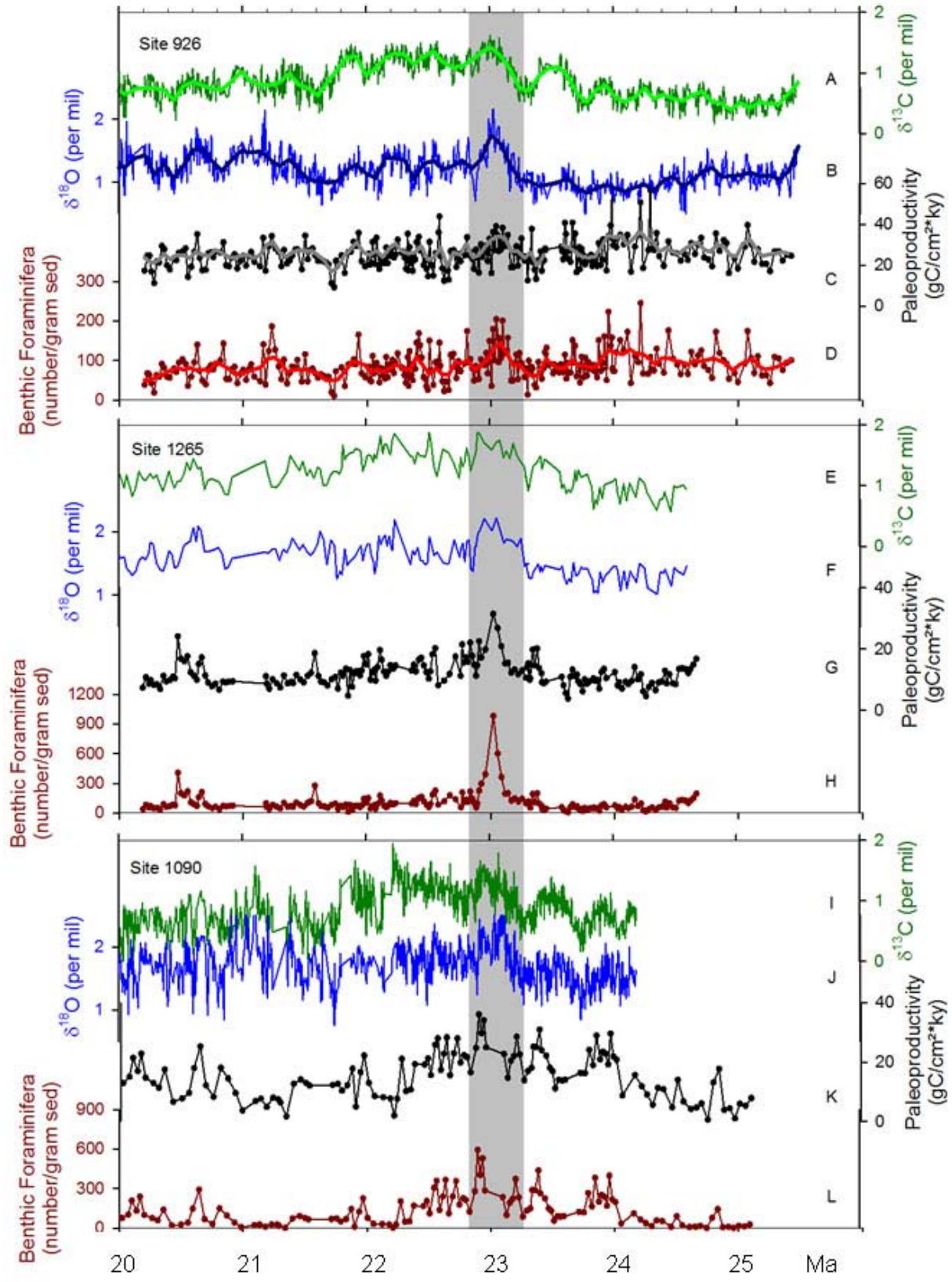

Fig. 1: Stable isotope and paleoproductivity records. The upper panel shows the benthic foraminiferal $\delta^{13}C$ (A), $\delta^{18}O$ (B), benthic foraminiferal accumulation rates derived productivity (C), and the number of benthic foraminiferal tests per gram sediment (D) for tropical Atlantic Site 926. The middle panel shows the benthic foraminiferal $\delta^{13}C$ (E), $\delta^{18}O$ (F), benthic foraminiferal accumulation rates derived productivity (G), and the number of benthic foraminiferal tests per gram sediment (H) for southeastern subtropical Atlantic Site 1265. The lower panel shows the benthic foraminiferal $\delta^{13}C$ (I), $\delta^{18}O$ (J), benthic foraminiferal accumulation rates derived productivity (K), and the number of benthic foraminiferal tests per gram sediment (L) for subantarcitc Southern Ocean Site 1090. The vertical grey bar highlights the increase in productivity that occurs across the Oligocene to Miocene boundary at all sites.

ICDP

Source rocks of crustal-scale magnetic anomalies in the upper crust of Eastern Finland

FRANK DIETZE[1], AGNES KONTNY[1], CHRISTOPHER VIRGIL[2]

[1]Institut für Angewandte Geowissenschaften, Universität Karlsruhe (KIT), Germany
[2]Institut für Geophysik und Extraterrestrische Physik, TU Braunschweig, Germany

The boundary of the Proterozoic and the Archaic plate in East Finland belongs to a region with extremely high crustal magnetic anomalies on Earth. Such anomalous regions often lie adjacent to the continent-ocean boundary of Precambrian provinces (western Africa, NW Africa, northern Baltic Shield, NE Guyana Shield, southern America, eastern India and Western Australia) and host prominent ore deposits. In the aeromagnetic total field anomaly map of this area, weakly to non-magnetic regions related to metasedimentary rocks and high-amplitude magnetic signatures were recognized (e.g. Airo & Loukola-Ruskeeniemi 2004). The latter are related to black shales, serpentinized ultramafic rock units, and gabbroic-wehrlitic dike rocks. Pyrrhotite is the main magnetic mineral in the black shales and magnetite is reported in the mafic to ultramafic lithologies. The banded aeromagnetic anomaly pattern in the Outokumpu region is related to different magnetized, gently towards SE dipping rocks of the Outokumpu assemblage (Airo et al. 2007). In the vicinity of these aeromagnetic anomalies the 2516 m deep (continuously cored) Outokumpu (OKU) deep drill hole is located within the Paleoproterozoic Outokumpu formation, which is famous for its polymetallic massive sulfide deposits, and which intersected a crustal-scale geophysical anomaly zone between 1314 and 1515 m. The ophiolite-derived altered ultramafic rocks with associated black schists of this depth interval are the host rocks of the Outokumpu-type massive Cu-Zn-Co-Ni-(Au-Ag) sulfide deposits of the area.

The polygenetic Outokumpu type deposits is interpreted by Peltonen et al. (2008) to be the result of mixing of two genetically distinct end-member sulfide reservoirs. First, a pretectonic Cu-rich proto-ore formed within peridotitic sea floor at about 1.95 Ga. Second, syntectonic disseminated Ni-sulfides formed through chemical interaction between obducting ultramafic massifs and adjacent black schists some 40 Ma after deposition of the Cu-rich proto-ore. The locally occurring carbonate-silica alteration of the serpentinite post-dated the initial tectonic emplacement of the mantle fragments but predated the earliest regional deformation. Five stages (D1 - D5) of the tectonic-metamorphic evolution are described in Kontinen et al. (2006), which are interpreted as a result of a continuum process under a sustained NNE-SSW orogenic compression during the Svecofennian orogeny.

The aim of this project is to provide basic petrophysical, rock and paleomagnetic data, which help (1) to understand rock magnetic properties in terms of the polygenetic Outokumpu ore formation, (2) to understand formation of magnetic minerals during serpentinization and carbonatization in a complex tectonic environment, and (3)

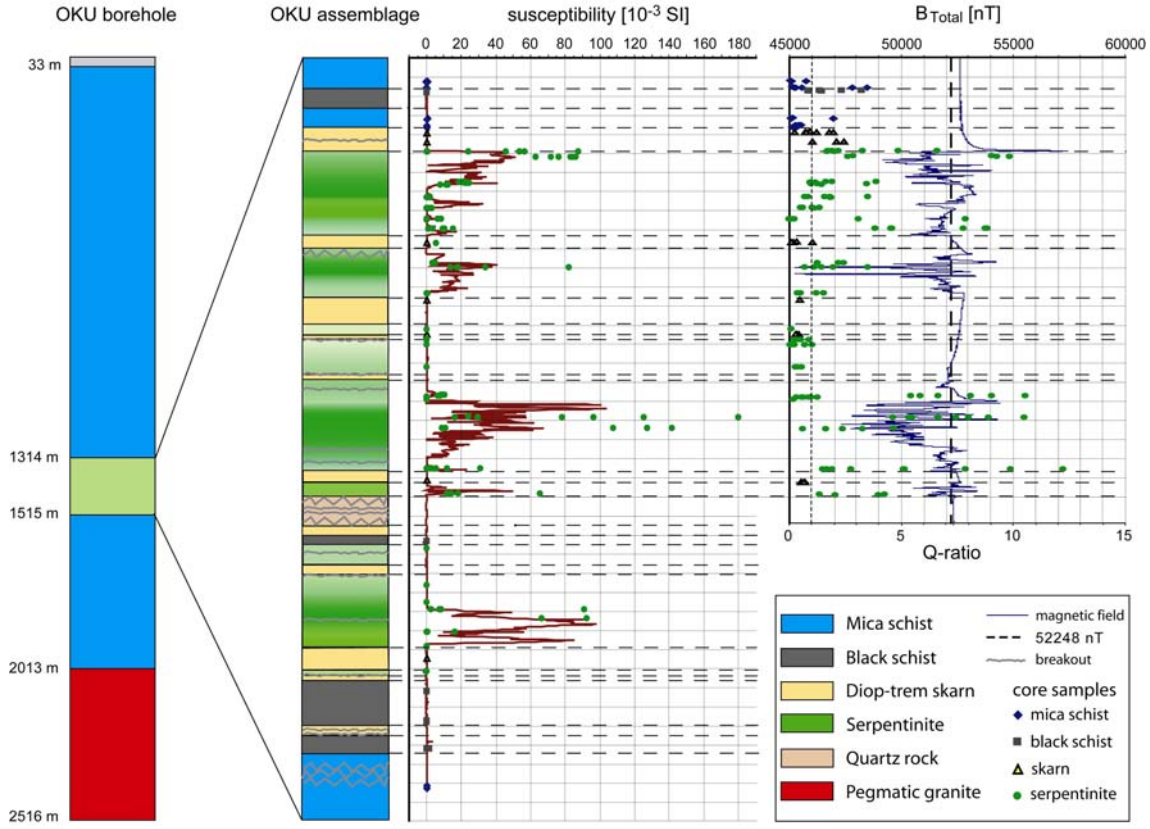

Fig. 1: Lithology of the Outokumpu borehole (left) and the OKU assemblage (right) with magnetic susceptibility from core data (measured with a handheld kappameter ZH30). Dots are data from core samples taken for detailed rock magnetic measurements.

to explain and interpret the magnetic logging measurements.

Magnetic susceptibility (χ) measurements every 20 cm along the cores revealed that the rocks of the Outokumpu assemblage vary significantly from dia- and paramagnetic values below 0.7*10-3 SI to ferrimagnetic ones above that value. We investigated 50 core samples including 241 single specimens (diameter of 2.5 cm and height of 2.1 cm), and measured a significant scattering of rock magnetic properties (Fig. 1), which indicates a heterogeneous distribution of ferrimagnetic minerals. Generally a positive correlation between χ and NRM of the ferrimagnetic serpentinites has been observed, indicating that the amount of magnetic minerals is responsible for the NRM variation.

Königsberger (Q) ratios (ratio between remanent and induced magnetization) are above 1 for most of the black schist and below 1 for the mica schist and most of the skarn rocks, indicating remanent and induced magnetization, respectively. Serpentinite layers show a large variation of Q ratios and only strongly serpentinized samples with NRM values above 0.01 A/m show a remanent magnetization.

While temperature-dependent magnetic susceptibility measurements indicate magnetite as main carrier of thermal demagnetization of NRM sometimes reveals a second remanence carrier beside magnetite, which is pyrrhotite. Both magnetic minerals seem to carry the same direction of magnetization, suggesting a magnetic mineral formation prior to the main ductile deformation stage and a remagnetization probably during deformation.

Compared to rock magnetic properties of serpentinites reported in the literature, serpentinites from the OKU drill core show a large variation but the mean values are in good agreement with those reported from other occurrences worldwide (e.g. Toft et al. 1990, Oufi et al. 2002). The large variation in the Outokumpu serpentinites can be correlated with a complex and inhomogeneous serpentinization and carbonatization alteration history, which seems to be mirrored in their rock magnetic properties. While serpentinization (pre-tectonic) is related to magnetite formation, the carbonate-silica alteration of the serpentinites (during deformation stages D1 – D2) caused a decomposition of magnetite and a formation of (non-magnetic) pyrrhotite and pentlandite. Our comparison

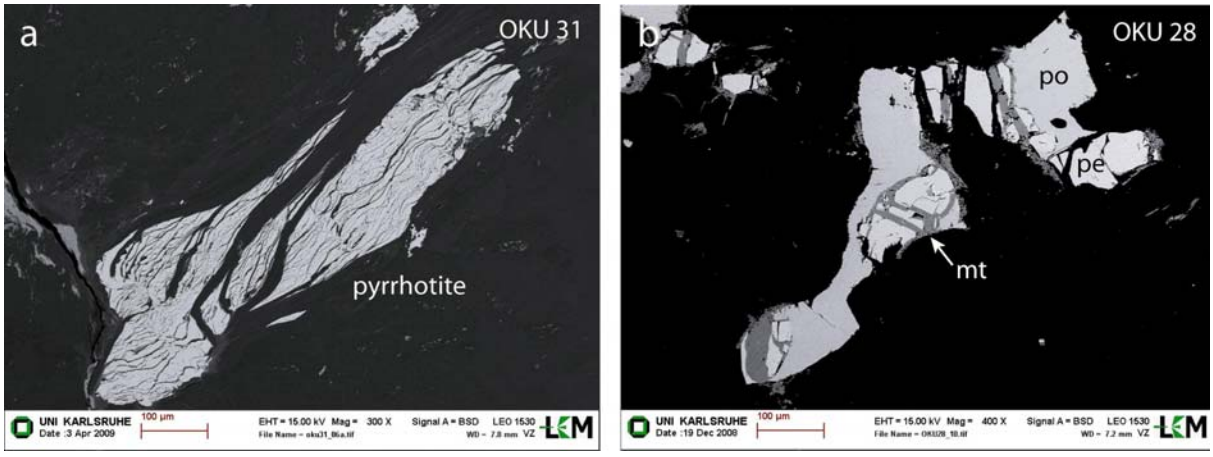

Figure 2: Backscattered electron (BSE) images of polished thin sections. (a) deformed pyrrhotite grain in a strong serpentinized sample, (b) magnetite (mt) along cracks in pendlandite (pe) and secondary formed pyrrhotite (po).

X-ray diffraction analyses have indicated that the mineralogy of the serpentinites is variable and can be correlated with the susceptibility intensity. In serpentinite with high magnetic susceptibility, lizardite is the dominating mineral. Chlorite (clinochlore), brucite and magnetite can also be identified. With decreasing magnetic susceptibility the magnetite and lizardite content decreases and dolomite and tremolite are the main mineral phases (Dietze et al. 2009a).

Magnetite as well as pyrrhotite shows corrugation lamellae (Fig. 2a), which have formed from an originally homogeneous individual during strong mechanical stresses. This observation indicates that these minerals have been formed previous to or in between of the regional deformation stages. Magnetite also forms elongated or rhomb-shaped non-deformed aggregates. In some samples, magnetite forms along microcracks of pyrrhotite (po) – pentlandite (pe) aggregates (Fig. 2b). Such sulfide aggregates (po-pe or po-niccolite) are mostly homogeneous and show sutured grain boundaries, which might indicate recrystallisation during the metamorphic events.

between lithologies of the Outokumpu assemblage with rock magnetic properties, mineralogy and the γ-ray log (kindly provided by J. Kück, GFZ Potsdam) revealed a clear relationship with the low-temperature listwaenite-birbirite-type carbonate-quartz alteration of the peridotite body margins, which is most likely related to the Ni proto-ore formation of the obduction stage as suggested by Peltonen et al. (2008). This low-temperature alteration caused the decomposition of magnetite and is responsible for low magnetic susceptibilities within the serpentinite sequence (Kontny and Dietze, 2009). A second magnetic generation, often formed along cracks in the Fe-Ni sulfides, must have formed during a subsequend fallowing deformation stage. The syn to late orogenic granitoid emplacement (1.87-1.85 Ga) with accompanying hydrothermal fluid circulation and metamorphic peak temperatures of 550 °C in this area probably caused a remagnetization of the magnetic minerals.

The subproject magnetic logging uses the high-resolution “Göttinger Bohrloch Magnetometer” (GBM) to compute the declination of rock magnetization by measuring the x-, y- and z-component of the magnetic field

based on a 2D model of homogeneously magnetized layers (Virgil et al., this vol.). Before using this declination, a depth correction between borehole and core depth is necessary because the magnetic susceptibility and NRM core data were used for calculation of the borehole magnetization. The depth correction was done using the γ-ray and susceptibility borehole data provided by the ICDP-OSG as reference depth and by correlation with the magnetic field data measured in the borehole with the GBM and with the rock magnetic data measured on core samples using anomaly jumps at lithological boundaries and within serpentinite units. Up to now, this correlation was done for the depth interval 1300-1530 m.

Strong magnetic inhomogeneity becomes evident from the aeromagnetic map (see Airo et al. 2007) and the borehole magnetic field, which has been measured until a depth of 1440 m (Fig. 1). Most of the magnetic anomalies are limited to the serpentinite units and are characterized by Königsberger ratios distinctly above 1 indicating that remanent magnetized serpentinite units cause the magnetic field anomalies (Dietze et al. 2009b). Interestingly, the magnetic anomalies are mostly negative suggesting a stable magnetic field vector in a direction different to the recent magnetic field. Further studies of the vector of remanent magnetization will help to establish a geological model for the magnetic borehole data.

References:

Airo M.-L. and Loukola-Ruskeeniemi K. (2004) Characterization of sulfide deposits by airborne magnetic and gamma-ray responses in eastern Finland. Ore geology reviews, 24, 67-84.

Airo M.-L., Elbra T., Kivekäs L., Laine T., Leino M., Mertanen S., Pesonen L., Vuoriainen S., Säävuori H. (2007) Petrophysical laboratory measurements of the Outokumpu deep drill core samples. In: Kukkonen I.T., (Editor), 2007. Outokumpu Deep Drilling Project, Sec. International Workshop, May 21-22, 2004, Espoo, Finland. Programme and Extended Abstracts. Geological Survey of Finland, Report Q10.2/2007/29, 35-40.

Dietze F., Kontny A., Airo M-L., Kramar U. (2009a) Rock magnetic properties and their correlation with mineralogy / geochemistry for the serpentinite sequence of the OKU drillhole (Eastern Finland). Abstract 08261, EGU Assembly.

Dietze F., Kontny A., Virgil C., Kück J., Hördt A., Airo M.-L. (2009b) Correlation of petrophysical logging data with core data for the depth interval 1300 – 1530 mof the OKU drilling. Abstract. Outokumpu Deep Drilling Project, Third International Workshop, Espoo, 86-90.

Kontinen A., Peltonen P., Huhma H. (2006) Description and genetic modelling of the Outokumpu-type rock assemblage and associated sulphide deposits. GTK report M10.4/2006/1.

Kontny A. and Dietze F. (2009) Rock magnetic properties of the Outokumpu rock type assemblage as function of mineralization process. Abstract. Outokumpu Deep Drilling Project, Third International Workshop, Espoo, 77-80.

McEnroe S.A., Langenhorst F., Robinson P., Bromiley G.D., Shaw C.S.J. (2004) What is magnetic in the lower crust? Earth and Planetary Science Letters, 226, 175– 192.

Oufi O. and Cannat M. (2002) Magnetic properties of variably serpentinized abyssal peridotites. J. Geophys. Res., 107, No. B5, 2095, 10.1029/2001JB000549.

Peltonen P., Kontinen A., Huhma A. and Kuronen U. (2008) Outokumpu revisited: New mineral deposit model for the mantle peridotite-associated Cu-Co-Zn-Ni-Ag-Au sulphide deposits. Ore Geology Reviews, 33, 559-617.

Toft P.B., Arkani-Hamed J., Haggerty S. (1990) The effects of serpentinization on density and magnetic susceptibility: a petrophysical model. Phys. Earth Planet. Inter., 65, 137-157.

Virgil C., Hördt A., Ehmann S., Leven M., Steveling E., Kück J., Dietze F. (2010) Drei komponentige Magnetfeldmessungen in der Outokumpu-Bohrung (Finnland), Abstract, this vol.

IODP

In-situ iron isotope ratio determination and thermo-oxibarometry in Fe-Ti oxides of IODP Hole 1256D (ODP Leg206 and IODP Exp. 309 & 312, East Pacific Rise)

W. DZIONY[1], I. HORN[1], J. KOEPKE[1,] F. HOLTZ[1]

[1]Institut für Mineralogie, Leibniz Universität Hannover

The formation of the oceanic crust is one of the main fundamental processes building our planet. IODP multi-cruise mission "Superfast Spreading Crust" successfully drilled a complete section of the upper oceanic crust into the underlying gabbros (Site 1256; eastern equatorial Pacific; 15 Ma crust formed at the East Pacific Rise). The recovered rocks now representing the first reference profile through fast-spreading upper oceanic crust, provide us with the good opportunity to improve our understanding of the formation and evolution of the crust. Complex interplay between magmatic and metamorphic processes, such as primary crystallization; low- and high-temperature alteration; contact-metamorphism; partial melting/assimilation; magma mixing can be observed. The petrographic record of the whole section reveals that all processes involve the formation of, or the reaction with, Fe-Ti oxides, which can consequently be used as suitable proxies for monitoring the different stages in the magmatic-metamorphic evolution of fast-spreading oceanic crust.

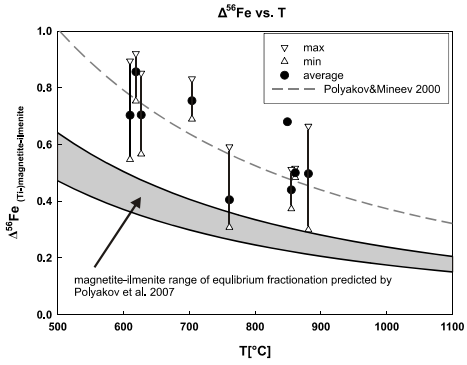

Fig. 1: Inter-mineral fractionation observed between coexisting pairs of ilmenite-magnetite from this study (black dots). Minimum and maximum values obtained from multiple measurements on one mineral pair are connected with vertical lines. The dashed curve shows the predicted values based on former data from Polyakov and Mineev 2000 and the solid curves are based on the revised data of Polyakov et al. 2007.

In situ iron isotope determination: We have determined Fe isotope ratios of oxides and sulphides of basalts and gabbros in order to gain basic knowledge of the Fe isotope cycle in the ocean crust, and to investigate if their isotopic signatures can be used as a proxy for hydrothermal alteration or as a geothermometer. The invesitgated samples are basalts from the uppermost unit, a~74m thick lava pond, a metamorphic overprinted dike and several gabbros (see units below in Fig. 3).

In this approach we are using a deep UV-femtosecond laser ablation system coupled to a MC-ICP-MS (multiple collector inductively coupled plasma mass spectrometer). This method allows us to determine iron isotope ratios in-situ with a precision of ±0.1 ‰ (2σ) for the δ^{56}Fe (δ^{56}Fe = (^{56}Fe/^{54}Fe$_{sample}$/^{56}Fe/^{54}Fe$_{IRMM-14}$-1)*1000). It has been shown in several studies (Horn et al. 2006, and within this project) that the influence of the matrix on the calibration of the δ^{56}Fe values is negligible. Furthermore UV-femtosecond laser ablation provides a spatial resolution that can not be reached with conventional aqueous solution mass spectrometry. Analytical and methodical techniques are given by Horn et al. (2006).

Most igneous rocks normally have a very destricted range in δ^{56}Fe, except for some high silica granitoids (Poitrasson and Freydier, 2005; Schoenberg and von Blanckenburg, 2006), mantle xenoliths and carbonatites (e.g. Weyer et al, 2005, Johnson and Beard, 2006). Large variations in δ^{56}Fe can be observed in both, magnetite and ilmenite as well as in pyrite within the investigated samples, even at very small scale. However, Δ^{56}Femagnetite-ilmenite values (δ^{56}Femagnetite - δ^{56}Feilmenite) of coexisting pairs of magnetite and ilmenite are in agreement with the general trend of temperature-dependent fractionation, but are shifted towards higher Δ^{56}Fe values compared to the predicted values, which implies that they are isotopically out of equilibrium. This could be explained by the influence of hydrothermal alteration, since all investigated samples show signs of typical hydrothermal alteration. Fe isotope compositions of hot fluids (> 300 °C) from mid-ocean-ridge spreading centers define a narrow range that is shifted to lower δ^{56}Fe values by 0.2‰–0.5‰ as compared to igneous rocks (Fig. 1, see Beard et al., 2003; Rouxel et al., 2003; Beard and Johnson, 2004). It has been shown that Cl-bearing

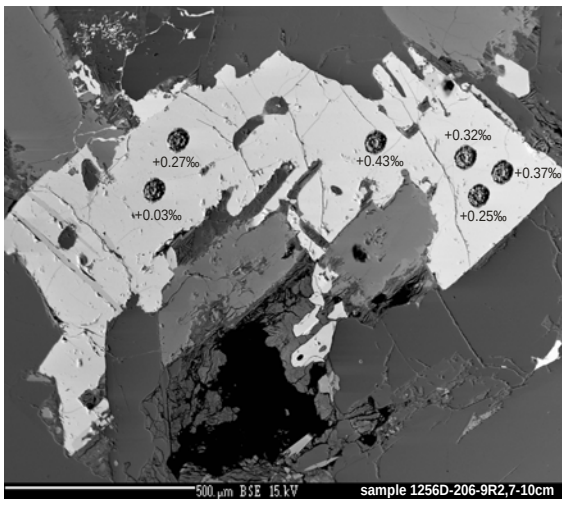

Fig. 2: Photomicrograph of a primary magmatic magnetite cristallized in a basalt of the the lava pond (sample 1256-206-9R2,7-10cm), showing an example of the variations of the δ56Fe. Lasered spots are around 40µm in diameter.

supercritical fluids can contain considerable amounts of divalent iron (Chou and Eugster, 1977). Such Fe^{2+}-bearing solutions tend to favor mobilization of isotopically light iron. Assuming that magnetite is more sensitive to exsolution of iron than ilmenite in the presence of Cl-bearing fluids, this would increase the δ^{56}Fe of magnetite and therefore the Δ^{56}Fe. Variations of up to 0.4‰ δ^{56}Fe within one single grain of magnetite (see Fig.2) also show that isotopic alteration can be extremely localized.

Pyrites are, with one exception, generally isotopically light. In the gabbros and the basalts of the lava pond they show relatively low δ^{56}Fe values between -1.1‰ and -0.6‰, identicating that they were formed by secondary precipitations from a hydrothermal fluid. In contrast, we observed a δ^{56}Fe for pyrite coexisting with ilmenite in a sample of the granoblastic dikes of about +0.3‰, which is close to the predicted fractionation with respect to the coexisting ilmenite (Polyakov and Mineev, 2000). Since all phases in the granoblastic dikes seem to be completely recrystallized, it is not clear so far, whether this pyrite is preserving its initial primary magmatic isotopic signature or has been formed by secondary precipitation and then isotopically re-equilibrated during the ongoing contact-metamorphic overprint, that the granoblastic dikes have suffered (see next paragraph).

Thermo-oxibarometry: Chemical data of the oxide minerals based on several thousands of microprobe analyses (Dziony et al., 2008, Koepke et al, 2007) were also applied to reconstruct the redox and temperature conditions during the evolution of the oceanic crust at Site 1256D. We applied the two-oxide geothermo-oxibarometer of Sauerzapf et al. (2008) to the rocks of IODP Hole 1256D. Since most magnetites show more or less pronounced exsolutions, different methods were used to estimate the initial composition prior to exsolution. In those cases where exsolutions were large enough to be measured separately, the initial compositon was recalculated by image analysis. In the case of very narrow exsolutions, a broad beam of 20 µm diameter was used. For fresh basalt and the gabbro directly at the dike/gabbro contact we estimated relatively reducing redox conditions, as expected for the MOR petrogenesis ($\log(fO_2) \sim \Delta$NNO -1log unit, with NNO corresponding to the $\log(fO_2)$ of the Nickel-Nickeloxide oxygen buffer). For the lowermost dikes ("granoblastic dikes"), which were affected by a contact-metamorphic event due to the thermal imprint of an underlying magma chamber (Koepke et al., 2008), a dramatic shift of the $f(O_2)$ (nearly 4 orders of magnitude) towards more oxidizing conditions (Fig. 3) is observed. The combination of the geothermometry and geo-oxybarometry indicates that this metamorphic event lead to a strong oxidation of the overprinted granoblastic dikes.

The apparent high temperatures for the uppermost gabbros could be explained by faster cooling rates at the contact to the sheeted dikes, whereas a re-equilibration of the oxides via Fe-Ti exchange could have occurred during slow cooling in the lower gabbros. This further indicates that the gabbros reacted with oxidizing fluids during cooling.

Future objectives: The basalts drilled at depths between ~ 350 and ~1300 meters (between the lava pond and the granoblastic dikes) are not suitable for two-oxide thermometry due to the lack of ilmenite. They are not suitable for laser ablation either, since the magnetites are too tiny and mostly skelettal. Therefore in our further work we will focus especially on the lava pond basalts as well as

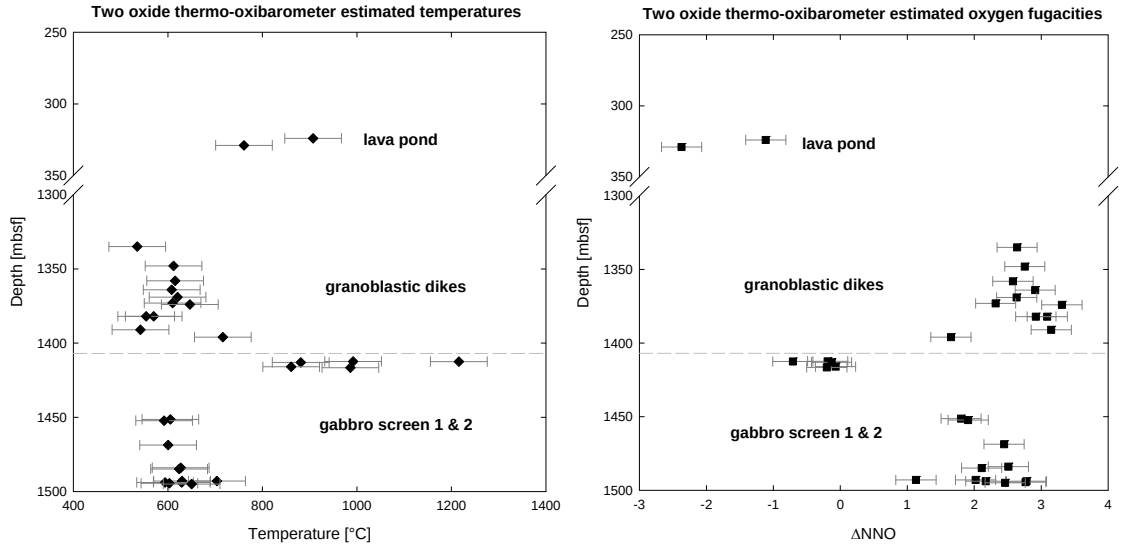

Fig. 3: Temperature and oxygen fugacity estimations by using the magnetite / ilmenite geothermo-oxibarometer by Sauerzapf et al. (2007). The dashed line corresponds to the dike/gabbro transition. mbsf=meters below sea floor; ΔNNO=f(O2) in log units compared to the Ni/NiO oxygen buffer.

the granoblastic basalts and the gabbros. For example, the application of the laser ablation technique to the oxide inclusions within the relictic crystalloblastic domains of some gabbros can solve the important question whether these relics underwent hydrothermal alteration prior to incorporation into the magmatic cycle or not. Furthermore we plan to extend our work on the determination of Fe-isotopes of the sulfides as well as the iron-bearing silicates (cpx, opx, ol). This information will be useful to understand Fe isotope fractionation as well as mechanisms of Fe isotopic exchange between minerals at high temperature (especially exchange between oxides, sulfides and silicates).

References:

Beard, B.L., Johnson, C.M., Von Damm, K.L., Poulson, R.L., 2003. Iron isotope constraints on Fe cycling and mass balance in oxygenated Earth oceans. Geology 31, 629-632.

Beard, B.L., Johnson, C.M., 2004. Fe isotope variations in the modern and ancient earth and other planetary bodies. Rev. Mineralogy & Geochemistry 55, 319-357.

Chou I.-M. and Eugster H. P., 1977. Solubility of magnetite in supercritical chloride solutions. Am. J. Sci. 277, 1296–1314.

Dziony, W., Koepke, J., and Holtz, F., 2008. Data report: petrography and phase analyses in lavas and dikes from Hole 1256D (ODP Leg 206 and IODP Expedition 309, East Pacific Rise). In Teagle, D.A.H., Alt, J.C., Umino, S., Miyashita, S., Banerjee, N.R., Wilson, D.S., and the Expedition 309/312 Scientists, Proc. IODP, 309/312: College Station, TX (Integrated Ocean Drilling Program Management International, Inc.)(doi:10.2204/iodp.proc.309312.201.2008)

Koepke, J., D. M. Christie, W. Dziony, F. Holtz, D. Lattard, J. Maclennan, S. Park, B. Scheibner, T. Yamasaki, and S. Yamazaki (2008), Petrography of the dike-gabbro transition at IODP Site 1256 (equatorial Pacific): The evolution of the granoblastic dikes, Geochem. Geophys.Geosyst.,9,Q07O09.(doi:10.1029/2008GC001939)

Horn, I., von Blanckenburg, F., Schoenberg, R., Steinhoefel, G., Markl, G., 2006. In situ iron isotope ratio determination using UV-femtosecond laser ablation with application to hydrothermal ore formation processes. Geochim. Cosmochim. Acta 70, 3677–3688.

Johnson C. M. and Beard B. L., 2006. Tracing metasomatic and crystallization processes in the mantle through Fe isotopes. Geochim. Cosmochim. Acta 70(1), A295.

Poitrasson F. and Freydier R., 2005 Heavy iron isotope composition of granites determined by high resolution MC-ICP-MS. Chem. Geol. 222, 132–147.

Rouxel, O., Dobbek, N., Ludden, J., Fouquet, Y., 2003. Iron isotope fractionation during oceanic crust alteration. Chem. Geol. 202, 155-182.

Sauerzapf, U, Lattard, D, Burchard, M, Engelmann, R., 2008. The titanomagnetite-ilmenite equilibrium; new experimental data and thermo-oxybarometric application to the crystallization of basic to intermediate rocks. Journal of Petrology 49(6):1161-1185

Schoenberg R. and von Blanckenburg F., 2006. Modes of planetary-scale Fe isotope fractionation. Earth Planet. Sci. Lett. 252, 342–359.

Weyer S., Anbar A. D., Brey G. P., Münker C., Mezger K. and Woodland A. B., 2005. Iron isotope fractionation during planetary differentiation. Earth Planet. Sci. Lett. 240, 251–264.

IODP

The Eemian sapropel – geochemical signatures and paleoenvironmental interpretation of the penultimate interglacial in the Black Sea

S. ECKERT[1], B. SCHNETGER[1], C. MONTOYA-PINO[2], S. WEYER[3], H. ARZ[4], H.-J. BRUMSACK[1]

[1] Mikrobiogeochemie, Insitut für Chemie und Biologie des Meeres (ICBM), Universität Oldenburg, P.O. Box 2503, D-26111 Oldenburg, Germany (sebastian.eckert@uni-oldenburg.de)

[2] Institut für Geowissenschaften, Universität Frankfurt, Altenhofer Allee 1, D-60431 Frankfurt a. M., Germany

[3] Institut für Geologie und Mineralogie, Universität zu Köln, Zülpicher Straße 49b, D-50674 Köln, Germany

[4] Geoforschungszentrum Potsdam (GFZ), Telegrafenberg, D-14473 Potsdam, Germany

During DSDP Leg 42B (Site 379A) in the Black Sea a sapropel of presumably Eemian age was recovered 99 m below the recent (Holocene) one (Ross, 1978). This was the first and only time this second sapropel was recovered until R/V *Meteor* cruise M72/5 in 2007, where this second sapropelic layer was again retrieved in two gravity cores (22-GC-3/7) at only 8 m depth. These sapropels were sub-sampled at high-resolution (2 to 6 mm). Because only one bulk sapropel sample was analyzed during the DSDP cruise (sample 19 in Ross, 1978) the sapropel was resampled at high-resolution in the Bremen Core Repository from the archive half. In all samples major and trace metals (e.g. Co, Cr, Cu, Fe, Mo, Ni, Re, U and V) were determined by XRF, ICP-OES and HR-ICP-MS. Organic and inorganic carbon as well as total sulfur were measured with standard techniques. In selected samples $\delta^{238}U$ and $\delta^{97}Mo$ were determined by MC-ICP-MS. In addition to a general inorganic-geochemical characterization, including a

lithological unit classification analogous to the Holocene one, a paleoenvironmental study by means of the vertical distribution of selected trace metals besides U and Mo isotopes was accomplished. The results show that the change from glacial to interglacial conditions slightly differs from the initial Holocene ingression of the Mediterranean Sea water over the Marmara Sea into the Black Sea. One reason might be the different situation in the Eastern Mediterranean Sea during the Eemian and the Holocene. While during the Eemian sapropel deposition in the Black Sea and Mediterranean Sea (*S5*) was synchronous, this is not the case during the Holocene (Units I and II in the Black Sea are not time equivalent to *S1*). On the basis of $\delta^{238}U$, $\delta^{97}Mo$, Fe/Al, Mo/Al and Re/Mo ratios an anoxic but less euxinic water column is indicated during the initial deposition of the Eemian sapropel. This might be due to a reservoir effect owing to the synchronous deposition of sapropel *S5* in the Eastern Mediterranean. For this reason sea water which enters the Black Sea during the Eemian might have been depleted in redox-sensitive trace metals. Therefore the Eemian sapropel is less enriched in trace metal than the Holocene one. Paleoproductivity proxies (e.g. Cu/Al, Ni/Al, P/Al, Sr_{xs}/Ca_{xs}, Ti/Ca and TOC,) suggest an increase in paleoproductivity during the Eemian interglacial due to an increased riverine nutrient inflow. To validate our new results a spatiotemporal comparison with the recent Black Sea sapropel (same location) and the Eastern Mediterranean *S5* sapropel (same time period) was undertaken. Our study implies that repeated sapropel formations in the Black Sea are linked to interglacial periods and reflect the global sea level rise and marine ingression through the Bosporus sill.

References:
Ross, D. A., 1978. Initial reports of the Deep-Sea Drilling Project Vol. XLII. U.S. Government Printing office, Washington D.C.

IODP

Viral infections as controlling factors of the deep biosphere?

T. ENGELHARDT, M. SAHLBERG, H. CYPIONKA, B. ENGELEN

Institut für Chemie und Biologie des Meeres, Carl-von-Ossietzky Universität Oldenburg,
Carl-von-Ossietzky Straße 9-11, D-26111 Oldenburg, Germany, http://www.pmbio.icbm.de

The marine deep biosphere represents the largest biotope on Earth harbouring about 70% of the total prokaryotic biomass. The "unseen majority" in the subsurface is involved in all main global biogeochemical cycles. Huge cell numbers are prone to extreme starvation leading to doubling times in the range of years to centuries. How life and death in this environment are regulated is not yet understood. Organisms from higher trophic levels appear to be absent in anoxic and highly compressed deep sediments. Whether viruses could be a factor for microbial mortality is unknown. Viral infections have been found to have a major impact on pelagic environments and on the microflora of the top 1-cm of the seafloor (Danovaro et al. 2008). Under the specific conditions in deep-subsurface sediments, bacteriophages might take over the role of the main predators, as anoxia and oligotrophy favour the importance of viruses as mortality factors. Furthermore, the fact that the viral shunt recycles organic compounds might be of special relevance to this severely nutrient-depleted habitat. In that case, the viral shunt within the deep subseafloor could make a significant contribution to the global carbon cycling and might have an impact on biogeochemistry, microbial diversity and evolution.

In our previous phage-induction experiments, representative isolates from our ODP Leg 201 culture collection (Batzke et al. 2007) were screened for the presence of lysogenic phages using the antibiotic mitomycin C (Chen et al. 2006). Six out of thirteen cultures from various phylogenetic groups, sampling sites and sediment depths showed a drop in cell density after virus induction. The phage morphology was visualized by transmission electron microscopy (TEM). Different morphotypes of myoviruses and siphovirus were identified, all with variations in size and shape. This morphologic diversity was confirmed by a size separation of phage-genomes. Three bacterial strains harboured even more than one prophage. While two DNA bands of different lengths were found for the two Vibrio-affiliated strains, five discrete DNA bands were detected for P. glucanolyticus strain P073A (Engelen et al. 2010).

A detailed analysis of phages from Rhizobium radiobacter populations is currently performed in the frame of a Master thesis (see poster M. Sahlberg et al.) All isolated phages were sent to the Broad Institute for complete genome sequencing. The resulting sequence information will be used to generate specific PCR-primers for an in-situ quantification of these phages. Additionally, we have investigated freshly collected sediments from IODP Exp. 323 to quantify the abundance of free viruses along a depth profile of IODP Site 1344. Furthermore, we have applied to sail on the "South Pacific Gyre Microbiology Expedition" to cultivate new host strains and to induce their prophages.

References:
Batzke A, Engelen B, Sass H, Cypionka H (2007) Phylogenetic and physiological diversity of cultured deep-biosphere bacteria from Equatorial Pacific Ocean and Peru Margin sediments. Geomicrobiology J 24:261-273
Chen F, Wang K, Stewart J, Belas R (2006) Induction of multiple prophages from a marine bacterium: a genomic approach. Applied and Environmental Microbiology 72: 4995-5001.
Danovaro R, Dell'Anno A, Corinaldesi C, Magagnini M, Noble R, Tamburini C, Weinbauer M (2008) Major viral impact on the functioning of benthic deep-sea ecosystems. Nature 454: 1084-U1027.
Engelen B, Engelhardt T, Sahlberg M, Cypionka H (2010) Bacteriophages as a component of the marine deep biosphere. Environ Microbiol (submitted, 22.01.2010)

IODP

Strengthening of the Walker and Hadley atmospheric circulations during the Pliocene-Pleistocene climate transition, 2.2-2.0 million years ago

J. ETOURNEAU [1], R. SCHNEIDER[1], T. BLANZ[1], P. MARTINEZ [2]

[1]Institut für Geowissenschaften, Universität zu Kiel, Ludewig-Meyn-Str., 24118 Kiel, Germany
[2] UMR CNRS 5805 EPOC, Université Bordeaux 1, Avenue des Facultés, 33405 Talence, France

In this study, we generated a new alkenone-based sea surface temperature (SST) gradient during the Pliocene-Pleistocene climate transition along the equatorial Pacific, between the IODP (Intergated Ocean Drilling Program)

Sites 806 and 1239. We found that the west-to-east SST gradient over the entire tropical Pacific irreversibly increased by 2 to 3°C between 2.3 and 1.8 Ma, in agreement with previous studies ([Jia et al., 2008; Wara et al., 2005), thus supposing a pronounced increase in atmospheric circulation from weak to strong zonal Walker circulation (WC) from Latest-Pliocene into Early-Pleistocene. Comparatively, evidence from other areas in, both, low-latitude Pacific and Atlantic Oceans, e.g. California, Peru and Benguela eastern boundary currents (Dekens et al., 2007; Liu et al., 2008; Etourneau et al., 2009), suggest an overall reorganization of the meridional Hadley circulation (HC), with its intensification ~2.2-2.0 Ma ago. We therefore emphasize that the evolution of both atmospheric circulation patterns in the tropical and subtropical regions during the Plio-Pleistocene transition were intimately coupled, probably tied to a narrowing of the tropical warm pool, and to the increase of the pole to equator temperature gradient. As supported by recent modelling studies (Haywood et al., 2007; Brierley et al., 2009) the intensification of both WC and HC was probably a result of the global cooling rather than a cause of the initiation of continental ice sheet formation at high latitudes, since the onset of extensive Northern Hemisphere glaciation (NHG) occurred much earlier, ~3.0 Ma ago, in the Early- to Mid-Pliocene. The establishment of strong WC and HC may have had in turn a strong impact on global climate change, acting as a negative feedback mechanism, by increasing the CO_2 release from the deep ocean to the atmosphere, and thus contributing to the slowdown in Plio-Pleistocene cooling 2.2-2.0 Ma ago.

References:
Brierley, C.M., Fedorov, A., Liu, Z., Herbert, T.D., Lawrence, K.T., & LaRiviere, J.P., Science, 323, 1714-1718 (2009).
Dekens, P.S., Ravelo, A.C. ,and M.D. McCarthy, Paleoceanography, 22, doi:10.1029/2006PA001394 (2007).
Etourneau, J., Martinez, P., Blanz, T., & Schneider, R. Geology, G25733 (2009).
Haywood, A.M., Valdes, P.J., & V.L. Peck, Paleoceanography, 22, doi:10.1029/2006PA001323 (2007).
Jia, G., Chen, F., & Peng, P. GRL, 35, doi: 10.1029/2008GL034792 (2008).
Liu, Z., Altabet, M.A., & Herbert, T. G3, doi: 10.1029/2008GC002044 (2008).
Wara, M., Ravelo, A.C., & Delaney, M.L. Science, 316, 1303-1307 (2005).

IODP

Biogeochemistry of North Pond Sediments: Results from the R/V M.S. Merian Site Survey in Support of IODP Proposal 677-Full "Mid-Atlantic Ridge Microbiology"

T.G. FERDELMAN[1], W.ZIEBIS[2], J. MCMANUS[3], A. PICARD[1,4], J. MURATLI[3], M. MORANDO[2], F. SCHMIDT-SCHIERHORN[5], SEBASTIAN STEPHAN[5], W. BACH[4,5], H. VILLINGER[5] & K.J. EDWARDS[2]

[1]Max-Planck-Institute for Marine Microbiology, Bremen, Germany
[2]Dept. of Biological Sciences, University of Southern California, Los Angeles, CA, USA
[3]College of Oceanic and Atmospheric Sciences, Oregon State University, Corvallis OR, USA
[4]MARUM, Centre for Marine Environmental Sciences, University of Bremen, Bremen, Germany
[5]Department of Geosciences, University of Bremen, Bremen, Germany

The North Pond sediment package (70 km^2) is centered at approximately 22° 46' N and 46° 06' W along the Mid-Atlantic Ridge. The western flank of the Mid-Atlantic Ridge, at 22°45'N is characterized by depressions filled with sediment and surrounded by high relief topography of 7 Ma old basement. The largest depressions are 5 km to 20 km wide and sediment thickness varies but can reach 400 m. This sediment pond lies below the oligotrophic central North Atlantic with sediments that are typically less than 0.3% organic carbon and about 50% calcium carbonate. Linear sedimentation rates are approximately 0.03 m a-1. Furthermore, this site lies on roughly seven million year old crust and appears to maintain active fluid circulation below the sediment package through the underlying permeable rock (Langseth et al., 1992). This location harbors significant potential as a microbial observatory, and is the target of both past and future ocean drilling expeditions.

North Pond was revisited in Spring 2009 with the German research vessel M.S. Merian (MSM 11/1) as part of an IODP site evaluation. Investigations included heat-flow, single-channel seismic and bathymetry surveys, as well as gravity coring. Oxygen measurements and pore water sampling (25 cm depth intervals) were performed directly on intact sediment cores, which were subsequently sampled for microbiological analyses, as well as for incubation experiments to test for autotrophic and heterotrophic microbial activity. The entire sediment column down to > 8 m sediment depth contained oxygen, the deepest penetration of oxygen that has been measured in the seafloor of the Atlantic. The steepest decrease in oxygen concentrations occurred within the top ~ 60 cm surface layer, and was consistent across all stations. In the central part of the sediment pond oxygen decreased continuously with depth, indicating an active aerobic microbial community while nitrate concentrations increased. In contrast, along the northern and western rims of North Pond, oxygen concentrations remained surprisingly constant with depth at values around 170 µM. Moreover, at 3 locations along the north shore, oxygen increased towards the bottom of the cores, indicating an upward supply of oxygen from the underlying basaltic basement. The straight oxygen profiles, beneath the surface layer, can be explained by a balance between upward diffusion and consumption of oxygen within the sediment column. Nutrient profiles confirmed that, in contrast to the central part of the pond where concentration profiles (nitrate, silica) reflected diagenetic processes, the sediment cover at the edges seemed to be influenced by transport processes. This is the first evidence that oxygen can be used as a tracer for deeply situated oxygen-rich reservoirs at the sediment-basalt interface. Evidence of upward transport of oxidants from basaltic aquifers to deeply buried sediments has raised questions on microbial respiration and energy cycling within the deep biosphere. Pore water nutrient profiles and incubation experiments confirmed active microbial communities throughout the sediment layer, as well as the influence of upward transport of oxidants on microbial processes in deeply buried sediments.

References
Langseth, M.G., K. Becker, R.P. Von Herzen, and P. Schultheiss. 1992. Heat and fluid flow through sediments on the western flank of the Mid-Atlantic Ridge: A hydrogeological study of North Pond. Geophys. Res. Lett. 19: 517-520.

ICDP

Development of an ultra-high resolution neutron computed tomography system for the characterisation of drill cores

A. FLAWS[1], K.-U. HESS[1], B. SCHILLINGER[2], Y. LAVALLE[1], D.B. DINGWELL[1]

[1]Geo- und Umweltwissenschaften, Ludwig-Maximilians-Universität, Theresienstr. 41, 80333 Munich, Germany
[2]Forschungsreaktor FRM-II, Technische Universität München, Lichtenbergstr. 1, 85747 Garching, Germany

In recent years, Neutron Computed Tomography (NCT) has established itself as a mature technique for non-destructive 3D imaging. The long neutron penetration length has long been used for industrial imaging of large objects and those with high metal contents. However, until now it has not enjoyed extensive application in general research due to its limited availability and spatial resolution. Today, the application of state of the art detector systems at the high flux, high collimation ANTARES beamline has lead to significant improvements in spatial resolution and contrast for geomaterial imaging. A resolution of 30 µm is now possible with a field of view of 65 mm, a level which is now comparable with X-ray computed tomography (XCT) and useful for geomaterial analysis. Although smaller nominal pixel resolutions are achievable for smaller view fields, they are ultimately limited by the scintillation screen. Thin 10 µm scintillators have been applied for a limited number of ultra-high resolution (order 10 µm) studies. However, the increased exposure time and image noise makes this an unattractive option. We have begun the development of new thin scintillator screens to combat this problem and have begun testing the first prototypes.

A software suite has been developed for reconstruction, image processing, segmentation and quantification, using fast algorithms which have been optimised for the unique challenges posed by geomaterial research. This software allows us to distinguish between the many different mineral phases present in natural samples, even in cases with high image noise or low phase contrast. It allows the user to build a database of objects: such as crystals, cracks and pores. This database can then be characterised, yielding particle size distributions, anisotropy, crack width and orientation. This has proved to be a valuable tool for geomaterial research and is now being used to test models of rheological processes quantitatively.

Samples from the drilling and the dome on Unzen have been studied by NCT. The methods sensitivity to hydrogen results in excellent phase contrast between hydrous and non-hydrogeous minerals. Due to the rarity of Unzen drill core samples, preliminary deformation experiments have been carried out on similar material from the Colima volcano, providing us with new insights into the process of magma fragmentation. We have also obtained the first XCT images of the Unzen samples. The information provided by NCT and XCT imaging is complimentary, meaning that by combining the two methods we will be able to distinguish between more mineral phases than by using either method individually. At this stage the comparison is being done manually. However, the XCT information will soon be incorporated into the tomography analysis suite.

ICDP

Holocene Dust Storms and Flood Events in the Dead Sea Region -

Reconstructing high resolution records of climatic variability by means of thin-section microscopy and µ-XRF-analysis of Dead Sea sediments

U. FRANK, M. J. SCHWAB, S. PRASAD, P. DULSKI & A. BRAUER

Helmholtz-Zentrum Potsdam, Deutsches GeoForschungsZentrum, Telegrafenberg, D-14473 Potsdam

During the last years, several joint projects were carried out by Israel and German scientist focussing on the reconstruction of the climatic variability and evolution in the Dead Sea and Jordan region. Sedimentological, microstratigraphical, palynological and magnetic methods were used to enhance the knowledge about the interactions between climate and environmental response in this climate sensitive region, as recorded in lacustrine sediments.

The sediment in the Dead Sea basin is composed of alternating fine layers of detrital clay layers and authigenic aragonite, with intercalated sand, halite and gypsum layers. The succession, composition and thickness of these layers are mainly controlled by changes in precipitation/evaporation ratio and runoff/evaporation ratio, thus making it an ideal candidate for paleoclimatic studies. Detailed microscopical analysis of a varved sediment succession from the Lisan-formation (Prasad et al., 2009), the precursor of the Dead Sea, already revealed, that North Atlantic Heinrich events, multidecadal NAO, and solar cyclicality are reflected in laminae thickness during MIS2 (Prasad et al., 2004). A first record of limnological changes in the Dead Sea basin, in terms of sea level variations reflecting regional paleoclimate variations during the last 10 ka, has also been reconstructed, using multiple, well dated sediment cores and profiles recovered from three sites on the western Dead Sea shore (Ken-Tor et al., 2001; Migowski et al. 2004, Migowski et al., 2006). The available data clearly demonstrate the unaltered nature of these sediments indicating their suitability for palaeoenvironmental reconstruction.

The main objective of this new investigation is to apply a novel methodological approach to identify flood and dust storm layers in Dead Sea sediments and to establish Holocene time series of these event deposits. To achieve this goal, the different phases of sedimentation (clastic to evaporitic) which are related to periods of abrupt seasonal changes in rainfall/evaporation in the northern Dead Sea region will be identified by means of petrographic thin section analyses, X-ray fluorescence element scanning and high-resolution magnetic susceptibility measurements. The geochemical investigations will reveal the element composition of the sediment laminae. This discrimination allows the characterization of different types of sediment sequences (i.e. limnic, fluvial, eolian sediment) in respect of their origin. The resolution of the resulting set of multi-proxy data will be below 1.0 mm thus allowing identification of individual dust storm and flood layers down to microscopic scale. The material chosen for investigations will be taken from the sediment cores from Ein Feshka, Ein Gedi and Ze'elim on the western shore of

the Dead Sea. All these records are located along a North-South climatic gradient at the western shore of the Dead Sea. Results from previous low resolution studies on these cores will be integrated. Cores from all three sites will be correlated and synchronized in great detail in order to disentangle local from regional signals. In addition to establishing long time series of individual extreme events, the expected data will allow for recognising decadal-scale variability in the eastern Mediterranean climate system during the Holocene. A particular focus will be on deciphering the influence of the North Atlantic Oscillation (NAO) and solar irradiation changes.

Detailed correlation of all records should also allow for an extension of the seismic history record integrating the seismites identified in the Ein Feshka sediment core. A further aim of this study is to calibrate the rock magnetic records, especially the magnetic susceptibility record with its high temporal resolution, versus the sedimentological and geochemical results, thus enabling the use of this parameter as a proxy for arid periods in further studies of Dead Sea sediments.

Following this research plan, a scientific procedure will be established, that will be adjusted to the specific problems generated by the uniqueness of the sediments from the Dead Sea. This study will therefore not only contribute to the scientific objectives of the Dead Sea Deep Drilling Project as applied to the ICDP, but will deliver tools to reach this goal.

References:

Ken-Tor, R., A. Agnon, Y. Enzel, M. Stein, S. Marco & J. F. W. Negendank (2001). "High-resolution geological record of historic earthquakes in the Dead Sea basin." J. Geophys. Res. 106: 2221-2234.

Migowski, C., A. Agnon, R. Bookman, J. F. W. Negendank & M. Stein (2004). "Recurrence pattern of Holocene earthquakes along the Dead Sea transform revealed by varve-counting and radiocarbon dating of lacustrine sediments." Earth Planet. Sci. Lett. 222: 301-314.

Migowski, C., Stein, M., Prasad Sushma, and Negendank J.F.W. (2006b). Holocene climate variability and cultural evolution in the Near East. Quaternary Research, 66(3), pp: 421-431.

Prasad, S., H. Vos, J. F. W. Negendank, N. Waldmann, S. L. Goldstein & M. Stein (2004). "Evidence from Lake Lisan of solar influence on decadal- to centennial scale climate variability duirng marine oxygen isotope stage 2." Geology 32: 581-584.

Prasad Sushma, Negendank, J.F.W., Stein, M. (2009). Varve counting and its potential for determining reservoir age fluctuations in palaeolake Lisan. Journal of Quaternary Science 24(7), pp: 690-696.

IODP

Millennial-scale changes in ice volume and North Atlantic SST during MIS 100 (latest Pliocene)

O. FRIEDRICH[1,2], C.T. BOLTON[2], C. BEER[2], P.A. WILSON[2], R. SCHIEBEL[3]

[1]present adress: Institut für Geowissenschaften, Goethe Universität Frankfurt/Main
[2]National Oceanography Centre Southampton, University of Southampton
[3]Laboratoire des Bio-Indicateurs Actuels et Fossiles, Universite d'Angers

Given its proximity to the large dynamic ice-sheets of the northern hemisphere and the role in deep-water formation the North Atlantic represents one of the climatically most sensitive regions on Earth. Hence, data sets in key areas like the North Atlantic are extremely useful in order to e.g. quantify and reconstruct the paleoceanographic dynamics of the latest Pliocene. The broad objective of this study is to quantify, at millennial time-scales, paleoclimatic and paleoceanographic changes during the Late Pliocene (MIS 99 to 101). These objectives will be met by the integration of planktic and benthic $\delta^{18}O$ and the Mg/Ca paleotemperature method and its use to allow a differentiation between changes in global ice-volume and SST.

The recently drilled Integrated Ocean Drilling Program Site 1313 from the central North Atlantic (50°N) provides an ideal opportunity to tackle these questions. A demonstrably complete Mid to Late Pliocene section for Site 1313 was recovered, consisting mainly out of nannofossil ooze and nannofossil silt. A very high sedimentation rate and the abundant and well-preserved microfossils provide the requirements for high-resolution studies on planktic foraminifera and optimal reconstruction of the phasing of SST records and their relationship to salinity and ice-sheet changes on a high temporal resolution.

For this study 145 samples in 2-cm spacing (resulting in a ~400 years resolution) of isotope stages MIS 99 to 101 were prepared for parallel Mg/Ca and stable isotope analyses of benthic (O. umbonatus, C. wuellerstorfi) and planktic foraminifera (G. ruber). Our sub-millennial Mg/Ca and stable isotope record indicates millennial-scale sea-surface temperature fluctuations in the North Atlantic during marine isotope stage 100 (Late Pliocene). These temperature fluctuations occur with a cyclicity of ~1,500 years, strongly related to Dansgaard-Oeschger-cycles of the cooler Pleistocene climate regime. Abundance peaks in IRD as well as ice-volume fluctuations are shown to occur on an approximately 8000 year spacing.

Our data show that latest Pliocene millennial-scale climate fluctuations occur on the same spacing than compared to the Late Quaternary, but with much smaller amplitudes.

ICDP

The Archaean-Palaeoproterozoic transition as recovered in the FAR-DEEP drill cores: First results of detrital U-Pb geochronology and provenance

C. GÄRTNER[1], H. BAHLBURG[1], V.A. MELEZHIK[2,3], A. LEPLAND[2], J. BERNDT[4], E. KOOIJMAN[4] AND THE FAR-DEEP SCIENTISTS

[1]Institut für Geologie und Paläontologie, Westfälische Wilhelms-Universität Münster, Germany
[2]Geological Survey of Norway, Trondheim, Norway
[3]Centre for Geobiology, University of Bergen, Norway
[4]Institut für Mineralogie, Westfälische Wilhelms-Universität Münster, Germany

The Archaean-Palaeoproterozoic transition is characterized by several events that were important for the evolution of the Earth system (e.g. Melezhik et al., 2005b). The break-up of the supercontinent Kenorland and other plate tectonic reorganisations coincided with major global environmental changes. During the Fennoscandian Arctic Russia - Drilling Early Earth Project (FAR-DEEP), which is part of the International Continental Scientific Drilling Program (ICDP), relevant volcano-sedimentary successions of early Palaeoproterozoic age, representing a 500 Ma interval, were drilled in the Pechenga and Imandra-Varzuga Greenstone belts (Kola Peninsula Province), as well as in the Onega basin in Russian Fennoscandia

(Karelian Province, Fig. 1; Melezhik et al, 2005b). We applied U-Pb-geochronology on detrital zircons by LA-ICP-MS to investigate provenance of the sedimentary rocks and to improve age constraints on the duration of three of these events: 1) the Huronian Glaciation, which is the first known worldwide glaciation from 2.45-2.22 Ga (Young et al, 2001), 2) the Lomagundi-Jatuli event, occurring from 2.3-2.06 Ga (Karhu & holland, 1996; Shields & Veizer, 2002, Melezhik et al., 2007), therefore following the glaciation and being characterized by a large positive excursion of $\delta^{13}C$ in sedimentary carbonates, and subsequently 3) the Shunga event, which was the first deposition of very Corg-rich sediments, so-called "shungites" (Melezhik et al, 2005a). Hitherto 14 samples of sandstone, greywackes, siltstone and tuffs from five formations in the Pechenga and Imandra-Varzuga Greenstone belts were analysed.

The results of detrital zircon dating for all samples provided an age range from 3.5 to 1.85 Ga having one prominent age-group of 2.9-2.5 Ga in all but two samples (Fig. 2). The youngest ages in individual samples vary due to their stratigraphic position. The youngest zircons from the Seidorechka Sedimentary Formation below Huronian glacial deposits in the Imandra-Varzuga Greenstone Belt yielded ages around 2.42 Ga (Fig. 2a), which are interpreted as an age close to the onset of the Huronian Glaciation and as the maximum depositional age for this formation. Similar ages for the Seidorechka Formation have been also reported by Amelin et al. (1995). Another age-peak in this formation is at 2.5 Ga, related to detrital zircons from the underlying Archaean basement. Zircon ages from the Polisarka Sedimentary Formation above Huronian diamictites in the Imandra-Varzuga Greenstone Belt and from the Neverskrukk Formation in the Pechenga Greenstone Belt indicate that the glaciation had apparently ended at 2.22 Ga (Fig. 2b). Young et al. (2001) reported similar ages for the Huronian Supergroup in Canada, where diamictites related to this glaciation were found. The results from the Fennoscandian Shield provide independent evidence for a simultaneous glaciation on both the Canadian and Fennoscandian shields. However, the age distributions of the Neverskrukk and Polisarka formations are significantly different. The zircon grains from the Neverskrukk Formation yielded much less zircons in the range of 2.7-2.4 Ga, in contrast to the Polisarka Formation, which provided less zircon ages around 2.8 Ga and populations around 2.5-2.4 Ga and 2.7-2.6 Ga respectively (Fig. 2a,b).

The youngest zircon ages from the sequence containing isotopically heavy carbonates of the Kuetsjärvi Sedimentary Formation in the Pechenga Greenstone Belt suggest that the Lomagundi-Jatuli event started around 2.32 Ga and that its end is younger than 2.06 Ga (Fig. 2c). A similar age constraint for the Kuetsjärvi Sedimentary Formation has also been reported by Melezhik et al. (2007). The main age group for the lower Kuetsjärvi Sedimentary Formation ranges from 2.6-3.0 Ga (Fig. 2c), the younger ages indicate a maximum depositional age of 2.32 Ga, which is considered as the beginning of the Lomagundi-Jatuli event. One sample from the middle Kuetsjärvi Sedimentary Formation has a prominent age group around 2.06 Ga, but contains some ages of 2.9-2.4 as well. The absence of zircons with ages of 2.3-2.1 Ga is remarkable (Fig. 2c).

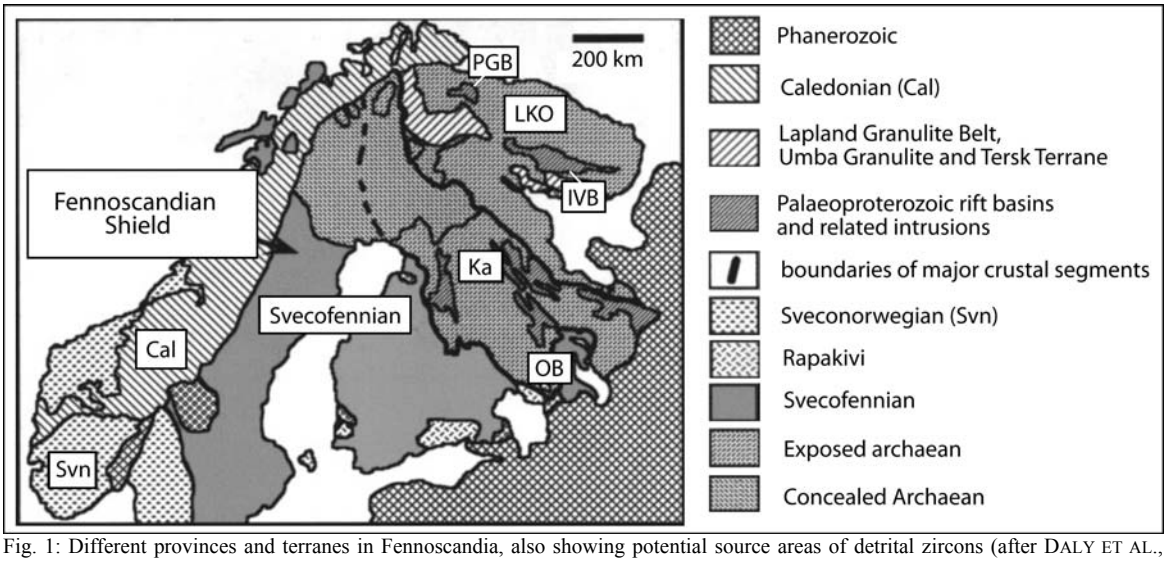

Fig. 1: Different provinces and terranes in Fennoscandia, also showing potential source areas of detrital zircons (after DALY ET AL., 2001). IVB – Imandra-Varzuga Greenstone Belt, Ka – Karelian Province, LKO – Lapland-Kola-Orogen/Kola Province, OB – Onega Basin, PGB – Pechenga Greenstone Belt.

Age constraints of ca. 2.0-1.9 Ga (Fig. 2d) for the beginning of the Shunga Event were obtained by dating zircons from the Kolasjoki Sedimentary Formation in the Pechenga Greenstone Belt. As the Shunga event followed the Lomagundi-Jatuli event and the latter had ended at 2.06 ga, these zircon ages confine the transition from the Lomagundi-Jatuli event to the Shunga event at 2.06-2.0 Ga, considering an analytical error. The two samples from the Kolasjoki Sedimentary Formation derive from similar stratigraphic positions, only seperated by a carbonate layer. This position is reflected in distinct age groups of ca. 2.1-2.0 Ga and 3.0-2.7 Ga below the carbonate layer and ca. 1.9 Ga above (Fig. 2d). Both samples show a lack of ages from 2.4-2.1 Ga, similar to the Neverskrukk and Kuetsjärvi Sedimentary formations, which include all samples from the Pechenga Greenstone Belt.

Another aim of the study is to investigate provenance and source areas of the analysed detrital zircons. The largest age group around 2.9-2.5 Ga points to orogenic processes during the formation of the Fennoscandian

Shield. Due to collisional and accretional processes during the Saamian (3.1-2.9 Ga) and Lopian orogeny (2.9-2.6 Ga; Gaál & Gorbatschev, 1987) recycled detritus from surrounding Archaean granitoid sources in the Kola Belt and the Neverskrukk, Kuetsjärvi and Kolasjoki Sedimentary formations from the Pechenga Greenstone Belt, whereas input into the Pechenga Greenstone Belt must have been rather limited.

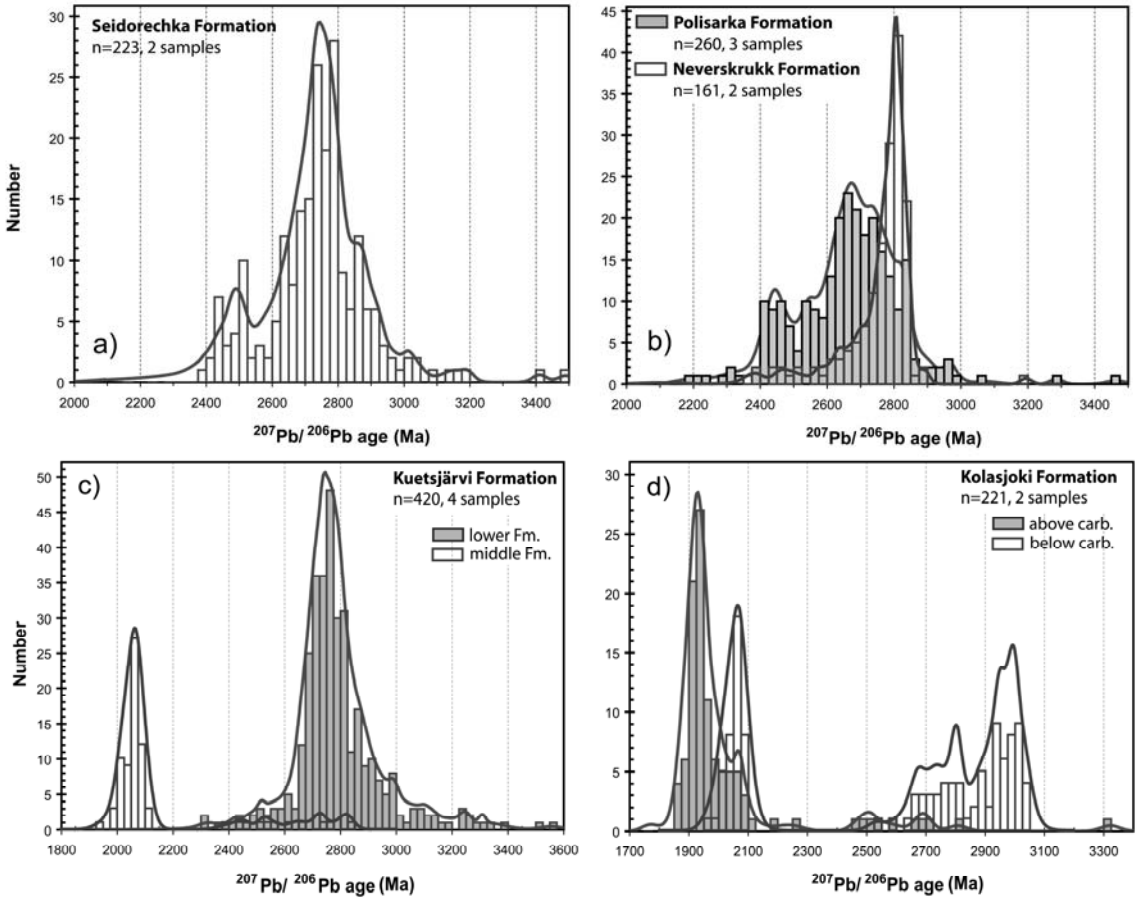

Fig. 2: a) Zircon ages for the Seidorechka Sedimentary Formation, b) Zircon ages for the Polisarka and Neverskrukk formations, c) Zircon ages for the middle and lower Kuetsjärvi Sedimentary Formation, d) Zircon ages for the Kolasjoki Sedimentary Formation (shown are only ages with >90% concordance).

Peninsula Province was transported into the study area (Fig. 1). These granitoids form the basement of the greenstone belts and its presence is also suggested in the Kola Peninsula Province on the northern Fennoscandian Shield (Gaál & Gorbatschev, 1987). The age interval of 2.5-2.4 Ga mainly occurs in samples from the Imandra-Varzuga Greenstone Belt (Seidorechka and Polisarka Sedimentary formations), in the Pechenga Greenstone Belt such ages are significantly less common. At 2.50 and 2.44 Ga, two periodes of earliest Palaeoproterozoic magmatism occurred (Amelin et al., 1995), which might be a source area for detrital zircons from the Seidorechka and Polisarka Sedimentary formations, as well as the basement below. After the break-up of the supercontinent Kenorland, dispersed terranes reassembled to the Lapland-Kola orogen in the Paleoproterozoic. Additionally, terranes of juvenile Palaeoproterozoic crust generated in an island-arc setting were accreted (Daly et al., 2001). This period of rifting from 2.5-2.1 Ga is marked by mafic plateau volcanicsm, intracratonic sedimentation and continental rift systems (Gaál & Gorbatschev, 1987). During these processes detrital material from several terranes was supplied to the stratigraphically younger sedimentary successions like the Polisarka Formation from the Imandra-Varzuga Greenstone

Zircon grains with ages of 2.1-1.9 Ga derived from sources connected to the formation of the Lapland-Kola orogen and the evolution of the composite Svecofennian orogen, a collage of microcontinents, inducing island arc/oceanic plateau associations and island arc magmatism in the Kola region.

References:

Amelin, Yu.V., Heaman, L.M., Semenov, V.S. (1995): U-Pb geochronology of layered mafic intrusions in the eastern Baltic Shield: implications for the timing and duration of Paleoproterozoic continental rifting. Precambrian Research, 75, p.31-46.

Daly, J.S., Balagansky, V.V., Timmerman, M.J., Whitehouse, M.J., de Jong, K., Guise, P., Bogdanova, S., Gorbatschev, R., Bridgwater, D. (2001): Ion microprobe U-Pb zircon geochronology and isotopic evidence for a trans-crustal suture in the Lapland-Kola Orogen, northern Fennoscandian Shield. Precambrian Research, 105, p. 289-314.

Gaál, G. & Gorbatschev, R. (1987): An Outline of the Precambrian Evolution of the Baltic Shield. Precambrian Research, 35, p. 15-52.

Karhu, J.A. & Holland, H.D. (1996): Carbon isotopes and rise of atmospheric oxygen. Geology, v. 24, p. 867-870.

Melezhik, V.A., Huhma, H., Condon, D.J., Fallick, A.E., Whitehouse, M.J. (2007): Temporal constraints on the Paleoproterozoic Lomagundi-JAtuli carbon isotopic event. Geology, v. 35, no. 7, p. 655-658.

Melezhik, V.A., Kump, L., Strauss, H., Fallick, A.E., Hanski, E., Hawksworth, C.J., Lepland, A., Prave, A., Philippov, N. (2005a): Fennoscandian Arctic Russia – Drilling Early Earth Project (FAR – DEEP). Full proposal to the International Continental Scientific Drilling Program.

Melezhik, V.A., Fallick, A.E., Hanski, E., Kump, L., Lepland, A., Prave, A., Strauss, H. (2005b): Emergence of the Modern Earth System during the Archean-Proterozoic Transition. GSA today, 15, p. 4-11.

Young, G.M., Long, D.G.F., Fedo, C.M., Nesbitt, H.W. (2001): Paleoproterozoic Huronian basin: product of a Wilson cycle punctuated by glaciations and a meteorite impact. Sedimentary Geology, 141-142, p. 233-254.

ICDP

Origin and development of maar Laguna Potrok Aike, Southern Patagonia, Argentina – seismic data

A. C. GEBHARDT[1], M. DE BATIST[2], F. NIESSEN[1], F. S. ANSELMETTI[3], D. ARIZTEGUI[4], T. HABERZETTL[5], C. OHLENDORF[6], B. ZOLITSCHKA[6]

[1]Alfred Wegener Institute for Polar and Marine Research, 27568 Bremerhaven, Germany
[2]Renard Centre of Marine Geology, University of Gent, 9000 Gent, Belgium
[3]Eawag, Swiss Federal Institute of Aquatic Science and Technology, Department of Surface Waters, 8600 Dübendorf, Switzerland
[4]Section of Earth and Environmental Sciences, University of Geneva, 1205 Geneva, Switzerland
[5]GEOTOP Research Centre, P. O. Box 8888, Succ. Centre-ville, Montréal, Québec, Canada
[6]Institute of Geography, University of Bremen, 28359 Bremen, Germany

Seismic reflection and refraction data provide insights into the sedimentary infill and the underlying volcanic structure of Laguna Potrok Aike, a maar lake situated in the Pali Aike Volcanic Field, Southern Patagonia. The lake has a diameter of ~3.5 km, a maximum water depth of ~100 m and a presumed age of ~770 ka. Its sedimentary regime is influenced by climatic and hydrologic conditions related to the Antarctic Circumpolar Current, the Southern Hemispheric Westerlies and sporadic outbreaks of Antarctic polar air masses. Multiproxy environmental reconstructions of the last 16 ka document, that this terminal lake reacts highly sensitive to climate change. Laguna Potrok Aike has recently become a major focus of the International Continental Scientific Drilling Program (ICDP) and was drilled down to 100 m below lake floor in late 2008 within the PASADO project.

Seismic reflection data show relatively undisturbed, stratified lacustrine sediments at least in the upper ~100 m of the sedimentary infill but are obscured possibly by gas and/or coarser material in larger areas. A model calculated from seismic refraction data reveals a funnel-shaped structure embedded in the sandstone rocks of the surrounding Santa Cruz Formation. This funnel structure is filled by lacustrine sediments of up to 370 m in thickness. These can be separated into two distinct subunits with low acoustic velocities of 1500-1800 m s-1 in the upper subunit pointing at unconsolidated lacustrine muds, and enhanced velocities of 2000-2350 m s-1 in the lower subunit. Below these lacustrine sediments, a unit of probably volcanoclastic origin is observed (>2400 m s-1). This sedimentary succession is well comparable to other well-studied sequences (e.g. Messel and Baruth maars, Germany), confirming phreatomagmatic maar explosions as the origin of Laguna Potrok Aike.

Seismic reflection data of the uppermost 100 m of the sediments reveal a rather dynamic development of the lake: on top of pelagic sediments a desiccation horizon is found, probably with sand dunes in the eastern part of the lake basin. These are overlain by a series of paleo shorelines documenting the history of lake level rise in this early stage of the newly formed lake. While this new lake formed in the central and eastern part of the maar depression, the western part probably was filled by stacked coarse-grained, delta-type sediments. The latter quite likely derive from the hinterland of the only inlet that is sporadically active at present. After this early lake stage, a stage of probably rapid lake level rise can be observed in the seismic reflection data.

ICDP

School project about paleoclimate research:

ICDP expedition at Lake El´gygytgyn enters the class room

J. GOTTSCHALK[1], A. J. KOPF[2], M. MELLES[3] AND EL´GYGYTGYN SCIENTIFIC PARTY

[1]University of Bremen, Faculty of Geoscience, Bibliothekstrasse 1, 28359 Bremen, Germany; gottscha@uni-bremen.de
[2]University of Bremen, Center for Marine Environmental Sciences, Leobener Strasse, 28359 Bremen, Germany
[3]University of Cologne, Institute of Geology and Mineralogy, Zuelpicher Str. 49a, 50674 Cologne, Germany

In the spring of 2009, Lake El´gygytgyn in northeast Siberia was the location of an ICDP expedition, which undertook tremendous efforts to recover the longest climate archive of the terrestrial Arctic. Its value is immeasureable due to an absence of desiccation and glaciation in the lake history. One of the major achievements is a 315 m long sedimentary record, that largely documents the climate and environmental history since the Early Pliocene. Since it is also a difficult task to make climate research accessable for non-scientists, especially for pupils, we arranged a school project in the High school of Wittstock (Brandenburg, Germany) for 60 pupils at the age of 16 years during the period 26.01. to 28.01.2010. Particular emphasis was put on the scientific background, life, work and safety aspects of the ICDP expedition at Lake El´gygytgyn, that stem from my personal experience during my participation in that expedition. To make the pupils get acquainted with the approaches of paleoclimate research we cored sediment records from the frozen surface of a pond ("Dosseteich") in the vicinity of the school. Thanks to the North German winter this year, weather conditions during coring at Dosseteich were almost equivalent to El´gygytgyn conditions. The obtained gravity cores were used for sediment analyses by different pupil groups, to study e.g. the microfossil content, chemical properties and geological features. The pupils´ task was to concentrate on one method in analysing the cores and report results back to their fellow pupils. The results were then compared to three ODP core sections representing different climatic regions, i.e. from Western Spitzbergen, the Eastern Mediterranean and offshore Namibia, all kindly provided by the IODP Core Repository of Bremen University. The school project was a great success and the major outcome for the pupils was that Lake El´gygytgyn should be favored over Dosseteich Wittstock as an important climate archive recording the distant past.

More information can be found at http://www.gymwk.de/faecher/geografie/geo_index.htm.

ICDP

Microbial driven methane dynamic in the Siberian Arctic during glacial-interglacial climate changes

J. GRIESS[1,2], K. MANGELSDORF[2], D. WAGNER[1]

[1]Alfred Wegener Institute, Research Unit Potsdam, Telegrafenberg A45, 14473 Potsdam, Germany
[2]Helmholtz Centre Potsdam, GFZ German Research Centre for Geosciences, Telegrafenberg B423, 14473 Potsdam, Germany

Arctic permafrost environments play an important role within the global methane cycle. Thawing of permafrost and the suggested release of this climate relevant trace gas, due to an increased microbial turnover of organic carbon and from ancient methane reservoirs, represent a potential risk to global warming. For the prediction of a future development of the permafrost environment and its contribution to the global atmospheric carbon budget, it is important to understand how this system reacted to environmental changes in the past. These changes in climate may cause chemical and physical variations in sedimentary column and thus, we expected changes in the composition of key microorganisms being implicated in methane cycle. Therefore, quantitative and qualitative analyses of the variations in composition of bacterial and archaeal communities involved in the Siberian methane cycle in Holocene and Late Pleistocene were conducted.

The El'gygygtgyn permafrost core and lake sediments of 142 m and 517 m length, respectively, were recovered within the ICDP project "Scientific Drilling in El'gygytgyn Crater Lake" from November 2008 to May 2009. In addition to that, a 23 m long permafrost core drilled in 2002 on Kurungnakh Island, Lena-Delta, Siberia, was examined. Permafrost environments can be quite different. Whereas the terrestrial core from El'gygytgyn represent a dry and TOC poor habitat, the permafrost core drilled on Kurungnakh Island was taken in a water saturated and TOC rich environment. These two sites will be compared. However, in the current abstract we will focus on the results of the Kurungnakh permafrost core.

Our studies on the reconstruction of the methane cycle in Siberian permafrost deposits combines biogeochemical and molecular microbiological methods. As a general result it was shown, that it was possible to recover lipid biomarker and intact DNA throughout the Kurungnakh permafrost sequence that comprises sediments of the holocene and late pleistocene. First analyses of intact glycerol dialkyl glycerol tetraethers (GDGTs) were conducted. GDGTs provide paleo-signals of archaeal and bacterial communities, since these core lipids are relatively stable outside intact cells. Highest amounts of ether lipids were found in the upper layer and at the bottom of the core. Generally, the results of GDGT analyses correlate to measured contents of total organic carbon (TOC) and concentrations of in-situ methane of the deposits. Total GDGT contents show highest concentrations with 495 ng/g sediment at 122 cm depth, with of 70 ng/g sediment at 1184 to 1745 cm and with about 400 ng/g sediment at 2320 cm depth. Furthermore, these biomarkers can be distinguished between biomarkers representing signals of paleo-archaeal and paleo-bacterial communities (depending on the tetraether alkyl bridges). Archaeol concentration varied between 3.84 and 62.5 ng/g sediment. The highest amounts were measured on top and bottom of the core and at a peak at 1745cm depth.

Additionally, the presence of aerobic methane oxidizing bacteria (MOB) was analyzed using diploptene (Hop-22(29)ene), a biomarker that can be found in methane oxidizing bacteria. The variability of the diploptene distribution correlates to measured rates of methane and content of TOC. Diploptene can be regarded as a paleo-signal for MOBs being present during time of sedimentation of the respective deposits (upper "aerobic" active layer). The fact that sedimentary intervals with high amounts of trapped methane (presumably intervals with in-situ methane production) also contain high contents of diploptene suggests that these sediments released also high amounts of methane in the past being the host of considerable aerobic methanotrophic communities.

To complete our information on the qualitative composition of microbial communities, DNA-based analyses were conducted using archaeal and methanotrophic specific primer combinations, whereas amplicons were subsequently analyzed by DGGE and clone libraries. Fingerprints of archaeal 16 S rRNA gene sequences of the different permafrost samples show variations within the vertical profile. Sequence analyses showed a distinct diversity of methanogens affiliated with Methanobacteriaceae, Methanosarcinaceaea and Methanomicrobiaceae. Highest diversity of methanogens could be detected at depth of 1507 cm and 1745 cm, which were also characterized by high amounts of archaeol.

Both biogeochemical as well as molecular methods revealed variation within the composition of past and present microbial communities and showed indications of response to climate changes.

IODP

Millennial Scale Changes in Sediment Flux on the Blake-Bahama Outer Ridge During Marine Isotope Stage 3: Implications for Deep Current Variability

J. GRUETZNER[1,3], M. J. VAUTRAVERS[2]

[1]Alfred-Wegener-Institut für Polar- und Meeresforschung, Bremerhaven, Germany (Jens.Gruetzner@awi.de)
[2]British Antarctic Survey, Cambridge, UK
[3]formerly at MARUM - Zentrum für Marine Umweltwissenschaften, Universität Bremen, Germany

The most intense export of North Atlantic deep and intermediate water masses occurs within the Deep Western Boundary Current (DWBC) along the Canadian and North American continental margin. Measurements of DWBC transport velocities at the Blake Outer Ridge showed volume transport of ~18 Sv (1 Sv = 1 x 10^6 m^3 s^{-1}) for all water flowing equator ward below a potential temperature of 6C [*Stahr and Sanford*, 1999]. The depositional environment is strongly influenced by changes in the strength and position of the DWBC that preferentially eroded sediments at the Canadian continental margin [*Giosan et al.*, 2002] and led to the sediment drifts in the Blake-Bahama Outer Ridge (BBOR) region. A depth transect (2164 to 4775 m) of sites drilled into the BBOR during ODP Leg 172 document a detailed history of late Neogene changes of the DWBC over the entire deep and intermediate water column.

We studied terrigenous and biogenic fluxes at millennial scale resolution along the BBOR-transect (ODP Sites 1055 to 1061) for the time interval 20 to 65 kyr. The investigation is based on element (Ca, Ti, Fe, K) intensities measured with an X-ray fluorescence (XRF) core scanner at cm-resolution. Calcium (Ca) intensities were calibrated with carbonate measurements on discrete samples to derive the percentage $CaCO_3$ with high accuracy. A detailed age model for Site 1060 has been developed by correlating abrupt shifts in the percentage of a group of warm surface-dwelling planktonic foraminifera with abrupt changes in the oxygen isotopic composition of Greenland ice [Vautravers et al., 2004]. Ti/Ca ratios also show strong similarities with Greenland ice core records and are used for a high-resolution inter-site correlation along the depth transect. The resulting chronologies have an average resolution of 1800 years, are in agreement with AMS-^{14}C chronologies from the BBOR region [e.g. Hagen and Keigwin, 2002; Keigwin and Jones, 1994] and thus allow studying millennial scale changes in sediment accumulation.

In combination, XRF measurements and age models allow to construct high resolution mass accumulation rate records of biogenic and terrigenous components. The pattern of terrigenous sediment fluxes indicates a continuous drift growth driven by a vigorous DWBC. The core of the DWBC was always focused below 3000 m but millennial scale changes in water mass and vertical extend of the current occurred that exhibit three different hydrographic modes as suggested by Sarnthein et al., [1994]: (1) an "interstadial mode" with a DWBC dominated by lower North Atlantic Deep Water (lower NADW) and a core flow between 3000 and 3500 m similar to today, (2) a "stadial mode" with a deep core flow consisting of Southern Ocean Water (SOW) below 3500 m and a shoaling of the upper limit of the DWBC due to enhanced lower NADW production, (3) a "Heinrich mode" with dominating SOW influence over a very broad depth range suggesting a very diminished or even ceased NADW production.

References:

Giosan, L., R. D. Flood, J. Grützner, and P. Mudie (2002), Paleoceanographic significance of sediment color on western North Atlantic Drifts: II. Late Pliocene-Pleistocene sedimentation, Marine Geology, 189(1-2), 43-61.

Hagen, S., and L. D. Keigwin (2002), Sea-surface temperature variability and deep water reorganisation in the subtropical North Atlantic during Isotope Stage 2-4, Marine Geology, 189, 145-162.

Keigwin, L. D., and G. A. Jones (1994), Western North Atlantic evidence for millenial-scale changes in ocean circulation and climate, Journal of Geophysical Research, 99, 12397-12410.

Sarnthein, M., K. Winn, S. J. A. Jung, J. C. Duplessy, L. Labeyrie, H. Erlenkeuser, and G. Ganssen (1994), Changes in east Atlantic deep-water circulation over the last 30,000 years: Eight time slice reconstructions, Paleoceanography, 9, 209-267.

Stahr, F. R., and T. B. Sanford (1999), Transport and bottom boundary layer observations of the North Atlantic Deep Western Boundary Current at the Blake Outer Ridge, Deep Sea Research II, 46, 205-243.

Vautravers, M. J., N. J. Shackleton, M. C. Lopez, and J. O. Grimalt (2004), Gulf Stream variability during marine isotope Stage 3, Paleoceanography, 19(2), 12. 2004.

.

IODP

Fluctuations of the oceanic Ca-isotopic budget and environmental changes during highly dynamic transitions of the Cenozoic

NIKOLAUS GUSSONE[1], BARBARA M.A.TEICHERT[2], KATHARINA RABE[1] AND IODP EXPEDITIONS 320/321 SHIPBOARD PARTY

[1]Institut für Mineralogie, Universität Münster, Corrensstr. 24, 48149 Münster, Germany
[2]Institut für Geologie und Paläontologie, Universität Münster, Corrensstr. 24, 48149 Münster, Germany

IODP Expeditions 320 and 321 retrieved well preserved continuous core material from the equatorial eastern Pacific that provides an excellent archive for reconstructions of Cenozoic climate, a period which is known for its times of rapid and extreme climate variability. Besides reconstruction of temperature and salinity fluctuations, a main aim of this expedition was to enhance the understanding of carbon cycling, in particular the interplay of carbonate compensation depth (CCD), $CaCO_3$-dissolution and productivity.

Shipboard results revealed sharp carbonate concentration fluctuations at ~44, 41, 39, and 36 Ma, refining the carbonate accumulation events described by Lyle et al. (2005). Additional drastic changes in the carbonate chemistry are revealed by strong changes in carbonate content indicating a CCD-rise around 49 Ma, between 23-27 Ma, a Neogene CCD minimum between 17 and 18 Ma, the 'carbonate crash' interval around 10 Ma, and a newly delineated CCD minimum at about 4 Ma (Pälike et al., in press). These events reveal not only dramatic changes in the carbonate but also in the Ca budget of the ocean. The exact role of Ca is yet unclear.

An ideal tool to study the changes of the Ca budget is the Ca isotopic composition of the paleo-seawater which is recorded in marine biogenic carbonates. Reconstructions of paleo-seawater $\delta^{44/40}$Ca values exist for the Neogene. Few studies exist for the Mesozoic, Paleozoic and Precambrian. For the Paleogene however, no continuous seawater Ca isotope reconstruction is available. Such a record is needed to better constrain the mechanisms of rapid and intense changes in the oceanic $CaCO_3$ balance during the key phases of climate changes. The aim of our project is to reconstruct the fluctuations of $\delta^{44/40}$Ca of the paleo seawater with microfossil records, model the oceanic Ca budget during key periods of climate change, and better constrain the role of Ca in terms of input, redistribution and output during times of massive CCD changes and important stratigraphic transitions.

References

Lyle M. W., Olivarez Lyle A., Backman J., and Tripati A. (2005) Biogenic sedimentation in the Eocene equatorial Pacific: the stuttering greenhouse and Eocene carbonate compensation depth, in Proc. ODP, Sci Res 199, edited by Lyle, M., Wilson, P., Janecek, T.R., and Firth, J., College Station, TX, Ocean Drilling Program: 35 pp.

Pälike H., Lyle M., Nishi H., Raffi I., Gamage K., Klaus A., and the Expedition 320/321 Scientists (in press) Proc. IODP, 320/321: Tokyo (Integrated Ocean Drilling Program Management International, Inc.).

ICDP

Seismic Reflection Images of the Central California Coast Ranges and the Tremor Region around Cholame from Reprocessing of Industry Seismic Reflection Profile "SJ-6"

S. GUTJAHR[1], S. BUSKE[1]

[1]Institut für Geologische Wissenschaften , Freie Universität Berlin, Malteserstraße 74-100, 12249 Berlin

The SJ-6 seismic reflection profile was acquired in 1981 by Western Geophysical Company. It extends over a distance of about 180 km from Morro Bay over the Coast Ranges and Great Valley to the Sierra Nevada foothills in South Central California. The profile runs across several prominent fault systems which separate major crustal blocks, e.g. the Rinconada Fault (RF) in the western part as well as the San Andreas Fault (SAF) in its central part. Crystalline rocks of the Salinian Block are separated from sedimentary rocks of the Franciscan Block by the RF in the southwest and the SAF in the northeast respectively. The latter includes the region of increased tremor activity near Cholame, as reported recently by several authors. Eastward of the SAF rocks of the Franciscan Block are overlain by Great Valley Sequence sediments.

The survey layout for each shot consisted of 48 receivers that were arranged in a split-spread geometry with a receiver spacing of about 67 m and an initial source-receiver offset of 268 m. We have recorrelated the original field data from 6 seconds to 26 seconds two-way traveltime which allows us to image the crust and uppermost mantle down to approximately 40 km depth. The preprocessing consisted of bandpass filtering , AGC and trace normalization. A 3D tomographic velocity model derived from local earthquake data (Thurber et al., 2006) was used. Kirchhoff prestack depth migration as well as Fresnel-Volume-Migration were applied to each shot gather separately. The absolute values of the single migrated shot gathers were stacked afterwards. Both imaging techniques were implemented in 3D by taking into account the true shot and receiver locations. The imaged subsurface volume itself was divided into three separate parts to correctly account for the significant kink in the profile line near the SAF.

The most prominent features in the resulting images are areas of high reflectivity down to 30 km depth in particular in the central western part of the profile corresponding to the Salinian Block between the RF and the SAF. Strong reflectors that are dipping slightly to the northeast at depths of around 15-25 km can be identified in the southwestern part. The eastern part consists of west dipping sediments at depths of 2-10 km that are folded and faulted in the region of the Kettleman Hills at the west end of the San Joaquin Valley. At depths of 10 km to 20 km west dipping reflectors with dip angles larger than those of the sediments show up. At the eastern end of the profile an almost horizontal reflector can be identified at a depth of 25 km below the Sierra Nevada foothills.

The resulting images are compared to existing interpretations (Trehu and Wheeler, 1987; Wentworth and Zoback, 1989; Bloch et al., 1993) and discussed in the frame of the suggested tremor locations in that area.

ICDP

Dust transport in Patagonia as recorded in "short" sediment cores from Laguna Potrok Aike – A preliminary study for the PASADO project

TORSTEN HABERZETTL [1], ANNEMARIE STOPP [2], CHRISTIAN OHLENDORF [3], BERND ZOLITSCHKA [3], HILMAR VON EYNATTEN [2], ILKA KLEINHANNS [4], PASADO SCIENCE TEAM

[1]Department of Physical Geography, Institute of Geography, Friedrich-Schiller-University Jena, Löbdergraben 32, 07743 Jena, Germany
[2]Sedimentology and Environmental Geology, Geoscience Center, University of Göttingen, Goldschmidtstr. 3, 37077 Göttingen, Germany
[3]Geomorphology and Polar Research, Institute of Geography, University of Bremen, Celsiusstr. FVG-M, 28359 Bremen, Germany
[4]Department of Earth Science, University of Bergen, Allegt. 41, 5007 Bergen, Norway

An increasing number of terrestrial paleoclimatic records from southern South America has been published during the last decade. However, these archives mostly cover the Lateglacial and/or the Holocene. Only little is known about the Patagonian climate before the Last Glacial Maximum (LGM). Here, we present a continuous, high-resolution magnetic susceptibility record for the past 48 ka from the maar lake Laguna Potrok Aike (51°58' S, 70°23' W, southern Patagonia, Argentina). Magnetic susceptibility serves as an excellent parameter for the parallelization of sediment cores all over Laguna Potrok Aike including sediment cores taken within the ICDP (International Continental Scientific Drilling Program) project PASADO (Potrok Aike maar lake Sediment Archive Drilling prOject). Additionally, magnetic susceptibility is assumed to be a proxy for dust deposition in this lake (Haberzettl et al. 2008, 2009). Distinct similarities were found between an independently dated magnetic susceptibility record from a "short" core (c. 12 m) from Laguna Potrok Aike and the non-sea-salt calcium (nss-Ca) flux from the EPICA Dome C ice core record (75°06'S, 123°24'E) the latter being a proxy for mineral dust deposition in Antarctica (Röthlisberger et al., 2002, 2004). Comparison of the two records and grain size analyses of the Laguna Potrok Aike sediment indicate a relatively high aeolian activity in southern South America during the glacial period. During the Holocene climatic conditions driving sediment deposition seem to have been more variable and less dominated by wind compared to glacial times. Although the source of the dust found in Antarctic ice cores often has been attributed to Patagonia (Delmonte et al. 2004, 2008), we present the first evidence for contemporaneity of aeolian deposition in both the target area (Antarctica) and the major source area (Patagonia). Considering the similarities of the two records, magnetic susceptibility might yield the potential for chronological information, i.e., the transfer of the ice core age-depth model to a lacustrine sediment record. This would be important as additional time control for the recently recovered sediment record within the ICDP deep drilling project PASADO. To support this idea of similar provenance, we performed Sr/Nd-isotopic analyses on the assumed aeolian fraction (63-200 µm) which is very well sorted and was deposited in Laguna Potrok Aike during the last glaciation. Additionally, we analysed the <5 µm

fraction which is commonly found as dust in Antarctica. Both grain size fractions were extracted from the same subsamples. Results are compared to the Sr/Nd-isotopic signatures measured directly on dust from Antarctic ice cores (Delmonte et al. 2004). The isotopic data field of sediments from Laguna Potrok Aike superposes a large part of isotopic data from Antarctic dust, although the $^{87}Sr/^{86}Sr$-data seems to show a slight offset to lower values.

In conclusion our analyses confirm previous studies that suggested southern South America to be the main source area for east Antarctic dust during glacial periods. However, this is the first evidence for a contemporaneous dust deposition pattern in the source and target area - Patagonia and Antarctica.

References:
Delmonte, B., I. Basile-Doelsch, J.R. Petit, V. Maggi, M. Revel-Rolland, A. Michard, E. Jagoutz, F. Grousset (2004): Comparing the Epica and Vostok dust records during the last 220,000 years: stratigraphical correlation and provenance in glacial periods. Earth-Science Reviews 66, 63-87.

Delmonte, B., P.S. Andersson, M. Hansson, H. Schöberg, J.R. Petit, I. Basile-Doelsch, V. Maggi (2008): Aeolian dust in East Antarctica (EPICA-Dome C and Vostok): Provenance during glacial ages over the last 800 kyr. Geophysical Research Letters 35, doi:10.1029/2008GL033382.

Haberzettl, T., B. Kück, S. Wulf, F. Anselmetti, D. Ariztegui, H. Corbella, M. Fey, S. Janssen, A. Lücke, C. Mayr, C. Ohlendorf, F. Schäbitz, G.H. Schleser, M. Wille, B. Zolitschka (2008): Hydrological variability in southeastern Patagonia and explosive volcanic activity in the southern Andean Cordillera during Oxygen Isotope Stage 3 and the Holocene inferred from lake sediments of Laguna Potrok Aike, Argentina. Palaeogeography, Palaeoclimatology, Palaeoecology 259, 213–229.

Haberzettl, T., F.S. Anselmetti, S.W. Bowen, M. Fey, C. Mayr, B. Zolitschka, D. Ariztegui, B. Mauz, C. Ohlendorf, S. Kastner, A. Lücke, F. Schäbitz, M. Wille (2009): Late Pleistocene dust deposition in the Patagonian steppe - extending and refining the paleoenvironmental and tephrochronological record from Laguna Potrok Aike back to 55 ka. Quaternary Science Reviews 28 (25-26), 2927-2939.

Röthlisberger, R., R. Mulvaney, E.W. Wolff, M.A. Hutterli, M. Bigler, S. Sommer, J. Jouzel (2002): Dust and sea salt variability in central East Antarctica (Dome C) over the last 45 kyrs and its implications for southern high-latitude climate. Geophysical Research Letters 29, doi:10.1029/2002GL015186.

Röthlisberger, R., M. Bigler, E.W. Wolff, F. Joos, E. Monnin and M.A. Hutterli (2004): Ice core evidence for the extent of past atmospheric CO2 change due to iron fertilisation. Geophysical Research Letters 31, doi:10.1029/2004GL020338.

ICDP

The performance of different infrared spectrometry techniques applied to core catcher samples from Laguna Potrok Aike, a maar lake in southernmost Argentina

A. HAHN[1], P. KLIEM[1], C. OHLENDORF[1], P. PERSSON[2], B. ZOLITSCHKA[1], P.ROSEN[3] AND THE PASADO SCIENCE TEAM

[1]Geomorphology and Polar Research (GEOPOLAR), Institute of Geography, University of Bremen, Celsiusstr. FVG-M, D-28359 Bremen, Germany
[2] Department of Chemistry, Umeå University, SE-901 87 Umeå, Sweden
[3] Climate Impacts Research Centre, Umeå University, SE-981 07 Abisko, Sweden

The analysis of sediment samples in visible to mid-infrared spectra is ideal for high-resolution records. It requires only small amounts (0.01-0.1g dry weight) of sample material and facilitates rapid and cost efficient analysis of a wide variety of biogeochemical properties on minerogenic and organic substances (Kellner et al. 1998). One of these techniques, the Diffuse Reflectance Fourier Transform Infrared Spectrometry (DRIFTS), has already been successfully applied to lake sediment from very different settings and has shown to be a promising technique for high resolution analyses of long sedimentary records on glacial-interglacial timescales (Rosén et al. 2009). However, the DRIFTS technique includes a time-consuming step where sediment samples are mixed with KBr. To assess if alternative and more rapid infrared (IR) techniques can be used, four different IR spectroscopy techniques are compared for core catcher sediment samples from Laguna Potrok Aike – an ICDP site located in southernmost South America. Partial least square (PLS) calibration models were developed using the DRIFTS technique. The correlation coefficients (R) for correlations between DRIFTS-inferred and conventionally measured biogeochemical properties show values of 0.80 for biogenic silica (BSi), 0.95 for total organic carbon (TOC), 0.91 for total nitrogen (TN), and 0.92 for total inorganic carbon (TIC). Good statistical performance was also obtained by using the ATR-FTIRS technique which requires less sample preparation. Two devices were used, the full-sized Bruker Equinox 252 and the smaller and less expensive Bruker Alpha. R for ATR-FTIRS-inferred and conventionally measured biogeochemical properties were 0.87 (BSi), 0.93 (TOC), 0.90 (TN), and 0.91 (TIC) for the Alpha, and 0.78 (TOC), 0.85 (TN), 0.79 (TIC) for the Equinox 252 device. As the penetration depth of the IR beam is frequency dependent, a firm surface contact of the sample is necessary. This could not be accomplished, therefore absorbance in higher wavelengths was not recorded correctly. As a result of the poor spectral quality no calibration model was established for BSi using the Equinox device. Since this is by far the most time-consuming and elaborate conventional measurement, results give clear advantages for the Alpha device.

Further calibration models were developed using spectra from the VNIRS region (400-2500 nm). Sample preparation for VNIRS analysis also is faster than for DRIFTS. However, FTIRS calibrations seem to perform better than those for VNIRS which show an R of 0.75 (BSi), 0.93 (TOC), 0.93 (TN), and 0.89 (TIC). NIRS primarily measures overtones of molecular vibrations and is typically used for quantitative measurement of organic functional groups. FTIRS is similar to NIRS, but uses longer wavelengths and directly monitors molecular vibrations. As a consequence, FTIRS allows more detailed structural and compositional analyses of both organic and inorganic compounds. Statistical analyses of the FTIRS-PLS models shows that the calibration depends on specific wave numbers, which compare well with spectra of pure compounds. The VNIRS technique gives rise to a spectrum with broad peaks and many overlapping signals which makes interpretation difficult without statistical analyses.

In conclusion, the DRIFTS technique shows the best statistical performance for the analysis of biogeochemical properties. However, the VNIRS techniques and especially the ATR-FTIRS Alpha device provide comparable results and can also be used as a rapid screening tool when time and costs are limiting factors.

References:
Kellner R, Mermet J-M, Otto M, Widmer HM (1998) Analytical chemistry. Wiley-VCH, Weinheim, etc.

Rosén P, Vogel H, Cunnigham L, Reuss N, Conley DJ, Persson P (2009) Fourier transform infrared spectroscopy, a new method for rapid

determination of total organic and inorganic carbon and biogenic silica concentration in lake sediments. J Paleolimnol 43:247-259

IODP

Testing a dynamic global vegetation model for pre-industrial and Last Glacial Maximum boundary conditions

DIAN N. HANDIANI[1,2], RIMA RACHMAYANI[1,2], ANDRÉ PAUL[1,2], LYDIE M. DUPONT[1]

[1]MARUM - Center for Marine Environmental Sciences, University of Bremen, Leobener Strasse, 28359 Bremen
[2]FB-Geowissenschaften,Universität Bremen, Klagenfurter Straße, 28359 Bremen

Achieving better comparison between dynamic global vegetation models (DGVM) with pollen or plant data is important for the climate-vegetation modeling community. Our study tried to find a scheme that can be applied consistently to compare DGVMs with pollen data sets. We tested two models, the Top-down Representation of Interactive Foliage and Flora Including Dynamics (TRIFFID) and the Community Land Model's Dynamic Global Vegetation Model (CLM-DGVM), which we both ran for pre-industrial boundary conditions. In addition, we ran the TRIFFID model using boundary conditions for the Last Glacial Maximum (LGM, ~19,000- 23,000 years before present). For comparisons, we used the modern vegetation of the BIOME4 model and the reconstruction for the year 18000 after pollen data from the BIOME6000 (Version 4.2) project. Differences in the number of PFTs in each DGVMs lead to different results of the biome distribution even if models and data qualitatively agree.

In the CLM-DGVM pre-industrial run, northern South America is covered by savanna or desert biome, which is associated with more growing degree days and lower rates of precipitation. Meanwhile, the TRIFFID model simulated a tropical forest in northern South America and a desert biome in Australia, probably because of higher values of growing degree days and different precipitation rates, which is higher in South America and lower in Australia. The climate parameters from both models show a similar pattern as in the BIOME4 model, but the values are higher in the DGVMs.

Biome distributions of the pre-industrial simulation show similarities and differences between dynamic vegetation modeling and data reconstructions. Both models reveal a fair agreement simulating savanna and desert biomes around the Sahel, tropical forest in western Africa, boreal forest in eastern North America, and tundra in northern Canada. Some discrepancies appear in South America and Africa, where pollen data indicate a combination of tropical forest, grassland, and savanna biomes whereas TRIFFID indicates a tropical forest biome and CLM-DGVM a savanna one. In Europe, both models failed to come up with temperate forest (i.e. combination of boreal forest and grassland biome) which is dominant in the pollen data set.

During the LGM, southern Europe is covered by grassland and shrubland biome according to the TRIFFID model and paleo-data. In southeast Africa the TRIFFID model simulates temperate and boreal forest, where the pollen reconstruction indicates savanna and grassland.

The results show that the CLM-DGVM model is insufficient in representing tree PFTs over South America and Europe, while at the same time the TRIFFID model exaggerates the amount of tree PFTs in South America and Africa. This suggests that the number of PFTs in DGVM influences the biome distribution, but is not necessarily correlated with the quality of the agreement between models and data. We hope that our results will contribute to the improvement of DGVMs by further incorporation of biological, physiological, and geophysical processes in these models.

IODP

Constraining the architecture of Hole U1309D (IODP Leg 304/305) through geospeedometry

ANETTE VON DER HANDT [1,2], ERIC HELLEBRAND[2], JÜRGEN KOEPKE[3], KEVIN JOHNSON[2]

[1]Albert-Ludwigs-Universität Freiburg, Institut für Geowissenschaften, Albertstrasse 23B, 79104 Freiburg (Anette.von.der.Handt@minpet.uni-freiburg.de)
[2]University of Hawaii, Department of Geology and Geophysics, 1680 East-West Road, 96822 Honolulu, HI
[3]Leibniz Universität Hannover, Institut für Mineralogie, Callinstrasse 3, 30167 Hannover

Although more than two-thirds of the Earth's surface are formed at mid-ocean ridges, the mechanism that controls crustal construction is still elusive. Several models are used to describe the architecture and timing of the crust formation along mid-ocean ridges; these include: (a) crystallization in large shallow level intrusions that are emplaced episodically; (b) emplacement of many small (m-scale) shallow level intrusions that cool separately; (c) crystallization in deep (20-30 km) plutons.

IODP Leg 304/305, drilling at 30°N Mid-Atlantic ridge, had the goal to illuminate accretionary processes of young, slow-spread oceanic lithosphere and drilled 1415 m into a complexly stacked gabbroic sequence (Hole U1309D). Recent petrological and geochemical studies resulted in conflicting models whether its architecture is formed by (i) cm-to-m scale intrusions (Godard et al., 2009) or (ii) hundred meter scale intrusions (Suhr et al., 2008). Radiometric dating on zircons indicates an earlier (and deeper?) formation of gabbros in the lower part of Hole U1309D (Grimes et al., 2008). It is unclear if the chemical variation in the upper and lower half of the core is related to either emplacement at different P-T conditions or changes in the melt compositions.

The different crustal accretion models predict very different thermal histories; deep crystallization in km-scale plutons will result in slow cooling due to the hot wall-rocks and the cooling rate will be largely controlled by the uplift rate. In the case of shallow crystallization in smaller intrusions (i.e. sheeted sills), cooling rates will depend on the size of the intrusion, the thermal structure at shallow levels and the extent of hydrothermal cooling. Thus by determining the cooling rate of lower crustal rocks, it is possible to test these different models and constrain the architecture of Hole U1309D.

In particular, the Calcium-in-olivine geospeedometer has been successfully used to calculate cooling rates from olivine-bearing gabbros from mid-ocean ridges and ophiolites. We applied the Calcium-in olivine

geospeedometer in a short interval of Hole U1309D which contains magmatic contacts between different lithological units. Our results allow us to establish younger/older relationships between the units which is not possible from mineral and whole-rock chemistry alone. Hence, in conjunction with other established and new geospeedometers, by extending this approach to the entire hole it is possible to provide spatially as well as lithologically controlled cooling rates and provide new insights into lithosphere formation at slow-spreading ridges.

References:
Godard, M. et al. (2009). Geochemistry of a long in-situ section of intrusive slow-spread oceanic lithosphere: Results from IODP Site U1309 (Atlantis Massif, 30°N Mid-Atlantic Ridge). Earth and Planetary Science Letters 279, 110-122.
Grimes, C.B., et al. (2008). Protracted construction of gabbroic crust at a slow spreading ridge: Constraints from $^{206}Pb/^{238}U$ zircon ages from Atlantis Massif and IODP Hole U1309D (30°N, MAR). Geochemistry, Geophysics Geosystems 9, doi:10.1029/2008GC002063.
Suhr, G. et al. (2008). Stacked gabbro and intervening mantle: A detailed look at a section of IODP Leg 305, Hole U1309D. Geochemistry Geophysics Geosystems 9, doi:10.1029/2008GC002012.

IODP

Pore water geochemistry from IODP Expedition 320/321 „Pacific Equatorial Age Transect (PEAT)“ reveals coupling of carbonate and non-carbonate diagenesis

E.C. HATHORNE [1], M.L. DELANEY [2], N. GUSSONE [3], K. KIMOTO [4], AND THE EXPEDITION 320/321 SCIENTISTS

[1]IFM-GEOMAR, Leibniz Institute of Marine Sciences at the University of Kiel, Wischhofstrasse 1-3, D-24148 Kiel, Germany
[2]Institute of Marine Sciences, University of California, Santa Cruz, 1156 High Street, Santa Cruz, CA 95064, USA
[3]Institut für Mineralogie, Westfälische Wilhelms-Universität Münster, Corrensstrasse 24, 48149 Münster, Germany
[4]Institute of Observational Research for Global Change (IORGC), Japan Agency for Marine-Earth Science and Technology, 2-15 Natsushima-Cho, Yokosuka 237-0061 Japan

Integrated Ocean Drilling Program (IODP) Expeditions 320 and 321, “Pacific Equatorial Age Transect” (PEAT) drilled Sites located on oceanic crust ranging in age from ~17 to 50 Ma [Pälike et al., in press] and most of the sediment thickness was deposited when the Sites were a few degrees either side of the palaeo-equator. The PEAT Sites display variable subsidence, sedimentation rates, and geothermal gradients [Pälike et al., in press] which all combine to produce distinctive diagenetic histories for coeval sediments from different sites. This makes the PEAT sediments attractive for the study of diagenesis and we illustrate this here with shipboard and preliminary shore-based analyses of pore water samples.

The enrichment of pore water Sr^{2+} concentrations compared to the seawater concentration often indicates the recrystallisation of biogenic carbonates [e.g. Baker et al., 1982] and the distinct diagenetic histories of the PEAT carbonate sediments are evident in the contrasting pore water Sr^{2+} profiles. There is a general trend with age as Sites on older crust display no or only slight enrichments in pore water Sr^{2+} with depth (Sites U1331-U1334), Sites on intermediate age crust have intermediate enrichments (U1335) and the Site on the youngest crust shows the strongest increase in Sr^{2+} with depth (U1338). Superimposed on this simple pattern is complex downcore behavior like that of Site U1337 (located on slightly older crust than U1338) where the upper section displays only a slight Sr^{2+} enrichment but below a small chert layer a significant Sr^{2+} enrichment is found. At all sites with a downcore Sr^{2+} enrichment, except for U1336 which was unfortunately not sampled entirely, Sr^{2+} returns to seawater values towards the bottom of the section indicating the flow of seawater in the basement. The Li^+ profile at all Sites generally mirrors that for Sr^{2+}, with Li^+ becoming increasingly depleted in pore waters with depth followed by a return to seawater values near the basement. This implies the source of Sr^{2+} and the sink of Li^+ are related and such a coupling of pore water Li^+ and Sr^{2+} was observed in the sediments from this region during ODP Leg 138 [Mayer et al., 1982]. However, measurement of bulk carbonate reveals no significant Li enrichment in the carbonate phase precluding carbonate recrystallisation from being both the source of Sr^{2+} and the sink for Li^+. Instead coupling of the Li^+ and Sr^{2+} in pore waters must also involve a non-carbonate phase, most likely clays, as the sink for Li^+.

During the PEAT Expeditions Rhizon pore water sampling [e.g. Dickens et al., 2007] was conducted for the first time on the JOIDES Resolution. This technique allows high-resolution (up to every 10cm) sampling of pore waters with a minimal disturbance of the core. Rhizon sampling was used to sample the pore waters across a diatom rich interval at Site U1338 before the core was split. The data from these unique samples reveal small but significant increases in both porewater Sr^{2+} and H_4SiO_4 in the diatom rich interval, suggesting the coupling of opal and carbonate diagenesis at the decimeter scale.

References:
Baker P. A., Gieskes J. M., and Elderfield H. (1982). Journal of Sedimentary Petrology 52, 71-82.
Dickens, G. R., Kölling, M., Smith, D. C., Schnieders, L., and the IODP Expedition 302 Scientists (2007) Scientific Drilling, No. 4, 22-25.
Mayer, L., Pisias, N., Janecek, T., et al. (1992). Proceedings of the Ocean Drilling Program, Initial Reports, Vol. 138.
Pälike, H., Lyle, M., Nishi, H., Raffi, I., Gamage, K., Klaus, A., and the Expedition 320/321 Scientists (in press). Proc. IODP, 320/321: Tokyo (Integrated Ocean Drilling Program Management International, Inc.).

IODP

Prediction of sub-seafloor gas hydrate inventories using a general transfer function

C. HENSEN[1], M. MARQUARDT[1], E. PINERO[1], M. HAECKEL[1], K. WALLMANN[1], R. GEHRMANN[2], C. MÜLLER[2]

[1]Leibniz_Institute of Marine Sciences, IFM-GEOMAR, Kiel, Germany
[2]Federal Institute for Geosciences and Natural Resources (BGR), Hannover, Germany

A number of recently published estimates of the global inventory of marine methane hydrate are based on diagenetic models, which were run for each grid point of a homogeneous grid of the seafloor. Since this is a very complex approach, which may also be limited by data availability, we invented a simple transfer function, which calculates the amount of gas hydrates based on easily accessible data. The transfer function was derived from a large set of systematic runs of a numerical diagenetic model covering the wide range of environmental conditions that are typically met along continental margins. The diagenetic model essentially predicts the formation

potential of methane and methane hydrate by microbial degradation of organic matter using the approach of Wallmann et al. (2006). The model runs have been constrained by field data derived from various ODP drill sites located at active and passive continental margins. An exhaustive parameter analysis established that the formation of gas hydrates from biogenic methane production can be sufficiently described by the total organic carbon accumulation rate (POCar) and the thickness of the gas hydrate stability zone (GHSZ). The following general equation to determine the gas hydrate inventory (GHI) was derived by Marquardt et al. (submitted):

$$GHI = a \cdot POCar \cdot GHSZ^{b} \cdot Exp[-GHSZ^{c} / POCar / d] + e$$

with a = 0.00214, b = 1.234, c = -3.339, d = 0.3148, e = -10.265

The above transfer function was applied to derive global estimates of the distribution and the total inventory of submarine gas hydrates. Global grids were calculated based on available datasets of 1x1-degree resolution of seafloor bathymetry (GEBCO), organic carbon input (Seiter et al., 2004), bottom water temperature, and geothermal gradient (estimated from heat flow (Stein & Stein, 1992; Hamza et al., 2008). The global amount of gas hydrate is predicted to be in good agreement with some previously published results (e.g. Archer et al., 2009). So far, our calculations do only consider microbially produced gas, and hence represent a minimum estimate. The tests, however, indicate that the transfer function gives a realistic approximation to the global submarine gas hydrate inventory essentially stored in low gas flux systems (LGF).The overall advantage of the function presented above is its simplicity compared to complex numerical models. Only two easily accessible parameters are required.

In addition the function has been used to estimate gas hydrate inventories along a transect across the convergent (Pacific) margin offshore Costa Rica. Limiting parameters like regional variability of thermal conditions (depth of the BSR) and the overall sediment thickness along the lines have been derived from post-stack seismic sections. Gas hydrate concentrations range in total from 0 to 10 g CH_4 per cm^2 (seafloor). The highest amounts of GH are expected at mid-slope depths, where optimal conditions with respect to organic matter input, sediment thickness and stability conditions are met. In addition, the model was tested against estimates based on seismic velocity analysis along the transects. Overall, seismic velocity analysis predicted significantly higher gas hydrate inventories than were obtained by the transfer function. One reason for the observed discrepancy is that the seismic velocities in this convergent margin setting are not very well contrained due to the lack of sufficient reflection events in the seismic sections. Another reason can be upward fluid advection, which is known to have a positive effect on the rates of gas hydrate formation. Based on additional test runs with the numerical model the general equation could be modified for a range of reasonable upward flow velocities that occur along convergent margins. Using this approach a good match between the geophysical and the geochemical model could be obtained. Integration of gas hydrate concentrations along the profiles may yield up to 60 x 10^{12} g(CH_4) are stored in gas hydrates on trench-parallel section (normalized to 1 km) of the Central American continental margin.

References:
Wallmann, K., Aloisi, G., Haeckel, M., Obzhirov, A., Pavlova, G., Tishchenko, P. (2006) Kinetics of organic matter degradation, microbial methane generation, and gas hydrate formation in anoxic marine sediments.- GCA, 70, 3905.3927.
Archer, D., Buffett, B., Brovkinc V. (2008) Ocean methane hydrates as a slow tipping point in the global carbon cycle. PNAS 106 (49), 20596-20601.
Hamza V.M., Cardoso, R.R., Ponte Neto, C. F. (2008) Spherical harmonic analysis of the Earth's conductive heat flow.- Intern. J. Earth Sci., 97, 205-226.
Marquardt M., Hensen, C., Piñero, E., Wallmann, K., Haeckel, M. (2010) Estimation of gas hydrate inventories in marine sediments: derivation and testing of atransfer function.- Biogeosciences, submitted.
Seiter, K., Hensen, C., Schröter, J., Zabel, M. (2004) Organic carbon content in surface sediments defining regional provinces.- Deep Sea Res. 51, 2001-2026.
Stein, C. Stein, S. (1992) A model for the global variation in oceanic depth and heat flow with lithospheric age.- Nature, 359, 123-128.

IODP

Early Pliocene ice sheet dynamics, ice sheet collapse and evidence for reduction of bottom water circulation along the West Antarctic Peninsula margin (ODP Site 1095)

D.A. HEPP[1], T. MÖRZ[1], K. NÖTHEN[2]

[1]MARUM – Center for Marine Environmental Sciences and Department of Geosciences, University of Bremen, Leobener Strasse, 28359 Bremen, Germany
[2]Alfred Wegener Institute, Am Handelshafen 12, 27570 Bremerhaven, Germany

Ice has been present on Antarctica since the Eocene/Oligocene transition. Starting with the late Miocene (~10 Ma) the West Antarctica has been covered by a waxing and vanishing ice sheet that periodically extended to the shelf edge. The sedimentary response to Antarctic Peninsula ice sheet dynamics and changes in the

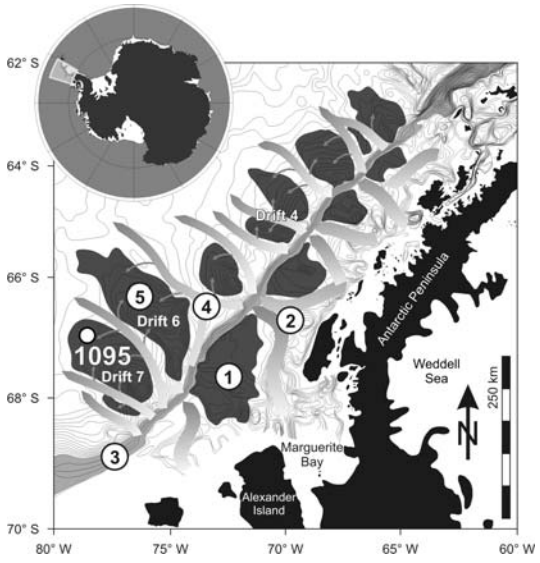

Fig. 1: Bathymetric map of the Pacific continental margin off the Antarctic Peninsula. The map shows a glacially driven sediment feeder system of (1) lobes and (2) troughs on the outer shelf, (3) an oversteepened slope, (4) deep-sea channels and (5) sediment drifts on the continental rise and the location of ODP Site 1095 on the distal part of Drift 7 (Hepp and Mörz, 2009).

regional oceanographic realm during the latest Miocene-early Pliocene warming phase is well documented in distal

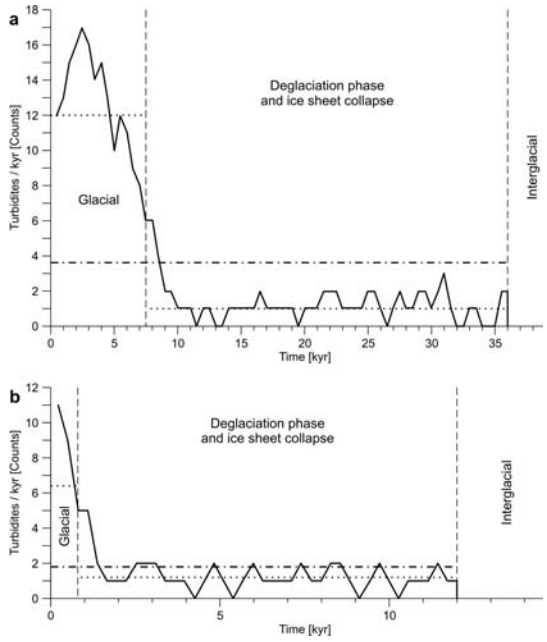

Fig. 3: Early Pliocene turbidite frequency for ODP Site 1095 core section between a. 105.64–104.02 mcd, and b. 168.93–168.27mcd. The diagram shows a decrease in turbidite frequency during the deglaciation and the ice sheet collapse phase. The number of turbidites per 1 kyr was plotted on the ordinate. The dotted line shows the mean average turbidite ratio for the glacial interval and the deglaciation phase respectively. The chain line shows the mean average of the total turbidite interval.

records from the Pacific continental rise off the Antarctic Peninsula (ODP Site 1095, Drift 7, Fig. 1). Such changes, especially enhanced primary productivity and accumulation of biogenic components, are reflected in paleoenvironmental proxies, e.g. the magnetic signal in the sedimentary record.

Pliocene ice sheet dynamics: In Hepp and Mörz (2009) we investigated the interaction of ice sheet dynamics, slope loading slope failure as reflected in turbidity sediment depositions along the Pacific continental margin of the Antarctic Peninsula during the early Pliocene.

We have linked the turbidite frequency (Fig. 2) and the average time period between two consecutive turbidite events to reaction rate constant measurements on reworked biogenic opal to derive an indirect measure of the slope retention times for two core intervals of ODP Site 1095 by using the long term sedimentation rate dependency of the marine carbon burial efficiency in Antarctic drift sediments, it was possible to calculate a ratio of glacial to interglacial sedimentation rates for the Pliocene. Pliocene glacial-interglacial periodicities were determined by using sparse magneto and bio-stratigraphic tie points and counts of glacial and interglacial intervals. Together with the decompacted average length of glacial and interglacials, a set of linear equations for the glacial and interglacials half periods and thus absolute half cycle sedimentation rates were calculated.

The deglaciation phase required a special adjustment because a diagenetic imprint on the organic carbon preservation prevents the organic carbon-sedimentation rate correlation approach for the calculation of the duration of the deglaciation phase. Even for this shelf-proximal site the glacial and interglacial half periods have on average equal durations of 63.98 kyr and 57.38 kyr, respectively (Fig. 3).

Derived average glacial turbidite recurrences of ~375 yr are interpreted as short and rapid ice sheet advances at relatively regular intervals resulting in continuous and periodic slope failures in the late Miocene/early Pliocene warm phase. Frequent turbidite recurrences imply short retention times between slope loading and slope failure. This finding is supported by low reaction rate constants of opal leaching experiments during early Pliocene glacials. A significant increase of the leaching rate from silt layer samples is associated with a decrease of the turbidite frequency during the deglaciation phase. The complex opal dissolution behavior observed in the laboratory is explained with a conceptual model of opal exposure, transport and burial.

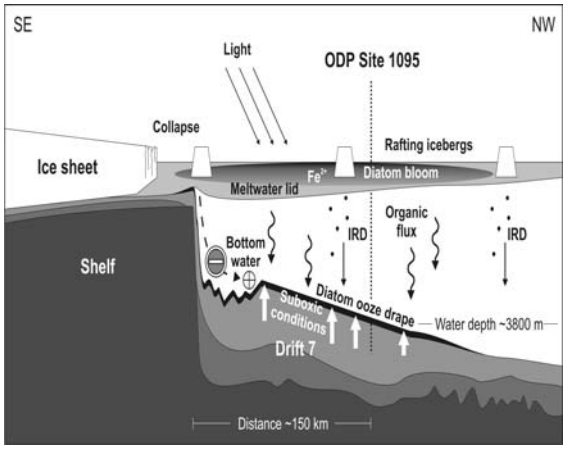

Fig. 1. During intense ice sheet collapse, the retreating ice sheet and a large meltwater lid leads to increased iron fertilization, a short-term diatom bloom and the stratification of the water column. Reduced bottom water ventilation and high export productivity foster the preservation of a diatom ooze drape on the drift resulting in periodic suboxic conditions in surface sediments.

The findings from silt layer frequency distribution and biogenic silica leaching rates imply a close interaction between ice sheet dynamics, sediment discharge, slope loading and slope failure. The ~120 kyr Pliocene glacial-interglacial periodicities correspond to data from wavelet and power spectra analyses from ODP Site 1095 on the Pacific continental rise of the Antarctic Peninsula. The previously predicted combined effect of precession and obliquity periodicity of ~60 kyr from magnetic susceptibility data suggest to correspond rather to glacial or interglacial half-cycles respectively.

Evidence for reduction of bottom water circulation: In Hepp et al. (2009) we present a unique late Miocene–early Pliocene record of sixty-four zones with prominent losses in the magnetic susceptibility signal (MSMZ). The MSMZs were identified in the magnetic susceptibility signal of ODP Site 1095 cores. The MSMZs, caused by reductive dissolution of magnetite under suboxic

conditions, are comparable in their shape and magnitude and occur commonly at glacial-to-interglacial transitions and are linked to the decrease in turbidite frequency during the deglaciation and the ice sheet collapse phase.

With detailed analyzes of organic matter, magnetic and clay mineral compositions we could show that, during early Pliocene times, exceptionally high organic matter fluxes in combination with weak bottom water currents produced temporary oxygen-depleted/suboxic conditions in the uppermost sediments. Other processes like dilution effects or changes in source and provenance of the sediments are insufficient to produce the MSMZs.

We speculate that at the end of the deglaciation (Fig. 4), during times of rapid shelf ice sheet break down, an increased freshwater discharge, a stratified water column and fertilization of the ocean by terrigenous and dust-bound iron could have enhanced export productivity under sea ice free conditions. Moreover, stratification, nearly stagnant deepwater conditions and the absence of bioturbation are possible causes for the preservation of current sensitive diatom oozes on the flank of an elevated topographic feature like Drift 7. High organic carbon export rates and reduced bottom water ventilation during the break down of the shelf ice sheet provided the framework for the development of suboxic conditions in surface sediments and most likely even for sulfate reduction ocurring close to the sediment water interface Fig. 4).

magnetic anomalies occur under glacial environmental conditions. During these times low organic fluxes influence the mixture of magnetite and pyrrhotite.

In search of additional evidence for the proposed anoxia in near surface sediments, well established export proxies like the $^{231}Pa/^{230}Th$, which are limited to an age window of 0-350 ky, are not applicable to the early Pliocene sediments of Site 1095. The characterization of the paleo-watermasses with carbon and oxygen isotopes from benthic forams is also difficult since the western Antarctic continental rise was most of the time below the CCD.

The redox sensitive element Uranium (^{234}U and ^{238}U compositions) is a possible candidate to characterize the redox potential of the sediment during meltwater pulses. Under oxic conditions in seawater, Uranium is stably dissolved as U^{+VI} with a concentration of 3.3 ppb. The Uranium concentration is related to salinity in seawater. Under suboxic to anoxic conditions, authigenic Uranium is precipitated in the sediment and becomes insoluble. This leads to a net diffusion of Uranium into the sediment from the water column above. In turn, analysis of the authigenic Uranium content can be taken as a measure of the sedimentary redox conditions. Reducing conditions would lead to a stronger Uranium content in the sediment. Therefore, the Uranium content is a potential proxy for the characterization of anaerobic sediment conditions during deglaciation phases and ice sheet collapses.

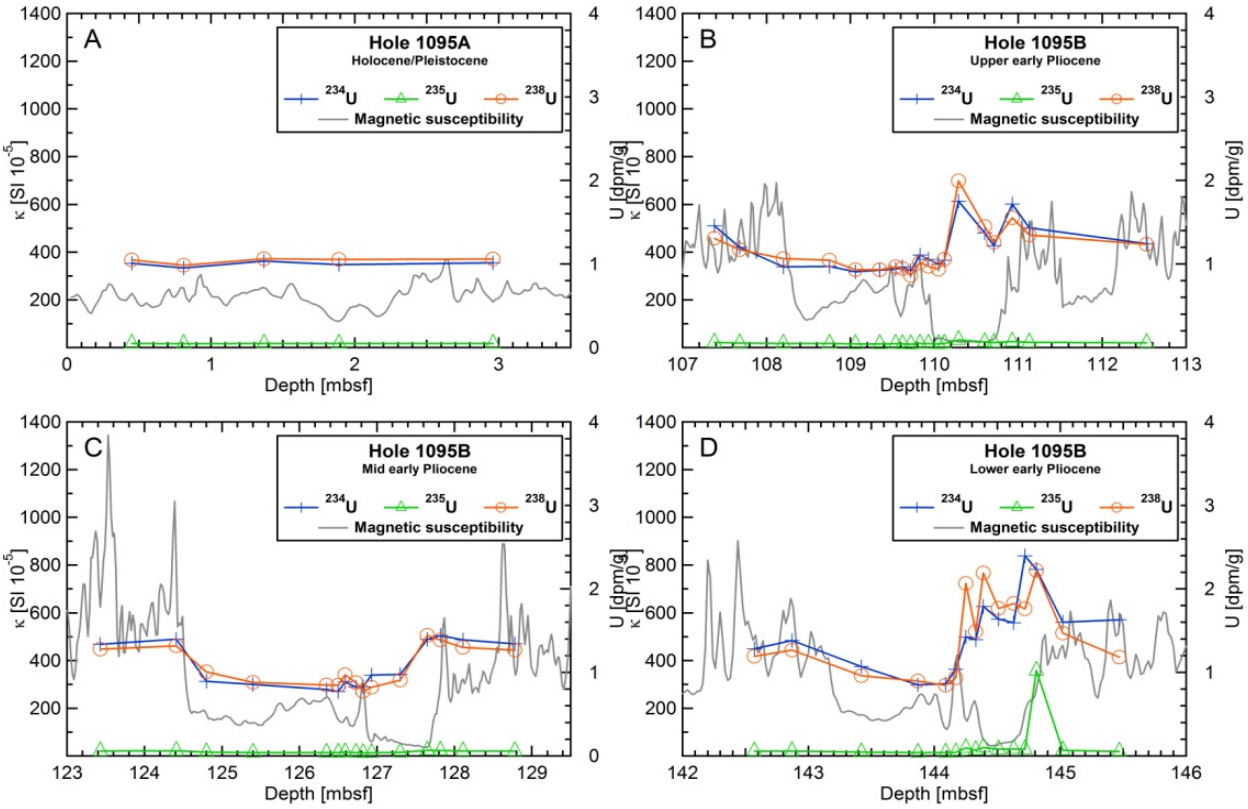

Fig. 2. ^{234}U and ^{238}U measurements on (A) one Pleistocene-Holocene reference interval and (B-D) three Pliocene intervals with zones of losses in the magnetic signal (unpublished data).

The findings for the Pliocene deposits differs clearly from scenarios proposed for late Pleistocene-Holocene sedimentary sequences of Drift 7, where repeated sediment

^{234}U and ^{238}U measurements on three Pliocene intervals with MSMZs and one reference interval showing changes in the sedimentary depositional regime (Fig. 2). The

Uranium concentration varies in general about 1 dpm/g, with higher values in glacial intervals. The relation of ^{234}U and ^{238}U in the sediment is also linked to lithological changes in glacial and interglacial intervals, with high ^{234}U values or low ^{238}U values, respectively, in glacial intervals and the opposite proportion in interglacials. Beside this general observations ^{234}U and ^{238}U concentration in Fig. 2B and D show an enrichment, up to 2.5 dpm/g, in zones where a loss in the magnetic signal was observed. In contrast, the Pleistocene-Holocene reference interval shows no significant changes in ^{234}U and ^{238}U concentration (Fig. 2A). Comparable to the interglacial intervals of the early Pliocene, ^{238}U values are higher than ^{234}U values. The ^{234}U and ^{238}U enrichments at early Pliocene MSMZs confirm the hypothesis of the evidence for anoxic conditions.

References:
Hepp, D.A. and Mörz, T., 2009. An approach to quantify Pliocene ice sheet dynamics via slope failure frequencies recorded in Antarctic Peninsula rise sediments. Ant. Sci., 21(6): 619-631.
Hepp, D.A. et al., 2009. A late Miocene-early Pliocene Antarctic deepwater record of repeated iron reduction events. Mar. Geol., 266(1-4): 198-211.

IODP

Nankai Trough Seismogenic Zone Experiment (NanTroSEIZE) Stage 2: Microbially mediated transformation of carbon in sediments entering an active subduction zone

V.B. HEUER[1], K.-U. HINRICHS[1], AND THE SHIPBOARD SCIENTIFIC PARTY OF IODP EXPEDITION 322

[1]Fachbereich Geowissenschaften, Universität Bremen, 28359 Bremen, Germany

With the Nankai Trough Seismogenic Zone Experiment (NanTroSEIZE), the Integrated Ocean Drilling Program (IODP) aims to drill, sample, and deploy instruments in the seismogenic portion of a convergent margin subduction zone where great earthquakes have repeatedly occurred (Tobin and Kinoshita, 2006). Along a transect of drill sites across the Nankai accretionary complex off southwestern Japan, NanTroSEIZE covers key elements of the active plate-boundary system, including the inputs to the subduction conveyor belt, the megasplay (one single fault that is continuous from the deep seismogenic zone up to the surface), and the main plate interface at a depth of ca. 6 km below the seafloor (Fig. 1). NanTroSEIZE is extending over several years and expeditions with D/V Chikyu that are grouped in four operational stages. In 2009, Stage 2 was completed.

While NanTroSEIZE is a central part of the Seismogenic Zone Initiative, it also enables us to address central topics related to The Deep Biosphere and the Subseafloor Ocean, i.e., another major theme identified in the IODP Initial Science Plan (IPSC, 2001). On the one hand, NanTroSEIZE opens a rare window to investigate microbial communities in great depths. On the other hand, it provides unique opportunities to elucidate the cycling of carbon in a subduction zone, where the elevated temperatures and hydrogeological complexity of the accretionary complex might exert control over biogeochemical and geological processes that (a) supply carbon and energy to the deep biosphere, (b) produce hydrocarbon-rich fluids that migrate through the accretionary prism, and (c) alter organic materials during their subduction to the crust. With this project, we are aiming to add more insight into the distribution of microbial biomass, carbon metabolism of subsurface microbial communities, and carbon flow in the deep subsurface system of the Nankai subduction zone.

During Stage 2, IODP Expedition 322 (September 1 - October 10, 2009) aimed to characterize the incoming sedimentary strata and the top of igneous basement prior to the plate entering the subduction zone. Two reference sites were drilled in the Shikoku Basin on the subducting Philippine Sea plate (Fig. 1): Site C0012 at the crest of a bathymetric high (Kashinosaki Knoll) and Site C0011 at the northwest flank of the knoll. Though still unaffected by subduction processes, these inputs are potentially influenced by lateral fluid migration from zones of deeper seated dehydration reactions (Fig. 2). Shipboard results point to the intriguing possibility of two fluids from different sources migrating through the sedimentary strata seaward of the trench. One regime is driven by expulsion of fluids from the subducting sediment and updip migration through high permeability horizons in the subduction inputs. The other flow regime, observed at the crest of the Kashinosaki Knoll, is driven by migration of a seawater-like fluid through the upper oceanic crust into the sandstone turbidites of the overlying sediment pile (Underwood et al., 2009). At the interface of both fluid regimes, microbial activity appears to be stimulated. At the Kashinosaki Knoll (Site C0012) this stimulating effect is evident at a sediment depth of 417 mbsf where we find indications for active anaerobic oxidation of methane (AOM): peak methane concentrations coincide with the complete consumption of sulfate and go along with a marked increase in pore-water sulfide and abundant pyrite in the sediment's solid phase over a comparable depth range (Underwood et al., 2009) as well as with a nearly

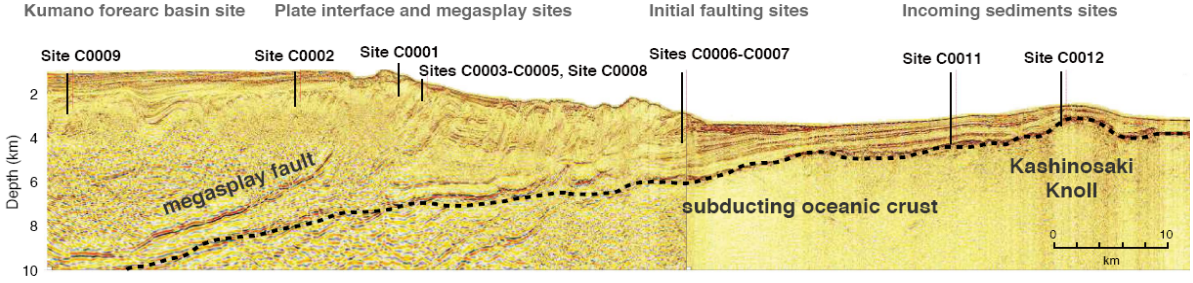

Fig. 1: Sites C0012 at the crest of a bathymetric high (Kashinosaki Knoll) and C0011 at the northwest flank of the knoll are shown together with other NanTroSEIZE drilling sites on a spliced composite profile of a representative depth section from NanTroSEIZE 3-D data volume (Moore et al., 2009) and Line 95 from IFREE mini-3-D seismic survey (Park et al., 2008) (modified from Underwood et al., 2009).

five-fold increase of total extracted DNA concentrations (John Moreau, personal communcation 2010).

The geochemical fingerprints of the updip migrating fluid component are fluid freshening and the presence of methane and higher hydrocarbons (Underwood et al., 2009). The freshening is thought to result from the dehydration of clay minerals at elevated temperatures (~100 to 150°C) in the subduction zone. Originating from deeper sources landward of the prism toe, the freshened fluid migrates updip through highly permeable horizons and terminates where the turbidite intervals pinch out against Kashinosaki Knoll (Underwood et al., 2009). However, the ultimate sources of the hydrocarbon gases remain to be explored. The presence of ethane, very low C_1/C_2 ratios (<450 at Site C0011; <100 at Site C0012), and the additional finding of propane and iso-butane at Site C0011 suggest a thermogenic source of the hydrocarbon gases (hypothesis 1). Moreover, the presence of thermogenic gases in the accretionary prism has been shown in earlier studies (Gamo et al., 1993, Berner and Faber, 1993; Horsfield et al., 2006). Therefore, the expulsion of freshend fluids which also contain thermogenic hydrocarbon gases from deep thermogenic sources is a plausible scenario. However, the results of our post-cruise carbon isotope analysis suggest a predominantly biogenic source of methane (hypothesis 2). At Site C0011, δ^{13}C-values of methane increase linearly with depth from -86‰ vs VPDB at 360 meters below seafloor (mbsf) to -61‰ vs VPDB at 858 mbsf (Fig 3.). This range of δ^{13}C-values points to biogenic CO_2 reduction as the dominant methane source (Whiticar, 1999). The linear increase of methane in ^{13}C with depth is possibly related to a parallel isotopic change of the DIC pool as a result of a progressive influence of methanogenesis as observed at other subsurface settings (e.g. Heuer et al., 2009; Pohlman et al., 2009). At Site C0012, δ^{13}C-values of methane increase with depth from -58‰ vs VPDB at 302 mbsf to -43‰ vs VPDB at 662 mbsf (Fig. 4). The enrichment in ^{13}C relative to Site C0011 could partly result from the preferential consumption of $^{12}CH_4$ by AOM or from a stronger contribution of methane from acetoclastic methanogenesis.

Further support for the second hypothesis comes from the observation that the concentration maxima of methane and ethane at Site C0012 correspond to a zone with elevated organic carbon contents and a relatively high contribution of terrigenous organic matter (Fig. 4), which might fuel the activity of deeply buried microorganisms and result in the in situ formation of methane and ethane. We suggest that the higher hydrocarbon gases ethane and propane could have a biogenic origin as well (Hinrichs et al., 2006).

In the final stage of the project we are aiming to characterize the dissolved organic carbon pool and to conduct laboratory incubations in order to address the following questions:

To what degree does the delivery of organic substrates by fluid flow stimulate microbial activity and influence the formation and cycling of volatile fatty acids and gaseous hydrocarbons?

Does the presence of organic-rich layers in lithological Unit V of Site C0012, especially at 410 to 450 mbsf, stimulate the metabolic activity of deeply buried microorganisms, which in turn results in the in situ formation of methane, or is the metabolic activity of deeply buried microorganisms stimulated by hydrocarbon gases that have migrated laterally over several tens of kilometers from a deep, hot source in the subduction zone to the crest of the Kashinosaki Knoll?

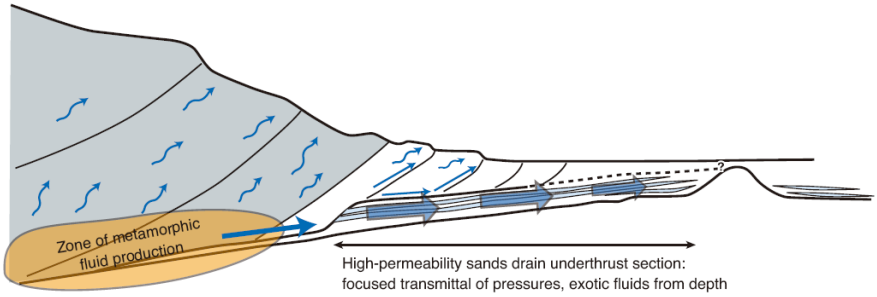

Fig. 2: Conceptual diagram showing fluid migration from zones of deeper seated dehydration reactions (Saito et al., 2009; after Saffer et al., 2008). In subduction zones, fluid flow is driven by the simultaneous compaction of sediments and dehydration of clay minerals. Fluids from overpressured regions are transported vertically or laterally along tectonic and sedimentary conduits, such as the décollement, faults or sand horizons. The evolution of fluid systems in subduction zones is closely linked to temperature (Moore and Saffer, 2001), since the primarily thermally driven phase transition from smectite to illite occurs between ~100 and 150°C. Interestingly, this temperature range is correlated with the updip limit of the seismogenic zone (Hyndman et al., 1995). Moreover, it overlaps with (a) the onset of petroleum generation (Quigley and Mackenzie, 1988), and (b) the upper temperature limit of life (121°C) (Kashefi et al., 2003).

Acknowledgements – We thank the crew and technical staff of the DV Chikyu for their support at sea. This research used samples provided by the Integrated Ocean Drilling Program (IODP), which is sponsored by the US National Science Foundation and participating countries under management of Joint Oceanographic Institutions (JOI), Inc. V.B.H. and K.-U.H. gratefully acknowledge funding of their research by the Deutsche Forschungsgemeinschaft (project grant Hi 616/9-1).

References:

Berner U., E. Faber (1993). Proceedings of the Ocean Drilling Program, Scientific results, Leg 131, p. 185-195.

Gamo, T.,M. Kastner, U. Berner, J. Gieskes (1993) Proceedings of the Ocean Drilling Program, Scientific results, Leg 131, p. 159-163.

Heuer, V.B., J.W. Pohlman, M.E. Torres, M. Elvert, K.-U. Hinrichs (2009) Geochimica et Cosmochimica Acta, 73, 3323-3336.

Hinrichs, K.-U., Hayes, J.M., Bach, W., Spivack, A., Hmelo, L.R., Sylva, S.P., Holm, N., Johnson, C.G. (2006) PNAS 103, 14684-14689.

Horsfield B., Schenk H. J., Zink K., et al. (2006) Earth and Planetary Science Letters 246(1-2), 55-69.

Hyndman R.D., Wang K., Yamano M. (1995) Journal of Geophysical Research-Solid Earth 100(B8), 15373-15392.

IPSC (2001) Integrated Ocean Drilling Program Initial Science Plan, 2003-2031. http://www.iodp.org/pdf/IODP_Init_Sci_Plan.final.pdf.
Kashefi K., Lovley D.R. (2003) Science 301 (5635), 934-934.
Moore J.C. and Saffer D. (2001) Geology 29(2), 183-186.
Moore, G.F., Park, J.-O., Bangs, N.L., et al. (2009). Proc. IODP, 314/315/316: Washington, DC. doi:10.2204/iodp.proc.314315316.102.2009
Park, J.-O., Tsuru, T., No, T., Takizawa, K., Sato, S., Kaneda, Y. (2008).

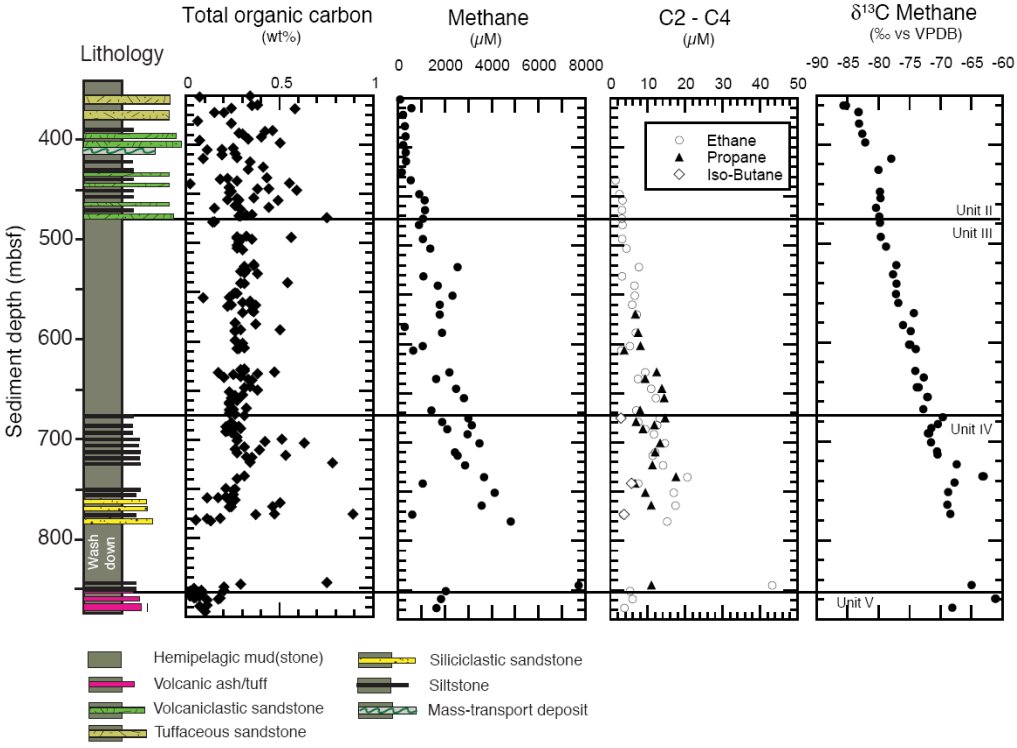

Fig. 3: Site C0011 – depth profiles of sedimentary total organic carbon, concentrations of dissolved methane, ethane, propane and iso-butane (shipboard data, Underwood et al., 2009) and carbon isotopic compositions of dissolved methane (this study) compared to lithology (Underwood et al., 2009)

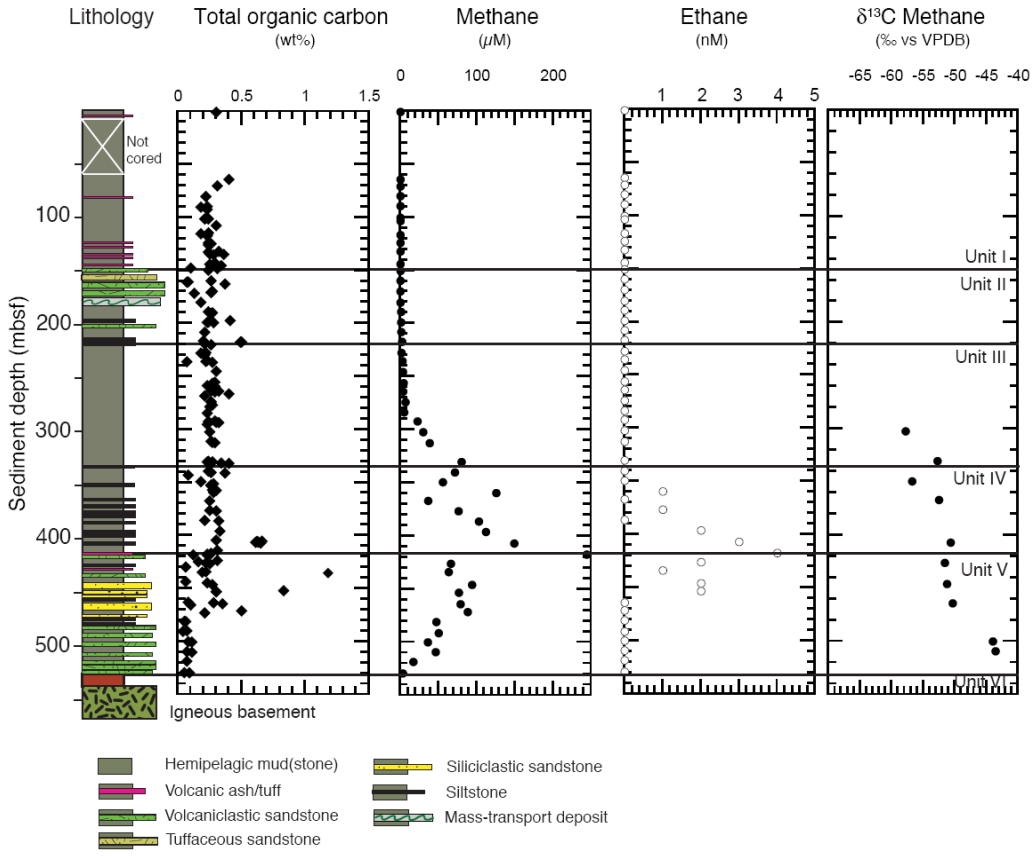

Fig. 4: Site C0012 – depth profiles of sedimentary total organic carbon, concentrations of dissolved methane, ethane, propane and iso-butane (shipboard data, Underwood et al., 2009) and carbon isotopic compositions of dissolved methane (this study) compared to lithology (Underwood et al., 2009)

Butsuri Tansa, 61:231–241. (in Japanese with English abstract)
Pohlman, J.W., M. Kaneko, V.B. Heuer, R.B. Coffin, M. Whiticar (2009) Earth and Planetary Science Letters. 287, 504-512.
Quigley T.M., Mackenzie A.S. (1988) Nature 333 (6173), 549-552.
Saffer, D.M., Underwood, M.B., McKiernan, A.W. (2008). Isl. Arc, 17(2):208–230. doi:10.1111/j.1440-1738.2008.00614.x
Saito, S., Underwood, M.B., Kubo, Y. (2009) NanTroSEIZE Stage 2: subduction inputs. IODP Sci. Prosp., 322. doi:10.2204/iodp.sp.322.2009.
Tobin, H.J., M. Kinoshita, M. (2006) NanTroSEIZE Stage 1. IODP Sci. Prosp., doi:10.2204/iodp.sp.nantroseize1.2006.
Underwood, M.B., Saito, S., Kubo, Y., and the Expedition 322 Scientists (2009) IODP Prel. Rept., 322. doi:10.2204/iodp.pr.322.2009
Whiticar, M. J. (1999) Chem. Geol. 161, 291-314.

ICDP

Geophysical and sedimentary studies to reveal the Quaternary evolution of the coast line of Lake Ohrid (FYROM/Albania)

N. HOFFMANN[1], K. REICHERTER[1]

[1]Institute of Neotectonics and Natural Hazards, RWTH Aachen University, Lochnerstr. 4-20, 52056 Aachen, Germany; Corresponding author: Nadine Hoffmann, mail: n.hoffmann@nug.rwth-aachen.de

The planned ICDP deep drilling site within the Lake Ohrid (FYROM/Albania, SCOPSCO initiative) needs a certain assessment of the tectonic framework and evolution of the site. The lake is situated in a karstic environment in the active tectonic region in the Balkanides, as evidenced by several moderate to strong earthquakes. It is located in an extensional back-arc setting, which is mainly controlled by the roll-back of the subducted slab and the migration of the Northern Hellenic Trench. Relatively straight shorelines are linked to N-S trending active normal faults. To understand the mechanisms controlling the basin and lake evolution, especially to understand possible fluctuations of the lake level, we studied the coastal areas. For the investigation of the Holocene shoreline-evolution extensive parts of the coastline including locations in the northern and southern plains as well the steep coastlines to the east and west of the lake, the deltas of the inflowing rivers and mass movement bodies at the east coast have been taken into account.

Ground Penetrating Radar and electric resistivity have been applied as non-invasive shallow subsurface mapping methods to image the sedimentary and tectonic structures. Sediment cores were taken at most of the sites, and grain size, fossil content and sediment composition were analyzed. Also, magnetic susceptibility measurements of the drill cores were carried out in the lab.

The main structural features encountered are:

- several S-ward dipping foreset-like structures in the northern Struga and southern Sveti Naum plains
- sets of channels revealing a meandering river system in the southern Sveti Naum plain
- a coastal marsh/lagoon environment on the fault-dominated eastern shore close to the Velestovo creek
- at the Velestovo site (east coast) a change in the drilled sediments from peat to clayey marls at a depth of 8 m suggests a change in the depositional environment.

Taking all this into account no evidence for a much higher lake-level was found in the plains north and south of the lake (except rare temporal floodings). The sudden change in sediment composition in the core of the east coast can be related to a sudden lake level drop, enhanced discharge of the karstic springs or to tectonic activities. We favor a tectonic event, possibly earthquake-related. The plains (north and south of the lake) are dominated by clastic input related to climate variations and uplift/erosion, whereas the steep western and eastern margins controlled tectonically by normal faulting. Mapping of the limestone cliffs around Lake Ohrid yielded no evidence for abrasional platforms or notches as indicator for past higher lake-levels.

IODP

A warming pulse in the subtropical North Atlantic during Oceanic Anoxic Event 1a, ODP Site 641C Galicia Margin

P. HOFMANN[1], L. HANDLY[2], H. M. TALBOT[2], T. WAGNER[2]

[1]Institut für Geologie und Mineralogie, Universität zu Köln (peter.hofmann@uni-koeln.de)
[2]School of Civil Engineering, Newcastle University, UK

Perturbations of the global carbon cycle during the Mesozoic on the order of 40 kyr to approximately 1 Myr are known as Oceanic Anoxic Events (OAEs, Arthur et al., 1990). They resulted in extreme environmental conditions including widespread deep ocean anoxia and deposition of organic matter-rich sediments. OAEs are recognized on the basis of their distinct carbon isotope signatures and have been attributed to the episodic release of large quantities of CO_2 .The source of these additional quantities of CO_2 in the atmosphere is still under dispute. However, recent studies show that the long lasting (>1 Myr) lower Aptian OAE 1a and the OAE 2 at the Cenomanian/Turonian boundary appear to coincide with a significantly increased flux of non radiogenic osmium (Os) to the oceans. These osmium isotope anomalies have been attributed to the formation of large igneous provinces (LIPs) such as the Ontong Java Plateau, the Colombian-Caribbean igneous plateau and the Madagascar flood basalts (Turgeon and Creaser, 2008; Tejada et al., 2009) suggesting a direct link between volcanic CO_2 emission and OAE occurrence. Other, more short lived OAEs, in particular those associated with distinct negative carbon isotope excursion in the sedimentary record, such as the Lower Albian OAE 1b and the initial phase of OAE 1a have been linked to the short term decomposition of large amounts of gas hydrates (Jahren et al., 2001; Wagner et al., 2007; 2008).

The environmental consequences of large scale CO_2 release into the ocean-atmosphere system during OAEs are thought to include: increased surface water and air temperatures, reduced temperature gradients between the poles and the equator, increased alkalinity of the oceans, an overall acceleration of the global hydrological cycle, intensified weathering conditions on the continents associated with extensive export of nutrients to the ocean, leading to the widespread deposition of marine organic matter-rich strata (e.g., Jenkyns et al., 2003). We present a new TEX_{86}-derived SST record from Ocean Drilling Program (ODP) Site 641 (Fig. 1), extending from the Upper Barremian to the Lower Aptian allowing us to test SST variability across OAE 1a at a North Atlantic location and to further explore environmental impacts related to an

increase in pCO_2. These impacts include alkalinity fluctuations in the ocean expressed in sedimentary carbonate content and weathering intensity on the adjacent continental landmass approximated by a chemical index of alteration (CIA) along the Galicia Margin.

excess volcanic CO_2 emission in the Pacific area coupled with a global scale perturbation of marine carbonate burial may have served as the ultimate driver for atmospheric and ocean surface warming. The new SST and carbonate records from Site 641 are consistent with such a coupled mechanism but still do not exclude any additional short-

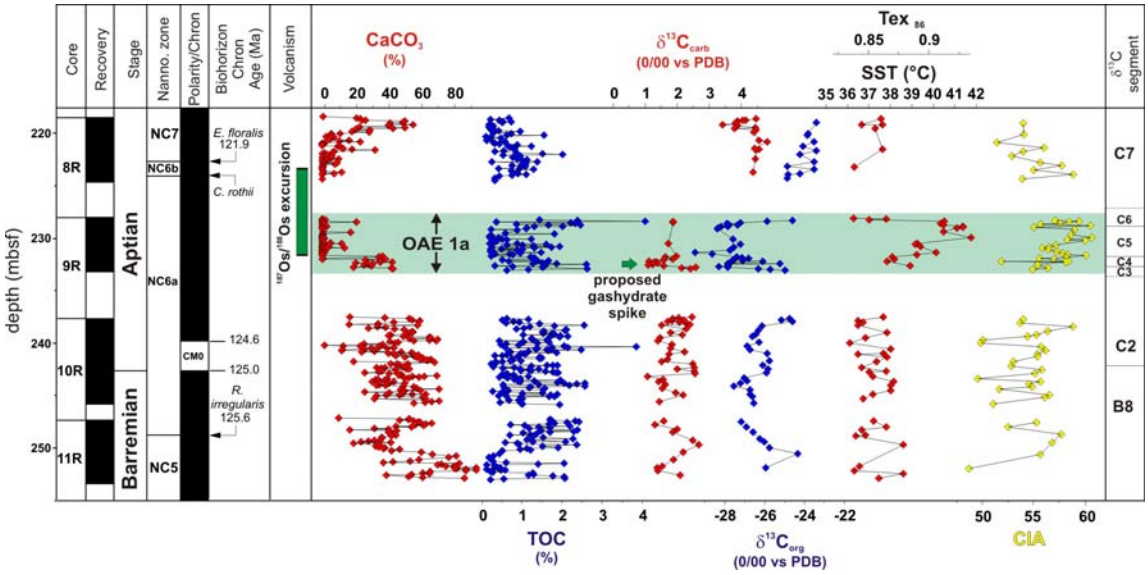

Fig 1: Summary of selected records reflecting environmental parameters of the upper Barremian to lower Aptian section recovered at ODP Site 641C in a chronostratigraphic framework modified after Shipboard Scientific Party Leg 103 (1987).

The TEX_{86} record from Site 641 does not show a quasi-synchronous increase in SST that parallels the negative $^{13}C_{carb}$ spike at the base of OAE 1a. Instead, if anything, temperatures decrease slightly within the interval of the negative $^{13}C_{carb}$ isotope excursion, with the marked SST increase occurring after the proposed methane emission event (cycle 1 in Fig. 2). A synchronous shift in of SST and ^{13}C values, however, is to be expected if methane emission would have been the cause of the onset of sea surface warming, as has been shown for example for OAE 1b (Wagner et al., 2008). Furthermore, a SST response should be observed at Site 641 given its location in a relatively subtropical small ocean basin with large surrounding continental landmasses (Fig. 1). Consequently, the lack of any SST rise coinciding with a negative carbon isotope excursion strongly argues against methane emission as a primary forcing mechanism for the temperature profile of OAE 1a (cycle 1; Fig. 2).

We do recognize, however, the coincidence between the onset of SST increase at Site 641 and the onset of submarine plateau basalt formation in the Pacific Ontong Java region. The $^{187}Os/^{188}Os$ isotope record from the OAE 1a type location in Italy (Tejada et al., 2009) shows a marked negative isotope excursion in $^{187}Os/^{188}Os$ ratios starting at the base of OAE 1a ($\delta^{13}C$ segment C5) and extending to the vicinity of the base of nannofossil zone NC 7 (Fig. 1). This Os anomaly has been attributed to an increased flux of non-radiogenic Os during a long-lasting phase of marine volcanism in the Ontong Java region (Tejada et al., 2009). Additional indirect support for a volcanic mechanism comes from a globally recognized marked drop in carbonate levels in OAE 1a sediments (e.g. Li et al., 2008). Both observations together argue that term (millennia or shorter) forcing mechanism, including local/regional gas hydrate destabilization. There is, however, no direct evidence that confirms such additional mechanisms and allows quantifying their impacts.

The Galicia Margin record shows that OC burial in the eastern North Atlantic was not affected by these large scale perturbations of the ocean-climate system (Fig. 1). This suggests that TOC supply in the area was largely governed by local/regional factors including variations in productivity, terrestrial organic matter supply and/or conditions changing the preservation potential of OM within the water column and at or in surface sediments. The significant surface water cooling at Site 641 by more than 5°C at the end of OAE 1a, paralleled by a large 4‰ drop in $\delta^{13}C_{org}$ (section 4; Fig. 3), may well document extensive and widespread marine OC burial, but not necessarily in the eastern North Atlantic region. A large marine OC sink would have induced a global drop in pCO_2 that would have been almost instantaneously translated into cooling of surface waters. More SST records covering this critical terminal phase of OAE 1a are required to draw any final conclusion from the Site 641 data. A likely area of enhanced OC burial, however, was the Pacific Ocean, considering the exceptional TOC-rich black shale at Shatsky Rise (ODP Site 1207, Dumitrescu et al., 2006) and, to a minor extent, in the Mid-Pacific Mountains region. These observations testify to the effectiveness of OCburial processes as modulators of global climate, even if they were focused in the most remote area of the Cretaceous Pacific.

Enhanced OC burial continuing beyond the termination of OAE 1a is suggested by generally heavier carbon isotopes at Site 641 (Fig. 2) and other locations worldwide

(e.g. Li et al., 2008; Wissler et al., 2003; Menegatti et al., 1998). The occurrence of lower and more stable SSTs between 36.4°C and 37.7°C in core 8R at Site 641C argue that greenhouse conditions were attenuated in the aftermath of the event despite the continued release of CO_2 inferred from the Os anomaly (Fig. 2), thus suggesting that the rate

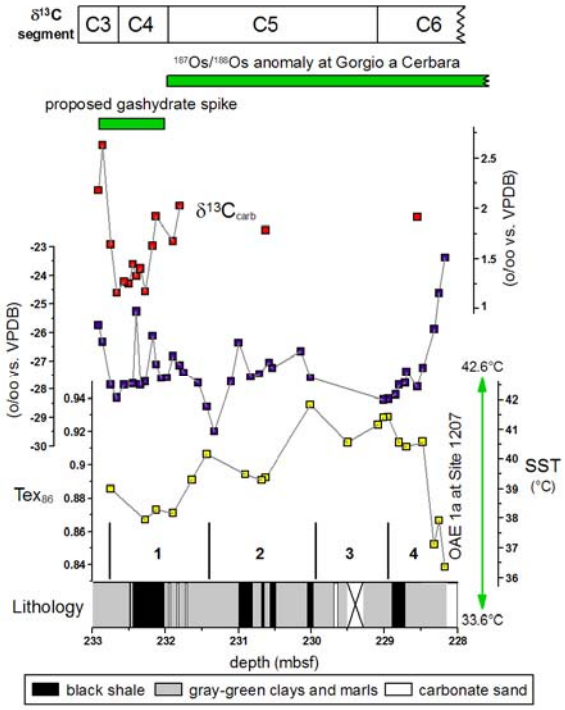

Fig. 2: 13C isotope and TEX86 records across OAE 1a at Site 641C (details see text). The SST range for the Pacific Site 1207 is based on TEX86 values published by Dumitrscu et al. (2006) and adjusted using the calibration of Kim et al. (2008). Position of the proposed gashydrate spike is from Jahren et al. (2001). Position of the osmium anomaly is from Tejada et al. (2009).

of carbon export and burial exceeded the rate of CO_2 release by volcanism.

Due to the lack of adequate records from all main ocean basins, a direct global comparison of SST development across the entire OAE 1a is not currently possible. Still, it is intriguing to compare SST trends before and during the initial and central parts of OAE1a to explore (North) Atlantic-Pacific interrelationships and possible response mechanisms.

In stark contrast with the Galicia Margin record, the SST profile from the central Pacific at Shatsky Rise (Fig. 3, Dumitrescu et al. 2006) does not exhibit an overall warming trend across the onset and during the main part of the OAE period. In the central Pacific, TEX86 values remain greater than 0.9, corresponding to SSTs above 40°C, before and during the event, with a possible moderate decline to around 0.85 (37°C) above this interval. We consider the open ocean setting at Shatsky Rise close to the paleo-Equator to be the primary reason for such invariable conditions: fully oceanic conditions in the tropics and the location in a large body of water would have attenuated or even suppressed further warming of central Pacific surface waters above the already very high background values. Unlike this setting the North Atlantic region was much smaller in size, in a landlocked position at

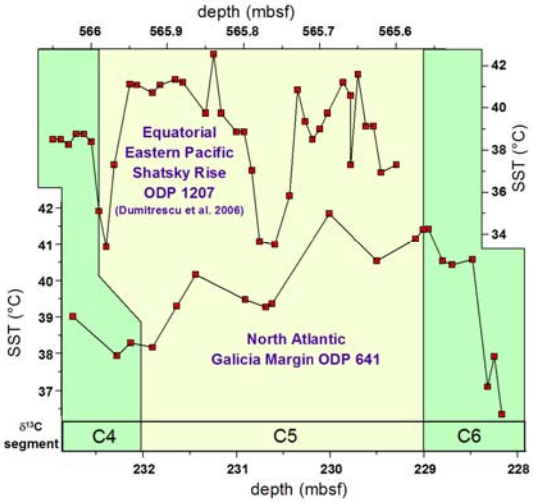

Fig. 3: Comparison of SST records across OAE 1a at Site 641 Galicia Margin and the Pacific Site 1207 (Dumitrscu et al. 2006).

sub-tropical latitudes. In such a setting, the SST response to increased atmospheric pCO_2 would likely have been amplified compared to the open ocean waters of the Pacific.

The SST record at DSDP Site 641C provides, for the first time, evidence for a warming of North Atlantic surface waters over the course of OAE 1a. The major phase of SST warming appears to be synchronous with an osmium isotope excursion reported from the Cismon section in Italy, which has been linked to an extensive episode of volcanism in the Pacific Ontong Java Plateau region. Warming of North Atlantic surface waters was accompanied by a shoaling of the local CCD and the development of intensified weathering conditions along the Galicia Margin, suggesting an overall amplification of greenhouse conditions and elevated pCO_2. We suggest that fluctuations in SST during OAE 1a were coeval in the Atlantic and Pacific region and may reflect changing pCO_2 levels during this period, which likely induced a reorganization of the global ocean-atmosphere system. Other high resolution records from other OAE 1a successions will be required to test to what extent the observed fluctuations in SST in both the Pacific and the North Atlantic were synchronous or diachronous. Elucidating such regional climatic couplings is essential for our understanding of regional climate instability and response under enhanced greenhouse climate conditions.

References:

Dumitrescu, M., Brassell, S.C., Schouten, S., Hopmans, E.C., Damste, J.S.S., 2006, Instability in tropical Pacific sea-surface temperatures during the early Aptian: Geology, v. 34, p. 833-836.

Jahren, A.H., Arens, N.C., Sarmiento, G., Guerrero, J., and Amundson, R., 2001, Terrestrial record of methane hydrate dissociation in the Early Cretaceous: Geology, v. 29, p. 159-162.

Jenkyns, H. C., 2003, Evidence for rapid climate change in the Mesozoic-Palaeogene greenhouse world: Philosophical Transactions of the Royal Society London A, v. 361, p. 1885-1916.

Kim, J.-H., Schouten, S., Hopmanns, E.C., Donner, B., and Sinninghe-Damsté, 2008, Global sediment core-top correlation of the Tex_{86} paleothernometer in the ocean: Geochimica Cosmochimica Acta, v. 72, p. 1154-1173.

Li, Y.-X., Bralower, T., Montanez, I.P., Osleger, D.A., Arthur. M.A., Bice, D.M., Herbert, T.D., Erba, E., and Premoli Silva, I., 2008, Towards an orbital chronology for the early Aptian Oceanic Anoxic Event (OAE 1a, ~120 Ma): Earth and Planetary Science Letters, v. 271, p. 88-100.

Menegatti, A.P., Weissert, H., Brown, R.S., Tyson, R.V., Farrimond, P., Strasser, A., and Caron, M., 1998, High-resolution $\delta^{13}C$ stratigraphy

through the early Aptian "Livello Selli" of the Alpine Trias: Paleoceanography, v. 13, p. 530-545.
Shipboard Scientific Party Leg 103, 1987, Site 641, *in* Boillot, G., Winterer, E.L., et al., Proceedings of the Ocean Drilling Program, Scientific Results, 103: College Station, Texas, Ocean Drilling Program, p. 571-649.
Tejada L.G., Suzuki, K., Kuroda, J. Cocconi, R., Mahoney, J.J., Ohkouchi, N., Sakamoto, T., and Tatsumi, Y., 2009, Ontong Java Plateau eruption as trigger for the early Apltian oceanic anoxic event: Geology, v. 37, 855-858.
Turgeon, S., and Creaser, R., 2008, Cretaceous anoxic event 2 triggered by a massive magmatic episode: Nature, v 545, p. 323-325.
Wagner, T. Wallmann, K, Herrle, J.O., Hofmann, P., and Stüsser, I., 2007, Consequences of moderate ~ 25,000 yr lasting emission of light CO2 into the mid-Cretaceous ocean: Earth and Planetary Science Letters, v. 259, p. 200-211.
Wagner, T., Stüsser, I., Hofmann, P., Schouten, S., Sinninghe Damsté, J.S., Herrle, J.O., 2008, Instant heating of Cretaceous surface waters off subtropical Africa in response to light carbon emission to the atmosphere: Geology, v. 36, 203-206.
Wissler, L, Funk, H, and Weissert, H., 2006, Response of early Cretaceous carbonate platforms to changes in atmospheric carbon dioxid levels: Palaeogeography Palaeoclimatology Paleoecology, v. 200, p. 187-205.

.

IODP

Reconstructing East Asian climate history between 12.5 and 7 Ma: Linkages to tectonic events, cryosphere evolution and orbital forcing

A. HOLBOURN[1], W. KUHNT[1], S. CLEMENS[2], W. PRELL[2], N. ANDERSEN[3]

[1]Institute of Geosciences, Christian-Albrechts-University, D-24118 Kiel, Germany
[2]Geological Sciences, Brown University, Providence, RI 02912, USA
[3]Leibniz Laboratory for Radiometric Dating and Stable Isotope Research, Christian-Albrechts-University, D-24118 Kiel, Germany

The late Miocene climate transition towards modern boundary conditions is still poorly resolved, mainly due to the scarcity of continuous, well-dated climate archives. Developing an astronomically-tuned chronology over this time interval has proven particularly challenging, as the $\delta^{13}C$ and $\delta^{18}O$ stable isotope signals generally exhibit low amplitude variations. Our primary targets are 1) to develop a high-resolution, orbitally-tuned chronology in an expanded clay-rich Miocene sedimentary archive recovered from the mid-continental slope of the northern South China Sea (ODP Site 1146, water depth: 2092 m), and 2) to provide a synthesis of climate and ocean chemistry proxies (benthic and planktic stable isotopes supplemented by carbonate dissolution indices) that targets the temporal evolution of both surface and bottom water masses. We focus on the punctuated evolution of global climate cooling between 12.5 and 7 Ma, in particular the timing and amplitude of late Miocene ice growth events (Mi5-Mi7 events of Miller et al., 1991), and test the hypothesis that these events coincided with low amplitude variations in the 1.2 Myr obliquity cycle. We additionally investigate the evolution of the East Asian monsoon in response to tectonic events, cryosphere evolution and orbital forcing by monitoring planktic $\delta^{18}O$ variations and contrasting the variance and phase relationships in our high/low latitudes climate proxy records.

Coring with the Extended Core Barrel (XCB) system at ODP Site 1146 recovered a continuous Miocene sequence of carbonate-rich hemipelagic sediments, which grade from unlithified green nannofossil clay in the lower Miocene to light brownish gray foraminifers and nannofossil clay in the upper Miocene. The average sedimentation rate for the Miocene succession is ~ 0.020-0.025 m kyr and the carbonate concentration within the sampled interval ~ 60 wt%. The shipboard splice of ODP Site 1146 corresponding to ~ 12.5-7 Ma was sampled in 5 cm (~ 2-2.5 kyr time resolution). The use of splice samples ensures that the sedimentary succession is continuous without sediment gaps at core breaks. We measured $\delta^{18}O$ and $\delta^{13}C$ in the near surface dwelling planktic foraminifer Globigerinoides trilobus and the benthic epifaunal species Cibicidoides wuellerstorfi and Cibicidoides mundulus. Ten to 20 well-preserved planktic tests from the size fraction 250-350 µm and 3-8 benthic tests in the size fraction >250 µm in each sample were broken into large fragments, cleaned in alcohol in an ultrasonic bath, then dried at 40 °C before analysis. In rare samples, where species abundance was low, a smaller number of specimens was analyzed. Measurements were made with the Finnigan MAT 251 mass spectrometer at the Leibniz Laboratory, Kiel University. The instrument is coupled on-line to a Carbo-Kiel Device (Type I). Samples were reacted by individual acid addition (99% H_3PO_4 at 73 °C). Standard external error is better than ±0.07 ‰ and ±0.05 ‰ for $\delta^{18}O$ and $\delta^{13}C$, respectively. Replicate measurements on ~5 % of samples indicate mean reproducibility of 0.1 ‰ for $\delta^{18}O$ and $\delta^{13}C$. Results were calibrated using the National Institute of Standards and Technology (Gaithersburg, Maryland) carbonate isotope standard NBS 20 and NBS 19 and 18, and are reported on the PeeDee belemnite (PDB) scale.

We originally developed an astronomically-tuned chronology over the interval 12.1-8.1 Ma by correlating the ODP Site 1146 benthic $\delta^{18}O$ signal to the Laskar et al.'s orbital solution (2004), following the strategy detailed in Holbourn et al. (2005; 2007). The revised biostratigraphy in Li et al. (2004) provided the preliminary chronological framework. Although astronomical tuning of the Late Miocene interval is challenging due to the low amplitude (~ 0.5 ‰) in $\delta^{18}O$ variations, we benefited from several plus points: (1) ODP Site 1146 $\delta^{18}O$ generally exhibits higher amplitude variations than the global average; (2) we minimized "noise" in the isotope signals through use of single species measurements; (3) we analyzed in parallel the core logging and coarse fraction data, which also show strong cyclicities, to test the robustness of interpretations. Initial benthic isotope results based on single species measurements reveal prominent 41 kyr and 100 kyr variability in the $\delta^{18}O$ signal with amplitude of up to 0.9 ‰ (Fig. 1). A salient feature of the $\delta^{18}O$ record is the transition from eccentricity-paced fluctuations to obliquity-paced variations, dominant between ~ 9.7 and 9.2 Ma during an interval of low 100 kyr eccentricity variance and high amplitude obliquity. In contrast, the benthic $\delta^{13}C$ record is characterized by lower frequency fluctuations (approximating 400 kyr), which suggests that the long eccentricity cycle influenced the carbon cycle and modulated Miocene long-term climate evolution (Fig. 1). The coarse fraction residue >63 microns, consisting almost exclusively of biogenic carbonate, exhibits a spectacular fine-scale cyclicity, which appears linked to changes in monsoonal regime on a precessional and/or semi-precessional timescale (Fig. 1). We are presently extending the benthic and planktic $\delta^{18}O$ and $\delta^{13}C$ records to fully cover the Miocene interval 12.5-7 Ma. Integration of

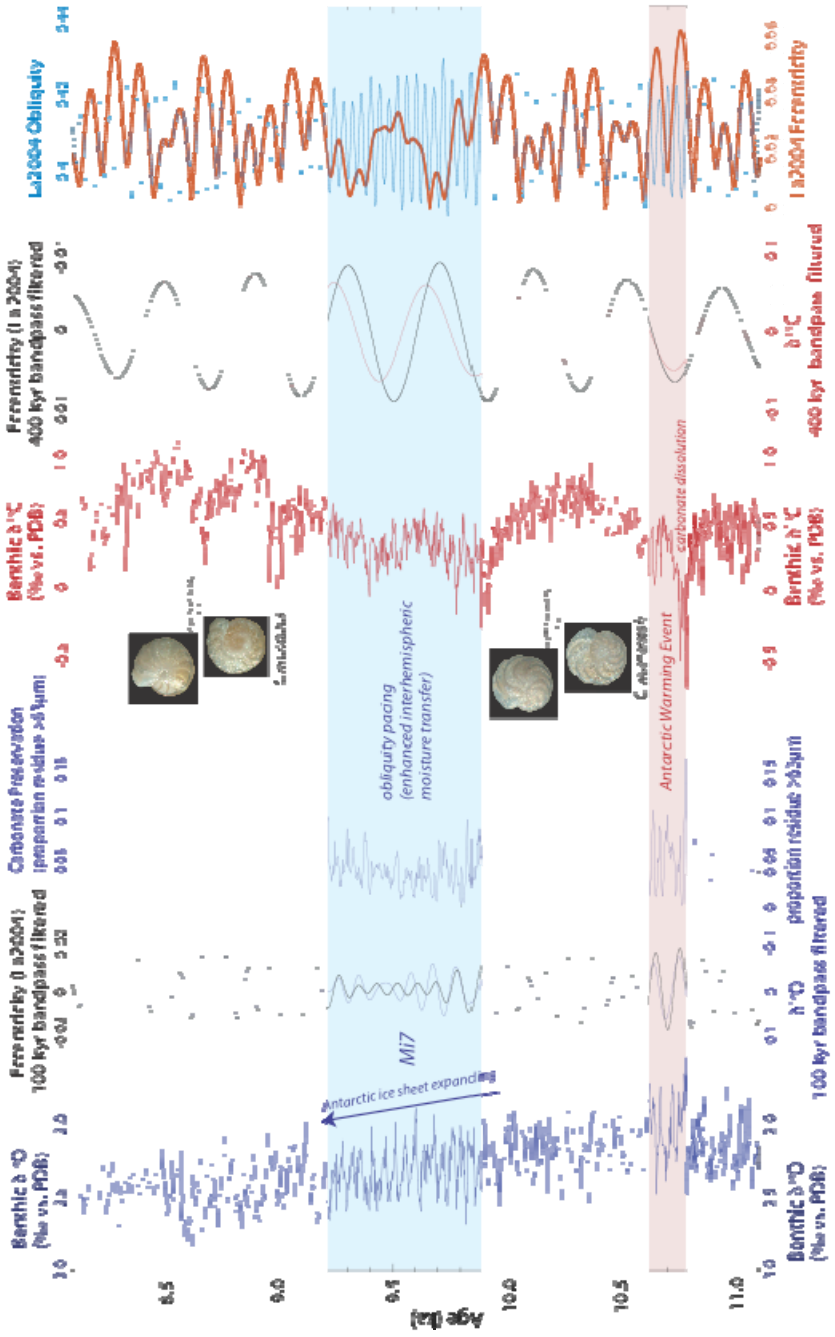

Figure 1: Benthic stable isotope and coarse fraction residue records from ODP Site 1146 closely tracking subtropical West Pacific paleoceanography during the late Miocene. Tuning of the benthic $\delta^{18}O$ series to the La2004 orbital solution provides a robust chronological framework. The benthic $\delta^{13}C$ record, characterized by prominent 400 kyr fluctuations, reveals eccentricity pacing of the carbon cycle.

planktic and benthic stable isotope data with carbonate dissolution indices will allow to tease out high and low latitudes signals and to monitor climatic events and upper ocean evolution in the South China Sea from the middle to late Miocene. This project complements previous work undertaken in ODP Site 1146 over the younger late Miocene to Pleistocene time slice (Clemens et al., 2008) and over the older middle Miocene time slice (Holbourn et al., 2005; 2007; submitted). Together, these collaborative efforts will ultimately contribute a continuous high-resolution Neogene climate archive for the subtropical West Pacific region.

References:

Clemens, S.C., Prell, W.L., Sun, Y., Liu, Z, and Chen, G., Paleoceanography, 23, PA4210, doi:10.1029/2008PA001638 (2008).

Holbourn, A.E., Kuhnt, W. and Schulz, M. and Erlenkeuser, H., Nature, 438(7067), 483-487, doi:10.1038/nature04123 (2005).

Holbourn, A.E., Kuhnt, W., Schulz, M., Flores, J.-A. and Andersen, N., EPSL, 261, 534-550. http://dx.doi.org/10.1016/j.epsl.2007.07.026 (2007).

Holbourn, A.E., Kuhnt, W., Regenberg, M., Mix, A. and Andersen, N., Geology (submitted).

Laskar J., Robutel, P., Joutel, F., Gastineau, M., Correia, A. C. M. and Levrard, B., Astronomy and Astrophysics, 428, 261-285 (2004).

Li, Q., Li, B., Zhong, G., McGowran, B., Zhou, Z., Wang, J. and Wang, P., Palaeogeography, Palaeoclimatology, Palaeoecology, 237, 465-482 (2004).

Miller, K. G., Wright, J. D. and Fairbanks, R. G., Journal of Geophysical Research, 96, 6829-6848 (1991).

IODP

Compaction tests of deep sea sediments at elevated temperatures: implications for physical properties and pore water geochemistry of subducting sediments

A. HÜPERS & A.J. KOPF

MARUM - Center for Marine Environmental Sciences, University of Bremen, P.O. Box 330440, 28334 Bremen, Germany.

Since the advent of plate tectonics, soil mechanical models were applied to study subduction zone dynamics. These models predicted pore fluid overpressures in underthrust sediments long before evidence from drilling, seismic imaging etc confirmed this assumption. In recent years temperature modelling revealed that great subduction zone earthquakes nucleate at depths where the temperature ranges from 125°C to350°C. This recent finding suggests that thermal behaviour has to be incorporated into soil mechanical models where it is commonly neglected. Refined models may shed light on how high fluid pressures affect the evolution and strength of the plate boundary or the onset of the seismogenic zone at convergent margins.

The present study aims at a lithological differentiated approach to study how different stratigraphic layers of the incoming sequence to the Nankai subduction system (Japan) contribute to dewatering during subduction in response to increasing depth and temperature. The laboratory study also includes chemical pore water analyses, because solutes such as chloride can provide useful insights in fluid flow.

Here, we present first results of heated consolidation tests on a clayey sediment sample similar to the smectite-rich hemipelagic facies ant the Nankai margin. Aliquots of the remolded sample were loaded up to 70MPa at temperatures of 20°C, 60°C, and 100°C. Investigation of mechanical data reveals that at similar stresses the pore space decreases with increasing temperature. This observation suggests that the grain contacts are weakened by the higher temperature and additional strain takes place until sufficient grains contacts are formed to bear the stress. An important parameter for excess pore fluid pressure modeling is the coefficient of consolidation (cv). It describes the rate at which a saturated clay undergoes consolidation when subjected to increasing stress. In previous studies this parameter was assumed to be constant. However, the present study shows that cv varies with temperature and stress. The coefficient increases with temperature, which can be directly linked to the temperature dependence of the hydraulic conductivity. A higher coefficient implies a higher rate of consolidation and thus pore pressure cannot as easily build up. In contrast, the cv decreases with increasing stress mostly at low stresses and stresses >30MPa. Future modeling using this data will investigate how the combination of the described trends may affect excess pore pressure generation in underthrust sediment.

Preliminary results of geochemical pore water analyses show a decrease of chlorinity at higher stresses for all tests. This observation is in accordance with previous studies and is generally interpreted as stress dependent release of water from smectite interlayers. However, chlorinity is higher for the heated tests. This observation is contrariwise to the expected temperature-dependent release of additional water from the smectite interlayer. Interaction of the charged clay surface and the pore water may one explanation for this result but further investigation is needed. Despite the observed freshening a wide range of solutes is increased in the expelled fluids at higher temperatures (e.g. B, Ba, Ca, K, Si), while some show retention (e.g. Mg). Possible reasons may be adsorption/desorption reaction at the clay surface, dissolution of mineral phases and illitization of smectite. The latter two are documented by XRD analyses of consolidated pucks after the experiments. The data reveals a decrease of plagioclase and initial smectite transformation with increasing temperature.

To sum up, the preliminary data reveals a pressing need to revise previous soil mechanical models to determine excess pore pressure in underthrust sediments. The data sows that the rate of consolidation is temperature and stress dependent which has to be taken into account. Further, geochemical data documents fluid freshening and an increase of distinct solutes which may provide further insights to fluid flow in the shallow subduction system.

ICDP

Molecular and organic carbon isotopic evidence for the evolution of key metabolic pathways during the Archean-Proterozoic transition

C. ILLING[1], H. STRAUSS[1], R. SUMMONS[2], A. LEPLAND[3], V. MELEZHIK[3,4] & THE FAR-DEEP SCIENTISTS

[1]Westfälische Wilhelms-Universität Münster, Institut für Geologie und Paläontologie, Corrensstr. 24, 48149 Münster, Germany
[2]Massachusetts Institute of Technology, Earth and Planetary Siences, 77 Massachusetts Ave E34-246, Cambridge, MA 02139-4307, USA
[3]Geological Survey of Norway, Leiv Eirikssons vei 39, N-7491, Trondheim Norway
[4]Center for Geobiology, University of Bergen, N-5020 Bergen, Norway

This work aims at reconstructing of the ancient microbial ecosystems and the evolution of key metabolic pathways during the Archean-Proterozoic transition (APT). The substantial rise of the Earth's atmospheric oxygen level around 2350 million years ago brought about large-scale environmental changes (e.g. Farquahr et al., 2000). The redox state of the oceans changed from a completely anoxic to a likely stratified water column with an upper oxic and a lower anoxic layer.

These changes affected microbial ecosystems and recycling of carbon, and have left characteristic geochemical traces, so called chemofossils including diagnostic organic biomolecules in the rock record (e.g. Brocks et al., 2005; Waldbauer et al., 2009). In addition, processes like autotrophic carbon fixation and/or the subsequent carbon recycling are associated with characteristic carbon isotopic fractionation (e.g. Eigenbrode, 2004) that can be tracked by studying the organic remnants.

The Fennoscandian Artic Russia-Drilling Early Earth Project (FAR-DEEP) provides a unique rock succsession of the Archean-Paleoproterozoic transition from the Fennoscandian Shield. This gives the possibility to examine the fundamental changes that occured in the

carbon cycle over approximatelly 700 Ma. 15 drillholes (fully cored, total length of ~3650 m), located on the Kola Peninsula and in Karelia have been succesfully completed in 2007. These are subjected to an international multidisciplinary study which includes the search for the remains of the ancient biosphere.

Organic carbon isotope data (δ^{13}_{Corg}) have been obtained on archive samples, collected from selected core intervals. However those are mainly focused on the organic-rich strata representing the Shunga-Event (e.g. Melezhik et al., 2009). Based on the previous work, the record of the organic carbon isotopic composition will be refined to identify promising intervalls for additional high resolution analysis.

Furthermore the analysis of biomarker abundance is part of the analytical scheme. However performing biomarker analysis in Precambrian rocks is still a challanging issue (e.g. Brocks, 2009) because of the high risk of contaminantion. To avoid possible post-drilling contamination a strict protocol (Sherman et al., 2007), will be followed and continously improved.

Initial sampling was performed during the FAR-DEEP Workshop in 2009. 121 archive samples were selected for δ^{13}_{Corg} measurements and ca. 30 samples for the biomarker analyses.

References:

Brocks J., Love G., Summons R., Knoll A., Logan G. & Bowden S. (2005): Biomarker evidence for green and purple sulfur bacteria in an intensely stratified Paleoproterozoic sea. Nature, 437, 866-870.

Brocks, J. (2009): The succession of primary producers in Proterozoic oceans. Goldschmidt Conference Abstracts 2009, A161. Abstract

Eigenbrode, J. (2004): Late archean microbial ecology: an integration of molecular, isotopic and lithologic studies. PhD Thesis Pennsylvania State University 326p

Farquahr, J., Bao, H. & Thiemens, M. (2000): Atmospheric Influence of Earth's Earliest Sulfur Cycle. Science 289, 756-758.

Melezhik, V., Huhma, H., Condon, D., Fallick, A., Whitehouse, M. (2007): Temporal constraints on the Paleoproterozoic Lomagundi-Jatuli carbon isotopic event. Geology, 35, 655-658.

Melezhik, V., Fallick, A., Filippov, M., Lepland, A., Rychanchik, D., Deines, J., Medvedev, P., Romashkin, A. & Strauss, H. (2009): Petroleum surface oil seeps from Palaeoproterozoic petrified giant oilfield. Terra Nova, 21, 119-126.

Sherman, L., Waldbauer, J. & Summons, R. (2007): Improved methods for isolating and validating indigenous biomarkers in Precambrian rocks. Organic Geochemistry 38, 1987-2000.

Waldbauer, J., Sherman, L., Sumner, D. & Summons, R. (2009): Late Archean molecular fossils from the Transvaal Supergroup record the antiquity of microbial diversity and aerobiosis. Precambrian Research 169, 28-47.

IODP

Influence of melt veins on the mineralogical and structural evolution of abyssal peridotites

N. JÖNS[1], W. BACH[1], F. KLEIN[1,2], T. SCHROEDER[1,2]

[1] Fachbereich Geowissenschaften, Universität Bremen, Klagenfurter Straße, 28359 Bremen, Germany

[2] present address: Geology and Geophysics Department, Woods Hole Oceanographic Institution, MA 02543, U. S. A.

[3] Faculty of Science and Mathematics, Bennington College, Bennington VT05201, U. S. A.

Hydration reactions are the major cause for changes in physical (rheology, magnetics, gravity,...) and chemical (mineralogy, trace element chemistry) properties of aging oceanic lithosphere. Such reactions are most effective where fault zones are present that facilitate seawater ingress into deeper parts of the lithosphere. Thus major locations for hydration are, on the one hand, close to subduction zones, where bending-related faulting produces deep trench-parallel faults, and on the other hand, transform faults intersecting the mid-ocean ridges. The latter ones are of particular interest as they occur in areas of comparatively high heat flow, enabling a pronounced hydrothermal activity with effective element transport and interaction with the ocean ridge magmatic system. A profound understanding of the underlying processes and pathways of fluid flow is of interest not only for economic geologists, but also for explanation of the fluid chemistry at hydrothermal vents and for estimating the bulk composition of the oceanic crust, the input into subduction zones. Our study is aimed at understanding the influence of magmatic melt impregnations on the hydration behavior of abyssal peridotites exposed at the seafloor, as well as the feedback mechanisms between mineralogical phase relations, shear zone formation and fluid flow.

Samples for this study are serpentinized abyssal harzburgites from Site 1270 of Ocean Drilling Program Leg 209 (Kelemen et al., 2004), which is located at the slow-spreading Mid-Atlantic ridge near the prominent 15°20'N fracture zone. Drill cores from Leg 209 consist mainly of peridotites and gabbros that are exposed in the footwall of major detachment faults on the flanks of the Mid-Atlantic ridge (Kelemen et al., 1998; Schroeder et al., 2007). We specifically chose peridotite samples that are crosscut by narrow (<15mm) shear zones (Fig. 1a). All studied samples are strongly serpentinized harzburgites (>90 vol.% of secondary minerals). Olivine is replaced by serpentine and magnetite making up a mesh texture, whereas orthopyroxene is pseudomorphously replaced by serpentine in almost magnetite-free bastite textures (Fig. 1a,b). The shear zones show a distinct mineralogy. Apart from some ultramafic material that has been sheared in, they consist of magnesium-rich chlorite (X_{Mg}=Mg/(Mg+Fe)=0.82–0.95) coexisting with Ti- and Al-poor tremolitic/actinolitic amphibole (X_{Mg}=0.85–0.93). Porphyroclasts of relict Ti- and Al-rich light-brownish magnesiohornblende are included in the chlorite matrix and are surrounded by needles of late-stage tremolite/actinolite. The occurrence of accessory zircon and apatite underlines that these "fault schists" likely formed from hydration of a melt impregnation veins crosscutting the peridotite. Based on whole-rock geochemistry, Ti-in-zircon thermometry (ca. 820°C; Ferry & Watson, 2007) as well as geochemical reaction path models (calculated using the EQ3/6 software package of Wolery, 2002), we propose that fault schists represent the hydrated remnants of former plagiogranitic melt impregnation veins (for further details see Jöns et al., 2009).

Whole rock oxygen isotope analyses of host rock serpentinites and separated fault schists (Jöns et al., 2009) indicate that shear zones were locations of enhanced fluid flow. Thus they are, although volumetrically insignificant, possibly of larger importance for hydrothermal vent fluid compositions. Their importance as major fluid pathways can be ascribed to the fact that the hydration behavior of plagiogranite differs strongly from that of the host peridotites. This leads to an early high-temperature (T≈500°C) hydration of plagiogranitic melt veins, when adjacent peridotites are still stable under hydrous conditions. In response to weakening due to formation of chlorite as breakdown product of primary plagiogranite

minerals, shear zones focus on former melt impregnations. This result is of major importance for the structural and hydrological evolution of detachment fault systems, as it shows that the basis for exhumation and for a pervasive lower-temperature serpentinization (T<350°C) is already established under comparatively high temperatures.

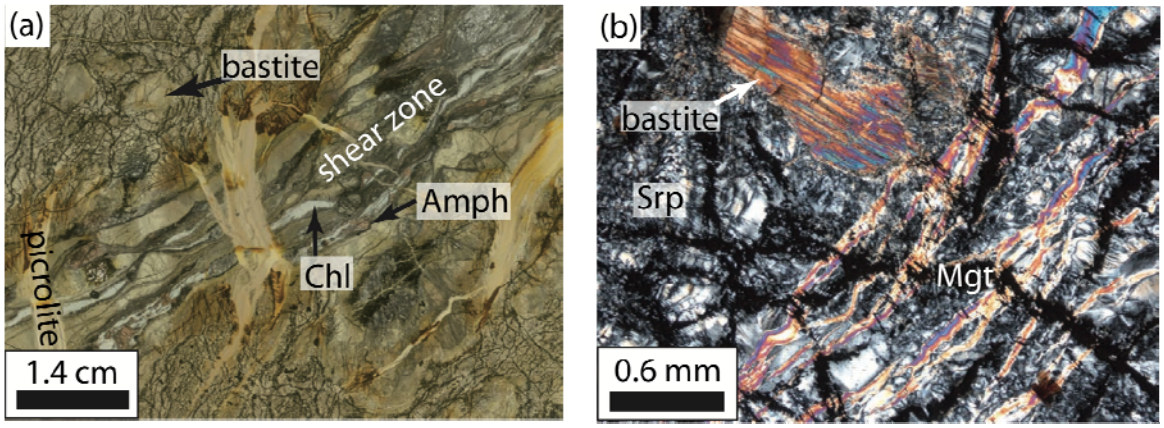

Fig. 1: Petrographical features of serpentinite samples from Leg 209, Site 1270: (a) Completely serpentinized harzburgite showing replacement of olivine (mesh texture) and orthopyroxene (bastite) by serpentine minerals and magnetite. The sample is crosscut by a shear zone containing chlorite and brownish amphibole porphyroclasts (plane polarized light). (b) Mesh texture formed from olivine breakdown and bastite after orthopyroxene. Small late-stage veins (high interference colours) crosscut the rock, indicating that fluid flow continued after serpentinization was complete (cross polarized light).

Apart from influencing the structural evolution of detachment fault systems, the melt-impregnated shear zones have also an impact on the chemical composition and phase relations of the ultramafic host rocks. We tried to assess the chemical changes due to melt impregnation and subsequent serpentinization using isocon diagrams (Grant, 1986). As no unaltered peridotite protolith is preserved, we compared the major and trace element contents of serpentinites occurring adjacent to altered melt veins with two melt-uninfluenced and variably serpentinized samples from the same ODP Leg (Paulick et al., 2006). This enables us to distinguish chemical changes due to melt impregnation from those related to serpentinization (Jöns et al., under review). The most obvious chemical influence of nearby melt veins is a strong enrichment in rare earth elements (REE). However, these elements remain mobile during serpentinization, as evidenced by more pronounced enrichment of the light REEs compared to the heavy REEs and an increased enrichment compared to more pervasively serpentinized samples. In contrast, the high field strength elements Zr and Nb are enriched in all samples, but show a constant degree of enrichment in comparison with assumed protolith compositions of variable serpentinization degrees. This indicates that enrichment of these elements took place before serpentinization started, i.e. by melt-rock interaction. Interestingly, there is also evidence for enrichment and mobility of aluminium during serpentinization.

The most obvious effect of melt impregnation veins on the mineralogy of serpentinites is the lack of brucite, which is explainable by increased silica activity close to melt veins. We used geochemical reaction path models to predict the mineralogical evolution of melt-influenced peridotites upon hydration (Fig.), and compared the results with petrographic observations. While serpentinization of pure harzburgite should lead to formation of brucite, serpentine and magnetite at T<350°C (Fig. a), brucite is almost absent in models simulating the influence of nearby plagiogranitic melt veins (Fig. b). The modeled fluid compositions show marked differences from the pure harzburgite model, which is reflecting the distinct mineralogy and mineral compositions. Such differences are more pronounced in the low-temperature area of the reaction paths, i.e. under typical serpentinization temperatures. As mineral assemblages are not only dependent on temperature and bulk rock composition, we used another model to study the influence of decreasing water-to-rock mass ratio. As we know that fluid flow is higher on shear zones, the mineral assemblages evolving under gradually decreasing water-to-rock mass ratios can be seen as equivalents for metasomatic zoning from the melt vein into the peridotite matrix. Isothermal models for 300°C – the assumed serpentinization temperature – are able to explain the absence of brucite in the serpentinites adjacent to melt-impregnated shear zones (Fig.). While amphibole-chlorite assemblages are able to form directly at the interface, brucite and magnetite are predicted to form more distal.

In the present study, we are able to show that the chemical and mineralogical evolution of serpentinites is strongly dependent on the nearby melt impregnation veins, which lead to development of distinct mineral assemblages prior to serpentinization and thus foster the shear zone development, exhumation and fluid flow in detachment fault systems. Furthermore, absence of brucite in abyssal peridotites will also influence the weathering behavior of the rocks when exposed to seawater under ambient P-T conditions.

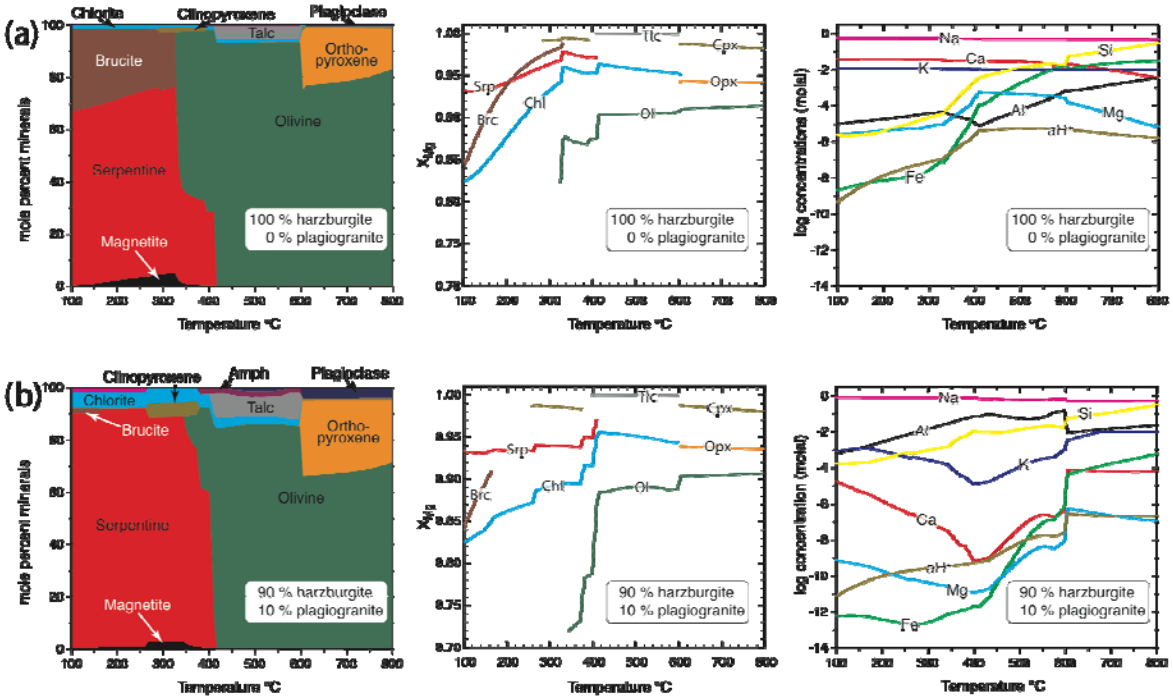

Fig. 2: Results of reaction path models. (a) Predicted mineralogy, mineral compositions and fluid compositions for hydrous alteration of a pure harzburgite. (b) Model for alteration of a 90:10 mixture of harzburgite and plagiogranite, simulating the presence of small amounts of plagionranitic melts in ultramafic hosted detachment faults. Notably, the amount of brucite is dramatically reduced. Concerning the fluid composition, a shift of the high pH region towards higher temperatures is observed.

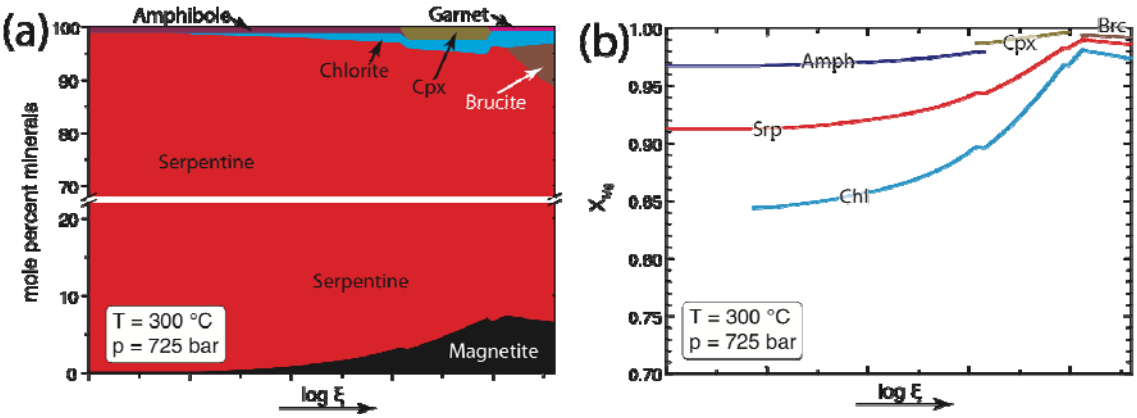

Fig. 3: Modeled mineralogy (a) and mineral compositions (b) for hydration of harzburgite with a fluid that had equilibrated on a melt-impregnated shear zone. In these diagrams ζ is a variable of reaction progress, and as it is a model-internal parameter no scale is given for the x axis. The diagrams reflect how mineral assemblages and compositions in serpentinites change with increasing distance from the melt vein: while chlorite and amphibole occur in vicinity to the melt vein (high flui/rock ratio), magnetite and brucite are predicted to form more distal (low fluid/rock ratio).

References:

Ferry JM, Watson EB (2007) New thermodynamic models and revised calibrations for the Ti-in-zircon and Zr-in-rutile thermometers. Contributions to Mineralogy and Petrology 154:429-437

Grant JA (1986) The isocon diagram - a simple solution to Gresens' equation for metasomatic alteration. Economic Geology 81:1976-1982

Jöns N, Bach W, Schroeder T (2009) Formation and alteration of plagiogranites in an ultramafic-hosted detachment fault at the Mid-Atlantic Ridge (ODP Leg 209). Contributions to Mineralogy and Petrology 157:625-639

Jöns N, Bach W, Klein F (under review) The influence of melt impregnations on reaction paths during serpentinization. Chemical Geology

Kelemen PB, Matsumoto T, Shipboard Scientific Party (1998) Geological results of Mode 98, Leg1: JAMSTEC/WHOI Shinkai 6500 cruise to 15°N, Mid-Atlantic Ridge. EOS Transactions 79 (Fall Meeting Suppl.):U22A-18

Kelemen PB, Kikawa E, Miller DJ, et al. (2004) Proceedings of the Ocean Drilling Program, Initial Reports, 209 [CD-ROM], vol. Ocean Drilling Program, Texas A&M University, College Station TX 77845-9547, USA

Paulick H, Bach W, Godard M, De Hoog JCM, Suhr G, Harvey J (2006) Geochemistry of abyssal peridotites (Mid-Atlantic Ridge, 15°20'N, ODP Leg 209): implications for fluid/rock interaction in slow spreading environments. Chemical Geology 234:179-210

Schroeder T, Cheadle MJ, Dick HJB, Faul U, Casey JF, Kelemen PB (2007) Nonvolcanic seafloor spreading and corner-flow rotation accommodated by extensional faulting at 15°N on the Mid-Atlantic Ridge: a structural synthesis of ODP Leg 209. Geochemistry, Geophysics, Geosystems 8:Q06015

Wolery TJ (2002) EQ3/6 - Software for geochemical modeling. In, vol. Lawrence Livermore National Laboratory, Livermore, California

ICDP

Quaternary mass movement events in Lake El´gygytgyn, northeastern Siberia – their effects on the ´pelagic´ sediment record and first results from the deep drilling project

O. JUSCHUS[1], V. WENNRICH[2], M. MELLES[2], C. GEBHARDT[3]

[1]Technische Universität Berlin, Institute of Applied Geoscience, Ackerstr. 76, Sek ACK 1-1, D-13355 Berlin
[2]University of Cologne, Institute of Geology and Mineralogy, Zuelpicher Str. 49a, D-50674 Cologne
[3]Alfred-Wegener-Institute for Polar and Marine Research, Am Alten Hafen 26, D-27568 Bremerhaven

Lake El´gygytgyn, located on Chukchi peninsula/NE Siberia, is a nearly circular lake with a diameter of 12 km and a water depth of 170 m. It was formed by an impact about 3.6 million years ago. Despite the fact that the lake is situated north of the Arctic Circle, geomorphological evidence suggests that the crater was never glaciated during the entire Late Cenozoic. Thus, a full-length sediment core from Lake El´gygytgyn would yield a complete record of Arctic climate evolution, back one million years prior to the first major glaciation of the Northern Hemisphere.

Pre-site surveys carried out in 1998 and 2003 recovered two 12.9 m and 16.6 m long sediment cores from the deepest part of the lake. They revealed a basal age of approximately 250 ka and 340 ka respectively and confirmed the lack of glacial erosion for the respective time period. The International Continental Scientific Drilling Program (ICDP) has provided funding for drilling operations on the lake and in its permafrost catchment. The drilling campaign took place in winter 2008/2009. The coring on the lake ice recovered more than 300 m of lake sediments. It probably represents a virtually complete Quaternary profile. The core-opening is still in progress. Thus, the results presented here are of preliminary nature.

In order to investigate the influence of gravitational sediment transport on the pelagic sediment record in the lake centre, two sediment cores were recovered in 2003 from the lower western lake slope. The cores penetrate a sub-recent mass movement deposit that was identified by 3.5 kHz echo sounding. In the proximal part of this deposit, deformed sediments reflect an initial debris flow characterized by limited sediment mixture. Above and in front of the debrite, a wide massive densite indicates a second stage with a liquefied dense flow. The mass movement event led to basal erosion of ca 1 m thick unconsolidated sediments along parts of its flow path. The event produced a suspension cloud, whose deposition led to the formation of a turbidite. The occurrence of the turbidite throughout the lake and the limited erosion at its base mainly suggest deposition by ‘pelagic rain’ following Stokes’ Law. Very similar radiocarbon dates obtained in the sediments directly beneath and above the turbidite in the central lake confirm this interpretation. When applying the depositional model for the Late Quaternary sediment record of Lake El´gygytgyn, the recovered turbidites allow reconstruction of the frequency and temporal distribution of large mass movement events at the lake slopes. In total, 28 turbidites and related deposits were identified in the sediment core covering approximately 300 kyr.

The new core, recovered in winter 2009, contain in the upper 50 m several mass movement deposits. Based on the core descriptions, the measured physical properties, and the results obtained from the 2003-cores, the following types of mass movement deposits can be distinguished as yet:

1. Small scaled, flood induced turbidites. The thickness is usually less than 0.1 cm. They occur in well laminated sediments only. These deposits were settled during cold and wet climatic stages like MIS 4 or 6.6.

2. Simple graded turbidites. The thickness range between 0.1 and 45 cm. The simple grading give evidence for the deposition by pelagic rain (see above). This type is the most common within the sediment succession. Sediment erosion by this type is of minor relevance.

3. Complex turbidites. Usually they are more than 10 cm thick. These turbidites are stratified, reflecting a stepwise (not continuous) upward fining. This is probably caused by current processes while deposition (possibly Lowe- or Bouma-Sequences). The base is mostly erosive.

4. Massive deposits with a graded top. These deposits are more than 15 cm thick. The base was settled by a dense flow, the top by turbidity currents. Erosion took place in the scale of mass movement thickness.

5. Massive deposits without a graded top. There is a broad thickness range from 2 cm upward. These deposits were settled by dense flows only. The base is usually erosive. The amount of erosion depends on mass movement thickness.

6. Deformed and displaced sediments inside a massive matrix. This type consists mainly of typical debris flow deposits. In the cores from the western shelf this type is overlain by densites and turbidites. The erosion is usually strong (up to 1 m).

7. Deformed and/or displaced sediments. The displacement took place as part of a slide or slump. Besides visible sediment deformation, evidences for this mass movement type are superpositions of the same sediment succession. Slides are usually less erosive but sediment duplication has to be subtracted for climatological interpretations.

References:

Juschus O., Melles M., Gebhardt C. & Niessen F. (2009): Late Quaternary Mass Movement Events in Lake El´gygytgyn, North-eastern Siberia. - Sedimentology, 56, 2155–2174. (DOI 10.1111/j1365-3091.2009.01074.x)

IODP

Mid-Pliocene restriction of the Indonesian Gateway and its implication on ocean circulation and climate

CYRUS KARAS[1], DIRK NÜRNBERG[1], RALF TIEDEMANN[2] AND DIETER GARBE-SCHÖNBERG[3]

[1] Leibniz Institute of Marine Sciences (IFM-GEOMAR), University of Kiel, Wischhofstrasse 1-3, D-24148 Kiel, Germany
[2] Alfred Wegener Institute for Polar and Marine Research, Am Alten Hafen 26, D-27568 Bremerhaven, Germany
[3] Institute of Geosciences, University of Kiel, D-24118 Kiel, Germany

Understanding the gradual global cooling during the mid-Pliocene (3.5–2.5 Ma ago) needs to consider the tectonical constriction of tropical seaways, which affected ocean circulation and the evolution of climate. Plate tectonic reconstructions show that the main reorganization of one such seaway, the Indonesian Gateway, occurred between 4 and 3 Myr ago. Model simulations have suggested that this would have triggered a switch in the source of waters feeding the Indonesian throughflow into the Indian Ocean, from the warm salty waters of the South Pacific Ocean to the cool and relatively fresh waters of the North Pacific Ocean. Here we show $\delta^{18}O$ and Mg/Ca ratios of planktonic foraminifera from different depth habitats to reconstruct the thermal structure at sensitive core sites in the Indian and Pacific Oceans from ~6 to 2 Myr ago: DSDP Site 214 in the tropical east Indian Ocean, ODP 763A in the subtropical east Indian Ocean under the influence of the Leeuwin Current, and DSDP Site 590B in the southwest Pacific Ocean at the Tasman front (Figure 1).

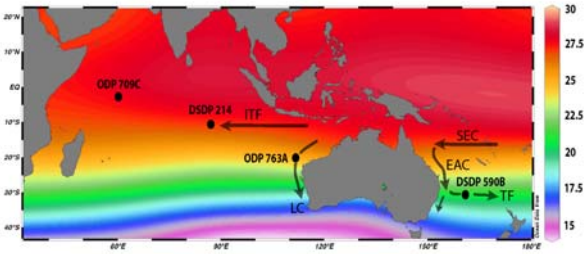

Fig. 1. Modern annual ocean temperatures (in °C) at 20 m water depth (Locarnini et al., 2006). Studied core sites 214, 709C, 763A and 590B (black dots) and surface ocean currents are indicated. ITF=Indonesian Throughflow, SEC=South Equatorial Current, LC=Leeuwin Current, EAC=East Australian Current, TF=Tasman Front.

In the outflow region of the Indonesian throughflow (DSDP Site 214), we find that sea surface conditions remained relatively stable throughout the mentioned Pliocene interval, while subsurface waters (300-450m water depth) freshened and cooled by about 4°C between 3.5 and 2.95 Myr ago. We suggest that the constriction of the Indonesian Gateway led to the cooling and shoaling of the thermocline in the tropical Indian Ocean and might have contributed to cooling in various (sub)tropical upwelling regions. At Site 763, we found evidence for a ~2°C decrease in sea surface temperatures during the Mid-Pliocene pointing to a Leeuwin Current, which weakened since ~3.3 Myr ago in line with the hydrographic changes in the Indonesian Throughflow region (Figure 2). Since

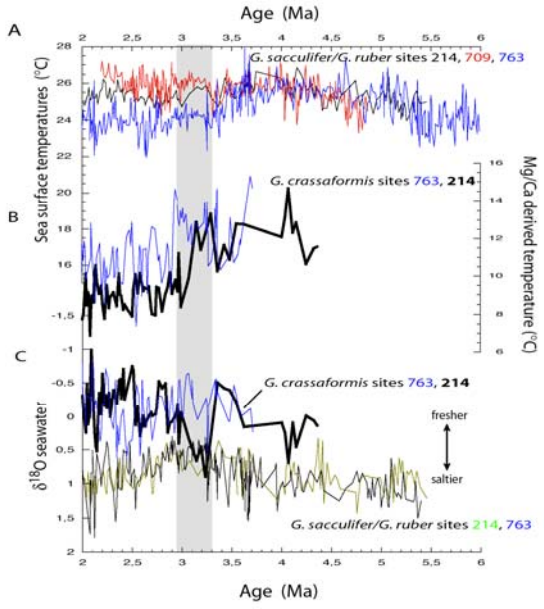

Fig. 2. Proxy data from Site 763 in relation to other paleoclimatic records across 6-2 Ma. (A) *G. ruber*/*G. sacculifer* $SST_{Mg/Ca}$ from Site 214 (black), Site 709C (red), Site 763A (blue). (B) Comparison of *G. crassaformis* Mg/Ca derived temperatures at the subsurface level from sites 214 (thick black) and 763A (blue). (C). (C) *G. sacculifer* (Site 214, green; Site 763A, blue) and subsurface *G. crassaformis* (Site 214, thick black; Site 763A, blue) $\delta^{18}O_{seawater}$ records.

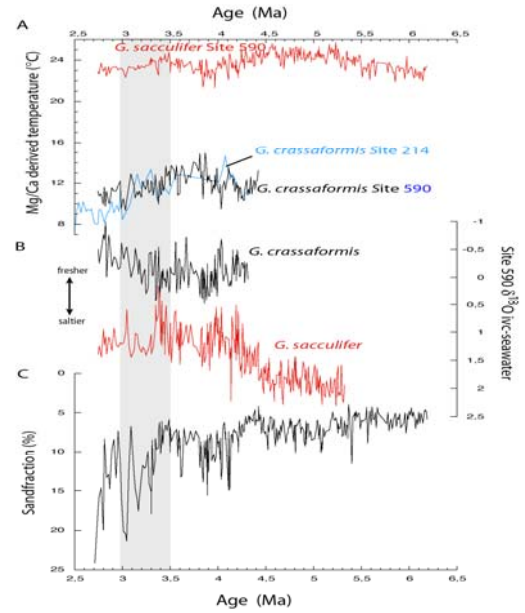

Fig. 3. Late Miocene to Pliocene proxy records of Southwest Pacific Ocean Site 590B in relation to other ocean areas (A) *G. sacculifer* $SST_{Mg/Ca}$ (red) and subsurface *G. crassaformis* Mg/Ca derived temperatures (black). Light blue line indicate *G. crassaformis* Mg/Ca derived temperatures from Site 214 (Karas et al., 2009). (B) *G. sacculifer* (red) and *G. crassaformis* (black) $\delta^{18}O_{ivc\text{-}seawater}$ values from Site 590B. (C) Site 590B Sandfraction data.

~3.5 Ma we observe a gradual subsurface cooling and freshening at the southwest Pacific Ocean (Site 590) whereas sea surface temperatures remained rather stable

(Figure 3). We suggest that the restricted Indonesian Gateway might have amplified the East Australian Current, allowing still warm sea surface temperatures at the southwestern Pacific Site 590B when the global climate gradually cooled. In contrast at the subsurface level the observed cooling and freshening points to a fostered northward flow of Subantartic Mode and Antartic Intermediate waters towards Site 590B, which is supported by an increase in the sanfraction indicating increased bottom currents (Figure 3). This possibly implies a first step towards the present Antarctic frontal system.

ICDP

Spatial sediment distribution at Laguna Potrok Aike, southern Patagonia, Argentina – An areal sediment survey to analyse the influence of late Holocene climate variability on sediment characteristics

S. KASTNER[1], C. OHLENDORF[1], T. HABERZETTL[2], A. LÜCKE[3], N.I. MAIDANA[4], C. MAYR[5,6], F. SCHÄBITZ[7], B. ZOLITSCHKA[1]

[1] Institute of Geography (Geopolar), University of Bremen, Germany – steka@uni-bremen.de
[2] Institute of Geography, Friedrich-Schiller-University Jena, Germany
[3] Institute of Chemistry and Dynamics of the Geosphere 4: Agrosphere (ICG 4), Energy & Environment, Research Center Jülich, Germany
[4] Department of Biodiversity and Experimental Biology, University of Buenos Aires, Argentina
[5] GeoBio-CenterLMU and Dept. of Earth & Environmental Sciences, University of Munich, Germany
[6] present address: Institute of Geography, Friedrich-Alexander-University Erlangen-Nuremberg, Erlangen, Germany
[7] Seminar for Geography and Education, University of Cologne, Germany

The Quaternary maar lake Laguna Potrok Aike (51°58'S, 70°23'W) is a palaeolimnological key site among the emerging southern hemisphere terrestrial climate archives and therefore was chosen as an ICDP drilling site in 2008 (Zolitschka et al., 2009) within the "Potrok Aike maar lake sediment archive drilling project" (PASADO). The lake and its catchment were investigated in detail during the past decade. On-site monitoring (Mayr et al., 2007a; Zolitschka et al., 2006), intensive seismic surveys (Anselmetti et al., 2009) and detailed studies of the lacustrine sediment infill were conducted. Short gravity cores (Haberzettl et al., 2005; Haberzettl et al., 2006) and long piston cores (Haberzettl et al., 2007; Haberzettl et al., 2008) were recovered from the 100 m deep lake. These sediments were investigated for sedimentological and geochemical proxy parameters as well as for pollen (Mayr et al., 2007b; Wille et al., 2007) and an stable isotopes (Mayr et al., 2009).

Situated in the dry steppe environment of southern Patagonia the lake is exposed to the influence of the prevailing Southern Hemispheric Westerly winds. Geomorphological features of the lake and multi-proxy reconstruction of the lacustrine sediment sequence document the sensitivity of the lake's hydrological budget to the varying intensity of the westerly winds, related pressure systems and thus precipitation changes (cf. Mayr et al., 2007b). Hydrological fluctuations correspond to lake level changes documented by aerial and sub-aquatic lake level terraces (Anselmetti et al., 2009) and depositional changes (Haberzettl et al., 2009). Thus, the lake provides a unique palaeoclimatic and palaeoenvironmental record of the late Holocene (Haberzettl et al., 2005) and early to mid to Holocene (Haberzettl et al., 2007) with its warm and dry or cold and wet periods .

In general, one point records of the lacustrine sediment infill are recovered to reconstruct long-term trends of palaeoenvironmental variations in high-resolution. However, only little is known about the spatial sediment variability of sedimentary proxies within lacustrine systems and thus the influence of climate variables on a spatial scale.

Laguna Potrok Aike represents a bowl shaped and nearly circular lake, about 3.4 km in diameter. The gently dipping and flat littoral zone is separated from the 100 m deep and flat profundal by steep slopes. In preparation of the PASADO deep drilling project a survey of the spatial sediment distribution was proposed to (A) develop an understanding of the dynamics of modern and sub-recent processes that control the areal sediment characteristic in the lake and (B) to improve the potential for interpretation of the long sediment record recovered by the PASADO project.

Analysing the influence of modern climate conditions on the areal sediment distribution a dense grid of 63 gravity cores was recovered in 2005 and 2008 from the lake floor. The cores were up to 49 cm in length and were recovered from water depths between 9 and 100 m. Additionally 40 near-shore samples were collected to represent modern sediment characteristics. Surface sediments of all cores were subsampled. Subrecent influences were analysed for selected time windows covering different hydrological settings (Haberzettl et al., 2005). The selected time windows – AD 1960, 1800, 1610, 1500 and 1380 – are supposed to represent the periods of the 20th century warming, the Little Ice Age (LIA) and the Medieval Climate Anomaly (MCA). All cores were scanned with X-ray fluorescence technique and magnetic susceptibility with 1 and 4 mm spatial resolution, respectively. Using the scanning data, all cores were correlated and thereafter linked to an established age-depth model (Haberzettl et al., 2005). The scanning profiles do not allow unequivocal correlation of profundal and littoral cores across the steep slopes. Thus, a correlation prior to the present sediment surface is solely based on cores from water depths exceeding 45 m. Samples of surface sediments were taken from all 63 cores while subsampling of the selected time intervals was only possible for up to 43 well correlated cores from the deep central basin. Thereafter, the sediment was analysed geochemically (for element concentrations of C, N, S, and P), sedimentologically (grain size), palynologically, diatomologically, and for stable isotopes of organic matter (C, N) and carbonates (C, O). Subsequently, distribution maps for all parameters and for each time window were compiled by an exact point kriging method.

The modern sediment distribution confirms pronounced differences between littoral and profundal cores (Kastner et al., submitted-a). Interpolated patterns of grain size, benthic diatoms, total inorganic carbon, Ti and Ca point to distinct internal depositional dynamics induced by the dominant westerly winds (Fig. 1). Frequent erosion, resuspension and redistribution of littoral sediment are

followed by transport to a profundal accumulation area. Hence, sedimentation within this lake is not only influenced by lake level changes, episodic inflows and the surrounding geology but also by wind driven wave action, resulting in internal currents and shoreline erosion.

the interpolation and thus on the quality of the recovered cores, the accuracy of the used age-depth model and the reliability and possibility of core correlation. Nonetheless, distribution patterns and sediment characteristics of modern and subrecent sediments reveal intensified

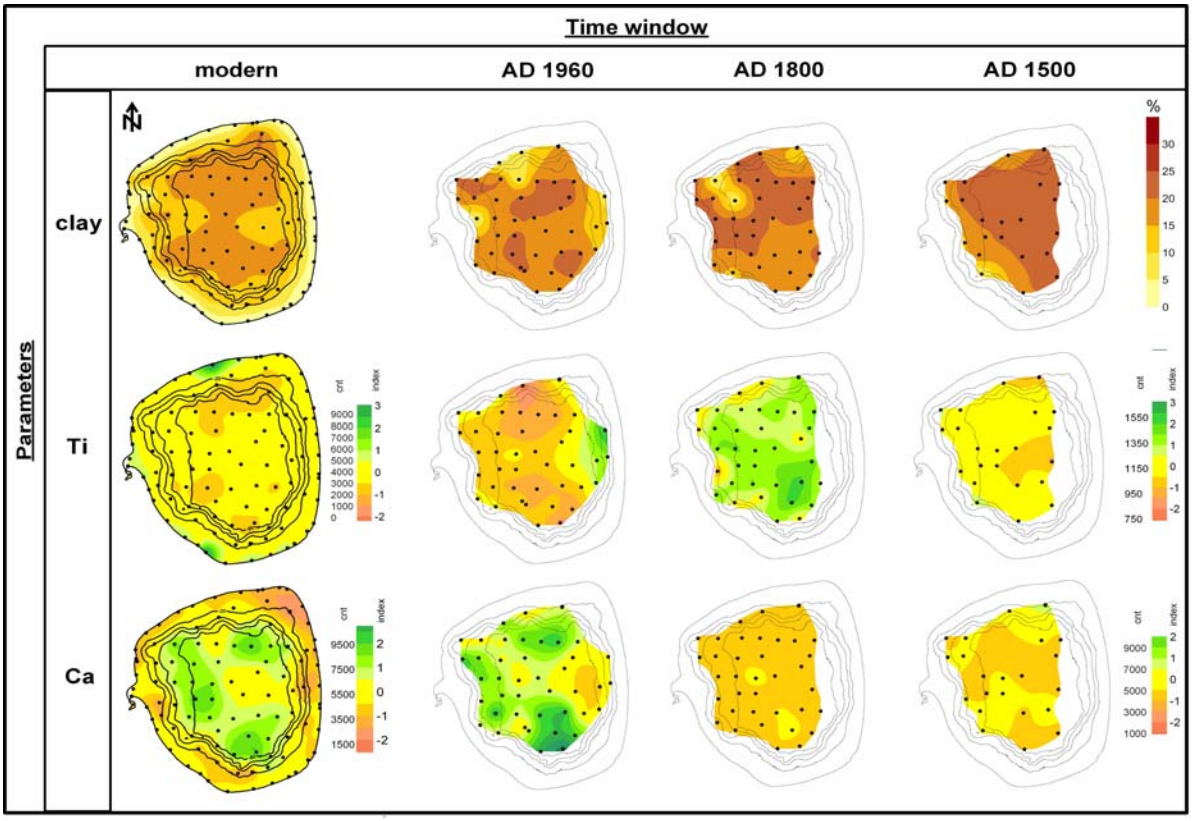

Fig 1: Distribution maps of clay (percentage), titanium (Ti: counts) and calcium (Ca: counts) for time windows of low lake levels (modern and AD 1960), high lake level (AD 1800: LIA) and an intermediate lake level stage (AD 1500). Contour map shows bathymetric information of Laguna Potrok Aike, black dots indicate coring locations. Note: values for Ca and Ti are standardised by a z-transformation. Values are reported as index-values (-5 to 5; mean = 0) and equivalent absolute counts (cnt). Due to data processing value ranges are slightly different for modern and subrecent time windows.

The subrecent spatial sediment distribution is evaluated and interpreted in the context of modern processes (Kastner et al., submitted-b). The aim of the analyses of time windows was to evaluate if the modern conditions could be identified for distinct past lake level stages. Due to difficulties with core correlation, the spatial resolution of the distribution maps is diminishing back in time. Thus, the interpretation is restricted to information of the deep central basin area. As a result information of the interpolated patterns becomes less clear with less data points available. Finally, distribution maps of the time window AD 1380, covering the MCA, could not be compared to modern low lake level conditions. Mineralogical parameters and stable isotope values of organic matter seem to be important proxies to evaluate the mechanisms of sediment distribution during selected hydrological settings. The data of the AD 1960 low lake level conditions explicitly indicate sediment reworking from the lake margins. In contrast, time windows of high lake level stages during the LIA (AD 1800 and 1610) indicate the influence of tributaries, especially at the western part of the lake (Fig. 1).

In conclusion, the interpretation of the distribution pattern strongly depends on the amount of cores used for sediment redistribution during low lake levels and strengthened winds, i.e. during post LIA times (around AD 1960) and around AD 1500. In contrast, LIA conditions (around AD 1800) with a lake level high stand and less intense westerly winds result in a more homogeneous sediment distribution within the deep central basin. Furthermore, spatial sediment distribution reveals distinct influences of the main western and smaller tributaries at the eastern shore.

Acknowledgements: We thank the SALSA- and PASADO-teams for help during coring in 2005 and 2008. This research is supported by the DFG priority program “International Continental Scientific Drilling Program” (ICDP) in the framework of the project "Analysis of sediment areal distribution in Laguna Potrok Aike” (ASADO).

References:

Anselmetti, F.S. et al., 2009. Environmental history of southern Patagonia unraveled by the seismic stratigraphy of Laguna Potrok Aike. Sedimentology, 56(873-892).

Haberzettl, T. et al., 2009. Late Pleistocene dust deposition in the Patagonian steppe - extending and refining the paleoenvironmental and tephrochronological record from Laguna Potrok Aike back to 55 ka. Quaternary Science Reviews, doi:10.1016/j.quascirev.2009.07.021.

Haberzettl, T. et al., 2007. Lateglacial and Holocene wet-dry cycles in southern Patagonia: chronology, sedimentology and geochemistry of a

lacustrine record from Laguna Potrok Aike, Argentina. Holocene, 17(3): 297-310.
Haberzettl, T. et al., 2005. Climatically induced lake level changes during the last two millennia as reflected in sediments of Laguna Potrok Aike, southern Patagonia (Santa Cruz, Argentina). Journal Of Paleolimnology, 33(3): 283-302.
Haberzettl, T. et al., 2008. Hydrological variability in southeastern Patagonia and explosive volcanic activity in the southern Andean Cordillera during Oxygen Isotope Stage 3 and the Holocene inferred from lake sediments of Laguna Potrok Aike, Argentina. Palaeogeography Palaeoclimatology Palaeoecology, 259(2-3): 213-229.
Haberzettl, T. et al., 2006. Environmental change and fire history of southern Patagonia (Argentina) during the last five centuries. Quaternary International, 158: 72-82.
Kastner, S. et al., submitted-a. Southern Hemispheric Westerlies control spatial distribution of modern sediments (Laguna Potrok Aike, Argentina). Journal of Limnology.
Kastner, S. et al., submitted-b. Spatial variability of Late Holocene sediment proxies controlled by lake internal depositional dynamics, Laguna Potrok Aike (southern Patagonia, Argentina). Holocene.
Mayr, C. et al., 2009. Isotopic fingerprints on lacustrine organic matter from Laguna Potrok Aike (southern Patagonia, Argentina) reflect environmental changes during the last 16,000 years. Journal of Paleolimnology, 42: 81-102.
Mayr, C. et al., 2007a. Precipitation origin and evaporation of lakes in semi-arid Patagonia (Argentina) inferred from stable isotopes (delta O-18, delta H-2). Journal Of Hydrology, 334(1-2): 53-63.
Mayr, C. et al., 2007b. Holocene variability of the Southern Hemisphere westerlies in Argentinean Patagonia (52 degrees S). Quaternary Science Reviews, 26(5-6): 579-584.
Wille, M. et al., 2007. Vegetation and climate dynamics in southern South America: The microfossil record of Laguna Potrok Aike, Santa Cruz, Argentina. Review Of Palaeobotany And Palynology, 146(1-4): 234-246.
Zolitschka, B. et al., 2009. The Laguna Potrok Aike Scientific Drilling Project PASADO (ICDP Expedition 5022). Scienctific Drilling, 8: 29-34.
Zolitschka, B. et al., 2006. Crater lakes of the Pali Aike volcanic field as key sites for paleoclimate and paleoecological reconstruction in southern Patagonia, Argentina. Journal of South American Sciences, 21: 294-309.

IODP

Major shifts in age control at ODP Site 982 near the Pliocene onset of Northern Hemisphere Glaciation – Composite depths and $\delta^{18}O$ stratigraphy revisited

N. KHÉLIFI[1], M. SARNTHEIN[1]

[1]Institute of Geosciences, University of Kiel, D-24118 Kiel, Germany (nk@gpi.uni-kiel.de)

ODP Site 982 at Rockall Plateau provided a key sediment section for reconstructing northeast Atlantic paleoceanography over the Late Pliocene to Quaternary onset of Northern Hemisphere Glaciation. By now, Site 982 served to monitor benthic $\delta^{18}O$ stratigraphy and the global $\delta^{18}O$ ice effect (Venz and Hodell, 2002; Lisiecki and Raymo, 2005), past changes in SST and SST phase relationships (Lawrence, 2009), trends in atmospheric pCO2 (Pagani et al., 2010), and the advection of Mediterranean Outflow Water and Atlantic Intermediate Water composition (N. Khélifi, in preparation). A detailed revision of composite depths and magnetostratigraphy, and a renewed fine-tuning of the benthic $\delta^{18}O$ record now led to a significant age shift (rejuvenation) of all proxy records by 20 to 150 ky during the onset of Northern Hemisphere Glaciation, an interval of major climate change (3.2–2.7 Ma ago). The revised new SST records well compare with coeval SST trends previously published from ODP sites elsewhere in the northern North Atlantic (e.g., Bartoli et al., 2005; Naafs et al., in preparation). Our study demonstrates the crucial significance of assembling with care composite-depth scales and a reliable $\delta^{18}O$ stratigraphy in ODP sediment records as backbone for correlations in paleoceanography.

References:
Bartoli et al., 2005: EPSL, 237, 33-44.
Khélifi N., 2010: PhD Thesis, Kiel University, in prep.
Lawrence et al., 2009: Paleoceanography, 24/2.
Lisiecki and Raymo, 2005: Paleoceanography, 20 PA1003.
Naafs, Khélifi et al., 2010: Pliocene changes in North Atlantic SST, in prep.
Pagani et al., 2010: Nature Geoscience, 3/1.
Venz and Hodell, 2002: Palaeo. Palaeo. Palaeo., 182, 197-220.

IODP

Time scales for vertically moving axial magma chambers at fast-spreading ocean ridges and involved magmatic reactions: Insights from IODP Site 1256

C. KIRCHNER[1], J. KOEPKE[1], H. BEHRENS[1]

[1]Institut fuer Mineralogie, Leibniz Universitaet Hannover, Callinstr. 3, 30167 Hannover, Germany, (c.kirchner@mineralogie.uni-hannover.de)

It is well accepted that AMCs ("axial magma chamber") under fast spreading ocean ridges located at the boundary between lower and upper crust are dynamic systems with the potential to move up and down. Nevertheless, the time scales of these vertical movements are poorly constrained up to now with very rough estimations, varying between 10 and 10000 years.

This project focuses on a close investigation on the gabbro/sheeted dike transition, which is part of a reference profile of the upper oceanic crust recently drilled by IODP multi-cruise mission „Superfast Spreading Crust" (Site 1256, equatorial East Pacific Rise). Of substantial interest is a specific horizon defined as CBL ("conductive boundary layer"), separating the AMC and the hydrothermally altered dikes. The ascent of the AMC leads to the formation of "granoblastic dikes" due to an intense metamorphic overprint under granulite-facies conditions [Koepke et al. 2008].

In order to quantify the vertical oscillations of the AMC described above, we plan to apply tools of diffusion profile modeling to relictic, zoned plagioclase and clinopyroxene phenocrysts within the granoblastic dikes, which were metamorphosed by the thermal imprint of the AMC (~1200°C) in a high position. Provided that the zoning patterns in the crystals studied are due to temperature-induced diffusion processes and the environmental conditions like temperature, volatile fugacities and diffusion coefficients are known, the detailed analysis and modeling of the concentration profiles allows us a quantification of the residence time of the heat source (AMC) in a high position and hence, temporal information about the vertical fluctuations of the AMC can be constrained.

At this stage of the project, we measured approximately 30 concentration profiles with respect to An content and selected trace elements in several relictic plagioclases with electron microprobe. Since many profiles are of irregular shape, obviously due to inhomogenities most likely caused by alteration reactions or inclusions, we identified that the measurement of acceptable profiles is a challenging task. Unfortunately, about two-third of the measured profiles up

to now exhibit irregularities and cannot be used for our modeling approach. By this observation, the necessity of our statistical approach in collecting a high number of diffusion profiles is emphasized. Nevertheless, about 10 profiles in a relictic plagioclase could be measured with satisfying results which show the typical shape of diffusion profiles resulting from the exchange between plagioclase and matrix as presented in Figure 1.

An-Profile lengths are slightly shorter (~5-7 µm) compared to previous works [Koepke et al. 2008]. All profiles were fitted using the diffusion equation [Crank, 1975] assuming constant diffusivity and an initially homogenous plagioclase (r^2=0.999). First estimations yield time scales of 33000 years for the development of the concentration profiles. In the future, we plan to model trace element profiles as well, because diffusion modeling is most reliable, when different elements with different diffusivities are included.

In addition to the diffusion modeling, an experimental subproject is planned, which aims on the simulation of melt/rock interactions occurring during the up-ward burning of the AMC into the previously altered sheeted-dike complex. With these experiments we attempt to extent our knowledge on the underlying magmatic reactions under fast spreading ocean ridges, regarding processes like stoping, assimilation and contamination.

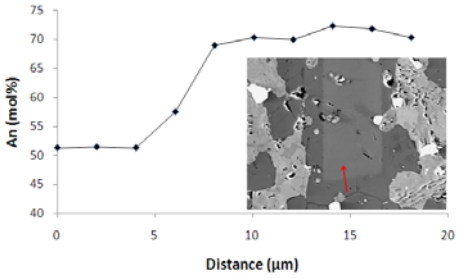

Fig. 1. Backscattered electron image showing a relictic plagioclase with idiomorphic shape (medium grey) surrounded by plagioclase of the granoblastic matrix (dark grey) within a typical granoblastic dike drilled at Site 1256D (sample number 312-1256D-203-1-10-14) The red arrow marks the location where the concentration profile was measured with the electron microprobe. The light grey and withish phases are hornblende, pyroxene, and oxides of the granoblastic matrix (including products of secondary alteration).

References:

Koepke, J. et al. (2008) Petrography of the dike-gabbro transition at IODP Site 1256 (equatorial Pacific): The evolution of the granoblastic dikes. Geochem.Geophys Geosyst, vol. 9, doi:10.1029/2008GC001939

Crank, J. (1975), The Mathematics of Diffusion, 414 pp., Oxford Univ. Press, Oxford, U. K.

IODP

A switch in recorded strain infered from magnetic fabric in an accretionary prism toe – results from IODP NanTroSEIZE Expedition 316, Nankai Trough, Japan

Y. KITAMURA[1], T. KANAMATSU[2], X. ZHAO[3]

[1]IFM-GEOMAR, Leibniz Institute of Marine Sciences at the University of Kiel, Wichhofstr. 1-3, 24148 Kiel

[2]Institute for Research on Earth Evolution, Japan Agency for Marine-Earth Science and Technology, 2-15 Natsushima-cho, Yokosuka, Kanagawa, 237-0061 Japan

[3]Department of Earth and Planetary Sciences, University of California Santa Cruz, 1156 High Street, Santa Cruz CA 95064, USA

The general goal of the Nankai Trough Seismogenic Zone Experiment (NanTroSEIZE) is to reveal active process in an accretionary subduction zone with recurrent large earthquakes. A key component of NanTroSEIZE is logging and sampling by the D/V Chikyu, as part of the Integrated Ocean Drilling Program (IODP). Stage 1 of NanTroSEIZE consisted of three continuous expeditions from 314 to 316 aimed at understanding the shallow parts of two major faults in the accretionary prism, the megasplay fault and the frontal thrust. During Expedition 316, fault rock samples from these two targets were successfully recovered [Kinoshita et al., 2009].

The strength of a material is a fundamental question in terms of its absolute value and special variation for faulting process in subduction zones. The key hypotheses on catastrophic faulting at the updip limit of seismogenic zone are; a change in thermal condition [e.g. Hyndmann and Wang, 1993] and following change in frictional behavior [e.g. Saffer and Marone, 2003], a change in shear strength controlled by fluid pressure [e.g. Moore and Saffer, 2001], and a change in strength due to lithification [e.g. Kimura and Ludden, 1995; Matsumura et al., 2003]. The Nankai Trough has lateral variation of prism taper angle which may induce different condition of basal friction on the décollement [Kimura et al. 2007]. To evaluate these hypotheses, we need to constrain stress, strain and strength variation in the accretionary prism. Recent observations of very low frequency (VLF) earthquake swarms in accretionary prisms near Kii Peninsula [Obara and Ito, 2005] reflect a poorly known dynamic process of the accretionary prisms. Those small events occur, interestingly, between updip limit of the seismogenic zone and trench, which indicate that the shallow accretionary prism is still active during the interseismic period.. However, structural studies on the evolution of shallow accretionary prism have mainly focused on in relation to long term tectonics but not to plate boundary earthquake or even VLF events. Further knowledge about the strain/stress condition in the shallow accretionary prism is necessary for us to understand the variation of such plate boundary processes. Here we performed anisotropy of magnetic susceptibility (AMS) analysis to evaluate the strain recorded in the prism toe material and to reveal the strain variation at initial deformation stage, which allow us to discuss strength variation. AMS is used as a strain indicator and is an unique technique especially for the rocks without any other strain marker or for limited volume of samples.

Two sites (C0006 and C0007) drilled during Integrated Ocean Drilling Program (IODP) Expedition 316 penetrated the sediment section, including intra wedge thrusts and the frontal thrust. Anisotropy of magnetic susceptibility (AMS) measurements provide insight into recorded strain during sedimentary and tectonic processes. Results from the upper part of the wedge show sedimentary acquired compaction fabric in general. In the lower part of the wedge, AMS fabrics occasionally rotate almost ninety degrees and suggest indicate horizontal compression. In contrast, magnetic fabrics did not show any correspondence to the thrusts or minor normal faults, which implies that those faults develop with concentrated shear deformation without disturbing surrounding sediments. Two adjacent drilling

sites and dense sampling demonstrated clearly the change in strain field which is reported by previous studies. Based on these results, we propose a model of structural evolution at the toe of the prism: 1) thrust faults observed in Site C0006 are already abandoned based on pore fluid chemistry data and appear to be kinked at a certain depth; 2) At the similar depth, AMS indicates a strain/stress detachment between vertical and horizontal compression and high porosity zone occurs below it; 3) deposition or erosion associated with mass movement on the surface was observed at both sites C0006 and C0007.

Many studies have presented strain and stress distribution within accretionary prism, which are rather in macroscopic scale. Commonly agreed features out of them are 1) vertical compaction near surface, 2) horizontal compression within accretionary wedge and 3) vertical loading again below plate boundary detachment. The question arises with the second condition; how does it initiate or extend? Expedition 316 drilled two sites within ~1km from the trench, and high resolution AMS data from almost all core sections made it possible to reveal comprehensive magnetic fabrics in the apex of the prism toe. Underthrusting marine sediments into deformation front are accountable for increasing in lateral stress and forming thrusts faults, and also for small scale debris on the surface. Those insights about the structural evolution fairly at the convergent margin between two plates contribute to understand further subduction processes starting from there.

References:

Hyndman, R.D., Wang, K., 1993, Thermal Constraints On The Zone Of Major Thrust Earthquake Failure - The Cascadia Subduction Zone, Journal of Geophysical Research-Solid Earth. 98, 2039-2060.

Kimura, G., Kitamura, Y., Hashimoto, Y., Yamaguchi, A., Shibata, T., Ujiie, K., Okamoto, S., 2007, Transition of accretionary wedge structures around the up-dip limit of the seismogenic subduction zone, Earth and Planetary Science Letters. 255, 471-484.

Kimura, G., Ludden, J., 1995, Peeling oceanic crust in subduction zones, Geology. 23, 217-220.

Kinoshita, M., Tobin, H., Ashi, J., Kimura, G., Lallemant, S., Screaton, E.J., Curewitz, D., Masago, H., Moe, K.T., Scientists, E., 2009, NanTroSEIZE Stage 1: investigations of seismogenesis, Nankai Trough, Japan, Proceedings of the Integrated Ocean Drilling Program. 314/315/316.

Matsumura, M., Hashimoto, Y., Kimura, G., Ohmori-Ikehara, K., Enjoji, M., Ikesawa, E., 2003, Depth of oceanic crust underplating in subduction zone -inference from fluid inclusion analysis of crack-seal veins-, Geology. 31, 1005-1008.

Moore, J.C., Saffer, D., 2001, Updip limit of the seismogenic zone beneath the accretionary prism of southwest Japan: An effect of diagenetic to low-grade metamorphic processes and increasing effective stress, Geology. 29, 183-186.

Obara, K., Ito, Y., 2005, Very low frequency earthquakes excited by the 2004 off the Kii peninsula earthquakes: A dynamic deformation process in the large accretionary prism, Earth Planets And Space. 57, 321-326.

Saffer, D.M., Marone, C., 2003, Comparison of smectite- and illite-rich gouge frictional properties: application to the updip limit of the seismogenic zone along subduction megathrusts, Earth And Planetary Science Letters. 215, 219-235.

ICDP

Dominance of remobilized sediment for the last glacial record of the South Patagonian maar lake Laguna Potrok Aike, Argentina

P. KLIEM[1], A. HAHN[1], C. OHLENDORF[1], B. ZOLITSCHKA[1] AND THE PASADO SCIENCE TEAM[2]

[1]GEOPOLAR, Institute of Geography, University of Bremen, Germany (kliem@uni-bremen.de)

[2]http://www.icdp_online.org/contenido/icdp/front_content.php?idcat=960

Laguna Potrok Aike is a 100m deep maar lake located in the dry steppe of southern Patagonia. The catchment area of >200km² mainly consists of till from the Bella Vista and Río Ciaike Glaciations as well as of alkali-olivine basalts from volcanism related to the Pali Aike Volcanic Field. Today's regional climate is affected by the Southern Hemispheric Westerlies and the rain shadow effect of the north-south striking Andean mountain chain. Since lakes are valuable terrestrial paleoclimate archives, sediments of Laguna Potrok Aike should reflect shifts of mid latitude wind and pressure fields as well as precipitation changes in southeastern South America. Aiming at the reconstruction of past climatic conditions, the deep drilling at Laguna Potrok Aike was accomplished in the framework of the ICDP project PASADO from September to November 2008.

By correlation of three holes drilled at Site 2 and located ca. 700 m south of the lake's center, a composite profile of 106.08 mcd (meters composite depth) was established. According to the lowermost ^{14}C age of aquatic macro remains from 80.6 mcd, the entire record comprises at least 50,000 years. The initial lithological description indicates that 50.74 m (i.e. 47.8%) of the sediment record consists of remobilized sediment (turbidity currents, homogenites, ball and pillow structures, gravel layers, slumps). Such deposits are almost absent in the top 12 mcd, where laminated clays and silts dominate. Correlation with an existing piston core allows a temporal relation of these topmost 12 m to the Holocene. Apart from obviously remobilized deposits Holocene sediments are distinguished from Late Glacial deposits by a lower frequency of coarse silt/fine sand layers within a silt/clay matrix.

Frequency and thickness of remobilized deposits increase with sediment depth. Most reworked sections are composed of three units: (1) a dark, coarse and fining upward base overlain by (2) a homogeneous layer of silt and (3) clay capped by a relatively thin and pale clay layer. Such sequences were often described as homogenites from marine sediments but are only rarely known from lakes. In the record from Laguna Potrok Aike homogenites reach up to 3 m in thickness. In contrast, turbidites are characterized by a fining-upward pattern of the entire sequence.

Homogenites in lake and marine sediments are generally regarded as representing a record of regional seismicity or tsunami activity. Since homogenites are not only triggered by seismotectonic activity and no such deposits are represented in the Holocene sediments of Laguna Potrok Aike, we hypothesize that homogenite generation could be linked to different climate conditions during glacial times. Reasons for this climate link may be (1) higher clastic input through the main tributary or (2) an extremely low lake level. The first option could be the

result of more intense geomorphodynamic processes in the catchment area compared to today due to the dominance of periglacial conditions with permafrost, forcing precipitation and melt water to run off superficially. Evidence for permafrost conditions in this region is given by an OSL-dated sand wedge in the catchment area yielding an age related to the ending Last Glacial Maximum (19.1 ± 1.4ka). The latter explanation is supported by the occurrence of coarse gravel layers at the bases of some homogenites as well as by one chaotic gravel-dominated unit between 87 and 89 mcd, considering that the distal core is located 1.8 km from the main tributary.

IODP

Palynological results from the New Jersey shallow shelf: site-shoreline distance, sea-level reconstruction, and vegetation development on the Atlantic Coastal Plain

KOTTHOFF, ULRICH[1*], MCCARTHY, FRANCINE M.G.[2], KATZ, MIRIAM E.[3], AND THE IODP EXPEDITION 313 SCIENTIFIC PARTY[4]

[1]Ulrich Kotthoff, Department of Geosciences, Hamburg University, Bundesstrasse 55, D-20146 Hamburg, Germany, e-mail: ulrich.kotthoff@uni-hamburg.de
[2]Francine M. G. McCarthy, Department of Earth Sciences, Brock University, 500 Glenridge Avenue, St. Catharines, Ontario, L2S 3A1, Canada
[3]Miriam E. Katz, Earth and Environmental Sciences, Rensselaer Polytechnic Institute, 110 8th St., Troy NY 12180, United States of America
[4]ECORD Science Operator, Edinburgh, United Kingdom
*corresponding author

The ratio between the cysts of marine (organic-walled dinoflagellates) and terrestrial palynomorphs (pollen & plant spores) found in Eocene to Miocene sediments of the New Jersey Atlantic Margin is used as a proxy to estimate the distance of two IODP drilling sites from the shoreline (Expedition 313 holes M0027A and M0029A). This ratio, combined with qualitative descriptions of the palynofacies, allows paleo-sea-level reconstruction. Estimates of paleo-depth based on benthic foraminiferal data show close agreement with the paleo-sea-level estimates derived from the palynomorphs. The combined use of these proxies provides great confidence in reconstructing sea-level change through time. Furthermore, the micropaleontology-based reconstructions of distance from the shoreline and paleodepth contribute to a pollen-transport model, and thus to more confident pollen-based reconstructions of the vegetation development in the hinterland of the New Jersey margin during the Miocene. Hickory-oak forests dominated the vegetation in the hinterland during the whole Miocene. The Aquitanian-Burdigalian boundary witnessed the presence of different hemlock (Tsuga) species, indicating humid, but probably cool conditions. Subsequently, the spreading of deciduous oaks and further broad-leaved tree taxa during the late Burdigalian, points to warmer temperatures. During the Langhian to Tortonian, grass- and herbs-dominated landscapes expanded, probably due to decreasing humidity.

ICDP

Sedimentary processes in Lake Van, Turkey – seismic pre-site survey and planned activities during the upcoming Lake Van Drilling Project

S. KRASTEL[1], D. WINKELMANN[1], D. CUKUR[1], T. LITT[2]

[1]Leibniz Institute of Marine Sciences (IFM-GEOMAR), Kiel, Germany
[2]Steinmann Institute of Geology, Mineralogy and Palaeontology, University of Bonn; Germany

Lake Van in Eastern Anatolia (Turkey) is the fourth largest of all terminal lakes in the world (surface area of 3,522 km², volume of 576 km³, maximum depth of 451 m, maximal length of 130 km WSW-ENE). Previous scientific work has shown that Lake Van has an excellent potential as a high resolution paleo-climate archive caused by the presence of annually laminated lacustrine sediments. As Lake Van can act as a key site for the investigation of the Quaternary climatic evolution of the Near East, an ICDP drilling campaign is scheduled for summer 2010. Five primary sites are proposed based on high resolution seismic data collected during a pre-site survey in 2004.

Three physiographic provinces were identified based on the seismic data: a lacustrine shelf, a lacustrine slope, and a deep, relatively flat lake basin province. The large Tatvan Basin is characterized by an alternating succession of well-stratified and chaotically reflecting layers representing widespread slide deposits. The basin is bounded by faults. A prograding sequence indicates the initial flooding of Tatvan Basin ~500ka BP caused by the construction of a major lava dam across Muş Basin during a volcanically active period of Nemrut volcano. The seismic data strongly supports a continuous existence of Lake Van since then. A sedimentary ridge (Ahlat Ridge) at the northern edge of Tatvan Basin represents an ideal location for the recovery of a complete section for paleoclimatic investigations of the past ~500ka. The elevated location of the ridge results in slightly reduced sedimentation rates but prevents this location from turbidite and slide deposits. After the initial flooding of Lake Van, significant lake level fluctuations are documented as clinoforms, channel systems and erosional unconformities on the lacustrine shelf and slope. Lake level was as high as 80m above and ~250m below the current lake level. Therefore lake level fluctuations exceed 300 m indicating extreme changes in water balances. Tatvan Basin with a depth of ~450m was not directly affected by these lake level fluctuations. 5 locations were selected as primary sites for the ICDP proposal.

Our main objective related to the upcoming drilling campaign is an integrated interpretation of the drilling and seismic data in order to reconstruct the genesis and evolution of Lake Van. Synthetic seismograms will be calculated for a correlation of seismic and drill data. An intensive logging program (core and downhole logging) will be the basis for this approach. The integration of logging and seismic data allows extrapolating the stratigraphy from the wells to 3D-space by using the seismic data. Special emphasis will be drawn on the timing of widespread mass wasting events, which might be used as proxy for estimating the paleo-seismicity and on lake-

level fluctuations, which played an important role for the sedimentary evolution of Lake Van.

IODP

Marine isotopic stage 11 in the eastern Mediterranean Sea

M. KUCERA[1], L. NUMBERGER[1], H. SCHULZ[1], U.RÖHL[2], A. MACKENSEN[3]

[1]Institut für Geowissenschaften, Universität Tübingen, Sigwartstrasse 10, 72076 Tübingen, Germany
[2]MARUM , Universität Bremen, 28359 Bremen, Germany
[3]Alfred-Wegener-Institut für Polar- und Meeresforschung, 27515, Bremerhaven, Germany

Marine isotopic stage 11 (MIS 11), centred on 400,000 years ago, provides the closest analogue to the Holocene in terms of the configuration of the Earth's orbit around the Sun. Despite the similarly low eccentricity of the Earth's orbit between the two interglacials, resulting in muted amplitude of insolation in the precessional band, it remains a hotly debated topic in the literature to what degree the climate trends of MIS 11 can be compared to the climatic development of the present interglacial. The eastern Mediterranean is in this context an ideal natural climate-amplifying laboratory that can be used to establish to which degree the climate of MIS 11 was comparable to the Holocene. Specifically, low-latitude insolation forcing is reflected in the eastern Mediterranean by periodic breakdown of deep water formation and the deposition of sapropel layers. Remarkably, there have been no detailed studies of the Mediterranean during MIS 11 as yet, most likely due to the inaccessibility of suitable sediments by conventional piston coring. In this project, we generated new high-resolution paleoclimate and sediment-properties records across MIS 11 and MIS 1 from ODP Site 964 (36°16'N, 17°45'E, 3658 m), supplemented by data from a lower-resolution piston core GeoTü-SL96 (32°46'N, 19°12'E, 1399 m).

Our multi-proxy high-resolution data from both cores allowed us to unambiguously identify the position of MIS 11. Whereas the isotopic data mostly followed known trends for this interval, the position of the sapropel (or sapropel equivalent) as well as the development of SST proxies showed unexpected patterns. The Holocene data as well as the MIS 11 data indicate a presence of a short but distinct negative oxygen isotopic excursion (<1 ‰) associated with the sapropel. This would indicate the presence of a significant freshwater discharge into the eastern Mediterranean at MIS 11, presumably from North Africa by enhanced monsoonal precipitation. This is interesting given the lower insolation forcing during MIS 11 compared to the Holocene. Remarkably, at ODP Site 964, the sapropel of MIS 11 is associated with a positive excursion of up to -1.8 ‰ in stable oxygen isotopes. Both the magnitude and the absolute values of the MIS 11 isotopic excursion at this site have no analog in the Holocene nowhere in the near region. A much more intense freshwater input during MIS 11 might be the reason for this higher peak, but since the Ionian Sea is far from the Nile source region, it remains unclear where this large freshwater flux would have come from. In terms of Ba concentrations and Ti/Al and K/Al ratios, MIS 11 and MIS 1 are highly comparable for this core. This indicates a similar source of particulates and presumably also freshwater for the two time intervals: the southern monsoonal and fluvial systems (mainly Nile river discharge and perhaps Saharan river courses at that time).

A robust stratigraphical model, based on stable oxygen isotopes in planktonic foraminifera has been developed for the interval from MIS 12 to MIS 9 in both sediment cores and the correlation between the two cores was further refined by faunal content and on the basis of the location of the MIS 11 sapropel or its equivalent. By tuning the oxygen isotope records to a global benthic stack, we show that the MIS 11 sapropel occurred during the second insolation maximum of MIS 11 at 409 ka. This stratigraphy implies that eastern Mediterranean planktonic foraminifera assemblages showed a delayed reaction to the isotopically recognised deglaciation in both records. The delayed reaction of the change from "cold" species to "warm" species abundances could be attributed to the exceptionally weak insolation forcing during Termination V. If the sapropel formation and associated freshwater spike in MIS 11 was triggered by the second insolation peak of MIS 11 after the deglaciation, then the entire paleoceanographic development of the basin during MIS 11 becomes non-analogous to the Holocene, where sapropel formation was triggered by the first insolation peak after the deglaciation. This second insolation peak and the precession minimum of MIS 11, around 408 kyr, thus appear to have been necessary to shift the ecological system of the eastern Mediterranean (planktonic foraminifera) into an interglacial mode although the polar ice caps have been melting for 20 kyr already. This alignment of MIS 11 is also more consistent with the presumed freshwater forcing from Africa: only the second insolation peak of MIS 11 has a magnitude similar to that of the Holocene and could be conceivably considered responsible for enhanced Monsoon over east African highlands.

The MIS 11 sapropel development differs significantly between the two investigated cores. Core GeoTü-SL96, just 260 sea miles away from ODP Site 964, shows a similar development of inferred conditions during MIS 11 and MIS 1. However, whereas the peak isotopic values reach -0.6 ‰ $\delta^{18}O$ during both sapropel intervals, Holocene element ratios appear rather different from MIS 11 sediments. The Sapropel in MIS 1 is marked by a distinct peak of Ba/Al, while relatively high concentration of Ba were consistently recorded throughout MIS 12 and early MIS 11 with no significant peak during the MIS 11 isotopic excursion. These data indicate that the lack of a distinct sapropel layer in this core is a primary signal and that no significant sapropel has developed at this shallower site in MIS 11. Similarly to data from ODP Site 964, elemental ratios in GeoTü-SL96 also indicate a common source of freshwater for the two time intervals and high concentrations of K support specifically an important influence of the Nile/north African discharge. Benthic foraminifera assemblages in ODP Site 964 and GeoTü-SL96 highlight the transition from MIS 12 to MIS 11. During MIS 12, high nutrient availability promoted the development of a dense population of low-oxygen tolerant taxa. Even in the deep core ODP Site 964 (3658 m), significant amounts of benthic foraminifera were found, despite a smaller amount of organic material reaching the bottom and lower oxygen content of bottom waters and

upper sediment layers at this depth. Like the planktonic fauna, benthic foraminifera also failed to react to the isotopically defined deglaciation and their abundance drops only at the time of the sapropel deposition. The early MIS 11 fauna is dominated by Bulimina spp., Pyrgo spp., Globobulimina affinis and Quinqueloculina spp. in both cores and persists until the period of sapropel formation. Coincident with the positive isotopic excursion in ODP Site 964, benthic faunal abundances decrease abruptly. In GeoTü-SL96, the benthic fauna also change after the isotopic excursion, but the population remains at this site throughout the isotopic excursion, confirming decisively the geochemical data that indicate that a sapropel (anoxia) has not reached these shallow depths during MIS 11.

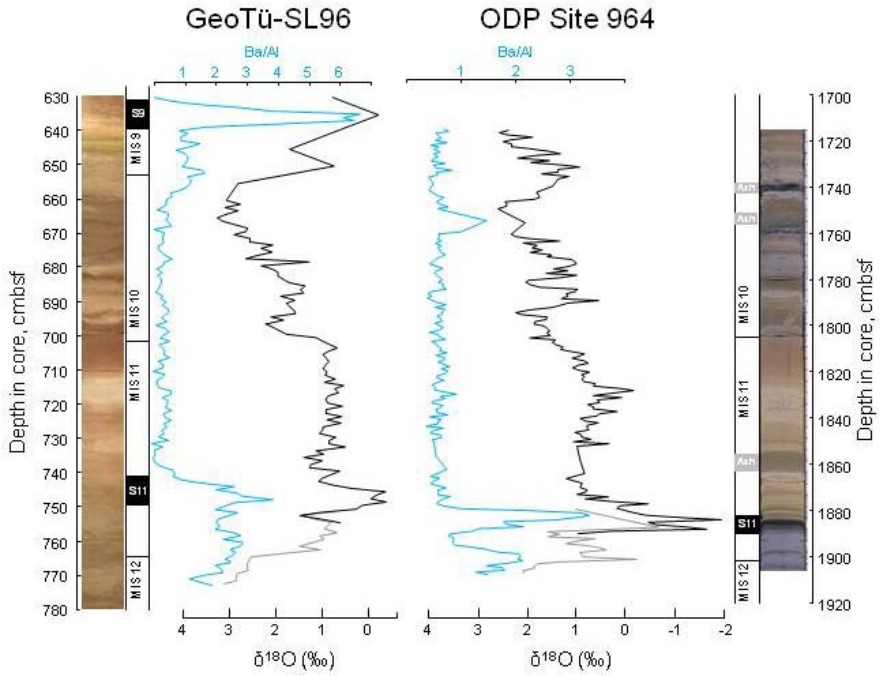

Figure 1. Sediment properties and oxygen stable isotope records from G. ruber (black lines) and G. bulloides (grey lines) for both GeoTü-SL96 and ODP Site 964 throughout MIS11. Position of MIS boundaries and sapropels is shown next to the core photographs. Note the distinct isotopic signature in both core associated with the MIS11 sapropel.

Continuous high-resolution planktonic foraminiferal records and organic biomarker results (alkenone unsaturation ratio) indicate that the entire 20 kyr long pre-sapropel interval of MIS 11 in the eastern Mediterranean was characterised by glacial planktonic foraminiferal assemblages and glacial temperatures. This is in stark contrast to the observed onset of the Termination V at 427 ka in all global proxy records and numerous records from the nearby northern Atlantic Ocean showing interglacial conditions soon after the deglaciation. Apparent deglaciation in the eastern Mediterranean coincided with the deposition of the sapropel after the 408 ka insolation peak. Peak interglacial fauna and alkenone temperatures, indicating values similar to those of the Holocene occurred first after the sapropel event and continued throughout the rest of the MIS 11, despite the gradual temperature decline observed in Northeastern Atlantic records. Interestingly, the alkenone-derived temperature is consistent with annual temperature reconstructed by artificial neural network (ANN) transfer functions from planktonic foraminifer assemblages during the end of MIS 12 and the whole MIS 11, whereas in MIS 10, the alkenone temperatures are closer to the reconstructed winter temperatures. Transfer-function and alkenone reconstructed SST values never exceed significantly the present-day temperatures at both sites, but remained high during much of the MIS 10 glacial. This glacial is known to have been exceptionally cold in the Mediterranean (expansion of mountain glaciers), an observation difficult to reconcile with the reconstructed paleotemperatures. Full glacial conditions of MIS 10 are observed only at the very end of this glacial, close to TIV, and even there the values are significantly warmer than those seen during MIS 12. This unexpected pattern is clearly seen in the planktonic foraminifer assemblages from both cores, with the abundance of G. ruber increasing throughout MIS 11 and reaching a peak in the second half of MIS 10, which is at odds with the behaviour of this species during later glacial cycles.

Although similar mechanisms and feedbacks appear to have been at play during the MIS 11 and the Holocene in the Mediterranean, we observe major changes in the behaviour of the Basin during the terminations and in the subsequent development of the planktonic foraminiferal fauna. This climatic development indicates a significant de-coupling from the oceanic system, presumably recording local circulation patterns and atmospheric conditions over the Mediterranean region. Our records further confirm a high sensitivity of the Mediterranean Sea to the amplitude of the insolation forcing, but the observed decoupling from global trends remains difficult to explain. The observed spatial and temporal differences, between MIS 1 and MIS 11 records indicate that these interglacials are not as comparable as expected from the orbital analogy alone. The MIS 11 interval is unique because of the exceptional

isotopic peak seen at ODP Site 964 and the much less developed anoxia associated with it. This appears completely counter-intuitive as enhanced freshwater flux should have acted to isolate the bottom waters more effectively. The alignment of sapropel intervals to the second insolation peak of MIS 11 makes it difficult to use the MIS 11 analogy to draw conclusions for future climate, because of the resulting decoupling of orbital forcing and climate response between MIS 11 and MIS 1 in the eastern Mediterranean after the deglaciation.

ICDP

Towards timescales of assimilation and magma mixing in the Large Igneous Province of Snake River Plain-Yellowstone, northwest United States: Why Deep-Drilling? Preliminary results.

Y. LAVALLÉE[1], C. P. DE CAMPOS[1], D. MORGAVI[1], R. HEISTEK[1], L. MORGAN[2], K. U. HESS[1], AND D.B. DINGWELL[1]

[1]Dept. of Earth and Environment, Germany;
[2]USGS, Denver, Colorado, USA;

Introduction: The Snake River Plain-Yellowstone (SRP-Y) volcanic province, western United States, consists of a layered sequence of Holocene to early Quaternary basalt units overlying northeastward-younging Miocene to Quaternary rhyolitic caldera complexes. Cyclic variations in the chemical composition of the basalts may be explained by successive cycles of magma replenishment and fractionation, with the minor assimilation of crustal material (Shervais et al., 2006). In contrast to this concept is the possibility that the passage of a high-heat flux mantle plume would heat the magma reservoirs to temperatures perhaps above that of the liquidus and thus outside the range of conditions in which fractionation takes place. Other processes must therefore be at work in the reservoirs to create the diversity of eruptive deposits observed.

The central SRP is transitional between the initial 14-17-Ma-volcanism which produced hundreds of thousands of km3 of widely distributed flood basalts and rhyolite in the most western part of the SRP-Y province and the later (<10 Ma), less voluminous, and more spatially restricted caldera-dominated volcanism to the east. Volcanism in the central CRP was sustained for up to 7 m.y. by heat generated by the detached plume head and upwelling plume tail (Pierce and Morgan, 2009) and generated up to 7-10 major caldera-forming events; ignimbrites erupted in the central SRP are compositionally diverse.

From surface information, rhyolites occur as the dominant component in the basalt-veneered SRP-Y volcanic province. In some areas the basalt lavas are intruded or overlain by ~15 km^3 of high-silica rhyolitic domes and flows (McCurry et al., 2008).

Snake River–type eruptions are known to have been voluminous and extraordinarily devastating (Branney et al., 2008). Massive, strongly welded ignimbrites with run-out distances over 150 km point towards low effective viscosities. Eruptive products in the SRP-Y province are generally described by high temperatures (>850°-1100° C) and relatively low water content (<5 wt.%). What physical or chemical mechanisms exactly drive these explosive super-eruptions through time remain unknown. Recent studies (including this work) have raised the possibility that high abundances of halogen may be key in decreasing the viscosity of the melt as well as providing the energy to drive explosive eruption (Barbara Nash, pers.com.). From a geodynamic point of view, it is imperative to understand magmatism and volcanic activity; most specifically to constrain the timescales for the maturation of magma reservoirs that lead to super-eruptions, and those encountered in the progression of these eruptions.

Why deep-drill the SRP? The SRP preserves a record of volcanic activity that spans over 16 Ma (Pierce and Morgan, 1992, 2009) and is still active today, with basalts as young as 200 ka in the west and 2 ka in the east. "The Snake River volcanic province represents the world-class example of active time-transgressive intra-continental hotspot volcanism" (Shervais et al., 2009; NSF research proposal for the Snake River Plain). The SRP is unique because it is young, relatively undisturbed tectonically, and contains the most complete record of volcanic activity associated with passage of a hotspot on continental crust. Hence, it is the best place in the world to test hypotheses for the evolution of a hotspot track on the continents, and, owing to the low rates of erosion, the complete volcanic record can only be sampled by drilling. In addition to this complete record of hotspot volcanism, the western SRP rift basin preserves an unparalleled deep-water lacustrine archive of paleoclimate evolution in western North America during the late Neogene.

The time is right for testing these hypotheses through drilling of the Snake River Plain for two primary reasons. First, as stated in the original proposal for deep drilling in the SRP, recently submitted to the American National Science Foundation by John Shervais, the productivity of recent geophysical studies focusing on seismic tomography, funded by Earthscope, has delineated the seismic structure of the deep mantle in unprecedented detail (e.g., *Yuan & Dueker 2005; Waite et al 2006;* Xue and Allen, 2007; James et al., 2009). A focused interdisciplinary study funded by Continental Dynamics has produced detailed tomographic images and geochemical data from the western part of the region (Roth et al., 2008). Other Earthscope Plate Boundary Observatory products are revolutionizing our understanding of upper mantle and lithospheric structure of the western United States (www.Earthscope.org).

Second, a recent proposal has been funded by DOE to core two drill holes in the central Snake River Plain at sites co-located in conjunction with the Project Hotspot initiative. With the additional funding from ICDP anticipated in early 2010, we will not need any funds for pre-drilling or logging operations associated with this project. As a result, drilling in the SRP requests only the funds needed to carry out the scientific studies, detailed in the cited recent proposal to the National Science Foundation in the USA, with the participation of the authors of this work.

Aims of this proposal in the general scope of the SRP-deep drilling project: In the global general scope of the SRP-deep drilling project, our project focuses on the development of new experimental methods to constrain the time scales of magmatic and volcanologic processes. Three sets of preliminary results will be presented, namely on: 1) the timescales of ignimbrite super-eruptions; 2) the

calibration and testing of a newly developed device for chaotic mixing (including the selection, characterization, and preparation of samples to be used as end-members); 3) the relation between rheology and halogen distribution, specially in the extracaldera Obsidian rholitic lava flow from Yellowstone.

To 1): Preliminary results from the determination of timescales ofvarious processes in ignimbrite super-eruptions in the Snake River Plain: The eruption and welding of ignimbrites requires the crossing of the glass transition temperature three times. Magma needs to: 1) fragment to ash during ascent at a rate exceeding its timescales of relaxation; 2) relax during deposition, agglutination, and welding at high temperatures, and lastly; 3) quench. Super-eruptions in the Snake River Plain generate thousands of cubic kilometres of hot ash particle density currents, which deposit and weld to form high-grade ignimbrite; the timescales and physico-chemical evolution of these events remain poorly understood. Lavallée et al., (in prep.) showed that welding is a rapid, syn-deposition process whereas the ignimbrite may be deposited for up to a day before quenching through its glass transition. Geospeedometry reveals that the basal vitrophyre underwent the glass transition at rate of 0.1 °C/min at 870°C; that is, 30-180°C below pre-eruptive temperature estimates. This temperature window and cooling rate constrain the timescale of explosive eruption, deposition, agglutination and welding of the basal vitrophyre to 5-30 hours. The vitrophyre revealed a Newtonian rheology, which suggests that ash particles have nearly entirely annealed during welding. The temperature dependence of the viscosity during cooling to glass transition coupled to an empirical welding model asserts the timescale of welding to the extent of lava-like behaviour to less than 8 hours, and possibly down to only tens of minutes. Our findings support the use of the term `lava-like' to describe the rheology of some Snake River-type ignimbrites, in addition to its use to describe the typical lithofacies manifested.

In order to support the consistency of these conclusions the use of geospeedometry will be carefully further tested for SRP-like glasses.

To 2) Preliminary results from the chaotic mixing device: In order to perform mixing experiments with Snake River Plain rhyolites, a new experimental device has been developed to perform chaotic mixing of high viscosity melts, under controlled fluid-dynamic conditions (De Campos et al., 2009). The apparatus is based on the Journal Bearing System (JBS). It consists of an outer cylinder hosting the melts of interest and an inner cylinder, which is eccentrically located. Both cylinders can be independently moved to generate chaotic streamlines in the mixing system. Both cylinders can be independently moved to generate chaotic streamlines in the mixing system. Two experiments were performed using as end-members different proportion of a peralkaline haplogranite and a mafic melt, corresponding to the 1 atm eutectic composition in the An-Di binary system. The two melts were stirred together in the JBS for ca. two hours, at 1,400°C and under laminar fluid dynamic condition (Re of the order of 10^{-7}). The viscosity ratio between the two melts, at the beginning of the experiment, was of the order of 10^3. Optical analyses of experimental samples revealed, at short length scale (of the order of μm), a complex pattern of mixed structures. These consisted of an intimate distribution of filaments; a complex inter-fingering of the two melts. Such features are thought to be produced by stretching and folding (mixing) processes, which generated wide compositional interfaces. In this way, chemical diffusion processes become more efficient, producing melts with highly heterogeneous compositions. A remarkable modulation of compositional fields has been obtained by performing short time-scale experiments and using melts with a high viscosity ratio. Our experimental device may replicate magma mixing features, typically observed in obsidians from the Snake River Plain and other natural rocks, opening new possibilities for the study of this important petrologic and volcanologic process.

The selection of natural SRP-samples to be used in the mixing experiments has been based on the most contrasting types known in the area. Fe-rich and Fe-poor end-members have been selected and already sampled in the Bruneau-Jarbridge volcanic field. Characterization and preparation of the samples are currently in progress.

The eruption age for the Bruneau-Jarbidge (BJ) eruptive center is estimated to be around 12.7 to 10.5 Ma (Cathey and Nash, 2004; 2009). Most of the eruptive activity consists of dominant rhyolitic and subordinate basalt flows. They have been emplaced during the Miocene (Branney et al., 2008). The Cougar Point Tuff (CPT) sample is characterized by polymodal mineral assemblages. This polymodal behaviour can be observed in both glasses and phenocrysts, such as pyroxene. Distinctive patterns of replicate glass and pyroxene assemblages from different eruptive units evidence this polymodality (Cathey and Nash; 2004). On the other hand the BJ sample is characterized by a unimodal pyroxene composition. Compared to the (CPT) the (BJ) presents clear FeO- and MgO-enrichments (Cathey and Nash, 2009). Distinguishing between physical features from the CPT and the BJ real lavas and lava-like ignimbrites is not trivial. Reasons for this difficulty are due to the lack of exposed units from the base of the deposits and to the similarity of many "lava-like" features such as basal breccias.

To 3) Preliminary results from the relation between rheology and halogen distribution in the extracaldera Obsidian rhyolite flow from Yellowstone :

The driver for explosive eruptions in the SRP is enigmatic as the magmas are considered to be too hot (> 900 °C) and dry to be explosive, although recent chemical analysis on the interstitial glass and melt inclusions reported the presence of the halogens, fluorine, and chlorine (Nash, pers. com.). Halogens may substitute for O^{2-} and alter the degree of polymerization of silicate melts, consequently affecting the rheology of magmas.

We performed chemical analysis for fluorine and chlorine present in the glass of several volcanic rocks from the SRP-Y volcanic province, using an electron microprobe. The glasses from Yellowstone are meta-aluminous rhyolites and some (e.g., Obsidian Cliff at Yellowstone) contain an unusually high content in Cl (up to ca. 1% wt) and absence of F. The high Cl-content in the volcanic products provides an opportunity to investigate the effects of this halogen on the rheology of natural magmas.

To date, the role of Cl has been studied on synthetic glass and is tied to the chemical composition. Cl slightly increases the viscosity of peralkaline melts, whereas it

decreases the viscosity of peraluminous melts; exceptions however exist at high temperatures where the presence of Cl increases the viscosity of peraluminous melts (Zimova and Webb, Am. Min. 2006). Here we present rheological measurements on the relationships between Cl and the viscosity of rhyolites from the Obsidian Cliff and test whether Cl has similar effects on natural magmas as on synthetic melts.

Conclusions: Drilling of two intermediate-depth (<2 km) boreholes (one targeted in basalt and the second targeted in rhyolite) into the central SRP will provide unprecedented insight into the mixing of basalt and rhyolite in the evolution of the large, hotspot-controlled volcanic fields. Questions that may be resolved include 1) the detailed stratigraphic history of several caldera-forming eruptions; 2) the interaction between pre- and post-caldera basaltic and rhyolitic eruptions with the main caldera-forming phases within the central SRP, 3) details regarding the models considering interaction between rhyolite and basalt in the subsurface will be evaluated; 4) details regarding processes in the rhyolites such as vapour-phase mineralization, welding, remelting, and decompression crystallization; 5) how anomalously high contents of Cl^- may influence the viscosity and explosivity of ignimbrite eruptions; and 6) how a high-heat flux from the mantle plume influences temperatures of the magma reservoirs higher than that of the liquidus and thus outside the range of conditions in which fractionation takes place. Our aim is to drill into a complete sequence of caldera-forming ignimbrites from the Twin Falls volcanic field (Pierce and Morgan, 1992) and penetrate the underlying basalts; this is unprecedented in the SRP or any continental hotspot to date.

References:

Branney, M., Bonnichsen, B., Andrews, G., Ellis, B., Barry, T., and McCurry, M., 2008, 'Snake River (SR)-type' volcanism at the Yellowstone hotspot track: distinctive products from unusual, high-temperature silicic super-eruptions: Bulletin of Volcanology, v. 70, no. 3, p. 293-314.

Cathey HE, Nash BP (2004) The Cougar Point Tuff: implications for thermochemical zonation and longevity of high-temperature, large volume silicic magmas of the Miocene Yellowstone hotspot. J. Petrol. 45:27–58

Cathey, Henrietta E. and Nash, Barbara P., (2009). Pyroxene thermometry of rhyolite lava, Bruneau-Jarbidge volcanic center. Journal of Volcanology and Geothermal Research 188 (2009) p. 173-185.

De Campos, C. P., Ertel-Ingrisch, W., Perugini, D., Dingwell, D. B. and Poli, G.(2009) Chaotic Mixing in the System Earth: Mixing Granitic and Basaltic Liquids. In: Skiadas, C.H. and Dimotikalis, I. Chaos Conference 2009. Book of Abstracts and Short Papers. (in press).

James, D, Roth, J, Fouch, M, and Carlson, R, 2009, Upper mantle velocity structure of the Pacific Northwest: Implications for geodynamical processes during the late Cenozoic, Abstract, Earthscope Nat. Meeting, Boise Idaho, 12-15 May 2009;

Lavallée, Y., Andrews, G., D., M., Von Aulock, F., Flaws, F., Hess, K.-U., Russel, J., K., Tuffen, H. dingwell, D., B., Timescale of ignimbrite super-eruption in the Snake River Plain (USA). (in prep.).

McCurry, M., Hayden, K., Morse, L., and Mertzman, S., 2008, Genesis of post-hotspot, A-type rhyolite of the Eastern Snake River Plain volcanic field by extreme fractional crystallization of olivine tholeiite: Bulletin of Volcanology, v. 70, no. 3, p. 361-383.

Pierce, K.L., and Morgan, L. A., 1992, The track of the Yellowstone hot spot: Volcanism, faulting, and uplift, in Link, P.K., Kuntz, M.A., and Platt, L.B., eds., Regional geology of eastern Idaho and western Wyoming, Geological Society of America Memoir 179, p. 1-53.

Pierce, Kenneth L. and Morgan, Lisa A., 2009, Is the Track of the Yellowstone Hotspot Driven by a Deep Mantle Plume? –Review of Volcanism, Faulting, and Uplift in Light of New Data in Journal of Volcanology and Geothermal Research, v. 188, issue 1, p. 1-25.

Roth, J.,B., Fouch, M., J., James, D., E., and Carlson, R., W., Three-dimensional seismic velocity structure of the northwestern United States. Geophysical Research Letters, Vol.35, L15304, doi:10.1029/2008GL034669, 2008.

Shervais, J.W., Vetter, S.K. and Hanan, B.B., 2006, A Layered Mafic Sill Complex beneath the Eastern Snake River Plain: Evidence from Cyclic Geochemical Variations in Basalt, Geology, v. 34, 365-368.

Shervais, JW and Vetter, SK, 2009, High-K Alkali Basalts of the Western Snake River Plain: Abrupt Transition from Tholeiitic to Mildly Alkaline Plume-Derived Basalts, Western Snake River Plain, Idaho, Journal of Volcanology and Geothermal Research, doi:10.1016/j.jvolgeores.2009.01.023.

Waite GP, Smith RB and Allen RM, 2006, VP and VS structure of the Yellowstone hot spot from teleseismic tomography: Evidence for an upper mantle plume. Jour Geophysical Research, 111, B04303.

Xue, M. and R.M. Allen (2007) The Fate of the Juan de Fuca Plate: Implications for a Yellowstone Plume Head, Earth Planet. Sci. Lett. 264, p266-276, doi:10.1016/j.epsl.2007.09.047.

Yuan H and Dueker K, 2005, Teleseismic P-wave Tomogram of the Yellowstone Plume, Geophysical Research Letters, vol. 32, L07304, doi:10.1029/2004GL022056.

Zimova, M., and Webb, S., 2006, The effect of chlorine on the viscosity of Na2O-Fe2O3-Al2O3 SiO2 melts: American Mineralogist, v. 91,p. 344–352, doi:10.2138/am.2006.1799.

http://www.Earthscope.org

IODP

Marine micropaleontology, round two: whole faunal surveys and their use in biostratigraphy and macroevolutionary research

D. LAZARUS[1], J. RENAUDIE[1], M. WEINKAUF[2]

[1]Museum f. Naturkunde, Invalidenstrasse 43, 10115 Berlin. david.lazarus@mfn-berlin.de; [2] Freie Universität, 74-100 Malteserstrasse, 12249 Berlin

Introduction: Antarctic Neogene sediments record major changes in oceanography linked to climate cooling and increased glaciation of the polar regions and are a key archive for paleoceanographic and paleoclimate studies. Because these sediments mostly lack carbonate microfossils and also because of widespread hiatuses and rapid changes in sedimentation rate, even with paleomagnetic stratigraphy it has been difficult to develop a robust, unambiguous geochronologic framework, the lack of which significantly hinders paleoceanographic/climatic research. In addition to the more widely employed diatoms, Antarctic Neogene sediments contain abundant well preserved radiolarians. These faunas are diverse, evolve rapidly and offer in principle a major resource for improved biostratigraphy and thus improved geochronology. However, studies to date have employed only a fraction of the fauna and the available biostratigraphic resolution is only moderate. Equally of interest is the increasing use in recent years of marine microfossil data in macroevolutionary studies, with several recent papers being published in high profile journals (Science, Nature, PNAS, etc). The hope is that the extraordinarily complete species-level fossil record of marine microfossils may circumvent problems with less-complete shallow marine or terrestrial macrofossil data. However, the same incompleteness of data collection that limits biostratigraphy also limits use of this record for evolutionary research.

The goals of a new project 'Antarctic Neogene Radiolaria' (AANR) are 1) to document as completely as possible the species level diversity of Antarctic Neogene radiolaria; 2) to determine the stratigraphic range of these species in several Neogene sections; 3) to analyze the patterns of species first and last occurrences using modern methods to increase biostratigraphic resolution in Antarctic

Neogene sediments; and 4) analyze the same data set to better understand patterns and processes of macroevolution in these faunas.

The project plan is divided into three approximately equal 1 year intervals. 2008/9-Taxonomic work (project catalog of taxa including synthesis of taxonomic literature); 2009/10-stratigraphic range determination (quantitative occurrence data for species in sample series from several sections); 2010/11-analysis of data. The taxonomic work has been largely completed; while quantitative occurrence data collection has begun. Only minimal data analysis has so far been done, although basic diversity calculations have been made. Below we describe in detail each of these aspects of the project work.

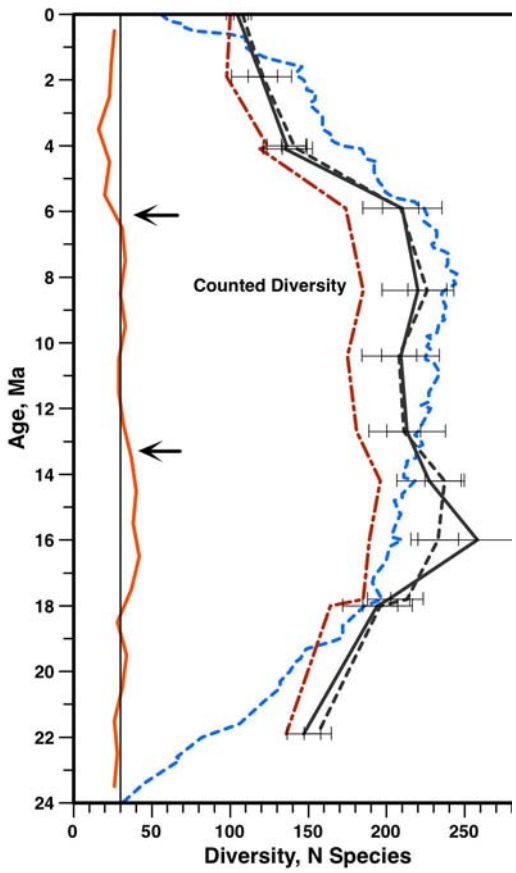

Fig. 1. Different estimates of primary diversity vs time in Antarctic Neogene radiolaria. Orange curve on left is synthesis of published ODP data by Lazarus (2002), with arrows showing diversity drops at ca 13 and 6 my. Blue dashed line - range through estimate of diversity based solely on photographed specimens used in internal taxonomic catalog. This may be expected to approach total diversity near middle of interval but will show major diversity loss near the top and bottom of the analyzed interval due to edge effects. Red dashed line - actual within sample counted diversity from initial set of Indian Ocean sector sample counts. Solid and dashed grey lines with error bars - estimated total diversity in samples with infinite sample size using two different extrapolation methods. Estimated within sample total diversity and range through diversity are in agreement except for top and bottom of interval where edge effects on range-through estimate are strong.

Taxonomic Results: After compiling an internal catalog of all species published as present in Antarctic Neogene sediments (ca 200 taxa), selected radiolarians slides from the Berlin MRC and our own collections were exhaustively scanned for species content. Digital images of known to be present as well as newly encountered taxa were taken (>5,000 images) and identified using existing radiolarian taxonomic literature. To make this work easier many older taxonomic papers were scanned, or if available in image pdf form, OCR'd to allow global searching of literature libraries for taxonomic name usage (using Spotlight in OS X). This taxonomic literature preparation work also benefited from complementary work being done developing a master taxonomic name list (TNL) for IODP as part of a separate project. Over 100 additional named species were identified in Antarctic Neogene sediments by this work, many of them having been reported previously only from North Pacific or Japanese on-shore sections. Lastly, more than 100 more species were identified which do not appear to have been described yet in the literature. These latter forms have been assigned open nomenclature names for internal use. In all, nearly 500 species have been identified and documented in our internal catalog for use in the project. As one of our goals is to improve the taxonomic documentation of Antarctic Neogene species we have been adding, for those taxa without entries, new detailed taxonomic catalog records for all named species at the international community's website radiolaria.org. To date we have added nearly 200 new records, nearly doubling the number of species so documented. Lastly, as many of the species newly documented at rad.org are present in the plankton, the records so added also improve documentation of modern biodiversity in general, as rad.org records are accessed and used to create taxonomic records at the Encyclopedia of Life project (www.eol.org).

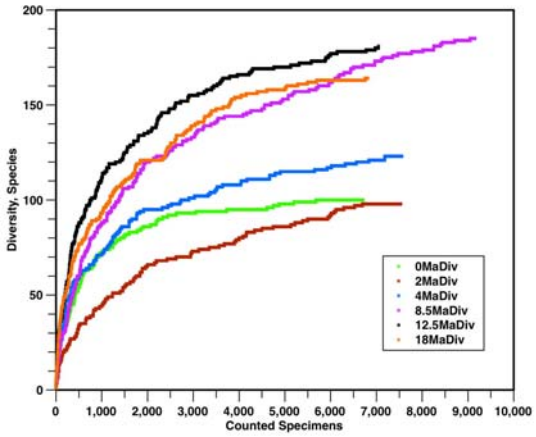

Fig. 2. Sample species diversity vs number of specimens counted for selected samples, based on output from 'DoriCount' program. Except for the 8.5 Ma sample (pink curve) all samples show a low slope at the end of the counting, indicating that most diversity has been captured. Projected total diversity error estimates are also relatively low due to the low slope/capture of curve shape in our counted data.

Although our results are still short of a 100% complete taxonomic documentation of this fauna (a few groups with problematic morphologies could not be included in our

taxa list), with diversity at the base and top of the study interval of ca 100 (Figure 1), we have well over 600 potential events to use in our analyses. Many of the new,

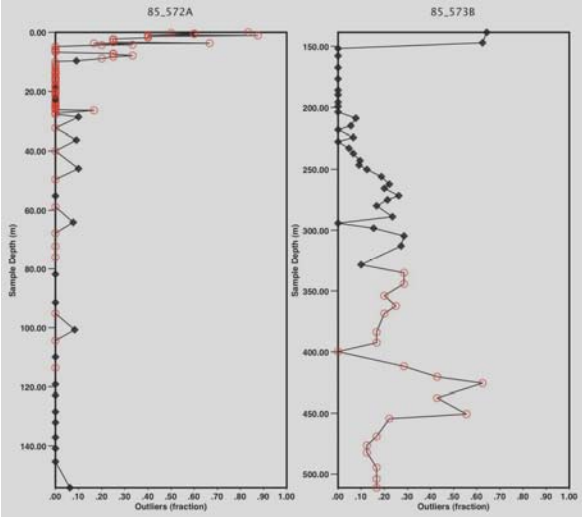

Fig. 3. Two examples of Pacman sample quality profiling using global Neptune radiolarian dataset and profiling results for two equatorial Pacific sections, from Lazarus and Weinkauf, in prep. These sections have (for current ODP reports) relatively taxonomy-rich radiolarian data (Nigrini, 1985, Leg 85 Initial Reports). Global mean outlier average is set analytically at 8% but individual samples and mean values for individual sections may have any fractional value. Sample points marked with open circles have <10 total taxa for calculating outlier fraction. a) Latest Miocene-Recent section with good data quality and relatively well constrained age model (Lazarus et al. 1995, also available at NGDC). Only topmost 10 m (uppermost core) appears to be disturbed or have older (reworked?) taxa, although original report (Nigrini, 1985) does not note this. b) Section with poor quality data. Interval below ca 220 m is mid Miocene-latest Eocene in age. The age model for this site (Lazarus et al. 1995) is poorly constrained by a small number of scattered planktonic foraminiferal datums in the Paleogene (300 m and deeper).

species or species formerly not reported as present in the Antarctic are from the Plagiacanthidae and are mostly small forms. Such smaller taxa were frequently overlooked in prior work, particularly in studies that used relatively coarse (63 µm) sieve sizes.

Occurrence Data: Using only the occurrences of the relatively small number of photographed specimens and a simple range-through calculation an initial rough diversity curve was computed and compared to the only previously published diversity curve of Lazarus (2002) (Figure 1). The comparison, despite the limited accuracy of the new curve, showed that the maximum diversity in the Neogene reached >200 species, and that, in contrast to Lazarus (2002), no diversity drop was observed in the mid-Miocene. A robust diversity curve however requires a detailed sequence of fully surveyed samples. Collecting this data is the main focus of year two of the project. Counting has been done using a new cross-platform Java program created in collaboration with Dorina Lenz and Jens Klump at the GFZ in Potsdam. This program has both full and rare-species-only counting modes and provides real-time feedback on diversity completeness of the counted data via an on-the-fly generated sample count-diversity curve. Rare-count mode allows the user to skip common taxa once these have been counted adequately and quickly scan a large population of specimens on a slide, counting only the remaining rare taxa. Generally, counting is continued until the diversity-sample size curve has largely flattened out (between 4 and 8 thousand specimens, including interpolated counts of common taxa in rare-count mode; Figure 2). Projection of curves to sample size of infinity using Chao1 and Jackknife1 methods suggest that ca. 80% of the taxa present in the sample are actually being recorded in the sample count data. Further, the projected total within-sample diversity estimates from the first set of samples counted agree very well with the much rougher range-through diversity curve calculated earlier, except at the upper and lower bounds of the section, where edge effects artificially reduce the range-through diversity values (Figure 1). We are thus confident that we are successfully capturing a reasonably complete quantitative dataset on the diversity history of this fauna, including the sequence of first and last species occurrences needed for later stratigraphic and evolutionary analysis.

Analyses: Although analytic work largely awaits a more complete dataset later this year, our goal is to use methods such as CONOP to optimally sequence our biostratigraphic events, use this result to cross-correlate sections, and use absolute age information (paleomagnetic reversals - correctly identified) to calibrate our

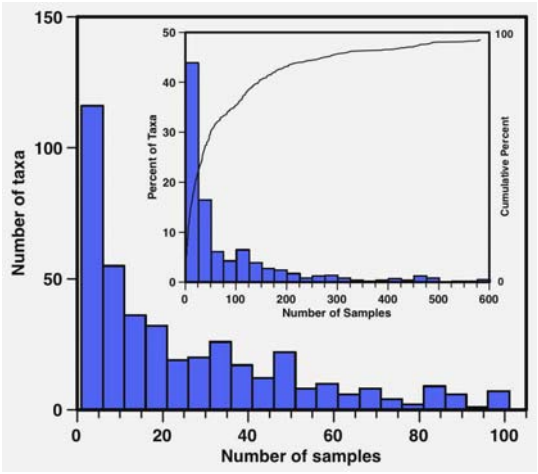

Figure 4 - Number of samples in which individual radiolarian species occur in the global Neptune database. Inset shows total distribution and cumulative curve, main shows detail for taxa with <100 occurrences in samples. Approximately half of all species have been reported from <20 samples and (not shown) just a few sections. From Lazarus and Weinkauf, in prep.

biostratigraphy. Raw data however can contain outliers (mis-identified or reworked specimens) which would seriously degrade the quality of the analysis. We have developed a method (Pacman profiling) to identify data outliers and extended this to sample quality profiling of entire sections. Exploratory work using existing global datasets in Neptune has given us confidence that the method will work well with our new data (Lazarus and Weinkauf, in prep.; Figure 3), but also has made clear that full faunal count data is badly needed for most sections. For example, most samples in the global published radiolarian literature of DSDP and ODP in reality have so few reported taxa in them (mean, global Cenozoic: 9 taxa; only ca 3% of the samples have >20 taxa) that accurate sample quality estimates based on outlier occurrences are

difficult to calculate. Equally, the stratigraphic ranges of most species are still not well known (Figure 4). Although perhaps less extreme, a similar deficit in high quality assemblage data exists for other microfossil groups as well. Macroevolutionary analyses of our data, not yet done, will compare in more detail our results to those of Lazarus (2002) based on incomplete biostratigraphic data, to determine to what degree such incomplete data can be employed too understand evolutionary patterns. These results may also have implications for the much larger body of studies of the traditional macrofossil record (e.g. Sepkoski and PBDB databases).

Outlook: Substantial work is still needed to document our new, more comprehensive taxonomy for Antarctic Neogene radiolaria. Our primary method for named species is to create (for those not already present) taxonomic catalog records at the community rad.org website. This work will continue well into year two, and will include preparing taxonomic papers for new species. Counting will continue throughout most of 2010, although by fall we should have enough data to begin a few initial CONOP and macroevolutionary analyses. Detailed analyses will occupy us in 2011.

References:
Lazarus, D.B., 2002, Environmental control of diversity, evolutionary rates, and taxa longevities in Antarctic Neogene Radiolaria: Paleontologica Electronica v. 5, p, ca 30 p. (web).

ICDP

Seismic stratigraphy of thick undisturbed sediment infill within ancient Lake Ohrid in preparation for the SCOPSCO ICDP-campaign

K. LINDHORST[1], S. KRASTEL[1], T. SCHWENK[2], G. DAUT[3], B. WAGNER[4]

[1]Leibniz-Institut für Meereswissenschaften (IFM-GEOMAR), Kiel, Germany, klindhorst@ifm-geomar.de
[2]Fachbereich Geowissenschaften, Universität Bremen, Germany
[3]Institut für Geographie, Friedrich Schiller Universität Jena, Germany
[4]Institute für Geologie und Mineralogie, Universität Köln, Germany

Lake Ohrid is a transboundary lake with approximately two thirds of its surface area belonging to the Former Yugoslav Republic of Macedonia and about one third belonging to the Republic of Albania. Lake Ohrid is considered to be the oldest, continuously existing lake in Europe, though the age and the origin are not completely unraveled to date. With more than 210 endemic species described, the lake is an unique aquatic ecosystem and a hotspot of biodiversity that is of worldwide importance (Albrecht and Wilke, 2008). The drilling proposal entitled SCOPSCO (Scientific Collaboration On Past Speciation Conditions in Lake Ohrid) is approved by ICDP and will be realized in summer 2011 or 2012. The planned deep drilling campaign will provide substantial information on age and origin of the lake, as well as a complete record of paleoenvironmental history and climate changes in the central northern Mediterranean region (incl. e.g. tephra deposition, evolutionary changes and their relation to geological events). A continuous record will also allow to investigate the impact of major geological/environmental events on general evolutionary patterns and shaping an extraordinary degree of endemic biodiversity as a matter of global significance. Five sites are proposed. The central DEEP-Site should provide a continious archive of maximal age. Four additional drill sites closer to the shore of the lake will shed light on (i) major changes of the hydrological regime, (ii) ages of ancient clinoforms that are linked to lake level fluctuations, as well as (iii) its neotectonic activity and associated mass wasting events.

In order to evaluate drill sites that are best for recovering long continuous records the sedimentary succession of the Lake Ohrid basin was investigated in detail. Beside a dense grid of shallow seismic (sediment echo sounder) data collected between 2004 and 2009 (Wagner et al., 2008), two multichannel seismic surveys were carried out using a 0.25l and 0.1l airgun in Sept. 2007 and June 2008, respectively. The energy was recorded with a 100m-long 16 channel streamer. Two compressors as commonly used for scuba diving provided air supply. A shot interval between 5000 and 7000ms was obtained. The processing procedure included trace editing, setting up geometry, static corrections, velocity analysis, normal moveout corrections, bandpass frequency filtering (frequency content: 35/60 - 600/900 Hz), stack, and time migration.

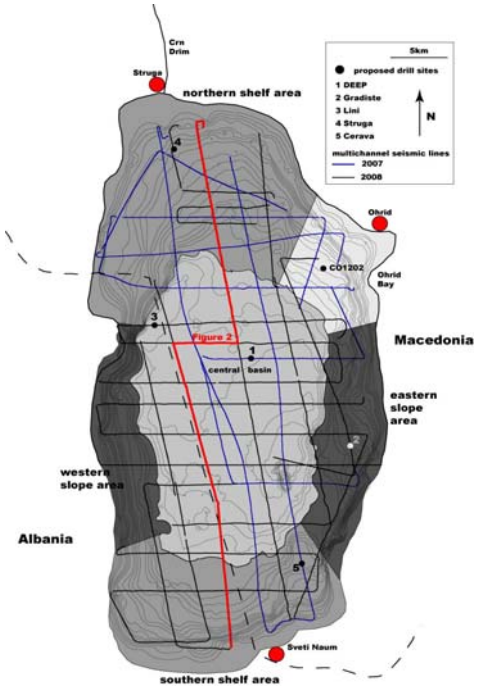

Fig. 1: Map of Lake Ohrid illustrating five primary morphological areas such as Ohrid Bay, eastern and western slope area, northern and southern shelf regions and central basin. Seismic lines recorded in 2007 and 2008 as well as proposed location for drill sites within the SCOPSCO campaign are marked.

An arbitrary seismic profile across Lake Ohrid nicely images main sedimentary features within the basin (Figure 2). The central basin is characterized by thick successions of mainly undisturbed sedimentation. The strata has been divided in six units marked from A to F (youngest to oldest) based on their seismic characteristics. Unit A is characterized by medium amplitude reflectors. We were able to correlate these sediment to core CO1202 (Vogel et

al., 2010) allowing to estimate an age of the lower base (MIS 5e) and subsequent calculate sedimentation rates for Lake Ohrid Basin. Additionally, a tephra layer most likely Y-5 (Vogel et al., 2010) has been mapped throughouth the seismic section. Finally, three sliding events (S1, S5, S6) have been identified within Unit A. Evidences for additinal slide deposits (S2, S3, S4) are further found in the southern part of the seismic profile within Units B and C. Whereas Unit B is characterized by more or less well stratified medium amplitude reflections within unit C there are very prominent high amplitude horizons striking out within the grid of the basement depth, however, has been calculated by combining lower frequency seismic data from 2007 with higher resolution data from 2008. Basement depth forms the basis for calculating the sediment thickness of Lake Ohrid basin. Sediment thickness reaches maximum values in the northern central basin within the area of undisturbed sedimentation (Figure 2).

Our primary drill site for the SCOPSCO campaign is located in the central basin water depth of 250m in order to recover a 700m long contionuous core providing substantial information for dating and to investigate the

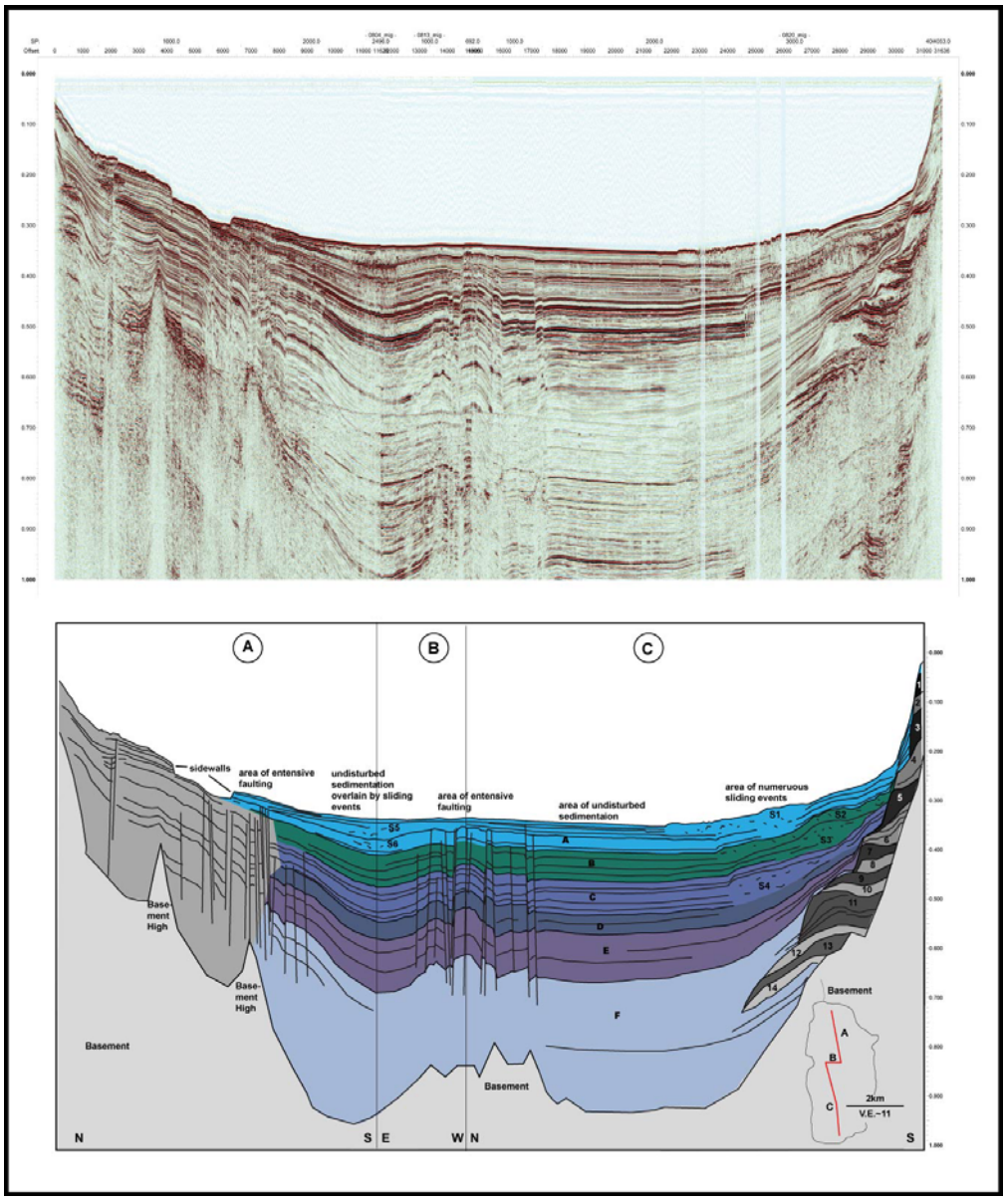

Fig. 2: Seismic cross section showing main sedimentary features of Lake Ohrid; (top) uninterpreted, (bottom) interpreted seismic line.

section. Units D and E have similar characteristics with medium amplitude reflections but each unit probably represents a flooding surface that onlaps on clinoform structures illustrated in the southern most part of the seismic line. The oldest unit F displays the thickest unit that infills and onlaps topographic highs and underlying basement. Multiple reflections within unit F impede tracing of primary reflections down to the basement of the basin. A

origin of the lake, the environmental history, tephra deposition, and the link between evolutionary changes with geological events.

Four additional sites have been proposed to ICDP in order to unravel tectonic activity, hydrological regime, and lake level fluctuations of Lake Ohrid. Two sites (Lini and Gradiste, Figure 1) are located at active lake-bounding major normal faults, one at the western and the other

located at the eastern site. Mass wasting bodies are found at both sites but probable trigger mechanism seem to be different. At the eastern part an earthquake is more likely to have initiated sliding. In contrast on the western side sliding is most likely in direct relation to neotectonic activity of the main boundary fault evidenced by two mass wasting deposits of mainly undeformed sequences that are rotated antithetically. These two mass wasting events vary significantly in thickness and extent, pointing to different magnitudes of seismogenic shocks.

Finally, two sites (Struga and Cerava, Figure 1) were depicted to shed light on the hydrological history of lake Ohrid as they are in the vicinity of clinforms structures. Numeruous clinoforms can be found in the southern part of the lake, the main water supply area, indicating major lake level fluctuations (Figure 2). Interestingly, in the north where at present time only an outflow (Crn Drim, Figure 1) exist, clinforms are present in depth of 0.25s TWT indicating a change of pathway for input of materials since the formation of the clinform. We hope to gain information about an exact age from the sediment core drilled at site Struga. Lake level lowstands as indicated by well preserved clinoforms in the southern region have dates most likely prior to MIS 5e as they are overlain by unit A. However only deep drill cores can provide substantial information needed for a reasable time/depth conversion that we aim to do as future tasks.

References:

Albrecht, C. & Wilke, T. 2008. Ancient Lake Ohrid: biodiversity and evolution. Hydrobiologia 615, 103-140.

Vogel, H., Wagner, B., Zanchetta, G., Sulpizio, R. & Rosén, P. 2010. A paleoclimate record with tephrochronological age control for the last glacial-interglacial cylce from Lake Ohrid, Albania and Macedonia. Journal of Paleolimnology.

Wagner, B., Reicherter, K., Daut, G., Wessels, M., Matzinger, A., Schwalb, A., Spirkovski, Z. & Sanxhaku, M. 2008. The potential of Lake Ohrid for long-term palaeoenvironmental reconstructions. Palaeogeography, Palaeoclimatology, Palaeoecology 259(2-3), 341-356.

IODP

Insights into the fine-grained fraction of serpentine mud from the Southern Chamorro seamount (ODP Leg 195): A combined XRD, XRF and TEM-EDX study

MARTIN LISCHKA[1], MARTIN MESCHEDE[1], LAURENCE N. WARR[1]

[1]University of Greifswald, Institut of Geography and Geology, Friedrich-Ludwig-Jahn-Straße 17a, 17487 Greifswald, Germany

Serpentine mud volcanoes in the outer forearc of the Izu-Bonin-Mariana subduction system occur in a restricted zone, 50km – 120 km away from the trench axis [Fryer et al. 1985]. The morphotectonic elements of the forearc are dominated by horst and graben structures, caused by extensional movements and normal fault systems related to seamount subduction [Fryer et al., 2000; Stern and Smooth, 1998]. These faults may provide conduits for the diapiric uprising of low density serpentine, extruding at the seafloor in stratovolcanic like structures. Released fluids from the subducted slab at estimated depths of approximately 30km are considered to hydrate the forearc mantle wedge along those fractures [Benton et al., 2001; Mottl et al., 2003; Rübke et al., 2004]. During the formation of the fault gauge, serpentine-bodies entrained xenoliths and xenocrysts from the surrounding rocks and are exhumed towards the surface [Fryer et al., 1990].

In our investigation we focus on the silty to clay-sized particle fraction of the serpentine mud matrix, drilled during ODP Leg 195 at site 1200E. We analysed the bulk mineral composition with X-ray diffraction methods on random powder samples, supplemented by X-ray fluorescence measurements on 25 samples. To obtain more insights into the mineralogy fabric and microstructure of the samples, electron microscopy and electron dispersive spectroscopy were used to determine the crystal-chemistry and alteration textures. Particular emphasis was given on determining serpentine polymorphs and the nature of other phyllosilicates and their geochemical composition and constraints. Geochemical observation of the secondary mineral phases should allow us to reconstruct the processes linked with the migration of fluids and volatile components during subduction related metamorphism affecting the mantle wedge. Based on the new data we characterize the conditions of alteration products within a subduction factory, related to the diapiric deposition of serpentine mud volcanoes.

ICDP

Scientific Collaboration On Past Speciation Conditions in Ohrid (SCOPSCO): Recent and fossil Ostracodes from Lake Ohrid as indicators of past environments: A coupled ecological and molecular genetic approach with deep-time perspective

J. LORENSCHAT[1], B. SCHARF[1], T. PETKOVSKI[3], F. VIEHBERG[2], M. LIST[1], A. SCHWALB[1]

[1]Institut für Umweltgeologie, Technische Universität Braunschweig, Langer Kamp19 c, 38106 Braunschweig, Germany (j.lorenschat@tu-bs.de)

[2]Institut für Geologie und Mineralogie, Universität zu Köln, Zülpicherstraße 49 a/b, 50674 Köln, Germany

[3]Macedonian Museum of Natural History, Boulevard Ilinden 86, MK-1000 Skopje, Macedonia

The group of Ostracoda is an ideal model group to study speciation by using extant species as well as fossil calcified valves from lake sediments. In the second deepest lake of Europe, Lake Ohrid in Mazedonia/Albania (289 m), 52 ostracode species are described in literature of which 33 are believed to be endemic to the lake itself (Albrecht and Wilke, 2008). A maximum of ostracode species diversity was found at around 40 m water depth (Mikulic and Pljakic, 1970).

On the basis of taxonomy, autoecology, molecular genetic methods on recent ostracodes, comparison of seasonal variation in the species assemblages, and by the use of studies on fossil assemblages, we contribute to the bundle project “Scientific Collaboration On Past Speciation Conditions in Ohrid (SCOPSCO)”. Overall goals are to (1) clarify the origin and the age of the ancient Lake Ohrid, and to (2) investigate the causes of speciation events.

Here we present preliminary data from the first two field campaigns in spring (March/April) and late summer (August/September) 2009. The third field trip took place in February 2010 (winter), and another will be realized in

early summer (May 2010) in order to assess seasonal variations in biodiversity. So far we identified 21 ostracode species based on adult specimen in the surface sediment samples. 14 out of these 21 species were identified using soft parts. All the other species were represented by isolated valves only. The diversity was slightly higher in spring (12 living species) than in late summer (11 living species). Adult specimen of Candona depressa, Candona triangulata and Candona holmesi occurred only in spring and adult specimen of Candona sp. 4 as well as Darwinula stevensoni were only found in late summer. The highest diversity in spring occured between 15 and 50 m and at around 100 m water depth. In summer, most of the species lived in the littoral zone and at around 50 m water depth. Diversity decreased during spring in the littoral zone. During summer, fewer species were found in higher water depths. Diverse fauna, however, was observed in water depths even below 130 m. In 282 m water depth, Candona hadzistei, Cypria lacustris and Cypria sp. are very common.

A preliminary study of DNA sequencing from ostracodes the mitochondrial cytochrome oxidase I (COI) gene from twelve ethanol-preserved ostracode species (two specimen per species) utilizing the protocol of Winnepenninckx et al. (1993) was extracted. This has delivered sequences for half of the determined ostracodes. In order to improve the DNA work following modifications will be conducted: Increasing the number of DNA amplification cycles (min. 40) and adding of bovines serum albumin (BSA) during the polymerase chain reaction (PCR). Because the choice of specific DNA markers for ostracodes is still rather limited and the mitochondrial 16S has been used successfully (Schön and Martens, 2003) provision is made for screening 16S instead of COI with the aid of universal primers for crustacean.

References:
Albrecht, C., Wilke, T., 2008. Ancient Lake Ohrid: biodiversity and evolution. Hydrobiologia 615: 103-140.
Mikulic, F., Pljakic, M.A., 1970. Die Merkmale der kvalitativen Distribution der endemischen Candonaarten im Ochridsee. Ekologija 5 (1): 101-115.
Schön, I., Martens, K., 2003. Phylogenetic reconstructions of ostracodes - a molecular approach. In: L.E. Park, A.J. Smith (eds), Bridging the Gap, Trends in the Ostracode Biological and Geological Sciences. Paleontological Soc. Papers 9: 71-88.
Winnepenninckx, B., Backeljau, T., De Wachter, R., 1993. Extraction of high molecular weight DNA from molluscs. Trends Genet. 9, 407.

ICDP

Carbon and nitrogen isotope composition of core catcher samples from the ICDP deep drilling at Laguna Potrok Aike (Patagonia, Argentina)

ANDREAS LÜCKE[1], HOLGER WISSEL[1], CHRISTOPH MAYR[2,3], MARKUS OEHLERICH[2], CHRISTIAN OHLENDORF[4], BERND ZOLITSCHKA[4] AND THE PASADO SCIENCE TEAM

[1]Institute of Chemistry and Dynamics of the Geosphere 4: Agrosphere (ICG 4), Energy & Environment, Research Center Jülich, Germany
[2]GeoBio-CenterLMU and Dept. of Earth & Environmental Sciences, University of Munich, Germany
[3]present address: Institute of Geography, University of Erlangen, Germany
[4]Institute of Geography (Geopolar), University of Bremen, Germany

The ICDP project PASADO aims to develop a detailed paleoclimatic record for the southern part of the South American continent from sediments of Laguna Potrok Aike (51°58'S, 70°23'W), situated in the Patagonian steppe east of the Andean cordillera and north of the Street of Magellan. The precursor project SALSA recovered the Holocene and Late Glacial sediment infill of Laguna Potrok Aike and developed the environmental history of the semi-arid Patagonian steppe by a consequent interdisciplinary multi-proxy approach (e.g. Haberzettl et al., 2007).

From September to November 2008 the ICDP deep drilling took place and successfully recovered in total 503 m of sediments from two sites resulting in a composite depth of 106 m for the selected main study Site 2. A preliminary age model places the record within the last 50.000 years. During the drilling campaign, the core catcher content of each drilled core run (3 m) was taken as separate sample to be shared and distributed between involved laboratories long before the main sampling party. A total of 70 core catcher samples describe the sediments of Site 2 and will form the base for more detailed investigations on the palaeoclimatic history of Patagonia.

We here report on the organic carbon and nitrogen isotope composition of bulk sediment and plant debris of the core catcher samples. Similar investigations were performed for Holocene and Late Glacial sediments of Laguna Potrok Aike revealing insights into the organic matter dynamics of the lake and its catchment as well as into climatically induced hydrological variations with related lake level fluctuations (Mayr et al., 2009). The carbon and nitrogen content of the core catcher fine sediment fraction (<200 µm) is low to very low (around 1 % and 0.1 %, respectively) and requires particular attention in isotope analysis (Fig. 1, 2). The carbon isotope composition shows comparably little variation around a value of -26.0 per mil. The positive values of the Holocene and the Late Glacial (up to -22.0 ‰) are only sporadically reached down core (Fig. 3). Compared to this, separated moss debris is remarkably ^{13}C depleted with a minimum at -31.5 ‰. The nitrogen isotope ratios of glacial Laguna Potrok Aike sediments are lower (2.5 ‰) than those of the younger part of the record (Fig. 4). The core catcher samples indicate several oscillations between 0.5 and 3.5 ‰. Data suggest a correlation between nitrogen isotopes and C/N ratios (Fig. 5), but no linear relation between carbon isotopes and carbon content and an only weak relationship between carbon and nitrogen isotopes. Increasing nitrogen isotope values from 8000 cm downwards could probably be related to changed environmental conditions of Marine Isotope Stage 3 (MIS 3) compared to Marine Isotope Stage 2 (MIS 2). Further analyses will increase the resolution in the composite profile and include the oxygen isotope composition of discrete plant debris layers as well as of phases bearing biogenic silica.

References:
Haberzettl, T. et al. (2007). Lateglacial and Holocene wet-dry cycles in southern Patagonia: chronology, sedimentology and geochemistry of a lacustrine record from Laguna Potrok Aike, Argentina. The Holocene, 17: 297-310.
Mayr, C. et al. (2009). Isotopic and geochemical fingerprints of environmental changes during the last 16,000 years on lacustrine organic matter from Laguna Potrok Aike (southern Patagonia, Argentina). Journal of Paleolimnology, 42: 81-102.

IODP

Paleoenvironmental history of the southern Bering Sea over the last 5 Million years (IODP Expedition 323, Site U1341) as recorded by sediment geochemistry

C. MÄRZ[1], H.-J. BRUMSACK[1], A.C. RAVELO[2], K. TAKAHASHI[3], C. ALVAREZ-ZARIKIAN[4], AND IODP EXPEDITION 323 SCIENTISTS

[1]AG Mikrobiogeochemie, Institut für Chemie und Biologie des Meeres (ICBM), Postfach 2503, 26111 Oldenburg, Germany
[2]Ocean Sciences Department, University of California, 1156 High Street, Santa Cruz CA 95064, USA
3Department of Earth and Planetary Sciences, Kyushu University, Hakozaki 6-10-1, Higashi-ku, Fukuoka 812-8581, Japan
[4]Integrated Ocean Drilling Program, Texas A&M University, 1000 Discovery Drive, College Station TX, 77845-9547, USA

IODP Expedition 323 recovered the first continuous sediment records covering the last 5 Ma from Bowers Ridge (southern Bering Sea). According to preliminary shipboard results, the sediment consists of a variable mixture of siliciclastic clay and silt, biogenic opal and minor carbonate, and volcanic ash. Sedimentation rates seem to range mostly between 10 and 15 cm/ka, but reach 45 cm/ka in some intervals. Although pore water data imply relatively weak present-day diagenesis, paleomagnetic records and authigenic precipitates prove higher diagenetic activity in Bowers Ridge sediments in the past. To resolve Pliocene-Pleistocene paleoenvironmental changes in the southern Bering Sea, including the amount and provenance of terrigenous material, biological productivity, bottom water redox conditions and diagenetic overprint of primary signals, around 200 bulk sediment samples were analysed for their elemental composition. We quantified major and some minor element contents using X-ray fluorescence (XRF), and total carbon and sulfur (TC, TS) via combustion and IR analysis. Here we will highlight some of the most interesting findings.

As exemplified by relatively low Al_2O_3 contents (~ 2-15 wt%), the terrigenous input to Bowers Ridge is generally of minor importance, which is consistent with its distance to potential source areas in a rather open marine environment. However, there is a clear trend to higher Al_2O_3 contents in younger sediments, most probably caused by the onset and intensification of Northern Hemispheric Glaciation and related sea ice formation in the Bering Sea. This effect is most probably related to lower diatom productivity, as indicated by decreasing SiO_2 contents and Si/Al ratios towards the top of the record. Notably, frequency and amplitude of variation of both, the Al and Si records, are relatively weak prior to ~ 2.7 Ma, but are much more pronounced in the overlying deposits. The cause of these patterns might be the shift from a relatively stable and warm Pliocene to a rather unsteady Pleistocene climate with major ice sheets and strong glacial-interglacial variation. This overall pattern is reflected in most element records we analysed.

The general enrichment of Si in Bowers Ridge deposits reflects the importance of opal productivity since the Pliocene, while biogenic carbonate is a minor component of the sediments. However, the record of Ba/Al, another popular geochemical paleoproductivity proxy, does not parallel the Si/Al pattern. While Ba enrichments in sediments older than ~ 3.5 Ma and younger than ~ 2.0 Ma hint to high paleoproductivity, its depletion to detrital background values in between these intervals calls for a different explanation. We assume that biogenic barite was originally deposited at Site U1341 between 3.5 and 2.0 Ma, but intense contemporaneous sulfate reduction caused barite dissolution and Ba depletion in the sediments. Based on our bulk geochemical data, we cannot explain the exact nature and timing of this biogeochemical process, but our hypothesis is supported by elevated total S contents, S/Al and Si/Al ratios indicating high opal productivity and S fixation via bacterial sulfate reduction.

Stronger sulfate reduction from 3.5 to 2.0 Ma indicates that bottom waters at Site U1341 were relatively oxygen-depleted or even anoxic. Despite only semi-quantitative results, the trace metals As and Mo are enriched within this interval while Mn is depleted, which supports our hypothesis of reducing bottom water conditions. However, trace metal data do not indicate prolonged anoxic to sulfidic bottom water conditions at Site U1341 during the last 5 Ma. Despite supposedly high opal productivity at Bowers Ridge, the sediments are relatively poor in total C (0.4 to 1.0 wt%) and are not enriched in the essential nutrient P. These findings suggest that either the productivity signal was diluted by detrital input (which is unlikely as stated above), or the element cycles of C and P were decoupled from the biogenic Si and Ba signals due to degradation in the water column or at the sea floor. Indeed, we find numerous sediment intervals at Site U1341 with finely dispersed or lithified authigenic precipitates rich in C and P (but also Ca, Mg, Mn and Fe), indicating formation of diagenetic carbonates and apatite.

ICDP

Rock magnetic properties from host rock and impact lithologies of drillings at the Chesapeake Bay impact structure, USA

CHRISTOPH MANG AND AGNES KONTNY

Karlsruhe Institute of Technology, Institut für Angewandte Geowissenschaften, Hertzstraße 16, 76187 Karlsruhe

The Chesapeake Bay Impact Crater, Virginia, USA, is characterized by irregular magnetic anomalies which are distributed over the whole crater structure and locally extend the crater rims. Positive magnetic anomalies at the western and eastern side of the crater differ from a regional NW - SW tending, negative magnetic anomaly pattern and are considered to be impact-related (Shah et al., 2009). Our work focuses on the magnetic minerals that cause these anomalies and how they have been affected by shock metamorphism, impact melting during the impact event or by post-impact hydrothermal systems.

Several drillings into the crater structure reveal different impact related units that fill up the impact crater. Beneath post impact sediments and a lithic impact breccia, suevitic rocks are interspersed with m to km scale megablocks. These megablocks exhibit uncoupled flinders of crystalline basement and consist of granitic and metamorphic rocks (gneiss, micaschist, amphibolite). So far, no impact related deformation has been found within the megablocks. Due to their irregular dispersion within the impact crater, the megablocks and impact related breccias are suggested to cause the deviation from the regional

magnetic anomaly pattern as each unit is characterized by distinct rock magnetic properties (Shah et al., 2009).

Previous measurements of rock magnetic properties (Elbra et al., 2009) show that post impact sediment layers and lithic impact breccia cannot be linked to the magnetic anomalies due to a lack of a significant amount of magnetic minerals.

As a consequence investigations about formation of the magnetic minerals were focussed on the basement units. Rock magnetic properties have been measured on cores from Eyreville, Cape Charles, Langley and Bayside boreholes. Each rock unit shows differences in its rock magnetic properties reflecting differences in the magnetic mineralogy. The main magnetic minerals causing the magnetic anomalies were determined to be magnetite/maghemite and pyrrhotite. They occour predominantly within the basement megablocks and the suevitic breccia.

The basement megablocks contain larger grains of magnetite/maghemite (granite block) and pyrrhotite (schist block). These grains are partly altered and their origin can clearly be linked with the regional geological history of the parent rock material. The suevite breccia contains µm to mm scale grains of maghemite and pyrrhotite.

In contrast to the magnetic minerals of the megablocks, most of the magnetic minerals within the suevite indicate a post impact formation since skeletal growth structures reflect a possible nucleation of new grains.

Magnetic Susceptibility measurements show the highest values in granitic, gneissic and schistose megablocks as well as in melt fragments and melt rich zones of the suevite breccia. However, granite and gneiss megablocks are dominated by induced magnetization and thus do not contribute a stable remanent magnetization (NRM). In contrast, schist, granite, gneiss and suevite breccia are dominated by a stable remanent magnetization.

NRM mean values published by Shah et al. (2009) and obtaining 2 – 6 A/m for a layer of impact melt cannot be confirmed by our measurements, as the measured values average 0.1 – 1 A/m. Thus we suggest magnetic contribution of the impact melt to be overestimated.

References:

T. Elbra, A. Kontny and LJ. Pesonen, Rock magnetic properties of the ICDP-USGS Eyreville core, 2009, Chesapeake Bay impact structure, Virginia, USA, Geological Society of America Special Paper 2009, p 119 – 137.

A.K. Shah, D.L. Daniels, A. Kontny and J. Brozena, 2009, Megablocks and melt pockets in the Chesapeake Bay impact structure constrained by magnetic field measurements and properties of the Eyreville and Cape Charles cores, Geological Society of America Special Paper 2009, p. 195 – 209.

IODP

Reconstruction of the Atlantic Circulation back to the Last Interglacial by a combined proxy approach from ODP Leg 172 Site 1063 sediments

A. MANGINI[1], J. LIPPOLD[1], E. BÖHM[1], S. WEYER[2], M. GUTJAHR[3], M. CHRISTL[4]

[1]Academy of Science, Heidelberg, Germany
[2]University of Köln, Germany
[3]University of Bristol, UK
[4]ETH Zürich, Switzerland

The Atlantic Meridional Overturning Circulation (AMOC) is believed to have crucial influence on global climate. It affects global temperatures due to the redistribution of heat energy to the high latitudes and by removing and releasing carbon from or into the deep sea. Reconstructions of past ocean circulation changes suggest a strong link between the strength of AMOC and climate especially in circum North Atlantic temperatures.

Theoretical studies and measured data suggest that the AMOC has different circulation modes and that transitions between these modes can be triggered by variations of freshwater runoff into the North Atlantic [Rahmstorf 2002; Rickaby and Elderfield 2005]. Further, glacial climate in the North Atlantic region was characterized by short term climatic cycles referred to as Dansgaard-Oeschger- and Heinrich- Events (HE), which are also believed to be tightly correlated to the strength of North Atlantic Deep Water formation and hence AMOC.

Within the last years two different proxies turned out to be promising in order to reconstruct past deep water provenance and strength of the AMOC, as both proxies are not subject to diagenetic processes. First, the ratio of the in seawater in situ produced ^{231}Pa and ^{230}Th in the sediment, and second the isotopic ratio of ^{143}Nd to ^{144}Nd (εNd hereafter) in the post depositional Fe-Mn coatings of the sediment (e.g. [Henderson and Anderson 2003; Frank 2002]). Due to the observation that in the Atlantic Ocean ^{231}Pa is subject to advective transport (while ^{230}Th is a constant flux tracer) the ^{231}Pa/^{230}Th ratio can be applied a tracer for the strength of AMOC in the past. By additionally using the water mass proxy εNd, complementary information about the source of the prevailing water mass is available. For this reason, a synthesis of both proxies from the same sediment samples holds the opportunity to provide new insights on the modes of deep ocean circulation in the past.

In this project samples of ODP Leg 172 Site 1063 will be investigated. The oceanic region of ODP Site 1063 on the northeast Bermuda Rise holds a key position in the interaction of Northern Component Water and Southern Component Water and is therefore ideal for detecting past changes in southward water mass export. These variations are recorded in marine sediments and can be reconstructed by analysing ^{231}Pa/^{230}Th and εNd. Site ODP 1063 displays constantly very high sedimentation rates (>10cm/ka) enabling a high time resolution.

This study is the first to directly compare water mass source changes, reconstructed by using εNd isotopes, with ^{231}Pa/^{230}Th ratios, which records the overturning rate, from identical samples on a timescale back to the last Interglacial (Eemian). The time interval of the planned

measurements (35 ka back to 130 ka) spans several severe climate incidents like Heinrich Events (HE-4 to HE-6), numerous Dansgaard-Oeschger Cycles, the Last Glacial Inception and the last Interglacial, which have not been addressed by $^{231}Pa/^{230}Th$ or εNd studies from the Western North Atlantic so far [McManus et al. 2004; Lippold et al. 2009; Gutjahr et al. 2008; Roberts et al. 2010]. It is assumed, that temperatures during the Eemian were partly higher than during the Holocene. Thus, in regard to a recent global warming, the reconstruction of the past Ocean circulation may serve to anticipate future developments.

References:
Frank, M. (2002), Radiogenic Isootpes: Tracers of Past Ocean Circulation and Erosional Input, Reviews of Geophysics 40(1).
Gutjahr, M., M. Frank, C. Stirling, L. Keigwin and A. Halliday (2008), Tracing the Nd isotope evolution of North Atlantic Deep and Intermediate Waters in the western North Atlantic since the LGM from Blake Ridge sediments, Earth and Planetary Science Letters 266: 61–77.
Henderson, G. and R. Anderson (2003), The U-series toolbox for paleoceanography, "Uranium Series Geochemistry", Reviews in Mineralogy and Geochemistry 128.
Lippold, J., J. Grützner, D. Winter, Y. Lahaye, A. Mangini and M. Christl (2009), Does sedimentary 231Pa/230Th from the Bermuda Rise monitor past Atlantic Meridional Overturning Circulation?, Geophyscial Research Letters 36: L12601.
McManus, J. F., R. Francois, J. M. Gherardi, L. D. Keigwin and S. Brown-Leger (2004), Collapse and rapid resumption of Atlantic meridional circulation linked to deglacial climate change, Nature 428: 834-837.
Rahmstorf, S. (2002), Ocean circulation and climate during the past 120,000 years, Nature(419): 207-214.
Rickaby, R. and H. Elderfield (2005), Evidence from the high-latitude North Atlantic for variations in Antarctic Intermediate water flow during the last deglaciation, Geochemistry Geophysics Geosystems 6: Q05001.
Roberts, N., A. Piotrowski, J. McManus and L. Keigwin (2010), Synchronous deglacial overturning and water mass source changes, Science, accepted.

ICDP

Carbonates from the ICDP-site Laguna Potrok Aike: Mineralogy, isotopic composition and sample pre-treatment effects

C. MAYR[1,2,3], M. OEHLERICH[1], A. LÜCKE[4], E. GRIESSHABER[1], S. KASTNER[5], O. OECKLER[6], C. OHLENDORF[5], W. SCHMAHL[1], B. ZOLITSCHKA[5] AND THE PASADO SCIENCE TEAM

[1]Earth and Environmental Sciences, LMU Munich, Germany (cmayr@geographie.uni-erlangen.de)
[2]Geo-Bio-Center, LMU Munich, Germany
[3]present address: Institute of Geography, University of Erlangen-Nuremberg, Germany
[4]Institute of Chemistry and Dynamics of the Geosphere 4: Agrosphere (ICG 4), Forschungszentrum Jülich, Germany
[5]GEOPOLAR, Institute of Geography, University of Bremen, Germany
[6]Department of Chemistry, LMU Munich, Germany

Endogenic carbonates occur in two different phases, calcite and ikaite at the International Continental Drilling Project (ICDP) site Laguna Potrok Aike (51°57´S, 70°23´W). Calcite ($CaCO_3$ of the trigonal crystal system) is abundantly present in Holocene sediment sections as finely dispersed crystals of less than 10 µm in size. These crystals resemble the features of endogenically precipitated calcites as known from many other lakes (e.g., Raidt & Koschel 1988). Ikaite was detected during the ICDP drilling campaign in September 2008. Up to ca. 3 mm large, transparent, sigmoidally shaped and idiomorphic crystals were found abundantly in the 4°C cool lake water, especially on submerged items like aquatic plants or ropes. Single crystal X-ray diffraction analyses on samples that were permanently kept cool document that these crystals were ikaite ($CaCO_3 \cdot 6H_2O$ of the monoclinic crystal system), a hydrated calcium carbonate mineral occasionally found in marine sediments but rarely reported from non-marine environments. Ikaite precipitation has been observed only at temperatures below 5-8°C (DeLurio & Frakes 1999). Because of the stability field of ikaite (Marland 1975), after air exposure, the crystals from Laguna Potrok Aike soon transformed to porous, polycrystalline, fragile pseudomorphs that rapidly disintegrated into µm-sized calcite crystals,

Calcite pseudomorphs after ikaite can be preserved by calcite cementation (e.g., Larsen 1994) and then their presence in the sedimentary record indicates cool water temperatures. So far no preserved pseudomorphs have been identified in the sediment record of Laguna Potrok Aike. However, the similar morphologies of originally precipitated calcite and calcite from disintegrated modern ikaite raise the question, if µm-sized ikaite-derived calcite crystals are also present in the lake sediment and how to distinguish between both carbonate sources. Stable isotope analyses were applied to resolve that question. Preliminary $\delta^{13}C$ and $\delta^{18}O$ results separate isotope values of calcites derived from ikaite from those of the surface sediments of the same lake. These first isotopic results suggest that the calcites from profundal sediments have a different origin than the ikaite-derived calcites from the littoral zone.

The sediment profile recovered during the ICDP drilling at Laguna Potrok Aike archives more than 50,000 years of environmental change in the steppe of southern Patagonia. The isotopic composition of carbonates can give information about past water temperatures and hydrological variability. First results show that the carbonate content is high (up to ~20 wt. %) in the Holocene, but low or even absent in the glacial interval of the sediment record. The presence of organic matter, especially in conjunction with low carbonate content, can bias carbonate isotope values due to the release of carbon dioxide from organic matter decomposition during the acidification necessary to produce measuring gas. Thus, a sample pre-treatment is often advised to remove organic compounds (e.g., Ito 2001). Therefore we tested several methods to pre-treat bulk samples for removal of organic compounds. First results show that the commonly used pre-treatment with sodium hypochlorite (NaOCl) to remove organic compounds from sediment samples leads to erroneous results. This is in accordance with recent investigations by Wierzbowski (2007). Our present efforts are to overcome these difficulties by (1) investigating which organic materials potentially affect carbonate stable isotope analyses and (2) testing alternative methods (e.g. H_2O_2 bleaching, no pre-treatment). The method with the least impact on isotope composition will then be applied for investigating the carbonate isotope record from Laguna Potrok Aike.

References:
De Lurio JL, Frakes LA (1999) Glendonites as a paleoenvironmental tool: Implications for early Cretaceous high latitude climates in Australia. Geochimica et Cosmochimica Acta 63:1039-1048.
Ito E (2001) Application of stable isotope techniques to inorganic and biogenic carbonates. In: Last WM & Smol JP (eds) Tracking Environmental Change Using Lake Sediments. Vol. 2. Kluwer Academic Publ., Dordrecht, The Netherlands, pp. 351-371.
Larsen, D (1994) Origin and paleoenvironmental significance of calcite pseudomorphs after ikaite in the Oligocene Creede Formation, Colorado. Journal of Sedimentary Research 64:593-603.
Marland G (1976) The stability of $CaCO_3 \cdot 6H_2O$ (ikaite). Geochimica et Cosmochimica Acta 39:83-91.

Raidt H, Koschel R (1988) Morphology of calcite crystals in hardwater lakes. Limnologica 19:3-12.
Wierzbowski H (2007) Effects of pre-treatments and organic matter on oxygen and carbon isotope analyses of skeletal and inorganic calcium carbonate. International Journal of Mass Spectrometry 268:16-29.

IODP

Sulphur- and carbon-isotopes document dynamic sulphate methane interface (Peru Margin, Leg 201 Site 1229)

PATRICK MEISTER[1], BENJAMIN BRUNNER[1], TIMOTHY G. FERDELMAN1, MICHAEL E. BÖTTCHER[2], AND BO BARKER JØRGENSEN[3]

[1] Max-Planck-Institute for Marine Microbiology, Celsiusstrasse 1, 28359 Bremen, Germany, pmeister@mpi-bremen.de
[2] Leibniz-Institute for Baltic Sea Research, Seestrasse 15, 18119 Rostock, Germany
[3] Center for Geomicrobiology, Aarhus University, Ny Munkegade 114-116, 8000 Aarhus, Denmark

Geochemical signatures in early diagenetic minerals may provide information necessary to understand the evolution of subsurface microbial activity and redox zonation over geological time periods. Because such signatures are preserved from the past, they may document changing conditions that are otherwise not obvious from microbiological or porewater geochemistry studies. In order to reconstruct past deep biosphere conditions in hemipelagic organic carbon-rich sediments of the Peru Margin, drilled during ODP Leg 201 (D'Hondt et al., 2003), we analyzed $\delta^{34}S$ values of pyrite (the chromium-reducible sulphide fraction) and compared them to a downcore record of $\delta^{13}C$-values from early diagenetic dolomite (Meister et al., 2007). The carbon isotope composition of dolomite and sulphur isotope composition of pyrite show a matching pattern. This is remarkable, because pyrite and dolomite represent two petrographically distinct diagenetic phases.

The interpretation of this relationship relies on the knowledge of time and depth of pyrite formation. In this particular case, a high degree of pyritization (ratio between pyrite and total reactive iron) was found throughout the stratigraphic column, indicating that the main part of the pyrite forms within the uppermost few meters below seafloor. This is consistent with the presence of free sulphide from the top meter below seafloor downcore, implying that pyrite formation at this site is controlled by the reactivity of iron bearing phases. Hence, pyrite-sulphur and its isotopic composition document a geological record of paleo-porewater sulphide composition near the sediment surface. The $\delta^{34}S$-value of sulphide near the sediment surface is likely to reflect the extent of organoclastic sulphate consumption, i.e. higher values indicating higher sulphate depletion, and consequently a shallower depth of the sulphate methane interface (SMI).

Carbon-13 values in diagenetic dolomite also represent a record of near surface porewater conditions. This is evidenced by calcium-isotopes (Teichert et al., this volume) and strontium-isotopes (Meister et al., 2007) showing both near surface signatures. Dolomite seems to form episodically within the uppermost 30 mbsf, when alkalinity is strongly increased along the SMI. Strong downcore variation of the $\delta^{13}C$ values in the dolomites, therefore, should represent varying conditions at the SMI in the past. Elevated $\delta^{13}C$ values would have been incorporated in the dolomite phase from an isotopically heavier DIC-pool that is likely produced by enhanced methanogenesis. More methane produced would then have driven the SMI upwards, which is consistent with the interpretation of the $\delta^{34}S$ values in pyrite. Vice versa, isotopically light dolomite would have been formed during less intense methanogenesis and a downward migration of the SMI.

The $\delta^{34}S$ in pyrite and $\delta^{13}C$ in dolomite provide evidence from two independent sources supporting dynamic changes in the depth of the sulphate methane interface over the past 2 Ma at Peru Margin Site 1229. The sediments from this site, which contain large amounts of early diagenetic dolomite and pyrite, are a unique archive of past deep biosphere evolution throughout the Plio-Pleistocene deposition history. This example demonstrates how changes of geochemical gradients, redox zonation, and the entire diagenetic system including the deep biosphere are preserved over geological times. Non-steady state subsurface conditions, therefore, have to be taken into account for a global assessment of the role the deep biosphere in Earth's system.

References:
D'Hondt, S.L., Jørgensen, B.B., Miller, D.J., et al. (2003) Proc. ODP, Init. Repts., 201: College Station, TX (Ocean Drilling Program). doi:10.2973/odp.proc.ir.201.2003
Teichert, B.M.A., Meister P., Ockert C., and Gussone N. (2010) Ca-isotopes of early diagenetic, primary dolomite from the Peru Margin. Abstract, this volume.
Meister, P., McKenzie, J.A., Vasconcelos, C., Bernasconi, S., Frank, M., Gutjahr, M., and Schrag, D.P. (2007) Dolomite formation in the dynamic deep biosphere: results from the Peru Margin. Sedimentology, 54, 1007-1031.

IODP

Quantification of the spatial enhancement of ocean anoxia during OAE2 and T-OAE using Mo and U isotope signatures

C. MONTOYA-PINO[1], S.WEYER[2], A. D. ANBAR[3], B. VAN DE SCHOOTBRUGGE[1], W. OSCHMANN[1], J. PROSS[1], H. W. ARZ[4]

[1]Institut für Geowissenschaften, Goethe Universität, Frankfurt am Main 60438, Germany
[2]Institut für Geologie und Mineralogie, Universität zu Köln 50674, Germany
[3]School of Earth and Space Exploration, Arizona State University, Tempe, Arizona 85287, USA
[4]Deutsches Geoforschungszentrum GFZ, Potsdam 14473, Germany

Introduction: Throught the Phanerozoic, the oceans are generally considered to be oxygenated. Nevertheless, episodes of depleted oxygen conditions in the oceans have been recorded. These episodes, known as oceanic anoxic events (OAEs; Schlanger and Jenkyns, 1976), are characterized by the widespread deposition of organic-rich sediments, e.g. black shales, of regional or even global extent, indicating a potentially global enhancement of oceanic anoxia. Here, combining the isotope composition of the redox sensitive trace metals Mo and U (i.e. variations in $^{238}U/^{235}U$) with redox sensitive trace metal concentrations in modern and ancient organic-rich

sediments, we present an approach to characterizing the redox conditions and determining the expansion of oceanic anoxia during such OAEs, compared to modern sediments from the Black Sea, the T-OAE and the OAE2. In contrast, low Fe_T /Al- and increased Mn/Al ratios indicate anoxic non-euxinic conditions during the

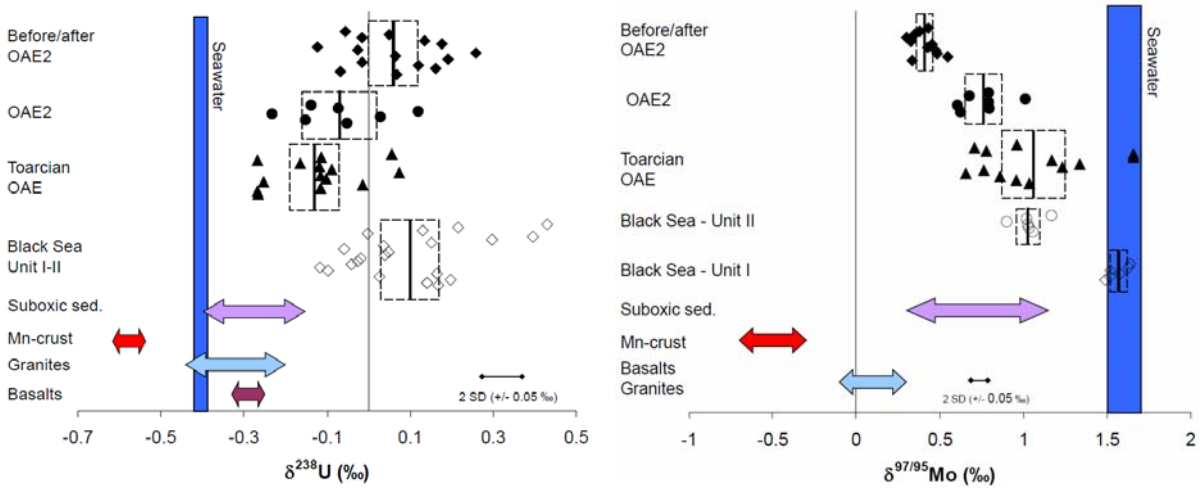

Fig. 1: Summary of U- (A) and Mo- (B) isotope compositions analysed in this study. Open symbols represent modern black shales from the Black Sea unit I and II. Solid symbols correspond to OAE black shales from the Toarcian OAE (triangles), the OAE2 (circles) as well as samples from the intervals before and after the OAE2 (diamonds). The U and Mo isotopic compositions of basalts, granites, suboxic sediments, manganese crusts (shown as colored arrows), seawater (blue rectangle) and 6 Black Sea black shales (open diamonds and circles) were taken from Weyer et al., 2008, Arnold et al., 2004; Siebert et al., 2003 and Barling et al. (2001), respectively. The mean U and Mo isotope compositions and 2 standard errors for each group of samples are displayed as solid lines and dashed rectangles.

oxygenated conditions. Both Mo and U are enriched in anoxic and euxinic environments and show systematic isotope variations between seawater, oxic- and anoxic sinks (Barling et al., 2001; Weyer et al., 2008). Accordingly, their isotopic budgets are sensitive to redox changes in the oceans (Arnold et al., 2004; Montoya Pino et al. in press). Moreover, using trace element compositions, we are comparing and characterizing the redox conditions of the anoxic/euxinic basins that are used for this study. Here, we focused on black shales from two well-recognized Mesozoic OAEs; the early Jurassic Toarcian OAE (T-OAE; ca. 183 Ma) and the mid-Cretaceous (Cenomanian-Turonian) OAE2 (ca. 93 Ma). Both had possibly a global extension (Erbacher et al., 2005; Pearce et al., 2008) and a long-enough duration (~900 ky and ~400-600 ky for the T-OAE and OAE2 respectively; Sageman et al., 2006; Voigt et al, 2008; Suan et al., 2008) that a global change in oceanic redox conditions should have affected the oceanic Mo and U isotope bugdet. For comparison, we also analysed black shales from periods devoid of OAEs, such as the black shales that were deposited prior to- and post OAE2, and also modern anoxic/euxinic sediments. The OAE2 samples, as well as those deposited before and after OAE-2 are from ODP Leg 207 Demerara Rise, Site 1261A, the T-OAE samples are from Western and Central Europe, and as modern equivalents we investigated sapropels from the Black Sea.

Results: The enrichment factors observed for redox sensitive trace elements like Re, Mo and U combined with redox proxies such as Fe_T/Al and Mn/Al ratios point to oxygen-depleted conditions at the time of black shale deposition in all the studied localities, in agreement with the findings from Brumsack (2006) and Hetzel et al. (2009). We used Fe_T /Al- and Mn/Al ratios to distinguish between euxinic and anoxic non-euxinic conditions. This proxy indicates euxinic conditions during the deposition of black shales before and after OAE2. The first attempts using Mo or U isotopes to quantify the extension of seafloor anoxia during periods of increased oceanic anoxic conditions like the OAE2 and the T-OAE were

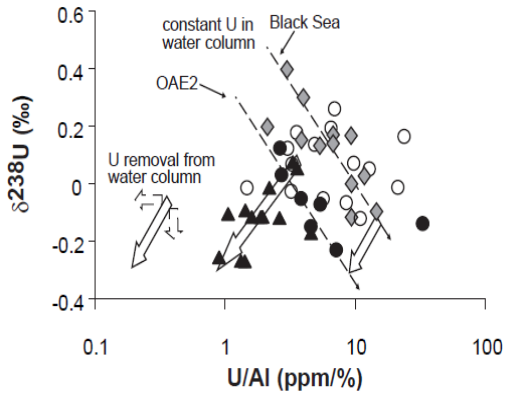

Fig. 2: Plot of $\delta^{238}U$ (‰) versus U/Al (ppm/%). Toarcian OAE samples yield a positive-, while Black Sea and OAE2 black shales yield a negative correlation.

Toarcian OAE: Triangles
OAE2: solid circles
Before/after OAE2: open circles
Black Sea Unit I-II: diamonds

made by Arnold et al. (2004), Pearce et al. (2008) and Montoya-Pino et al. in press. Here we use a similar approach as the one used by Montoya-Pino et al. in press to model the global change of anoxic and euxinic conditions during the OAE2 and the T-OAE using the combined signature of Mo and U isotope compositions (Fig. 1A and

B), compared to that of modern euxinic organic-rich sediments.

We observed a systematic shift of ≈0.2‰ and 0.6‰ towards lighter U and Mo isotope compositions respectively, between modern (Black Sea) and black shales from OAE2 and T-OAE. Black shales from the intervals before and after OAE2 display a similar U isotope

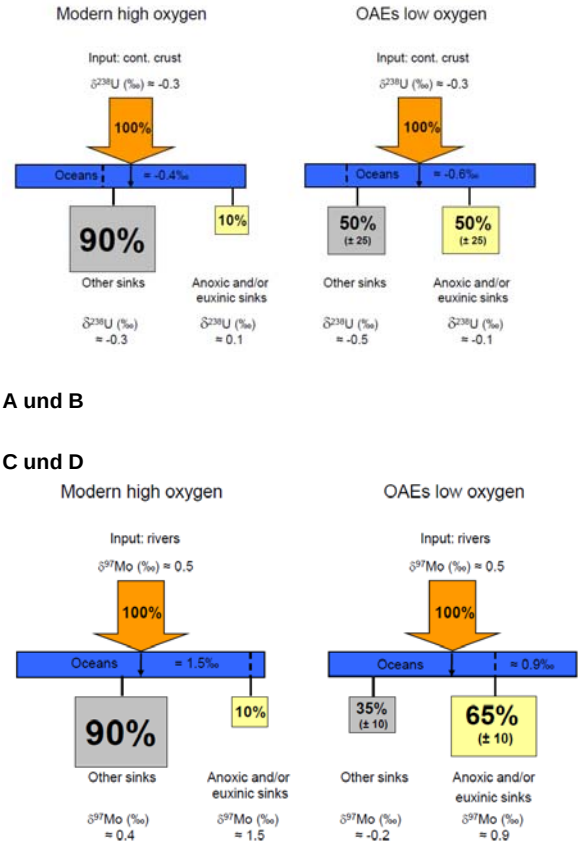

Fig. 3: Oceanic U and Mo mass balance for **(A, C)** modern oceans (little anoxia) and **(B, D)** oceans during the OAEs (enhanced anoxia). Low $\delta^{238}U$ and $\delta^{97}Mo$ of OAEs compared to modern black shales indicate enhancement of anoxic and/or euxinic sinks during the Toarcian OAE and the OAE2 if applying mass balance constrains.

$\delta^{238}U$ from seawater and oxic/suboxic/hydrothermal settings ("other sinks" in **A** and **B**) during OAE times were estimated assuming a constant fractionation factor between black shales and seawater (0.5‰; Weyer et al., 2008) and little fractionation between seawater and other sinks. In contrast, the $\delta^{97}Mo$ from seawater and oxic/suboxic settings ("other sinks" in **C** and **D**) were estimated assuming no fractionation between seawater and euxinic sediments and strong fractionation between seawater and oxic/suboxic environments. $\delta^{238}U$ and $\delta^{97}Mo$ (‰) for the U- (continental crust; Weyer et al., 2008) and Mo (rivers; Archer and Vance, 2008) input, respectively was assumed to be invariant with time.

composition as black shales from the Black Sea, i.e. heavier than OAE2 black shales. However, in contrast to U, Mo-isotope compositions of black shales from above and below the OAE2 interval are even lighter than those from the OAE2 black shales. Additionally, a shift of both OAEs towards lighter U-isotope compositions and/or U concentrations is also evident in a plot of U isotopes and U/Al (Fig. 2), where Black Sea and OAE2 black shales show a negative correlation, while those from the T-OAE show a positive correlation.

Discussion and Conclusions: The observed shift in the U and Mo isotope compositions between OAE and Black Sea black shales points to a lighter U and Mo isotopic composition of seawater during the OAE periods (compared to that of the present ocean), if assuming a constant fractionation factor between seawater and black shales (Montoya-Pino et al. in press), which indicates a global enhancement of seafoor anoxia during the OAEs. A similar enhancement is also indicated relative to periods before and after OAE2 by the U isotope compositions of black shales. In contrast, the Mo-isotope compositions of the before and after OAE2 samples are even lighter than the OAE2 black shales themselves.

However, the Mo-isotope composition of these samples is likely affected by changes in the local redox conditions as indicated by the Fe_T/Al ratios, resulting in Mo isotope fractionation towards lighter compositions (Poulson et al., 2006). Thus, a change from anoxic/non-euxinic to euxinic conditions at the onset of OAE2 (Hetzel et al., 2009) is likely responsible for the observed shift in Mo isotopes.We used the shift in the Mo and U isotope composition of black shales that formed during OAE2 and T-OAE to quantify the expansion of seafloor anoxia during these events compared to modern times, combining data from this study (Weyer et al., 2008 and Archer and Vance, 2008) and applying mass balance constraints. According to our model, we obtained an enhancement in seafloor anoxia of up to about 60% during the OAEs, compared to 10% at present day (Fig. 3) which occurred on a global scale if assuming unrestricted connection of the sample localities to the world ocean. Such an increase translates to ~1-2.5% anoxic and/or euxinic environments during both OAEs.

According to our U isotope results, seafloor anoxia during the T-OAE may have been even more enhanced than during the OAE2, which is opposite in direccion to what is indicated by Mo isotope signatures. However, the U-isotope shift between OAE2 black shales and Black Sea black shales may represent a minimun shift, as water mass exchange of the modern locality to the open ocean is very limited (in contrast to Demerara Rise during OAE2; Erbacher et al., 2004). This may result in U isotope fractionation in the water column. Limited water mass exchange (possibly even more than that of the modern Black Sea; McArthur et al., 2009) may also have affected T-OAE samples, which may be indicated by the positive trend of U isotopes and U/Al. However, this correlation may also indicate mixing of authigenic enrichment of redox sensitive trace metals with those from a detrital component, which may affect U- slightly more than Mo isotope signatures

References:

Archer C. and Vance D. (2008) The isotopic signature of the global riverine molybdenum flux and anoxia in the ancient oceans. Nature Geoscience 1, 597-600.

Arnold G. L., Anbar A. D., Barling J. and Lyons T. W. (2004) Molybdenum isotope evidence for widespread anoxia in Mid-Proterozoic oceans. Science 304, 87-90.

Barling J., Arnold G. L. and Anbar A. D. (2001) Natural mass dependent variations in the isotope compositions of molybdenum. EPSL 193, 447-457.

Brumsack H. –J. (2006) Trace metal content of recent organic carbon-rich sediments: Implications for Cretaceous black shale formation. Palaeo3 232, 344-361.

Erbacher J., Friedrich O., Wilson P. A., Birch H. and Mutterlose J. (2005) Stable organic carbon isotope stratigraphy across oceanic anoxic event

2 of Demerara Rise, western tropical Atlantic. Geochemistry Geophysics Geosystems 6, doi: 10.1029/2004PA001102.
Hetzel A., Böttcher M. E., Wortmann U. G. and Brumsack H. –J. (2009) Paleo-redox conditions during OAE 2 reflected in Demerara Rise sediment geochemistry (ODP Leg 207). Palaeo3 273, 302-328.
McArthur J. M., Algeo T. J., van de Shootbrugge B., Li Q. and Howarth R. J. (2009) Basinal restriction, black shales, Re-Os dating and the Early Toarcian (Jurassic) Oceanic Anoxic Event. Paleoceanography (in press).
Montoya-Pino C., Weyer S., Anbar A. D., Pross J., Oschmann W., van de Schootbrugge B. and Arz H. W. Global enhancement of ocean anoxia during Oceanic Anoxic Event 2: A quantitative approach using U isotopes. Geology (in press).
Pearce C. R., Cohen A. S., Coe A. L. and Burton K. W. (2008) Molybdenum isotope evidence for global ocean anoxia couple with perturbations to the carbon cycle during the Early Jurassic. Geology 36, 231-234..
Poulson R. L., Siebert C., McManus J. and Berelson W. (2006) Authigenic molybdenum isotope signatures in marine sediments. Geology 34, 617-620.
Sageman B. B., Meyer S. R. and Arthur M. A. (2006) Orbital time scale and new C-isotope record for Cenomanian-Turonian boundary stratotype. Geology 34, 125-128.
Schlanger S. O. and Jenkyns H. C. (1976) Cretaceous oceanic anoxic event: Causes and consequences. Geol. Mijnb 55, 179-184.
Suan G., Pittet B., Bour I., Mattioli E. and Duarte L. V. (2008) Duration on the Early Toarcian carbon isotope excursion deduced from spectral analysis: consequence for its possible causes. EPSL. 267, 666-679.
Voigt S., Erbacher J., Mutterlose J., Weiss W., Westerhold T., Wiese F., Wilmsen M. and Wonik T. (2008) The Cenomanian-Turonian of the Wunstorf section – (North Germany): Global stratigraphic reference section and new orbital time scale for the Oceanic Anoxic Event 2. Newsletters on Stratigraphy 43, 65-89.
Weyer S., Anbar A. D., Gerdes A., Gordon G. W., Algeo T. J. and Boyle E. A. (2008) Natural fractionation of $^{238}U/^{235}U$. GCA 72, 345-359.

IODP

Sediment Pore Water Chemistry from the New Jersey Shallow Shelf: IODP Expedition 313

MICHAEL J MOTTL[1], TAKESHI HAYASHI[2], SUSANNE STADLER[3,4], EXPEDITION 313 SCIENCE PARTY[5]

[1]Department of Oceanography, University of Hawaii, 1000 Pope Road, Honolulu HI 96822, USA, mmottl@soest.hawaii.edu
[2]Akita University, Tegata-gakuen-mach; 1-1, Akita City, Akita 010-850 2, Japan, t.hayashi@ed.akita-u.ac.jp
[3]Leibniz Institute for Applied Geophysics (LIAG), Stilleweg 2, 30655 Hannover, Germany
[4]Federal Institute for Geoscienes and Natural Resources (BGR), Stilleweg 2, 30655 Hannover, Germany, susanne.stadler@bgr.de
[5]ECORD Science Operator, Edinburgh, United Kingdom

Three holes were drilled in May to July 2009, to depths of 640-757 mbsf on the continental shelf in 34-36 m of water, 45-65 km off the coast of New Jersey, to investigate sea-level change since the late Eocene. Core recovery was ~80%. Pore water was extracted from the cores onboard the drill rig using rhizons under negative pressure and by squeezing of whole rounds in a piston-cylinder apparatus. 223 pore water samples were analyzed onboard for salinity by refractive index, pH, alkalinity, and ammonia, and onshore at the University of Hawaii for chlorinity with a precision of 0.5%.

Alkalinity and ammonia generally increase with depth in the three holes, to 9-27 and 1-6 mM, respectively, while pH decreases to 7.3-6.8. Chlorinity varies widely, from 19 to 930 mM. All samples from shallower than 630 mbsf in Holes 27A and 28A, and shallower than 350 mbsf in Hole 29A, are fresher than seawater (~550 mM), and most are much fresher, <100 mM within depth intervals in all three holes. Below these depths chlorinity increases above that of seawater, especially in the deepest Hole 29A, in which it rises steadily to ~930 mM near the bottom of the hole, at 690-750 mbsf. These data from the shallow shelf can be interpreted in the context of samples recovered across the shelf by the USGS AMCOR Project in 1976 in water depths of 22-300 m, and by ODP Sites 902-906 and 1071-1073 on the outer shelf and slope in water depths of 89-2700 m. These holes have established that there is a large and persistent tongue of freshwater beneath the New Jersey shelf, at depths up to 500-1000 m at the coast. They have also recovered brines with increasing depth, all of which reach but do not exceed 900-1000 mM chlorinity, from 250 mbsf at Site 906 to 1113 mbsf at Site 903, all from the upper to mid-slope at 445 to 1113 m water depth. Our Hole 29A, at 36 m water depth, is the first to encounter such brines beneath the shallow shelf. The shape of the chlorinity profiles, with frequent large swings over narrow intervals, indicates that both freshwater and seawater are largely confined to specific beds within the shallow sediment, and that permeable sandy layers permit lateral flow of both types, i.e., one or the other in a given bed. At the deeper sites, deeper in the holes, the profiles indicate localized upwelling of brine through deep vertical fractures in the sediment prism.

In addition, reactive chemical species such as sulfate, alkalinity, and ammonium provide clear evidence of microbial reactions at multiple depths. Microbes appear to have been much more successful in reducing sulfate within the fresher water layers than within the saltier ones, in the process of oxidizing organic matter in the sediment.

IODP

Climatic variations in the mid-latitude North Atlantic during the last 5 Ma

B. DAVID A. NAAFS[1,2], JENS HEFTER[1], RÜDIGER STEIN[1] AND GERALD H. HAUG[2,3]

[1]Alfred Wegener Institute for Polar and Marine Research, Columbusstrasse, 27568 Bremerhaven, Germany
[2]Leibniz Center for Earth Surface and Climate Studies, Institute for Geosciences Potsdam University, 14476 Potsdam, Germany
[3]Geological Institute, Department of Earth Sciences, ETH-Zentrum, Zürich, Switzerland

Global climate has changed significantly during the last five Ma [Zachos et al., 2008]. During the Pliocene global temperatures were several degrees higher compared to the present, with most of this warming centered in the North Atlantic, and ice sheets were small [Dowsett et al., 2009; Haywood and Valdes, 2004; Robinson, 2009]. In the Late Pliocene global climate began to cool as the glaciation of the Northern Hemisphere intensified (INHG) and the Quarternary-style climate began. The North Atlantic region was of particular importance for the INHG because of its ability to transport heat to the higher latitudes by means of the North Atlantic Current (NAC), which would prevent widespread glaciation [Lunt et al., 2008].

Here we report results from IODP Site U1313, a re-drill of DSDP Site 607, located in the mid-latitude North Atlantic at 41 oN. Site U1313 is located directly under the influence of the NAC, which provides warm surface waters and forms the boundary between the high productivity regions in the northern North Atlantic and the oligothrophic regions of the subtropical gyre. Hence, variations in SST and surface water productivity at this site

reflect changes in the strength and position of the NAC. Using the alkenone biomarker we reconstructed orbitally resolved (± 4 ka resolution) records of sea surface temperatures (SST) and surface water productivity. Our results for the first time provide insights into the variations of the NAC over the last five Ma. We show that the INHG was accompanied by drastic changes in surface water characteristics in the mid-latitude North Atlantic. Before

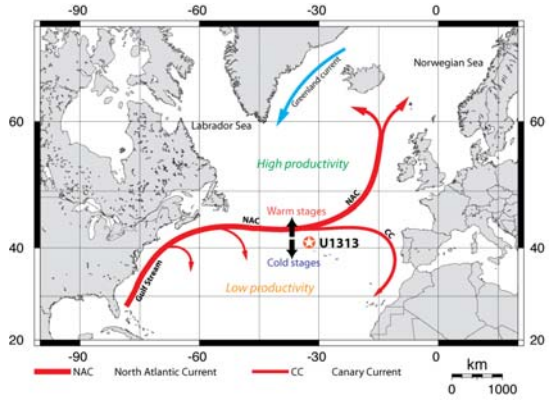

Fig 1; Map of the North Atlantic with the main surface currents. Nowadays, Site U1313 is located directly under the influence of the North Atlantic Current (NAC). The position and strength of the NAC varied between cold and warm stages, influencing surface water characteristics at our site.

the INHG, SST were up to 4 oC warmer and surface water productivity was low. During the INHG SST started to decrease. At the same time, surface water productivity increased during glacial periods as the nutrient availability increased. Following the INHG surface water characteristics varied on a glacial/interglacial basis. We interpret these changes to reflect a southward shift together with a weakening of the NAC during the INHG and following glacial periods. This decrease in heat being brought to the higher latitudes seems to have been critical for the development of the Quarternary-style climate.

References:
Dowsett, H. J., M. M. Robinson, and K. M. Foley (2009), Pliocene three-dimensional global ocean temperature reconstruction, *Clim. Past*, *5*(4), 769-783.
Haywood, A. M., and P. J. Valdes (2004), Modelling Pliocene warmth: contribution of atmosphere, oceans and cryosphere, *Earth and Planetary Science Letters*, *218*(3-4), 363-377.
Lunt, D. J., G. L. Foster, A. M. Haywood, and E. J. Stone (2008), Late Pliocene Greenland glaciation controlled by a decline in atmospheric CO2 levels, *Nature*, *454*(7208), 1102-1105.
Robinson, M. M. (2009), New quantitative evidence of extreme warmth in the Pliocene Arctic, *Stratigraphy*, *6*(4), 265-275.
Zachos, J. C., G. R. Dickens, and R. E. Zeebe (2008), An early Cenozoic perspective on greenhouse warming and carbon-cycle dynamics, *Nature*, *451*(7176), 279-283.

IODP

Interaction of Calcium with clay minerals and marine sediments

C. OCKERT[1], B.M.A TEICHERT[2], S. KAUFHOLD[3], N. GUSSONE[1]

[1]Institut für Mineralogie, Corrensstraße 24, 48149 Münster
[2]Institut für Geologie und Paläontologie, Corrensstraße 24, 48149 Münster
[3]Bundesanstalt für Geowissenschaften und Rohstoffe, Stilleweg 2, 30655 Hannover

Ca-isotope ratios of marine organic and inorganic mineral precipitates have been used to record changes in paleo-temperature, to monitor changes in the oceanic Ca-budget and as a proxy for the trophic level of organisms in the food chain (Zhu & Macdougall, 1998; Skulan et al., 1997). However, only little is known about processes that happen in marine porewaters which might have the potential to alter the primary Ca-isotope signature. Besides partial dissolution of calcareous fossils, diagenetic processes like release of organically bound Ca, ion exchange processes with clay minerals, Ca-complexation with carbonate or sulfate ions as well as Ca-release from altered volcanic material can introduce Ca into the porefluid and thus have the potential to affect the proxy signal of the respective archives.

The discovery of a correlation between ammonium and δ44/40Ca ratios in porewaters of the Cascadia accretionary margin (ODP Leg 204, Teichert et al., 2009) suggested a relationship between NH4+ and the release of isotopically light Ca into the porewater. A similar kind of relationship had been found by von Breymann et al. (1990) for Mg2+ and ammonium in marine porewaters and was attributed to interaction of the cations with sediment particles. While von Breymann et al. (1990) saw a correlation between Mg2+-concentration and NH4+-concentration, Teichert et al. (2009) could detect a correlation between ammonium concentration and Ca-isotope ratios, rather than Ca concentrations. This points to possible Ca-isotope fractionation as Ca is displaced from clay minerals by ammonium that is released during organic matter remineralization, while the Ca-concentration is influenced by other processes, like carbonate precipitation.

In order to approach Ca-fractionation mechanisms during adsorption and desorption to clay minerals laboratory experiments on well characterized clay minerals as well as analyses of natural porewaters from the North Atlantic were carried out.

Calcium exchange experiments on clay minerals

Since earlier findings suggested possible isotope fractionation of Ca during adsorption and desorption to clay minerals (Teichert et al., 2009), we conducted different adsorption and desorption experiments under controlled laboratory conditions.

One adsorption experiment was carried out at 21 °C and desorption experiments were carried out at three different temperatures (2, 6 and 21 °C) on a well characterized montmorillonite from Huancayo, Peru. As a desorbent for the desorption experiments Copper-triethylenetetramine (Cu-trien; Meier & Kahr, 1999; Kaufhold & Dohrmann, 2003), an organic complex which is known to remove all cations bound to the interlayer spaces in clay minerals, was employed. Two different experimental set-ups were designed for the desorption experiments: One was planned to release all Ca in one step (total Ca), while Ca was desorbed in 5 successive steps for the second experiment, in order to study incomplete desorption.

The adsorption experiment showed no evidence for Ca-isotope fractionation at 21 °C. In contrast, Ca-isotope fractionation of up to 0.3 ‰ (δ44/40Ca) was revealed for the step-wise desorption experiments and showed a temperature dependency. During the 6 °C experiment fractionation is evident with the first three steps releasing isotopically heavy Ca (1.43 ‰; SRM 915a) and the last

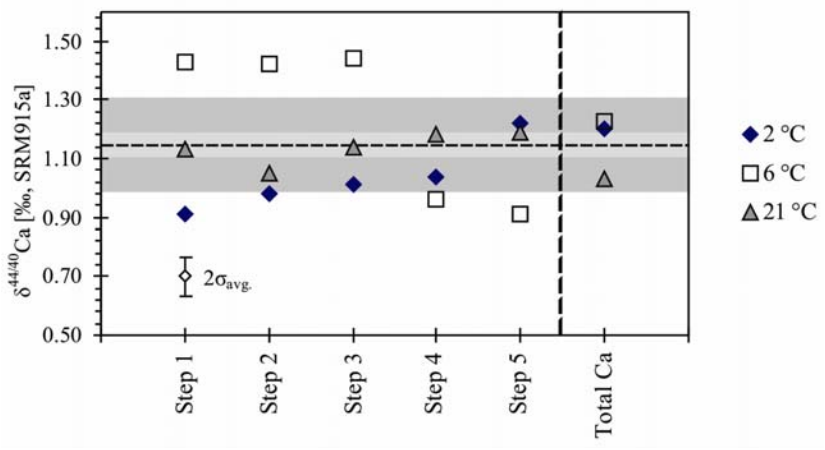

Fig. 1: Ca-isotope values of 5-step and total Ca-desorption experiments. Horizontal black dashed line: $\delta^{44/40}$Ca ratio of loaded $CaCl_2$; light grey boundaries: 2σ (±0.04) of measurement; dark grey boundaries: variation of ±0.16 implying a significant variation from $CaCl_2$.

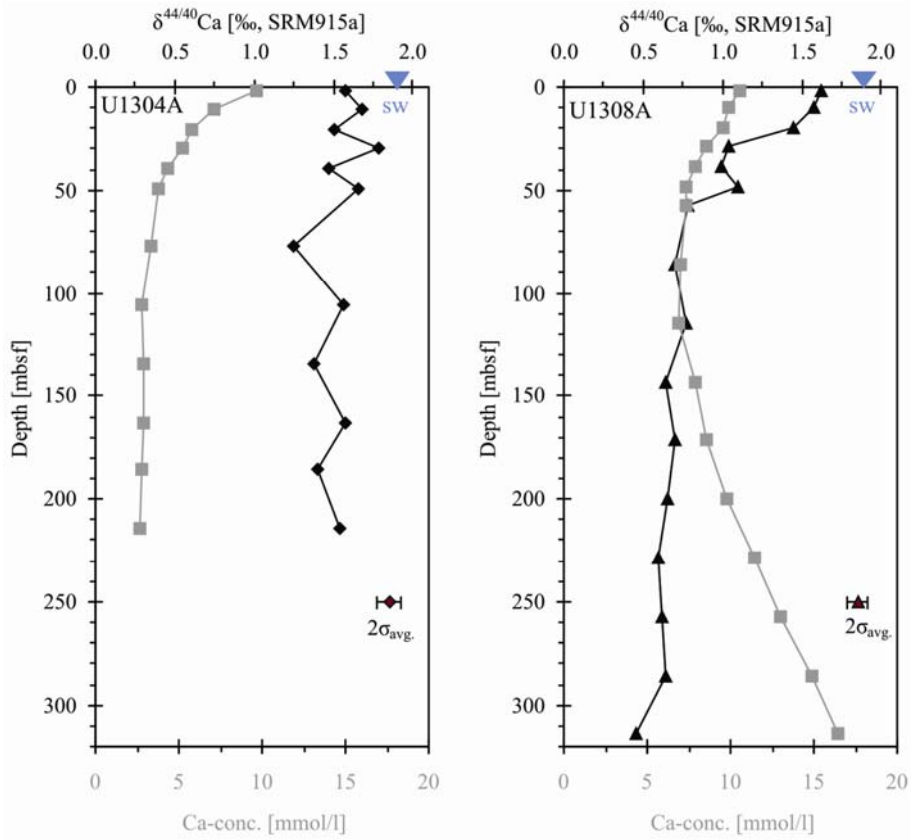

Fig. 2: Porewater profiles of Ca-concentration (Channell et al., 2006) and Ca-isotopic composition with depth for Sites U1304A and U1308A. Triangle indicates the $\delta^{44/40}$Ca of seawater (sw).

three steps releasing lighter Ca of about 0.95 ‰ (Fig. 1). Interestingly, the 2 °C experiment shows the reverse trend of increasing δ44/40Ca ratios with increasing step number. For the 21 °C experiment no significant isotope fractionation could be observed. The isotopic ratios for the total Ca-experiments correspond to the ratio measured for the Ca which was loaded onto the montmorillonite and thus display no fractionation effect (Fig. 1). These preliminary findings suggest that the step-wise desorption can cause a temperature dependent Ca-isotope fractionation, while Ca-adsorption does not show any fractionation. This has important implications for understanding processes in marine porewaters.

Calcium-isotopes in marine porewaters: With the newly gained insights on the ion exchange behavior of Ca, it is possible to better understand the natural occuring processes controlling Ca-isotope fractionation. Three Sites (U1304, U1306, U1308 from the North Atlantic sampled in 2004 during IODP Expedition 303 of Joides Resolution; Channel et al., 2006) with different lithology and porewater Ca-concentration development with depth, indicative of different diagenetic processes, were chosen for porewater

analyses. Ca-isotope analyses have been carried out on two sites already.

Sediments of Site U1304 are dominated by interbedded nannofossil ooze and diatom ooze (Channell et al., 2006). In the upper 100 mbsf (meters below sea floor) of the core a decrease of Ca from seawater concentration to lower concentration is evident. This low concentration remains approximately constant downcore (Fig. 2). Site U1308, on the other hand, reveals a lithology composed of mainly nannofossil ooze and minor silty clay. Here the Ca-concentration also decreases to a minimum in the upper 100 mbsf of the core and then increases to above sea water concentration (Fig. 2). The dissimilar Ca-concentration patterns for both Sites are also reflected in differing Ca-isotope ratio patterns with depth. The $\delta^{44/40}$Ca values for Site U1304 range around an average that is slightly lower than seawater and show only small excursions (Fig. 2). Data of Site U1308, however, demonstrate a trend from seawater-like to low (0.46 ‰) $\delta^{44/40}$Ca values (Fig. 2). This suggests a deep source of Ca either from $CaCO_3$ dissolution or from interaction with the basement. Sr-isotope data collected from the lowermost samples of Site U1308 identified the deep source of light Ca to be dissolution of marine biogenic $CaCO_3$. This finding is consistent with the Ca isotopic composition of biogenic marine carbonates of that age (Heuser et al., 2005).

For Site U1308 a striking negative correlation of NH_4^+-concentration and $\delta^{44/40}$Ca is evident, which supports the suggested interaction of Ca with clay minerals. During this interaction isotopically light Ca is displaced from sediment particle surfaces and interlayers by ammonium that is released during organic matter remineralization. For Site U1304 no strong correlation of ammonium and Ca isotope values is evident, although similar amounts of ammonium are present. According to these findings it can be proposed that the different behavior is caused by lithologic differences. At Site U1304, clay is almost absent and can therefore not provide light Ca through ion exchange. The data obtained in this study point to a global diagenetic process in siliciclastic, organic-bearing sediments where light Ca is released into the porewaters.

References:

Channell, J.E.T., Kanamatsu, T., Sato, T., Stein, R., Alvarez Zarikian, C.A., Malone, M.J., and the Expedition 303/306 Scientists (2006): Proceedings of the Integrated Ocean Drilling Program, 303/306: College Station TX (Integrated Ocean Drilling Program Management International, Inc.). doi:10.2204/iodp.proc.303306.2006

Heuser A., Eisenhauer, A., Böhm, F., Wallmann, K., Gussone, N., Pearson, P.N., Nägler, T.F., Dullo, W.-C. (2005): Calcium isotope (δ44/40Ca) variations of Neogene planktonic foraminifera. Paleoceanography 20(2). PA2013, doi:10.1029/2004PA001048,2005.

Kaufhold S. & Dohrmann R. (2003): Beyond the Methylene Blue Method: Determination of the Smectite Content using the Cutriene Method. Zeitschrift für Angewandte Geologie 2, 13-16.

Meier, L.P. & Kahr, G. (1999): Determination of the cation exchange capacity (CEC) of clay minerals using the complexes of copper (II) ion with triethylenetetramine and tetrahylenepentamine. Clays and Clay Minerals 47(3), 386-388.

Skulan, J., DePaolo D.J., and Owens T.L. (1997): Biological control of calcium isotopic abundances in the global calcium cycle. Geochimica et Cosmochimica Acta 61(12), 2505-2510.

Teichert, B.M.A., Gussone, N., Torres M.E. (2009): Controls on calcium isotope fractionation in sedimentary porewaters. Earth and Planetary Science Letters 279(3-4), 373-382.

von Breymann, M.T., Collier, R., Suess, E. (1990): Magnesium adsorption and ion exchange in marine sediments: a multi-component model. Geochimica et Cosmochimica Acta 54(12), 3295-3313.

Zhu, P. & Macdougall D. (1998): Calcium isotopes in the marine environment and the oceanic calcium cycle. Geochimica et Cosmochimica Acta 62(10), 1691-1698.

ICDP

Core processing procedures applied to the 106 m long lacustrine sediment record of Laguna Potrok Aike, Argentina (ICDP-project PASADO)

C. OHLENDORF[1], C. GEBHARDT[2], A. HAHN[1], P. KLIEM[1], B. ZOLITSCHKA[1] AND THE PASADO SCIENCE TEAM[3]

[1]Geopolar, Institute of Geography, University of Bremen, Germany (ohlen@uni-bremen.de)
[2]Alfred Wegener Institute for Polar and Marine Research, Bremerhaven, Germany
[3]PASADO Science Team as cited at: http://dc-app1-02.gfz-potsdam.de/site/contacts/contacts-search-all?select=3&term=pasado

Lake drilling in the framework of the ICDP project PASADO (Potrok Aike Maar Lake Sediment Archive Drilling Project) was carried out between September and late November 2008. From the maar lake Laguna Potrok Aike (52°S, 70°W; 116 m asl.; diameter: 3.5 km; water depth: 100 m) in southern Patagonia, Argentina, in total 510 m of lacustrine sediments have been recovered using the GLAD800 platform equipped with a CS-1500 drill rig. At two drillsites quadruplicate (site 1) and triplicate (site 2) cores down to a maximum depth of 101.5 m below lake floor have been recovered using mainly the hydraulic piston coring tool. Recovered core sections and core catcher samples were transferred to the shore-based fieldlab where first on-site measurements were done.

Owing to the great diversity of continental drilling projects, workflow in an ICDP deep drilling project seems to be much less standardised then is the case for IODP projects. For instance, according to our knowledge, PASADO was the first ICDP project where continuous subsamples were taken for the entire sediment sequence (106 m). Such an approach requires logistical preparations different from sub-sampling campaigns of cores drilled in the framework of most other projects. We therefore take this as an opportunity to present field and lab protocols that were applied during the PASADO drilling and subsampling campaigns. Sample handling begins already on-site as soon as the core is handed over from the drilling crew to the onboard scientists with cutting the core runs into sections and packaging the core catcher samples. For the latter, analysis in the on-site field lab included sample description, photography, smear slide preparation and the determination of water content, as well as producing a suspension and a HCl-extract in which conductivity, Ca^{2+}- and Cl^- concentration were measured. Core sections were weighted and magnetic susceptibility was logged.

For the off-site lab procedures it was important to design a workflow that accounts for the needs of all involved research groups. In 2009 all cores from Site 2 (southern part of the deep, central basin) and all except one core from Site 1 (central deep basin) were opened, described, documented by digital high resolution photography and scanned with different non-destructive techniques. Core scanning was performed at 5 mm resolution for all parameters and involved the following techniques: 1) color scanning with a handheld X-rite spectrometer, 2) magnetic susceptibility scanning with a Bartington MS2F-sensor, 3) XRF scanning and X-radiography with an ITRAX core scanner (COX analytical systems) and 4) p-wave velocity/transmission seismograms

and gamma ray absorption with a modified Geotek MSCL tool. Immediately after non-destructive scanning anaylses were finished, core halfs were covered with cling-film, vacuum sealed in tubular film and stored at 4°C to prevent drying and surface oxidation of sediments until sampling begun.

An essential task was to amalgamate all cores from one site to establish a composite profile that then could be sampled in consecutive steps. For Site 2, a 106.08 m long composite profile was composed based on visual core correlation and core scanning data. The working half of this composite profile was then sampled completely in consecutive 2 cm thick intervalls. Using an especially designed sampling device each sample was divided into 6 volumetric and one non-volumtric sub-samples during the sampling process, whereas smeared sediment close to the liner wall was discarded simultaneously. Subsamples were stored and processed according to the needs of the respective research groups. From the archive half a U-channel was taken, which is regarded as the archive sediment for the PASADO project, since only non-destructive rock- and paleomagnetic analyses will be performed on it. In the trench that was left behind from U-channel trepanning, samples for thin section preparation, grainsize analysis and micro magnetic properties were taken. Based on the core description and a detailed inspection during sampling 1) 18 samples of aquatic moss remains were sieved out for AMS 14C dating, 2) 16 samples of tephra layers were taken for geochemical fingerprinting and 3) a first identification of redeposited sediment sections was accomplished. According to first results from these samples, the sedimentary record from Laguna Potrok Aike reaches back to approx. 50 ky BP and exhibits contrasting lithologies downcore especially in the Pleistocene part of the record. First estimates indicate that up to 50% of the record consist of redeposited sediments.

Core series 1A, 1B and 1C from Site 1 were opened and sampled for rock- and paleomagnetic studies whereas core series 1D was reserved for OSL-dating. From the latter core series selected sections were split and sampled under red light. The sampled halves as well as the non-sampled archive halves were photographed digitally to assure 1) the exact positions of OSL samples and 2) the exact correlation with parallel cores from Site 1 and with the composite profile of Site 2. All not sampled core sections from 1D were then opened under red light. The archive half was immedeately sealed in black tubular film to conserve the possibility of later OSL sampling, whereas the working half was photographed digitally, vacuum sealed in tubular film and stored at 4°C. Through a thorough correlation of Site 1 cores with the Site 2 composite profile the OSL chronology will then be available for both sites.

IODP

Paleoclimatic drilling targets in the shelf canyon offshore Bangladesh using high-resolution seismostratigraphic records

L. PALAMENGHI[1,2,*], T. SCHWENK[1], H.-R. KUDRASS[3], C. FRANCE-LANORD[4], V. SPIEß[1]

[1]Department of Geosciences, University of Bremen, Klagenfurter Str. 28359 Bremen, Germany.

[2] Bremen International Graduate School for Marine Sciences (GLOMAR), University of Bremen, Leobener Straße, 28359 Bremen, Germany

[*] contact:lupala@uni–bremen.de

[3] MARUM — Center for Marine Environmental Sciences, University of Bremen, Leobener Straße, 28359 Bremen, Germany

[4]CRPG, Centre de Recherches Pe´trologiques et Ge´ochimiques, 15 rue Notre Dame des Pauvres, 54501 Vandoeuvre le`s Nancy, France.

The Swatch of No Ground (SoNG) is a canyon that deeply incises the Bengal shelf offshore Bangladesh and acts as a sediment trap in the source to sink system Himalaya–Bengal Basin–Bengal Fan (Fig. 1A). The suspended sediment flux in the order of one billion t/yr is thought to be equally distributed between the subaerial delta, the shallow subaqueous prodelta and the SoNG from where episodic turbidity currents feed the deep sea Bengal Fan (Goodbred and Kuehl, 1999; Curray et al., 2003; Schwenk et al., 2003). Despite the canyon is located 100 km west of the Ganges–Brahmaputra–Meghna river mouth, recent sedimentation rate estimated by 137Cs is 50 cm/yr at the head of the canyon decreasing to 15 cm/yr in 600 m water depth (Kudrass et al., 1998; Michels et al., 2003). The frequency and the trigger mechanism of the release of turbidity currents is unknown but according to the sedimentation rates and the efficient organic carbon burial found in the ODP Site 717, ODP Site 718 and cores from the surrounding of the active channel in the Bengal Fan (France Lanord and Derry, 1997; Galy et al., 2007), the canyon would be filled in around 1000 yr if there wouldn't be a constant drainage toward the Bengal Fan (Weber et al., 1997).

The sediment reaches the canyon through two main transport processes: (1) tidal currents generating low-salinity plumes during the monsoon rainy season and (2) tropical cyclones during pre and post monsoon causing resuspension plumes mobilized on the inner shelf (Kuehl et al., 1997; Michels et al., 1998). Additionally, high sediment load leads to an oversteepening of the flanks, which generates, together with excess pore pressure by gas, tectonic events and passage of tropical cyclones, frequent mass wasting processes from the flanks down to the canyon (Kottke et al., 2003). In general, the shelf including the canyon is highly influenced by the subduction of the Indian Plate to the north under the Eurasian Plate and to the east under the Burmese Plate, which is resulting in high and spatially variable subsidence rates creating accomodation space. Inland subsidence value varies from 4 to 1 mm/yr (Goodbred and Kuehl, 2000a) while offshore it ranges from 0,6 mm/yr (Wiedicke et al., 1998) to 0,4 mm/yr (Hübscher and Spiess, 2005).

Taken into account the enormous sedimentation rates for the last 50 years, the SoNG could be an outstanding ultra high-resolution archive of monsoon variability over different time scales including anthropogenic influences. The mechanisms driving the temporary or permanent storing vs sediment release toward deep sea could answer important questions on the offshore response to the Himalayas denudation and the sink of CO2 in the ocean. However, to use this potential archive it is necessary to understand first the filling architecture.

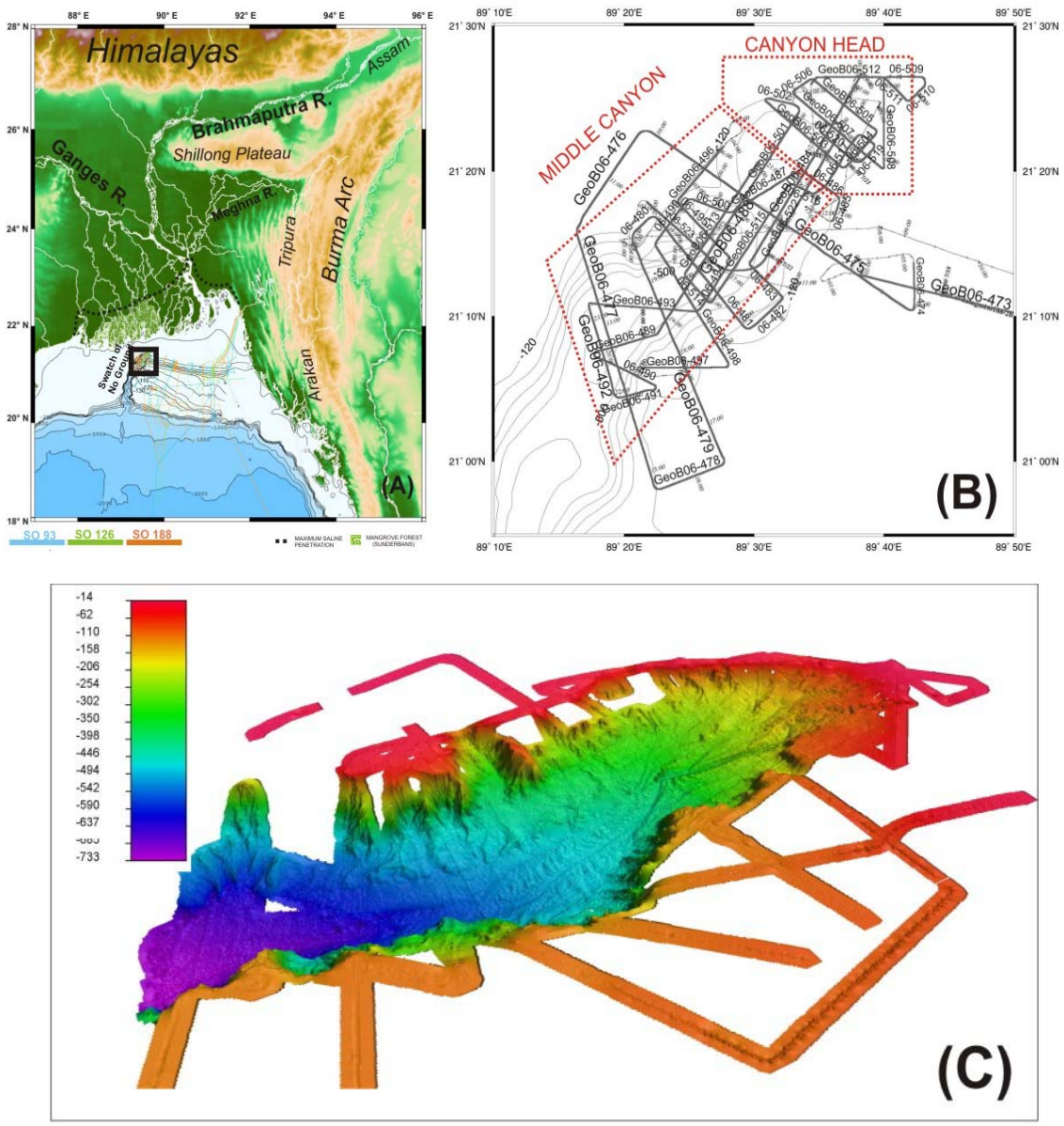

Fig. 1: (A) General map of the Bengal Basin, (B) location of the seismic survey at the head and middle canyon and (C) bathymetric chart from the eastern flank perspective.

High-resolution multichannel seismic data were collected in 2006 in the upper canyon with the German research vessel “Sonne” during cruise SO188-2 (Fig. 1B). Additionally, multibeam (Simrad EM120) and sediment echosounder (Parasound) data were gathered, together with gravity cores. Hydroacoustic data and cores collected on cruises in 1994 (SO93) and 1997 (SO 126) were compared with the new data set and consequently, some lines and stations were revisited to study the deposition within the last years.

At the head of the canyon the transition between topset deposits of the prodelta and canyon flanks is smooth and only deeply incised V-shaped channels are visible at the northern canyon rim. These incisions belong to a distributary system that possibly channelizes hyperpycnal flows deriving from the inner shelf to the main bottom channel that meanders on the canyon floor (Fig. 1C). Multichannel seismic profiles dipping the canyon axis present a vertical aggrading stacking with horizontal to sub-horizontal major horizons. Higher and lower amplitude reflections distribution seems to indicate a migration pathway of the main bottom channel.

Three major seismic facies are visible: stratified, wavy and chaotic (Fig. 2). Relatively undisturbed and stratified sequences around 100 m thick are mostly found in the upstream sections of the main bottom channel. A gravity core, collected during SO93 (96 KL) in a pocket like incision sampled the uppermost 15 m. It consists of interlayering of fine-grained laminated mud and coarse-grained graded silty to sandy layers. These graded layers closely correlate with the passages of the tropical cyclones crossing this region. The repetition of the core during the SO188 expedition (336 KL, 18.5 m) confirms the active sedimentation rate in the same order of magnitude for the last 12 yr. Analysing the new data collected in 2006, more promising locations with extended stratified sections compared to the location of Core 96 KL exists. Assuming constant sedimentation rates, such stratified sequences

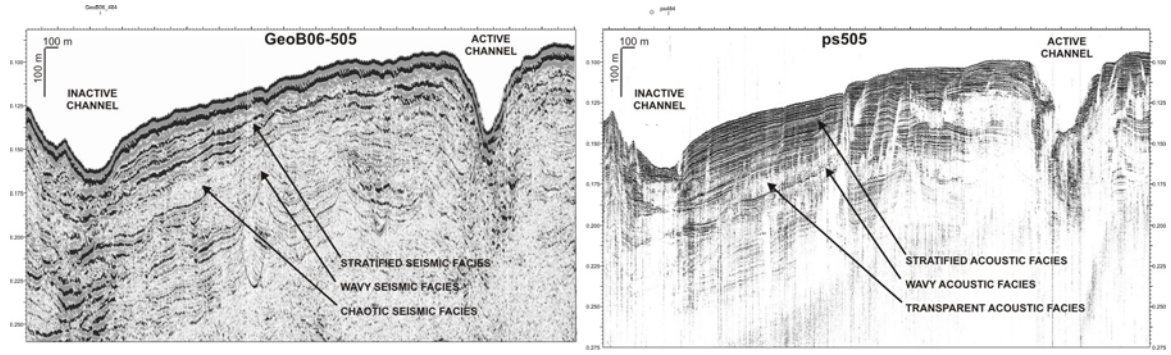

Fig. 2: Details of the seismic (left) and parasound (right) line GeoB06 505. See fig. 1B for profile location.

would cover 250-200 yrs making them a good target to identify changes of the cyclone frequency and additionally changes of the sedimentary regime produced by mankind activity.

Beside the stratified sediments, also wavy deposits are found at the surface and in the subsurface. They were previously interpreted as blocks deformed by slow moving rotational slides. The repetition of this acoustic facies in the subsurface and the proximal position to the bottom channel support also the hypothesis they are mud waves generated by spill over during the passage of the hyperpycnal flows. Chaotic seismic facies characterizes units of variable thicknesses from few to several metres and shape from lenticular to sheet-like. In the parasound records chaotic facies appears as acoustically transparent indicating an absence of internal structure caused by a homogenization. Acoustic transparent units are very frequent in the shelf region and are interpreted as liquefaction flow deposits. Further investigations are necessary to characterize more exactly what kind of processes are causing them in the SoNG.

Further south in the study area the canyon's thalweg is around 10 km wide and 300 to 700 m deep (see Fig. 1C). The canyon margin is frequently faulted and numerous gullies are incised. Blocks of sediments with chaotic seismic facies are found at the flanks foots representing individual mass wasting events there. As a first seismostratigraphic approach, some horizons can be traced further into the shelf and in particular the transgressive surface of erosion representing the flooding of the Bengal Shelf after Last Glacial Maximum can be identified in the canyon thalweg and used as first time marker.

In all seismic profiles two pronounced, nearly horizontal discontinuities are found at a depth 1000 and 1100 m. The thickness of the sedimentary sequence above ranges from 900 mbsf at the head of the canyon to 550 mbsf moving downward. The filling of the canyon above these unconformities shows sedimentary units characterized by different reflection amplitudes and seperated by unconformities. U-shaped channels 1-2 km wide may probably represent former channel pathways. Nevertheless well stratified, undisturbed sequences can be found especially in the southern part of the study area, beside all other features that indicate a complex deposition history in the canyon. If the two main discontinuities found in the canyon are rebounded to the sea surface by an average subsidence rate of 0.5 mm/yr, their age would fit into the early Pleistocene. If this rough estimation is realistic, the sequence has the potential of recovering the entire Quaternary environmental evolution of the Himalaya-Bengal Basin system.

Outlook:The main aim of this ongoing project is the understanding of the SoNG´s filling architecture to identify locations which are suitable to use this outstanding archive for drilling. Such a drilling could give new insights into the climate evolution of south east Asia with special emphasis on the anthropogenic impact. For this target, a careful analysis of all available data has to be carried out to decipher between the numereous processes affecting the deposition within this canyon, mainly sedimentary input, tectonics, and sea-level changes. On the other hand, by choosing the optimal coring sites, all these processes could be studied in detail. For example, the last glacial-interglacial cycle has been investigated on-shore and the most relevant emerging issues are that (1) an intensification of monsoon strength at early Holocene time corresponds to doubling of the transported sediments by the rivers (Goodbred and Kuehl, 2000a) and (2) the location of the river main flow and major estuarine or deltaic output migrated frequently and over great distances (Goodbred and Kuehl, 2000b; Allison et al., 2003). It is not precisely known if and when any river was ever directly coupled with the head of the canyon during low or high stands of sea level. Since this significantly affect the amount of the transported material into the canyon, the deposition history in the canyon can reveal not only informations about monsoonal development, but also about related transport processes and how it results in the constructution of continental margin. As mentioned above, another main issue within the deposition history in the canyon are mass wasting events. However, since mass wasting events needs both, a potentially unstable slope and a trigger, a seismo-stratigraphic classification of these events can be used to evaluate these factors. Unstable slopes are the result of high sediment accumulations rates, which in turns depend on the sediments input and thereby on the intensity of the monsoon. Potential triggers in this region are earthquakes and cyclones, therefore mass wasting deposits can be utilized as recorders of them.

To gather the targets of this project, available seismic and parasound data have been or will be processed to load them into an interpretation software. In order to identify possible drilling locations a careful seismic and acoustic analysis will be conducted. Seismostratigraphic studies, including tracing the major horizon from the canyon into the continental shelf, should give an idea about ages of the

different depositional units. Integrating results from onshore studies and from the deep-sea fan as well as using the present day conditions as analog for past reconstruction it will hopefully emerge a clearer picture of the sedimentary and transport processes that had exported the greatest flux of sediment to the ocean and built the greatest submarine fan on earth.

References:

ALLISON, M.A., KHAN, S.R., GOODBRED JR, S.L.., KUEHL, S.A., (2003). Stratigraphic evolution of the late Holocene Ganges–Brahmaputra lower delta plain. Sedimentary Geology 155 317–342.

CURRAY, J.R., EMMEL, F.J., MOORE, D.G., (2003). The Bengal Fan: morphology, geometry, stratigraphy, history and processes. Marine and Petroleum Geology 19, 1191–1223.

GALY, V., FRANCE-LANORD, C., BEYSSAC, O., FAURE, P., KUDRASS, H., PALHOL F., (2007). Efficient organic carbon burial in the Bengal fan sustained by the Himalayan erosional system. Nature Vol 450, 407-410.Goodbred and Kuehl, 1999;

GOODBRED JR., S.L., KUEHL, S.A., (1999). Holocene and modern sediment budgets for Ganges–Brahmaputra river: evidence for highstand dispersal to floodplain, shelf, and deep-sea depocenters. Geology 27, 559–562.

GOODBRED, S.L., KUEHL, S.A., (2000a). Late Quaternary evolution of the Ganges–Brahmaputra River delta: significance of high sediment discharge and tectonic processes on margin sequence development. Sedimentary Geology 133, 227– 248.

GOODBRED, S.L., KUEHL, S.A., (2000b). Enormous Ganges–Brahmaputra sediment load during strengthened early Holocene monsoon. Geology 28,1083-1086.

HUBSCHER, C., SPIEß V., (2005). Forced regression systems tracts on the Bengal Shelf. Marine Geology 219, 207–218.

KOTTKE, B., T. SCHWENK, M. BREITZKE, M. WIEDICKE, H.R. KUDRASS, and V. SPIESS (2003) Acoustic Facies and Depositional Processes in the Upper Submarine Canyon Swatch of No Ground (Bay of Bengal). Deep-Sea Research II, 50, 979-1001.

KUEHL, S.A., LEVY, B.M., MOORE, W.S., ALLISON, M.A., (1997). Subaqueous delta of the Ganges–Brahmaputra river system. Marine Geology 144, 81–96.

KUDRASS, H.R., MICHELS, K.H., WIEDICKE, M., SUCKOW, A., (1998). Cyclones and tides as feeders of a submarine canyon off Bangladesh. Geology 26, 715–718.

MICHELS, K.H., KUDRASS, H.R., HUBSCHER, C., SUCKOW, A., WIEDICKE, M., (1998). The submarine delta of the Ganges–Brahmaputra: cyclone-dominated sedimentation patterns. Marine Geology 149, 133–154.

MICHELS, K.H., SUCKOW, A., BREITZKE, M., KUDRASS, H.R., KOTTKE, B., (2003). Sediment transport in the shelf canyon ''Swatch of No Ground'' (Bay of Bengal). Deep-Sea Research II 50, 1003–1022.

SCHWENK, T., SPIEß, V., HÜBSCHER, C. AND BREITZKE, M., (2003). Frequent channel avulsions within the active channel-levee system of the middle Bengal Fan - an exeptional channel-levee development derived from Parasound and Hydrosweep data. Deep Sea Research II, 50(5): 1023-1045.

WEBER, M. E., WIEDICKE, M. H., KUDRASS, H. R., HÜBSCHER, C. & ERLENKEUSER, H., (1997). Active growth of the Bengal Fan during sea-level rise and highstand. Geology 25, 315–318.

WIEDECKE, M., KUDRASS, H. R., HÜBSCHER, C., 1999. Oolitic beach barriers of the last glacial sea-level lowstand at the outer Bengal shelf. Marine Geology 157, 7–18.

ICDP

Environmental History of Lago Petén Itzá, Guatemala during the Deglacial and Last Glacial Maximum

L. PEREZ[1], J. LORENSCHAT[1], M. BRENNER[2], B. SCHARF[1], A. SCHWALB[1]

[1]Institut für Umweltgeologie, Technische Universität Braunschweig, Langer Kamp 19c, 38106, Braunschweig, Germany

[2]Department of Geological Sciences & Land Use and Environmental Change Institute, University of Florida, Gainesville, Florida, 32611, USA

We present late Glacial climate and environmental reconstructions using non-marine ostracodes (microscopic bivalved crustaceans called "mussel-shrimps") in sediments from Lago Petén Itzá, Guatemala. Ostracodes are sensitive to changes in lake variables conductivity, pH, temperature, aquatic macrophyte cover, energy environment, water depth and sediment type. They are therefore excellent bioindicators. Holocene oxygen isotope records from ostracode valves provided evidence that the terminal Classic Maya collapse in the 9th Century AD was tempotrally correlated with drought in the lowland Neotropics (Hodell et al. 1995). Little, however, is known about the ecology of ostracodes from the Yucatán Peninsula. We collected modern ostracodes and limnological information to better understand the ecological factors that determine species relative abundance in water bodies on the peninsula. Our objective was to develop a calibration data set that would permit interpretation of fossil ostracode assemblages in Lago Petén Itzá sediment cores. Lago Petén Itzá has a surface area of ~100 km^2 and lies at ~110 m asl. It is the deepest lake on the Yucatán Peninsula, with a maximum depth of 165 m (Fig. 1, Pérez et al. 2010a). Sediment cores taken as part of an International Continental Scientific Drilling

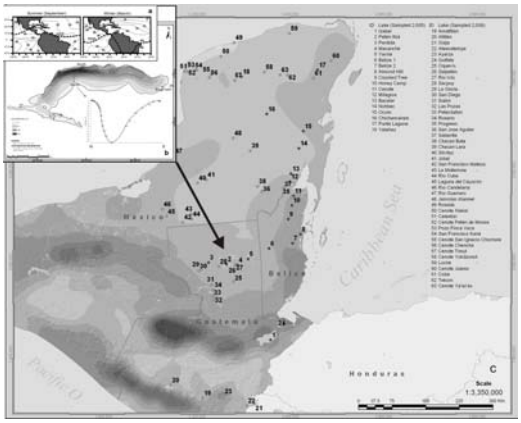

Fig. 1: (a) Position of the Intertropical Convergence Zone (ITCZ) over South America, (b) Lago Petén Itzá, northern Guatemala, and (c) aquatic systems sampled across the Yucatán Peninsula.

Program project penetrated to a maximum of ~133.2 m below lake floor (> 200 ka).

Our calibration data set includes information from 63 aquatic environments (i.e. freshwater and saline lagoons, lakes, ponds, rivers and sinkholes) sampled across the precipitation gradient on the Yucatán Península from the dry region in the northwest to the wetter areas to the east and south (Petén) (Fig. 1c). We analyzed the geochemistry of surface sediments and the physico-chemical properties of the waters.

Multivariate statistics (Canonical Correspondence Analysis, CCA) were used to calibrate ostracode occurrence and environmental factors. The main factors that best explain the ostracode species distribution are conductivity and water depth (Figs. 2 and 3). We found a total of 30 living ostracode species distributed in the Yucatán Peninsula. Most of the species have a Neotropical distribution, a few possess a Nearctic range, and others display a worldwide distribution. The ostracode fauna is composed of freshwater and brackish water species. The ordination diagram displays species assemblages typical of the highlands (Pérez et al. 2010b), lowlands and aquatic

environments close to the coast (Fig. 2). The fauna of the Yucatán Peninsula coast is similar to the fauna of southwestern Florida, suggesting that both environments

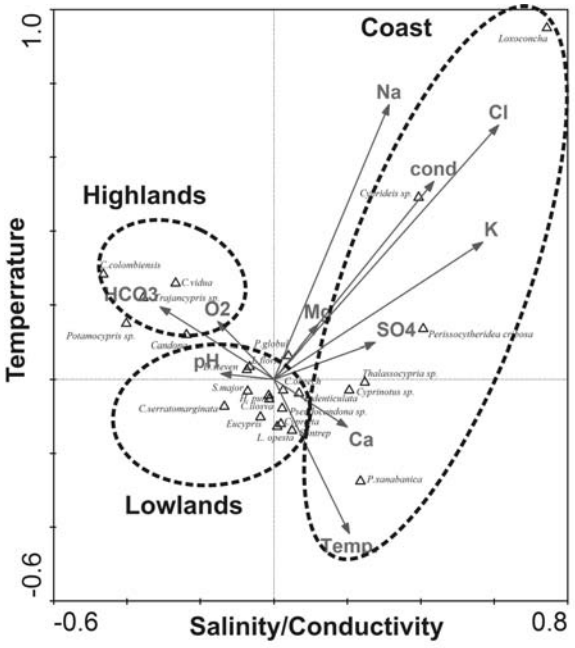

Fig. 2: Canonical Correspondence Analysis of non-marine ostracode species and 63 aquatic environments in the lowlands, highlands, and coast of the Yucatán Peninsula. Conductivity is the main variable that influences ostracode distribution.

display similar environmental conditions, e.g. vegetation and seasonal precipitation.

Twenty-seven surface sediment samples collected across a N-S water-depth transect in Lago Petén Itzá provide information about the ecological preferences and spatial distribution of ostracodes (Pérez et al. 2010a).

We found eleven extant species in the lake (Pérez et al. 2010c). A cluster analysis (Fig. 3) revealed three water depth ranges in Lago Petén Itzá important to ostracode distribution: 1) littoral zone (0.1-3 m), 2) water depths from the base of the littoral zone to the base of the thermocline (3-40 m), and 3) water depths below the thermocline (40-160 m, Pérez et al. 2010a).

Fossil ostracode assemblages were selected from a 70-m-long, PI-6 (Fig. 4), retrieved from a water depth of 71 m. Age at the core base is approximately 85 ka,. The LGM (~23-18 ka) was characterized by a lake level of ~50 m at the coring site, low ostracode species richness (4 spp.), periods of low ostracode abundance (2-188 valves/g dry), and core depths without ostracodes (22.34-22.75 and 24.91 m). This period was also characterized by the presence of an ostracode species indicative of deep waters (Physocypria globula) and clay-rich sediments. The Deglacial (~18-10 ka) was characterized by lake levels <20 m at the core site, higher ostracode species richness (6 spp.) and abundances (385 valves/g dry), sediments rich in gypsum sands, and presence of shallow-water and littoral-zone indicators such as Heterocypris punctata and Strandesia intrepida. Our results suggest that climate was cold and wet during the LGM, and dry and warm during the Deglacial. This is consistent with results from lithologic and seismic studies (Müller et al. in press [2010]), and

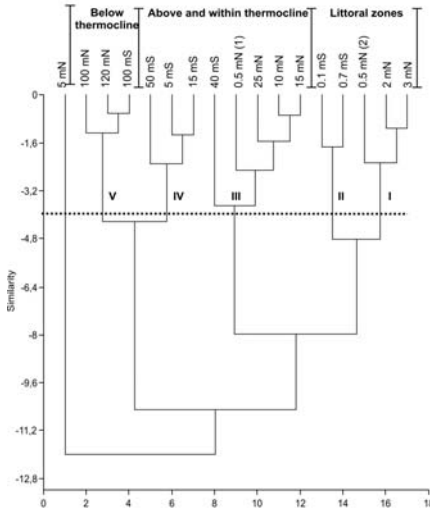

Fig. 3: Cluster analysis of ostracode species and 27 surface sediment samples collected at different water depths in Lago Petén Itzá, Guatemala showing the three water depth ranges of importance to ostracode distribution.

pollen records (Bush et al. 2009). Ostracodes provide important additional information that cannot be inferred from other bioindicators. For example, ostracode taphonomy and adult/juvenile ratios shed light on the energy of the environment. LGM sediments possess mostly ostracode broken valves, resulting from erosion and transport, suggesting increased precipitation and higher lake levels. Whereas diatoms and chironomid remains are absent in many parts of the studied record, ostracodes are present throughout, enabling reconstruction of a continuous record of lake conductivity and water depth for the Deglacial and LGM. This highlights the importance of multi-proxy paleolimnological studies.

References:

Bush, M. B., A. Correa-Metrio, D. A Hodell, M. Brenner, F. S. Anselmetti, D. Ariztegui, A. D. Müller, J. H. Curtis, D. Grzesik, C. Burton & A. Gilli. 2009. Re-evaluation of climate change in Lowland Central America during the Last Glacial Maximum using new sediment cores from Lake Petén Itzá, Guatemala. 113-128 In: F. Vimeux et al. (eds.). Past Climate Variability in South America and Surrounding Regions. Vol 14. Developments in Paleoenvironmental Research.

Hodell, D.A., J.H. Curtis & M. Brenner. 1995. Possible role of climate in the collapse of Classic Maya civilization. Nature, 375:391-394.

Müller, A. D., F. S. Anselmetti, D. Ariztegui, M. Brenner, D. A. Hodell, J. H. Curtis, J. Escobar, A. Gilli, D. A. Grzesik, T. P. Guilderson, S. Kutterolf & M. L. Plötze. In press [2010]. Late Quaternary Paleoenvironment of Northern Guatemala: Evidence from Deep Drill Cores and Seismic Stratigraphy of Lake Petén Itzá. Sedimentology (accepted).

Pérez, L., J. Lorenschat, M. Brenner, B. Scharf & A. Schwalb. 2010a. Distribution, diversity and ecology of modern freshwater ostracodes (Crustacea), and hydrochemical characteristics of Lago Petén Itzá, Guatemala. Journal of Limnology 69 (1).

Pérez, L, J. Lorenschat, M. Brenner, B. Scharf & A. Schwalb. 2010b. Non-marine ostracodes (Crustacea) of Guatemala. In: Enio Cano (ed.) Biodiversidad de Guatemala (Tomo 2).(accepted).

Pérez, L., J. Lorenschat, M. Brenner, B. Scharf &A. Schwalb 2010c. Modern freshwater ostracodes (Crustacea: Ostracoda) from Lago Petén Itzá, Guatemala. Revista de Biología Tropical (accepted).

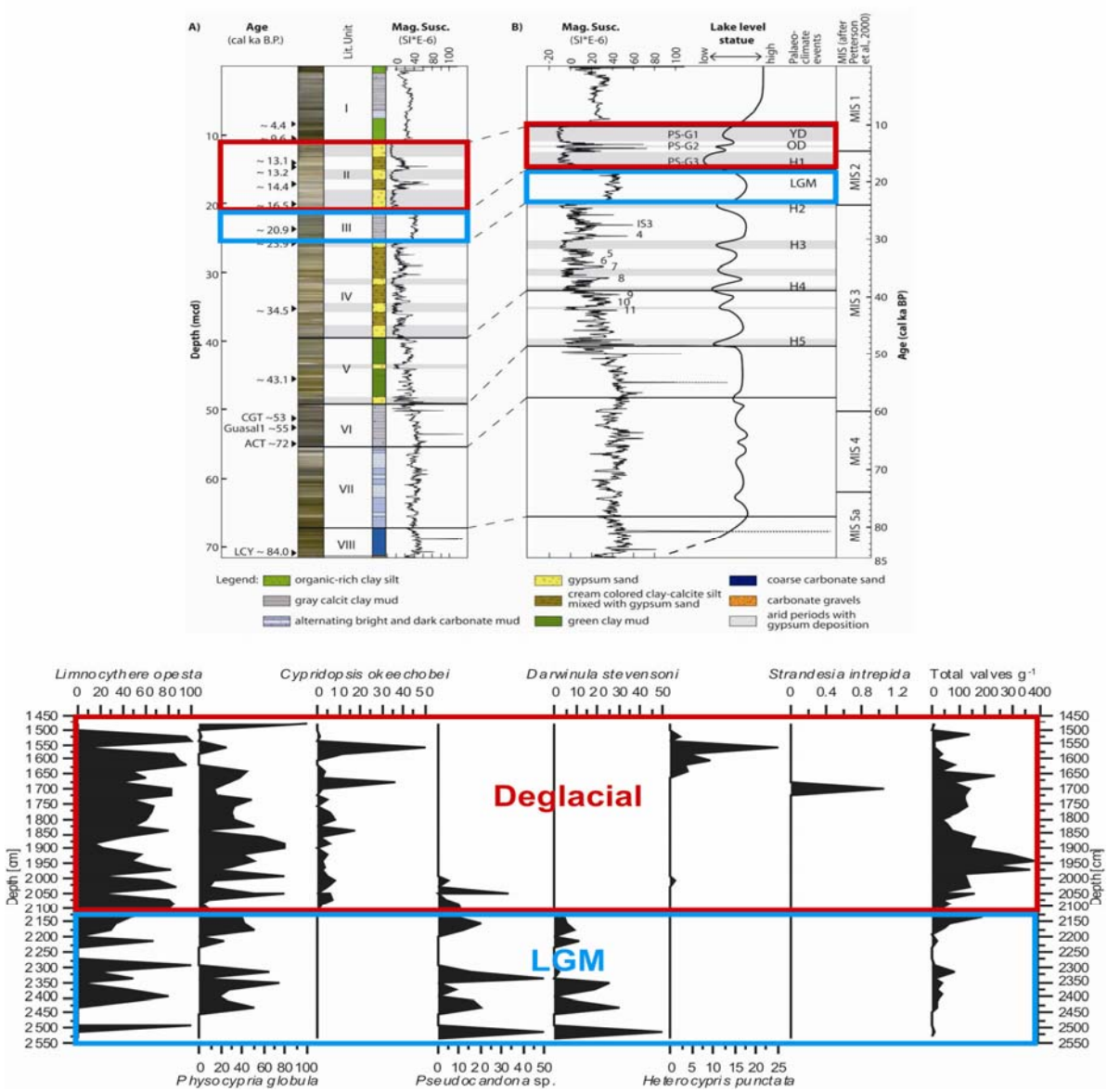

Fig. 4: Long core PI-6 retrieved at a water depth of 71 m from Lago Petén Itzá (modified from Müller et al. 2009), Guatemala and ostracode species assemblages from the Last Glacial Maximum and Deglacial.

IODP

Fluid flow systems offshore Costa Rica revealed by 2-D seismic MCS data (IODP proposal 633)

L. PLANERT[1], D. KLÄSCHEN[1], C. BERNDT[1], W. BRÜCKMANN[1], C. HENSEN[1]

[1]IFM-GEOMAR, Leibniz-Institut für Meereswissenschaften an der Universität Kiel, Wischhofstr. 1-3, D-24148 Kiel.

Quantification of the global carbon and water cycle requires improved understanding of complex forearc dewatering processes of erosive subduction zone systems. The same processes are furthermore pertinent to the functioning of seismogenic zones in erosive subduction settings. Such processes can be best studied at seafloor mounds which are related to mud diapirism/volcanism and precipitation of authigenic carbonates, and at large-scale slides related to the subduction of seamounts. These areas are windows to the deep parts of the subduction zones as they are cold seeps where fluids from different depths of the subduction zone system get expelled into the water column and can be sampled.

Because of their size and high fluid expulsion rates Mound Culebra and Mounds 11&12 on the Pacific continental margin of Costa Rica, are targets for fluid sampling proposed in IODP drilling proposal 633-Full2. Analysis of 2-D MCS seismic data across these mounds constrains the architecture and formation mechanisms of mound structures and provides information on how the ascending fluids interact with gas hydrate formation and dissociation.

The conditions for the formation of mounds at the erosive margin off Costa Rica seem to be fundamentally different from those described for many accretionary prisms and passive margin settings. This is attributed, in this area, to a lack of high sedimentation rates, which are generally assumed as a pre-requisite for the generation of

overpressured mud. Geochemical analyses of methane hydrate and chloride anomalies as well as heat flow modeling of the mounds indicate deeply sourced fluids discharged by clay dehydration at the decollement [Hensen et al., 2004; Grevemeyer et al., 2004; Schmidt et al., 2005]. At Mounds 11&12, an observed preferred NW-SE orientation on the scale of individual carbonate outcrops [Klaucke et al., 2008] as well as of both mounds coincides with the observed general slope-parallel trend of normal faulting at the Costa Rica margin [Hensen et al., 2004]. Hence, the fracture porosity of faults which extend through the overriding plate and provide the paths for fluids liberated by early dehydration reactions from the plate boundary appears to dominate the hydrogeological system and may also control the long-term tectonics at erosive margins, e.g. the onset of seismogenic behaviour [Ranero et al., 2008].

In order to test the hypothesis of deeply sourced and fault-controlled dewatering sites and to better understand the interactions between gas hydrate formation and dissociation with fluid ascent from deep sources, new pre-site survey seismic profiles were acquired using the 36-gun four-string linear gun array of R/V Marcus Langseth, and a 240-channel streamer comprising 3000 m of active length. MCS seismic data processing included cmp crooked line binning with 6.25 m, bandpass filtering 4/8-180/240 Hz, resampling from 0.5 ms to 2 ms, spherical divergence correction using the smoothed depth migration velocity field, and a shot gather consistent predictive deconvolution. The seismic lines were prestack depth migrated, in which the velocity model is iteratively improved from top to bottom using depth focussing analysis and residual moveout correction on common image point gathers. Additionally, a true amplitude prestack time migration was applied to the data.

Data processing and analysis of the uppermost portions of the subsurface beneath BSR depths reveal an upbending of the bottom-simulating reflection (BSR) towards the mounds and an absence of the reflection in the area of the fluid conduit, which may indicate a build-up of free gas within the gas hydrate stability zone, probably due to increased fluid flow and associated hydrate dissociation [Wood et al., 2002]. Improvement of the deep imaging currently involves multiple attenuation (radon transformation, wavefield extrapolation methods) and detailed velocity analysis for the lower sedimentary portions and beneath the basement. We are investigating the role of the acoustic basement for the fluid ascent and the location of fault structures with respect to surface features. The selected mound sites are both related to deep-reaching fault systems, corroborating preliminary estimates of the source depth of fluids and extruded material. In addition, the new seismic data shows differences in terms of the mounds' activity and stage of development.

References:

Grevemeyer I., Kopf A., Fekete N., Kaul N., Villinger H., Heesemann M., Wallmann K., Spiess V., Gennerich H.-H., Müller M., and Weinrebe W., (2004), Fluid flow through active mud dome Mound Culebra offshore Nicoya Peninsula, Costa Rica: evidence from heat flow surveying. Mar. Geol. 207, 145-157.

Hensen C., Wallmann K., M S., Ranero C. R., and Suess E (.2004), Fluid expulsion related to mud extrusion off Costa Rica - a window to the subducting slab. Geology 32(3), 201-204.

Klaucke, I., Masson, D.G., Petersen, C.J., Weinrebe, W., Ranero, C.R., (2008), Multifrequency geoacoustic imaging of fluid escape structures offshore Costa Rica: Implications for the quantification of seep processes. Geochem. Geophys. Geosyst., 9, Q04010, doi:10.1029/2007/GC001708.

Ranero, C. R., Grevemeyer, I., Sahling, H., Barckhausen, U., Hensen, C., Wallmann, K., Weinrebe, W., Vannucchi, P., von Huene, R., McIntosh, K. (2008), Hydrogeological system of erosional convergent margins and its influence on tectonics and interplate seismogenesis. Geochem. Geophys. Geosyst., 9, Q03S04, doi:10.1029/2007/GC001679.

Schmidt M., Hensen C., Mörz T., Müller C., Grevemeyer I., Wallmann K., Mau S., and Kaul N. (2005), Methane hydrate accumulation in "Mound 11" mud volcano, Costa Rica forearc. Mar. Geol. 216, 83-100.

Wood W.T., Gettrust, J.F., Chapman, N.R., Spence, G.D., Hyndman, R.D. (2002), Decreased stability of methane hydrates in marine sediments owing to phase-boundary roughness. Nature, 420, 656-660

IODP

Clay mineral alteration of Cretaceous sediments intruded by volcanic sills, ODP Site 1276, Newfoundland Margin

T. PLETSCH[1], R. PETSCHICK[2]

[1]Bundesanstalt für Geowissenschaften und Rohstoffe, Stilleweg 2, 30655 Hannover

[2]Institut für Geowissenschaften, Goethe-Universität Frankfurt, Altenhöferallee 1, 60438 Frankfurt am Main

Situated at the toe of the SE facing Newfoundland Margin, ODP Hole 1276A provided access to more than six hundred metres of mid-Cretaceous, deep-marine, organic-rich mudstones with intercalated mass flow deposits (Shipboard Scientific Party, 2004). A 10 meter basaltic sill with a radiometric age around 105 Ma (Hart & Blusztajn, 2006) was recovered at 1612 metres below the seafloor (mbsf), intercalated with upper Aptian to lower Albian (105 - 113 Ma) mudstones. Another sill, approximately 20 metres thick and recovered some 100 metres deeper in the section, is 8 M.y. younger than the upper sill. Metamorphosed sediments with metamorphic minerals, porphyroblastic textures and mineralised veins were recovered from the upper contact zone (66 cm) of the upper sill. Further away from this narrow contact zone, thermal alteration of the sediment cannot be detected visibly, but is recorded as an aureole of several metres thickness that is characterised by its unusual organic maturity and mineral composition. Similar aureoles with variable thicknesses occur at the other sill contacts, wereas the immediate contact metamorphic zones were not or incompletely recovered. To investigate the effect of intrusive heating on the adjacent sediments we studied the mineral composition of the bulk sediment and the separated clay size-fraction from these thermal aureoles using X-ray diffraction.

Clay mineral assemblages between 1100 and 1500 metres (i.e. 100 – 500 m above the upper sill) are dominated by smectite and irregular illite-smectite (IS) mixed-layer minerals which, together, comprise about 80% of the clay fraction. The composition of these assemblages is interpreted to result from the depositional input without major recognisable clay mineral alteration. Smectite percentages rapidly drop downhole from around 60% to zero, between 1500 – 1550 mbsf whereas the concentrations of mixed-layer minerals, including regular and irregular IS increase from 10-20 to 40-60%. This is a common feature in shaly lithologies which is thought to result from the transformation of original smectite into the mixed-layer clay minerals and often occurs in a palaeo-temperature range from 60° – 100°C. Organic maturity indicators corroborate this temperature range (Pross et al.,

2007). It is not clear to what extent this abrupt transition in clay minerals is governed by a) illitization of smectite intermediate layers engendered by downward increasing potassium concentration of the fine-grained sediments, or b) changing primary sediment composition.

From about 3 – 0.3 m distance to the upper sill, the IS mixed-layer mineral and illite concentrations decreases down to zero, but chlorite-smectite (CS) mixed-layer mineral concentration, a trace ingredient in the section above, become more abundant and co-occur with chlorite. Within the contact metamorphic zone, however,, the bulk of the clay size-fraction (80 – 95%) is made up of kaolinite. This mineral likely formed in relation to low-pH solutions produced by the interaction of the sill with the organic-rich host sediment. Clay mineral assemblages return to IS mixed-layer dominated compositions shortly beneath the upper sill. The reduced thickness of the lower clay mineral alteration aureole is in line with a narrower aureole suggested by organic maturity and is thought to result from incomplete recovery of this contact. Nontronite (an iron-rich smectite) is unusually abundant in one sample from the lower aureole of the upper sill, where it co-occurs with abundant chlorite. This assemblage was probably formed by the alteration of minor apophyses from the overlying sill. Ion-enrichment within this interval was likely favoured by the sealing effect of the sill.

The mineral alteration aureole of the lower sill is more extensive: its upper boundary lies between 26 – 12 m above the recovered lower sill contact and is characterised by the disappearance of IS mixed-layer minerals and illite, and by the concurrent increase in chlorite and CS mixed-layer minerals, much in the way as it was observed above the upper sill. As in the contact zones of the upper sill, porosity is reduced by intensive silicate mineral growth and carbonate cementation adjacent to the lower sill.

Strikingly, however, the organic maturity indicators (vitrinite reflectance, Rock-Eval Tmax) do not correspond with the trend seen in mineral alteration. Maturity reaches a minimum around 34 m where clay mineral assemblages would indicate substantial alteration This discrepancy may be related to the unusually elevated porosity: Whereas overlying sediment was compacted to a porosity around 20%, porosity values of 30% – 44% were retained in an interval between the two sills. Pore-water overpressure may have delayed the maturation of organic matter whereas mineral transformation was probably favoured by the supply of ions form alteration of the underlying sill through the open pore framework. The poorly compacted, high-porosity sediments between the two sills yielded elevated concentrations of gaseous hydrocarbons that were likely generated at the lower sill contact or in the underlying sedimentary section. The intercalation of undercompacted sediments with the igneous sills creates a high-amplitude seismic reflector that was previously attributed to a basinwide unconformity ("U" reflector; Tucholke et al., 1989) and mapped over large parts of the Newfoundland Basin. Given the regionally extent of igneous intrusions in the Newfoundland Basin, we expect that sills emplacement and cementation of their aureoles created vertically stacked and large low-permeability barriers to the upward migration of hydrocarbons.

References:

Hart, A.D. & Blusztajn, J., 2006. Age and geochemistry of the mafic sills, ODP site 1276, Newfoundland margin. Chem. Geol. 235: 222–237.

Pross, J., Pletsch, T., Shillington, D.J., Ligouis, B., Schellenberg, F. & Kus, J., 2007. Thermal alteration of terrestrial palynomorphs in mid-Cretaceous organic-rich mudstones intruded by an igneous sill (Newfoundland Margin, ODP Hole 1276A). Int. J. Coal Geol. 70: 277-291.

Tucholke, B.E., Austin, J.A.J. & Uchupi, E., 1989. Crustal structure and rift-Drift evolution of the Newfoundland Basin. In: Tankard, A.J. and Balkwill, H.R. (Eds): Extensional Tectonics and Stratigraphy of the North Atlantic Margins. AAPG Mem. 46: 247-263.

Tucholke, B.E. et al. (Eds), 2004. Proc. ODP, Init. Rept., 210, College Station TX (Ocean Drilling Program).

IODP

Isotope Signature of calcareous Organisms from upper and Lower carbonate mound sediments

J. RADDATZ[1], W.-CHR DULLO[1], V. LIEBETRAU[1], A. RÜGGEBERG[1,2], A. EISENHAUER[1]

[1]IFM-GEOMAR Leibniz-Institute of Marine Sciences, Wischhofstrasse 1–3, D-24148 Kiel, Germany.
[2]Renard Centre of Marine Geology, Ghent University, Krijgslaan 281, S8, B-9000Gent, Belgium

The project ISOLDE (Isotope Signature of calcareous Organisms from upper and Lower carbonate mounD sEdiments) started in June 2008. The overall focus of the project is the study of carbonate mound development off Europe with special focus on the initiation of mound growth. Further aspects concern the "switch-on" and "switch-off" mechanisms leading to interruptions of carbonate mound growth.

The Integrated Ocean Drilling Program Expedition 307 sailed in 2005 to the Porcupine Seabight in order to investigate for the first time sediments from the base of a giant carbonate mound (155 m, Challenger mound, Fig. 1). First results indicate that initiation and start-up phase of this carbonate mound coincides with the beginning of the Northern Hemisphere Glaciation (NHG) at ~2.7 Ma. Further carbonate mound development seems to be strongly dependent on rapid changes in paleoceanographic and climatic conditions at the Pliocene-Pleistocene boundary, especially characterized and caused by intermediate water masses.

The aim of our investigations was to reconstruct paleo-environmental parameters using well-developed paleoceanographic proxies in calcareous tests of benthic and planktonic foraminifera in order to better understand the onset and early development of deep-water carbonate mounds in the NE Atlantic. For this purpose we used grain size analyses and stable isotopes ($\delta^{13}C$ and $\delta^{18}O$) on five different, well-preserved benthic and one planktonic foraminifera species from the base of Challenger mound (142-152 m). Our results show that all benthic foraminifers provide reliable isotopic information, except $\delta^{13}C$ values of Discanomalina coronata, probably influenced by species-specific vital effects, which needs to be studied in another project. In a paleoceanographic context we can demonstrate that temperature, nutrients and bottom currents changed during the onset of the NHG and became favourable for cold-water corals to grow. As a consequence initial coral settlement began and the carbonate mound growth started. These results are integrated into the manuscript "Paleo-environmental reconstruction of deep-water carbonate mound initiation in the Porcupine Seabight, NE Atlantic" (Raddatz et al., in review: Appendix 3). Since we know

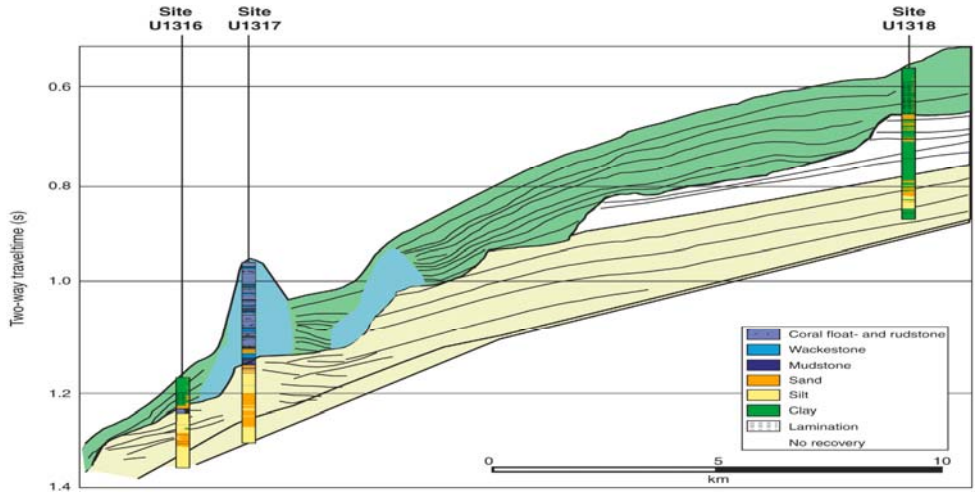

Figure 1: Litho-stratigraphy of the three sites projected on the seismic profile of Challenger mound along a north-northwest to south-southeast transect (from Expedition Scientists, 2005). Site U1317 has five drill holes with recovered sediment cores (A–E).

that the current conditions of carbonate cold-water coral mound growth are governed by a distinct density contrast of the ambient water masses (Dullo et al., 2008: Appendix 4), we are presently working on a proxy based approach for the ISOLDE project as a paleotemperature proxy.

Nevertheless, these initial results were still accompanied with a quiet large range of uncertainty. In order to deduce a

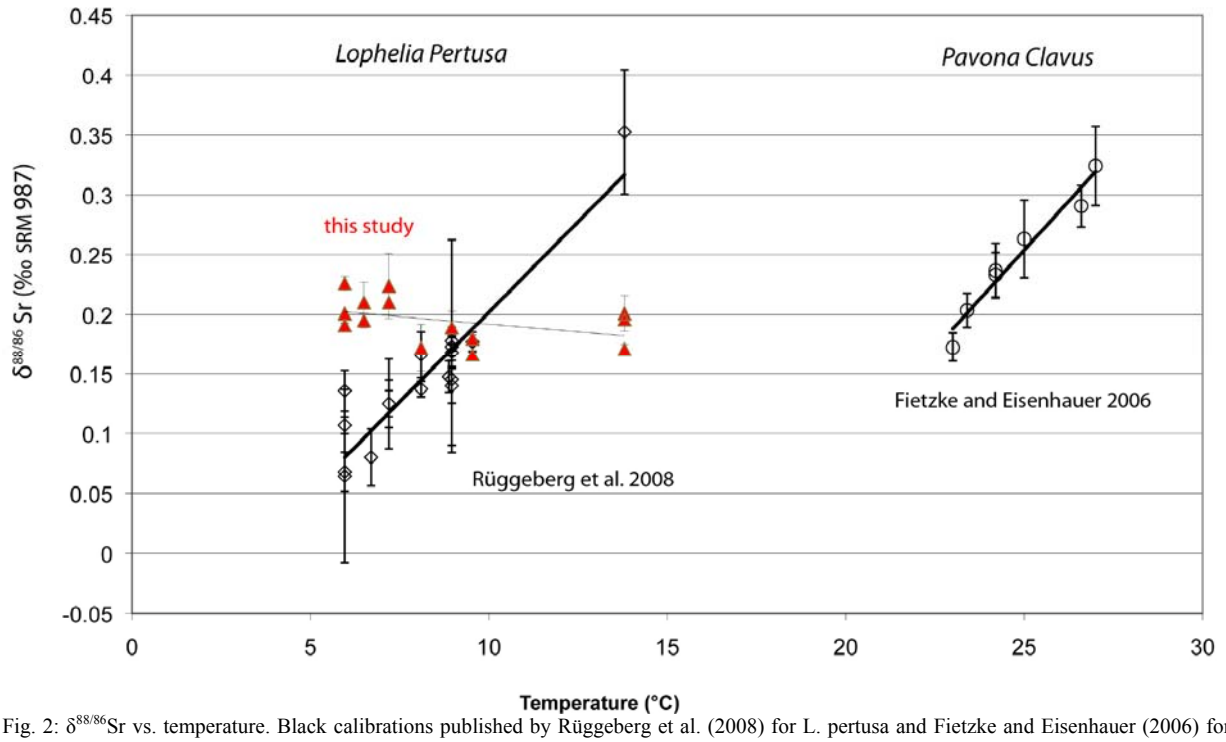

Fig. 2: $\delta^{88/86}$Sr vs. temperature. Black calibrations published by Rüggeberg et al. (2008) for L. pertusa and Fietzke and Eisenhauer (2006) for Pavona clavus. Red diamonds calibration is based on DS-TIMS measurements of this study implying no straight temperature dependent fractionation for stable δ88/86Sr. Correlation coefficients of previous studies are R2=0.59 for Rüggeberg et al. (2008) and R2=0.96 for Fietzke and Eisenhauer (2006).

reconstruction for paleo-densities.

The aim of paleotemperature reconstruction, a major task of the ISOLDE project, required application of most recent developments in proxy research. A promising perspective in this field was provided by findings of systematic correlations between ambient temperature and stable Sr isotope signatures ($\delta^{88/86}$Sr) in tropical and cold-water corals (Fietzke and Eisenhauer, 2006; Rüggeberg et al. 2008: Appendix 5), respectively (Fig. 2). As a pioneering work on cold-water corals the latter demonstrated directly the potential of the stable Sr significant temperature correlation this first attempt required a rather statistical and time-consuming analytical approach. This challenge for a routine proxy application was circumvented by the development of a new and more robust method (Krabbenhöft et al. 2009: Appendix 6), applying double spike instead of bracketing standard technique. Simultaneously to the stable Sr ($\delta^{88/86}$Sr) proxy information this method provides the radiogenic Sr (^{87}Sr/^{86}Sr) isotope ratio as monitor of the related seawater Sr isotope evolution stage. This indirect, on the considered range of 3 Ma rather imprecise, but important age estimate

is crucial for the determination of mound initiation phases and the detection of major changes in rate of mound accumulation. Consequently, beside the fundamental and established reconstruction using a multi species foraminifera approach (Raddatz et al. in review: Appendix 3), the first period of ISOLDE was focused to combine the new double spike Sr isotope measurement technique with the findings of Rüggeberg et al (2008). As prerequisite for a significant achievement in temperature resolution, this first down-core case study started with major efforts on a refinement approach for the temperature calibration of the $\delta^{88/86}$Sr isotope signature in recent to subrecent Lophelia pertusa.

The new, from methodical point of view, more robust results (Fig. 2) are not supporting a straight temperature dependence of the $\delta^{88/86}$Sr ratio solely.

Fig. 3 documents the range in δ88/86Sr signature related to different sampling sites and coral species. At the actual stage of the project the data set reflects only a very narrow range of variation, implying a rather similar δ88/86Sr signature for different recent Lophelia pertusa habitats, from the Mediterranean Sea up to the Norwegian Margin. The presented arithmetic weighted mean δ88/86Sr value of 0.188 ± 0.016 ‰ (2SEM) is almost identical with the value for the JCp-1 coral standard of 0.197 ± 0.008 ‰ (2SEM; Krabbenhöft et al., 2009).

As an important contribution to the understanding of the range covered in different habitats and their temperatures between 6 to 14°C (Fig. 3).

Note, the slope within the Irish Margin sample implies an increase from the inner to the outer part. Therefore, an apparent slope within a data set of different bulk samples could be theoretically induced by varying cleaning, preparation and sampling strategies. Whether vital effects like varying calcification rates and/or changes of ambient temperatures during different growth stages are controlling factors is topic of ongoing research at the IFM-GEOMAR.

The first down-core $\delta^{88/86}$Sr application on cold-water coral specimens from the basal part of IODP Site 1317C (Challenger Mound, Fig. 3) did not show any significant variation from values of recent habitats. In order to exclude as far as possible secondary alteration as overprinting process introducing modern isotope signatures, each sample was carefully pre-investigated by X-ray diffraction. All analyzed specimens showed pure aragonitic mineralogy. The lack of calcite as potential tracer of early recrystallisation processes implied no significant diagenetic influences. Therefore, the Sr isotope ratios are considered as primary signatures.

These new insights and the related achievement in Sr isotope systematic were presented on the AGU Fall Meeting 2009 in San Francisco and is topic of recent publication activity within ISOLDE (Raddatz et al. in prep.) Nevertheless, due to the fact that no straight

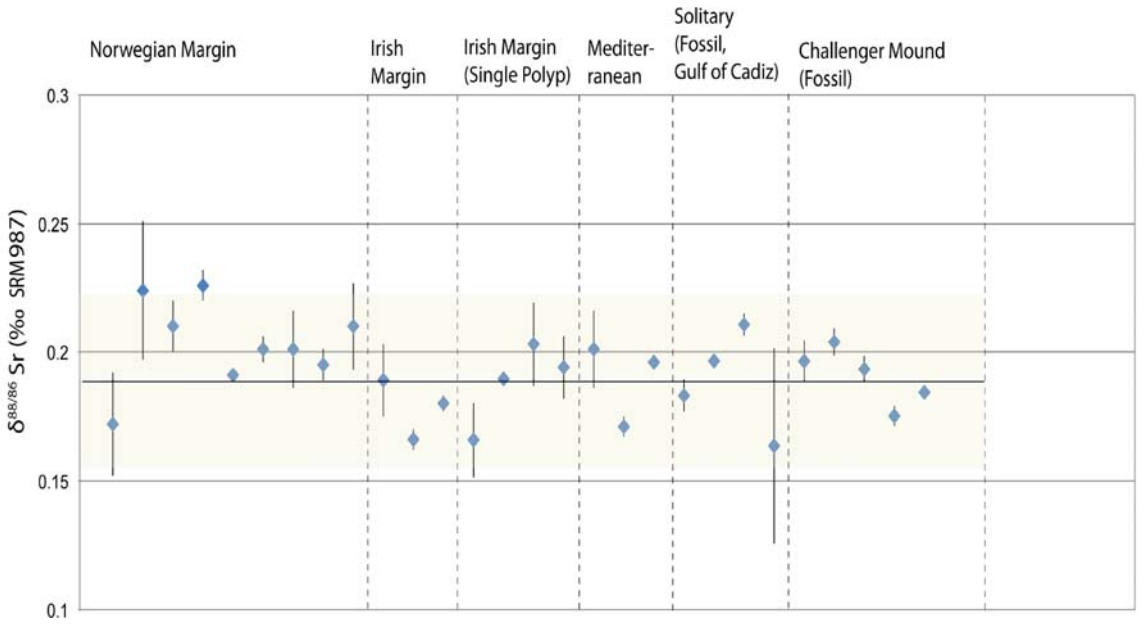

Figure 3: $\delta^{88/86}$Sr from cold-water coral (Lophelia pertusa) from various sites (Norwegian margin – recent, Irish margin – recent, Irish margin – one single polyp – cross section analysis from the inner to the outer part, Mediterranean Sea- recent, Gulf of Cadiz - solitary and fossil, Challenger mound – fossil. The black line indicates the arithmetic weighted mean of 0.188 ‰ with a 2SEM (grey bar).

stable Sr systematic in cold-water corals detailed micromill based subsampling was conducted within ISOLDE. A recent single Lophelia pertusa polyp from the Irish Margin and a fossil solitary one (Dendrophyllia sp.) from the Gulf of Cadiz were analyzed (Fig. 3), each by 4 subsamples from different growth zones.

Both heterogeneity tests document a variation during the calcification processes of single polyps of different species as almost similar in $\delta^{88/86}$Sr values and amplitude to paleotemperature reconstruction can be expected at the actual state of knowledge, the biogeochemical topic of Sr isotope fraction during carbonate precipitation of corals will be not in the focus of the final period of ISOLDE.

The results in Fig. 3 imply comparable environmental conditions concerning the potential $\delta^{88/86}$Sr controlling factors like temperature, calcification rate or ambient water mass signature throughout the last ~2.6 Ma of Lophelia pertusa reef formation. Therefore, alternative, partly more established approaches will be major goal for the final

project phase as described above in the proposal. In addition to the reconstruction of environmental conditions of mound initiation and the resettling after hiatuses these independent parameters will still contribute to the verification of $\delta^{88/86}$Sr controlling parameters.

References
Dullo C., Flögel S. and Rüggeberg A., (2008) Cold-water coral growth in relation to the hydrography of the Celtic and Nordic European continental margin.Marine Ecology Progress Series, Vol. 371: 165-176 , DOI 10.3354/meps07623
Expedition Scientists, 2005. Modern carbonate mounds: Porcupine drilling. IODP Prel. Rept., 307. doi:10.2204/iodp.pr.307.2005
Fietzke J., and Eisenhauer, A. (2006) Determination of temperature dependent stable strontium isotope (^{88}Sr/^{86}Sr) fractionation via bracketing standard MC-ICP-MS. Geochem. Geophys. Geosyst., 7, Q08009, doi:10.1029/2006GC001243.
Krabbenhöft, A., Fietzke, J., Eisenhauer, A., Liebetrau, V., Böhm, F., and Vollstaedt, H., 2009. Determination of radiogenic and stable strontium isotope ratios (^{87}Sr/^{86}Sr/d$^{88/86}$Sr) by thermal ionization mass spectrometry applying an ^{87}Sr/^{84}Sr double spike. J. Anal. At. Spectrom., 24: 1267–1271.
Raddatz, J., Rüggeberg, A., Margreth, S., Dullo, W.-Chr., and IODP Expedition 307 Scientific Party (in review.) Paleoenvironmental reconstruction of deep-water carbonate mound initiation in the Porcupine Seabight, NE Atlantic. Marine Geology, Special Volume COCARDE
Raddatz J., Liebetrau, V., Rüggeberg, A., Dullo, W.-Chr., Eisenhauer, A., et al., in prep. Stable strontium isotope ratios in scleractinian corals.
Rüggeberg A., Fietzke J., Liebetrau V., Eisenhauer A., Dullo W.-Chr., Freiwald A. (2008) Stable strontium isotopes (d$^{88/86}$Sr) in cold-water corals – A new proxy for the reconstruction of intermediate ocean water temperatures. Earth Planet. Sci. Lett., 269:569-574, doi:10.1016/j.epsl.2008.03.002

IODP

Paleoenvironmental reconstruction of deep-water carbonate mound initiation in the Porcupine Seabight, NE Atlantic

J. RADDATZ[1], A. RÜGGEBERG[1,2], S. MARGRETH[3], W.-CHR DULLO[1] AND IODP EXPEDITION 307 SCIENTIFIC PARTY

[1]IFM-GEOMAR Leibniz-Institute of Marine Sciences, Wischhofstrasse 1–3, D-24148 Kiel, Germany.
[2]Renard Centre of Marine Geology, Ghent University, Krijgslaan 281, S8, B-9000Gent, Belgium
[3]University of Fribourg, Department of Geosciences, Ch. du Musée 6, Fribourg, Switzerland.

The understanding of the paleoenvironment during initiation and early development of deep-water carbonate mounds in the NE Atlantic is currently focus of international research. The Integrated Ocean Drilling Program (IODP) Expedition 307 drilled the 155 m high Challenger Mound in the Porcupine Seabight in order to investigate for the first time sediments from the base of a giant carbonate mound. The initiation and start-up phase of this carbonate mound coincides with the beginning of the Northern Hemisphere Glaciation (NHG) at around 2.7 Ma. Further carbonate mound development seems to be strongly dependent on rapid changes in paleoceanographic and climatic conditions at the Pliocene-Pleistocene boundary, especially characterized and caused by intermediate water masses. This study focuses on the investigation of this specific time interval of ~ 2.7 Ma using established proxies such as δ^{18}O and δ^{13}C of planktonic (*Globigerina bulloides*) and of benthic foraminifera (*Fontbotia wuellerstorfi*, *Discanomalina coronata*, *Lobatula lobatula*, *Lobatula antartica*, and *Planulina ariminensis*) as well as grain size parameters to determine the paleoenvironmental and paleoecological setting favourable for the initial coral colonization. Stable oxygen and carbon isotope records of the benthic foraminiferal 35 assemblages indicate that *Lobatula lobatula* provides a reliable isotopic signature for paleoenvironmental reconstructions and that enhanced bottom currents of intermediate water masses of southern origin (Mediterranean, Bay of Biscay) intensified at the start-up of the NHG. Temperatures of these intermediate waters decreased to favourable 9 °C supporting the growth of cold-water corals. During the early mound development, reconstructed phosphate and nitrate concentration stayed in range of reported tolerance. Concluding, temperature and nutrient availability caused by a vigorous hydrodynamic regime supported development of cold-water coral, and hence rapid growths of carbonate mounds at early stage.

ICDP

ICDP Project „Lake El´gygytgyn“ (2008/09)

Core curation of impact rocks

U.RASCHKE[1], W.U. REIMOLD[1], R.T.SCHMITT[1], C. KOEBERL[2]

[1]Museum für Naturkunde, Invalidenstr. 43, 10115 Berlin
[2]Department of Lithospheric Research, Center for Earth Sciences, University of Vienna, 1090-Vienna, Austria

ICDP El´gygytgyn drill core 1C was obtained between January and April 2009, to a depth of 517 m blf (meters below lake floor). The core was separated into two

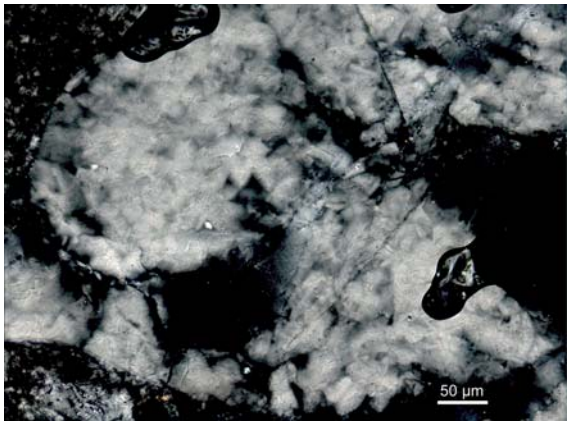

Fig.1: Mosaicism in shocked Quartz grain (20x zoom, cross pol., 491 m blf)

Fig.2: Self-built equipment for opening of the the core liner

different parts. The upper 318 m consist of lake sediments and are curated and analyzed at the University of Cologne and at the University of Massachusetts at Amherst (USA), with the main research focus being sedimentological analysis aimed at paleoclimate reconstruction. The lower ca. 200 m are being pre-processed at the Museum für Naturkunde Berlin. This section consists entirely of impactites that will be analyzed for better understanding the impact process in volcanic rocks.

Processing started with software (DIS) training and instruction in core curation by ICDP personnel. This is followed by full examination of the content of the core boxes and liners. The liners have to be opened and in most cases the contents (much of it in form of aggregate) need to be washed to remove the drilling mud. Afterwards the core sections were scanned with a GFZ core scanner and photographed. Due to the extent of brecciation it is only possible to obtain slabbed scans of many sections and not 3-D unrolled scans. All data are entered into the DIS database.

Next, the lithological description of the different impact rocks is made, with the assistance of a standardized DIS data sheet. Parameters such as clast lithology and textural aspects, presence of veining and of melt, or matrix composition are recorded. This cores ection comprises about 50 m of suevite (317 to 370 m) above brecciated basement rocks (370 to 517 m). Suevite is a melt-bearing polymict breccia with mineral and lithic clasts that show all stages of shock metamorphism (unshocked to melted: 0 - >50 GPa shock pressures) set in a clastic matrix. The degree of brecciation in the basement section decreases notably with depth. An international sampling party for the impactite core section is planned to take place at the Museum für Naturkunde in Berlin during May 2010.

IODP

Carbonate veins as recorder of seawater-crust interaction

S. RAUSCH[1], A. KLÜGEL[1], W.BACH[1], F. BÖHM[2]

[1]Geoscience Department, University of Bremen, Petrology of the Oceanic Crust, Klagenfurter Str.2, 28359 Bremen, Germany, srausch@uni-bremen.de
[2]IfM-GEOMAR, Wischhofstr. 1-3, 24148 Kiel, Germany, fboehm@ifm-geomar.de

Fluid circulation through the ocean crust plays a major role in the chemical and heat exchange between crust and oceans and for regulating seawater chemistry (Staudigel et al. 1996; Alt and Teagle 2000).Chemical exchange between seawater and ocean crust starts immediately after the formation of the new crust at mid-ocean ridges and continues for several million years. The seawater flow inside the ocean crust decreases with increasing spreading rate, for that the main part of vein formation and oxidation of the crust takes place in the first 10-15 Ma of crustal evolution (e.g. Bach and Edwards 2003). The overall fluid flux decreases with age because of decreasing permeability of the crust and increasing sediment cover. Nevertheless, crust-seawater exchange associated with circulation in off axis crust >1 Myrs old is critical in setting ocean chemistry. While high-temperature axial hydrothermal systems act as a source of alkalis and carbon to the oceans, low-temperature alteration at ridge flanks provide a sink for these elements; usually the off-axis uptake flux overwhelms the axial leaching flux (Hart and Staudigel 1982).

In this study we examine the role of the oceanic crust as a sink for CO_2, precipitated as carbonate in veins and vugs in the basement rock. The timing and magnitude of CO_2 uptake, is not well understood, however. One set of studies suggests that the net oceanic crustal CO_2 sink is comparable to the global atmospheric CO_2 input by subaerial volcanism and subaerial hydrothermalism in subduction zone settings, based on estimated global oceanic uptake flux of $2–4 \cdot 10^{12}$ mol CO_2/yr for Mesozoic crust (Staudigel et al. 1989; Alt and Teagle 1999). Younger ridge flanks in the East Pacific, however, indicate CO_2 uptake-fluxes that are an order of magnitude smaller (Sansone et al. 1998; Bach et al. 2003).

In order to better constrain these fluxes and understand processes during carbonate veining we comprehensively investigated carbonates abundance in twenty-three drill cores from North Atlantic and Pacific crustal basement, which included samples from crust of different age and spreading rates. We integrated oxygen and strontium isotope analyses with measurements of trace element concentrations at high spatial resolution by laser-ablation ICP-MS to gather information about the evolution of circulating seawater composition recorded in single carbonate veins.

The visual core logging data show that carbonate abundance principally increases with increasing basement age, which had been proposed before by (Alt and Teagle 1999). The oldest samples are of Jurassic to Cretaceous age (Holes 417A, 417D, 418A, 801C, and 1149D) showing a carbonate proportion of 2.3 to 5.5 vol.%, whereas younger

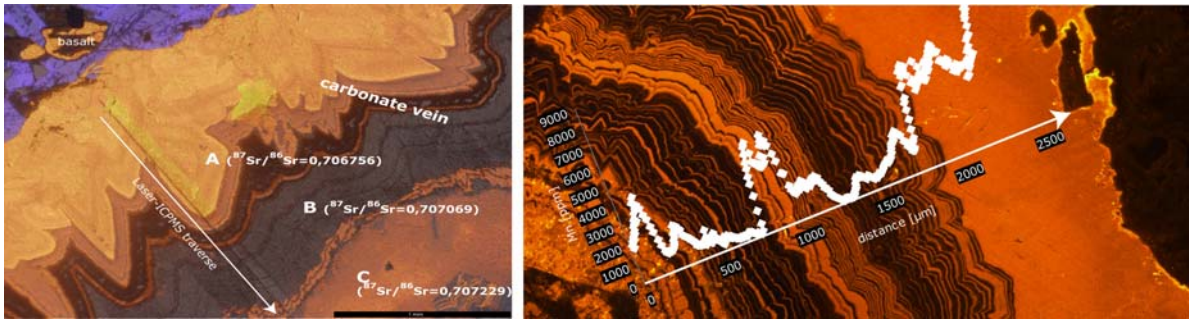

Fig.1: a) Cathodoluminescence picture (801B-43-2) showing a complex zonation and locations of Sr-isotope measuements; b) CL (417A-46-2) displays Laser-ICPMS traverse (Mn) across the carbonate vein.

samples (Holes 332A, 332B, 334, 395, 396, 396B, 407, 409, 504B, 553A, 597C, 896A, 1032A, 1027C, and 1224F) show significantly lower carbonate percentages between 0.1 and 1.2 vol.%. We also recognized a general trend of decreasing carbonate abundance with increasing depth below the sediment-basement interface. We calculated an average proportion of carbonate veins and vugs in the upper 600-700 m of oceanic crust on the order of 2-4

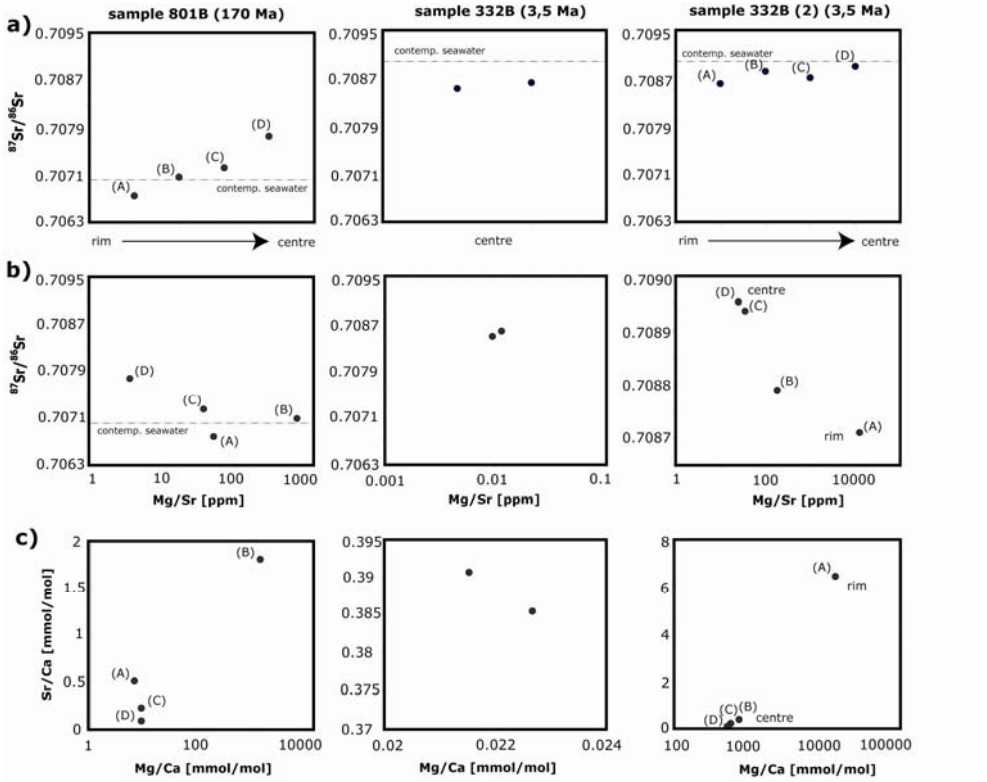

Fig.2: $^{87}Sr/^{86}Sr$ analyses confirm the compositional zonation in selected carbonate veins refered to Mg/Sr and Sr/Ca vs. Mg/Ca at the same positions inside the vein.

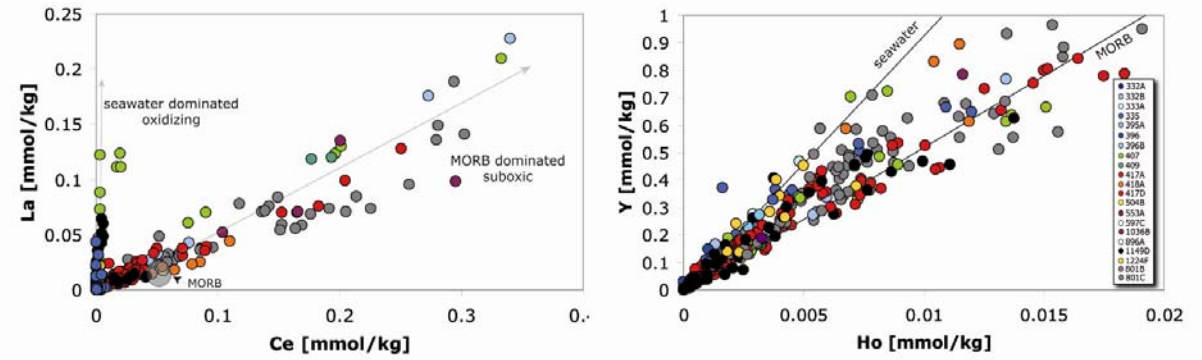

Fig.3: On a La versus Ce diagram most analyzed carbonate veins fall either on a seawaterdominated trend with high La/Ce and a negative Ce anomaly, or on a basement dominated trend with low La/Ce.
Fig.4: On a Y against Ho diagram most carbonate vein samples plot in the range between average seawater (after Nozaki et al. 1997) and MORB.

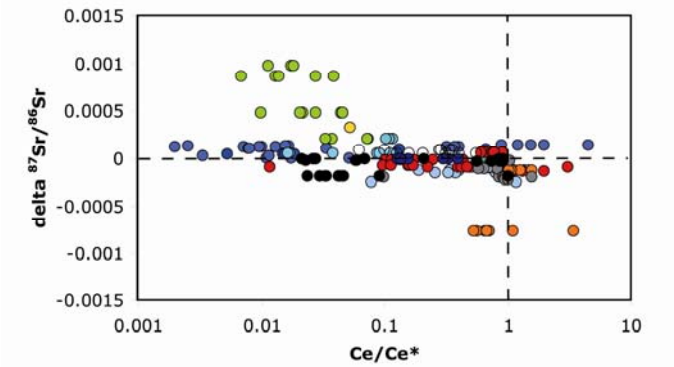

Fig.5: Plot of delta $^{87}Sr/^{86}Sr$ deviation from contemporanepus seawater versus Ce/Ce* (Ce* = (LaN+PrN)/2). Sites with positive $^{87}Sr/^{86}Sr$ tend to display negative Ce anomalies (i.e. Ce/Ce*<1).

vol.%, which is equivalent to a global CO_2 uptake of 1-2 · 10^{12} mol/yr. Our data are thus intermediate between earlier estimates based mainly on investigations of drill cores from >110 Myrs old ocean crust (Staudigel et al. 1989; Alt and Teagle 1999) and for <7Ma sedimented ridge flanks (Sansone et al. 1998; Bach et al. 2003).In addition to petrographic observations, we used cathodoluminescence microscopy to reveal zonations and textures of carbonate veins caused by variable trace element concentrations. The orange cathodoluminescence shown in Fig. 1 is caused by the presence of Mn^{2+} cations that replaces Ca^{2+} in distorted octahedral sites of the calcite structure and cause radiative transition (Cazenave et al. 2003). Our LA-ICP-MS traverse data show highly variable Mn contents consistent with the cathodoluminescence images (Fig.1). Many veins show fine and complex zoning and several generations of carbonate cements, some of which indicate that circulating fluids used cracks in pre-existing veins. In some samples cathodoluminescence reveal whole-sale replacement of aragonite by calcite.

Age dating of carbonate veins may under favorable conditions be obtained using their Sr istope ratios. This is because the $^{87}Sr/^{86}Sr$ ratio of global seawater has strongly increased during the past 40 Ma and the $^{87}Sr/^{86}Sr$ ratio in carbonate veins can be compared with this record to estimate formation age (Hart and Staudigel 1978; Hart et al. 1994). This methods works if isotopic exchange between circulating fluid and basement rock can be ignored. $^{87}Sr/^{86}Sr$ of the analyzed samples (see companion paper by Böhm et al.) indicate that carbonate veins in some sites (335, 395, 396, 407, and 1224) formed much later than the basement, which suggests prolonged (up to 20 Ma) open circulating of seawater. In contrast, samples with $^{87}Sr/^{86}Sr$ below that of contemporaneous seawater indicate hydrothermal uptake of Sr from the basaltic basement (Sites: 332, 333, 409, 418, 801, and 1149) and impair their use as a chronometer. In addition to Sr isotope analyses of bulk veins, we analyzed both trace element concentrations and Sr isotope ratios across single veins traverses by laser ablation ICP-MS and MC-ICP-MS, respectivley. $^{87}Sr/^{86}Sr$ in some veins (Fig.2a, Site 801B) increases with distance from the basalt contact, which may reflect open circulation over a very long period during which seawater $^{87}Sr/^{86}Sr$ increased. Alternatively, this trend could indicate decreased intensity of seawater-crust exchange when the centre of the vein formed. Veins from younger sites such as Hole 332B (3.5 Ma) show either similar $^{87}Sr/^{86}Sr$ ratios as contemporaneous seawater, or increasing $^{87}Sr/^{86}Sr$ with distance from the basalt contact. A plot of $^{87}Sr/^{86}Sr$ ratio versus Mg/Sr ratio shows a negative trend (Fig.2b), indicative of low-temperature water-rock interactions during which Mg is depleted in the circulating seawater and is taken up by the crust, which releases low-$^{87}Sr/^{86}Sr$ to the fluid. Coggon et al. (2004) showed a systematic trend in Mg/Ca vs. Sr/Ca of carbonate veins from the Juan de Fuca Ridge flank. Our data for different zones in single carbonate veins show similar variations with high Mg/Ca and Sr/Ca ratios near to the basalt contact and much lower ratios in the vein center (Fig.2c). These co-variations may imply continuous growth of carbonate recording change in fluid composition. Our bulk-data show that low-temperature carbonate veins from open circulation sites do not show any sign of seawater exchange with basement in Mg/Ca and Sr/Ca. Overall, the intensity of basement exchange recorded in the vein composition is fairly minor. Carbonate veins, for which exchange with basement can be ruled out, can therefore be used to reconstruct the Mg/Sr evolution of seawater.

The rare earth element (REE) patterns of the investigated carbonate veins define to distinct groups, one with a pronounced Ce depletion and one without a Ce depletion (Fig.3). Cerium is typically depleted in oxic seawater, hence a Ce depletion in the carbonates is an indication of oxidative conditions during carbonate precipitation. Ce depletions are commonly observed in carbonates from veins with high $^{87}Sr/^{86}Sr$ (i.e., sites with open circulation). In contrast, all sites where low $^{87}Sr/^{86}Sr$ ratios indicate considerable exchange with basement show no Ce depletion, suggesting that conditions during carbonate precipitation were less seawater-dominated and less oxidizing than seawater. Suboxic to anoxic conditions prevail in case of restricted circulation where exchange with the ocean is strongly limited, as is also indicated by celadonite and pyrite in vein halos. The Y/Ho ratio of carbonate veins is another sensitive indicator for the extent of seawater-basement interaction. Unlike Mg/Sr, it responds to even minor extents of exchange with basement, because REE and Y concentrations of seawater are 5-6 orders of magnitude lower than those of basalt and the Y/Ho ratio of seawater is about twice that of basalt. Our combined analyses of ~75 veins indicate a large range of Y/Ho, which reflects highly variable extents of basement-seawater interaction, that were not discernible from Mg and Sr concentrations (Fig.4). Veins with negative Ce anomalies and contemporaneous seawater Sr isotope ratios tend to have seawater-like Y/Ho, while those revealing basement exchange show chondritic Y/Ho.

Many investigated carbonate veins often show a strong compositional zonation for some trace elements including Mn, Y and the REE (Fig. 1). Concentrations may simply increase towards the contact to the basalt, whereas other veins show different and more complex zonations. Some veins show MORB-like rare earth element concentrations near the contact to the host basalt that but distinctly lower values and seawater-like Y/Ho ratios near the vein centers. Apparently these changes reflect a systematic variation of seawater-basement interaction during the formation of the veins. It appears likely that early carbonate formation along fracture walls reduce the contact area between fluid and basement thereby limiting chemical exchange during subsequent fluid flow and carbonate precipitation.

In summary, microanalyses of $^{87}Sr/^{86}Sr$ ratios and trace element concentrations in carbonate veins in oceanic crust provide conclusive evidence for an open system behavior and therefore a continuous growth of the veins. Moreover, REE concentrations and Y/Ho ratios and Sr isotopes of carbonate veins are highly sensitive indicators for the extent of seawater-basement interaction during vein formation.

References:

Alt, J. C. and D. A. H. Teagle (1999). "The uptake of carbon during alteration of the ocean crust." Geochimica et Cosmochimica Acta **63**(10): 1527-1535.

Alt, J. C. and D. A. H. Teagle (2000). "Hydrothermal alteration and fluid fluxes in ophiolites and the ocean crust." Geological Society of America, Special Paper **349**: 273-282.

Bach, W. and K. J. Edwards (2003). "Iron and sulfide oxidation within the basaltic ocean crust: Implications for chemolithiautotrophic microbial biomass production." Geochimica et Cosmochimica Acta **67**: 3871-3887.

Bach, W., B. Peucker-Ehrenbrink, et al. (2003). "Geochemistry of hydrothermally altered oceanic crust:DSDP/ODP Hole 504B - Implications for seawater-crust exchange budgets and Sr- and Pb-isotopic evolution of the mantle." Geochemistry, Geophysics, Geasystems **4**.

Cazenave, S., R. Chapoulie, et al. (2003). "Cathodoluminescence of synthetic and natural calcite: the effects of manganese and iron on orange emission." Mineralogy and Petrology **78**: 243-253.

Cicero, A. D. and K. C. Lohmann (2001). "Sr/Mg variation during rock-water interaction:Iplications for secular changes in the elemental chemistry of ancient seawater." Geochimica et Cosmochimica Acta **65**(5): 741-761.

Coggon, R. M., D. A. H. Teagle, et al. (2006). "10. Data Report: Composition of Calcium Carbonate Veins from Superfast Spreading Rate Crust, ODP leg 206." Proceedings of the Ocean Drilling Program, Scientific Results **206**.

Coggon, R. M., D. A. H. Teagle, et al. (2004). "Linking basement carbonate vein compositions to porewater geochemistry across the eastern flank of the Juan de Fuca Ridge, ODP Leg 168." Earth and Planetary Science Letters **219**: 111-128.

Hart, S. R., J. Blusztajn, et al. (1994). "Fluid circulation in the oceanic crust: Contrast beween volcanic and plutonic regimes." Journal of Geophysical Research **99**: 3163-3173.

Hart, S. R. and H. Staudigel (1978). "Oceanic crust: age of hydrothermal alteration." Geophys. Res. Lett. **5**: 1009-1012.

Hart, S. R. and H. Staudigel (1982). "The control of alkalies and uranium in seawater in seawater by ocean crust alteration." Earth and Planetary Science Letters **58**: 202-212.

Sansone, F. J., M. J. Mottl, et al. (1998). "CO2-depleted fluids mid-ocean ridge-flank hydrothermal springs." Geochimica et Cosmochimica Acta **62**(13): 2247-2252.

Staudigel, H., S. R. Hart, et al. (1989). "Cretaceous ocean crust at DSDP Sites 417 and 418: Carbon uptake from weathering versus loss by magmatic outgassing." Geochimica et Cosmochimica Acta **53**: 3091-3094.

Staudigel, H., T. Plank, et al. (1996). "Geochemical fluxes during seafloor alteration of the basaltic upper crust: DSDP Sites 417 and 418." Geophysical Monograph **96**: 19-38.

ICDP

The global sulfur cycle across the Archean-Paleoproterozoic transition: Evidence from FAR-DEEP

M. REUSCHEL[1], H. STRAUSS[1], V.M. MELEZHIK[2, 3], A. LEPLAND[2], P. CARITGNY[4], L.R. KUMP[5], Y. DEINES[6], A. ROMASHKIN[6], D. RYCHANCHIK[6]

[1]Westfälische Wilhelms-Universität Münster (Germany)
[2]Geological Survey of Norway (Norway)
[3]Centre for Geobiology, University of Bergen (Norway)
[4]Institut de Physique du Globe Paris (France)
[5]Pennslvanina State University, Department of Geosciences (United States of America)
[6]Russian Academy of Sciences, Karelian Research Center, Institute of Geology (Russia)

The time interval between 2.5 and 2.0 Ga, the Archean-Paleoproterozoic transition (APT), represents one of the most critical periods in Earth history. Fundamental changes in the biogeochemical cycles of redox sensitive elements like carbon, sulfur, iron or phosphorus characterize this time period together with geotectonic and climatic upheavals. However the most important event was likely the rise in atmospheric oxygen concentration round 2.4 Ga ago. Mass independent fractionation of sulfur isotopes (MIF-S) is by now the most reliable tool to reconstruct atmospheric oxygen concentration (Farquhar et al., 2000, Pavlov and Kasting, 2002). The loss of the MIF-S signal is thought to mirror the rise in atmospheric oxygen, as far as MIF-S can only be produced, transferred and archived in Earth surface environments in an anoxic atmosphere and hydrosphere.

As a consequence of Earth's atmospheric oxygenation and the concomitant onset of oxidative weathering of sulfides, the oceanic sulfate concentration began to rise. Likely stimulated by enhanced sulfate availability the importance of microbial sulfur cycling increased.

The Russian part of the Fennoscandian Shield provides exceptional rock successions of the Paleoproterozoic, spanning nearly 700 Ma of Earth history. The rocks provide a unique record of the APT and thus help to further investigate the geotectonic, climatic and biochemical changes during that time (Melezhik et al., 2005).

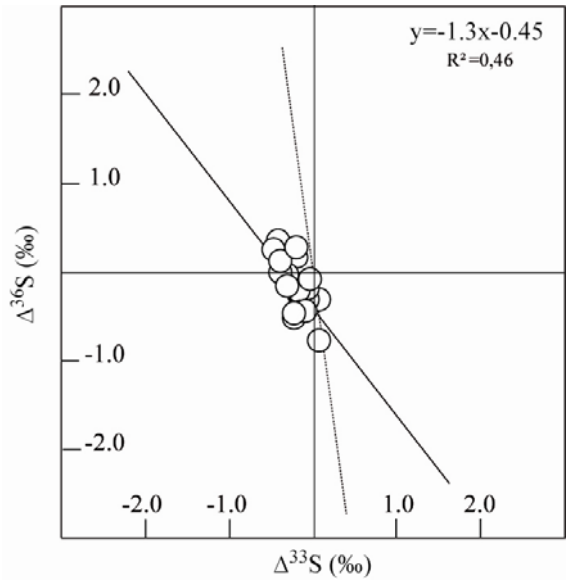

Fig. 1. Relationship between $\Delta^{33}S$ and $\Delta^{36}S$ for sulfides of the Seidorechka Sedimentary Formation. The black line shows the slope for the Seidorechka sulfides, the dashed line shows the slope that reflect mass dependent fractionated sulfur species.

In summer 2007, the ICDP FAR-DEEP (Fennoscandian Arctic Russia - Drilling Early Earth Project) drilled 15 holes in three areas of the Fennoscandian Shield. Two of the three drilling sites are situated in the Kola Peninsula. These include the Pechenga Greenstone Belt located in the north-west, close to the Norwegian boarder, and the Imandra/Varzuga Greenstone Belt, in the south-east. The third drilling area, the Onega basin, is located in Karelia. A total of 3650 m of drill core has been stored and archived at the Norwegian Geological Survey in Trondheim. More than 500 archive samples (samples were taken approximately each 7 m) are available for multidisciplinary research. The first sampling party in spring 2008 gave the possibility to study the cores more in detail for their geochemical parameters and to take additional research samples.

To date, 250 samples have been studied for their sulfur geochemistry, including total sulfur abundances and sulfur isotope measurements for monosulfide sulfur, pyrite sulfur and carbonate-associated sulfate (CAS). In addition to the archive samples, 73 research samples were selected from drillcores 1A, 3A, 10A, 10B and 11A to study specific intervals in more detail and for the extraction of CAS.

The oldest formation of the FAR-DEEP succession is the Seidorechka Sedimentary Formation from the Imadra/Varzuga Greenstone Belt with an age of ca. 2.44 Ga (U-Pb, Amelin et al., 1995). This formation could still capture the interval of Earth's initial oxygenation of the Earth's surface environments (Great Oxidation Event, GOE, Holland, 2002). Hence, 50 samples (archive and research samples and outcrop material) have been analyzed

for their sulfur isotopic composition. Sulfide $\delta^{34}S$ varies between -15.1 and +3.3 ‰ with distinct temporal variations. In contrast to the outcrop material, the $\delta^{34}S$ values of the drill core show two excursions, at around 160 m and at around 140 m depth with values of -4.4 ‰ and +3.3 ‰ respectively. The overall range in $\delta^{34}S$ throughout the succession indicates bacterial sulfate reduction in the depositional environment with low sulfate concentrations. The deviations to more positive values could indicate a progressive sulfate limitation in the sedimentary realm. For a subset of 16 samples multiple sulfur isotopes (^{32}S, ^{33}S, ^{34}S amd ^{36}S) have been measured. MIF-S (i.e $\Delta^{33}S$) values range between 0.06 and -0.42 ‰ (with an average of -0.20±0.15 ‰). These small, but still significant deviations from mass dependent fractionated signatures in $\Delta^{33}S$, combined with a $\Delta^{33}S/\Delta^{36}S$ plot clearly reveal the influence of MIF-S producing reactions in the atmosphere for the Seidorechka sulfides (Fig. 1). It is therefore suggested that the atmospheric oxygen concentration was still below 10^{-5} PAL, low enough for UV induced photochemistry of SO_2 to cause MIF-S in atmospheric sulfur species. The largely negative character of the $\Delta^{33}S$ suggests a dominance of oxidized sulfur species in the atmosphere, since the reduced species and elemental sulfur carry a positive anomaly in $\Delta^{33}S$. The negative $\Delta^{33}S$ signature could thus be a sign of low concentrations of elemental sulfur in the atmosphere and this in turn could point to a low concentration of reduced gases like CH_4 and H_2 in the atmosphere.

The dominance of oxidized sulfur species in the atmosphere and subsequently in the hydrosphere has likely stimulated bacterial sulfate reduction together with increasing availability of sulfate in the depositional environment. This in turn triggered the anaerobic oxidation of methane, which would have drawn down the methane concentration of the hydrosphere and finally in the atmosphere. Because methane is a greenhouse gas, its drawdown would lead to a cooling of Earth's surface and may have triggered the onset of the Huronian Glaciation, represented by the glacial deposits of the overlying Polisarka Sedimentary Formation on the Fennoscandian Shield and elsewhere in the world. The Polisarska Sedimentary Formation overlies the 2.44 Ga Seidorechka Volcanic Formation and its sedimentary rocks are thought to be of glacial origin, reflecting the Fennoscandian equivalent of the Huronian glaciation. The isotopic composition of the sulfides range between -30.7 and -2.4 ‰. However, the upper part of the succession is dominated by volcanic rocks displaying δ34S signatures close to zero (-1.6±1.5 ‰). Some intercalated siliciclastic rocks also show sulfur isotopic compositions close to zero indicating a volcanic sulfur source and no microbial activity. In contrast, the lower part shows evidence for microbial sulfur cycling with an average δ34S of -16.7±7.5 ‰.

The oldest rocks of the Pechenga Greenstone Belt, drilled by the FAR-DEEP, is a weathering crust of the Ahmalahi Formation (drillhole 5A). The drillholes 6A intersected the Kuetsjärvi Volcanic Formation dated to 2.06 Ga (Melezhik et al. 2007), whereas drillholes 7A,8A and 8B cover the overlying Kolasjoki Sedimentary Formation. The Kuetsjärvi volcanic rocks are highly oxidized, and may carry a fingerprint of oxidized upper mantle (Kump et al., 2001). The sedimentary succession of the Kuetsjärvi Sedimentary Formation includes quartz arenites, dolostones, red beds and hot spring travertines, whereas the Kolasjoki Sedimentary Formation is composed of greywackes, jaspers, dolostones and schists. The sulfur isotope data within the sedimentary sulfides of the Kolasjoki and Kuetsjärvi Sedimentary Formations reveals variations between-7.6 and +8.7 ‰.

A middle part of the Kolasjoki Volcanic Formation with a thin black schist interval was the target of drillhole 9A. The δ34S for the sulfides displays small-scale stratigraphic variation between -1.7 and +5.7 ‰. Rocks recovered in the Onega basin during FAR-DEEP drilling include the Tulomozero Formation dolostones and shales with abundant Ca-sulfates, and the overlying Zaonega Formation with its unique accumulations of organic matter. 32 research samples of the Tulomozero Formation from the drillcores 10A, 10B and 11A have been selected for CAS extraction. However only 8 samples yielded measurable amounts of CAS. The CAS content varies between 65 and 310 ppm and $\delta^{34}S$ ranges between + 8.3 and +15.8 ‰ with an average of 10.9±2.7 ‰. The CAS sulfur isotopic composition refelcts the sulfate isotopic composition of ancient seawater sulfate (e.g. Burdett et. al., 1989, Kampschulte et al., 2001, Gellatly and Lyons, 2005, Guo et al., 2009). Furthermore, in situ (multiple) sulfur isotope analyses have been performed on seleceted samples from the Tulomozero Formation that contain pseudomorphed bedded sulfates.

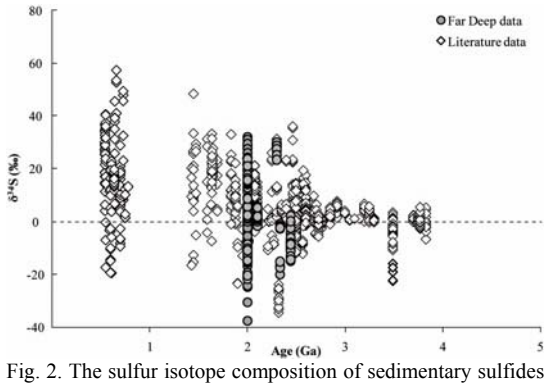

Fig. 2. The sulfur isotope composition of sedimentary sulfides over time. White diamonds represent literature data (Bao et al., 2007, Bekker et al., 2003, Kaufman et al., 2007, Mojzsis et al., 2003, Ohmoto et al., 2006, Ono et al., 2006, 2009a,b, Papineau et al., 2005, 2006, 2007, Patridge et al., 2008, Poulton et al., 2004, Philippot et al., 2008, Shen et al., 2008, Whitehouse et al., 2005) and grey circles show the sulfur isotope compositions of FAR-DEEP sulfides.

The drillcore 13A is the third hole, in addition to 12A and 12B that intersects the organic-rich rocks of the Zaonega Formation. All sulfide-bearing archive samples of the Zaonega Formation (n=104) have been analyzed for their sulfur isotopic composition. The sulfur isotopic compositions range between -7.7 and +32.4 ‰ throughout the Zaonega Formation. However the sulfides represent a mixture of different generations, and specifically-targeted research project is requested for further research.

All together the sulfur isotopic composition of the sulfides within the FAR-DEEP strata displays variations between -37.7 and +32.4 ‰. This is consistent with the known record of $\delta^{34}S$ for that time interval (Fig. 2).

References:

Amelin, Y.V., Heaman, L.M., Semenov, V.S. (1995) U-Pb geochronology of layered mafic intrusions in the eastern Baltic Shield: implications for the timing and duration of Paleoproterozoic continental rifting. Precambr. Res. 75, 31-46.

Bao, H., Rumble, D., Lowe, D.R. (2007) The five stable isotope compositions of Fig Tree barites: implications on sulfur cycle in ca. 3.2. Ga oceans. Geochim.Cosmochim. Acta 71, 4868-4879.
Bekker, A., Holland, H.D., Wang, P.L., Rumble, D., Stein, H.J., Hannah, J.L., Coetzee, L.L., Beukes, N.J. (2004) Dating the rise of atmospheric oxygen. Nature 427. 117-120.
Burdett J. W., Arthur M. A. and Richardson M. (1989) A Neogene seawater sulfur isotope age curve from calcareous pelagic microfossils. Earth Planet. Sci. Lett. 94, 189–198.
Farquhar, J., Bao, H.M., Thiemens, M. (2000) Atmospheric influence of Earth's earliest sulfur cycle. Science 289, 756–758.
Gellatly A. M., Lyons T. W. (2005) Trace sulfate in mid-Proterozoic carbonates and sulfur isotope record of biospheric evolution. Geochim. Cosmochim. Acta 69, 3813–3829.
Guo, Q., Strauss, H., Kaufman, A.J., Schröder, S., Gutzmer, J., Wing, B., Baker, M.A., Bekker, A., Jin, Q., Kim, S., Farquhar, J. (2009) Reconstructing Earth's surface oxidation across the Archean Paleoproterozoic transition. Geology 37, 399-402.
Holland, D. (2002)
Kampschulte A., Bruckschen P. and Strauss H. (2001) The sulphur isotopic composition of trace sulphates in Carboniferous brachiopods: implications for coeval seawater, correlation with other geochemical cycles and isotope stratigraphy. Chem. Geol. 175, 149–173.
Kaufman, A.J., Johnston, D.T., Farquhar, J., Masterson, A.L., Lyons, T.W., Bates, S., Anbar, A.D., Arnold, G.L., Garvin, J. Buick, R. (2007) Late Archean biospheric oxygenation and atmospheric evolution. Science 317, 1900-1903.
Kump, L.R., Kasting, J.F., Barley, M.E. (2001) Rise of atmospheric oxygen and the "upside-down" mantle. Geochem. Geophy. Geosyst 2, 1025.
Melezhik, V.A., Fallick, A.E., Hanski, E.J., Lepland, A., Prave, A.R., Strauss, H. 2005: Emergence og the aerobic biosphere during the Archean-Proterozoic transition: Challenges of future research. GSA Today,15,4.
Melezhik, V.A., Huhma, H., Condon, D.J., Fallick, A.E., Whitehouse, M.J. (2007) Temporal constraints on the Palaeoproterozoic Lomagundi-Jatuli carbon isotopic event. Geology 35, 655-658.
Mojzsis, S.J., Coath, C.D., Greenwood, J.P., McKeegan, K.D., Harrison, T.M (2003) Mass-independent isotope effects in Archean (2.5 to 3.8 Ga) sedimentary sulfides determined by ion microprobe analysis. Geochim. Cosmochim. Acta 67, 1635-1685.
Ohmoto, H., Watanabe, Y., Ikemi, H. Poulson, S.R., Taylor, B.E. (2006) Sulphur isotope evidence for an oxic atmosphere. Nature 442, 908-911.
Ono, S., Eigenbrode, J.L., Pavlov,A.A., Kharecha, P., Rumble, D., Kasting, J.F., Freeman, K. (2003) New insights into Archean sulfur cycle from mass-independent sulfur isotope records from the Hamersley Basin, Australia.
Ono, S., Beukes, N.J., Rumble, D. (2009a) Origin of two distinct multiple-sulfur isotope compositions of pyrite in the 2.5 Ga Klein Naute Formation, Griqualand West Basin, South Africa. Precambr. Res. 169, 48-57.
Ono, S., Kaufman, A.J. Farquhar, J., Summer, D.Y., Beukes, N.J.(2009b) Lithofacies control on multiple sulfur isotope records and Neoarchean sulfur cycles. Precambr. Res. 169, 58-67.
Papineau, D., Mojzsis, S.J. (2006) Mass-independent fractionation of sulfur isotopes in sulfides from the pre-3770 ma Isua Suprecrustal Belt., West Greenland. Geobiol. 4, 227-238.
Papineau, D., Mojzsis, S.J., Coath, C.D., Karhu, J.A., McKeegan, K.D. (2005) Multiple sulfur isotopes of sulfides from sediments in the aftermath of Paleoproterozoic glaciations. Geochim. Cosmochim. Acta 69, 5033-5060.
Papineau, D., Mojzsis, S.J. Schmitt, A.K. (2007) Multiple isotopes from Paleoproterozoic interglacial sediments and the rise of the atmospheric oxygen. Earth a. Planetary Science Letters 255, 188-212.
Patridge, M.A., Golding, S.D., Baublys, K.A., Young, E.(2008) Pyrite paragenesis and multiple sulfur isotope distribution in late Archean and early Paleoproterozoic Hamersley Basin sediments. Earth and Planetary Science Letters 272, 44-49.
Pavlov, A.A., Kasting, J.F., 2002. Mass-independent fractionation of sulfur isotopes in Archean sediments: strong evidence for an anoxic Archean atmosphere. Astrobiology 2, 27–41.
Poulton, S.W., Canfield, D.E. (2004) The transition to a sulphidic ocean ~1.84 billion years ago. Nature 341, 173-177.
Philippot, P., van Zuilen, M., Lepot, K., Thomazo, C., Farquhar, J., van Kranendonk, M. (2007) Early Archean Microorganisms preferred elemental sulfur not sulfate. Science 317, 1534-1537.
Shen, B., Xiao, S., Kaufman, A.J., Bao, H, Zhou, C., Wang, H. (2008) Stratification and mixing of a post glacial Neoproterozoic ocean: evidence from carbon and sulfur isotopes in a cap dolostone from Northwest China. EPSL 265, 209-228.
Whitehouse, M.J., Kamber, B.S., Fedo, C.M., Lepland, A. (2005) Integrated Pb- and S-isotope investigation of sulphide minerals from the Early Archean of southwest Greenland. Chem.Geol. 222, 112-131.

ICDP

Einflüsse prähistorischen Vulkanismus auf die Vegetationsgeschichte Ostanatoliens. Vorläufige Untersuchungsergebnisse holozäner Sedimente des Vansees (Türkei)

NILS RIEDEL & THOMAS LITT

Steinmann-Institut, Abt. Paläontologie, Universität Bonn

Hochauflösende Untersuchungen an kontinentalen Archiven ermöglichen nicht nur die Rekonstruktion klimatischer Zustände der Vergangenheit, sondern auch das Studium katastrophaler geologischer Ereignisse und ihre Auswirkungen auf Ökosysteme.

Die Folgen rezenter Vulkaneruptionen (z. B. Mt. St. Helens, Krakatau) auf die Vegetation waren bereits mehrfach Objekt wissenschaftlicher Untersuchungen. Hierbei konnten wichtige Erkenntnisse zu Vegetationszerstörungen, sowie anschließende Stadien der Wiederbesiedlung gewonnen werden. Auswirkungen von prähistorischen Vulkanereignissen auf die Vegetation konnten dagegen bisher jedoch nur selten nachgewiesen werden.

Der Vansee in Ostanatolien (Türkei) ist einer der größten Terminalseen der Welt. Seine Lage in einer klimasensitiven Region, sowie seine jahreszeitlich geschichteten Sedimente machten ihn bereits mehrfach zum Ziel wissenschaftlicher Forschungskampagnen. Ostanatolien befindet sich im Bereich der Kollisionszone zwischen Arabischer Platte und den Pontidenterranen und zeichnet sich durch hohe tektonische Aktivität aus. Vulkanismus lässt sich bereits seit dem jüngeren Paläogen nachweisen. In der direkten Umgebung des Vansees befinden sich mehrere quartäre Vulkanzentren, von denen drei bis in das Holozän aktiv waren. Bohrungen, die im Jahr 2004 im Rahmen einer Voruntersuchung zum ICDP-Projekt *Paleovan* im Vansee abgeteuft wurden, erbrachten Sedimentkerne, die etwa die vergangenen 20.000 Jahre abdecken. Die Untersuchung der Bohrkerne ergab neue Einblicke in die Entwicklung des Klimas und der Vegetation Ostanatoliens seit dem Weichselhochglazial. Die Bohrkerne enthalten zudem 16 Tephren die durch geochemische Untersuchungen ihren Ursprungsvulkanen zugeordnet werden konnten. In dieser Arbeit konnten mit Hilfe hochauflösender (< 5 Jahre/Probe) palynologischer Analysen der deutliche Einfluss der Vulkaneruptionen auf die Vegetation, sowie Stadien und Dauer der anschließenden Sukzession nachgewiesen werden. Jüngste Untersuchungen vulkanischer Ablagerungen im Vanseegebiet, die z. T. Mächtigkeiten von über 10 m erreichen, lassen für die im Sommer 2010 stattfindende ICDP-Bohrkampagne im Vansee neue, spektakuläre Einblicke in die Vulkan- und Vegetationsgeschichte der letzten Jahrhunderttausende erwarten.

IODP

Late Miocene biomarker and pollen records in Southeast Atlantic Ocean sediments indicate environmental changes

F. ROMMERSKIRCHEN[1], L. DUPONT[1], T. CONDON[2], G. MOLLENHAUER[3], E. SCHEFUß[1]

[1]Marum - Center for Marine Environmental Sciences, University of Bremen, P.O. Box 330 440, D-28334 Bremen, Germany
[2]Department of Earth & Planetary Sciences, Havard University, 20 Oxford Street, Cambidge, MA 02138 USA
[3]Alfred Wegener Institute for Polar and Marine Research, D-27570 Bremerhaven, Germany

The Late Miocene epoch is characterized by fundamental changes in Earth's climate system: sea-level variability, changes in surface- und deep-water circulation, increase in upwelling intensity along the coasts and turnover in marine and terrestrial biota [1,2]. It is thought that plants using the CO_2 concentrating C_4 mechanism for photosynthesis potentially evolved during times of a global drop in atmospheric CO_2 content and at relatively hot and dry habitats. During the Late Miocene C_4 plants expanded nearly simultaneously at different places in the world, while temperatures declined and global CO_2 levels exhibited no corresponding change [1,3]. Our objectives concern the climatic and environmental change of Miocene Southwest Africa between ~14 to ~5 Myrs BP and how these conditions may be linked to the C_4 plant expansion.

We use a variety of organic geochemical techniques combined with palynology on sediments of ODP Site 1085. The site is situated in the Cape Basin at the south-west African continental margin, within the today's upwelling zone of the Benguela Coastal Current. Miocene sea surface temperature (SST) estimates applying two indices (TEX_{86} and $U^{K'}_{37}$) suggest a transition to cooler temperatures from above 27 to 18°C over a time period from ~14 to ~5 Myrs BP, but are different in rate and timing. Increased upwelling leads to cooler SSTs and enhanced marine primary production as implied by a small but clear overall shift in total organic carbon content after 11 Myrs BP. Concurrently, the abundance of both marine cysts and terrestrial pollen and spores increase and the relative contribution river run-off from the nearby Orange River declines, as indicated by the BIT-index (from ~0.8 to <0.1). We connect these findings to a change in strength and the predominant direction of the wind combined with an intensification of the Benguela upwelling current bringing cold, nutrient-rich waters from the South Atlantic and the Antarctic circumpolar current, probably driven by the formation of the West Antarctic ice sheet [1,2]. The transport way for terrestrial organic matter, pollen and spores changed from riverine to predominantly airborne contribution potentially accompanied by a change of the source area. However, pollen records and molecular stable carbon and hydrogen isotopic measurements of plant leaf wax n-alkanes exhibit spreading grassy vegetation due to a stepwise growing aridity in South Africa. After 8 Myrs BP terrestrial floral assemblages got more affinity to those of the Pleistocene and mark the beginning of the floral change towards C_4-dominance (oder "the beginning of C4-expansion"). We infer that by the end of the Miocene C_4 grasslands became important in Southwest Africa.

References:
[1] Zachos, J. et al. (2001) Science 292, 686-693.
[2] Diester-Haass, L.D., et al. (1990) Paleoceanogr. 5, 685-707.
[3] Tipple, B.J., Pagani, M. (2007) Annu. Rev. Earth Planet. Sci. 35, 435-461.

IODP

Diversity of phages from deep-biosphere populations of Rhizobium radiobacter

M. SAHLBERG, T. ENGELHARDT, H. CYPIONKA, B. ENGELEN

Institut für Chemie und Biologie des Meeres, Carl-von-Ossietzky Universität Oldenburg, Carl-von-Ossietzky Straße 9-11, D-26111 Oldenburg, Germany, http://www.pmbio.icbm.de

Throughout the last years, we have obtained interesting insights into the microbial community composition of the marine deep biosphere while the viral inventory of deep-subsurface sediments was not studied so far. Viruses might be the main "predators" for indigenous microorganisms and probably have a major impact on deep biosphere populations in providing labile organic compounds for this generally nutrient depleted habitat.

More than 70% of all known bacterial genomes contain prophage sequences (Canchaya et al. 2003). Prophages can be induced to become free phage particles if the host cells are set under certain stress situations such as a treatment with DNA-damaging antibiotics (Chen et al. 2006). Therefore, culture collections from a respective habitat represent an archive of its viral diversity.

We have cultivated several deep biosphere organisms from ODP Leg 201 (Batzke et al. 2007) and have recently performed a study on the presence of prophages within the genomes of representative isolates (Engelen et al. 2010). Among others, this culture collection comprises a number of fourty isolates of R. radiobacter from different ODP sites and sediment depths of the Equatorial Pacific and the Peru margin. Rhizobium radiobacter was shown to be a highly abundant inhabitant of Mediterranean subsurface sediments (Süß et al. 2006). This was proven for Leg 201 sediments by applying quantitative PCR (qPCR). Therefore, R. radiobacter was chosen as a model organism to identify the intra-species diversity and the biogeography of phages that infect deep biosphere populations of this species.

In this study, we want to test whether our isolates contain the same viruses or if they exhibit distribution patterns that are correlated to certain sampling sites or sediment layers. Beforehand, the isolated strains were grouped into four clusters by a molecular technique (ERIC-PCR) to differentiate them below the species level. Fifteen representative isolates of the different clusters were chosen for phage induction experiments using the antibiotic mitomycin C. All of the investigated strains were tested positively for inducible phages. A further molecular study on the phage diversity by pulsed-field gel electrophoresis (PFGE) revealed the presence of several phages with varying genome sizes. The different morphotypes were visualized by transmission electron microscopy (TEM).

In a future project, we will extend our investigations to R. radiobacter strains that were isolated from Mediterranean subsurface sediments. As most of these isolates derived from sapropel layers, their origin can be correlated to the time period and environmental conditions

of sediment deposition. These investigations focus on the question whether viral infections took place in the water column by virioplankton or specifically within the subsurface. As R. radiobacter is ubiquitous, a comparison with isolates from terrestrial habitats will furthermore elucidate if they were already infected when they entered the marine environment.

References:
Batzke A, Engelen B, Sass H, Cypionka H (2007) Phylogenetic and physiological diversity of cultured deep-biosphere bacteria from Equatorial Pacific Ocean and Peru Margin sediments. Geomicrobiology J 24:261-273
Canchaya C, Proux C, Fournous G, Bruttin A, Brussow H (2003) Prophage genomics. Microbiology and Molecular Biology Reviews 67: 238-276.
Chen F, Wang K, Stewart J, Belas R (2006) Induction of multiple prophages from a marine bacterium: a genomic approach. Applied and Environmental Microbiology 72: 4995-5001.
Engelen B, Engelhardt T, Sahlberg M, Cypionka H (2010) Bacteriophages as a component of the marine deep biosphere. Environ Microbiol (submitted, 22.01.2010)
Süß J, Schubert K, Sass H, Cypionka H, Overmann J, Engelen B (2006) Widespread distribution and high abundance of Rhizobium radiobacter within Mediterranean subsurface sediments. Environ Microbiol 8:1753-1763

IODP

Mid-Pliocene North Atlantic palaeoceanography based on palynology, Mg/Ca of planktonic foraminifers and alkenones

S. DE SCHEPPER[1], M.J. HEAD[2], J. GROENEVELD[3], D. NAAFS[3]

[1]Fachbereich Geowissenschaften, Universität Bremen, Postfach 330 440, D-28334 Bremen <sdeschepper@uni-bremen.de>
[2]Department of Earth Sciences, Brock University, 500 Glenridge Avenue, St. Catharines, Ontario L2S 3A1
[3]Alfred Wegener Institute, Columbusstrasse, D-27570 Bremerhaven

The mid-Pliocene was an episode of prolonged global warmth and strong North Atlantic thermohaline circulation, interrupted briefly at ca. 3.30 Ma by a global cooling event corresponding to Marine Isotope Stage (MIS) M2. We have combined Mg/Ca ratios and $\delta^{18}O$ from Globigerina bulloides with dinoflagellate cyst assemblage data from three IODP/DSDP sites to reconstruct the palaeoceanography of the eastern North Atlantic between ca. 3.4 and 3.2 Ma.

Sea-surface temperature reconstructions indicate warm waters at IODP Site 1308 and DSDP Site 610 before and after MIS M2, but a cooling of ca. 2–3˚C during MIS M2. A dinoflagellate cyst assemblage overturn, characterized by a significant decline in Operculodinium centrocarpum at those sites, points to a reduced northward heat transport and weakened influence of the NAC. The reduced northward heat transport at the northerly sites occurs about 23–35 ka in advance of the maximum global ice volume of MIS M2. Hence, it has been suggested that changes in North Atlantic circulation led to the expansion of the Greenland ice-sheet during MIS M2 (De Schepper et al., 2009). Preliminary results from the more southerly IODP Site U1313 apparently do not record the marked changes of the northerly site. Our foraminiferal Mg/Ca data and the dinoflagellate cyst assemblages show minor variability and no expressed cooling around MIS M2, suggesting that only the higher latitudes experienced significant cooling. In contrast, cooling is reflected around that time in an alkenone based sea-surface temperature record from the same site.

Our multiproxy approach also allows a first attempt at unravelling the ecological preferences of extant and extinct Pliocene dinoflagellate cysts. For at least one species, Impagidinium pallidum, a contradiction is apparent between its present and Pliocene spatial and temporal distributions, which could be explained by changes in seasonality, transport paths, and/or ecological preference.

References:
De Schepper, S., Head, M. J. & Groeneveld, J., 2009. North Atlantic Current variability through marine isotope stage M2 (circa 3.3 Ma) during the mid-Pliocene. Paleoceanography 24(4), PA4206, doi:10.1029/2008PA001725

IODP

Geophysical results from an IODP site survey for planned investigation of the deep biosphere at North Pond (Mid-Atlantic-Ridge).

F. SCHMIDT-SCHIERHORN[1], U. BECKERT[1], N. KAUL[1], A. POLSTER[1], A. SCHWAB[1], S. STEPHAN[1], H. VILLINGER[1] AND MSM 11/1 SHIPBOARD SCIENTIFIC PARTY

[1]Fachgebiet Meerestechnik/Sensorik,FB Geowissenschaften, Universität Bremen,Postfach 330 440,D-28334 Bremen Germany

North Pond is an isolated small sediment pond (8 km by 14 km) located on the western flank of the Mid-Atlantic Ridge (23°N) which offers the opportunity to study microbial communities and their activities in deeply-buried sediments and the underlying basement. One important argument for choosing North Pond was that the geochemistry, hydrology, and geologic setting of North Pond had been previously studied by a series of DSDP and ODP drill holes and seafloor observatories. However the existing site survey data are not sufficient for the approved North Pond IODP drilling expedition, scheduled to take place in FY 2011. Therefore we proposed a site survey of North Pond in order to be able to position the new planned IODP holes precisely. These surveys compromise a detailed seismic mapping of the sediment-basement interface of North Pond, additional heat flow data and geochemical and microbial sampling of the sediments. The site survey cruise on RV Maria S. Merian (MSM 11/1) took place from February 17 – March 12, 2009 (Fort-de-France, Martinique to Dakar, Senegal). Due to an accident on board the scheduled working days on site were reduced from 14 to 6 days. Therefore a number of detailed investigations especially in the southern part of the basin had to be abandoned.

The mapping of bathymetry, sediments and basement topography confirms the existing results based on two seismic profiles from 1989 but the new data show much more detail. The new bathymetry of the pond reflects in part the topography of the sediment covered basement ridges which are also seen in the high-resolution sediment echosounding records (Parasound). They also reveal a number of turbidites and a large slump body which originated on the south-western basement highs. Unfortunately the 14 single channel seismic records do not show the sediment-basement interface very clearly probably due to the small scale topographic relief of this

boundary and also maybe due to insufficient acoustic energy. However, the records allow mapping the basement topography to a much greater detail than before. In total 52 successful heat flow measurements complement the existing heat flow coverage of Langseth et al. (1992) and confirm the hydrothermal circulation pattern with inflow of cold seawater at the southern rim of the basin and upflow of warm water at the north/north-eastern boundary. The new detailed geophysical data set will allow to position the proposed drillholes and constrain hydrogeological modeling of the circulation in the upper crust.

References:

Langseth, M., Becker, K., Von Herzen, R., Schultheiss, P., 1992. Heat and fluid flux through sediment on the western ank of the mid-atlantic ridge: a hydrogeological study of North Pond. Geophysical Research Letters 19, 517-520.

IODP

Palynostratigraphy and Paleoenvironment of Arctic and Subarctic Neogene Sediments:

A magnetostratigraphic calibration of ODP Site 907A dinocyst events

M. SCHRECK, J. MATTHIESSEN

Alfred Wegener Institute for Polar and Marine Research (AWI), Bremerhaven, Germany

The High Northern Latitudes are a sensitive region for climate change on various timescales and played an important role on Earth's final way from the "Greenhouse World" into the fully glaciated, so called "Icehouse World". Superimposed on this long-term climate development frequent short-term climate changes occurred leading to rather variable climate conditions during the Neogene and finally to the pronounced glacial-interglacial cycles in the Pleistocene (e.g. Flower and Kennett 1994). In the Miocene the Nordic Seas experienced a reorganisation of ocean circulation due to the opening of the major arctic gateway, Fram Strait. The Pliocene is an important epoch because it marks the transition from rather restricted local to extensive regional scale glaciations on the circum-arctic continents between 3.6 and 2.4 Ma. Despite these facts the exact timing of certain paleoclimatic events is still a matter of intensive debate due to the inconsistent chronostratigraphic framework of northern high latitude Neogene sequences. The chronostratigraphy is principally based on magnetostratigraphy supported by age datums of various microfossil groups whereas stable isotope records on benthic and planktic foraminifers play only a subordinate role because of strongly discontinuous records due to the low content of biogenic carbonate in the hemipelagic sediments. A consistent biostratigraphy that allows placing magnetostratigraphy and beryllium isotope stratigraphy into an absolute temporal framework is still not available. Therefore the long-term paleoenvironmental evolution of the Nordic Seas and the Arctic Ocean is still virtually unknown although Neogene sequences have been successfully drilled during ODP Legs 104, 105, 151 and 162.

To overcome this obstacle we investigate marine palynomorphs (e.g. dinoflagellate cysts and acritarchs) within the project „Palynomorphs in the Northern High Latitude Cold Water Domain: A Neogene Stratigraphic and Paleoenvironmental Transect across the Fram Strait" (DFG-MA3913/2). Dinoflagellate cysts (dinocysts) are the only microfossil group continuously present in subarctic sediments and occurring irregularly in Arctic Ocean sediments throughout the Neogene. They have been proven valuable in solving correlative and chronostratigraphic problems related to ODP/IODP drillings as well as for paleoecological and paleoenvironmental reconstructions in the High Northern Latitudes.

The studied transect consists of ODP Sites 907 and 909 in the seasonally ice-covered Nordic Seas and IODP Site M2A in the perennial ice-covered Arctic Ocean. Site 907A in the Icelandic Sea, with an almost continuous Neogene sequence recovered, is our standard reference section for the past 16 Ma. Its revised high-resolution magnetic polarity stratigraphy (Channel et al. 1999) based on the composite section of three holes is well dated and additionally tied to an independent diatom biostratigraphy (Koç and Scherer 1996). Therefore it provides one of the best Neogene high northern latitude chronostratigraphic records and was used to calibrate our palynomorph datums to the Astronomical Tuned Neogene Timescale (ATNTS 2004) of Lourens et al. (2005). We follow Gibbard et al. (2009) for the newly ratified position of the Pliocene–Pleistocene boundary.

In an initial study Poulsen et al. (1996) established an informal dinocyst zonation for ODP Leg 151 Sites 907-909 with an average resolution of 60-300kyr consisting of three dinocyst zones for Site 907. Based on the established age-model and in order to improve the temporal resolution Hole 907A was initially sampled at 100kyr intervals from the base up to 2.58 Ma. With our study we extend the dinocyst record of Poulsen et al. (1996) up to the Piacenzian/Gelasian boundary. A careful study of 907A dinocysts and comparison with Poulsen et al. (1996) revealed several discrepancies in the taxonomy, and estimates of abundances are partly not reproducible. As a result of our investigation on Site 907A it is evident that taxonomic concepts of more high latitude dinocyst taxa must be reevaluated than expected in order to make reliable interpretations on their stratigraphic value and paleoenvironmental significance.

The analysed section from 11.8 to 2.58 Ma (137.5-49.1 mbsf) is characterized by a distinct three-step decrease of both dinocyst abundances and diversity clearly reflecting the general long-term cooling trend since the Middle Miocene. This long-term dinocyst evolution is punctuated by numerous short-term variations and we identified different assemblages and distinctive suites of acmes possibly indicating considerable changes in the physical characteristics of water masses.

1) From 11.4 to 8.3 Ma (137.5-104 mbsf) dinocyst abundance and diversity are highest throughout the entire section analysed but decreasing rapidly at the top of this interval. The species richness varies from 19 to 45 species per sample with an average of 30 species per sample. Nevertheless, dinocyst concentration (cysts/g sediment) varies significantly which might be caused by the statistical error of the marker grain counts. Baticasphaera species (mainly B. minuta) associated with H. tectata and the Spiniferites/Achomosphaera complex are dominating the assemblages. Protoperidinium spp. recorded only sporadically in the upper part is common and peridinioid cysts like C. cristatoserratum, Selenopemphix spp.,

Lejeunecysta spp. and B. graminosum are recorded frequently. Protoperdinioid and peridinioid species are considered to be heterotrophic and thus may indicating increased nutrient availability in the surface waters. Between 122.7 to 104.5 mbsf the occurrence of warm water taxa e.g. L. machaerophorum, M. choanophorum and D. pastiellsii in association with the frequently recorded cold water sensitive O.? eirikanum may display a temporary pronounced inflow of warmer proto North Atlantic Current water into the Icelandic Sea. Nevertheless cold-water indicator I. pallidum and cold-water tolerant H. tectata are still abundant supporting a temporal nature of these possible events.

Since the Neogene comprises a considerable number of extinct species (e.g. D. martinheadii, B. minuta), their paleoecological affinities cannot simply be inferred from a modern distribution. Therefore a different approach using the relationship between their paleogeographic distribution and the known paleoclimate evolution is additionally applied.

In addition we recognised several first appearance and last appearance datums (FAD, LAD) within this section e.g. C. cristatoserratum (FAD, LAD), L. truncatum (LAD), D. martinheadii (FAD), D. pastiellsii (LAD), H. obscura (LAD), O. piaseckii (LAD), Impagidinium sp. 3 of Manum et al. 1989 (LAD) and different undescribed Operculodinium und Spiniferites species. The LAD of L. truncatum and C. cristatoserratum are located close to the top of this interval and their disappearance might be associated with the subsequent cooling near the Miocene/Pliocene boundary

2) The following section from 103.5 to 99.5 mbsf (9 samples, approx. 900 kyr) is complete barren of dinocysts and pollen and bisaccates are absent. This might be due to sample resolution and the samples recorded intervals with unfavourable conditions, e.g. glacials or periods with limited productivity due to sea ice cover. Preservational effects must also be considered as a possible explanation although preservation is good to moderate throughout the complete core. This interval is designated for resampling at higher resolution to explain causes for the absence of palynomorphs.

3) Within the 7.2 to 4.2 Ma (99.0-71.2 mbsf) interval assemblage diversity decreases and the richness varies between 3 to 19 species with an average of 10.5 species per sample. This interval is characterized by huge variations in both dinocyst abundances and diversity possibly reflecting short-term changes in the environmental setting and water mass properties. Besides decreasing dinocyst abundance and diversity we recognised a distinct shift in assemblage composition. The assemblages are now dominated by N. labyrinthus, an outer neritic to oceanic species with arctic to tropical distribution today (Marret and Zonneveld 2003). It is often associated with I. pallidum and I. cf. japonicum. Impagidinium species are considered to be oceanic and I. pallidum is typical for cold environments where seasonal sea-ice cover occurs (Marret and Zonneveld 2003). We recognized several range tops of stratigraphically valuable species in the upper part of this interval, e.g. B. minuta and R. actinocoronata. Their disappearance is likely to have been associated with the subsequent cooling around the mid Pliocene transition.

Between 5.2 to 4.7-Ma (81.2-76.2 mbsf) the abundance of N. labyrinthus drops to 5-7% whereas the dinocyst concentration reaches maximum values in this part. N. labyrinthus is mainly replaced by B. minuta, S. elongatus, S. ramosus group, O. tegillatum and Protoperidinium spp. Both may indicate an increased productivity and nutrient-rich surface water conditions. We found a single specimen of M. choanophorum and 3 specimen of O. israelianum in this specific interval. Both are considered to be warm-water species but the low abundance may suggest reworking. In addition the acritarch C.? invaginata reaches highest abundance in this interval.

4) The interval from 4.2 to 2.58 Ma (71.2-49.1 mbsf) yielded only very small amounts of dinocysts and the species richness varies between 1 to 5 species per sample with an average of 2.4 species per sample. The dinocyst concentration is very low with only a few specimens recorded. In addition, we found several barren samples containing not a single specimen, possibly reflecting a cold environment in the Late to Middle Pliocene. This interval coincide with the first major IRD peaks at Site 907 around 3.5-3.3 Ma marking an expansion of the Greenland ice sheet (Jansen et al. 2000). Statistically significant counts of 350 dinocysts were not practicable except for two neighbouring samples (7H7 41-43; 7H6 87-89). Both samples are almost monogeneric Spiniferites sp. assemblages with abundances of 99.5% and 98.3% respectively and are calibrated to 3.41 and 3.34 Ma. The genus Spiniferites is known to prefer a more neritic setting and this acme is difficult to reconcile with a scenario in which these dinoflagellates thrived in pelagic, offshore surface waters. This acme of a near-shore indicator might be the result of increased transportation in response to sea level falls as suggested by Pross et al. (2009) and might have caused a basinward shift of the optimum habitats of neritic taxa.

As already mentioned this study identified several useful marker species and datums at Site 907A which are calibrated to the ATNTS 2004. The identification of these datums in Holes 909C and M2A from the Fram Strait and the Central Arctic Ocean reveal that previous age models must be revised, having implications for published paleoenvironmental reconstructions that were based on these sites. These datums are used to establish a biozonation in detail that surpasses earlier studies in the Neogene of the High Northern Latitudes. Due to the detailed character of this study several undescribed or open nomenclature species and morphotypes (e.g. Impagidinium sp. 3 of Manum et al. 1989) with so far unknown stratigraphic range and paleoecological requirements are recorded and their stratigraphic value must be evaluated by comparison with other high latitude dinocyst studies. Many of our identified marker species are used in the Norwegian-Greenland Sea Zonation (NGSZ) of Smelror et al. (unpubl. manuscript) but are often rare in 907A and only two of them (D. martinheadii and F. filifera) are recorded in IODP Site M2A so far (Matthiessen et al. 2009). This is partly due to the more temperate-warm water affinities of the stratigraphic markers proposed by Smelror et al. (unpubl. manuscript). We attempt to incorporate as many zonal markers of the NGSZ into our coldwater zonation to allow correlation between the Nordic Seas and Arctic Ocean but nevertheless it displays that new marker species are required to establish a consistent and comprehensive high resolution palynostratigraphic framework for the cold-

water as well as for the warm-water domain of the Nordic Seas and the Arctic realm.

For example, the assemblages between 93.5 to 94.4 mbsf are dominated by an acme of D. martinheadii. Based on the magnetostratigraphy the last appearance datum (LAD) is fixed at approx. 6.2 Ma at Site 907A which is similar to its maximum concentration in the Arctic Ocean. Furthermore our study calibrates the first appearance datum (FAD) tentatively at approx. 10.53 Ma and supports a FAD in sediments younger than 13 Ma as proposed by Matthiessen et al. (2009). Of special interest might be the stratigraphic range of B. minuta. Its one of the few species recorded in the Neogene of the Central Arctic Ocean and its used in the previously published Pliocene eastern North Atlantic Zonation of De Schepper and Head (2009). De Schepper and Head used the highest occurrence of B. minuta at 3.83 Ma to define the top of their RT2 interval zone. In 907A the LAD of B. minuta is tentatively calibrated at approx. 3.41 Ma. The causes for this asynchrony disappearance are not evaluated yet but a well-defined range might allow for spatial and temporal correlation between these different marine realms. Furthermore, the persistent occurrence of several palynomorphs with unclear biological affinity (acritarchs) might be of stratigraphic use in the High Northern Latitudes and will be evaluated in more detail.

References:

Channell, J. E. T., Amigo, A. E., Fronval, T., Rack, F. and Lehman, B. 1999. Magnetic stratigraphy at Sites 907 and 985 in the Norwegian-Greenland Sea and a revision of the Site 907 Composite section. In: M.E. Raymo, E. Jansen, P. Blum and T.D. Herbert (Editors), Proceedings *of the Ocean Drilling Program, Scientific Results*. 131-148.

De Schepper, S. and Head, M.J. 2009. Pliocene and Pleistocene dinoflagellate cyst and acritarch zonation of DSDP Hole 610A, Eastern North Atlantic. *Review of Palaeobotany and Palynology*. 179-218

Flower, B.O. and Kennett, J. P. 1994. The middle Miocene climate transition: East Antarctic ice sheet developpment, deep ocean circulation and global carbon cycling. *Palaeogeography, Palaeoclimatology, Palaeoecology*. 108: 537-555.

Jansen, E., Fronval, T., Rack, F. and Channel, J.E.T. 2000. Pliocene-Pleistocene ice rafting history and cyclicityin the Nordic Seas during the last 3.5 Myr. *Paleoceanography*. 709-721.

Koç, N. and Scherer, R.P. 1996. Neogene diatom biostratigraphy of the Icelandic Sea Site 907. In: J. Thiede, A. Myhre, J.V. Firth, G.L. Johnson and W.F. Ruddiman (Editors), *Proceedings of the Ocean Drilling Program, Scientific Results.* 151, 61-74.

Manum, S.B., Boulter, M.C., Gunnarsdottir, H., Rangnes, K. and Scholze, A. 1989. Eocene to Miocene Palynology of the Norwegian Sea (ODP Leg 104). In: O. Eldholm, J. Thiede and E. Taylor (Editors), *Proceedings of the Ocean Drilling Program*, *Scientific Results* 104, 611-662.

Marret, F. and Zonneveld, K. 2003. Atlas of organic-walled dinoflagellate cyst distribution. *Review of Palaeobotany and Palynology*. 1-200

Matthiessen, J., Brinkhuis, H., Poulsen, N., Smelror, M. 2009. Decahedrella martinheadii – a stratigraphic and paleoenvironmental acritarch indicator species for the high norther latitude Late Miocene. *Micropaleontology*

Poulsen, N.E., Manum, S.B., Williams, G.L. and Ellegard, M. 1996. Tertiary dinoflagellate biostratigraphy of Site 907, 908, and 909 in the Norwegian-Greenland Sea. In: J. Thiede, A. Myhre, J.V. Firth, G.L. Johnson and W.F. Ruddiman (Editors*), Proceedings of the Ocean Drilling Program, Scientific Results.* 151, 243-253.

Pross, J., Houben, A.J.P., van Simaeys, S., Williams, G.L., Kotthoff, U., Coccioni, R., Wilpshaar, M. and Brinkhuis, H. 2010. Umbria-Marche revisited: A refined magnetostratigraphic calibration of dinoflagellate cyst events for the Oligocene of the Western Tethys. *Review of Palaeobotany and Palynology*. 213-235

Smelror, M. and Anthonissen, E.: A Neogene dinoflagellate cyst biozonation for the Norwegian-Greenland Sea. (unpubl. manuscript)

IODP

Oceanographic and climate changes during the Latest Danian event in the Atlantic: Evidence for a hyperthermal event?

P. SCHULTE[1], A. BORNEMANN[2], R.P. SPEIJER[3]

[1]GeoZentrum Nordbayern, Universität Erlangen, Schlossgarten 5, D-91054 Erlangen, Germany
[2]Institut für Geophysik und Geologie, Universität Leipzig, D-04103 Leipzig, Germany
[3]Department of Earth and Environmental Sciences, K.U. Leuven, B-3001 Leuven, Belgium

The Paleocene to early Eocene is punctuated by several transient, 20-200 ky lasting hyperthermal events of which the Paleocene-Eocene Thermal Maximum (PETM) was the most prominent one. Abrupt shallowing of the lysocline/CCD, negative carbon isotope excursions, and benthic faunal turnover all imply a major perturbation of the ocean system during these events. Our recent research at the Southern Tethyan shelf suggests the presence of an additional hyperthermal event associated with sea-level fluctuations, the Latest Danian Event (LDE; Speijer, 2003; Bornemann et al., 2009). At Zumaia, Northern Spain, a negative 0.5 per mil carbon isotope excursion is present in the uppermost Danian that may correlate to the LDE (Arenillas et al. 2008). Moreover, cyclostratigraphic studies have shown that several deep-sea sites are characterized by a prominent peak in both Fe and MS data at cycle Pc100-38 in the uppermost Danian: This applies to all Walvis Ridge (Atlantic) and Shatsky Rise (Pacific) sites as well as Site 1001 in the Caribbean Sea (Top Chron C27n Event; Westerhold et al., 2007). These results suggest that the LDE in the Tethys and the Top Chron C27n Event in the Atlantic may be correlative. We have conducted mineralogical, geochemical, and micropaleontological investigations to characterize this event in the Western Atlantic.

The first results of this pilot project successfully revealed that at ODP Leg 165 Site 1001A the "Top Chron 27n Event" (Westerhold et al., 2007) does correspond to (i) a ~0.5 ‰ negative carbon isotope excursion, (ii) a brief phase of deep-sea carbonate dissolution, and (iii) changes in the terrigeneous detritus input that may reflect an amplified hydrological cycle. In more detail, at Site 1001 the Top Chron 27n Event is reflected by a 12 cm thick clay layer. The biostratigraphic analysis of the enclosing interval shows that the preservation of calcareous plankton is extremely poor and only the FAD of Sphenolithus primus (base NTp8) has been identified, but seems to be diachronous to the standard nannofossil zonation scheme (e.g., Bernaola et al., 2009; Sprong et al., 2009). Therefore the existing magnetostratigraphy in combination with the XRF core scanning data of Westerhold et al. (2007) are much more promising for correlating the clay layer in core with other deep-sea sections. Although there is some scatter in the data, the general trend of the stable isotopes shows a sharp ~0.5 ‰ drop of the carbon isotopes that is followed by a gradual recovery (Fig. 1 and 2). The oxygen isotopes does show an about 1 ‰ positive anomaly correlative to the carbon isotope excursion, although the very negative values (about –4 ‰) of the oxygen isotopes indicate a strong diagenetic overprint that may have affected the clay-rich layers to a lesser degree than the calcium carbonate-rich background sediments.

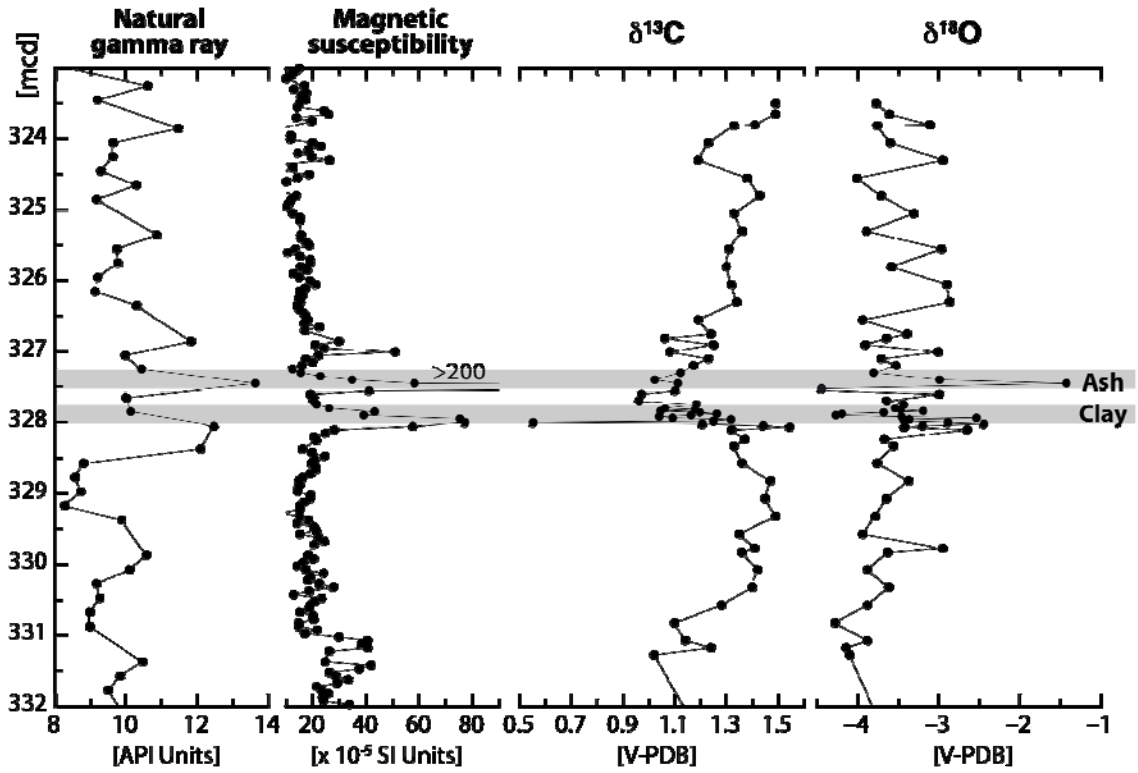

Fig. 1. Geophysical and bulk rock stable isotope data for core 1001A-36.

Mineralogical analyses reveal a sharp 50% drop of the carbonate content in the clay layer and a disproportionally high increase of the phyllosilicate content in the insoluble residue compared to the quartz and illite content. The magnitude and pattern of the carbon isotope excursion is very similar to the results for the LDE in the Tethys and at Zumaia. In conclusion, our results demonstrate a supra-regional transient perturbation of the carbon cycle during the LDE in the Tethyan realm, the Atlantic, and possibly the Pacific Ocean.

Our results suggest that the sharp peak in Fe intensity and magnetic susceptibility corresponding to the Top Chron C27n event at cycle Pc10038 found at Walvis Ridge (1262), Shatsky Rise (1209), and Zumaya (Dinarès-Turell et al., 2007; Westerhold et al., 2007) represents indeed a short term, possibly global perturbation of the carbon cycle. This interpretation is substantiated by recently published studies that indicate a correlative negative 0.5 ‰ carbon isotope anomaly correlative to the "Chron 27n event" in Zumaya (Arenillas et al., 2008) as well as high-resolution biostratigraphic studies that suggest a good correlation of this event at Zumaya to the Late Danian event in sections from the Tethys (Bernaola et al., 2009); see also Bornemann et al. (2009) for details. Various approaches to estimate the duration of the Latest Danian Event suggest that the carbon isotope anomaly lasted between 100 and 191 ka (Bornemann et al., 2009).

Our preliminary findings strongly support interpretations that hyperthermal events occurred multiple times during the early Paleogene and were indeed of global significance. The repeated occurrence of these events in the early Paleogene starting shortly after the K-Pg boundary has been interpreted as reflecting orbital pacing by Milankovitch cycles (e.g., Lourens et al., 2005; Westerhold et al., 2007). If this is the case, the orbital pacing eventually controls the timing and probably the intensity of these events. Although many characteristics of these pre- and post-PETM events are similar to those characterizing the PETM, they are all of shorter duration and of less intensity (Lourens et al., 2005; Nicolo et al., 2007; Agnini et al., 2009; Stap et al., 2009). Some authors hypothesize that the early Eocene hyperthermals result from repeated releases of methane hydrates, possibly triggered by precursor deep-sea warmings (Nicolo et al., 2007; Sluijs et al., 2007). However, it was also suggested that multiple occurrences of negative carbon isotope excursions with reduced magnitude and rapid rate of recovery compared to the PETM indicate that the carbon is not derived from deeply buried sources, but rather represent redistribution of carbon within the biosphere (Quillévéré et al., 2008).

The apparently prolonged recovery of the carbon isotopes during the LDE event is similar to the ELMO and X-events but differs from the stratigraphically older DAN-C2 event. Estimates of carbon sequestration times (Quillévéré et al., 2008) suggests that for these events (including the PETM) the CO_2 was possibly not derived from redistribution of carbon already in the ocean-atmosphere-biosphere system, but was injected from buried carbon reservoirs. These contrast with the DAN-C2 event which has a fairly symmetrical shape and is of significantly shorter duration, and thus may have triggered by carbon release from areas with expanded oxygen minimum zones or anoxic marginal seas, soils and peat, or surficial organic-rich sediments.

An additional aspect of this study is that the stable isotope chemostratigraphy (e.g., Weissert et al., 2008) may improve cyclostratigraphic studies by providing additional tie points beyond magneto and/or biostratigraphy (e.g.,

Westerhold et al., 2007). This may help to resolve differences for the absolute cycle counts for the Paleocene included for instance in Westerhold et al. (2007) and Dinarès-Turell et al. (2007).

Acknowledgments: We are grateful to the IODP for providing sample material and the DFG for funding (SCHU 2248/5).

References:

Agnini, C., Macrì, P., Backman, J., Brinkhuis, H., Fornaciari, E., Giusberti, L., Luciani, V., Rio, D., Sluijs, A., and Speranza, F., 2009, An early Eocene carbon cycle perturbation at ~52.5 Ma in the Southern Alps: Chronology and biotic response: Paleoceanography v. 24, p, PA2209.

Arenillas, I., Molina, E., Ortiz, S., and Schmitz, B., 2008, Foraminiferal and d^13^C isotopic event-stratigraphy across the Danian-Selandian transition at Zumaya (northern Spain): chronostratigraphic implications: Terra Nova v. 20, p, 38–44.

Bernaola, G., Martín-Rubio, M., and Baceta, J.I., 2009, New high resolution calcareous nanofossil analysis across the Danian/Selandian transition at the Zumaia section: Comparison with South Tethys and Danish sections: Geologica Acta v. 7, p, 79–92.

Bornemann, A., Schulte, P., Sprong, J., Steurbaut, E., Youssef, M., and Speijer, R.P., 2009, Latest Danian carbon isotope anomaly and associated environmental change in the southern Tethys (Nile Basin, Egypt): Journal of the Geological Society, London v. 166, p, 1135–1142.

Dinarès-Turell, J., Baceta, J.I., Bernaola, G., Orue-Etxebarria, X., and Pujalte, V., 2007, Closing the Mid-Palaeocene gap: Toward a complete astronomically tuned Palaeocene Epoch and Selandian and Thanetian GSSPs at Zumaia (Basque Basin, W Pyrenees): Earth and Planetary Science Letters v. 262, p, 450–467.

Dinarès-Turell, J., Baceta, J.I., Pujalte, V., Orue-Etxebarria, X., Bernaola, G., and Lorito, S., 2003, Untangling the Palaeocene climatic rhythm: An astronomically calibrated Early Palaeocene magnetostratigraphy and biostratigraphy at Zumaia (Basque basin, northern Spain): Earth and Planetary Science Letters v. 216, p, 501–514.

Lourens, L.J., Sluijs, A., Kroon, D., Zachos, J.C., Thomas, E., Röhl, U., Bowles, J., and Raffi, I., 2005, Astronomical pacing of late Palaeocene to early Eocene global warming events: Nature v. 435, p, 1083–1086.

Nicolo, M.J., Dickens, G.R., Hollis, C.J., and Zachos, J.C., 2007, Multiple early Eocene hyperthermals: Their sedimentary expression on the New Zealand continental margin and in the deep sea: Geology v. 35, p, 699–702.

Quillévéré, F., Norris, R.D., Kroon, D., Wilson, P.A., and Wilson, P., 2008, Transient ocean warming and shifts in carbon reservoirs during the early Danian: Earth and Planetary Science Letters v. 265, p, 600–615.

Sluijs, A., Brinkhuis, H., Schouten, S., Bohaty, S.M., John, C.M., Zachos, J.C., Reichart, G.-J., Sinninghe, D., Jaap S., Crouch, E.M., and Dickens, G.R., 2007, Environmental precursors to rapid light carbon injection at the Palaeocene/Eocene boundary: Nature v. 450, p, 1218–1221.

Speijer, R.P., 2003, Danian-Selandian sea-level change and biotic excursion on the southern Tethyan margin (Egypt), in Wing, S.L., Gingerich, P.D., Schmitz, B., and Thomas, E., ed., 369: p. 275–290.

Sprong, J., Speijer, R.P., and Steurbaut, E., 2009, Biostratigraphy of the Danian/Selandian transition in the southern Tethys. Special reference to the lowest occurrence of planktic foraminifera Igorina albeari.: Geologica Acta v. 7, p, 63–77.

Stap, L., Sluijs, A., Thomas, E., and Lourens, L., 2009, Patterns and magnitude of deep sea carbonate dissolution during Eocene Thermal Maximum 2 and H2, Walvis Ridge, southeastern Atlantic Ocean: Paleoceanography v. 24, p, PA1211.

Weissert, H., Joachimski, M.M., and Sarnthein, M., 2008, Chemostratigraphy: Newsletters on Stratigraphy v. 42, p, 145–179.

Westerhold, T., Röhl, U., Raffi, I., Fornaciari, E., Monechi, S., Reale, V., Bowles, J., and Evans, H.F., 2007, Astronomical calibration of the Paleocene time: Palaeogeography, Palaeoclimatology, Palaeoecology v. 257, p, 377–403.

ICDP

Quartz weathering in freeze-thaw cycles; experiment and application as a permafrost tracer to El'gygytgyn sedimentary records

G. SCHWAMBORN[1], G. FEDOROV[2], B. DIEKMANN[1], L. SCHIRRMEISTER[1], H.-W. HUBBERTEN[1]

[1]Alfred Wegener Institute for Polar and Marine Research, D-14473 Potsdam

[2]Arctic and Antarctic Research Institute, RUS-199937 St. Petersburg

Summary: Brittle and fragile sand and silt is produced in Siberian near surface permafrost. It makes up much of the regolith in permafrost areas such as Arctic Siberia. Microscopical grain features (e.g. angular outlines, surficial microcracks) stem from cryogenic destruction in the course of numerous seasonal freezing and thawing events in the uppermost soil. Even after a grain is transported off place (i.e. in mobile slope material, in seasonal melt-water run-off, into a lake basin), it still keeps the particular weathering traces in their single grain micromorphology.

This is also valid for a mineralogical peculiarity; frost weathering is a selective grain break-up. In contrast to lower latitudes, quartz is more sensitive to weathering in high latitudes. Quartz quickly reacts to cryogenic break-up and small grains disintegrate due to the explosive power of expanding ice in micro-meter scale fissures. This quartz enrichment in the fines also evolves from seasonal freeze-thaw (F/T) weathering and the grain break-up is demonstrated in an experimental set-up where >100 F/T cycles preferentially crack quartz grains (with reference to feldspar). Minerogenic debris in the upper 12 core meters from El'gygytgyn Crater lake, which is placed north of the Arctic circle in NE Russia, is characterised by silt abundance, cryogenic grain micromorphology, and quartz enrichment in the silt fraction. This argues for persistent permafrost conditions in the area back to 220.000 years as reflected by the continuous input of cryogenic weathering detritus into the basin. Even when periods were as warm as or warmer than today (i.e. during the Eemian Interglacial) the permafrost signal does not disappear.

Introduction: Up to now inference of permafrost history mostly relies on studying local sections providing insights into only restricted and mostly Late Quaternary time windows (e.g. Schirrmeister et al., 2002). More limits of studying the permafrost history arise from imprecise age determinations of permafrost due to reworked or out-of-range radiocarbon material, or an insufficient bleaching of OSL material, or the uncertainty of postdepositional permafrost formation (Krbetschek et al., 2002).

The questions we address are; (1) can quartz grain enrichment be confirmed in the silt fraction following numerous F/T cycles for samples from other (non-permafrost) areas (i.e. non pre-cracked grains). This would emphasize the geologic significance of this weathering signal and provide a measurable means for detecting permafrost conditions in historical geology. (2) How does quartz grain enrichment compare to a limnic record where the weathering debris is preserved in a continuous sequence. Hypothetically, lake sediments do approximately reflect surface soil when related to the minerogenic debris. Thus it is possible to trace the weathering signal along an archive with a robust age frame.

The aim is to reconfirm the potential of sensitive quartz weathering for tracing permafrost conditions. A second purpose is to apply the permafrost proxy data to the El'gygytgyn lake sediment record (ICDP project "Elgygytgyn Drilling Project"), a palaeoenvironmental archive that uniquely allows tracing late Cenozoic evolution of Arctic climate and the associated permafrost history (Nowaczyk et al., 2002, Brigham Grette et al., 2007). Backed up by laboratory experiments of frost weathering we develop a sediment-mineralogical data set that links production of cryogenic weathering in a

permafrost environment to a well-dated lake sediment column. This allows testing whether frost weathered quartz grains and their enrichment is a valuable proxy of cryogenic weathering.

Experimental testing and application to El'gygytgyn sediment samples:

For laboratory testing of quartz break-up eight samples have been selected and underwent >100 roundtrips of F/T between -20° to +30°C. Each cycle usually took about 24 hours, where the warming period took 16-18 hours and the freezing period 6-8 hours. Whereas seven samples were kept saturated using deionized water, one sample was kept dry. The samples have the following different geologic origins; samples (1) and (2) were from beach sands of El'gygytgyn Impact Crater lake, NE Russia. This periglacial basin is placed in the zone of continuous permafrost and samples were taken from a raised ancient beach terrace. The first sample was kept saturated; the second sample was kept dry for comparison. Samples (3) and (4) are from floodplains in the Lena River delta, whereby sample 3 contained organics and sample 4 was void of organics. Sample (5) derives from Algerian dune sands taken as a random surface sample; sample (6) is a mixed surface sample from modern surface wash as found in the mouth areas of intermittent creeks draining slopes around El'gygytgyn Crater Lake. Sample (7) is a typical Australian red sand and was taken as a random surface sample at the foot of Ayers Rock in the interior of the continent. Sample (8) derives from randomly sampled surface deposits belonging to an alluvial fan in the Death Valley, USA.

The laboratory scheme included (1) dry-sieving, (2) laser particle sizing (LPS), (3) quartz amounts assessments as measured by XRD (X-ray diffractometry), and (4) SEM (scanning electron microscopy) of single quartz grains. Quartz is assessed A quartz-to-feldspar ratio is calculated according to the "Cryogenic Weathering Index (CWI)" from Konishchev and Rogov (1993). Values >1 are indicative for quartz particle enrichment in the fines. This argues for preferential quartz grain split-up due to cryogenic widening in grain fissures when water freezes and expands to ice. Feldspar serves as a reference mineral, since it is ubiqiutous but less susceptible to frost cracking.

A similar laboratory scheme has been applied to samples from El'gygytgyn Crater surface and lake deposits. In order to make use of a well-dated and continuous archive, the study explores the uppermost 12 m of from El'gygytgyn Crater Lake, NE Siberia (core Lz1024, see Figure). For calibration with subrecent frozen ground deposits sandy lobes in the mouth areas of the intermittent creeks have been sampled and are taken as a reference for modern composition of minerogenic debris (white dots, see Figure 1). The present-day quartz mineralogical signal is compared to the lake record. As a second reference a short drill core (<5 m) into loose permafrost deposits covering a piedmont area in the northern crater margin is available (core P2, see Figure). Down to 2.26 m core depth the layers date back an accumulation of slope deposits to 13,100 cal. yr BP. The core further penetrates into weathered volcanic bedrock (Schwamborn et al., 2008).

Results and Interpretation: Experimental results:The grain size effect of frost action on the fine sandy material is obvious for all samples. After >100 F/T cycles grains are produced in the silt and smaller sized fractions (see Figure A). For samples 7 and 8 more F/T cycling was needed to crack the grains. Sample 8 shows high resistance against F/T grain break up even after an extended cycling time. Samples 1 and 2 show the same rate in silt production, although sample 2 run through thermal cycles only, whereas sample 1 was kept moist. It appears that the fluvial

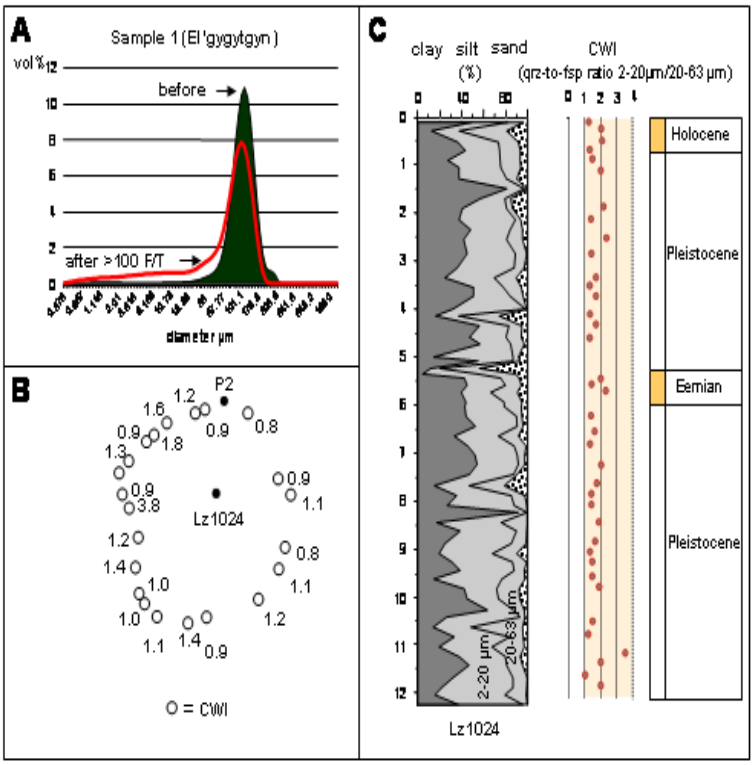

Fig. 1: A: Example of experimental grain break-up. "Before" marks the initial fine sand sample , whereas "after " shows the increase in the silt and clay portion after F/T cycling. B: Display of "Cryogenic Weathering Index (CWI)" measured from surface samples of El'gygytgyn Crater lake inlets. The lake diameter is 11 km. C: CWI values for lake sediment core Lz1024. Samples stretch over

sample 3, which contains Corg, was much more productive in breaking up grains than sample 2, which has no Corg. LPS curves comparing grain size distribution before and after the experiment show that samples after the experiment gain much in the silt fraction from 0.6 to 6.2 weight %. Only sample 1 also has a considerable amount of grains in the clay range.

From all samples semiquantitative amounts of quartz and feldspar in the fine sand and coarse silt fraction have been measured. This has been done before and after F/T cycling. The resulting values highlight the experimental quartz production in the fines by comparing the amounts of quartz in the silt fraction before and after. This is done by substracting the initial quartz occurrence from the experimentally evolved. Positive values show that quartz is enriched in the fines after the experiment. In fact, calculated values are all positive, thus demonstrating increased portions of silty quartz after >100 F/T. Remarkably, the dry sample 2 has more shattered quartz grains than the corresponding moist sample 1. Sample 8 though did not produce enough material for XRD analyses to be measured after F/T. SEM images from newly formed silt-sized particles exhibit angular outlines and conchoidal breakage as typical for quartz.

Experimental results are compatible with the classical 9% water-to-ice expansion view; silt and smaller sizes are produced and associated with the explosive power of ice growth in fissures. Quartz is more sensitive to F/T weathering with respect to feldspar irrespective from the geological origin. Konishchev and Rogov (1993) point out that cracks in quartz particle can also form as a result of freezing in gas-liquid inclusions. Nevertheless, also thermal stress is effective as obvious from sample 2, which also partly disintegrated into silt size grains. It has to be considered in contributing to grain break-up (Hall and Andrè, 2003).

Application to El'gygytgyn samples: bedrock, permafrost and lake record:In El'gygytgyn Crater most of the area (ca. 75 %) is built up by ignimbrites and tuffs. Ignimbrites are porphyric containing mainly embayed quartz and feldspar next to amphiboles, pyroxenes, and biotites. Remarkably, quartz macrocrystals are formed in the fine sand spectrum. They are bedded in a fluidal red to brownish microcrystalline groundmass. Eutaxitic texture is common. Tuffs have mainly feldspar types as macrocrystals. They are embedded in a microcrystalline green or red groundmass. Feldspar microprobe analysis shows an overall quantitative occurrence of albite-orthoclase (microcline, respectively)-anorthite in descending order.

When weathering detritus is released from bedrock an initial deposition occurs on the slopes. Sampling of frozen slope deposits in a foothill area reveals a mainly silty to sandy grain size composition. This is still true when penetrating into the underlying volcanic bedrock at about 2 m core depth. CWI values calculated from 27 core samples range around 1.2, the minimum value is 0.4 and the maximum value is 2.1. Most of the values are greater than 1, thus they fall into the indicative range of cryogenic weathering.

Similarly the CWI values measured from 22 surface samples taken from the inlets of El´gygytgyn Crater lake (white dots; see Figure) average around 1.3. The minimum value is 0.8 whereas the maximum value is 3.8. Quartz enrichment thus is evident in the fines.

SEM micrographs illustrate the fragility of quartz grains from permafrost where surface microcracking indicates source areas of silty particles. Some cracked grains are robust enough to survive slope and fluvial transport. Various features of brittle quartz break-up, which are associated with cryogenic destruction due to F/T cycles, exhibit for example angular, high relief and sharp edged grain shapes and rough and flaky weathered grain surfaces (Schwamborn et al., 2006).

El'gygytgyn lake sediments consist of clayey to silty layers. Laser particle sizing reveals a common major mode around 20 microns. CWI values are all greater than 1. The mean is 1.5 and values vary between 1.0 and 2.2. Thus, almost all values are placed in the range that is characteristic for cryogenic weathering.

First transport of grains and subsequent deposition on a slope implies that the in-situ weathering signal gets lost. Gravitational and hydrodynamic forces cause the separation of a particular grain composition. Still, quartz particles enrich in the fine fraction and are preserved and evident when comparing the in-situ signal of the weathered bedrock material with the overlying slope deposits in core P2. Furthermore, on average it can be found in the sampled fluvial surface sediments, too.

El´gygytgyn lake basin receives mineralogical debris from a fairly small and geologically fairly uniform catchment. This makes it a good natural laboratory to record pervasive minerogenic weathering signals dynamics assuming that the eroded bedrock does not change drastically in its composition over geologic time scales. The CWI values in core Lz1024 demonstrate a stable regime of cryogenic weathering for the last 220.000 years according to the age model (Juschus et al., 2007). Hence, permafrost is assumed to be stable in the area for that time period. Warm intervals such as the Eemian and the Holocene do not result in particular different CWI values than those from cold-climate periods. Based on the CWI values there is no offset of permafrost conditions in the record.

Conclusions: The combination of silt production, quartz enrichment and peculiar quartz grain micromorphology has been tested in an experimental set up and in sedimentary records for its potential as a sediment-mineralogical permafrost tracer. From the experiment it is obvious that F/T cycles break-up grains and that quartz is particular sensitive for grain break-up.

On average, quartz enrichment can be detected in El'gygytgyn permafrost and lake sediment sequences. The connection between silt production, CWI analysis and SEM features is most obvious, when medium- to high-relief grains become fragmented due to cryogenic cracking

However, cryogenic weathering is an in-situ process taking place during the intermediate time in the active layer. As soon as grains are transported, the mineralogical signal from in-situ weathering is blurred. The El'gygytgyn sedimentary archive records an integral signal of soil and surface conditions around the site on a long-term scale (multi kyr). It demonstrates persistent permafrost conditions in mountainous NE Asia back to at least marine isotope stage (MIS) 7.

When geologic conditions are favourable, i.e. in confined periglacial basins and where glacial grinding of

material can be excluded, we suggest a proxy data set of the three aforementioned sediment properties as a suitable method to infer frost weathering dynamics (i.e. active layer dynamics).

The effective production of silt caused by frost weathering has wider implications for interpreting Quaternary sections in the terrestrial Arctic and elsewhere. This includes the formation of loess-sized graines in permafrost deposits as well as questioning geochronological data sets, since grain break-up may alter micro physico-chemical environments thus modifying the ionising radiation and storage of the luminescence signal.

References:
Brigham-Grette, J. et al., 2007. Overview and significance of a 250 ka paleoclimate record from El'gygytgyn Crater Lake, NE Russia. J. Paleolim. 37, 1–16.
Hall, K., André, M.-F., 2003. Rock thermal data at the grain scale: applicability to granular disintegration in cold environments. Earth Surf. Proc. Landf. 28, 823-836.
Juschus, O. et al., 2007. Applying SAR-IRSL methodology for dating finegrained sediments from Lake El´gygytgyn, northeastern Siberia. Quat Geochron 2, 187-194.
Konishchev, V.N., Rogov, V.V., 1993. Investigations of cryogenic weathering in Europe and Northern Asia. Perm. Peri. Proc. 4, 49-64.
Krbetschek, M. et al., 2002. Luminescence dating results on sediment sequences of the Lena Delta, Polarforschung 70, 83-88.
Nowaczyk, N.R. et al., 2002. Magnetostratigraphic results from impact crater Lake El´gygytgyn, northeastern Siberia: a 300 kyr long high-resolution terrestrial paleoclimatic record from the Arctic. Geophys. J. Intern. 150, 109-126.
Schirrmeister, L. et al., 2002.Paleoenvironmental and paleoclimatic records from permafrost deposits in the Arctic region of Northern Siberia, Quat. Intern. 89, 97-118.
Schwamborn, G. et al., 2006. Ground ice and slope sediments archiving Late Quaternary paleoclimate and paleoenvironment signals at the margins of Lake El'gygytgyn impact crater, NE Siberia. Quat Res. 66, 259-272.
Schwamborn, G. et al., 2008. Periglacial sediment variations controlled by lake level rise and Late Quaternary climate at El'gygytgyn Crater Lake, Arctic Siberia. Boreas 37, 55–65.

ICDP

Magma storage conditions and degassing processes of low-K and high-Al island-arc tholeiites: Experimental constraints for Mutnovsky volcano, Kamchatka

T. SHISHKINA[1], R. BOTCHARNIKOV[1], R. ALMEEV[1], F. HOLTZ[1]

[1]Institut für Mineralogie, Universität Hannover, Callinstrasse 3, 30167 Hannover, Germany

Introduction: Mutnovsky volcano is located in the southern part the Eastern volcanic front of Kamchatka peninsula (Russia). The mafic lavas of the volcano are typical island arc high-Al, low-K tholeiitic basalts. Mutnovsky is the object of the proposed ICDP drilling project which is focused on the investigation of the interaction between active magmatic and adjacent hydrothermal systems. It has has two central scientific issues: (1) the identification of magmatic component in fluids proximal to conduits and (2) the determination of the overall volatile and thermal budget of the Mutnovsky volcano.

The experimental data and natural observations obtained in the course of our running DFG-project should provide new constraints on the pre-eruptive conditions, especially on the pressures (depths), temperatures and volatile contents in the magma chamber of Mutnovsky volcano. The project consists of three main parts: (1) experimental study of the H_2O-CO_2 solubilities in basaltic melts relevant to Mutnovsky primitive magmas, since H_2O and CO_2 contents in magmas can be used as indexes of magma storage conditions; (2) determination of pre-eruptive conditions and depths of basaltic magma chamber beneath Mutnovsky volcano based on crystallization experiments; and (3) the study of natural samples, in particular compositions and volatile abundances in glass inclusions.

The data obtained for Mutnovsky volcano have a broad application and can be used to constrain a general genetic model for the formation of island arc tholeiitic series and will provide estimates on the budget and contribution of magmatic volatiles to the magmatic-hydrothermal volcanic systems.

1. Experimental investigation of solubility of H_2O and CO_2 in basaltic melts: This part of the project is devoted to the quantitative determination on H2O-CO2 solubility in tholeiitic basaltic melts in the range of pressures (50-900 MPa) corresponding to the crustal depths of magma chambers and conduits beneath typical island arc volcanoes.

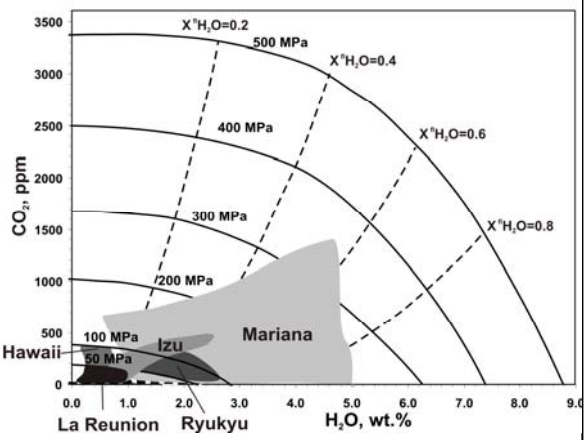

Fig. 1: Solubility plot for H_2O and CO_2 in basaltic melts at 1250°C. The solid lines represent isobars while the dashed lines are isopleths of constant fluid composition for the melts saturated with H_2O-CO_2-bearing fluids. Grey fields are concentrations of H_2O and CO_2 measured in natural melt inclusions in olivine from low- to mid-K tholeiitic basalts from different localities (see text). Natural data compared to that from experiments can provide pressure estimates of magma storage prior to volatile degassing.

As a starting composition for the experiments we used basaltic glass produced by air-melting of natural low-K high Al tholeiitic basalt from Mutnovsky volcano (sample N72, provided by M. Portnyagin; Duggen et al., 2007). Experiments were conducted in internally heated pressure vessel (IHPV) at pressures of 50 to 900 MPa and temperature of 1250ºC with Ar as pressure- medium. Five Au80Pd20-capsules, containing 50 mg of basaltic glass and H2O and CO_2 in different proportions (the mole fraction of H_2O in the fluid phase, XH2O from 0 to 1) were run simultaneously at isobaric and isothermal conditions. The duration of each run was about 24 hours. Afterwards samples were quenched isobarically using a rapid-quench method. The run products at 1250°C were bubble- and crystal-free glasses coexisting with a H_2O-CO_2-fluid phase. Glasses were analyzed using different methods: Karl-Fischer Titration (KFT), Infrared Spectroscopy (FTIR),

combustion and subsequent IR spectroscopy (CS), Microprobe (EPMA), wet chemical colorimetric method.

Concentrations of H_2O and CO_2 in the glasses considerably increase with increasing pressure and H_2O/CO_2 and CO2/H2O proportions in the coexisting fluid, respectively. The solubility of H2O in equilibrium with pure H_2O fluid increases from about 2.2 wt.% at 50 MPa to about 12.8 wt.% at 900 MPa. The concentration of CO_2 increases from about 200 to 6200 ppm in glasses which were in equilibrium with the most CO_2-rich fluids (XCO2 from 0.7 to 0.9). In general, the solubilities of both H_2O and CO_2 in basaltic melt show a non-linear dependence on the mole fraction of H_2O and CO_2 in the equilibrium fluid. Especially strong deviation from linearity is observed at high pressures (300 - 500 MPa).

Solubility data for tholeiitic basalt from Mutnovsky volcano are the first systematic and extensive dataset for the behaviour of mixed H_2O-CO_2-bearing fluid obtained for the same composition in wide range of pressures (50-900 MPa) in one Laboratory . Our data are in a good agreement with datasets of Dixon et al. (1995) obtained for MORB compositions at low pressures up to 100 MPa and of Botcharnikov et al. (2005) obtained for ferrobasalt at 200 MPa. Experimental data on H_2O-CO_2-solubility in tholeiitic basalt at pressures higher than 500 MPa do not exist, and can be only evaluated using thermodyanmic and empirical models. A comparison of new experimental data with existing numerical solubility models of Newman & Lowenstern (2002) and Papale et al. (2006) shows that model N&L (2002) is in agreement with experiments up to 200 MPa, but at higher pressures it considerably underestimates CO2 solubility. In opposite, the model of Papale et al. (2006) overestimates CO2 solubility in comparison with experimental data and at 500 MPa these overestimations reach a factor of 2 for CO_2-rich compositions. The reason of these deviation can derived from lack of experimental data at high pressures. Therefore our dataset can be used to recalibrate the existing models on volatile solubilities in silicate liquids.

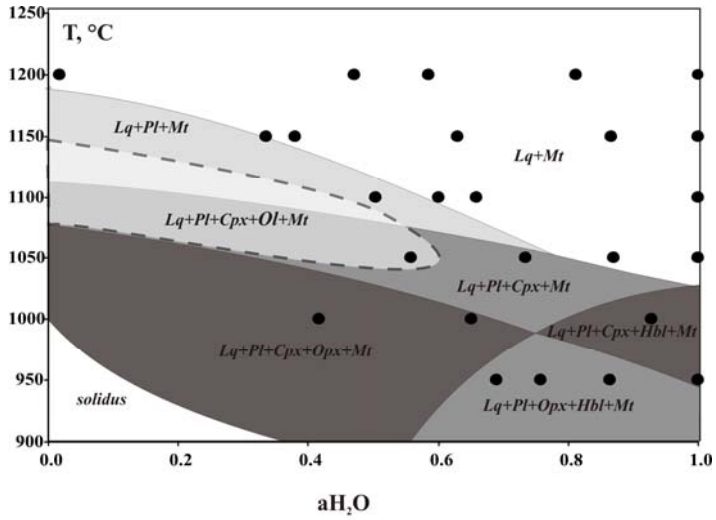

Fig. 2: Phase diagram (Temperature vs. water activity in the residual melt, aH_2O) for Mutnovsky tholeiitic basalt at 300 MPa. Mineral associations in equilibrium with melt (*Lq*) are shown by different colors.

A diagram containing fluid-saturation isobars and isopleths of constant fluid composition (Fig. 1) can be used as a tool for the evaluation of magma storage conditions and for the reconstruction of the dynamics of magma degassing. In particular, it can be applied for the determination of pressures and volatile compositions for natural basaltic glasses, for example, for melt inclusions in minerals. Determination of H_2O-CO_2 contents in the melt inclusions in olivines from Mutnovsky and application of our new solubility data are still in progress (see part 3). As example of employment of the solubility diagram for H_2O and CO_2 in tholeiites we plotted volatile concentrations measured in glass inclusions in olivines from low to mid-K basalts of several geographical and geological localities (Hawaii (Harris, 1983; Anderson, 1993), Mariana arc

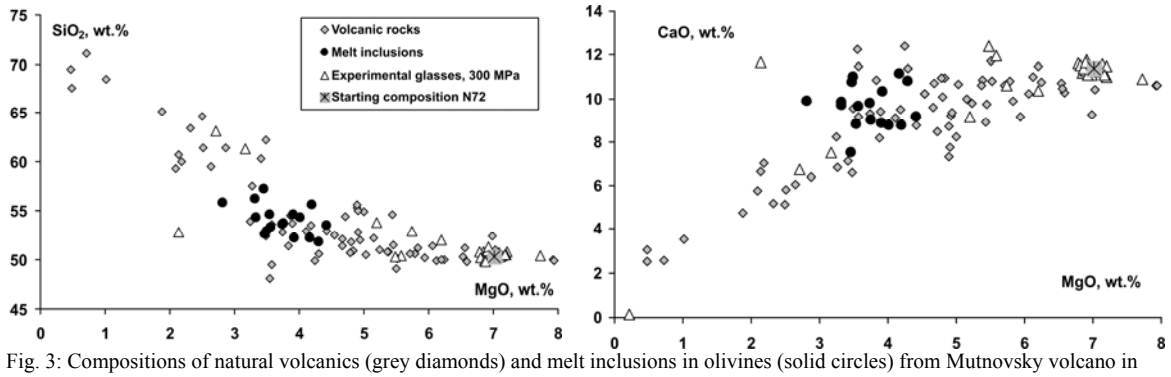

Fig. 3: Compositions of natural volcanics (grey diamonds) and melt inclusions in olivines (solid circles) from Mutnovsky volcano in comparison with residual melt (open triangles) compositions produced in experiments at 300 MPa on Mutnovsky parental basalt N72 (star in grey square) .

(Newman et al., 2000; Shaw et al., 2008), Ryukyu arc (Saito et al., 2001), Izu-Bonin arc (Nichols& Wysoczanski, 2007), La Reunion (Famin et al., 2009) (Fig.1). Determined volatile compositions of all melt inclusions lie below 500 MPa isobar, indicating that most melt inclusions were trapped in olivines at relatively shallow levels of the magmatic feeding systems (<15-20 km). The variations in compositional trends for different magmas presumably resemble different evolution and degassing histories of natural magmas.

The solubility data obtained in our project will be also used for the interpretation of the experimental results on crystallization/differentiation of Mutnovsky magmas and for the reconstruction of magma degassing conditions based on the study of natural samples.

2. Crystallization experiments: Phase relationships of the Mutnovsky parental magma are intended to be investigated as a function of pressure, fO_2 and aH_2O. The experimental results can be used to construct a set of phase diagrams at different pressures and temperatures for basaltic magma, coexisted with H_2O-CO_2 fluid phase. The obtained experimental data should provide quantitative information on the influence of pressure, aH_2O and fO_2 on stability fields of oxide and silicate phases, as well as on evolutionary trends of island-arc tholeiitic magma of Mutnovsky volcano. A first set of crystallization experiments was conducted at 300 MPa and between 950-1250°C on tholeiitic basalt (sample N72) previously investigated for H_2O-CO_2 solubilities. All experiments have been carried out in IHPV at intrinsic oxygen fugacity, corresponding to the value NNO+2.6 at water-saturated conditions, and to ~QFM at nominally dry conditions. The phase diagram (T vs. aH_2O at 300 MPa) constructed on the basis of experimental runs is shown in Fig. 2.

At 1200°C Mutnovsky basalt is above the liquidus for the whole range of investigated aH_2O. At 1150°C all runs with high aH_2O demonstrate crystallization of magnetite (Mt), whereas at low aH_2O (<0.35) crystallization of plagioclase (Pl) was also observed.

In general, with decreasing temperature, the crystallization sequence is as follows: Mt → Mt + Pl → Mt + Pl + Cpx → Mt + Pl + Cpx + Opx, where Cpx and Opx are high and low-Ca pyroxene respectively. At higher water activities this crystallization sequence is complicated by the stabilization of amphibole (Hbl). In the presence of Hbl, Cpx and Opx do not crystallize simultaneously. Crystallization of olivine (Ol) was observed only in one experiment at aH_2O ~ 0.5 and T=1050°C. Therefore, the stability field of Ol is shown in Fig. 2 by a dashed field indicating a preliminary position of phase boundaries for this mineral.. Interestingly, the mineral compositions in this run (Ol (Fo_{83}) – Pl (An_{82-84}) – Cpx (Mg# 79, $Fs_{12}En_{45}Wol_{42}$)) are very close to those observed in natural basalts. Moreover, petrographic observations and petrochemical trends for Mutnovsky volcano reported in the literature indicate cotectic Ol+Pl+Cpx precipitation from the initial stages of magma evolution. Therefore the presence of only Pl (together with Mt, but without Ol and Cpx) on the liquidus of Mutnovsky basalt at 300 MPa in the wide range of studied aH_2O may suggest that experimental conditions applied so far are not relevant for Mutnovsky magma chamber. However the final conclusion should be made after the analysis of experiments (which are in progress) at reduced conditions (low fO_2) and at very low aH_2O and dry conditions. At such conditiond Ol and Cpx can start to coprecipitate with plagioclase due to the different effect of H_2O on crystallization temperatures of these minerals (e.g. Almeev et al., 2007).

In Fig. 3 the compositions of the experimental glasses, volcanic rocks and glass inclusions in olivines from basalts of Mutnovsky volcano have been plotted. The experimental glass compositions at 300 MPa reproduce the Mutnovsky liquid lines of descent , indicating a genetic link between parental basaltic compositions and their differentiates. Thus, our opreliminary experiments show that crystal fractionation rather than magma mixing may be recponcible for the genesis of Mutnovsky lavas.

3. Study of natural samples from Mutnovsky volcano: Due to the lack of samples from delayed ICDP drilling on Mutnovsky volcano, short fieldworks have been conducted in the end of July – beginning of August 2009 with the aim to collect natural samples for our project. The major task of this field trip was to collect less-altered most primitive basalts from Mutnovsky volcano, which can be further used as starting composition for our crystallization experiments and for investigation of the olivine-hosted melt inclusions. We have sampled several young fresh cinder cones on the south-west slope of Mutnovsky volcano. The lavas of these cones are composed of clinopyroxene-olivine-plagioclase-bearing basalts (8 wt.% MgO, 50 wt.% SiO_2). For studying of melt inclusions in olivines we also collected basaltic tephra (porous basaltic bombs, pieces of scoria and ash). Due to the fast eruption and rapid cooling, olivines from tephra usually contain naturally quenched glassy inclusions with very well preserved pre-eruptive volatile abundances.

The study of glass inclusions from tephra of Mutnovsky volcano (with diameter more than 20 μm in olivines (Fo 75-80)) was started at the end of 2009 and is still in progress. Major element compositions and S, Cl content were determined by electrone microprobe. All glasses have basaltic composition and overlap with the general petrochemical trend of Mutnovsky volcanic series (Fig. 3). Using the experimentally calibrated H_2O-CO_2 saturation pressures (see part 1, Fig.1), the analyses of H_2O (SIMS) and CO_2 (FTIR) in glass inclusions will be helpful to providing quantitative estimates on the depth(s) at which Mutnovsky magmas started to degass.

Further objectives:

Crystallization experiments required for the simulation of phase diagrams at pressures 100, 300 and 500 MPa are scheduled. To reconstruct crystallisation history and magma storage conditions of Mutnovsky volcano new experimental observations will be compared with compositions of natural minerals, their proportions and with compositions of glass inclusions. Volatile contents of glass inclusions in olivines from Mutnovsky basalts will provide complementary information on fluid compositions as well as on depths of magma reserviors.

The data on magma degassing combined with the estimates on the magma production during eruptions (Melekestsev et al., 1987; Selyangin, 1993), emission of volcanic gases (e.g., Taran et al., 1992) and information obtained in the framework of the ICDP drilling project will be useful to constrain the total budget and contribution of magmatic volatiles to the magmatic-hydrothermal system of Mutnovsky volcano.

In the course of our field trip we contacted two principle investigators of the ICDP project on Mutnovsky volcano. These meetings at the Institute of Volcanology and Seismology in Petropavlovsk-Kamchatsky with Dr. Alexey Kiryukhin (Russia) and Dr. Pavel Izbekov (USA) resulted in fruitful discussions of our experimental data and were very helpful in coordination of our research plans in the frame of future ICDP drilling.

References:

Almeev, R.R., Holtz, F., Koepke, J., Parat, F. and Botcharnikov, R.E. (2007) The effect of H_2O on olivine crystallization in MORB: Experimental calibration at 200 MPa. American Mineralogist, 92 (4), 670-674.

Botcharnikov, R.E., Freise, M., Holtz, F., Behrens, H. (2005) Solubility of C-O-H mixtures in natural melts: new experimental data and application range of recent models. Annals of Geophysics 48, 633-646.

Dixon, E.J., Stolper, E.M., Holloway, J.R. (1995) An experimental study of water and carbon dioxide solubilities in mid-ocean ridge basaltic liquids. Part 1: Calibration and solubility models. Journal of Petrology 36, 1607-1631.

Duggen, S., Portnyagin, M.V., Baker, J., Ulfbeck, D., Hoernle, K., Garbe-Schonberg, D., Grassineau, N. (2007) Drastic shift in lava geochemistry in the volcanic-front to rear-arc region of the Southern Kamchatkan subduction zone: Evidence for the transition from slab surface dehydration to sediment melting. Geochim. Cosmochim. Acta 71, 452-480.

Melekestsev, I.V., Braizeva, O.A., Ponomareva, V.V. (1987) The activity dynamics of Mutnovsky and Gorely volcanoes in Holocene and volcanic hazards for surrounding areas. Volcanology and Seismology, 3-18 (in Russian).

Newman, S., Lowenstern, J.B. (2002) VolatileCalc: a silicate melt–H_2O–CO_2 solution model written in Visual Basic for Excel. Comput. Geosci. 28, 597–604.

Papale, P., Moretti, R., Barbato, D. (2006) The compositional dependence of the saturation surface of H_2O + CO_2 fluids in silicate melts. Chemical Geology 229, 78-95.

Selyangin, O.B. (1993). New data on Mutnovsky volcano: Structure, evolution and prediction. Volcanology and Seismology 1, 17-35 (in Russian).

Taran, Y.A., Pilipenko, V.P., Rozhkov, A.M., Vakin, E.A. (1992) A geochemical model for fumaroles of the Mutnovsky volcano, Kamchatka, USSR. Journal of Volcanology and Geothermal Research 49, 269-283.

ICDP

Carbonation of porous volcanic rocks by interaction with magmatic and hydrothermal fluids - a case study on Unzen volcano, Japan

SIMONYAN, A.V.[1], DULTZ, S.[2], BEHRENS, H.[1], FIEBIG, J.[3]

[1]Institute of Mineralogy, Leibniz University of Hannover, Callinstr. 3, 30167 Hannover, Germany, (simonian@mineralogie.uni-hannover.de)

[2]Institute of Soil Science, Leibniz University of Hannover, Herrenhäuser Str. 2, D-30419 Hannover

3Institute of Geosciences, J.W. Goethe University of Frankfurt, Altenhöferallee 1, D-60438 Frankfurt am Main

The Unzen drilling project was the first attempt to get insights into the mechanisms of volcanic eruptions by drilling into an active volcano shortly after eruption. The project yielded a couple of unexpected results, i.e. the temperature in the borehole was much lower than expected, and the drilling cores were highly altered with large amounts of secondary minerals such as carbonates, chlorite and pyrite, supposed to be products of reactions of discharged volcanic fluids with the host rocks.

These surprising findings inspired us to use the drilling cores in combination with experimental work to identify the mechanisms of fluid-rock interaction, in particular the carbonation and decarbonation of rocks. This research is not only important for understanding the deep degassing of volcanoes, but it has also major impacts for storage of CO_2 in cavities or in porous/brecciated volcanic rocks. For instance the formation of carbonate immobilizes CO_2 and may strongly change the permeability of rocks by closing open paths.

Our planned research involves (i) a petrographical investigation of drilling cores with special focus on texture and composition of alteration products, (ii) the analyses of carbon isotopes and oxygen isotopes to get information about the origin of the COB2B bond in carbonates, (iii) the characterization of pore systems in differently altered rocks using impregnation with Wood's metal and analyzing thermally released water from pre-saturated samples, (iv) an experimental study of transport and reaction of volatiles in the pore space of rocks using in situ techniques, and (v) hydrothermal fluid-rock experiments at conditions relevant to the near-conduit region of the volcano (200 – 400°C and up to 100 MPa).

Petrographic investigations of natural rocks from drilled cores with electron microprobe (WDS and EDX) and with scanning electron microscope (SEM) show that carbonates are secondary minerals substituting amphiboles during alteration of volcanic rocks in the cooling magmatic conduit. The carbonates are mostly calcite with significant proportions of dolomite. Minor alteration products are clay minerals, pyrite, and quartz. The presence of clay minerals besides carbonates in the altered dacite indicates that the rock might be exposed to different weathering environments, as clay minerals usually form in long-term and carbonation by magmatic and hydrothermal fluids might proceed in much shorter time periods.

The oxygen isotopic composition of amphiboles that are supposed to be unaltered was analysed by CO2-laser fluorination. $\delta^{18}O$-values of these amphiboles is quite homogeneous, varying only between 6.6 and 7.0‰ vs VSMOW. Accounting for the fractionation factor between bulk dacite/andesite and amphibole at magmatic temperatures of about 1.3-1.6‰ (Zheng, 1993; Zhao&Zheng, 2003), the calculated $\delta^{18}O$ value for bulk rocks should be about 8‰ which is in perfect agreement with the typical isotopic signature of unaltered Unzen rocks (Chen et al., 1999). Isotopic analyses, therefore, imply that the oxygen within these amphiboles primarily derives from a magmatic source. The analysis of altered products for the isotopic composition of oxygen as well as for carbon isotopes is in progress and will reveal us the origin of carbon and oxygen contained in these secondary phases.

The porosity and the specific surface area (SSA) of unaltered and altered rocks was investigated by N2-absorption method and Hg-porosimetry. It was observed that altered rocks have a SSA which is more than one order of magnitude larger than that of unaltered dacite (~0.3 m2/g) and can reach values up to 5.2 m2/g. The typical diameter of pores in unaltered dacite is about 400 nm while pore size in altered rocks is significantly lower (~10 nm). Preliminary data show that the concentration of carbon in dome samples is about 0.08 wt% and about 1.74 wt% in altered samples. This corresponds to approximately 0.7 and 14.5 wt% carbonate, respectively. A decrease in porosity from 8.4 vol.% in the original dacite to 4.9 vol.% in the strongest altered (carbonated) sample is observed. Wood`s metal impregnation analysis of altered and unaltered samples is in progress.

The in-situ experimental determination of transport and reaction properties of volcanic samples requires accurate

characterization of starting material. The results of petrographic and textural analysis of altered and fresh rocks will provide information for further selection of samples.

Hydrothermal experiments on the interaction between dacitic rocks, fluids of different compositions (composed of H2O+CO2 in various proportions) and different mineral phases (CaCO3; Ca-rich plagioclase) were conducted at 300, 400 and 500°C and pressures of 100 and 150 MPa. First results demonstrate that carbon is indeed involved in the reaction between dacitic rock and fluid (in agreement with other experimental studies, e.g., Dufaud et al., 2009). However, individual carbon-rich phases (e.g. carbonate) were not detected in experimental products. Moreover, no measurable changes in the composition of amphiboles were observed. Additional experimental efforts (e.g., with smaller solid/fluid ratio) for the reproduction of alteration processes in natural rocks are in progress.

References:
Chen et al., 1999, JVGR, 89, 243-253. Dufaud et al., 2009, Chem. Geol., 265, 79-87. Zheng, 1993, EPSL 120, 247-263; Zhao & Zheng, 2003, Chem.Geol. 193, 59-80.

IODP

Warm Climates come with Colder Times

PETER P. SMOLKA[1]

[1]University Muenster(*),smolka@uni-muenster.de

Increasing input of CO_2 into the atmosphere is, based on physics, expected to increase atmospheric temperatures ("greenhouse effect"). In the runup to the climate conference in Copenhagen (cop15), hacked emails showed, that some people appeared to have been astonished about a less–than–expected increase of warming during the last decade. Others appeared to have been astonished about abundant snowfall in regions where they did not expect so much snow, such as Texas. Some used this as wrong argument against climate change.

Data from the Pliocene (Smolka, 2008 and submitted) and principles of physics show that the observed phenomena (regionally less warming, more snow) are the result of climate change:

Once the atmosphere starts to warm such that faster ice–melt occurrs, such as in Greenland during the last years, the energy that is used to melt the ice, not only at the surface but at the base of glaciers, lacks elsewhere. This applies to other climate–change related processes as well. Globally averaged temperature curves are then expected to rise less steep or even to show for a limited time a plateau. Once SSTs of the oceans increase, more moisture results. In moderate regions more floods result; in cold regions more snowfall is observed. This is consistent with data from the Pliocene: Higher SSTs in connection with Arctic Sea ice (IRD–data are different from PRISM–scenarios) resulted in large amounts of snow on the NH continents in winter. Although we are currently well below Pliocene conditions (no permanent El–Nino visible) groups of years might have similarities regarding the processes: less warming as result of enhanced icemelt (lacking energy in the system) plus more snow–fall in cold regions and more rain in warm regions resulting from the evaporated moisture from the oceans.

Long transient runs of coupled atmosphere–ocean models will either provide in the future correct modeled time–series or more insight into improvables for parametrizations.

References:
Smolka, P.P. 2008. Cold Aspects of past Neogene Warm Climates. IGC33.
Smolka, P.P. 200x. Cold Aspects of past Neogene Warm Climates. Submitted.

IODP

Evolution and variability of the East Asian summer monsoon during the Middle-Late Miocene: Evidence from combined planktonic foraminifera Mg/Ca and $\delta^{18}O$ (ODP Site 1146; northern South China Sea)

S. STEINKE[1], J. GROENEVELD[2], H. JOHNSTONE[1]

[1]MARUM – Center for Marine Environmental Sciences and Department of Geosciences, University of Bremen, Bremen, Germany
[2]Alfred Wegener Institute for Polar and Marine Research, Bremerhaven, Germany

The monsoon system represents one of the basic elements of the global atmospheric circulation that controls the redistribution of latent and sensible heat and its evolution and variability play a significant role in our understanding of global climate (Webster et al., 1998). One of the central questions in this context is how the monsoon has evolved over long periods of geologic time. In this study, we are focussing on the Middle to Late Miocene time interval from 13 Ma to 6 Ma.

The combined approach of measuring planktonic foraminiferal (G. sacculifer-quadrilobatus) Mg/Ca ratios and stable oxygen isotopes from northern South China Sea (SCS) Ocean Drilling Program (ODP) Site 1146 (19°27.40'N; 116°16.37'E; water depth of 2092 m) enabled us to reconstruct temperature independent seawater $\delta^{18}O$ (i.e. proxy for sea surface salinity) variations in order to reconstruct the hydrography in the northern SCS. Located offshore the Pearl (Zhujiang) River, or its predecessor, the location of ODP Site 1146 is considered to provide a most sensitive record for detecting potential changes in freshwater input/river-run off as a result of changes in continental humidity, and hence changes in East Asian summer monsoon (EASM) climate. The chronology for ODP site 1146 is based on a combination of planktonic foraminiferal and calcareous nannofossil first occurrence (FO) and last occurrence (LO) datums, and magnetostratigraphic datums.

Mg/Ca based sea surface temperature (SST) estimates were found to vary between 23.7°C and 30.1°C during the investigated time interval (Fig. 1). Following a period of relative constant SSTs (~28-30°C), the Mg/Ca-SST estimates suggest a distinct cooling trend from 10 Ma (~29-30°C) to 7.6 Ma (~26°C) that is followed by an abrupt increase in SSTs around ~7.6 Ma. Following again a period (7.5 Ma to 6.8 Ma) of relative constant SSTs of around 28°C, lower temperatures, ranging between 26°C and 27°C, are recorded for the time interval 6.8 Ma to 6 Ma. The overall decreasing trend in SST from ~30°C to ~26°C for the Middle-Late Miocene time interval 13-6 Ma supports the concept of Wei et al. (2006) for decreasing temperatures in south China since the Middle Miocene as

proposed from chemical weathering records at neighbouring northern SCS ODP Site 1148 (Wei et al., 2006). The decreasing SSTs for time interval 13-6 Ma are in general agreement with the previously described "global climate cooling" (Middle to Late Miocene) which was indicated by benthic foraminiferal oxygen isotopes and benthic foraminiferal Mg/Ca estimates (Zachos et al. 2001; Lear et al., 2000).

Local seawater $\delta^{18}O$ (hereafter $\delta^{18}O_{sw}$) reconstructions for ODP Site 1146 from 13 Ma to 6 Ma yield values varying between –0.3‰ and 1.8‰ (Fig. 1). Local $\delta^{18}O_{sw}$ reconstructions for the time interval 13 Ma to ~7.5 Ma reveal highly variable estimates between –0.3‰ and 1.46‰ with an average value of 0.61‰. Around ~7.5 Ma, the local $\delta^{18}O_{sw}$ estimates reveal a prominent shift towards higher (heavier) local $\delta^{18}O_{sw}$ values (an average value of

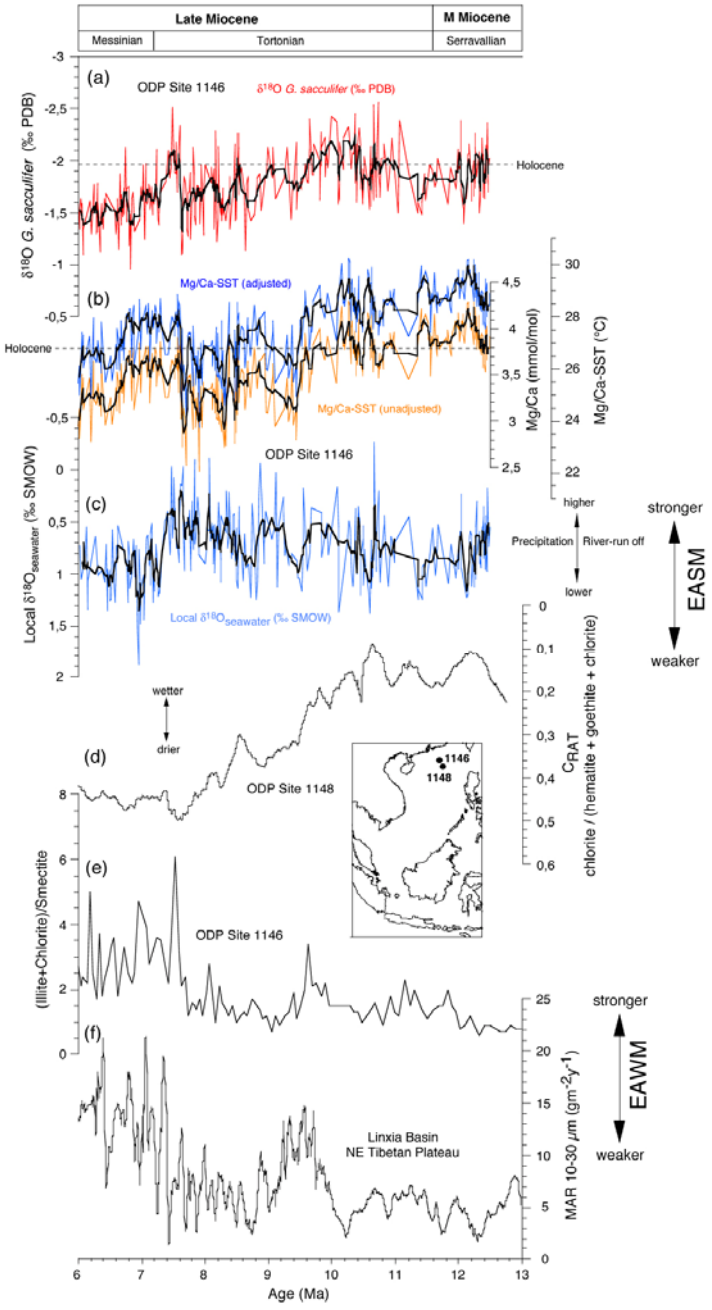

Fig. 1: (a) Oxygen isotope record of G. sacculifer-quadrilobatus of ODP Site 1146; (b) Mg/Ca ratios (mmol/mol) and Mg/Ca-SST estimates (blue; Mg/Ca-SST adjusted). Mg/Ca ratios were transformed to surface water temperatures by using the calibration equation for G. sacculifer of Nürnberg et al. (2000). The Nürnberg et al. (2000) calibration was modified in order to account for differences in seawater Mg/Ca ratios between the Middle-Late Miocene (4.5 mol/mol; Wilkinson and Algeo, 1989) and present (5.1 mo/mol; Broecker and Peng, 1982). Mg/Ca-SST estimates (orange; Mg/Ca-SST unadjusted) not corrected for seawater Mg/Ca changes; (c) Local δ18Osw estimates at ODP Site 1146. To calculate the δ18O of seawater (δ18Osw), firstly, the δ18Osw was estimated by removing the temperature driven component of changes in the planktonic foraminiferal δ18O record using the palaeotemperature equation given by Shackleton (1974). Secondly, an estimate of the Middle-Late Miocene (13 Ma to 6 Ma) ice volume signal was subtracted from the δ18Osw record in order to assess relative variations in local δ18Osw (= proxy for local surface water salinity changes). The Tian et al. (2008) benthic stable oxygen isotope record of northern SCS Site 1148 was used to approximate variations in Middle-Late Miocene ice volume. For the calculations, it was assumed that 70% of the amplitude of the benthic foraminiferal record is due to ice volume. A normalized (ice volume corrected) record was subtracted from the δ18Osw record, leaving a local δ18Osw record, which would provide an approximation of relative changes in surface water salinity in this area between 13 Ma and 6 Ma.The data in (a) – (c) were smoothed by a five-point moving average (black line); (d) Chemical weathering index CRAT of ODP site 1148 (Clift et al., 2008); (e) (Illite+Chlorite)/Smectite at ODP Site 1146 (Wan et al., 2007); and (f) Mass accumulation rates (MAR), Linxia Basin, NE Tibetan Plateau (Fan et al., 2006).

0.98‰). The variations of the local $\delta^{18}O_{sw}$ estimates during the time interval 13-6 Ma are interpreted to reflect changes in river run-off from the Pearl River (Zhujiang) River due to changes in continental humidity and/or decreased precipitation over the ocean and hence, changes in EASM intensity. As inferred from the local $\delta^{18}O_{sw}$ estimates, the EASM development between 13 Ma to ~7.5 Ma can be regarded as a period of alternating stronger and weaker EASM intensity rather than a continuous decrease in EASM intensity as deduced from chemical weathering records of ODP Site 1148 (Wei et al.; 2006; Clift et al., 2008). Only after ~7.5 Ma, a prominent shift towards heavier values is interpreted to reflect a notable decrease in EASM intensity. The conclusion that the EASM decreased notably around 7.5 Ma, agrees well with palaeobotanical and lithological data from numerous sites over China that reveal enhanced aridity around 8 Ma (Sun and Wang, 2005). This is further supported by terrestrial mollusk records from the Western Chinese Loess Plateau, indicating a dominance of the East Asian winter monsoon (EAWM) between 7.1 and 5.5 Ma (Li et al., 2008). This study suggests that a notable abrupt weakening of the summer monsoon around ~7.5 Ma was most likely the driving force for decreasing aridity in East and South Asia that resulted in widespread ecological (e.g. C_4 grass expansion) and environmental shifts during this time period as revealed by a number of terrestrial studies (stable isotopes of pedogenic carbonates, palynological studies; loess records; see Molnar, 2005 for details).

The strongest support for the integrity of our EASM proxy record, however, comes from the comparison with previously published proxy records of EAWM variability (Fig. 1). Grain-size records from the Linxia Basin (NE Tibetan Plateau; Fan et al., 2006) and clay mineral data of northern South China Sea ODP Site 1146 (Wan et al., 2007) reveal an abrupt intensification of the EAWM at ~7.5 Ma. The comparison of our EASM proxy data with these EAWM proxy records suggests an inverse behaviour of the EAWM and EASM between 13 Ma and 6 Ma. A weaker EAWM is associated with a relative stronger EASM from 13 Ma to 7.5 Ma. After 7.5 Ma, the prominent shift in the $\delta^{18}O_{sw}$ data reveal a shift towards weaker EASM that is associated with a shift towards a stronger EAWM (Wan et al., 2007; Fan et al., 2006). This likely suggests that an anti-phase relationship between summer and winter monsoon as observed for the Late Pleistocene and Holocene (e.g. Yancheva et al., 2007) is also valid for the Middle to Late Miocene. From the coincidence in timing between changes in the EASM and EAWM, we suggest that the anti-phase behaviour of the EAWM and EASM between 13 Ma and 6 Ma as inferred form our proxy data is a more likely scenario than the differential evolution of the EASM and EAWM as proposed by Wan et al. (accepted).

It is suggested from this study that changes in the long-term character of the East Asian monsoon during the Middle-Late Miocene may have been caused by a complex interplay of changes in the volume of the Artic and/or Antarctic ice sheets, tectonic factors, such as sea-land distribution and mountain uplift, SST and vegetation cover. While this study presented here does not resolve the controls on the EASM change, it does suggest e.g. that the profound ecological and environmental shifts in East and South Asia during the Late Miocene at 8-6 Ma are related to EASM changes.

IODP

Geotechnical experiments indicate deformation partitioning in the soft sediments of the Nankai accretionary prism (NEXT - NanTroSEIZE)

MICHAEL STIPP[1], YUJIN KITAMURA[2], JAN H. BEHRMANN[3] AND BERND LEISS[4]

[1] Marine Geodynamics, IFM-GEOMAR, Kiel, Germany, mstipp@ifm-geomar.de
[2] Marine Geodynamics, IFM-GEOMAR, Kiel, Germany, ykitamura@ifm-geomar.de
[3] Marine Geodynamics, IFM-GEOMAR, Kiel, Germany, jbehrmann@ifm-geomar.de
[4] GZG, University of Göttingen, Germany, bleiss1@gwdg.de

1. Introduction: The IODP-project NanTroSEIZE (Nankai Trough Seismogenic Zone Experiment) investigates plate boundary deformation, accretionary prism formation and the upper seismogenic zone of the Nankai trench at which the Philippine sea plate is subducted below the Japanese islands Honshu and Shikoku (Eurasian plate). In the course of the project it is planned to drill for the first time through an active plate boundary thrust fault. Along this thrust fault the so-called Nankai earthquake is supposed to originate that occurs approximately every 80-100 years. Its last incidence was a sequential rupture in 1944 and 1946 with magnitudes of 8.0 and 8.1, respectively, causing devastating tsunamis in addition.

IODP expeditions 315 and 316 investigated the shallow frontal thrusts, and the hanging wall to a major active splay fault of the active frontal thrust system. Expedition 322 was dealing with the characterization of composition, architecture, and state of pre-subduction sediments transported to the seismogenic zone. Coring was successful and we were able to acquire 28 whole round core samples with lengths between 70 and 220 mm onboard of the expeditions for geotechnical testing. Although the drilled cores from the accretionary prism consist of a relatively homogeneous sequence of variably consolidated silty clay and claystone, zones of higher and lower deformation strain have been observed and different fault generations discriminated. At present it is not clear if the involved sedimentary rocks are dominated by localized brittle deformation and related fault slip, or alternatively, by distributed deformation and strain weakening causing a slow creep-like behavior. To answer this question, we experimentally deform drill core samples of expeditions 315, 316 and 322 from a depth range of 48-853 m below sea floor within the frame of our follow-up work project "Natural and experimental faulting of rocks, Nankai Accretionary Prism (NEXT)" that started in July 2009. The first results of the laboratory part of the project are presented here demonstrating the importance of deformation partitioning within the Nankai accretionary prism.

2. Methods: Experiments have been carried out using sample cylinders (50 mm in diameter, up to 100 mm in length) under consolidated and undrained conditions at confining pressures of 400-1000 kPa, room temperature,

axial displacement rates of 0.005-0.1 mm/min and up to axial compressive strains of ~45%. After saturation and consolidation three different geotechnical deformation tests

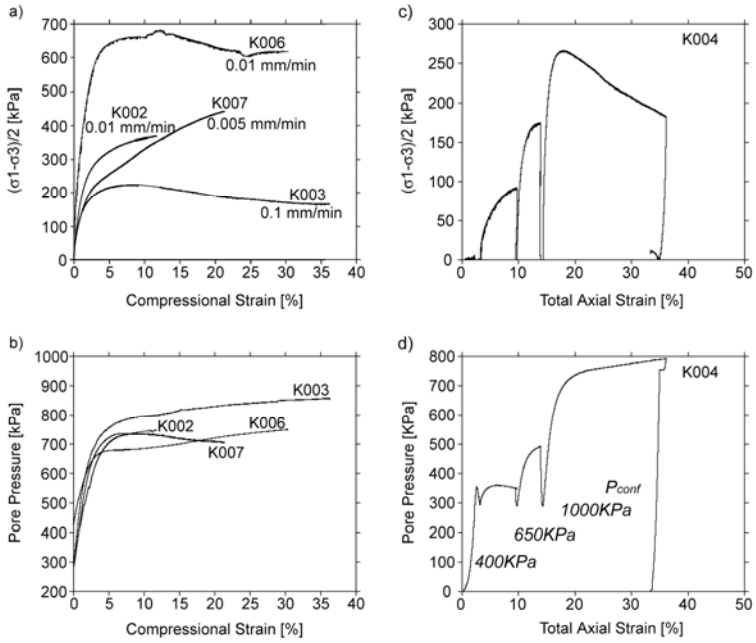

Fig. 1: Stress/strain-record and pore pressure/strain-records of single step compression experiments (a, b) and pressure stepping compression experiments (c, d). See text for further explanations. a,b) Experiments at a constant confining pressure of 1000 kPa; displacement rates and sample numbers are indicated. See Figure 2 for IODP core numbers. c,d) Single experiment at constant displacement rate (0.01 mm/min) and three different confining pressures (Pconf). Sample number is indicated.

were performed: (1) single step compression experiments at constant confining pressure and displacement rate, (2) pressure stepping compression experiments at constant displacement rate and three different confining pressures, and (3) displacement rate stepping compression

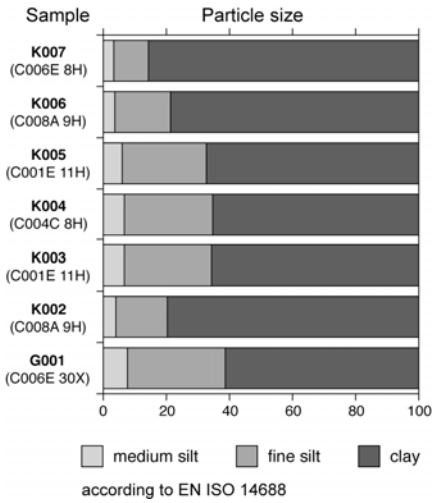

Fig. 2: Grain size distribution of the experimentally deformed samples as determined by laser particle sizer (see text for further explanation).

experiments at constant confining pressure and increasing displacement rate (Fig. 1). Single step compression experiments show the general stress/strain-record of a sample including elastic and plastic loading, peak or fracture strength, stress drop and residual strength in the brittle and creep strength, weakening or hardening in the plastic deformation case. Pressure stepping experiments allow to determine peak strength at three different confining pressures in one and the same experiment. From that we will plot Mohr diagrams and determine internal friction coefficients. The third group of experiments investigates velocity effects on sample strength.

3. Results: Experimental results show the expected low Vp- and Vs-velocities for the water-rich sediments. Despite the consistent low depth range and the lithological similarity of the so far deformed samples, the samples can be separated into two distinct 'rheological groups': The first sample group shows deviatoric peak stress after only a few percent of compressional strain (< 10%) and a continuous stress decrease after peak conditions (Fig. 1a). Simultaneous to this decrease there is a pore pressure increase indicating contractant behavior characteristic of structurally weak material (Fig. 1b). The second sample group reaches deviatoric peak stress after significantly higher strain (> 10%) and weakens only moderately to a relatively high residual strength level (Fig. 1a). These samples are structurally stronger, even though the pore pressure/strain-relationship deviates slightly from what is commonly expected for structurally strong material (Fig. 1b). This mechanical behavior has been observed over the range of applied displacement rates.

The actual cause of deformation partitioning has not yet been resolved. The small differences in grain size and composition are probably not the cause for the occurrence of the two rheological sample groups. The planned microstructural investigations and texture measurements of the undeformed and deformed samples may allow to elucidate this deformation phenomenon in the rather

monotonous rock sequence. A microstructural comparison between experimentally and naturally deformed rocks is intended to prove if our experimental results can be extrapolated to the actual deformation conditions and processes in the Nankai accretionary prism.

The further work plan includes experiments in a 1000 kN triaxial deformation apparatus to test the samples from greater drilling depth and the rock samples taken onshore from the exhumed Boso and Shimanto accretionary prisms. The deformation conditions ought to directly correspond to the updip end of the seismogenic zone. Additional ring shear tests allow deformation at faster strain rate and to higher shear strain. Microstructural investigations by light and scanning electron microscopy and texture analysis by synchrotron radiation and X-ray goniometry will be continued to compare our experimentally with naturally deformed samples from high strain zones of the drilled core sequence.

Furthermore, these investigations may elucidate the processes which cause deformation partitioning and which facilitate velocity weakening or strenghtening. Our results will finally be correlated with the core data base and with meso- and large-scale structures.

Increasing displacement rate stepping tests showed almost no strength increase from step to step, even though after each step the compressive piston was retracted and the differential stress was brought to a small value close to zero prior to advancing the compressive piston at an increased rate.

Grain size distribution of the experimentally deformed samples were determined by a laser particle sizer (Analysette-22 Nanotec). The grain sizes range from clay to fine sand, but the volume proportion of fine sand and coarse silt is well below 1%. Overall, the grain size distribution of the recovered sample material from the hanging wall of the frontal thrust system is very homogeneous (Fig. 2). The same is true for the mineral composition as determined by XRD analysis (cores from Sites C0001 and C0006; Underwood et al., unpublished data). The average composition (±5%) of almost all of the samples is 36% illite, 31% smectite, 21% chlorite, 7% quartz, 5% kaolinite.

Crystallographic preferred orientation (texture) measurements have been carried out by synchrotron radiation at HASYLAB (DESY, Hamburg) in a pilot study of a sample from low depth (C0001-B-4H, ~30 mbsl). This is the first time that a water-rich silty clay sample has been analyzed by synchrotron radiation. For that we had to develop a new preparation technique with cylindrical samples of a diameter of 20 mm being mounted inside a plexiglass capsule (Fig. 3a).

Synchrotron radiation allows for measurements of entire sample volumes including large amounts of water. Artifacts from sample polishing and preparation can be neglected because of the large sample volume in comparison to the little effect of the sample surface. Measurement results show a random texture indicating that initial compaction and consolidation have not caused a preferred orientation of the clay minerals at this low burial depth. There is also no evidence for any flow alignment due to sediment currents. Further measurements of the starting material, i. e. the undeformed sediments, are important to verify any pre-existing texture (e. g. compaction textures of phyllosilicates at greater depth). These results will be compared to measurements on our experimentally deformed samples as well as on naturally sheared samples from high strain zones of the drilled rock sequence.

We think that deformation of the entire sedimentary sequence causes strain concentration within layers of structurally weak material and maybe the formation of mechanical runaways. The capability of deformation partitioning is probably the key for understanding brittle faulting within the uniform silty and clayey sedimentary sequence of the Nankai accretionary prism. The velocity weakening behavior in the displacement rate stepping tests is different from what has been observed for single step compression experiments for which an increase in displacement rate comes along with a strength increase. Further tests are required to constrain this behavior and to check if it is a property inherently connected to the structurally weak material.

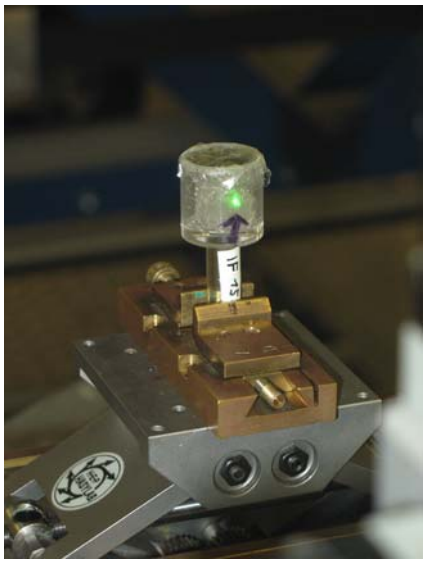

Fig. 3: a) Sample holder at the HASYLAB with plexiglass capsule and sample inside. b) Area detector diffraction image of sample C0001-B-4H with continuous Debye rings indicating a random texture (recorded at HASYLAB, DESY; measurements were carried out by Dr. Helmut Klein, GZG Göttingen).

The actual cause of deformation partitioning has not yet been resolved. The small differences in grain size and composition are probably not the cause for the occurrence of the two rheological sample groups. The planned microstructural investigations and texture measurements of the undeformed and deformed samples may allow to elucidate this deformation phenomenon in the rather monotonous rock sequence. A microstructural comparison between experimentally and naturally deformed rocks is intended to prove if our experimental results can be extrapolated to the actual deformation conditions and processes in the Nankai accretionary prism.

The further work plan includes experiments in a 1000 kN triaxial deformation apparatus to test the samples from greater drilling depth and the rock samples taken onshore from the exhumed Boso and Shimanto accretionary prisms. The deformation conditions ought to directly correspond to the updip end of the seismogenic zone. Additional ring shear tests allow deformation at faster strain rate and to higher shear strain. Microstructural investigations by light and scanning electron microscopy and texture analysis by synchrotron radiation and X-ray goniometry will be continued to compare our experimentally with naturally deformed samples from high strain zones of the drilled core sequence. Furthermore, these investigations may elucidate the processes which cause deformation partitioning and which facilitate velocity weakening or strenghtening. Our results will finally be correlated with the core data base and with meso- and large-scale structures.

IODP

Onland tephra record around Lake Van as a stratigraphic, compositional, temporal and alteration framework for the Palevan drilling project

M. SUMITA[1], H.-U. SCHMINCKE[1]

[1]Leibniz-Institute for Marine Science, IFM-GEOMAR, Wischhofstr. 1, 24148 Kiel, Germany

Goal: The importance of tephra layers for the *Paleovan drilling project* lies in (a) their enormous stratigraphic value – probably several hundred tephra layers – , (b) temporal framework ($^{40}Ar/^{39}Ar$ alkali feldspars) and (c) supply of elements, the alkalic rhyolitic glasses providing a major source for the alkalinity of Lake Van.

Results: A crude preliminary *tephrostratigraphy* was established over an area of >1000 km^2 from 40 km east of Tatvan, 20 km (Bitlis) to the southwest, Lake Nazik 20 km northwest of Ahlat and > 50 km east of Ahlat.

More than 10 *major and many tens of minor* fall deposits were erupted over the past ca. 210 - 300 (?) ka. Thickness > 2m, large diameter of pumice bombs (up to 50 cm (!) in some) reflect *large magnitude explosive eruptions*. One fallout blanket (AP-1) near Ahlat, up to ca. 15 m (!!) thick (Fig. 1a), likely derived from Nemrut, 30 km away, would have buried Ahlat if erupted today. Magma volumes of some of these eruptions must have amounted to several tens of km^3, in the range of some of the largest Plinian eruptions known worldwide.

The compositionally zoned *Nemrut Ignimbrite (NI)* (high-silica rhyolite to mafic trachyte), ca 30 ka old, consists of extremely variable facies and probably advanced over water for at least 10 km (!) across Tatvan Bay. Possibly as many as 7 different ignimbrites erupted from Nemrut since 210-300 (?) ka must have formed syn-ignimbrite turbidites after debouching into Lake Van. They are likely to represent excellent seismic reflectors and to show characteristic depositional structures contrasting with subaqueous fallout tephra.

Debris avalanche deposits, common on the lower slopes of Nemrut and Süphan, must have entered the lake and are probably generated tsunamis when impacting water.

EMP analyses of glass, feldspar, pyroxene, olivine and biotite for ca. 80 tephra units on land and 16 tephras in the short cores represent the first more comprehensive database for tephra from Nemrut and Süphan volcanoes. The *phenocrysts* of tephras likely erupted from Nemrut volcano are dominantly anorthoclase, hedenbergite clinopyroxene and fayalitic olivine apart from Fe/Ti-oxides, rare augitic cpx and highly corroded plagioclase in the mafic upper parts of ignimbrites. Süphan-derived tephras carry a complex mineral assemblage: andesine and ternary feldspars, augitic and, in some, slightly more Fe-rich clinopyroxene coexisting with hypersthene, in some units extremely inclusion-studded, biotite and amphibole in some. One tephra from Nemrut contains chevkinite. *Glasses* are dominantly (high-silica) rhyolitic but range to andesitic, the latter more common of Süphan tephras. Nemrut tephras are mainly peralkaline, as also reflected in their mineralogy. Chemical fingerprinting is common, i.e. individual tephra layers are characterized by narrowly defined compositional clusters (Fig. 1b,c), a major bonus in recognizing and correlating drilled tephra deposits to those on land by glass - when unaltered - or phenocryst composition.

Correlation land-lake: Several hundred tephra layers are likely to be drilled and major ones with sufficient feldspar phenocrysts will be dated providing a temporal framework for the cores over several hundred ka. Correlation with the land will be based on structural type (fallout, syn-ignimbrite turbidite, debris avalanche, reworked), particle textures and glass and mineral compositions. Thick tephra units on land will correspond to prominent seismic reflectors. A major, ca. 6 km-long eruptive fissure migrating from south to north from successively younger scoria cones to huge İncekaya hydroclastic tephra ring – a prominent landmark – may continue into Lake Van. The widespread distribution of the basaltic Incekaya hyaloclastite marker beds at least as far as Tatvan, 15 km west, must reflect a colossal phreatomagmatic underwater eruption. Fallout scoria beds from the co-eval precursor scoria cone extend for >5 km eastward, the basaltic tephras providing a widespread and compositionally distinct stratigraphic marker on land and likely in the cores as well. Textures and compositions of 16 *tephras drilled* show two major phases of explosive activity, an older Süphan overlain by a younger Nemrut phase, the oldest tephra (T16) being again Nemrut-related by glass and mineral compositions. The tephras comprise 10 primary fallout, 1 pyroclastic flow-related and 5 reworked tephras based on compositional homogeneity, abundance of lithics, rounding etc..

Incomplete soil development between tephra units indicates *dry climate* through at least 200-300 (?) ka. A wet episode is reflected in a small intramontane basin 25 km

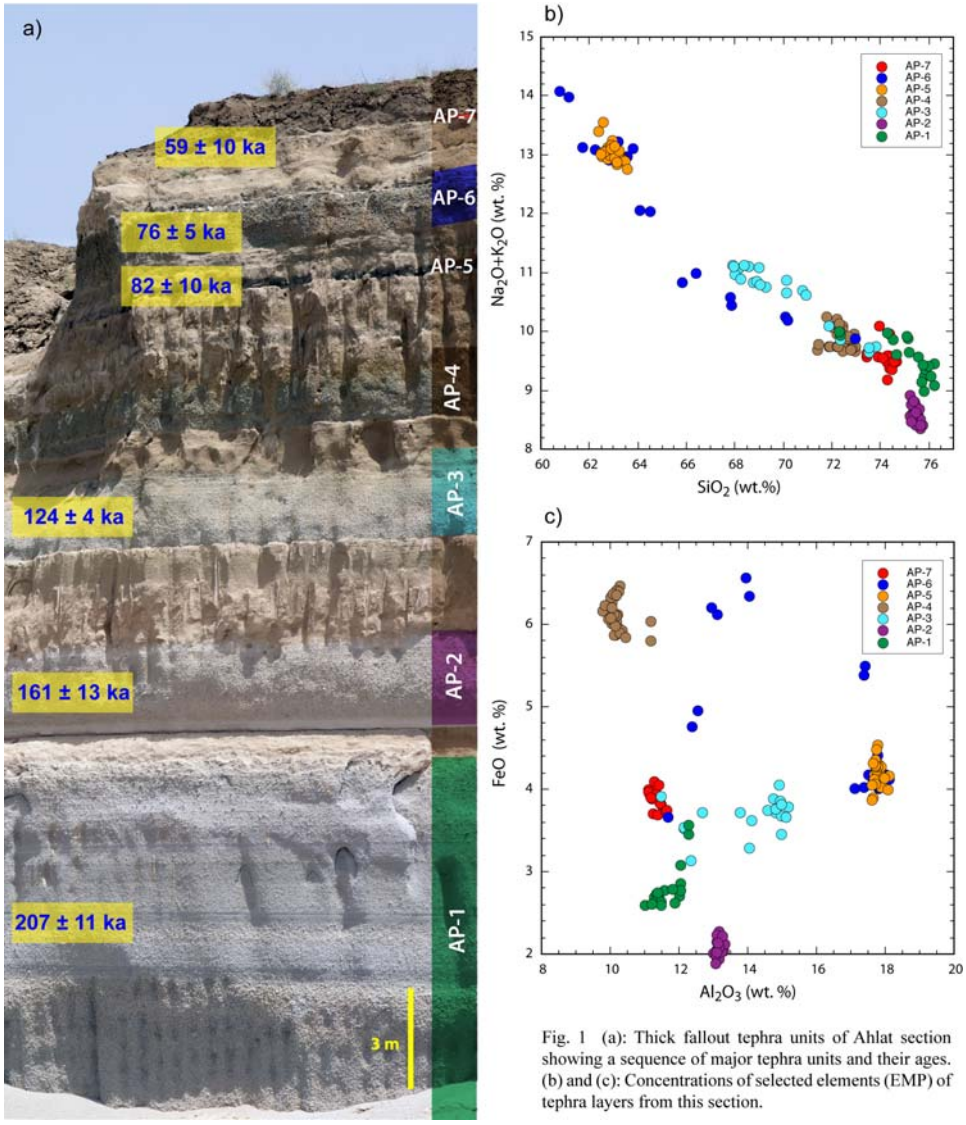

Fig. 1 (a): Thick fallout tephra units of Ahlat section showing a sequence of major tephra units and their ages. (b) and (c): Concentrations of selected elements (EMP) of tephra layers from this section.

east of Tatvan. The swamp section contains at least 8 tephra layers (two >10 cm thick) in a 1m (!) section reflecting a much higher preservation potential of water-deposited tephra. This would mean several hundred tephra layers if translated into the 240m deep planned core. Land evidence does suggest, however, that volcanism is episodic. Major fallout fans east of Tatvan reflect westerly, contrasted with dominant SW wind directions for tephra layers in the Ahlat area. Tephra deposits several m thick sealing thousands of km^2 around Lake Van for a long time will result in significant impact on the vegetation.

Major types of *volcanic hazards and risks* relevant for the populated areas bordering Lake Van (c. 0.7 million people), include (1) debris avalanches resulting from sector collapse of the volcanic edifices, (2) widespread inundation of the lowland and lake surrounding Nemrut by voluminous pyroclastic flows, (3) tsunamis generated by both types of mass flows, (4) massive tephra fallout.

The origin of closed Lake Van basin is commonly believed to be due to a lava flow blocking its drainage. We speculate that deposition of one or two huge pyroclastic flows issued from the southern part of Nemrut and/or intrusions and/or sector collapse were the main cause for drainage cutoff. The huge volume of alkaline glassy tephras in the lake sediments, probably increasing downwards based on seismic evidence, are likely a major factor in explaining the *alkalinity of the water*, a high Ph being the fundamental prerequisite for the breakdown of alkaline silicic glasses. A purely tectonic origin of *Tatvan Hole* is not entirely convincing. Alternatives: (a) Collapse spatially separated from the eruptive site (the largest historic eruption of last century, Katmai (1912), took place 10 km away from caldera collapse). (b) A real eruptive center in view of huge tephra fallout thicknesses near Ahlat.

References:

Litt T, Krastel S, Sturm M, Kipfer R, örcen S, Heumann G, Frany SO, Ülgen UB, Niessen F (2009) 'PALEOVAN', international continental scientific drilling program (ICDP): site survey result and perspectives. Quat Sci Rev 28: 1555-1567

IODP

Ca-isotopes of early diagenetic, primary dolomite from the Peru Margin

BARBARA M.A.TEICHERT[1], PATRICK MEISTER[2], CHARLOTTE OCKERT[3] AND NIKOLAUS GUSSONE[3]

[1]Institut für Geologie und Paläontologie, Universität Münster, Corrensstr. 24, 48149 Münster
[2]Max-Planck-Institut für Marine Mikrobiologie, Celsiusstr. 1, 28359 Bremen
[3]Institut für Mineralogie, Universität Münster, Corrensstr. 24, 48149 Münster

Early diagenetic dolomite beds were sampled during ODP Leg 201 on the Peru continental margin. The highly active 'deep biosphere' that was detected at different locations on the Peru Margin provides a new context in which dolomite formation in a hemipelagic environment can be evaluated. Since the mechanism of dolomite formation is still a controversial process this location bears the potential to shed new light on dolomite formation in deep-sea sediments and the factors controlling this precipitation.

In this study, we investigated dolomite samples from Site 1229 which is located in an upper shelf basin (Salaverry Basin) at about 150 m water depth. Previous studies by Meister et al. (2007) proved that the dolomites have a diagenetic origin and are primary precipitates. Precipitation from hydrothermal fluids or a formation through recrystallization of precursor carbonate could be excluded. Strontium- and carbon-isotope data of dolomite and porewater indicated that currently dolomite is only actively formed in the upper 30 mbsf (meters below seafloor) while dolomite layers at greater depth were formed in the past when they were located nearer to the sediment/water interface (Meister et al., 2007). The formation of dolomite in shallow sediments coincides with the current sulfate-methane-interface (SMI) at about 30 mbsf. This 'microbial hot-spot' with the highest bacterial cell count, high metabolic activity and maxima in alkalinity control the precipitation of dolomite (Meister et al., 2007).

Since Site 1229 is already very well characterized in respect to biogeochemistry, it is ideally suited to further investigate Ca-isotope systematics of diagenetic dolomite formation. A prerequisite for understanding the Ca-isotope composition of the dolomites, is knowledge of the Ca-isotopic composition of the porewaters from which the dolomites precipitated. The $\delta^{44/40}$Ca values in the upper 100 mbsf show a decrease of about 1 ‰ from seawater-like values. A similar decrease in $\delta^{44/40}$Ca in shallow marine sediments has previously been observed at the Cascadia Margin (Teichert et al., 2009) and the North Atlantic (Exp. 303, Site U1308, Ockert et al. (2010) and is always accompanied by a correlation with ammonium concentration in the porewater. Several hypotheses have been proposed to explain this observation (Teichert et al., 2009). The basic process is probably an ion exchange reaction caused by the production of ammonium through the degradation of organic matter. New results confirm this hypothesis (Ockert et al., 2010). In the deeper part of the sedimentary section, the upward diffusion of a brine dominates the Ca-isotopic composition of the porewater. The $\delta^{44/40}$Ca values get constantly heavier with depth.

The $\delta^{44/40}$Ca values of five dolomite samples show a rather similar isotopic composition of 1.13-1.24 ‰SRM915a except for one sample which shows a lighter value of 0.91 ‰SRM915a. Since these are the first Ca-isotope values for primary dolomites, we propose an apparent fractionation factor of -0.5 ‰ at about 14 °C (D'Hondt et al., 2003). This indicates that dolomites have a rather heavy Ca-isotopic composition compared to other authigenic (Teichert et al., 2005) and inorganic carbonates (e.g. Gussone et al., 2005). The influence of precipitation rate and temperature will need a separate evaluation. The results from Ca-isotopes also confirm that the dolomite is currently precipitated at about 8 mbsf while the deeper samples (64 – 105 mbsf) are buried dolomites that were precipitated in much shallower parts of the sedimentary succession. The variation in the $\delta^{44/40}$Ca values of the dolomites indicate either that the Ca-isotopic composition of the porewater varied over time, possibly due to varying amounts in total organic matter or deepening of the SMI, or that precipitation rates differed.

References

D'Hondt, S.L., Jørgensen, B.B., Miller, D.J., et al. (2003) Proc. ODP, Init. Repts., 201: College Station, TX (Ocean Drilling Program). doi:10.2973/odp.proc.ir.201.2003

Gussone, N., Böhm, F., Eisenhauer, A., Dietzel, M., Heuser, A., Teichert, B.M.A., Reitner, J., Wörheide, G., and Dullo, W.-C. (2005) Calcium isotope fractionation in calcite and aragonite. Geochimica et Cosmochimica Acta, 69, 4485-4494.

Meister, P., McKenzie, J.A., Vasconcelos, C., Bernasconi, S., Frank, M., Gutjahr, M., and Schrag, D.P. (2007) Dolomite formation in the dynamic deep biosphere: results from the Peru Margin. Sedimentology, 54, 1007-1031.

Ockert, C., Teichert, B.M.A., Kaufhold, S., and Gussone, N. (2010) Interaction of Calcium with clay minerals and marine sediments. IODP/ICDP-Kolloquium 2010, Frankfurt.

Teichert, B.M.A., Gussone, N., Eisenhauer, A., and Bohrmann, G. (2005) Clathrites: Archives of near-seafloor pore-fluid evolution ($\delta^{44/40}$Ca, δ^{13}C, δ^{18}O) in gas hydrate environments. Geology, 33, 213-216.

Teichert, B.M.A., Gussone, N., and Torres, M.E. (2009) Controls on calcium isotope fractionation in sedimentary porewaters. Earth and Planetary Science Letters, 279, 373-382.

IODP

Results of a high resolution seismic IODP Pre-Site Survey in the south-western Baltic Sea: Anholt Loch and Hanö Bay / Bornholm Basin

A. F. TRAMPE[1], V. SPIESS[1], S. KRASTEL[2], T. ANDRÈN[3], R. ENDLER[4], J.HARFF[4,5]

[1]Department of Geosciences, University of Bremen, Klagenfurter Str., 28359 Bremen, Germany
[2]Leibniz Institute of Marine Sciences (IFM-GEOMAR), Wischhofstr. 1-3, 24148 Kiel, Germany
[3] Department of Geology and Geochemistry, Stockholm University, SE-106 91 Stockholm, Sweden
[4] Marine Geology Section, Baltic Sea Research Institute, Seestraße 15, Warnemuende 18119 Roststock, Germany
[5] Institute of Marine Sciences, University of Szczecin, Ul. Mickiewicza 18 PL-70-383 Szczecin, Poland

The Baltic Sea Basin (BSB) is one of the world's largest intra-continental basins. The BSB has served as depositional sink throughout its geological history. The accumulated sediments comprise a unique high-resolution paleoenvironmental archive where the history of the drainage area and the basin itself is preserved. Present knowledge of the development of the BSB is based on results from short cores (up to 20 m long), but seismic data

and onshore drillings indicate much thicker apparently undisturbed sediment sequences (Eiriksson et al., 2005; Jensen et al., 2002; Lykke-Andersen et al., 1993; Kristensen et al., 2005).

In 2004 the IODP Pre-Proposal "Paleoenvironmental evolution of the Baltic Sea Basin trough the last glacial cycle" was submitted by Andrèn et al. (2004). The general aim of the project is to reconstruct the climatic response of Northern Europe to the forcing of the Northern Atlantic is to study possible links between thermohaline circulation changes and freshwater outburst from the Scandinavian ice sheet during the last deglaciation and early Holocene (MIS 2 and MIS 1). The planned drill sites in the working areas of Hanö Bay / Bornholm Basin shall be used to study the complexities of the last glacial (MIS 4 – MIS 2) (Andrèn et al., 2009).

The seismic data, which were used to search for adequate drilling locations, were collected with the Bremen

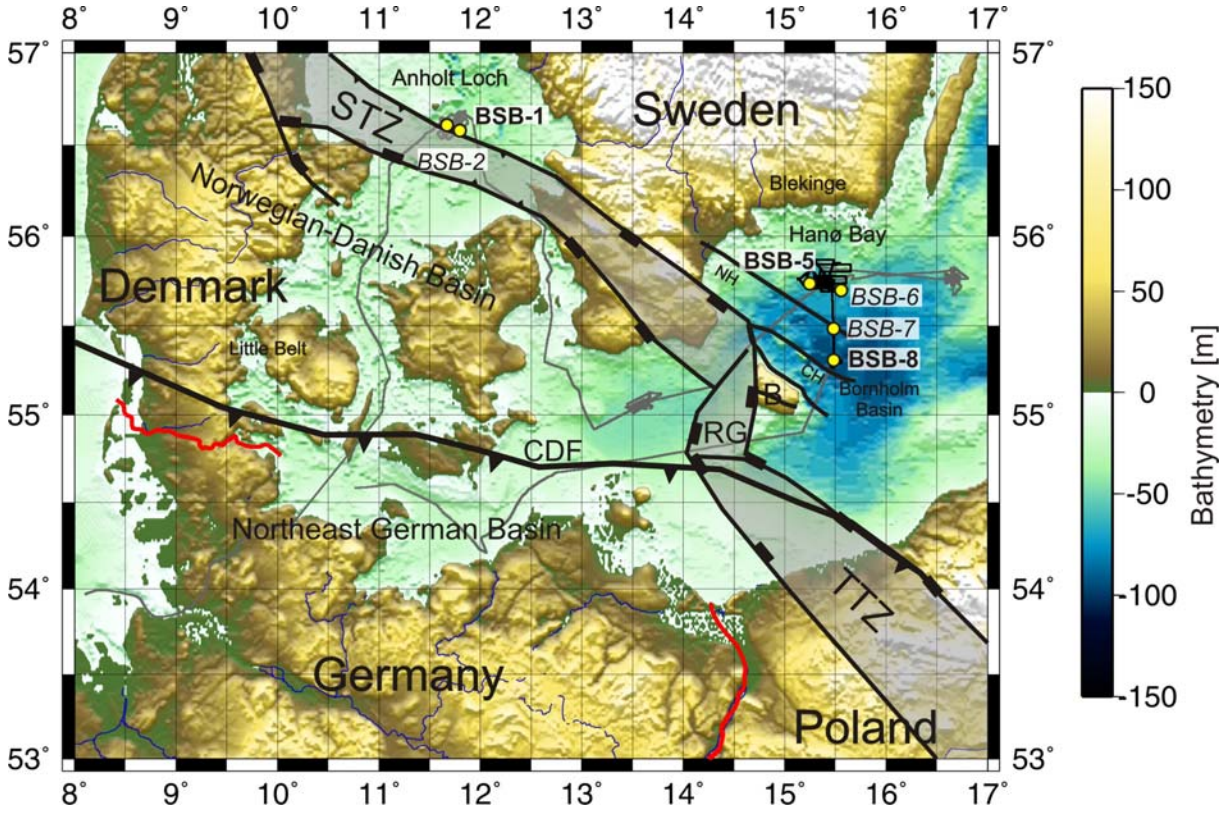

Fig. 1: Bathymetric map of the southern Baltic Sea and track chart of R/V Heincke He244 seismic Pre-Site Survey cruise. BSB-1 and BSB-2 are located in the so called Anholt Loch (Kattegat), BSB-5 to 8 are located in the area of Hanø Bay and Bornholm Basin (italics=alternae sites of. Structural features are taken from Hansen et al. (2005). ***STZ*** – Sorgenfrei-Tornquist Zone; ***RG*** – Rønne Graben; ***TTZ*** – Tornquist-Teisseyre Zone; ***CDF*** – Caledonian Deformation Front; ***NH*** - Nävlingeåsen Horst; ***CH*** – Christiansö Horst; ***B*** – Bornholm (Denmark)

atmospheric and oceanic circulation system during the last glacial cycle (Holocene, Weichselian and Eemian) by using the sedimentary record of the BSB. During a seismic pre-Site Survey in February 2006 with the R/V Heincke, high-resolution seismic data and sediment echosounder data were collected in the south-western Baltic Sea. This pre-Site Survey was an important step for submitting a Full-Proposal in October 2007 (Andrèn et al., 2007) by demonstrating that suitable drill sites and sediments exist. The revised proposal version (672-full3) was accepted by the IODP Science Steering and Evaluation Panel (SSEP) in July 2009 and was forwarded to the Science Planing Committee (SPC) with a three star grouping (1 to 5 stars). The SPC will review the proposal in March 2010 and rank it for possible scheduling as drilling expeditions in 2012 or beyond. In total, 11 sites are proposed based on our and other seismic data (Fig. 1). Our data were collected around Sites BSB-1 and -2 (Anholt Loch) and BSB-5 to -8 (Hanö Bay / Bornholm Basin), whereas the BSB-1, -5 and -8 are primary sites and BSB-2, -6 and -7 are alternate sites. The primary aim for the sites in the vicinity of the island Anholt high-resolution seismic system. Two different streamer systems were used simultaneously during data acquisition: a 300 m long 48 channel streamer and a 50 m long 48 channel shallow water streamer. The long streamer was mainly used for velocity analysis, which is crucial to distinguish between Quaternary and Mesozoic sediments, as an unconformity between these sedimentary units is not clearly visible in most parts of the profiles because of almost parallel layering. Therefore, only a velocity analysis can reveal this boundary due to the very different consolidation state. In both study areas Anholt Loch as well as Hanö Bay and Bornholm Basin this approach was successfully applied. An example of a seismic velocity model for a full profile across Anholt Loch is shown in Fig. 2. The high resolution data of the shallow water streamer were used for a structural and seismic facies analysis. The objectives of our investigations are to reconstruct the quaternary history of the Anholt Loch and of Hanö Bay / Bornholm Basin in order to verify a sufficiently thick Quaternary sediment cover at these sites. All drill sites were picked at local depressions which may have preserved

sediment from glacial erosion during various late Quaternary glacial advances and favour increased sedimentation rates.

depression is incised into the lowermost facies A, characterized by tilted reflectors and a sharp increase in seismic velocity (Fig. 2). Facies A is interpreted as Pre-

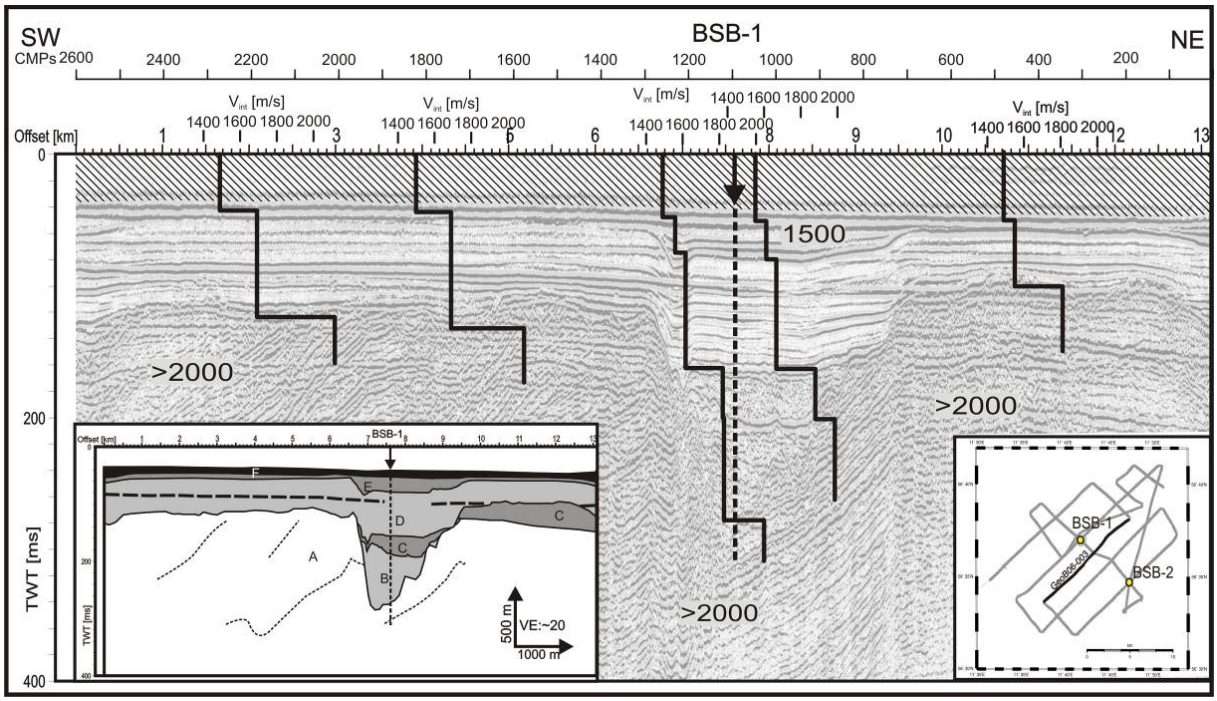

Fig. 2: Profile GeoB06-003: Velocity model of the profile, which runs perpendictular to the valley Anholt Loch. The velocity profiles are embedded over the migrated seismic data. The box in the bottom left corner of the velocity model shows the interpretation of this profile.The location of the profiles is shown in the inserted map. BSB-1 and BSB-2 are the proposed drill sites. BSB-1 is located north-west of profile 003 and is projected on this profile. **III:** A: Jurassic, B: Saalian and Eemian C: Weichselian till, D: Weichselian, glacio-marine sediments, E: late Weichselian, F: Holocene. Dashed line: Multiple of the seafloor reflector, dotted lines: tilted reflectors in facies A. For location of the study area and the proposed drill sites see Fig. 1.

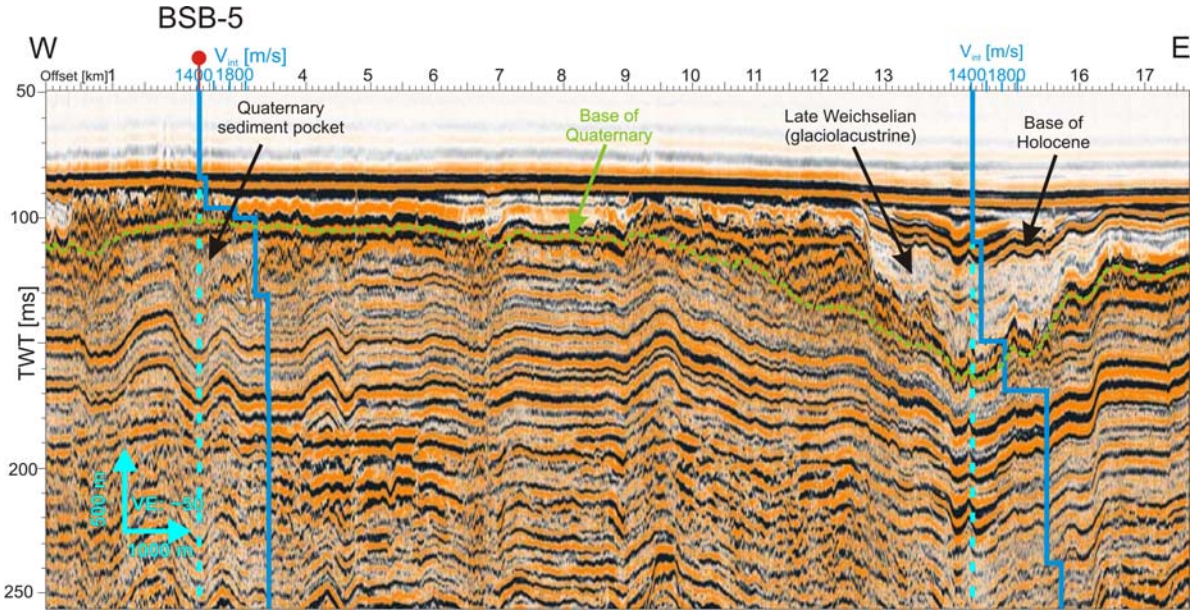

Fig. 3: Migrated E-W trending profile GeoB06-057 in the working area of Hanö Bay. The velocoty profiles, which were used for the detection of the boudary between Quaternary and Mesozoic sediments (green, dashed line), are shown in blue. Marked are also the Holocene and Late Weichselian units as well as the sediment pockect, filled with Weichselian to Eemian sediments. Additionally the location of of the drilling site BSB-5 is marked in red. For location of the study area and the proposed drill sites see Fig. 1

The Anholt Loch is located in the Kattegat, the westernmost area of the Baltic Sea (Fig. 1). The elongated

Quaternary sediments. A drilling on the island of Anholt shows that the Pre-Quaternary sediments are Jurassic in

age (Lykke-Andersen et al., 1993). The detection of the boundary of the Pre-Quaternary and Quaternary sediments is based on a facies analysis and a detailed velocity analysis. The NW-SE trending elongated depression was probably eroded by the drainage of subglacial meltwater. This tunnel valley is filled with a more than 230 m thick sedimentary succession, in which five different seismic units (B-F) could be identified. Unit B to F are interpreted as Quaternary sediments: Holocene, Late Weichselian glaciomarine sediments and a glacial till, which is probably deposited during the Last glacial Maximum (LGM) in Weichselian times. The lowermost unit must be older than the Weichselian glacial till. One possible explanation is that the lowermost Quaternary sedimentary unit in the study area was deposited in the Early or Middle Weichselian. Another possibility might be that this unit contains older sediments, e.g. Saalian till and Eemian sediments, which were deformend by the glaciers during the Weichselian glacial by glaciers. This interpretatino was supported by the sediments which were found by drilling on the island of Anholt, an 8 m-thick unit of late Saalian and Eemian age in 76 m drilling depth (Lykke-Andersen et al., 1993). In this case, sediments of the complete last glacial cycle may be present at these proposed Anholt Loch sites (Trampe et al., in prep.).

The second study area of Hanö Bay/Bornholm Basin is situated in south-western Sweden, east of the province of Skåne. To the north and northeast the Hanö Bay is bordered by the province of Blekinge. Southwest of the bay lies the Danish island Bornholm (Fig. 1). It can be subdivided in two parts: the northern area Hanö Bay near the mainland and the southern area within the Bornholm Basin. The study area Hanö Bay/Bornholm Basin constitute a tectonically influenced sedimentary basin. The study areas are located at the south-western margin of the Fennoscandian shield, bordered by the prominent the Tornquist Zone (TZ) (Fig. 1). The TZ defines the border between the Precambrian shield of Fennoscandia and Eastern Europe and the younger lithosphere of Central Europe. The area nearby the TZ was tectonically influenced by the NW-SE trending fault zone for the last 440 million years (Gregersen et al., 2009). The basement, the mature sub-Mesozoic peneplain, was interpreted by Kumpas (1980) as Lower Cambrian sandstone and as crystalline Precambrian basement. The basement dips from the mainland (0 mbsf) in the northeast to Christiansö Horst in the southwest, where the basement rises abruptly from -1000 to -100 mbsf (Fig.1). In both study areas, Hanö Bay and Bornholm Basin, the Precambrian basement was covered completely by Mesozoic sediments (Kumpas, 1980). The Mesozoic sediments were deposited with major interruptions from the Late Triassic (Rhaetian) to the Late Cretaceous (Campanian-Maastrichtian). With decreasing age of the Mesozoic sediments the covered area increases (KUMPAS, 1980).

The reflectors of the Mesozoic sediments are running almost parallel to the overlying Quaternary reflectors, which are present throughout the complete working area. The challenge to distinguish between these two sedimentary successions of totally different age but with similar reflection patterns was approached by a detailed velocity analysis (Fig. 3). The uppermost, thin and transparent unit (Fig. 3) is present in the whole working area and was interpreted as Holocene Mud and Clay. The reflection pattern indicates a relative homogenous material, which confirms this interpretation. The thickness of this unit increases basinwards (southwards). The Seafloor shows in the working area a gentle south-easterly dipping bottom surface. In Hanö Bay, the greatest thickness of the Holocene unit can be found in a shallow NNW-SSE trending depression (Fig. 3). Beneath this unit, a relatively thick transparent unit with some internal reflectors is present (Fig. 3). This unit increases, as the Holocene Mud and Clay, basinwards. Again, the greatest thickness of this unit is found within the NNW-SSE trending valley, which has acted as sediment trap. The parallel reflectors in the nearly transparent unit indicate a deposition under relative quiet conditions. These deposits were interpreted as glaciolacustrine sediments of Late Weichselian age, after the recession of the last glacial advance. In contrast to the uppermost two units, the unit beneath the glaciolacustrine sediment shows a chaotic reflection pattern with highly variable thickness and is not present in the whole area. This is in a glacially influenced area an indicator for glacial till, most probably deposited during the last advance during Weichselian times. In both areas, Hanö Bay and Bornholm Basin, some sediment pockets beneath the Weichselian till were identified. These sediments were probably deposited in the lake stage from Eemian to the last Weichselian ice advance with sediments of the same age. This will provide the opportunity to study the lake development both in littoral phases in Hanö Bay and in deep lake phases in the Bornholm Basin. The four sites BSB-5 to -8 (36 to 93 m thick Quaternary sediment succession) in Hanö Bay and Bornholm Basin are located in sediment pockets, as an example Site BSB-5 is shown in Fig. 3, where sediments may be less affected by glacial processes. Sites were chosen close to the shore in the area of Hanö Bay and also in the deeper Bornholm basin along a transect in order to compare records in environments with different glacial influence.

References:

ANDRÈN T., BITINAS A., BJÖRK S., EMELYANOV E., HARFF J., JAKOBSON M., JENSEN J. B., KNUDSEN K. L., KOTILAINEN A., LEMKE W., USCINOWICZ S., VESKI S., and ZELCHS V. (2004) Paleoenvironmental evolution of the Baltic sea basin through the Last Glacial Cycle (Pre-Proposal).

ANDRÈN T., BJÖRCK S., JØRGENSEN B. B., KNUDSEN K. L., HARFF J., BITINAS A., EMELYANOV E., JAKOBSON M., JENSEN J. B., KOTILAINEN A., SPIESS V., USCINOWICZ S., VESKI S., and ZELCHS V. (2007) Paleoenvironmental evolution of the Baltic sea basin through the Last Glacial Cycle (Full-Proposal – 672-full3).

ANDRÈN T., BJÖRCK S., JØRGENSEN B. B., KNUDSEN K. L., HARFF J., BITINAS A., EMELYANOV E., JAKOBSON M., JENSEN J. B., KOTILAINEN A., SPIESS V., USCINOWICZ S., VESKI S., and ZELCHS V. (2009) Paleoenvironmental evolution of the Baltic sea basin through the Last Glacial Cycle (Full-Proposal – 672-full3).

EIRIKSSON J., KRISTENSEN P.-H., LYKKE-ANDERSEN H., BROOKS K., MURRAY A., KNUDSEN K. L., and GLAISTER C. (2005) A Sedimentary record from a deep Quarternary valley in the southern Lillebaelt area, Denmark: Eemian and Early Weiselian lithology and chronology at Mommark. Boreas 35, 320-331.

GREGERSEN, S., VOSS, P., NIELSEN, L. V., ACHAUER, U., BUSCHE, H., RABBEL, W., and SHOMALI, Z. H., 2009. Uniqueness of modeling results from teleseismic P-Wave tomography in Project Tor. Tectonophysics, 9.

HANSEN, M. B., LYKKE-ANDERSEN, H., DEHGHANI, A., GAJEWSKI, D., HÜBSCHER, C., OLESEN, M., and REICHERTER, K., 2005. The Mesozoic-Cenozoic structural framework of the Bay of Kiel area, western Baltic Sea. International Journal of Earth Science 94, 12.

JENSEN J. B., PETERSEN K. S., KONRADI P., KUIJPERS A., BENNIKE O., LEMKE W., and ENDLER R. (2002) Neotectonics, sea-level changes and biological evolution in the Fennoscandian Border Zone of the southern Kattegat Sea. Boreas 31, 133-150.

KRISTENSEN P.-H. and KNUDSEN K. L. (2005) Palaeoenvironments of a complete Eemian sequence at Mommark, South Denmark: foraminifera, ostracods and stable Isotopes. Boreas 35, 349-366.

KUMPAS, M., 1980. Seismic Stratigraphy and tectonics in Hanö Bay, southern Baltic, Unitversity of Stockholm.
LYKKE-ANDERSEN H., SEIDENKRANTZ M.-S., and KNUDSEN K. L. (1993) Quarternary sequences and their relation to the pre-Quarternary in the vicinity of Anholt, Kattegat, Skandinavia. Boreas 22, 291-298.
TRAMPE, A. F, KRASTEL, S., SPIESS, V. (in prep.) High resolution seismic investigation of the Pleistocene valley Anholt Loch in the Kattegat, south-western Baltic Sea

IODP

Eirik Drift: Archive of palaeoenvironmental information of climate development and oceanic circulation in the Greenland and Labrador Seas

G.UENZELMANN-NEBEN[1]

[1]Alfred-Wegener-Institut für Polar- und Meeresforschung, Am Alten hafen 26, 27568 Bremerhaven

The Eirik Drift has been documenting the sedimentation near southeast Greenland since the Miocene. This sediment drift forms an important archive for the depositional processes in this region, which have been shaped by the Western Boundary Undercurrent (WBUC), the Greenland ice sheet and the material input from the Labrador Sea/Davis Strait. The incorporation of high resolution seismic reflection data acquired during RV Maria S. Merian cruise MSM 12/2 in June/July 2009 with geologic information from ODP and IODP sites (ODP Leg 105 and IODP Expedition 303) will lead to information on the development of the WBUC as well as the dimensions and expansion/retreat of the Greenland ice sheet and a much clearer understanding of the evolution of the climate southwest of Greenland. A comparison with sediment drifts from the southern hemisphere will further allow conclusions regarding global climate variations.

ICDP

Drei komponentige Magnetfeldmessungen in der Outokumpu-Bohrung (Finnland)

C. VIRGIL[1], A. HÖRDT[1], S. EHMANN[1], M. LEVEN[2], E. STEVELING[2], J. KÜCK[3], F. DIETZE[4]

[1]Institut für Geophysik und extraterrestrische Physik, Technische Universität Braunschweig
[2]Institut für Geophysik, Georg-August-Universität Göttingen
[3]Helmholtz-Zentrum Potsdam Deutsches GeoForschungsZentrum GFZ, Potsdam
[4]Institut für Angewandte Geowissenschaften - Strukturgeologie und Tektonophysik, Universität Karlsruhe (TH)

Einleitung: Bisherige Verfahren zur Messung von magnetischen Anomalien in Bohrlöchern bestimmen meist nur das magnetische Totalfeld. Jedoch erlauben Messungen, die auf dem Totalfeld beruhen, nur eine sehr eingeschränkte Aussage über die räumliche Ausdehnung und die magnetischen Eigenschaften von Störkörpern. Es existieren aber viele theoretische Arbeiten, die den Vorteil von vektoriellen Bohrlochmagnetfelddaten gegenüber Totalfelddaten beschreiben, um Störkörper eindeutiger zu charakterisieren (z.B. Silva und Hohmann, 1981). Dazu können auch Oberflächenmagnetikmessungen zusammen mit dreikomponentigen Bohrlochmessungen mittels Joint Inversion kombiniert werden (Li und Oldenburg, 2000; Lelièvre und Oldenburg, 2009). Eine weitere Anwendung besteht in der Modellierung von Schichtungen, die von der Bohrung durchdrungen werden (Bosum et al., 1988; Pozzi et al. 1988; Gallet und Courtillot, 1989). Aus dreikomponentigen Magnetfelddaten lassen sich in diesem Fall zusätzlich zur Amplitude auch die Richtung der Magnetisierung der Schichten berechnen. Diese vektoriell bestimmten Magnetisierungen liefern wichtige Informationen für paläomagnetische Polbestimmungen (Bosum und Scott, 1988) und geben Aufschluss über die tektonische Entwicklung der Region. Weiterhin können Bohrkerne durch Vergleich der „In-Situ“ bestimmten, und der im Labor am Kern gemessenen Magnetisierung reorientiert werden.

Um diesen starken theoretischen Hintergrund nutzen zu können, wird eine Bohrlochsonde benötigt, welche das Magnetfeld in drei Komponenten, sowie die Orientierung in Bezug auf ein geographisches Referenzsystem aufzeichnet. Die Schwierigkeit hierbei liegt in der exakten Orientierungsbestimmung. Bosum et al. (1988) entwickelten eine Bohrlochsonde, die mit Hilfe von Inklinometern und einem mechanischen Kreisel die Lage der Sonde aufzeichnete. Allerdings erwies sich der Kreisel als zu ungenau, um eine kontinuierliche Vektormessung durchzuführen.

Unsere Sonde, das „Göttinger Bohrlochmagnetometer“ (GBM) verfügt als Orientierungssystem über drei orthogonal zueinander angebrachte, optische Faserkreisel (Fibre Optic Gyro, FOG). Diese zeichnen sich durch eine hohe Auflösung von 9 · 10-5 ° und durch eine geringe Drift von 1.5 °/h aus. Zusammen mit einem Förstersonden Tripel, ist es uns so möglich, das Magnetfeld kontinuierlich in drei Komponenten zu messen und in das geographische Referenzsystem zu übertragen. Die erreichte Genauigkeit dieser Reorientierung ergibt sich zu 0.14 ° in der Inklination und 1.4 ° in der Deklination. Mit dieser Sonde wurde im September 2008 eine Messreihe in der Tiefbohrung Outokumpu (Finnland) (Kukkonen, 2007) durchgeführt. Das Ziel dieser Messungen war die Bestimmung der Magnetfeldanomalie in drei Komponenten. Mit diesen Daten wurde die Magnetisierung der Gesteinsschichten berechnet, um Aufschluss über die geologische Entwicklung der so genannten „Outokumpu-Formation“ und den Entstehungsprozess der darin enthaltenen Erzlagerstätten zu erhalten. Innerhalb der heterogenen Formation lassen sich zwei Teufenbereiche identifizieren, die unterschiedliche Vorzugsrichtungen in der Magnetisierung aufweisen. Dies steht vermutlich mit einer unterschiedlichen tektonischen Entwicklung im Zusammenhang.

Vorbereitung und Datenverarbeitung: Eine Vorraussetzung für die Bestimmung der Gesteinsmagnetisierung war die Optimierung der Messprozedur und der Weiterentwicklung der Datenverarbeitung. Dazu sind zunächst umfangreiche Kalibriermessungen durchgeführt worden. Die Kalibrierung der Magnetfeldsensoren wurde in dem magnetischen Laboratorium „Magnetsrode“ (Glassmeier et al., 2007) mittels des dort vorhandenen Braunbekspulensystems ausgeführt. Dieses Spulensystem besitzt eine aktive Kompensation des Erdmagnetfeldes, so dass ein beliebig orientiertes Magnetfeld von bis zu 120000 nT erzeugt werden kann. Die Genauigkeit des erzeugten Feldes liegt bei 1 nT. Für die Kalibriermessung wurden in allen drei Achsen Magnetfelder von -50000 nT

bis 50000 nT in 10000 nT Schritten angelegt. Aus dem Vergleich zwischen den Kalibrierfeldern und den von der Sonde aufgezeichneten Daten ließen sich so die Offsets, die Skalenfaktoren und die Schiefstellung der Sensoren untereinander bestimmen.

Mit dem Braunbekspulensystem war es auch möglich, die kombinierte Übertragungsfunktion der Magnetfeldsensoren und der verbauten Tiefpassfilter der Sonde zu bestimmen. Diese Filter haben eine Cutoff-Frequenz von ca. 0.3 Hz. Besonders bei schnellen Drehungen um die z-Achse können dadurch die horizontalen Komponenten des Magnetfeldes beeinflusst werden. Um nun die genaue Filtercharakteristik zu ermitteln, wurden stufenförmige Magnetfelder sukzessive in allen drei Raumrichtungen erzeugt und aus der Differenz zwischen anliegendem und von der Sonde aufgezeichnetem Feld mittels eines Wienerfilters die Übertragungsfunktion ermittelt.

Ein weiterer wichtiger Schritt bei der Kalibrierung der Sonde betrifft die Faserkreisel. Diese weisen eine temperaturabhängige Drift auf, die einer tatsächlich auftretenden Rotation überlagert ist, und die vor der Reorientierung von den Messdaten abgezogen werden muss. Durch Labormessungen wurde die Driften in dem Betriebstemperaturbereich von 35°C bis 45°C zu 1.4 °/h für den x-Kreisel, 1.7 °/h für den y-Kreisel und 2 °/h für den z-Kreisel bestimmt. Es zeigte sich außerdem, dass die Kreisel nicht exakt senkrecht aufeinander stehen. Dies führt dazu, dass bei einer Rotation um die z-Achse auch eine scheinbare Bewegung um die x- und y-Achse von dem jeweiligen Kreisel registriert wird. Um die Fehlwinkel zu bestimmen, wurde die Sonde drehbar gelagert und langsam um 720 ° entlang der z-Achse rotiert. Aus einer Korrelationsanalyse konnten dann die Winkel zu 0.19° zwischen x- und z-Kreisel, bzw. 0.02 ° zwischen y- und z-Kreisel bestimmt werden.

Um die in den Kalibriermessungen ermittelten Eigenschaften der Magnetfeldsensoren und Faserkreisel auf die Messdaten anwenden zu können, mussten die bestehenden Programme zur Datenauswertung angepasst, bzw. ergänzt werden. Eine wichtige Änderung wurde auch bei dem eigentlichen Reorientierungsprozeß umgesetzt. Bei der Reorientierung der Magnetfelddaten aus dem Sondensystem x, y, z in das geographische Referenzsystem Nord, Ost und Vertikal werden zunächst die Rohdaten um die oben beschriebenen Fehler korrigiert. Anschließend wird für jeden Messpunkt aus den drei Faserkreiselwerten eine Rotationsmatrix berechnet, die mit dem Magnetfeldvektor multipliziert wird. In dem bisherigen Algorithmus wurde diese Matrix nach der Roll-Yaw-Pitch Konvention berechnet. Diese geht davon aus, dass die einzelnen Drehungen zeitlich separiert in einer festen Reihenfolge ablaufen. Bei realen Messungen finden die von den Kreiseln registrierten Winkeländerungen in einer Messperiode aber meist gleichzeitig statt. Um dies zu berücksichtigen wurde zur Berechnung der Rotationsmatrix nun die „Direct Cosine Matrix“ verwendet, die eine kontinuierliche Drehung beschreibt.

Eine weitere Verbesserung in der Reorientierungsgenauigkeit wurde durch das „Einnorden“ der Sonde erreicht. Zu Beginn und am Ende einer jeden Messung wurde die Sonde über der Bohrung hängend mit Hilfe einer neu entwickelten Zieleinrichtung auf eine feste Marke ausgerichtet. Die Genauigkeit hierbei beträgt 0.05 °. Durch vorherige Differential GPS Messungen ist auch der Winkel der Strecke Bohrung/Marke zu Nord mit einem Fehler kleiner als 0.01 ° bekannt. Mit der Kenntnis der genauen Lage der Sonde im Raum kann man den Einfluss der Erdrotation auf die Faserkreisel sehr präzise berechnen. Ein weiterer Vorteil liegt darin, dass man die aus den Faserkreiseldaten berechnete Ausrichtung der Sonde zu diesen beiden Zeitpunkten vergleichen kann. Aus diesen Daten lassen sich Driftkorrekturen für die Kreisel berechnen. Mit diesen zusätzlichen Driftkorrekturen wird

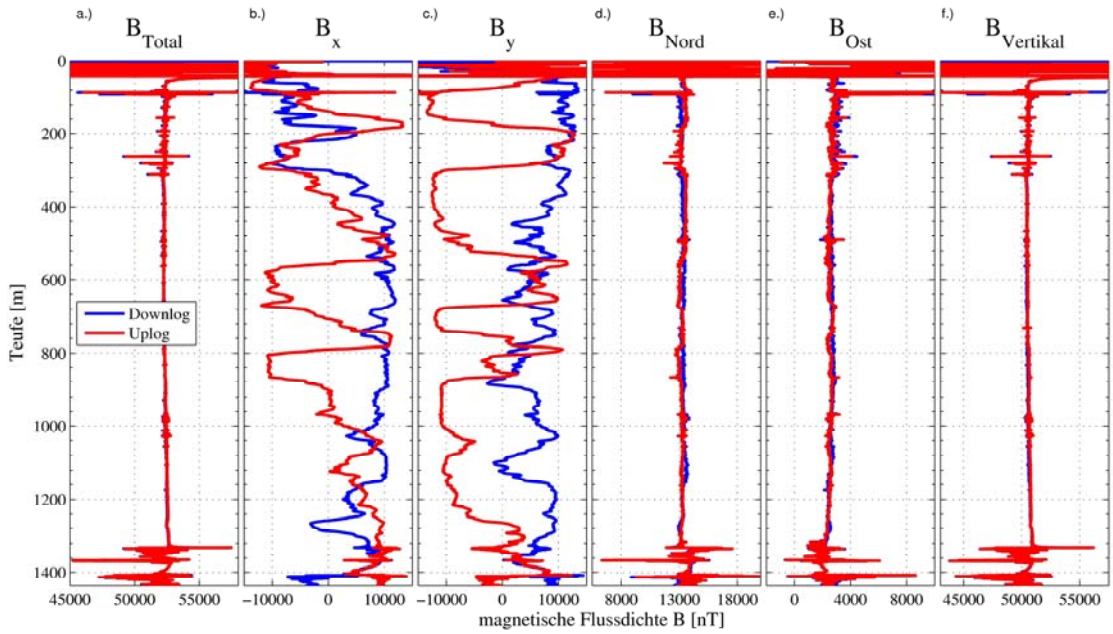

Abbildung 1: Vergleich zwischen den gemessenen Magnetfeldern vor und nach der Reorientierung. a.) Totalfeld, b.), c.) Magnetfeld im Sondenkoordinatensystem, d.)-f.) Reoreintiertes Magnetfeld im geographischen Referenzsystem

der Reorientierungsalgorithmus ein letztes Mal angewandt. In Abbildung 1 ist ein Vergleich zwischen Rohdaten im

Sondensystem x, y, z und den reorientierten Magnetfelddaten im geographischen Referenzsystem Nord, Ost, Vertikal (abwärts gerichtet) aufgetragen. Der RMS-Wert der Differenz zwischen Down- und Uplog nach der Reorientierung (Abb. 1, d.), e.), f.)) beträgt RMS_{Nord}=250 nT, RMS_{Ost}=180 nT and $RMS_{VertiKal}$=75 nT.

Auswertung: Um das Verständnis über die geologische Entwicklung der Region um Outokumpu (Finnland) zu erweitern, ist es nötig, ein Modell der die Bohrung umgebenen magnetisierten Schichten zu erstellen. Um aus den gemessenen und reorientierten Magnetfeldern die Magnetisierung der umgebenen Schichten zu berechnen, mussten zunächst die magnetischen Anomalien entlang der Bohrung bestimmt werden. Dazu wird ein dreikomponentiges Hintergrundfeld mittels eines gleitenden Mittelwertes mit einer Fensterbreite von 10 m aus den reorientierten Magnetfelddaten berechnet. Dieses wird von den Magnetfelddaten subtrahiert, um die Anomalien zu extrahieren. Aus den magnetischen Anomalien wurde dann unter Verwendung eines Modells nach Bosum et al. (1988) die Magnetisierung der Umgebung des Bohrlochs in drei Komponenten berechnet. Das Modell beschreibt das Magnetfeld im Inneren einer Bohrung durch einen horizontalen, homogen magnetisierten Hohlzylinder.

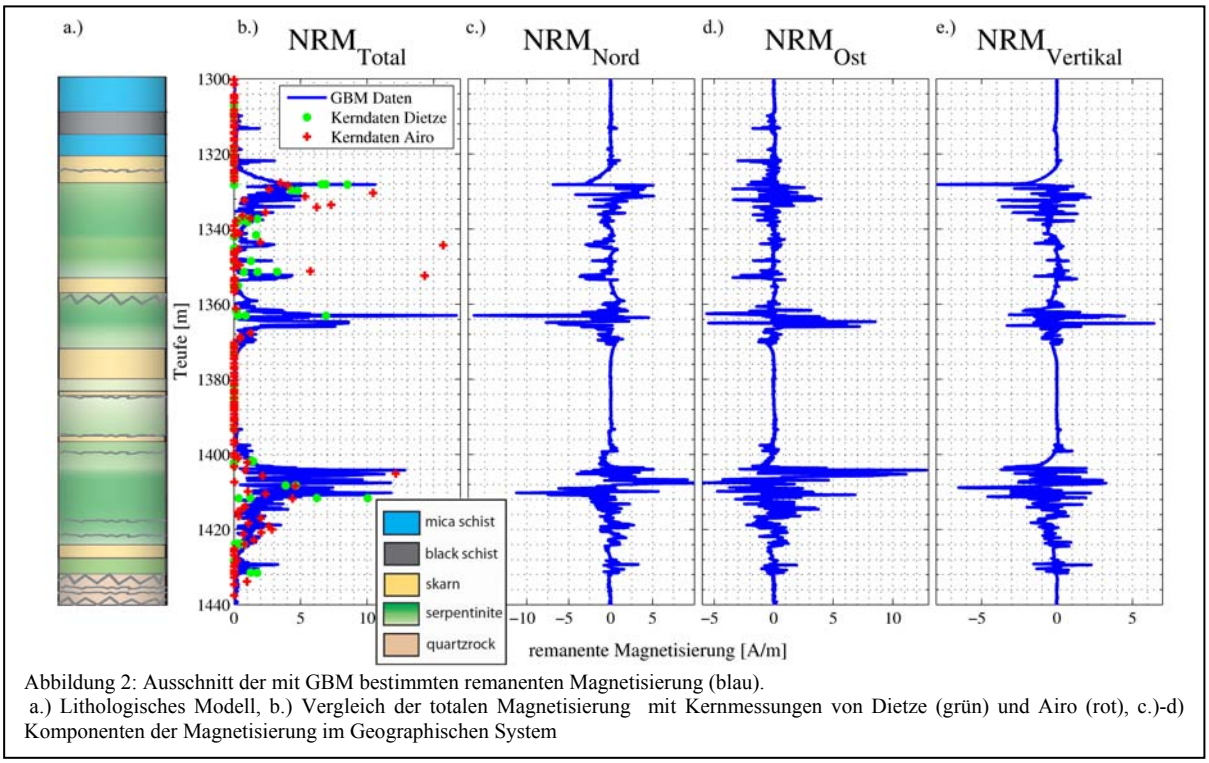

Abbildung 2: Ausschnitt der mit GBM bestimmten remanenten Magnetisierung (blau).
a.) Lithologisches Modell, b.) Vergleich der totalen Magnetisierung mit Kernmessungen von Dietze (grün) und Airo (rot), c.)-d) Komponenten der Magnetisierung im Geographischen System

In einem ersten Ansatz wurden die Schichten als unendlich ausgedehnt angenommen. Ausgehend von einem Startmodell wurden die drei Komponenten der Magnetisierung für jede Schicht so lange iterativ angepasst, bis die aus dem Modell berechneten Magnetfelder den gemessenen magnetischen Anomalien im Rahmen der Sensorauflösung entsprachen. Damit ergibt sich ein räumlich hoch aufgelöstes Schichtmodell. Mit Hilfe einer zusätzlichen Suszeptibilitätsmessung durch eine Sonde der Operational Support Group des GFZ wurde aus dem Referenzfeld die induzierte Magnetisierung berechnet. Die Differenz aus dem Magnetisierungsmodell und der induzierten Magnetisierung ergibt ein Modell der remanenten Magnetisierung (Natural Remanent Magnetization, NRM).

Ein Ausschnitt der berechneten remanenten Magnetisierung in einem stark magnetisierten Bereich ist in Abbildung 2 zu sehen. Hier sind außerdem auch Messungen der totalen Magnetisierung an Kernproben von Dietze und des GTK (zur Verfügung gestellt von M.-L. Airo), sowie ein lithologisches Profil aufgetragen. Ein Vergleich der totalen Magnetisierung mit den Kerndaten gibt eine qualitativ gute Übereinstimmung, ein quantitativer Vergleich ist aber schwierig, da zum Einem die räumliche Dichte der Kernproben sehr viel geringer ist und zum Anderen das Gestein und die Magnetisierungen in diesem Teufenbereich starke Inhomogenitäten auf kleinen Skalen aufweisen. Dies zeigt sich in den Variationen der aus den Kernproben bestimmten Magnetisierungen von bis zu 9.7 A/m auf einem Teufenbereich von weniger als 10 cm (Dietze et al., diese Ausgabe). Mit dem GBM wird die magnetische Anomalie aus einem sehr viel größeren Volumen aus der Umgebung der Bohrung ermittelt. Durch diese unterschiedlichen räumlichen Auflösungen ergänzen sich die Kernmessungen hervorragend mit den Magnetometermessungen bei der Interpretation der Daten. Dies stellt neben den dreikomponentigen Daten und der hohen räumlichen Auflösung einen weiteren Vorteil der „In-Situ“ Messung mit dem GBM dar.

Die Ergebnisse der Magnetisierungsberechnungen zeigen in den drei Teufenbereichen (1328 m – 1355 m, 1355 m – 1370 m, 1400 m – 1440 m) deutliche Anomalien. Allerdings weisen diese, wie schon aus den Kernproben zu erwarten, keine gleichmäßige Schichtstruktur auf, sondern zeigen auch in einem größeren Bereich starke Variationen mit der Tiefe. Dies weist auf eine komplexe geologische Entwicklung der angebohrten Gesteinsabfolgen hin. Ein Vergleich des lithologischen Modells mit den GBM-Daten zeigt, dass stark serpenitisierte Einheiten, die nur wenig oder garnicht karbonatisiert wurden, als Träger der magnetischen Minerale fungieren.

Der Vergleich der Reproduzierbarkeit der Ergebnisse unter verschiedenen Messungen ergab für die Magnetisierung in der Nord- und Ostkomponente eine Genauigkeit von 0.2 A/m und in der vertikalen Komponente 0.1 A/m. Für eine statistische Auswertung der Richtung der Magnetisierung in den drei Teufenbereichen werden nur Datenpunkte berücksichtigt, deren Magnetisierung über diesen Werten liegt. In dem ersten Teufenbereich ist die bevorzugte Inklination 0°. Die Deklination hat mit 10° und -170 ° zwei Vorzugsrichtungen. Die Inklination des zweiten Bereichs ist ebenfalls 0°, allerdings ändert sich die Deklination auf -10 bzw 170 °. In dem dritten Bereich ist die häufigste Inklination -20 °, während die Deklinationsverteilung keine klare Vorzugsrichtung zeigt. Die Richtungen der Magnetisierungen deuten darauf hin, dass sich die tektonischen Entwicklungen der Teufenbereiche 1328 m – 1370 m und 1400 m – 1440 m voneinander unterscheiden.

Danksagung

Wir danken vielmals Ilmo Kukkuonen (GTK Finland) für die Ermöglichung der Messungen und die organisatorische Unterstützung; Martin Töpfer und Christian Carnein (Operational Support Group OSG/ICDP, GFZ) für den logistischen und technischen Beitrag; Meri-Liisas Airo (GTK Finland) für die Bereitstellung der zusätzlichen Bornkerndaten, sowie Johannes Stoll (Metronix) für die Hilfe bei der Verbesserung des Reorientierungsalgorithmus. Dieses Projekt wird von der DFG unterstützt (DFG, Ho 1506/16-1).

References:

Bosum, W., Eberle, D. und Rehli, H.-J. 1988. A Gyro-orientated 3-component Borehole Magnetometer for Mineral Prospecting, with Examples of its Application. Geophysical Prospecting 36, 933-961

Bosum, W. und Scott, J. H. 1988. Interpretation of Magnetic Logs in Basalt, Hole 418A. Proceedings of the Ocean Drilling Program, Scientific Results, Vol. 102

Dietze, F., Kontny, A., und Virgil, C. 2010. Source rocks of crustal-scale magnetic anomalies in the upper crust of Eastern Finland. Abstract, Diese Ausgabe

Gallet, Y. und Courtillot, V. 1989. Modeling magetostratigraphy in a borehole. Geophysics 54, No. 8, 973-983

Glassmeier, K.-H., Richter, I., Diedrich, A., Musmann, G., Auster, U., Motschmann, U., Balogh, A., Carr, C., Cupido, E., Coates, A., Rother, M., Schwingenschuh, K., Szegö, K. und Tsurutani, B. 2007. RPC-MAG The Fluxgate Magnetometer in the ROSETTA Plasma Consortium. Space Science Reviews, Vol. 128, 649-670

Kukkonen, I. T. 2007. Outokumpu Deep Drilling Project, Second International Workshop. Programme and Extended Abstracts, siehe: http://www.gsf.fi/projects/o_k_deepdrilling/

Lelièvre, P. G. und Oldenburg, D. W. 2009. A 3D total magnetization inversion applicable when significant, complicated remanence is present. Geophysics, Vol. 74, No.3, L21-L30

Li, Y. und Oldenburg, D. W. 2000. Joint inversion of surface and three-component borehole magnetic data. Geophysics 65, No. 2, 540-552

Pozzi, J. P., Martin, J. P., Pocachard, J., Feinberg, H. und Galdeano, A. 1988. In-situ magnetostratigraphy: interpretation of magnetic logging in sediments, Earth and Planetary Science Letters, 88, 357-373

Silva, J. B. C. und Hohmann, G. W. 1981. Interpretation of three-component borehole magnetometer data. Geophysics 46, No. 12, 1721-1731

IODP

The Campanian – Maastrichtian (Late Cretaceous) climate transition: the history of palaeoceanographic changes

VOIGT, S.[1], JUNG, C.[1], FRIEDRICH, O.[1], FRANK, M.[2]

[1]Goethe-University of Frankfurt, [2]IFM-GEOMAR Kiel

The latest Cretaceous was characterised by the transition of the Earth´s system from the Cretaceous greenhouse to the cooler Cenozoic climate that includes several perturbations in the global carbon cycle. The aim of this project is to investigate the history of changes in ocean circulation and deep-water formation in the tropical Pacific relative to the late Campanian to early Maastrichtian carbon isotope events (LCE, CMBE, and MME). The climatic and oceanographic processes involved in the Campanian–Maastrichtian transition are not well understood to date, especially because of the low temporal resolution of biostratigraphy and the pronounced provincialism between tropical and temperate taxa. We intend to develop an orbitally tuned high-resolution carbon isotope stratigraphy at Shatsky Rise (DSDP Site 305, ODP Site 1210B) using bulk-carbonates to decipher short-lived climatic events between 76-68 Ma. Presently, two new high-resolution carbon isotope records derived from the boreal shelf-sea section at Lägerdorf-Kronsmoor-Hemmoor, northern Germany and the tropical Pacific at DSDP-Site 305, Shatsky Rise can be correlated in high resolution (Fig. 1; Voigt et al. subm.). The generation of the $\delta^{13}C$ record for ODP-Site 1210B is currently underway. The correlated $\delta^{13}C$ records from northern Germany and Site 305 display distinct carbon isotope events in the late Campanian and the early Maastrichtian to represent global carbon cycle perturbations. Especially, the one-million-year-lasting negative carbon isotope excursion in the early Maastrichtian, a pronounced feature of open-ocean records

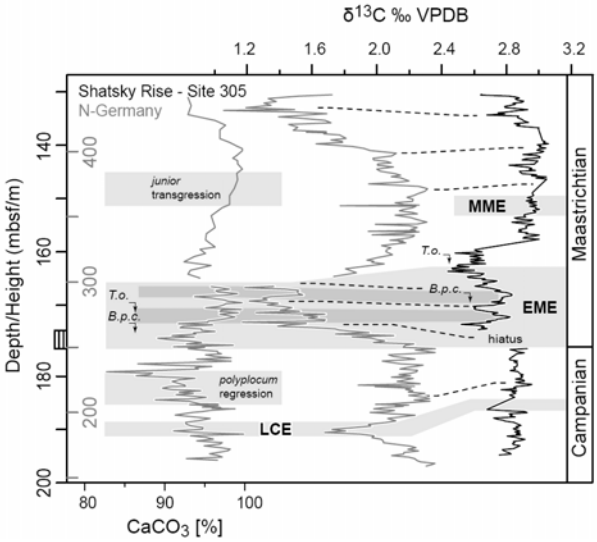

from the Pacific and Southern oceans, is recognized for the first time at a shelf-sea locality related to the North-Atlantic Ocean. Furthermore, two superimposed occurring short-term positive excursions indicate oceanographic variability acting on orbital time scales.

In the course of this project, the history of changes in surface- and deep-water temperature will be reconstructed for the carbon isotope events using high-resolution benthic and planktic foraminiferal stable isotope analyses. Changes in ocean circulation and the source regions of different deep and intermediate water masses will be deciphered by using radiogenic isotopes (Nd). Nd isotope analyses of fish teeth and early diagenetic ferromanganese coatings of bulk sediments from the tropical Pacific and the Southern Ocean. By comparison of different locations the data will allow a reconstruction of past water mass flow in the tropical Pacific and its relationship to carbon cycle perturbations.

References:
Voigt, S., Friedrich, O., Norris, R .D. & Schönfeld, J. submitted. Campanian – Maastrichtian carbon isotope stratigraphy: shelf–ocean correlation between the European shelf sea and the tropical Pacific Ocean. Geochemistry, Geophysics, Geosystems. Submitted on 13/11/2009

IODP

Orbital chronology for the Cenomanian-Turonian Oceanic Anoxic Event 2 and its environmental implications

S. VOIGT, Y. WEBER, D. BRÜNSCH

Goethe-University Frankfurt

The Cenomanian – Turonian Oceanic Anoxic Event 2 (OAE 2) is reflected by one of the most extreme carbon cycle perturbations in Earth's history. Severe short-termed climatic, oceanographic and biotic changes are supposed to have occurred during and in response to OAE 2. The immense acquisition of palaeoenvironmental data for OAE 2 improved our knowledge about the response of climate, ocean and fauna in a broad variety of depositional setting from coastal and shallow environments to the open ocean. However, the nature of these changes as well as their spatial and temporal dimension is discussed controversial for more than two decades.

While the duration of OAE 2 is well constrained by the development of regional orbital age models at four sites from shelf settings on both sides of the Central Atlantic Ocean (Gale et al. 2000, Sageman et al. 2006, Voigt et al. 2008, Kuhnt et al. 2009), the temporal framework of these age models can not be correlated to the more condensed sites in the open ocean so far. We this project we intend to generate a time series from the most extended site (ODP Site 1261) at Demerara Rise, tropical Western Atlantic using high-resolution XRF core scanning. The measurements will be performed in the second half of February this year. The relative changes in XRF element concentrations will be analysed by spectral analysis and calibrated against published records of the OAE 2 $\delta^{13}C$ anomaly. First results will be presented during the March-Colloquium in Frankfurt. The inter-site comparison of dominant orbital periodicities will significantly improve the orbital time scale for OAE 2. Such a new time scale provides the unique opportunity to establish high-resolution correlations between the Atlantic and Western Tethys as well as adjacent shelf seas (e. g. Wunstorf, N-Germany) and to recognize leads and lags between the regional changes in the formation of oxygen deficiency, ocean circulation and temperature in different oceanic settings.

ICDP

The sediment record of Lake Ohrid, Albania and Macedonia – modern and past sedimentation and inferences of climatic and environmental change over the last glacial-interglacial cycle

B. WAGNER[1], H. VOGEL[1], AND THE SCOPSCO SCIENCE TEAM

[1]Institute of Geology and Mineralogy, University of Cologne, Zülpicher Str. 49a, 50674 Köln, Germany

Lake Ohrid, a transboundary lake shared by the former Yugoslav Republic of Macedonia and the Republic of Albania is with its likely Pliocene age (Albrecht & Wilke 2008) considered to be the oldest existing lake in Europe. Since 2004 numerous sediment successions and surface sediments have been recovered from Lake Ohrid in order to investigate modern and past sedimentation patterns, to establish a tephrostratigraphic and chronological framework, and to infer past climatic and environmental changes.

The sound understanding of the modern sedimentation pattern is needed to better understand the past sedimentation conditions in the lake. Modern sedimentation in the Lake Ohrid basin is controlled by a complex interaction of multiple processes. Analysis of biogeochemical bulk parameters, selected metals, pigment concentrations as well as grain size distributions revealed a significant spatial heterogeneity in surface sediment composition. Sedimentation in Lake Ohrid is controlled by an interaction of multiple natural and anthropogenic factors and processes. Major factors controlling modern surface sediment composition are related to differences in geological catchment characteristics, anthropogenic land use, and the existence of a counterclockwise rotating surface water current (Vogel et al. in prep.).

Despite distinct spatial differences, Lake Ohrid appears to have reacted relatively uniformly to climatic forcing on changes in catchment configuration, limnology and hydrology in the past as evidenced by contemporaneous changes in sediment composition in long sediment successions from different parts of the lake basin (Vogel et al. 2010, Wagner et al. in prep.). Occurrences of well-dated tephra and cryptotephra layers as well as radiocarbon, electron spin resonance, and luminescence dating allowed the establishment of a chronological framework for the recovered sediment successions (Wagner et al. 2008; Vogel et al. 2009; Lindhorst et al. in prep.; Sulpizio et al. in prep.). These data revealed that the sediment successions recovered so far from Lake Ohrid in part reach well back into MIS 6.

The recovered sediment successions are characterized by distinctly different sediment successions during glacial and interglacial phases, thus indicating large variations in the interplay of climatic forced factors. Glacial sediments are dominated by clastic clayey-sandy silt, whilst interglacial sediments appear as calcareous clayey-sandy silt (Wagner et al. 2008, Vogel et al. 2010). Apart from this general pattern tied to high amplitude climate fluctuations, short-term climatic fluctuations of reduced amplitude are also recorded in the sediment successions and generally well correlated to other paleoclimate records in the Mediterranean (Wagner et al. 2008, Vogel et al. 2010, Holtvoeth et al. in prep., Leng et al. in prep., Wagner et al. in prep.).

In order to complement this rather qualitative information on past climatic and environmental change, proxies and/or methods allowing a more quantitative inference are required. Dating and sedimentological analyses of sediment successions recovered from subaquatic terrace levels at 32 and 55 m water depth point to significant lake level low stands and thus a significantly drier climate during MIS 6, MIS 5.5, and during the last glacial inception (Lindhorst et al. in prep.). Initial quantitative inferences of past lake surface temperatures

(LST) on 11 samples over the last glacial-interglacial cycle using the TEX_{86} paleothermometer (Schouten et al. 2002; Powers et al. 2004) revealed c. 5-6°C lower temperatures during glacial compared with interglacial periods. The reconstructed glacial and interglacial temperatures from Lake Ohrid correspond relatively well with temperature anomalies derived from sea surface temperature reconstructions in the marine (-4°C) and pollen-based temperature reconstructions in the terrestrial (-9°C) vicinity. This initial dataset on fluctuations of past LST´s using the TEX_{86} paleothermometer is currently been complemented by 190 additional samples allowing an estimate of temperature changes at submillenial resolution over the last glacial-interglacial cycle.

These data gathered from the existing sediment successions in combination with a proposed sediment fill of more than 600 m and its likely Pliocene age highlight Lake Ohrids potential for investigations of past climatic and environmental change and ash dispersal over long time scales in the northern Mediterranean region. In order to recover longer sediment succession extending back into Pliocene times from this promising site an ICDP deep drilling campaign is envisaged for 2011.

References:

Albrecht C, Wilke T (2008) Ancient Lake Ohrid: biodiversity and evolution. Hydrobiol 615:103-140

Holtvoeth J, Vogel H, Wagner B, Wolfe G (in prep.) Environmental change in the Lake Ohrid Basin - evidence from organic-geochemical proxy records. Biogeoscience (special issue)

Leng M, Zanchetta G, Baneschi I, Vogel H, Wagner B (in prep.) Late Quaternary palaeoenvironmental reconstruction from Lakes Ohrid and Prespa in the Mediterranean using stable isotopes. Biogeoscience (special issue)

Lindhorst K, Vogel H, Hilgers A, Zander A, Krastel S, Wagner B, Wessels M, Daut G (in prep.) Subaquatic terrace formation and coastline evolution of Lake Ohrid: a morphological perspective. Biogeoscience (special issue)

Powers LA, Werne JP, Johnson TC, Hopmans EC, Sinninghe Damsté JS, Schouten S (2004) Crenarcheotal membrane lipids in lake sediments: A new paleotemperature proxy for continental paleoclimate reconstruction? Geology 32, 613-616

Schouten S, Hopmans EC, Schefuß E, Sinninghe Damsté JS (2002) Distributional varaiations in marine crenarcheotal membrane lipids: a new organic proxy for reconstructing ancient sea water temperatures? Earth and Planetary Science Letters 204, 265-274

Sulpizio R, Zanchetta G, D´Orazio, Vogel H, Wagner B (in prep.) Tephrostratigraphy and tephrochronology of the lakes Ohrid and Prespa, Balkan area. Biogeoscience (special issue)

Vogel H, Zanchetta G, Sulpizio R, Wagner B, Nowaczyk N (2009) A tephrostratigraphic record for the last glacial-interglacial cycle from Lake Ohrid, Albania and Macedonia. Journal of Quaternary Science. DOI: 10.1002/jqs.1311

Vogel H, Wagner B, Zanchetta G, Sulpizio R, Rosén P (2010) A paleoclimate record with tephrochronological age control for the last glacial-interglacial cycle from Lake Ohrid, Albania and Macedonia. Journal of Paleolimnology, DOI: 10.1007/s10933-009-9404-x

Vogel H, Wessels M, Stich H-B, Wagner B (in prep.) Spatial variability of recent sedimentation in Lake Ohrid (Albania/Macedonia) - a complex interplay of environmental and anthropogenic factors and their possible impact on biogeographical patterns. Biogeoscience (special issue)

Wagner B, Vogel H, Sulpizio R, Zanchetta G, Lotter A, Valsecchi V (in prep.) Heinrich events on the Balkans recorded in the sediments from lakes Prespa and Ohrid. Biogeoscience (special issue)

Wagner B, Lotter AF, Nowaczyk N, Reed JM, Schwalb A, Sulpizio R, Valsecchi V, Wessels M, Zanchetta G (2009) A 40,000-year record of environmental change from ancient Lake Ohrid (Albania and Macedonia). Journal of Paleolimnology 41, 407-430

ICDP

Dust transport from Patagonia to Antarctica – a perspective from the Scotia Sea for the last glacial cycle

M. E. WEBER[1], D. SPRENK[1], G. KUHN[2]

[1]Institute of Geology and Mineralogy, Zuelpicher Str. 49a, 50935 Cologne, Germany, michael.weber@uni-koeln.de
[2]Alfred-Wegener-Institute for Polar and Marine Research, Am Alten Hafen 26, 27568 Bremerhaven, Germany

Dust records of Antarctic ice cores provide important information on past atmospheric circulation. They can be used to evaluate global circulation models and to infer the paleoenvironmental conditions of the surrounding continents. East Antarctic ice cores (e.g., EPICA-DML) indicate southern South America as a major source of dust during Late Quaternary glaciations. There, the cold periods provided drier conditions with increased physical weathering and intensified glacial erosion in combination with a more persistent westerly circulation. We retrieved a deep-sea sediment core from the Scotia Sea, which lies between the presumed source area of the Patagonian loess (e. g., ICDP project PASADO) and East Antarctica (e. g., planned IODP drilling projects for the southeastern Weddell-Sea margin; see Antarctic Climate Evolution (ACE) white paper for IODP; De Santis, 2009), to study the dust history along the trajectory to the Antarctic continent.

Core MD07-3134 was retrieved during cruise MD160 with RV Marion Dufresne II in March 2007 in the Scotia Sea. The core is 58.08 m long and originates from 3663 m water depth. We used core-logging techniques to measure a number of sediment-physical and –optical properties as well as relative paleointensity. Also, we determined biogenic opal, major and minor element concentration, and the amount of ice-rafted debris. Correlation of the dust (nssCa2+) record from the EPICA-DML ice core to the magnetic susceptibility record (MS) of site MD07-3134 provides a one-to-one reproduction of virtually every single increase during the last glacial cycle. Therefore, there is sustained evidence that the MS record is a dust indicator. The oceanic record has, on average, higher amplitudes of variability with elevated contents during glacial stages because it is located closer to the Patagonian source area. Specifically during the Last Glacial Maximum, the upper parts of Marine Isotopic Stage 3 and 4, the Scotia Sea record exhibits strong atmospheric dust signals that did not fully reach the Antarctic continent.

The one-to-one correlation provides a sound age model for the last 92.5 ka. Accordingly, the Scotia Sea site has relatively high average sedimentation rates of roughly 65 cm/ka. We established up to 20 confident age control points within the boundaries given by the relative paleointensity record and other stratigraphic indicators. The fact that we phase-locked nssCa2+ and MS seems reasonable because both signals are atmospheric and, hence, we assume no major leads or lags. With the establishment of a high-resolution age model, upcoming studies will relate in detail the temperature record over East Antarctica to the paleoclimate proxies determined at site MD07-3134 in order to distinguish between atmospheric and oceanic signals.

IODP

Microbial respiration and diagenetic redox cycling in sediments of the high-productivity Bering Sea (IODP Expedition 323)

L.M. WEHRMANN[1], T.G. FERDELMAN[1], B. BRUNNER[1], C. MÄRZ[2], Y. HUH[3], M. IKEHARA[4], N. RISGAARD-PETERSEN[5], H. SCHRUM[6], E.A. WALSH[6], S. D'HONDT[6], A.C. RAVELO[7], K. TAKAHASHI[8], C. ALVAREZ-ZARIKIAN[9] AND IODP EXPEDITION 323 SCIENTISTS

[1]Max Planck Institute for Marine Microbiology, Bremen, Germany
[2]Institute for Chemistry and Biology of the Marine Environment (ICBM), Oldenburg University, Germany
[3]Seoul National University, Korea
[4]Kochi University, Japan
[5]Center of Geomicrobiology, Aarhus University, Denmark
[6]University of Rhode Island, USA
[7]University of California, Santa Cruz, USA
[8]Kyushu University, Fukuoka, Japan
[9]IODP-USIO, Texas A&M University, College Station, USA

At present, the Bering Sea is among the most productive areas of the world. High productivity is, however, largely constrained to the "Green Belt" propagating along the shelf break under the influence of the Bering Slope Current (BSC). Nevertheless, the Bering Sea is regarded as an effective atmospheric CO_2 sink in the modern carbon cycle due to the efficient biological pump involving high biogenic opal contents. Integrated Ocean Drilling Program (IODP) Expedition 323 to the Bering Sea afforded the opportunity to study carbon cycling and microbially-mediated diagenetic pathways in a wide range of productivity regimes that diverge in sedimentation rates and lithology. A drilling depth of >700 m combined with high-resolution sampling in the top 36 m allowed for a unique approach to deepen the understanding of organic-fueled microbial activity in the deep biosphere of this high latitude-high productivity area as proposed by Ancillary Project Letter 739-APL (S. D'Hondt, T.G. Ferdelman, J. Kallmeyer, A.J. Spivack, R. Pockalny: "Microbial respiration, biomass and community composition in subseafloor sediment of the very high-productivity Bering Sea"). Furthermore, it allows deciphering the effect of spatial and temporal variability of regional productivity linked to Pleistocene-Pliocene paleoenvironmental changes of this highly climate-sensitive region expressed in variable microbial respiration rates and pathways in the sediment.

We present results from two sites that show different extents of microbially-mediated redox diagenesis. Site U1344 located at 3220 m water depth in the northern Aleutian Basin shows the influence of the Green Belt manifested in rapidly accumulating organic-rich sediments (29-50 cm/kyr). Biogeochemical processes at this site are strongly influenced by the presence of high methane concentrations that lead to the installation of a shallow sulfate-methane transition zone (SMTZ) at 8.3 m driven by sulfate reduction coupled to the anaerobic oxidation of methane (AOM). Dissolved inorganic carbon and alkalinity concentrations up to 74 mM and ammonium concentrations as high as 11.4 mM likewise reflect the high rates of organic matter turnover at this site. The initial data show that the deeply buried sediments at the Bering Sea margin continue to function as a microbially active repository for organic carbon. The occurrence of very high concentrations of biogenic methane and a shallow STMZ highlight the importance of methanogenesis during carbon mineralization.

Site U1341 located at 2177 m water depth on Bowers Ridge shows deep sulfate penetration, low dissolved inorganic carbon and alkalinity concentrations (~12 mM), and low ammonium values (5.1 mM), indicating low present-day microbial respiration. The sulfur isotope composition of sedimentary pyrite, however, recorded strong ^{34}S-enrichment in the sediment interval deposited between ~ 2.0 and 3.8 Ma. These data suggest a period of enhanced sulfate reduction probably as a result of high paleoproductivity in the Bowers Ridge region (see also Poster by C. März et al.). The occurrence of distinct authigenic layers of dolomite supports the assumption that microbial carbon respiration rates were elevated during this time period. Diagenetic conditions between ~ 2.0 and 3.8 Ma may have resembled the present-day biogeochemistry at Site U1344 and may have involved a prominent role of methanogenesis and the concomitant installation of a SMTZ. Intriguingly, the pore-water concentration and sulfur isotope composition of sulfate from this site still carries the imprint of the former AOM-driven sulfate depletion. Increasing sulfate concentrations below the former location of the SMTZ suggest that a deep sulfate source is impinging on the pore-water sulfate signal.

ICDP

The ICDP Deep Drilling at Lake El'gygytgyn, NE Siberia: Operational Success and First Results

V. WENNRICH[1], M. MELLES[1], JULIE BRIGHAM-GRETTE[2], PAVEL MINYUK[3], CHRISTIAN KOEBERL[4] & ELGYGYTGYN SCIENCE PARTY

[1]University of Cologne, Institute of Geology and Mineralogy, Zuelpicher Str. 49a, D-50674 Cologne, Germany
[2]University of Massachusetts, Dept of Geosciences, 611 N. Pleasant Street, Amherst, MA 01003, USA
[3]Russian Academy of Sciences, Northeast Interdisciplinary Scientific Research Institute, Portovaya 16, Magadan, 685000 Russia
[4]University of Vienna, Center for Earth Sciences, Althanstrasse 14, 1090 Vienna, Austria

High arctic Lake Elgygytgyn (67°30' N, 172°05' E) is a 3.6 Ma old meteorite crater lake located in Chukotka/NE Siberia. From Oct. 2008 until Mai 2009 an ICDP drilling campaign was conducted at Lake Elgygytgyn, achieving its three major objectives.

First of all, drilling from the ice cover in the lake center penetrated the complete 315-m long sediment sequence of Lake Elgygytgyn. The sediments show no obvious indications for hiatuses due to glaciation or desiccation. Hence, their temporal length and geologic significance is absolutely unprecedented, for the first time providing deep and widely continuous insights into the climatic and environmental evolution of the terrestrial Arctic since Pliocene times. First preliminary results suggest highly variable climatic and/or environmental conditions in NE Siberia during the Quaternary, which was drilled with almost 100 % recovery. Within the Pliocene, corresponding to the lower app. 200 m of the core, various distinct climatic variations are indicated. The Pliocene climate

record seams to be partly masked by an enhanced rate of mass movement deposits.

Second, a ca. 200 m thick, almost complete section of impact breccias was recovered underneath the lake sediments, consisting of a 60 m thick suevite layer above monomictic breccia and broken and fractured volcanic basement rocks. Investigation of this core sequence promises new information concerning the El´gygytgyn impact event, including the composition and nature of the meteorite, the energy released, and the shock behaviour of the volcanic basement rocks.

And third, a 142 m long sequence was recovered from the permafrost deposits in the western lake catchment, only a few hundred meters from the lake shore. The core consists of sandy and gravelly alluvial fan deposits, which are continuously frozen and rich in ground ice. The sediment and ice composition promises to provide complementary information on the regional climatic history and lake-level fluctuations. Besides, a thermistor chain installed in the drill hole as part of the "Thermal State of Permafrost Network" of the International Permafrost Association will contribute to the understanding of the permafrost behaviour under the currently changing climatic settings.

In summary, the drilling operation at Lake El´gygytgyn in winter 2008/09 has kept behind the expectations with regard to the quantity of core material, however, it is regarded as great success taking the potential the high-quality material has to address the three major scientific goals of the project. The presentation will summarize the operational success of the drilling campaign and highlight the scientific results obtained so far based on the limited onsite and ongoing offsite core processing.

IODP

First time real-time mud gas monitoring during riser drilling in Nankai Trough (IODP Exp319)

T. WIERSBERG[1], J. ERZINGER[1], AND THE EXPEDITION 319 SCIENTISTS

[1]Helmholtz-Zentrum Potsdam, Deutsches GeoforschungsZentrum , Telegrafenberg, 14473 Potsdam

Chikyu Expedition 319 was the first cruise of the IODP when riser drilling was performed scientifically and while real-time mud gas monitoring was conducted. Conventional IODP drilling uses mainly sea water as drilling fluid which is not recirculated, however, during riser drilling the drill mud returns back to the ship through a riser pipe which encases the drill pipe. The dissolved gas is extracted from returning drill mud and analyzed in real-time, furthermore sampled for off-line noble gas and stable isotopes studies. This technique has been applied in the past on several scientific continental drilling projects of e.g. ICDP.

Expedition 319 was part of the NanTroSEIZE project, a multiexpedition, multistage IODP drilling program focused on understanding the mechanics of seismogenesis and ruptures propagation along the Nankai accretionary prism. Riser drilling was carried out on Site NT2-11, located approx. 60 km SE of Shingu harbor. This site was chosen (i) to collect drill core and cutting samples of the upper basin fill sediments in the hanging wall of the plate boundary fault, (ii) to measure in situ pore pressures and stress states downhole, and (iii) for installation of a long-term borehole monitoring observatory. Hole C0009A intersects the cover sediments of the Kumano Basin and probably penetrates into the accretionary prism below.

Real-time mud gas monitoring was performed in Hole C0009 during drilling from 703 to 1594 mbsf (meter below sea floor) and during hole enlargement from 703 to 1569 mbsf. Both datasets show similar gas distribution at depth. Gas was furthermore extracted, sampled and analyzed from 24 drill cutting samples.

Drill mud gas is mainly composed of air in addition to gases that derive from the formation. The principal formation gases from both drilling phases and in cuttings were hydrocarbons, mainly methane. Up to 14 vol % CH_4 was detected during drilling and up to 3 vol % during hole enlargement. Down to 800 mbsf and below 1280 mbsf, the methane concentration in drill mud is lower than in the interval between where methane peaks at several depths. At 1280 mbsf an unconformity is indicated from lithology, in seismic and paleobiostratigraphic data, and from physical property measurements.

During hole enlargement, the mud gas was also analyzed for heavier hydrocarbons. Traces of ethane (up to 16 ppmv) and propane (up to 3 ppmv) were detected, however, the Bernhard parameter $CH_4/[C_2H_6 + C_3H_8]$ was always higher than 500, mostly in the range of 1000. The molecular composition of hydrocarbons and the isotope composition of methan ($\delta^{13}C$ from -63.3 to -67.4‰ PDB) are clear evidences for a microbial source. Furthermore, the distribution of methane with depth correlates with the presence of coal and wood fragments found in drill cuttings. The hydrocarbons are probably located in the pore space, as suggested from Vp/Vs data, and do not enter the hole through fractures or permeable faults.

To estimate the gas concentration in drill mud, a defined amount of CaC_2 (500g) was dropped in the hole for calibration purpose. Integration of the resulting C_2H_2 peak that corresponds to 175.000cc (STP) acetylen gas enables the determination of the absolute methane concentration from drill-mud gas vs. time. From this data, gas concentration per volume of drilled rock was calculated by using the known rates of penetration (ROP) and the effective borehole areas.

The methane concentration was also determined in drill cuttings. Known amounts of cuttings were placed in gas-tight bags and spiked with 10cc of Kr. After 100h of gas extraction, the accumulated gas phase was sampled and analyzed. To prove that gas release was completed, three samples from 896, 967 and 1060 mbsf were also treated 270h. Methane concentration were similar at all times, suggesting that no additional gas was liberated after 100h.

Methane in drill mud and in drill cuttings show similar depth profiles, but gas concentrations are about two order of magnitude lower in drill cuttings. The methane concentration per rock mass, calculated from mud gas, ranges from approx. 0.1 to 0.5 cc/g [STP] in the depth interval 967 to 1305mbsf. Between 1329 and 1585 mbsf, methane concentrations are between approx. 0.02 and 0.1 cc/g [STP].

ICDP

Vegetation history in southern Patagonia: first palynological results of the ICDP lake drilling project at Laguna Potrok Aike, Argentina

M. WILLE[1], F. SCHÄBITZ[1], PASADO SCIENCE TEAM"

[1]Seminar für Geographie and Education, University of Cologne, Gronewaldstr. 2, 50931 Cologne, Germany
[2]http://dc-app1-02.gfz-potsdam.de/site/contacts/contacts-search-all?select=3&term=pasado

Laguna Potrok Aike located in southern Argentina is one of the very few locations that are suited to reconstruct the paleoenvironmental and climatic history of southern Patagonia. In the framework of the multinational ICDP deep drilling project PASADO several long sediment cores to a composite depth of more than 100 m were obtained. Here we present first results of pollen analyses from sediment material of the core catcher. Absolute time control is not yet available. Pollen spectra with a spatial resolution of three meters show that Laguna Potrok Aike was always surrounded by Patagonian Steppe vegetation. However, the species composition underwent some marked proportional changes through time. The uppermost pollen spectra show a high contribution of Andean forest and charcoal particles as it can be expected for Holocene times and the ending last glacial. The middle part shows no forest and relatively high amounts of pollen from steppe plants indicating cold and dry full glacial conditions. The lowermost samples are characterized by a significantly different species composition as steppe plants like Asteraceae, Caryophyllaceae, Ericaceae and Ephedra became more frequent. In combination with higher charcoal amounts and an algal species composition comparable to Holocene times we suggest that conditions during the formation of sediments at the base of the record were more humid and/or warmer causing a higher fuel availability for charcoal production compared to full glacial times.

IODP

$^{34}S/^{32}S$ and $^{18}O/^{16}O$ ratios of dissolved sulfate from interstitial water samples above gas hydrate bearing sediments of IODP Expedition 311, Cascadia margin

U. G. WORTMANN, B. M. CHERNYAVSKY, M. TORRES, M. KASTNER

Dept. of Geology, University of Toronto, Canada, uli.wortmann@utoronto.ca
Institute of Integrated Energy Systems, University of Victoria
College of Oceanic and Atmospheric Sciences, Oregon State University, Corvallis, Oregon, USA.
Scripps Institution of Oceanography, University of California San Diego, La Jolla, California, USA.

Microbially mediated sulfate reduction affects the isotopic composition of dissolved and solid sulfur species in marine sediments. Although several details of the fractionation process remain controversial, the overall process is well understood and can be described as the sum of several mass dependent fractionations during the enzymatically catalyzed stepwise reduction of sulfate to sulfide. The overall istope effect is a function of the ratio between the forward and backward fluxes of sulfur between the individual reduction steps and across the cell-membrane. In order to express large isotopic effects the ratio between forward and backward fluxes must be >=1. While it is difficult to quantify these fluxes, recent developments in CF-IRMS techniques together with advances in reaction transport modeling facilitate the routine determination of bulk forward and backward flux ratios of SO4 in porous sediments. Here we report measurements from deep-sea sediments offshore Vancouver Island (IODP Expeditiopn 311, Cascadia Margin). These sediments are characterized by high net sulfate reduction rates near the benthic boundary layer and within the sulfate methane interface. In between these two zones, carbon limitation causes net sulfate rates to drop by 3 orders of magnitude. However, backward fluxes change only on the order of one magnitude and are of similar magnitude as previously reported fluxes. We therefore hypothesize that backward fluxes have a natural upper limit which is independent of the magnitude of the forward fluxes. This assumption readily explains why fractionation factors higher then 46\% have only been observed in environments where forward fluxes are very small, and thus allow for flux ratios close to unity. Furtermore, we use these results to constrain the rates of organotrophic versus methanotrophic sulfate reduction. Our results show that even in cases where sulfate concentration decline in a linear fashion, up to 50\% of all sulfate is consumed by organotrophic sulfate reduction.

ICDP

Characterisation of the 106 m long lacustrine sediment record from Laguna Potrok Aike, Argentina (ICDP-project PASADO)

B. ZOLITSCHKA[1], C. OHLENDORF[1], C. GEBHARDT[2], A. HAHN[1], P. KLIEM[1], AND THE PASADO SCIENCE TEAM[3]

[1]Geopolar, Institute of Geography, University of Bremen, Celsiusstr. FVG-M, 28359 Bremen, Germany
[2]Alfred Wegener Institute for Polar and Marine Research, Bremerhaven, Germany
[3]http://www.icdp-online.org/contenido/icdp/front_content.php?idcat=960

Laguna Potrok Aike is located in the South-Patagonian province of Santa Cruz (52°58'S, 70°23'W; 116 m a.s.l.; diameter: 3500 m, water depth: 100 m) and was formed by a volcanic (maar) eruption in the late Quaternary Pali Aike Volcanic Field several hundred thousand years ago (Zolitschka et al., 2006). This archive holds a unique record of climatic and environmental variability (Mayr et al., 2009) from a region sensitive to fluctuations in southern hemispheric wind and pressure systems, which provide a cornerstone for the understanding of the entire global climate system (Mayr et al., 2007; Wagner et al., 2007). Moreover, Laguna Potrok Aike is close to many active volcanoes allowing a better understanding of the history of volcanism in the Pali Aike Volcanic Field as well as in the Andean mountain chain. The latter is located in a distance of less than 150 km to the west with volcanic ash layers being deposited as far away as the Antarctic continent (Narcisi et al., 2010). Additionally, Patagonia is

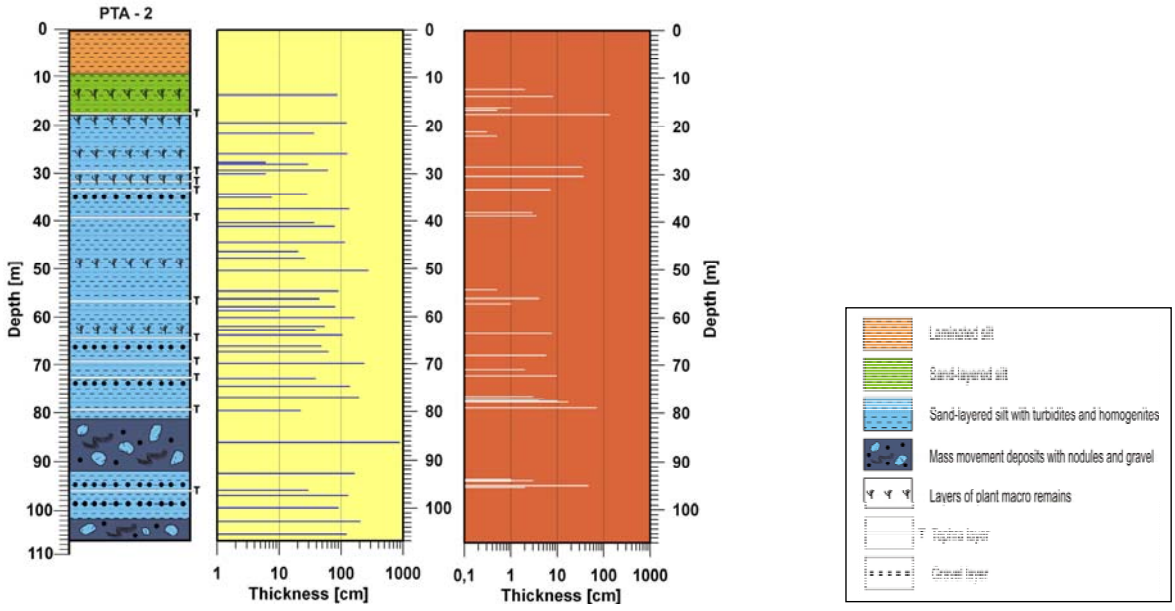

Fig. 1: Lithology of the composite profile (left) from Site 2 of Laguna Potrok Aike (PTA-2) with the thickness of redeposited sediment layers (center) and volcanic ash layers (right).

the source region of eolian dust blown from the South American continent into the South Atlantic and onto the Antarctic ice sheet (Delmonte et al., 2010; Gabrielli et al., 2010; Haberzettl et al., 2009). The currently ongoing global climate change, the threads of volcanic hazards and the regional dust storms are of increasing socio-economic relevance and thus challenging scientific themes that are tackled for southernmost South America with an interdisciplinary research approach in the framework of the ICDP-funded "Potrok Aike Maar Lake Sediment Archive Drilling Project" (PASADO).

Drilling operations for this southernmost ICDP project PASADO are dedicated to terrestrial climatic and environmental reconstruction. Field work was completed in late November 2008 (Zolitschka et al., 2009). From the maar lake Laguna Potrok Aike in total 510 m of lacustrine sediments have been recoverd using the GLAD800 platform equipped with a CS-1500 drill rig. Quadruplicate

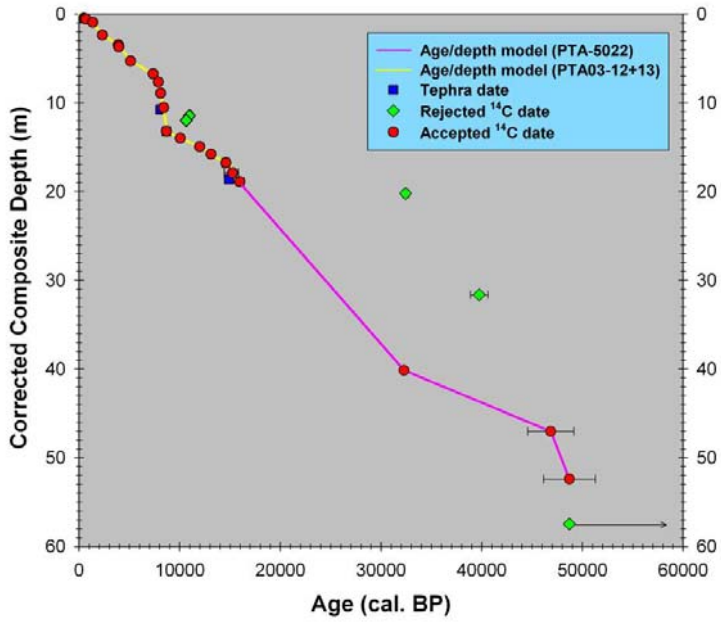

Fig. 2: Age-depth plot for the composite profile of Site 2 from Laguna Potrok Aike. Note that the "corrected composite depth" refers to the fact that all redeposited sediment sections have been substracted from the entire length of the record. The age-depth model for core PTA 03-12 and -13 is from Haberzettl et al. (2007, modified).

and triplicate cores down to a maximum hole depth of 101.5 m blf (below lake floor) have been taken mainly using the hydraulic piston coring tool. Total core recovery was 94,4 % from two drillsites located 700 m apart from each other in the central deep and profundal plane of the lake. In 2009 cores were opened, described and documented by digital high-resolution photography and scanned with different non-destructive techniques. A 106 mcd (meters composite depth) long profile was constructed for Site 2 based on visual core correlation (Fig. 1) and thereafter subsampled in consecutive 2 cm thick intervalls. Core scanning was performed with 5 mm spatial resolution for all parameters and involved the following techniques: (1) color scanning with a handheld X-rite spectrometer, (2) magnetic susceptibility scanning with a Bartington MS2F-sensor, (3) XRF scanning and X-radiography with an ITRAX core scanner (COX analytical systems) and (4) p-wave velocity/transmission seismograms and gamma ray absorption with a modified Geotek multi sensor core logger tool (MSCL).

The composite profile consists of undisturbed laminated and sand-layered lacustrine silts with an increasing number of coarse gravel layers, turbidites and homogenites at depth (Fig. 2). Below 80 mcd two mass-movement deposits of 10 m and 5 m in thickness are recorded. These deposits show tilted and distorted layers as well as nodules of fine-grained sediments and randomly distributed gravel. Such features either indicate an increased seismicity that cannot be completely excluded for this late Quaternary backarc volcanic field or they are the result of hydrologically induced lake level variations and hence relate to changes in hydrological conditions within the catchment area. Intercalated throughout the record are 24 macroscopically visible volcanic ash layers (Fig. 2) that document the regional volcanic history and open the possibility to establish an independent time control through tephrochronology supported by Ar/Ar dating. Moreover, these isochrones potentially act as links to marine sediment records from the South Atlantic and to Antarctic ice cores. Preliminary extrapolation of the mean sedimentation rate of 1.1 mm/a determined for the upper 16 ka (Haberzettl et al., 2007) indicates that a continuous and high quality record may go back in time to approximately 50,000 years (Fig. 2). Such a time frame is supported by first radiocarbon dates obtained from aquatic mosses.

According to this preliminary age model, the sedimentary record from Laguna Potrok Aike reaches back to Oxygen Isotope Stage 3 and exhibits contrasting lithologies downcore especially in the Pleistocene part of the record. Moreover, first estimates indicate that up to 50% of the record consist of redeposited sediments. Element profiles acquired by XRF core logging document these pronounced downcore lithological changes.

As a terminal lake, the sedimentary record of Laguna Potrok Aike is well suited to trace temporal changes in the hydrological cycle. Subaerial and subaquatic terraces evidence large lake level variations of more than 50 m (from +21 m to -35 m) during Holocene and Late Glacial periods (Anselmetti et al., 2009). These have been recorded as variations of inorganic carbon percentages and of XRF counts for calcium (Ca) in the sedimentary record. However, while the element profile of Ca is controlled by the proportion of authigenically precipitated calcite in the lake since the Lateglacial this seems to be different during earlier periods of the Pleistocene. Hence, XRF Ca counts in this older intervall, which represents more than 80% of the sediment thickness recovered during the PASADO drilling campaign, seem to be controlled by different mechanisms.

References:

Anselmetti, F., Ariztegui, D., De Batist, M., Gebhardt, C., Haberzettl, T., Niessen, F., Ohlendorf, C., Zolitschka, B., 2009. Environmental history of southern Patagonia unraveled by the seismic stratigraphy of Laguna Potrok Aike. Sedimentology 56: 873–892.

Delmonte, B., P.S. Andersson, H. Schöberg, M. Hansson, J.R. Petit, R. Delmas, D.M. Gaiero, V. Maggi, M. Frezzotti, 2010. Geographic provenance of aeolian dust in East Antarctica during Pleistocene glaciations: preliminary results from Talos Dome and comparison with East Antarctic and new Andean ice core data Quaternary Science Reviews 29: 256–264.

Gabrielli, P., Wegner, A., Petit, J.R., Delmonte, B., De Deckker, P., Gaspari, V., Fischer, H., Ruth, U., Kriews, M., Boutron, C., Cescon, P., Barbante, C., 2010. A major glacial-interglacial change in aeolian dust composition inferred from Rare Earth Elements in Antarctic ice. Quaternary Science Reviews 29: 265–273.

Haberzettl, T., Corbella, H., M. Fey, S. Janssen, A. Lücke, C. Mayr, C. Ohlendorf, F. Schäbitz, G.-H. Schleser, E. Wessel, M. Wille, S. Wulf, B. Zolitschka, 2007. A continuous 16,000 year sediment record from Laguna Potrok Aike, southern Patagonia (Argentina): Sedimentology, chronology, geochemistry. The Holocene 17: 297-311.

Haberzettl, T., F.S. Anselmetti, S.W. Bowen, M. Fey, C. Mayr, B. Zolitschka, D, Ariztegui, B. Mauz, C. Ohlendorf, S. Kastner, A. Lücke, F. Schäbitz, M. Wille, 2009. Late Pleistocene dust deposition in the Patagonian steppe - extending and refining the paleoenvironmental and tephrochronological record from Laguna Potrok Aike back to 55 ka. Quaternary Science Reviews 28: 2927-2939.

Mayr, C., M. Wille, T. Haberzettl, M. Fey, S. Janssen, A. Lücke, C. Ohlendorf, G. Oliva, F. Schäbitz, G.-H. Schleser, B. Zolitschka, 2007. Holocene variability of the Southern Hemisphere westerlies in Argentinean Patagonia (52°S). Quaternary Science Reviews 26: 579-584.

Mayr, C., A. Lücke, N.I. Maidana, M. Wille, T. Haberzettl, H. Corbella, C. Ohlendorf, F., Schäbitz, M. Fey, S. Janssen and B. Zolitschka, 2009. Isotopic and geochemical fingerprints on lacustrine organic matter from Laguna Potrok Aike (southern Patagonia, Argentina) reflect environmental changes during the last 16,000 years. Journal of Paleolimnology 42: 81-102.

Narcisi, B, Petit, J.R., Delmonte, B., 2010. Extended East Antarctic ice-core tephrostratigraphy. Quaternary Science Reviews 29: 21–27.

Wagner, S., M. Widmann, J. Jones, T. Haberzettl, A. Lücke, C. Mayr, C. Ohlendorf, F. Schäbitz, B. Zolitschka, 2007. Transient simulations, empirical reconstructions and forcing mechanisms for the Mid-Holocene hydrological climate in Southern Patagonia, Climate Dynamics 29: 333-355.

Zolitschka, B., Schäbitz, F., Lücke, A., Clifton, G., Corbella, H., Ercolano, B., Haberzettl, T., Maidana, N., Mayr, C., Ohlendorf, C., Oliva, G., Paez, M.M., Schleser, G.H., Soto, J., Tiberi, P., Wille, M., 2006. Crater lakes of the Pali Aike Volcanic Field as key sites of paleoclimatic and paleoecological reconstructions in southern Patagonia, Argentina. Journal of South American Earth Sciences 21: 294-309.

Zolitschka, B., F. Anselmetti, D. Ariztegui, H. Corbella, P. Francus, C. Ohlendorf, F. Schäbitz and the PASADO Scientific Drilling Team, 2009. The Laguna Potrok Aike Scientific Drilling Project PASADO (ICDP Expedition 5022). Scientific Drilling, 8: 29-34.

IODP

Drilling and monitoring of natural and man-made landslide trigger mechanisms at the Ligurian slope (W'Mediterranean Sea): the Nice Airport Landslide NAIL

STEGMANN, S., HENRY, P., KOPF, A., SULTAN, N., SPIESS, V., DE LANGE, G., MORAN, K., MORGAN, J.K., MIGEON, S., CAMERLENGHI, A., YAMADA, Y., SOLHEIM, A., TINTI, S., CHARVIS, P.

Concerning geohazards, the current IODP Initial Science Plan expiring in 2013 refers mainly to earthquakes and gas hydrate dissociation. However, submarine landslides represent a major societal threat and an exciting research target given the wealth of trigger mechanisms and their interaction at both active and passive ocean margins.

Hence we have recently submitted a mission-specific drilling proposal at the Ligurian Margin off Nice (Eastern Mediterranean) where a large number of trigger mechanisms of slope failure can be addressed in a small area, e.g. seismicity, sedimentary/tectonic loading, creep of weak clays, groundwater-charging as well as man-mad construction. Drill sites aim to characterize the metastable slope beside of the former collapse structure, and the re-deposited material partly occupying the present-day landslide scar. The target depth at each site will provide reconnaissance data and characterization of the underlying strata down to ~150mbsf. Geotechnical drilling (coring, in situ sonic CPTU) will identify mechanically weak vs. strong layers, hydraulically active horizons, and zones of overpressure owing to groundwater-charging or vertical loading. Long-term objectives include borehole observatory installations and monitoring of the governing physical parameters affecting slope failure (pore pressure, temperature, strain, seismicity) in this socio-economically relevant part of the French Riviera.